

# IRRIGATION WITH POOR-QUALITY MINE WATER IN MPUMALANGA

*JG Annandale, PD Tanner and SN Heuer*



**WATER  
RESEARCH  
COMMISSION**

TT 855/1/21



# IRRIGATION WITH POOR-QUALITY MINE WATER IN MPUMALANGA

Report

to the Water Research Commission

by

JG Annandale, PD Tanner and SN Heuer (editors)

Department of Plant and Soil Sciences  
University of Pretoria

Report No. TT 855/1/21  
ISBN 978-0-6392-0267-9

**July 2021**



**WATER**  
RESEARCH  
COMMISSION

Obtainable from:

Water Research Commission

Lynnwood Bridge Office Park

4 Daventry Street

Lynnwood Manor

Pretoria

0081

[orders@wrc.org.za](mailto:orders@wrc.org.za) or download from [www.wrc.org.za](http://www.wrc.org.za)

#### **DISCLAIMER**

This report has been reviewed by the Water Research Commission (WRC) and approved for publication. Approval does not signify that the contents necessarily reflect the views and policies of the WRC, nor does mention of trade names or commercial products constitute endorsement or recommendation for use.

## EXECUTIVE SUMMARY

---

The mining industry in South Africa produces large volumes of mine-impacted water and the agricultural industry requires large water inputs to improve and maximise crop yields. A noteworthy opportunity, therefore, arises for the use of mine water for irrigation, if monitored and correctly managed, to facilitate sustainable mine closure. It could also provide an alternative strategy for operating mines, and for the use of mine water, with or without treatment, depending on the quality.

Success with mine water irrigation has been demonstrated in several previous Water Research Commission (WRC) studies. However, this approach to using suitable mine water has not received traction, partly due to the difficulty of authorising such use, which is partially due to a lack of confidence in the viability of this practice. Chapter 1 gives a brief overview of irrigation with mine-impacted waters, and the objectives of this project to address key issues regarding this practice.

This project evaluates and demonstrates successful irrigation with untreated mine water on a single unmined site, and evaluates issues associated with setting up irrigation on a rehabilitated site. In addition, factors that are likely to affect the success of using untreated acid mine drainage (AMD) and partially treated AMD for irrigation are investigated in depth. The economic viability of mine water irrigation projects is analysed, which leads to the development of a technical guideline to assist mines and regulators to establish irrigation projects using mine water.

Chapter 2 reports on the monitoring results of three successful summer maize cropping seasons and one winter rye season at the Mafube pivot on unmined land. The Mafube unmined pivot provides a platform for the longer-term quantification, monitoring and modelling of salt and water balances when irrigating with poor-quality mine water.

The recently developed irrigation water quality decision support system (DSS) makes use of soil-water balance (SWB) model simulations to predict the long-term water and salt balances of site-specific scenarios. It can, therefore, predict the sustainability of irrigation with different types of mine-impacted water under various cropping system and water management scenarios. Chapter 3 covers the DSS modelling of two cropping systems using the water quality supplied for irrigation at Mafube. Long-term estimates of salt and water balances were made using weather data from a nearby weather station, showing that roughly a third of the salt applied to the profile is expected to precipitate as gypsum, thereby keeping these salts out of adjacent water sources. In addition, if the water quality were to remain unchanged over time, no meaningful reduction in crop yield is expected using this particular water for irrigation.

Many mines have large areas of rehabilitated lands. These often have complex soil profiles with large spatial variability in chemical and physical properties. It is important to ascertain what is required to get rehabilitated land to an irrigable potential as, apart from the availability of such land in close proximity to mine water, the impact of irrigating such fields with mine water may be considered more environmentally responsible than the irrigation of unmined lands. This is because it is easier to control the fate of solutes moving beyond the root zone on rehabilitated profiles. Chapter 4 summarises the progress of the establishment of the pivot on rehabilitated land at Mafube over the project period. Although no crop production has taken place on this pivot on rehabilitated land yet, a better understanding of the field conditions required to commence irrigation on rehabilitated land has been obtained. Specifically, it is important to fill in any surface depressions resulting from subsidence in order to ensure that the water will not pond in the field, but rather be able to run off site in a controlled manner. In addition, filling and levelling can cause compacted layers that need to be ripped to at least 300 mm with heavy mine equipment. Normal agricultural tractors and rippers are likely to be ineffective. This valuable research site is now almost ready to test the irrigation of such fields.

Chapter 5 outlines the planning, design, equipment installation and field plot establishment at the Kromdraai mine site, where irrigation with untreated AMD or limed, but unclarified mine waters would have occurred. Unfortunately, due largely to safety and deteriorating security situations, the site was never irrigated, so no field trial results could be obtained. Using limed soil as the “treatment plant” for AMD under field conditions, if feasible and sustainable, could eliminate the need for a high-density sludge (HDS) processing plant. This would save enormous capital and some of the running costs of operating an HDS plant. If this is not feasible, and there is still a need to neutralise AMD in a liming plant, irrigating with unclarified, neutralised mine water, if feasible and sustainable, would eliminate the need for the clarification of limed water and sludge disposal (which is an expensive operation). Studies on crop and soil response to irrigation with AMD and with unclarified and clarified, neutralised mine water for irrigation are clearly still needed, and the planning, design and installation done so far will aid in setting up future trials of these novel concepts.

Because the research team experienced difficulties accessing the site and establishing a safe environment in which to work, many detailed laboratory and glasshouse studies were executed in support of the concept of irrigating crops with untreated or partially treated AMD.

Chapter 6 outlines the use of high-density sludge as a soil amendment in support of the concept of irrigating crops with unclarified, neutralised AMD, where large loads of sludge will accumulate in soil profiles. A detailed study is made of the hazardous status of several local HDS products to assess their potential impact on crops and soils. South African hazardous waste guidelines were found to be somewhat impractical, with several published thresholds against which to measure constituents of concern being below typical method detection limits. In addition, the inclusion of manganese in local guidelines may be unnecessary, with several leading international guidelines not considering this element. Using HDS products as soil amendments can improve soil fertility through the increase of the soil pH by the residual lime they contain and can increase calcium and sulphur concentrations in deficient soils. In addition, potentially toxic transition metals may be sequestered by iron hydroxides. It is clear that careful attention will need to be paid to crop nutrition under irrigation with unclarified, neutralised AMD, as the availability of phosphorus may be reduced.

The possibility of irrigating crops directly with AMD on soils that are strategically limed has been identified as a potentially fruitful research area. One of the questions that arises when considering this unusual practice is whether or not crop foliage will be scorched, thereby reducing photosynthetic leaf area, and reducing production to below economic levels. Chapter 7 considers the scorching of two monocotyledonous and two dicotyledonous crops in the seedling and later growth stages. It is concluded that cowpea, soybean and sorghum exhibit significant morphological defects as a result of foliar wetting with simulated AMD in the early seedling stage, but field-planted crops were resistant to foliar wetting with synthetic AMD after the seedling stage, and no reduction in crop growth was observed. Possible methods to restrict seedling damage in the early stages are suggested, as are future research opportunities.

Chapter 8 evaluates the water quality guidelines and food safety implications when irrigating with water rich in arsenic and lead. Crops grown in soils or irrigated with water-containing, elevated levels of potentially hazardous trace elements, such as arsenic and lead, have repeatedly exceeded international food safety guidelines. The primary objective of this study was to evaluate whether the uptake of arsenic or lead present in irrigation water, or built up in the soil as a result of irrigation, results in edible plant parts exceeding food safety thresholds for those elements. The outcome indicated that the South African Irrigation Water Quality Guidelines (Department of Water Affairs and Forestry, 1996) for arsenic and lead need to be revised, so as to negate all possible future contamination of fresh produce resulting from irrigation inputs. Of specific concern is that published food safety guidelines did not exist when the irrigation water quality guideline thresholds were established. In addition, foliar uptake of constituents of concern was shown to be an important uptake pathway. This is not included in any water quality guideline.

The strategic liming of the field before irrigation is essential if crops are to be irrigated with untreated AMD. In essence, the idea is to turn the limed field into an AMD neutralisation reactor. To optimise such management practices, one needs to better understand the neutralisation reactions. Chapter 9 summarises key findings around the limestone neutralisation of synthetic acids in an aqueous environment and sand columns. This study assesses calcitic limestone as a neutralising agent and whether a soil profile containing limestone can act as a reactor and aid the neutralisation of acid mine water percolating through soil columns. Limestone particle size is crucial in determining the efficiency of neutralisation, and the surface application of limestone ensures the effective neutralisation of infiltrating AMD.

Manganese is present in many mine-affected waters. There are widely adopted, but costly processes to remove manganese from mine-impacted waters, and more affordable alternative options are required. Irrigation with Mn(II)-rich water on soils that are able to immobilise manganese is possibly one such alternative solution. Chapter 10 summarises the quantification and comparison of the abilities of different soils to oxidise and immobilise Mn(II). Soils have varying Mn(II)-oxidising potential (MOP). The MOP of soils is an index that indicates the Mn(II) oxidation effectiveness of different soils. A soil's MOP and its ability to accept electrons will determine how effective it is in immobilising Mn(II), as is required when irrigating with manganese-rich mine waters.

A key consideration when selecting a mine water treatment or utilisation option is that of cost effectiveness. Chapter 11 provides a summary of the economic feasibility of irrigating with mine-impacted water. Irrigating with poor-quality mine water is economically viable but may not always be financially feasible without additional capital contributions. It was also noted that increasing salinity levels leads to decreased yields, which proves, as one would expect, to have a negative impact on economic viability. It is clear from this economic study that productive use can be made of mine water suitable for irrigation, and that sustainable livelihoods can be created.

It is concluded that, based on available evidence, suitable mine water, if well managed, can be used to successfully and sustainably irrigate crops. The technical guidelines developed provide a tool for defining how to approach such projects. Additional research is urgently required to develop guidelines for the irrigation of complex rehabilitated soil profiles. In addition, the novel concept of irrigation with untreated or partially treated mine water on suitably limed soils appears to be a very promising research opportunity that will pay great dividends if successful.

## REFERENCES

DEPARTMENT OF WATER AFFAIRS AND FORESTRY (DWAF) (1996) *South African irrigation water quality guidelines, Vol. 4: Agricultural use: Irrigation*, 2<sup>nd</sup> ed., DWAF, Pretoria, South Africa.

## ACKNOWLEDGEMENTS

---

The project team would like to acknowledge the Water Research Commission, the Mine Water Coordinating Body (MWCB), Anglo American, through the Green Engine Project, Mafube Colliery, Khwezela Colliery, South32, Exxaro and the Strategic Water Partnership for providing funding and resources for this very important study on irrigation with mine-impacted waters.

Special thanks go to the research managers of this project, initially Dr Jo Burgess, and then Mr Yazeed van Wyk and Dr John Zvimba.

Furthermore, the valuable inputs of the Reference Group members are acknowledged, specifically:

- Mrs Ritva Muhlbauer (Anglo American)
- Mrs Carla Hudson (Mine Water Coordinating Body)
- Mr Nkateko Kubayi (Water Research Commission)
- Mr Bashan Govender (Department of Water and Sanitation)
- Mr Edwin Mametja (Department of Agriculture, Forestry and Fisheries)
- Mrs Nosipho Mosito (South32)
- Mr Ian Midgley (Eskom)
- Dr Kai Witthüser (Delta H)
- Ms Michelle Proude (Strategic Water Partners Network)

The assistance of the staff at Mafube and Kromdraai collieries, as well as Beestepan Boerdery, which assisted with the day-to-day running of the project, are also gratefully acknowledged.

- Mr Max Kane Berman (farmer)
- Mr Peter Kane Berman (farmer)
- Ms Ingrid Sithole (Mafube)
- Ms Zamantshali Mtshali (Mafube)
- Ms Jackie Hlomuka (Mafube)
- Mr Martin Platt (Kromdraai)

The assistance of the following people is also gratefully acknowledged.

- Meiring du Plessis (University of Pretoria)
- Mike Butler (iThemba Labs)
- Charl Hertzog (University of Pretoria – ICP-AES Laboratory)
- Lucas Nonyane (University of Pretoria)

# TABLE OF CONTENTS

---

EXECUTIVE SUMMARY .....	iii
ACKNOWLEDGEMENTS .....	vi
TABLE OF CONTENTS .....	vii
LIST OF FIGURES.....	1
LIST OF TABLES.....	6
ACRONYMS AND ABBREVIATIONS.....	9
CHAPTER 1: INTRODUCTION .....	12
CHAPTER 2: DEMONSTRATING THE SUSTAINABLE USE OF UNTREATED CIRCUM-NEUTRAL MINE WATER FOR IRRIGATION: UNMINED LAND.....	13
2.1 INTRODUCTION .....	13
2.2 TRIAL OVERVIEW .....	13
2.3 WATER QUALITY MONITORING .....	16
2.3.1 Groundwater quality .....	10
2.3.2 Irrigation water quality .....	15
2.3.3 Downstream surface water quality.....	18
2.3.4 Stable isotope study.....	21
2.4 CROP GROWTH AND YIELDS.....	23
2.5 COSTING REPORT: SEED, FERTILIZER AND PESTICIDE REGIME.....	29
2.6 GRAIN ANALYSES.....	30
2.7 SOIL ANALYSES.....	32
2.8 CONCLUSION.....	36
2.9 REFERENCES .....	37
CHAPTER 3: IRRIGATION WITH MINE-IMPACTED WATERS: CROP, SALT AND WATER BALANCE MODELLING .....	38
3.1 INTRODUCTION .....	38
3.2 SOIL-WATER BALANCE MODEL.....	38
3.3 MODELLING MINE WATER IRRIGATION AND CROP GROWTH.....	40
3.4 IRRIGATION WATER FITNESS-FOR-USE ASSESSMENT – DECISION SUPPORT SYSTEM .....	49
3.5 CONCLUSIONS.....	53
3.6 REFERENCES .....	54
CHAPTER 4: DEMONSTRATING THE SUSTAINABLE USE OF UNTREATED CIRCUM-NEUTRAL MINE WATER FOR IRRIGATION: REHABILITATED LAND .....	55
4.1 INTRODUCTION .....	55
4.2 SITE SELECTION AND REHABILITATED FIELD DESCRIPTION .....	56
4.3 WORK DONE TO ESTABLISH A FUNCTIONING PIVOT SYSTEM ON A SUITABLE SECTION OF REHABILITATED LAND AT MAFUBE COLLIERY .....	58
4.4 RECOMMENDATIONS AND CONCLUSION.....	60

4.5	REFERENCES .....	60
CHAPTER 5: IRRIGATION WITH UNTREATED OR PARTIALLY TREATED ACID MINE DRAINAGE		
	.....	61
5.1	INTRODUCTION .....	61
5.2	CROP SCREENING FIELD TRIAL.....	62
5.2.1	Site selection.....	62
5.2.2	Crop screening trial layout .....	63
5.2.3	Seedbed establishment, plot demarcation and fertilization .....	66
5.2.4	Design and installation of irrigation system .....	69
5.2.5	Crop schedule and growth .....	70
5.2.6	Summary of challenges encountered at Kromdraai.....	71
5.3	REFERENCES .....	72
CHAPTER 6: HIGH-DENSITY SLUDGE AS A SOIL AMENDMENT .....		
		73
6.1	EXECUTIVE SUMMARY .....	73
6.2	INTRODUCTION .....	73
6.3	THE SOLUBILITY OF CONSTITUENTS OF HIGH-DENSITY SLUDGE FROM ACID MINE DRAINAGE NEUTRALISATION AND POSSIBLE ENVIRONMENTAL RISK.....	74
6.3.1	Materials and methods.....	74
6.3.2	Results and discussion .....	75
6.4	THE PHYSICAL PROPERTIES OF HIGH-DENSITY SLUDGE GENERATED BY ACID MINE DRAINAGE TREATMENT .....	82
6.4.1	Materials and methods.....	82
6.4.2	Results and discussion .....	83
6.4.3	Conclusions.....	87
6.5	THE HAZARDOUS WASTE CLASSIFICATION STATUS OF HIGH-DENSITY SLUDGE FROM ACID MINE DRAINAGE NEUTRALISATION, AS DETERMINED BY VARIOUS CLASSIFICATION SYSTEMS .....	87
6.5.1	Materials and methods.....	87
6.5.2	Results and discussion .....	88
6.5.3	Conclusions.....	95
6.6	THE SOIL AMELIORATION EFFECTS OF HIGH-DENSITY SLUDGE AS A SOIL AMENDMENT .....	95
6.6.1	Materials and methods.....	95
6.6.2	Results and discussion .....	96
6.6.3	Conclusions.....	103
6.7	THE CROP RESPONSE OF HIGH-DENSITY SLUDGE AS A SOIL AMENDMENT .....	103
6.7.1	Materials and methods.....	103
6.7.2	Results and discussion .....	106
6.7.3	Conclusions.....	115

6.8	REFERENCES .....	115
CHAPTER 7: RESPONSE OF SELECTED CROPS TO FOLIAR APPLICATION OF SIMULATED ACID MINE DRAINAGE..... 120		
7.1	INTRODUCTION .....	120
7.2	MATERIALS AND METHODS.....	121
7.2.1	Location of study.....	121
7.2.2	Crop selection and synthesis of acid mine waters.....	121
7.2.3	Part 1: Pot trial .....	122
7.2.4	Part 2: Field trial.....	123
7.2.5	Data collection.....	123
7.3	RESULTS .....	124
7.3.1	Part 1: Pot trial .....	124
7.3.2	Part 2: Field trial.....	128
7.4	CONCLUSION .....	129
7.5	RECOMMENDATIONS.....	130
7.6	REFERENCES .....	130
CHAPTER 8: EVALUATION OF IRRIGATION WATER QUALITY GUIDELINES FOR ARSENIC AND LEAD, WITH IMPLICATIONS FOR FOOD SAFETY ..... 133		
8.1	INTRODUCTION .....	133
8.2	GLASSHOUSE FOLIAR ADSORPTION TRIAL.....	134
8.3	GLASSHOUSE ROOT UPTAKE TRIAL.....	139
8.4	CONCLUSION .....	146
8.5	REFERENCES .....	146
CHAPTER 9: LIMESTONE NEUTRALISATION OF SYNTHETIC ACIDS IN AN AQUEOUS ENVIRONMENT AND SAND COLUMNS..... 148		
9.1	INTRODUCTION .....	148
9.2	MATERIALS AND METHODS – NEUTRALISATION OF THE SYNTHETIC ACIDS IN AN AQUEOUS ENVIRONMENT .....	148
9.2.1	Preparation of synthetic acids.....	149
9.3	MATERIALS AND METHODS – NEUTRALISATION OF SYNTHETIC ACID METAL CATION MINE WATER IN SAND COLUMNS .....	150
9.2.2	Soil column components.....	150
9.3.2	Estimating the dosage of limestone applied to the columns.....	151
9.3.3	Treatments and experimental procedure .....	152
9.4	RESULTS .....	152
9.4.1	Effect of limestone particle size on the neutralisation (increasing of pH) of sulphuric acid	152
9.4.2	Effect of limestone particle size on the neutralisation (increasing of pH) of synthetic acid metal cation mine water.....	155
9.4.3	Neutralisation of a synthetic acid metal cation mine water in a sand column.....	157

9.5	CONCLUSIONS.....	159
9.6	REFERENCES .....	160
CHAPTER 10: MANGANESE(II) OXIDISING POTENTIAL OF SELECTED SOILS UNDER DIFFERING OXIDATION CONDITIONS .....		162
10.1	INTRODUCTION .....	162
10.2	MATERIALS AND METHODS.....	162
10.2.1	The soil's physical and chemical characterisation .....	163
10.2.2	Manganese batch sorption experiment.....	164
10.2.3	Soil monitoring, analyses and extractions .....	166
10.3	RESULTS .....	168
10.3.1	Soil physical and chemical characterisation .....	168
10.3.2	Manganese batch sorption experiment.....	168
10.3.3	Soil monitoring, analyses and extractions .....	171
10.3.4	Manganese (II) oxidising potentials .....	177
10.4	CONCLUSION .....	180
10.5	REFERENCES .....	181
CHAPTER 11: ECONOMIC FEASIBILITY AND ANALYSIS OF MINE WATER-IRRIGATED CROPPING SYSTEMS.....		186
11.1	INTRODUCTION .....	186
11.2	COMPARATIVE ECONOMIC VIABILITY SCENARIOS.....	187
11.3	CONCLUSION .....	191
11.4	REFERENCES .....	191
CHAPTER 12: CONCLUSION .....		192
12.1	PROJECT OVERVIEW.....	192
12.2	RECOMMENDATIONS.....	192
12.3	REFERENCES .....	192
APPENDICES.....		194

## LIST OF FIGURES

---

Figure 2.1: Monitoring stations on Mafube unmined land. The letter S denotes soil monitoring stations, BH refers to borehole monitoring sites, and Pz to piezometers.....	14
Figure 2.2: Typical field monitoring station setup at the dryland and pivot sites. An automatic and manual rain gauge, as well as the waterproof enclosure to house a data logger and battery for automated soil water and salinity measurements of the profile can be seen. ....	15
Figure 2.3: Weather station situated at the Mafube unmined site .....	15
Figure 2.4: The location of surface and groundwater monitoring stations, as well as Beestepan Dam, used for surface water quality monitoring on the Mafube unmined land .....	16
Figure 2.5: A west-to-east cross-section from the coal mine stockpile through the adjacent wetland and across the Mafube unmined pivot indicating the various shallow and deep groundwater monitoring points.....	17
Figure 2.6: Water level (in cm) measured for the upstream shallow piezometer at the Mafube unmined field over the project period.....	10
Figure 2.7: Water level (in cm) measured for the downstream shallow piezometer at the Mafube unmined field over the project period.....	11
Figure 2.8: (i) Eroded slopes of the stockpile next to the unmined pivot; and (ii) the acid water runoff ponding on the surface near the downstream piezometer (PZm 2).....	13
Figure 2.9: Piper diagram of the four on-site monitoring boreholes for the Mafube unmined pivot.....	15
Figure 2.10: Piper diagram of the irrigation water (Void 3) used for irrigation at the Mafube unmined pivot .....	16
Figure 2.11: Change in pH and electrical conductivity of the Void 3 water from October 2014 to August 2020 .....	17
Figure 2.12: Change in major cation concentrations of Void 3 irrigation water from October 2014 to August 2020 .....	17
Figure 2.13: Change in electrical conductivity and sulphate concentration in the Void 3 irrigation water from October 2014 to August 2020 .....	18
Figure 2.14: Changes in the pH and electrical conductivity (mS/m) in Beestepan Dam from December 2016 to August 2020 .....	19
Figure 2.15: Changes in the major constituents in Beestepan Dam from December 2016 to August 2020. The horizontal blue line represents the established threshold value for sulphate.....	<b>Error!</b>
<b>Bookmark not defined.</b>	
Figure 2.16: Stable isotope data relative to the global meteoric water line (Craig, 1961). ....	22
Figure 2.17: Seasonal rainfall and irrigation throughout the maize-growing seasons at the Mafube unmined site .....	23
Figure 2.18: Phenological growth stages for the maize crop (He et al., 2010).....	25
Figure 2.19: Average leaf area index of irrigated and dryland white maize on the Mafube unmined field over the project period .....	27
Figure 2.20: Average fractional interception of photosynthetically active radiation for white maize grown at the Mafube unmined field.....	28
Figure 2.21: Crop height measured for pivot and dryland areas for white maize grown at the Mafube unmined field .....	29
Figure 2.22: Elemental distribution of irrigated maize from the Mafube unmined pivot.....	31
Figure 2.23: Elemental distribution of irrigated maize from the Mafube unmined pivot.....	32

Figure 2.24: Map of soil sampling locations on the Mafube unmined land.....	32
Figure 2.25: Soil profile at the Mafube unmined pivot indicating the change in pH, electrical conductivity (mS/m) and SO <sub>4</sub> (mg/l), over an irrigation period of three years, at three depths (30, 60 and 90 cm) .....	34
Figure 2.26: Soil profile at the Mafube unmined pivot indicating the change in Ca (i), Mg (ii), Na (iii) and K (iv) (mg/l), over an irrigation period of three years, at three depths (30, 60 and 90 cm).....	35
Figure 3.1: Radiation use efficiency as the slope of the relation between cumulative dry matter production and cumulative interception of solar radiation.....	42
Figure 3.2: Measured (symbols) and simulated (lines) LAI (top), and top and harvestable dry matter (bottom) simulating the effect of saline water irrigation. ....	45
Figure 3.3: Measured (symbols) and simulated (lines) LAI (top), and top and harvestable dry matter (bottom) simulating a dryland season. ....	45
Figure 3.4: Soil-water balance simulation of yields (t ha <sup>-1</sup> ) for a maize/wheat rotation over a 50-year period .....	46
Figure 3.5: Simulated wheat yield (t ha <sup>-1</sup> ) over a 50-year period for two different water qualities using soil-water balance .....	47
Figure 3.6: Soil profile salinity (EC <sub>e</sub> in mS m <sup>-1</sup> ) predicted for 50 years of irrigation with four different water qualities using soil-water balance. Salinity thresholds (Maas and Hoffman, 1977) for maize, wheat and soybean are also indicated.....	47
Figure 3.7: Gypsum precipitation (t ha <sup>-1</sup> ) and percentage salt removed as predicted by soil-water balance over a 50-year period for three different water qualities.....	48
Figure 3.8: The decision support system's 45-year simulation for the soil saturated paste electrical conductivity (EC <sub>e</sub> ) for a single maize crop using Void 3 water. The 2018, 2019 and 2020 EC <sub>e</sub> soil measurements and the salinity thresholds for maize, wheat and soybean are included. ....	52
Figure 3.9: The decision support system's 45-year simulation for the soil gypsum precipitation (tons/ha) for a single maize crop using Void 3's average water quality. ....	53
Figure 4.1: Google Earth image of the four potential pivot sites considered, with the preferred rehabilitated and unmined sites indicated.....	56
Figure 4.2: Representative soil profile of a rehabilitated site with a Witbank soil form.....	57
Figure 4.3: Cross-section of the soil depth of the rehabilitated site from north to south .....	57
Figure 4.4: Cross-section of the soil depth of the rehabilitated site from west to east .....	58
Figure 4.5: Unassembled pivot on the rehabilitation site, mid-2017 .....	58
Figure 4.6: Dr Phil Tanner at the centre pivot on the Mafube rehabilitated field with clear signs of water ponding after the heavy rains.....	59
Figure 4.7: A bulldozer with a ripper reducing compaction to 300 mm.....	60
Figure 4.8: The rehabilitation pivot at the end of the research project (January 2021) .....	60
Figure 5.1: Acid mine drainage treatment process and resultant high-density sludge generation.....	61
Figure 5.2: A: Source for neutral mine water (unclarified and clarified); B: Source for AMD; and C: Rehabilitated land (Source: Theo van Rensburg, 2017 – irrigation engineer).....	63
Figure 0.3: Crop screening trial layout.....	64
Figure 5.4: a) Disc-harrowing and ripping operation; b) Field ready for marking of blocks and sub-plots .....	66
Figure 5.5: a) Marked blocks and sub-plots; b) Rotovating within blocks.....	67
Figure 5.6: Buffer curve used to determine lime requirement.....	68

Figure 5.7: a) Liming of plots; b) Lime applied per block .....	69
Figure 5.8: Sites for the installation of pump units: A: Sources of neutralised mine water (clarified and unclarified); B: Acid mine drainage (Lopies Dam).....	70
Figure 5.9: Irrigation system installed for each block.....	70
Figure 5.10: Fire melted A) pipes and B) connectors .....	70
Figure 6.1: High-density sludge phosphate sorption curves.....	81
Figure 6.2: Particle size distribution with demarcations for D0.1 (particles at 10%), D0.5 (median particles at 50%) and D0.9 (particles at 90%) for A): GypFeMn; B): GypB; C): Gyp; and C): GypFe sludges .....	84
Figure 6.3: Cumulative particle size distribution curves for the sludges GypFeMn, GypFe, GypB and Gyp .....	85
Figure 6.4: Particle size distribution of sludges and particle size boundaries for clay-, silt- and sand- sized particles .....	85
Figure 6.5: Proportions of sand-, silt- and clay-sized particles for each sludge. ....	85
Figure 6.6: Relationship between total iron concentration in gypsum products (GypFe, GypFeMn, GypB, Gyp) and particle density .....	86
Figure 6.7: Water characteristic curves .....	87
Figure 6.8: A): Exchangeable acidity reduction, dotted line indicates initial exchangeable acidity; B): Exchangeable hydrolysable cations, dashed line indicates initial exchangeable hydrolysable cations.....	99
Figure 6.9: Selected major plant nutrients, total and available: A): sulphur; B): calcium; C): phosphorus .....	101
Figure 6.10: Total and available trace elements: A): manganese; B): iron; C): zinc .....	102
Figure 6.11: Total and available metals: A): nickel; B): lead.....	103
Figure 6.12: Germination (percentage) in the pot trial with different sludge-soil treatment combinations .....	106
Figure 6.13: Plant height for: A: Soil + GypFe; B: Soil + Gyp; C: Soil only; D: Limed soil.....	107
Figure 6.14: Total plant biomass comparisons .....	108
Figure 7.1: Cowpeas grown in sliced plastic discs to prevent acid drip into soil during foliar wetting	122
Figure 7.2: Fraction of injured leaves as a percentage of total leaves per plant for crops sprayed with synthetic acid mine water at a pH of 2 at 24 days after planting .....	125
Figure 7.3: Percentage of scorched leaves visually estimated for crops sprayed with synthetic acid mine water at a pH of 2.....	125
Figure 7.4 (clockwise): Scorched maize, cowpea, soybean and sorghum at 20 days after planting following wetting with synthetic acid mine water at a pH of 2 .....	126
Figure 7.5: Percentage of scorched leaves calculated using ImageJ for crops sprayed with synthetic acid mine water at a pH of 2 .....	127
Figure 7.6: Number of days to showing signs of leaf scorching for crops sprayed with synthetic acid mine water at a pH of 2 .....	127
Figure 8.1: Arsenic accumulation on a dry mass basis, within edible plant parts of crops wetted with arsenic-enriched water every one to three days throughout the growing period, in relation to food safety thresholds .....	137
Figure 8.2: Lead accumulation, dry mass basis, within edible parts of crops wetted with lead-enriched water every two days throughout the growing period in relation to food safety thresholds .....	139

Figure 8.3: Arsenic accumulation on a dry mass basis, within edible parts of crops grown in arsenic-enriched soil at 43.5 mg kg<sup>-1</sup> (simulating 99 years of irrigation at 0.1 mg l<sup>-1</sup>) and 168.9 mg kg<sup>-1</sup> (19 years of irrigation at 2.0 mg l<sup>-1</sup>) in relation to food safety thresholds ..... 143

Figure 8.4: Lead accumulation, dry mass basis, within edible parts of crops grown in lead-enriched soil at 88.1 mg kg<sup>-1</sup> (simulating 99 years of irrigation at 0.2 mg l<sup>-1</sup>) and 168.9 mg kg<sup>-1</sup> (19 years of irrigation at 2 mg l<sup>-1</sup>) in relation to food safety thresholds ..... 146

Figure 9.1: The column ensemble, which consists of a polyethylene tube and its base, with a gridded sieve to allow leachate to exit the column and prevent the loss of soil ..... 151

Figure 9.2: The ensemble that was utilised for the percolation and collection of the synthetic acid mine water that was passed through sand columns containing limestone ..... 151

Figure 9.3: Surface application of 12.6 g limestone with a particle size of larger than 4 mm, but less than 10 mm (left) and less than 0.1 mm (right) ..... 152

Figure 9.4: Neutralisation of sulphuric acid with an initial pH of 2 as influenced by a series of limestone particle sizes ..... 154

Figure 9.5: Neutralisation of sulphuric acid with an initial pH of 3 as influenced by a series of limestone particle sizes ..... 154

Figure 9.6: Neutralisation of synthetic acid metal cation mine water with an initial pH of 2 as influenced by a series of limestone particle sizes ..... 156

Figure 9.7: Neutralisation of synthetic acid metal cation mine water with an initial pH of 3 as influenced by a series of limestone particle sizes ..... 156

Figure 9.8: The precipitation of ferric hydroxide, represented by the orange-rust-like colour at a pH of about 5.5 ..... 157

Figure 9.9: Neutralisation of synthetic acid metal cation mine water according to two leaching procedures (LP1 and LP2) in a sand column with limestone of less than 0.1 mm and less than 10 mm in size that is mixed with sand ..... 158

Figure 9.10: Neutralisation of synthetic acid metal cation mine water according to two leaching procedures (LP1 and LP2) in a sand column with limestone of less than 0.1 mm and less than 10 mm in size applied to the surface of the columns ..... 158

Figure 10.1: Basic experimental set-up of the Mn(II) batch sorption trial ..... 165

Figure 10.2: Samples after measurements were taken, before daily aeration; (ii) daily measurements using an ORP probe ..... 166

Figure 10.3: A simplification of the soil-solution system as seen in the manganese batch sorption experiment, showing the concept of manganese mass balance determination ..... 167

Figure 10.4: Linearised Langmuir isotherm for the adsorption of Mn(II) for the four selected soils ... 170

Figure 10.5: The redox potential (mV) vs the pH of the four soils over the 40-day aeration/oxidising period (A and B), as well as for the four soils over the 15-day aeration/oxidising followed by 25-day reducing period (C and D) ..... 172

Figure 10.6: Easily reducible fraction of manganese in the four soils for the three different oxidising regimes ..... 174

Figure 10.7: Easily oxidisable fraction of manganese in the four soils for the three different oxidising regimes ..... 176

Figure 10.8: Easily oxidisable and reducible fractions of manganese making up the total manganese ..... 177

Figure 10.9: A simplified breakdown of how measuring adsorption and the oxidisable and reducible fraction of manganese can be used to determine a soil's manganese oxidising potential ..... 178

Figure 10.10: The MOP percentage of the soils in correlation with the change in Eh (mV) of the different soil systems over the period of the batch sorption experiment..... 179

## LIST OF TABLES

Table 2.1: Summary of average elemental concentrations observed at the two piezometers of the Void 3 irrigation water and discard dump runoff water.....	12
Table 2.2: Summary of constituent concentrations of the four on-site boreholes for the Mafube unmined pivot .....	14
Table 2.3: Average water quality of Void 3 used for irrigation at the Mafube unmined field over the project period.....	15
Table 2.4: Average water quality of Beestepan Dam used for monitoring irrigation impacts over the five-year project period .....	19
Table 2.5: A summary of seasonal irrigation and rainfall the Mafube unmined pivot has received over the last three irrigated maize seasons and a shortened stooiling rye growing season .....	24
Table 2.6: Maize phenological stages.....	24
Table 2.7: Summary of yields, total dry mass, Harvest Index and average cob length observed at the end of each growing season .....	26
Table 2.8: Average tonnage, cost per hectare, maize price, profit or loss per hectare with and without pumping costs for each cropping season. ....	30
Table 2.9: International guidelines and thresholds of selected elements for grain food and feed safety .....	31
Table 2.10: Detailed soil analyses performed.....	33
Table 3.1: Crop parameters required for SWB modelling.....	38
Table 3.2: Daily weather parameters required for SWB modelling.....	39
Table 3.3: Soil parameters and initial conditions required for SWB modelling.....	40
Table 3.4: Crop input parameters used for simulations .....	42
Table 3.5: Soil chemical initial conditions and hydraulic parameters used for simulations .....	43
Table 3.6: Weather station locations and data provided.....	43
Table 3.7: Different water qualities in the vicinity of Mafube Colliery.....	46
Table 3.8: Tier 1 results of irrigating with Void 3 irrigation water quality .....	50
Table 3.9: Tier 2 results of irrigating only white maize with Void 3 irrigation water quality.....	51
Table 3.10: Cumulative salt balance and gypsum retained in the soil profile after a 45-year simulation of irrigation with Void 3 water .....	53
Table 5.1: Selected crops' and pastures' acidity and salinity tolerance (adapted from Jovanovic et al., 1998, AGRICOL, 2016; Pannar Product Catalogue, 2013).....	65
Table 5.2: List of selected biofuel crops (Poaceae sp.) planned to be planted at Kromdraai .....	66
Table 5.3: Soil chemical composition per block.....	67
Table 5.4: Concentrations of plant available macro and micronutrients in the soil.....	68
Table 5.5: Fertilizers and quantities procured per block.....	68
Table 6.1: Total concentration of selected major and trace elements in HDS.....	77
Table 6.2: Selected water-soluble elements in the sludges (cumulative of five water extractions).....	77
Table 6.3: Selected soluble elements extracted with diluted HCl at a pH of 4 (five cumulative extractions) .....	78

Table 6.4: Selected TCLP extractable elements.....	79
Table 6.5: Selected elements extractable with EDTA and NH <sub>4</sub> OAc.....	80
Table 6.6: Particle size, surface area, particle density and uniformity of sludges .....	83
Table 6.7: South African waste classification limits and analytical status of six HDS samples.....	89
Table 6.8: Classification results obtained from Table 6.5 using the South African Guidelines .....	90
Table 6.9: Assessment of sludge hazardous status based on both TCLP and SCC thresholds (first and second screening stages) (New South Wales Environment Protection Authority, 2014).....	91
Table 6.10: Assessment of HDS based on leachable concentrations using regulatory guidelines for Canada, US EPA and China (Zinck et al., 1997 and US EPA (1990)).....	93
Table 6.11: Summary of elements affecting classification of high-density sludge by the different systems .....	94
Table 6.12: Selected physicochemical soil properties .....	96
Table 6.13: Selected chemical sludge properties and selected total elemental content .....	97
Table 6.14: Effect of treatments on soil pH.....	98
Table 6.15: Effect of treatments on salinity (mS m <sup>-1</sup> ) in soil-sludge mixtures .....	100
Table 6.16: Treatments .....	104
Table 6.17: Final height (cm) of maize plants in a pot trial with different sludge-soil treatment combinations as growth medium.....	106
Table 6.18: Sludge, lime and phosphate effects on calcium concentration (mg kg <sup>-1</sup> ) in maize stems, leaves and tassels.....	109
Table 6.19: Sludge, lime and phosphate effects on sulphur concentration (mg kg <sup>-1</sup> ) in leaves, stems and tassels of maize.....	109
Table 6.20: Sludge, lime and phosphorus effects on phosphorus concentration (mg kg <sup>-1</sup> ) in maize leaves, stems and tassels .....	110
Table 6.21: Iron (mg kg <sup>-1</sup> ) in biomass of maize.....	110
Table 6.22: Manganese (mg kg <sup>-1</sup> ) in biomass of maize .....	111
Table 6.23: Sludge and phosphate influence on nickel (mg kg <sup>-1</sup> ) in biomass.....	112
Table 6.24: Sludge, lime and phosphate influence on lead (mg kg <sup>-1</sup> ) in biomass .....	112
Table 6.25: Yield of maize planted in different sludge-soil mixtures (g pot <sup>-1</sup> ).....	113
Table 6.26: Major elements in maize grain (mg kg <sup>-1</sup> ).....	113
Table 6.27: Manganese and iron in maize grain (mg kg <sup>-1</sup> ) .....	114
Table 6.28: Nickel and lead (mg kg <sup>-1</sup> ) in grain .....	114
Table 7.1 Minimum and maximum soil pH requirements of the selected crops .....	121
Table 7.2: Treatments and sulphuric acid volumes added to water .....	121
Table 7.3: Plant height for crops sprayed with synthetic acid mine water .....	128
Table 7.4: Above-ground dry mass (kg/ha) of crops sprayed with acid mine water .....	129
Table 7.5: Leaf Area Index of crops sprayed with synthetic acid mine water.....	129
Table 7.6: Chlorophyll content (SPAD units) of crops sprayed with synthetic acid mine water .....	129
Table 8.1: Yield response of crops following irrigation with arsenic- or lead-enriched irrigation water .....	134

Table 8.2: Mean arsenic accumulation in dry mass following irrigation with arsenic-enriched irrigation water in relation to food and feed thresholds .....	135
Table 8.3: Median arsenic accumulation in dry mass following irrigation with arsenic-enriched irrigation water in relation to food and feed thresholds .....	136
Table 8.4: Lead accumulation in dry mass following irrigation with lead-enriched irrigation water in relation to food safety thresholds .....	137
Table 8.5: Median lead accumulation in dry mass following irrigation with lead-enriched irrigation water in relation to food and feed thresholds .....	138
Table 8.6: Effect of arsenic and lead treatments on soil pH and EC .....	140
Table 8.7: Bioavailability of arsenic and lead 22 weeks after soil application .....	140
Table 8.8: Yield response of crops grown in arsenic- or lead-enriched soil .....	141
Table 8.9: Mean arsenic accumulation in the dry mass of crops grown in arsenic-enriched soils in relation to food and feed thresholds.....	142
Table 8.10: Median arsenic accumulation in the dry mass of crops grown in arsenic-enriched soils in relation to food and feed thresholds .....	143
Table 8.11: Mean lead accumulation in the dry mass of crops grown in lead-enriched soil in relation to food and feed thresholds.....	144
Table 8.12: Median lead accumulation in the dry mass of crops grown in lead-enriched soils in relation to food and feed thresholds.....	145
Table 9.1: The required volume of stock solution needed per litre to produce the target pH levels and actual pH values obtained .....	149
Table 9.2: The mass of each sulphate salt required to produce a litre of synthetic acid metal cation mine water for each target pH level and the concentration of metals present in the acids .....	150
Table 10.1: General soil sample description and classification .....	163
Table 10.2: Texture analyses of the selected soils .....	168
Table 10.3: Basic chemical characterisation of the selected soils .....	168
Table 10.4: Summary of the Mn(II) adsorption efficiencies (as a percentage) for the four selected soils in the batch experiment.....	169
Table 10.5: Summary of adsorption coefficients for Mn(II) of the four selected soils for the three different oxidising regimes .....	169
Table 10.6: Summary of linearised Langmuir isotherm parameters for Mn(II) on the four selected soils .....	170
Table 10.7: Easily reducible manganese fractions for the four soils under three different oxidising regimes .....	173
Table 10.8: The regression analysis and coefficient of determination for the total electron demand and hydroxylamine values of the four soils under three oxidising regimes.....	175
Table 10.9: Easily oxidisable manganese fractions for the four soils under three different oxidising regimes .....	175
Table 10.10: Manganese adsorption efficiency percentage and manganese oxidising potential percentage for the four soils under three different oxidising regimes .....	178
Table 11.1: Comparative indicators for Scenario 1 (monocrop) and Scenario 2 (crop rotation) .....	188
Table 11.2: Sensitivity analysis .....	190

## ACRONYMS AND ABBREVIATIONS

---

AMD	Acid mine drainage
ARC	Agricultural Research Council
BDL	Below detection limit
CaCO <sub>3</sub>	Limestone
CaSO <sub>4</sub>	Gypsum
Ca(OH) <sub>2</sub>	Hydrated lime
CCE	CaCO <sub>3</sub> (limestone) equivalents
CEC	Cation exchange capacity
CRD	Completely randomised design
CV	Coefficient of variation
DAFF	Department of Agriculture, Forestry and Fisheries
DAP	Days after planting
DM	Dry matter
DSS	Decision support system
DWR	Dry matter to water ratio
E <sub>c</sub>	Radiation use efficiency
EC	Electrical conductivity
EC <sub>e</sub>	Soil profile salinity
EC <sub>e</sub>	Soil saturated paste electrical conductivity
EDTA	Ethylenediaminetetraacetic acid
Eh	Redox potential
EHC	Exchangeable hydrolysable cations
ET	Evapotranspiration
ET <sub>0</sub>	Reference crop evaporation
EIL	Environmental Isotope Laboratory
EPA	Environmental Protection Agency
FAO	Food and Agricultural Organisation
FC	Field capacity
FeS <sub>2</sub>	Pyrite
FI	Fractional interception
GDD	Growing degree days
GMWL	Global meteoric water line

GSW	General solid waste
GypB	Gypsum with brucite
GypFe	Gypsum with iron oxides
GypFeMn	Gypsum with iron oxides and manganese
HDM	Harvestable dry matter
HDPE	High-density polyethylene
HDS	High-density sludge
HI	Harvest Index
HW	Hazardous waste
IAP	Ion activity product
ICP-AES	Inductively coupled plasma atomic emission spectroscopy
ICP-OES	Inductively coupled plasma optical emission spectrometry
IRR	Internal rate of return
KCl	Potassium chloride
Ksp	Solubility product
LAI	Leaf Area Index
LAN	Limestone ammonium nitrate
LC	Leachable concentration
LCT	Leachable concentration threshold
LDM	Leaf dry matter
LGR	Los Gatos Research
LP	Leaching procedure
LSD	Least significant difference
MAE	Mean absolute error
MDL	Method detection limit
MOP	Manganese-oxidising potential
MSE	Manganese-sorption efficiency
MWCB	Mine Water Coordinating Body
MWCO	Molecular weight cut-off
NPV	Net present value
ORP	Oxidation reduction potential
PAR	Photosynthetically active radiation
PWP	Permanent wilting point
RCBD	Randomised complete block design

RGR	Relative Growth Rate
RMSE	Root mean square error
RO	Reverse osmosis
RSW	Restricted solid waste
RUE	Radiation use efficiency
SANAS	South African National Accreditation System
SAWQI	South African Water Quality Guidelines for Irrigation
SCC	Specific contaminant concentration
SLA	Specific leaf area
SMOW	Standard mean ocean water
SPAD	Chlorophyll content meter
SSA	Specific surface area
SSP	Single superphosphate
SWB	Soil-water balance
TC	Total concentration
TCLP	Toxicity characteristic leaching procedure
TCT	Total concentration threshold
TDM	Total dry mass
TDS	Total dissolved solids
TED	Total electron demand
TLB	Tractor-loader-back
UP	University of Pretoria
VPD	Vapour pressure deficit
WRC	Water Research Commission
XRD	X-ray diffraction
XRF	X-ray fluorescence

## CHAPTER 1: INTRODUCTION

---

**JG Annandale, PD Tanner and SN Heuer**

A major water management problem, in addition to water scarcity, is that South Africa has large volumes of decanting mine-impacted waters. The coalfields of Mpumalanga are critical to the production of electricity for South Africa. This large energy requirement has major knock-on environmental effects. One such effect is the production of acid mine drainage. There is large uncertainty regarding the volumes of mine-impacted water being produced in coal mines in Mpumalanga and the rate at which these mine-impacted waters are being decanted into catchments. In cases where mine water from operating and closed coal mines is of too poor a quality to be discharged into rivers, water treatment processes such as high-density sludge plants and reverse osmosis are often used. The degradation of river water quality has been observed in Mpumalanga, and can, at least partly, be attributed to mining activities in the Crocodile and Olifants river catchments.

The South African mining industry produces large volumes of mine-impacted waters, and the agricultural industry requires large water inputs to improve and maximise crop yield. Therefore, a noteworthy opportunity arises, providing consumptive use of the water, and any environmental impacts are acceptable. As a result of Mpumalanga's erratic rainfall, this region is highly dependent on irrigation to produce crops economically. The availability of large volumes of mine-impacted water and large tracts of unfarmed land owned by mines creates an opportunity to utilise this poorer-quality mine water for irrigation. The application and reuse of mine-impacted waters not only addresses some environmental issues, but also contributes to the growing demand for food, and provides much-needed employment. Irrigation with poor-quality mine water to sustainably produce a range of crops and reduce mine water salt loads to catchment water bodies through gypsum precipitation in the root zone has been well researched for coal mine water in South Africa.

Current water treatment technologies are energy intensive and expensive processes with a high carbon footprint. The generation of electricity for this process has additional environmental impacts and leads to the need for more mining. Using mine-impacted water for irrigation may alleviate water treatment costs during mining operations, as well as post-mine closure. An additional and supplemented water supply may assist in the reclamation of valuable agricultural lands. Due to the large scale at which irrigation with mine-impacted waters could be practiced in Mpumalanga, there is a need for more extensive information regarding the fate and impact on the environment due to such irrigation.

This research project had five main objectives:

- Demonstrate irrigation with mine water over a longer period in order to create a successful production site that others interested in mine water irrigation or needing to authorise such use can refer to.
- Investigate issues associated with the irrigation of rehabilitated land. This is important because there are large tracts of such land available in close proximity to mine water sources, and it is expected that the off-site environmental impact of mine water irrigation may be somewhat less than is expected when irrigating unmined lands.
- Evaluate the concept of irrigating with untreated or partially treated AMD on strategically limed soil profiles in order to save on water treatment costs.
- Establish the economic viability of mine water irrigation as a sustainable mine water management option, where water quality is suitable for irrigation.
- Generate technical guidelines for the establishment of mine water irrigation projects to assist potential irrigators and those required to authorise such practices.

In general, these objectives were largely met, except that much detailed laboratory and greenhouse work was required in lieu of some of the originally planned fieldwork, mainly due to challenges experienced with water supply, and the safety and security of the research sites.

# CHAPTER 2: DEMONSTRATING THE SUSTAINABLE USE OF UNTREATED CIRCUM-NEUTRAL MINE WATER FOR IRRIGATION: UNMINED LAND

---

SN Heuer, JG Annandale, PD Tanner, C McGladdery and ZD Ronquest

## 2.1 INTRODUCTION

Coal mining is known to produce acid mine drainage with high amounts of sulphate and potentially toxic trace elements (Johnson and Hallberg, 2005). Acid mine drainage is generated when sulphide-bearing minerals (such as pyrite, which is commonly associated with coal mining) are exposed to oxygen and water. This results in a reduction in pH, which allows metals to become more soluble (Mackie and Walsh, 2015). Fortunately, these waters can be treated by adding hydrated lime ( $\text{Ca}(\text{OH})_2$ ) or limestone ( $\text{CaCO}_3$ ) (Akcil and Koldas, 2006). The problem is that the treated water is now saline, often dominated by calcium and magnesium sulphate, potentially polluting the environment and other natural resources. However, studies on coal mines have shown that there is potential to use such mine waters for crop irrigation (Jovanovic et al., 1998; Annandale et al., 2001; Annandale et al., 2006).

The main premise is that much mine-affected water contains large quantities of calcium sulphate. When crops are irrigated with such gypsiferous waters, significant quantities of calcium sulphate are precipitated out in soils, primarily as gypsum. As much as 70% of salts contained in mine waters can be removed in this way, and the soils are not negatively affected by the presence of these precipitates (Du Plessis, 1983). Because large volumes of such mine-impacted water are available, with large tracts of unfarmed land available on both active and closing mines, with several key crops that are sufficiently tolerant to saline waters, a clear opportunity arises to utilise this water for irrigation. Not only will this drastically reduce mine water treatment costs, but it will enable sustainable livelihoods and food production, particularly in the post-mine closure situation.

The aims of the Mafube irrigation with mine water study were to monitor and model field-scale water and salt balances for a small-scale commercial mine water irrigation scheme in Mpumalanga in order to predict the long-term impact and sustainability of gypsiferous mine water irrigation. The intention was also to establish a demonstration site that could serve as a reference for potential mine water irrigators, and those needing to authorise such practices.

## 2.2 TRIAL OVERVIEW

A field experiment was conducted at an unmined site at Mafube Colliery in Middelburg, Mpumalanga. The trials took place from November 2016 to March 2020. The experimental site is located at latitude 25°48'25" S and longitude 29°45'48" E, and is 1,670 m above sea level. Soils in the northern section of the field are classified as deep Glencoe, where lateral subsurface flow is expected to occur as water reaches the deep hard Plinthic B horizon. The signs of wetness in this part of the field were not concerning, as the soils are deep, and all indications are that water should drain to the wetland to the west of the field. Soils in the southern and eastern areas of the field are deep Hutton soils, which have excellent drainage and are ideal for crop production under irrigation. Dr Johan van der Waals of Terra Soil conducted soil sampling and classification in September 2016.

A white maize, variety PHB 32B07BR (genetically modified with stacked gene for stalk borer and herbicide resistance), was planted at a population of 80,000 plants per hectare each season (2017/18, 2018/19 and 2019/20). Adjacent to the pivot, dryland maize was planted at a population of 50,000 plants per hectare to another white maize variety, DKC 7883R. In the 2016/17 season, only dryland maize was planted and monitored, as some delays were experienced in commissioning the irrigation system.

The Mafube unmined pivot summer cropping system was a long season white maize variety monocrop. This cropping system selection was made to suit the collaborating leading commercial farmers' needs and business plan. Stooling rye was planted for half of the winter season of 2018, upon the request of the research team, who were anxious to monitor the performance of a winter cereal small grain crop.

Four monitoring stations were established as far from the main road as possible to reduce the likelihood of theft or vandalism, while remaining within the well- to moderately drained areas of the field. Careful consideration was taken to protect monitoring stations from damage by farm machinery by placing them away from the implement tyre and centre pivot tracks. The four monitoring stations, denoted as S1 to S4 in Figure 2.1, comprise two stations within the pivot area and two within the adjacent dryland area. The stations were situated as follows: Station 4 was located in the well-drained dry land area of the field, stations 1 and 2 were in moderate drainage areas within the pivot, and Station 3 was located in the poorly drained dryland area.



Figure 2.1: Monitoring stations on Mafube unmined land. The letter S denotes soil monitoring stations, BH refers to borehole monitoring sites, and Pz to piezometers.

These stations were set up to provide information on both the dryland and irrigated water and salt balances and growth crop responses. The stations were all equipped with sensors (see Figure 2.2) to facilitate accurate monitoring of the various parameters that are required for modelling purposes.

Each monitoring station was equipped with the following:

- A weatherproof enclosure housing a Campbell Scientific CR300 data logger and battery. The data logger stored measurements from CS655 soil water and salinity/temperature probes at three depths, as well as rainfall or irrigation from a TE525 tipping bucket rain gauge every hour.
- An automatic TE525 tipping bucket rain gauge monitored irrigation and rainfall with a resolution of 0.254 mm per tip.
- Three CS655 probes at depths of 30 cm, 60 cm and 90 cm monitored soil water content, dielectric permittivity, bulk electrical conductivity (EC) and soil temperature.
- A manual rain gauge collected samples for water quality monitoring.

Soil analyses were performed before and after each cropping season to assess salt loading and accumulation within the soil as a result of mine water irrigation.



Figure 2.2: Typical field monitoring station setup at the dryland and pivot sites. An automatic and manual rain gauge, as well as the waterproof enclosure to house a data logger and battery for automated soil water and salinity measurements of the profile can be seen.

A weather station (Figure 2.3) was set up in open land near the pivot in order to accurately monitor changing weather conditions over the period of the growing season.

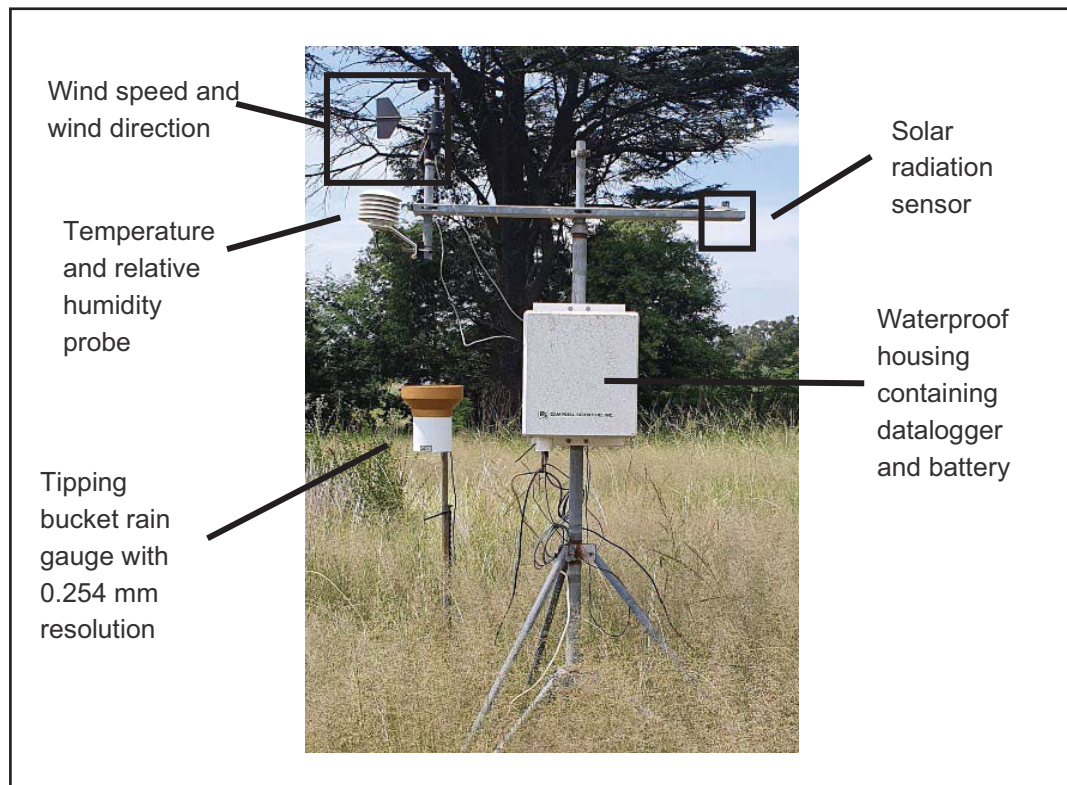


Figure 2.3: Weather station situated at the Mafube unmined site

Crop parameters (leaf area index, fractional interception of radiation, plant height, growth stage and plant component dry mass) were sampled and measured every two weeks at the four monitoring sites throughout the growing season. Along with crop data, chemical analyses were performed on irrigation water and groundwater (see boreholes and piezometers in Figure 2.1). Consultants from the mine analyse the water quality of the boreholes every quarter and the irrigation water every two weeks. The research team conducted spot checks of the irrigation water quality throughout the season to corroborate the chemical analyses.

### 2.3 WATER QUALITY MONITORING

The locations of the monitoring piezometers and boreholes, as well as the surface water monitoring point (Beestepan Dam) can be seen in Figure 2.4. Changes in the quality of the groundwater of the pivot and surrounds were monitored through four boreholes and two piezometers. Two boreholes were drilled upstream and two downstream of the pivot to monitor any changes in groundwater quality. The monitoring boreholes were denoted BH1 (upstream, deep  $\pm 30$  m), BH2 (upstream, shallow  $\pm 10$  m), BH3 (downstream, deep  $\pm 30$  m) and BH4 (downstream, shallow  $\pm 10$  m). There were two piezometers (PZm1 and PZm2) on the downstream side of the pivot. These piezometers were used to monitor shallow groundwater movement and qualities. The piezometers, along with the boreholes, allowed the research team to sample shallow and deep groundwater in order to analyse the potential impact of mine water irrigation on subsurface water flow and salt accumulation.

The yellow dashed line in Figure 2.4 indicates the west-east cross-section, which indicates the points of shallow and deep groundwater monitoring that is depicted in Figure 2.5.

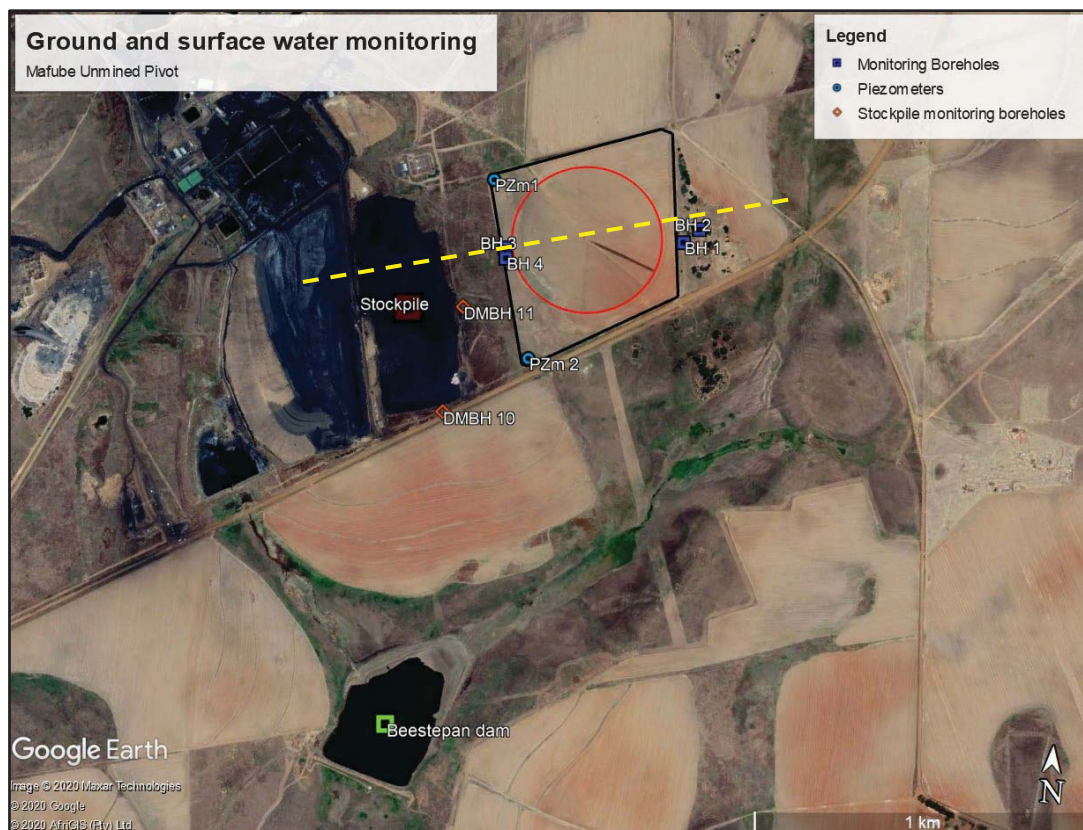


Figure 2.4: The location of surface and groundwater monitoring stations, as well as Beestepan Dam, used for surface water quality monitoring on the Mafube unmined land

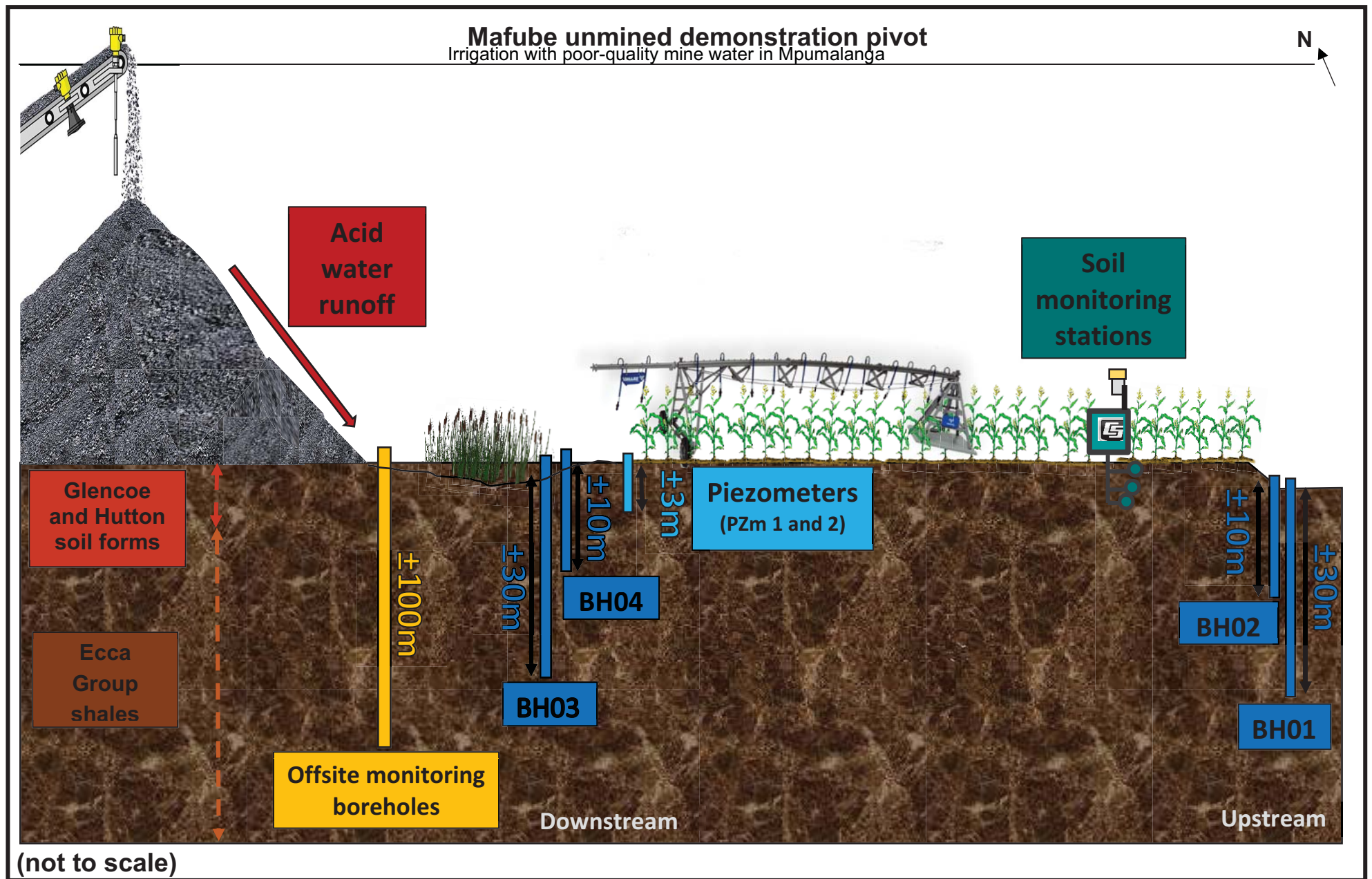


Figure 2.5: A west-to-east cross-section from the coal mine stockpile through the adjacent wetland and across the Mafube unmined pivot indicating the various shallow and deep groundwater monitoring points

### 2.3.1 Groundwater quality

#### **Monitoring piezometers**

Two piezometers were installed at depths of around 3 m. These piezometers were placed in an upstream (PZm 1) and downstream (PZm 2) location within the wet, westerly side of the field.

Water levels were measured using an electronic groundwater level detector and samples retrieved using a bailer. In Figure 2.6, the changes in the water level of the upstream piezometer (PZm 1) can be seen over the project period. For PZm 1, typical groundwater response curves are seen. The water level increases sharply due to the rainfall experienced in the summer rainy months, after which it drops and remains constant due to less precipitation in the winter months at a shallow groundwater level ( $\pm 140$  to  $170$  cm below ground level). Figure 2.7 shows the changes in the water level of the downstream piezometer (PZm 2) over the project period. The groundwater response is similar to that for PZm 1.

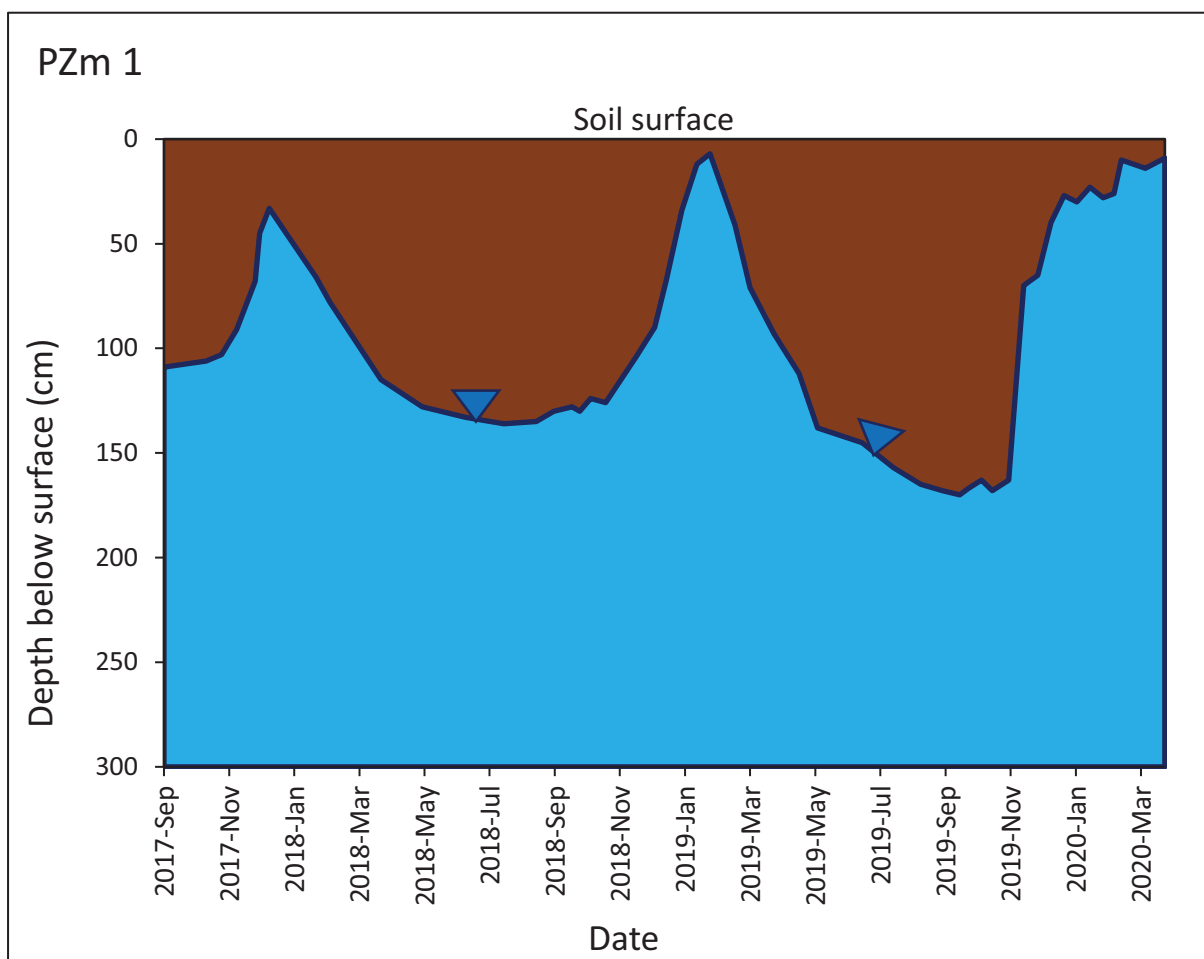


Figure 2.6: Water level (in cm) measured for the upstream shallow piezometer at the Mafube unmined field over the project period

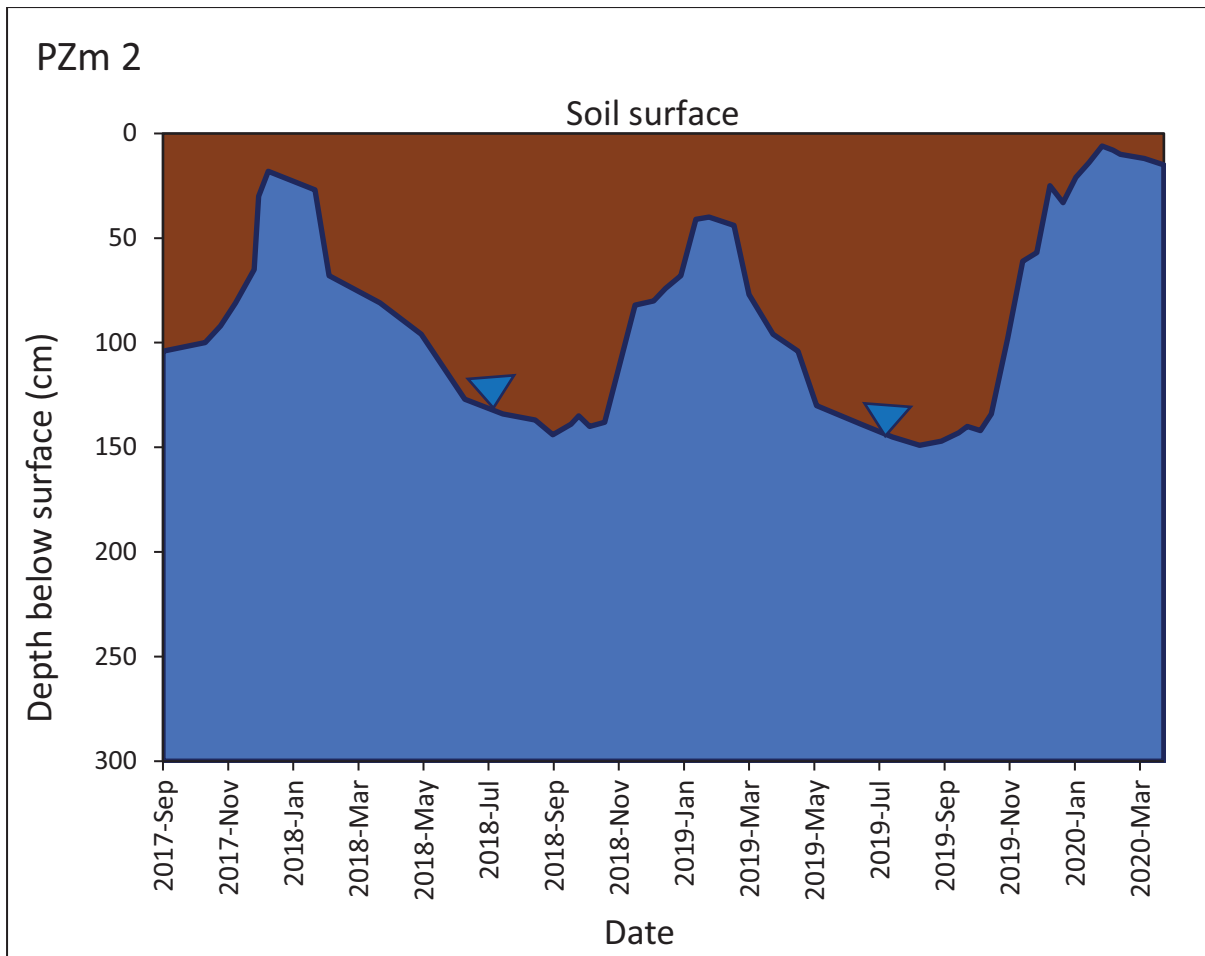


Figure 2.7: Water level (in cm) measured for the downstream shallow piezometer at the Mafube unmined field over the project period

In Table 2.1, average elemental concentrations of acidic runoff water from the discard dump, and from both upstream (PZm 1) and downstream piezometers (PZm 2), are reported. A different chemical concentration trend can be seen between the upstream and downstream piezometers. The concentrations of the different constituents were higher at the downstream piezometer than the upstream piezometer. This can be attributed to the acid surface runoff and water seepage through the discard dump, translocated laterally towards the topographically low point, expressed as a wetland and the maize field.

Figure 2.8(i) shows the eroded slopes of the coal stockpile situated next to the unmined field, caused by rains. This reaction between the discard dump material and the rainwater produces acid mine water runoff. Acid water runoff ponded near the downstream piezometer, combined with subsurface seepage from the discard dump, it probably caused the altered water quality (Figure 2.8(ii)).

Table 2.1: Summary of average elemental concentrations observed at the two piezometers of the Void 3 irrigation water and discard dump runoff water

Unit	Parameter	Piezometer		Void 3 water	Discard dump acid runoff water
		Upstream (PZm 1)	Downstream (PZm 2)		
	pH	6.3	5.7	7.8	4.3
	EC (mS/m)	78	293	198	331
	Suspended solids	13	61	54	87
mg/l	TDS	141	568	324	613
	K	1.8	3.1	100	4.7
	Mg	23	55	102	69
	Ca	34	87	153	107
	P	0.4	1.4	0.9	1.3
	SO <sub>4</sub>	72	204	1 098	179
	Na	24	252	93	261
	Cl	45	289	30	294
	Fe	0.02	0.7	0.06	1.2
	Al	0	0.1	0.12	0.3
	Mn	0	0.5	2.7	0.8
	Pb	0	0.02	0.005	0.04
Zn	0.02	0.05	0.01	0.06	

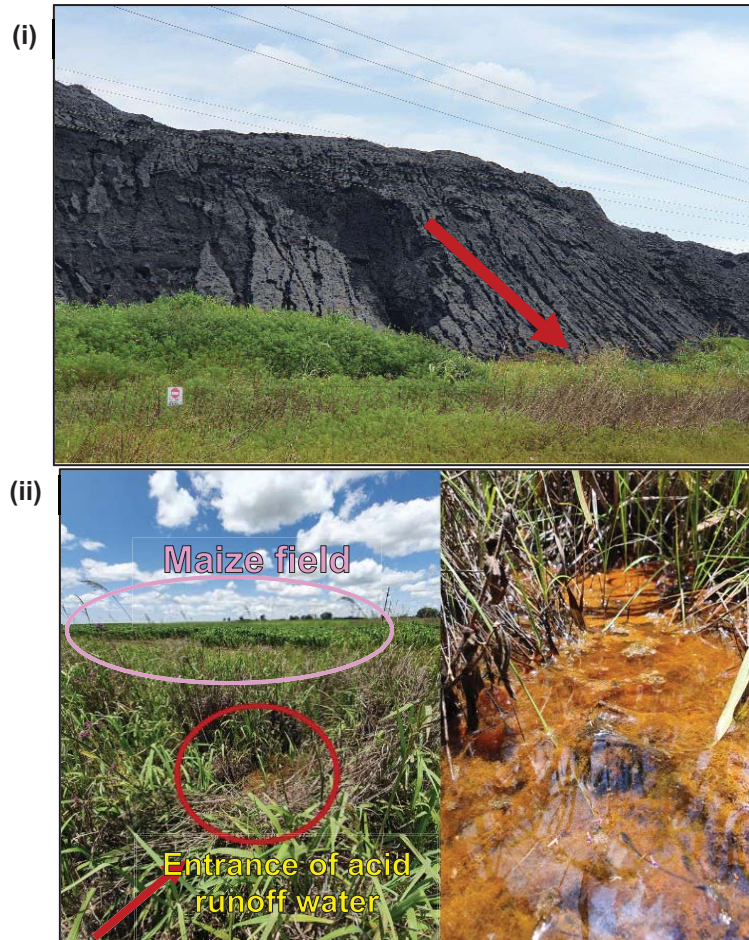


Figure 2.8: (i) Eroded slopes of the stockpile next to the unmined pivot; and (ii) the acid water runoff ponding on the surface near the downstream piezometer (PZm 2)

### Monitoring boreholes

Boreholes 1 and 2 are located in the well-drained eastern side of the field, and boreholes 3 and 4 are located in the poorly drained western side of the field. The shallow boreholes (boreholes 2 and 4, referred to as shallow upstream and shallow downstream, respectively) are about 10 m deep and the deep boreholes (boreholes 1 and 3, referred to as deep upstream and deep downstream, respectively) are around 30 m deep. These boreholes were sampled, analysed and reported on by Mafube Colliery every quarter.

Comparing the data for the shallow upstream and downstream boreholes, it was observed that they exhibited very similar chemical signatures. During the rainy season, when there were increased acid runoff rates, the downstream monitoring point (Borehole 4) had much higher concentrations of most constituents compared to any of the other boreholes. This can possibly be attributed to Borehole 4 intercepting acidic runoff from the adjacent coal stockpile and therefore increasing these concentrations. The deep upstream and downstream boreholes (boreholes 1 and 3) exhibited very similar groundwater chemistry, with slight variations in EC, total dissolved solids (TDS), sodium and chlorine contents. The most likely explanation for these observed elevated salt levels in the downstream boreholes (boreholes 3 and 4) can be due to the acid water runoff from the discard dump adjacent to these boreholes. In August 2018, Mafube Colliery installed two additional boreholes around the south-western border of the discard dump (discard dump boreholes marked DMBH 10 and DMBH 11 in Figure 2.4), which will enable groundwater closer to the discard dumps to be monitored, thereby reducing uncertainty around the impact of irrigation on groundwater resources.

Average constituent concentrations for each borehole can be seen in Table 2.2. Figure 2.9 presents a Piper diagram of the four borehole waters, indicating the hydrofacies in which each borehole falls. The boreholes show a similar groundwater chemical signature, mainly sodium chloride-dominated water, indicative of the Ecca Group's metamorphosed shales, mudstones and sandstones in which the boreholes are drilled. Therefore, after three seasons, there is no sign of impact on groundwater quality from the circum-neutral irrigation water.

Table 2.2: Summary of constituent concentrations of the four on-site boreholes for the Mafube unmined pivot

Unit	Parameter	Borehole			
		Borehole 1 (upstream – deep)	Borehole 2 (upstream – shallow)	Borehole 3 (downstream – deep)	Borehole 4 (downstream – shallow)
mg/l	pH	6.8	5.97	6.7	6.5
	EC (mS/m)	105	6.4	298	37.5
	TDS	652	50	1869	163
	Suspended solids	27	8.4	56	195
	SO <sub>4</sub>	72	2	427	65
	Ca	33	2.5	53	5.6
	Mg	20	1.6	56	6
	Na	135	5	459	80
	K	5.9	3.2	7.2	62
	Cl	238	7	628	158
	Total P	0.4	0.3	0.3	0.6
	Total N	6	1.9	3.6	6.5
	Al	0.2	0.08	0.16	0.1
	Fe	0.16	0.08	0.15	0.25
	Mn	0.05	0.05	1.96	0.02
	Zn	0.04	0.03	0.06	0.02
	F	0.3	0.5	0.35	0.2

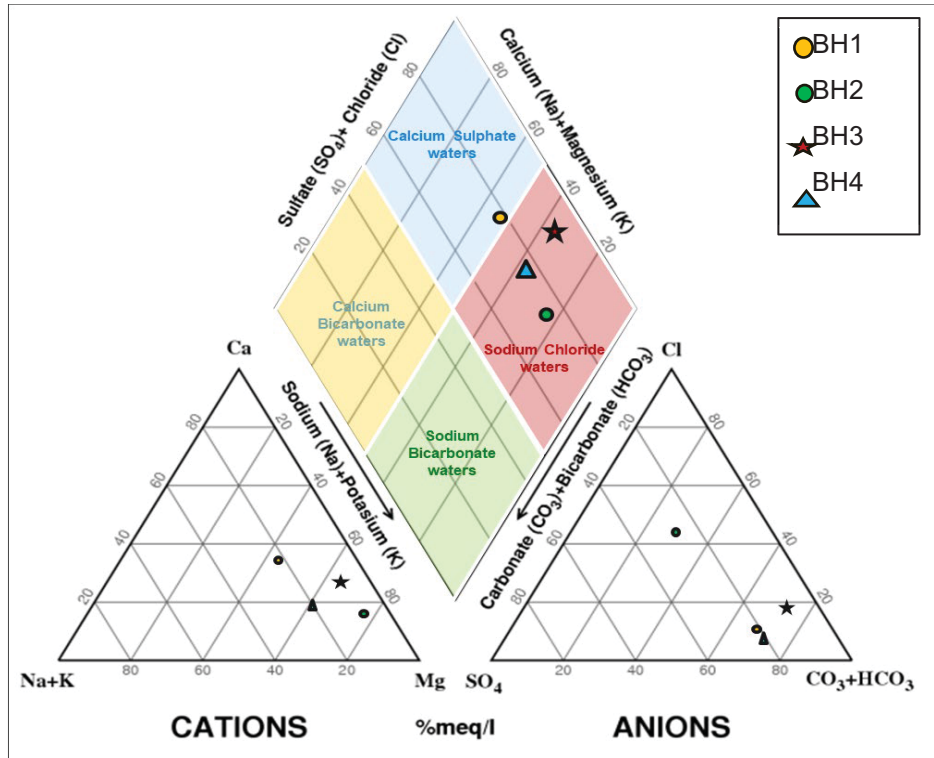


Figure 2.9: Piper diagram of the four on-site monitoring boreholes for the Mafube unmined pivot

### 2.3.2 Irrigation water quality

The irrigation water is sourced from the Mafube voids, more specifically Void 3. Fluctuations in water quality were observed due to dilution by rainfall, and at times the introduction of poorer-quality water from Arnot Colliery. Table 2.3 shows the average irrigation water quality for October 2014 to December 2019. The data reported in Table 2.3 is the water quality of the irrigation water used throughout the three maize-growing seasons. A Piper diagram (Figure 2.10) indicates that Void 3 water has calcium sulphate hydrofacies, confirming this to be a gypsiferous mine water quality.

Table 2.3: Average water quality of Void 3 used for irrigation at the Mafube unmined field over the project period

Unit	Parameter	Irrigation Void 3 water				
		October 2014 to September 2015	October 2015 to September 2016	October 2016 to September 2017	October 2017 to September 2018	October 2018 to December 2019
mS/m	EC	98.1	140.3	112.7	207.3	251.2
	pH	7.2	6.9	7.4	8	8.1
mg/ℓ	K	10.3	14.1	14.6	31,2	22.5
	Mg	57.2	93.7	71.4	153.5	84.4
	Ca	74	118.6	94.2	217	142.2
	Total hardness	-	-	743.4	1173.6	523.7
	Na	31.2	46,3	43.1	65.1	157.2
	Cl	20.9	27.0	23.6	21.7	40.4
	SO <sub>4</sub>	458	743.5	516.5	1098.6	1506.7

<b>Total N</b>	1	0.8	1.9	4.1	1
<b>Fe</b>	0.1	0.1	0.1	0.1	0.01
<b>Mn</b>	6.8	9.7	2.9	2.4	0.1
<b>Al</b>	0.1	0.1	0.1	0.1	0.2
<b>Pb</b>	-	-	-	0.005	0.006
<b>Zn</b>	-	-	0.03	0.01	0.006
<b>Ni</b>	-	-	-	0.01	0.4
<b>Cr</b>	-	-	-	0.003	0.006
<b>Cd</b>	-	-	-	0.003	0.008
<b>F</b>	0.5	0.8	0.7	0.5	0.6

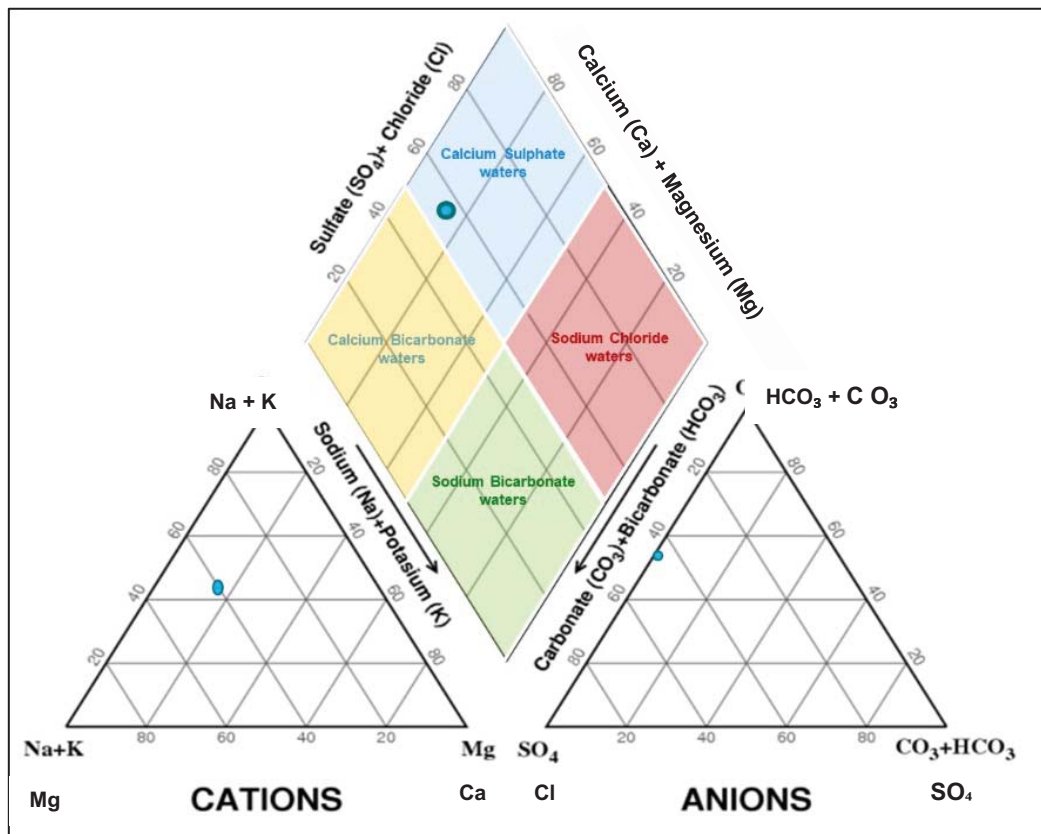


Figure 2.10: Piper diagram of the irrigation water (Void 3) used for irrigation at the Mafube unmined pivot

Figures 2.11 to 2.13 show the changing concentrations of various constituents of weekly Void 3 water over the period of five years. The data supplied by Mafube Colliery of the Void 3 irrigation water quality was assumed to be derived from correctly taken water samples that were accurately analysed, as these measurements were undertaken by an independent South African National Accreditation System (SANAS)-accredited laboratory.

The EC showed a steady increase from around 100 mS/m to almost 300 mS/m, while the pH remained fairly constant at around 7 to 8. Both calcium and magnesium saw a steady increase in concentration from October 2014 to August 2016, after which the concentrations dropped to a quarter of the peak concentration (from  $\pm 140$  mg/l to 35 mg/l). This can perhaps be attributed to no water being pumped into the void over this period. These two elements, along with the electrical conductivity and sulphate concentrations, have seen a steady increase in concentrations from September 2016 to August 2020. This is likely due to the importation of water from Arnot Colliery during times of water shortage at Mafube.

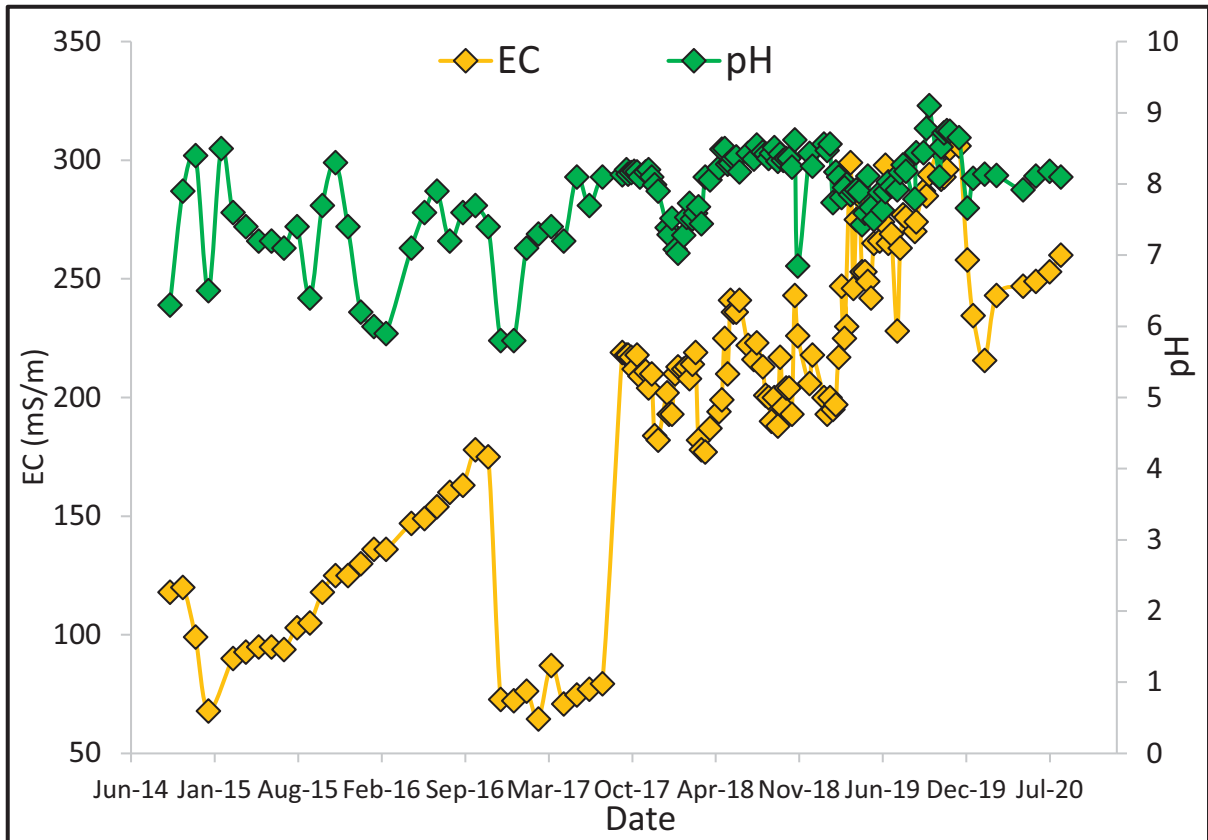


Figure 2.11: Change in pH and electrical conductivity of the Void 3 water from October 2014 to August 2020

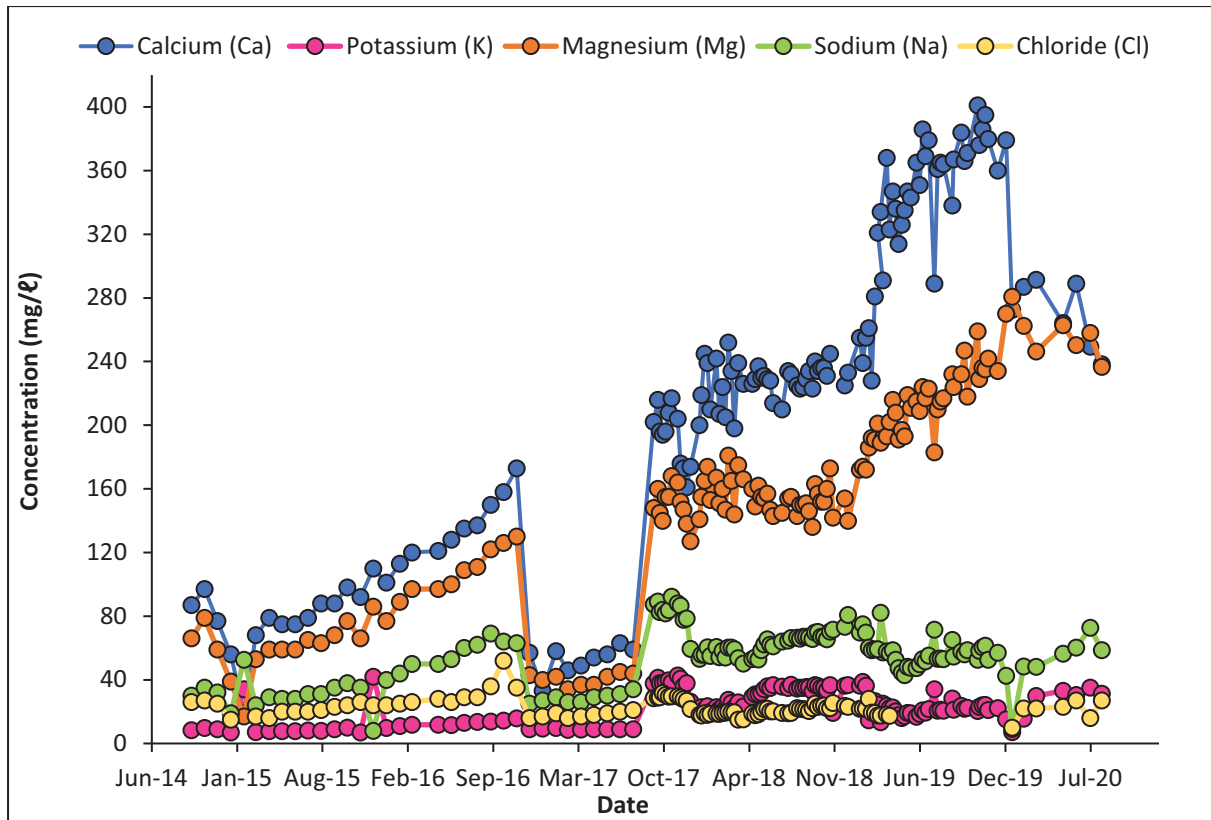


Figure 2.12: Change in major cation concentrations of Void 3 irrigation water from October 2014 to August 2020

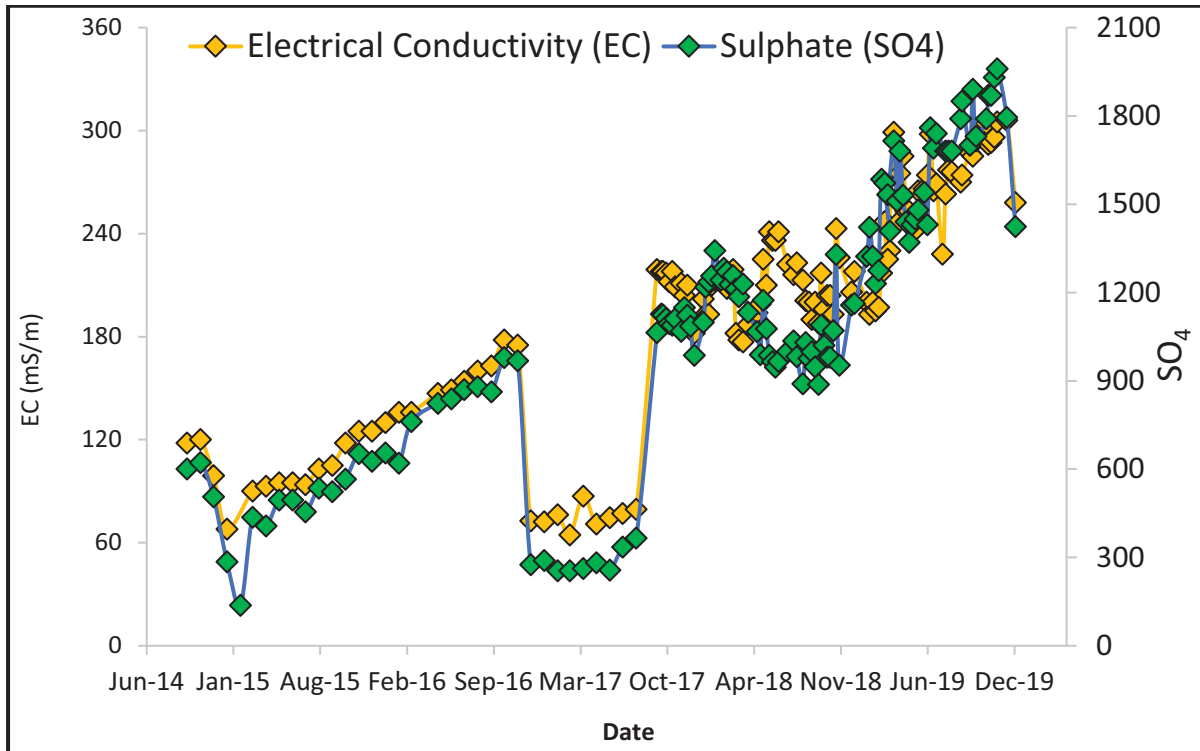


Figure 2.13: Change in electrical conductivity and sulphate concentration in the Void 3 irrigation water from October 2014 to August 2020

### 2.3.3 Downstream surface water quality

The identified downstream surface water monitoring point (Beestepan Dam) was chosen as the point where any potential impact of irrigation could be monitored. Sulphate was chosen as the identifiable “flagging” constituent, and if a 20% increase in original concentration (before irrigation), attributable to irrigation, was observed, irrigation would cease. This was, however, later realised to be a somewhat ambiguous threshold, as the monitoring point is also downstream from one of the mines’ discard dumps, and any increase in sulphate (or any other element) cannot easily be related to irrigation alone. In addition, the deterioration in irrigation water quality over time, due to the import of water from Arnot Colliery, confounds the situation still further. In practice, adaptive management will be required when responding to approaching or exceeding such downstream surface water thresholds. Adaptive management practices can include reducing the size of the irrigated area, intercepting the runoff or shallow groundwater flow and then reusing and/or treating such waters. Understanding a specific site’s local hydrogeology and hydraulic flow characteristics will allow for greater insight into setting site-specific thresholds.

Fortunately, the continuous monitoring has demonstrated that the threshold level was not reached, and no action was required. Table 2.4 shows the average annual water qualities, as well as before and after irrigation started in September 2017. Figures 2.14 and 2.15 show the changes in constituents of the water in Beestepan Dam from 2016 (before irrigation commenced) to August 2020. The dotted red line indicates when irrigation commenced.

Table 2.4: Average water quality of Beestepan Dam used for monitoring irrigation impacts over the five-year project period

		Average October 2014 to May 2017	Irrigation commenced	Threshold (20% increase)	Average September 2017 to May 2018	Average September 2018 to May 2019	Average September 2019 to May 2020	Average September 2020 to August 2020	
pH		7.1				8.1	7.93	7.7	7.59
EC (mS/m)		115				70	102	105	95
SO <sub>4</sub> <sup>2-</sup>	mg/l	535			<b>642</b>	282	406	402	378
Na		52				30	45	45	39
Total P		0.5				0.2	0.2	0.2	0.2
Total N		1.4				1.3	1.2	0.7	0.6

Figure 2.14: Changes in the pH and electrical conductivity (mS/m) in Beestepan Dam from December 2016 to August 2020

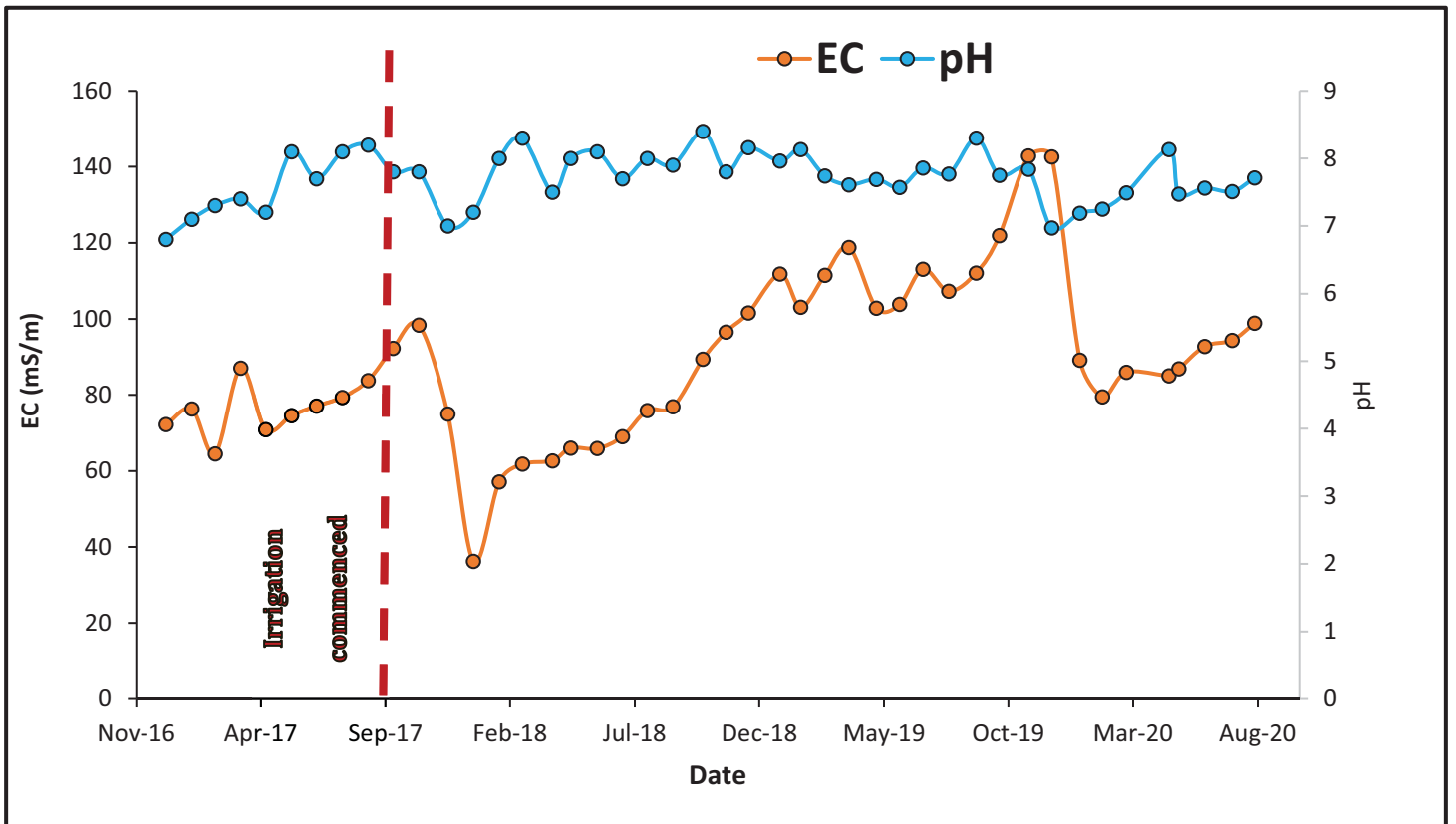


Figure 2.15: Changes in the pH and electrical conductivity (mS/m) in Beestepan Dam from December 2016 to August 2020

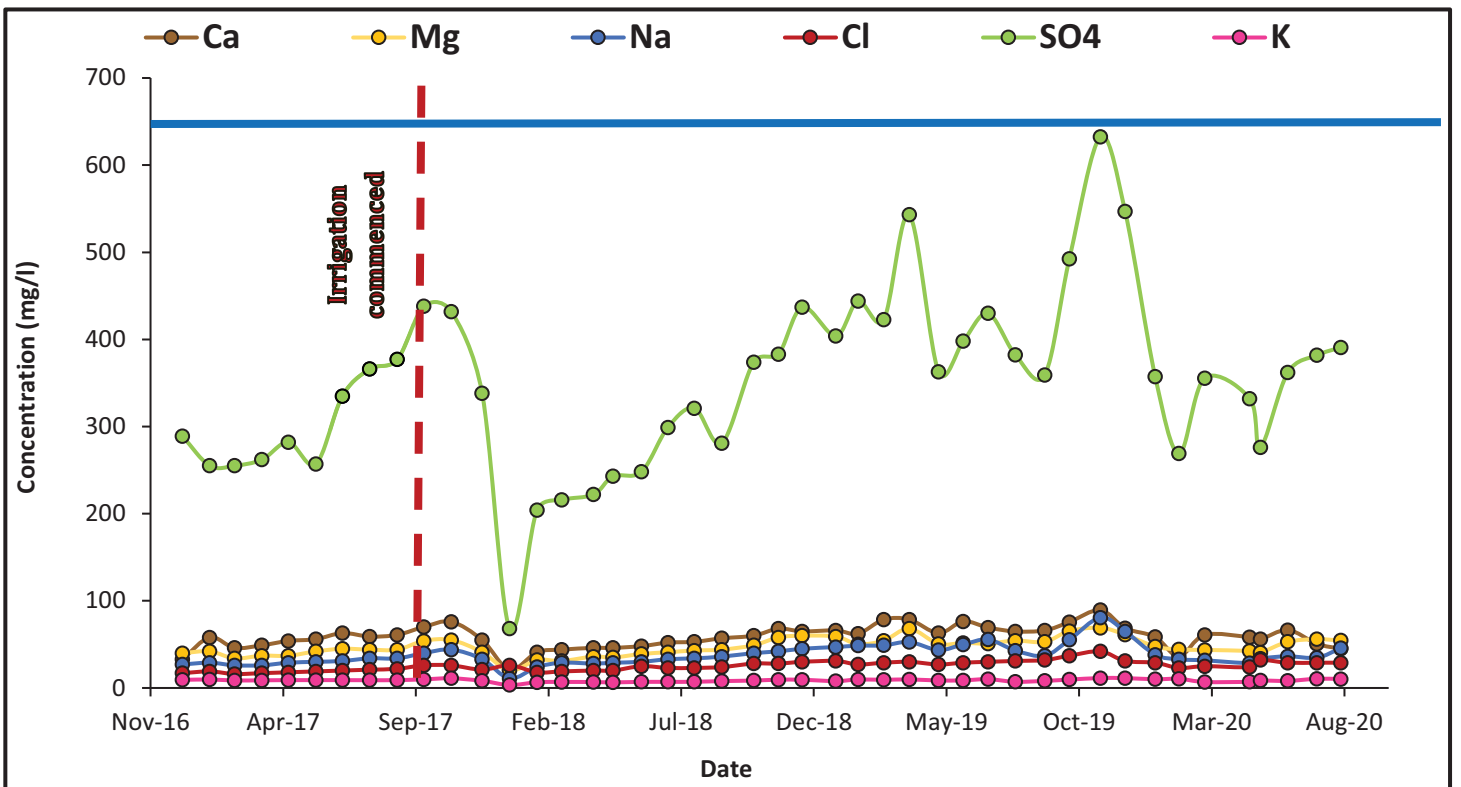


Figure 2.16: Changes in the major constituents in Beestepan Dam from December 2016 to August 2020. The horizontal blue line represents the established threshold value for sulphate.

### 2.3.4 Stable isotope study

Stable isotope studies help identify hydraulic connections between water sources. Changes in the isotopic signatures of water sources can be due to the source being base flow or rainfall fed, affected by evaporation rates, and surface and groundwater mixing (Mahlangu et al., 2020). Understanding the connection between Beestepan Dam and the Mafube irrigation pivot is crucial when looking at the transport and fate of constituents from the irrigation water (Void 3 water).

The underlying geology of the Mafube Colliery, unmined pivot and surrounding farmland is the Ecca Group metamorphosed shales, mudstones and sandstones (Brink, 1983). The area of the Mafube unmined pivot and surrounds is made up of the Glencoe and Hutton soil forms. The soil is generally quite deep ( $\pm 5\text{--}7\text{m}$ ), as identified by the borehole logs, has a high clay percentage ( $\pm 15\%$  kaolinitic clay) and cation exchange capacity ( $\pm 15\text{ cmol}(+)/\text{kg}$ ). This means that if there is significant movement of irrigation water from the unmined pivot towards the surface water resource (Beestepan Dam), it would most likely be through the vadose (unsaturated) zone, and less likely via the fractured rock system of the Ecca Group rocks.

Water D/H ( $^2\text{H}/^1\text{H}$ ) and  $^{18}\text{O}/^{16}\text{O}$  ratios were analysed in the laboratory of the Environmental Isotope Laboratory (EIL) of iThemba Labs, Johannesburg. The equipment used for stable isotope analysis consists of a Los Gatos Research (LGR) liquid water isotope analyser. Laboratory standards, which were calibrated against international reference materials, were analysed with each batch of samples. The analytical precision is estimated at 0.5‰ for O and 1.5‰ for H.

Analytical results are presented in the common delta notation:

$$\delta^{18}\text{O}(\text{‰}) = \left[ \frac{(^{18}\text{O}/^{16}\text{O})_{\text{sample}}}{(^{18}\text{O}/^{16}\text{O})_{\text{standard}}} - 1 \right] \times 1000$$

which applies to D/H ( $^2\text{H}/^1\text{H}$ ), accordingly. These delta values are expressed as per mil deviation relative to a known standard, in this case standard mean ocean water (SMOW) for  $\delta^{18}\text{O}$  and  $\delta\text{D}$ .

The stable isotope analyses for all the water samples were well reproduced within the expected analytical error limits. Figure 2.21 shows the water samples  $\delta^{18}\text{O}$  vs  $\delta\text{D}$  data, relative to the global meteoric water line (GMWL) (Craig, 1961).

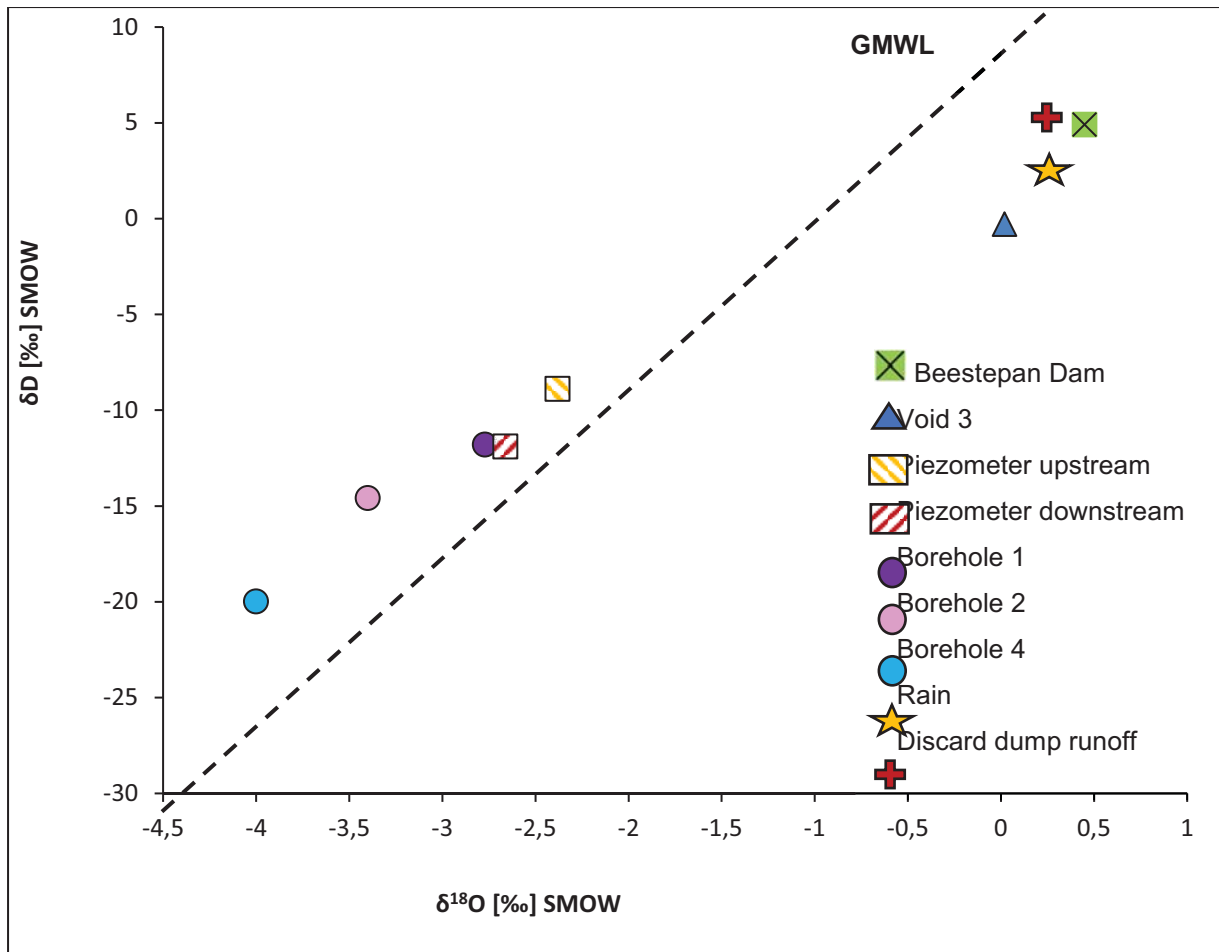


Figure 2.17: Stable isotope data relative to the global meteoric water line (Craig, 1961).

Both the Void 3 irrigation and Beestepan Dam waters are surface waters. These waters have been stored in open dams, and are both exposed to large amounts of evaporation. Both these samples plot in the light isotope-depleted region, right of the GMWL (Craig, 1961). The groundwater samples show less enrichment in lighter isotopes, indicative that these waters are not exposed to high rates of evaporation (Abiye et al., 2015; Akwensiogee et al., 2019; Butler et al., 2018).

The rainfall water is also enriched in light isotopes, providing evidence that both surface waters are rained or experience some degree of rainwater recharge. Both surface water samples can also be influenced by runoff recharge (Abiye et al., 2015). The isotopic signature of the discard dumps' runoff water is rainwater that now becomes acidic runoff water. This is the reason the discard dump runoff water has a similar isotopic signature to rainwater. No clear distinction is made between the isotopic signature of the rainwater, the discard dump water, irrigation water (Void 3) and the downstream surface water source (Beestepan Dam).

The groundwater's isotopic signature is due to base flow and not rainfall recharge, as their isotopic signatures are very different. It can also be concluded that the irrigation water is not from the same source water as the groundwater. With a fair amount of confidence, it can be concluded that the irrigation water is not interacting with the groundwater in its vicinity.

It is noted that the stable isotope analyses are a conservative approach to contaminant studies. Factors such as dilution, dissolution, mineral deposition, chemical reactions and cation exchange play a role in the accuracy of isotope results. It is also highlighted that the impact and interaction of the discard dumps' acidic runoff, located directly next to the Mafube pivot, are unknown and have not been quantified, as

this is on the mine’s property. Interaction from the direct runoff and groundwater seepage may play a role in the results of these isotope tracer tests.

Further recommendations for isotope tracer tests at the pivot include further seasonal interaction studies to assess and identify if any further interactions occur. Any additional water input into the system should be identified and samples analysed to increase the confidence in the findings of this study.

## 2.4 CROP GROWTH AND YIELDS

This section presents data on cumulative irrigation and rainfall, and the growth and development of the maize crop over the course of this project at the unmined Mafube site.

The annual cumulative rainfall and irrigation amounts can be seen in Figure 2.17. Table 2.5 summarises the total irrigation and rainfall the Mafube unmined pivot has received over the period of this project. In conjunction with the fertilization programme, the farmer should take the loading rates of salts applied to the irrigated field over the 28-month irrigated period into account and adjustments made to fertilizer application rates. The total salts applied to the Mafube unmined field over all the growing seasons are as follows: 19 034 kg/ha SO<sub>4</sub>, 2 709 kg/ha Ca, 1 746 kg/ha Mg, 1 596 kg/ha Na, 431 kg/ha Cl and 1 770 kg/ha K.

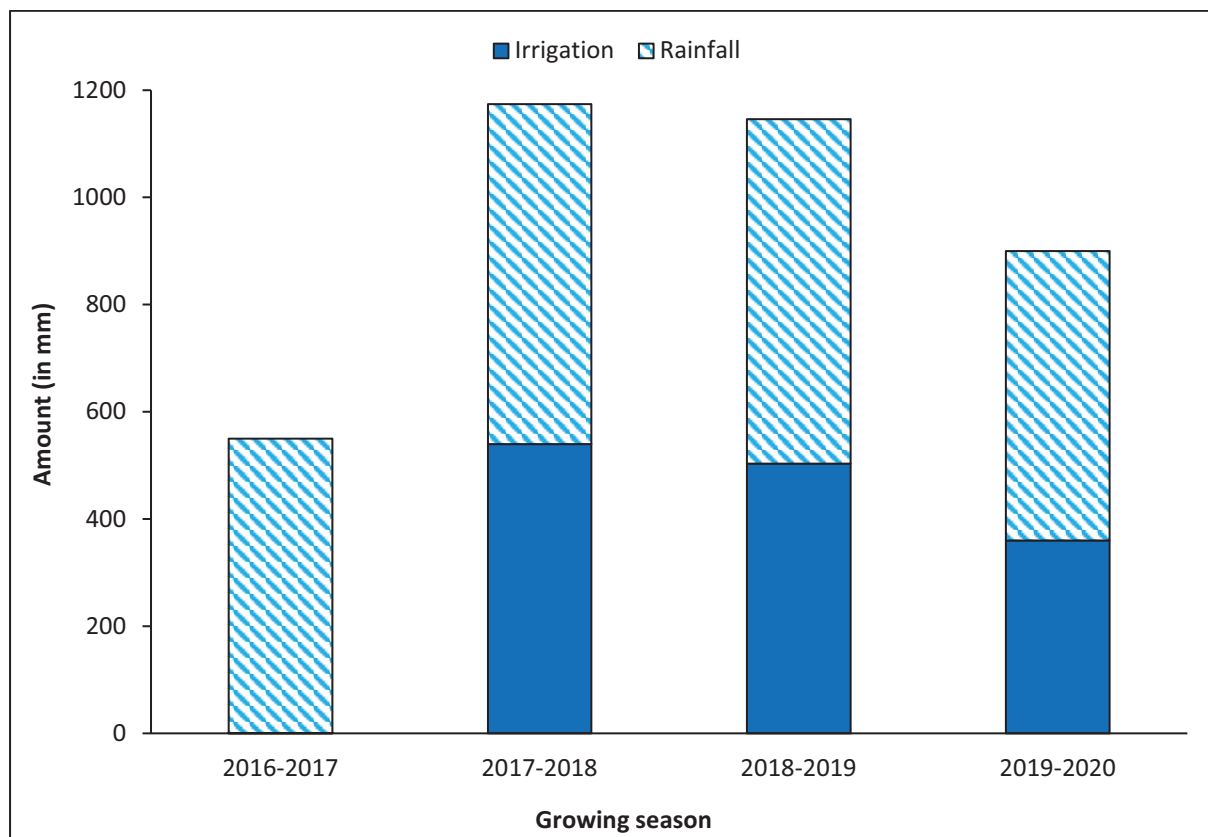


Figure 2.18: Seasonal rainfall and irrigation throughout the maize-growing seasons at the Mafube unmined site

Table 2.5: A summary of seasonal irrigation and rainfall the Mafube unmined pivot has received over the last three irrigated maize seasons and a shortened stooling rye growing season

Year	Growing season	Irrigation amount (mm)	Rainfall amount (mm)
2015/16	Dryland maize	-	480
2016/17	Dryland maize	-	550
2017/18	First irrigated maize	304 (summer)	634
2018	Half-season irrigated stooling rye	236 (winter)	-
2018/19	Second irrigated maize	503	643
2019/20	Third irrigated maize	360	540
<b>Total</b>		<b>1 403</b>	<b>2 847</b>

Along with Leaf Area Index (LAI) and fractional interception of radiation, plant height, total above ground dry mass and the phenological stage was observed every second week. Table 2.6 gives details regarding maize growth stages. Knowing the phenological growth stage (Figure 2.18) of the crop helps keep track of overall crop development. This is very important information when modelling crop growth and production. Pictures of the crop have been incorporated into this diagram from various seasons to indicate the visual status of the maize crop.

Table 2.6: Maize phenological stages

Physiological stage		
Planting		
VE (Coleoptile emergence from soil)		Vegetative growth stage
V3/V4		
V5/V6 (Visible collar of the fifth and sixth leaf)		
V(n) nth node visible		
VT (Tasseling stage)		
R1 (Silking stage)	Kernel filling	Reproductive growth stage
R2 (Blister stage)		
R3 (Milk stage)		
R4 (Dough stage)		
R5 (Dent stage)	Physiological maturity	

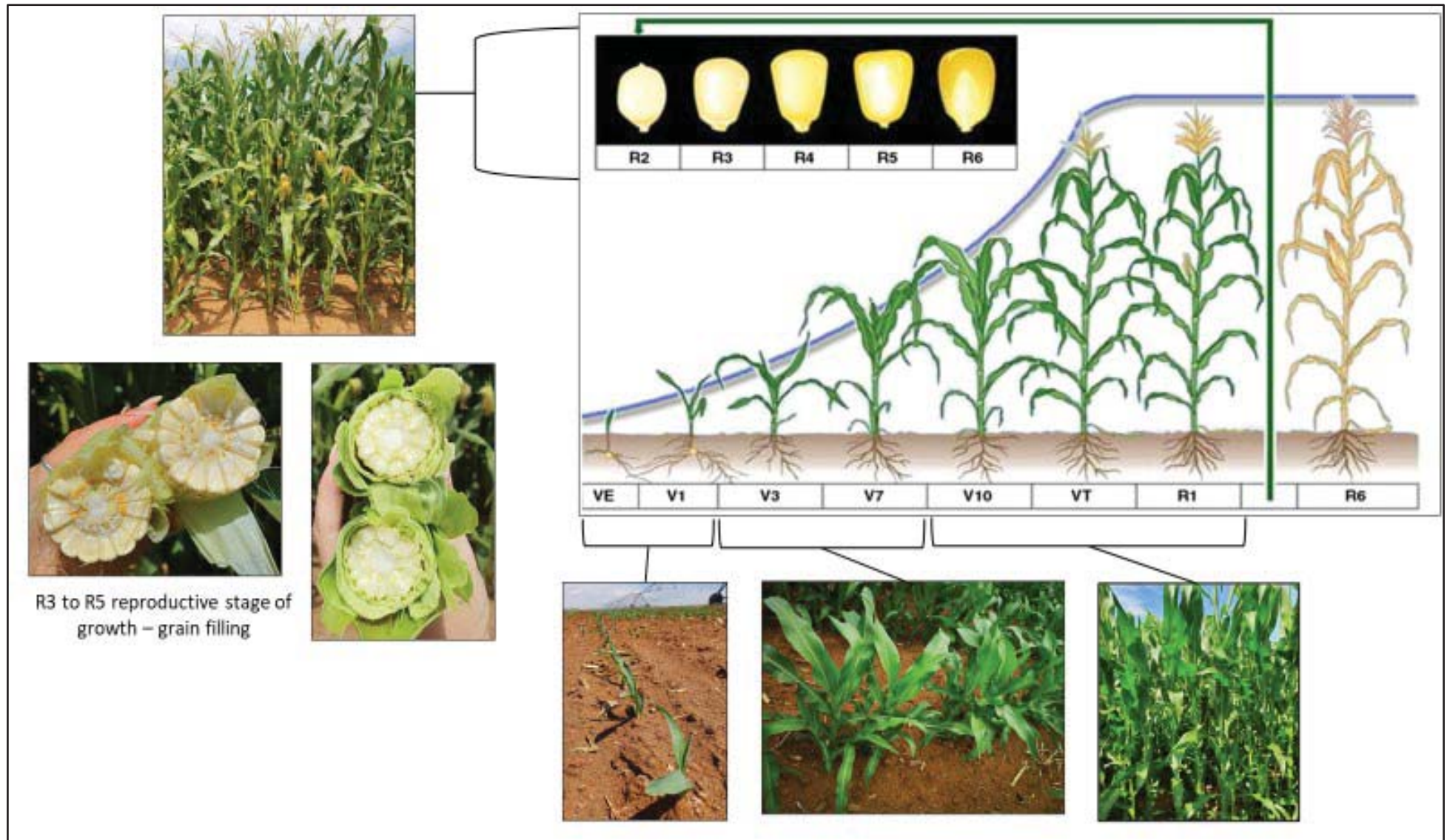


Figure 2.19: Phenological growth stages for the maize crop (He et al., 2010)

**Note:** VE = Emergence; V1-VT = Vegetative Phase; R1-R6 = Reproductive Phase

Total above-ground biomass or total dry mass (TDM), together with grain yield, provides some insight into the effect of mine water irrigation on crop production. Approximately 45% of the above-ground dry biomass at harvest is partitioned into the maize grain under non-stress conditions (the so-called Harvest Index) (HI). If the HI is much lower than this, it is indicative of stress (Unkovich et al., 2010). Under ideal growing conditions, without water stress, the rate of dry matter accumulation from V7 to V16 should increase exponentially until physiological maturity when there will be a sharp decline in the rate of dry matter accumulation as the crop matures. This is associated with functional and visual leaf senescence. This time period is critical to maintaining good yields, as all assimilates are partitioned to grain filling from silking to maturity. Table 2.7 gives a full summary of the yields, TDM, HI and average cob length for the three white maize irrigation growing seasons. A correction was made for the dry mass by 12.5% for moisture loss.

Table 2.7: Summary of yields, total dry mass, Harvest Index and average cob length observed at the end of each growing season

	2016/17	2017/18		2018/19 *Hail damage		2019/20	
	Dryland	Irrigated	Dryland	Irrigated	Dryland	Irrigated	Dryland
Yield (ton/ha)	4.1	13,5	4,5	11,6	5,5	14,3	4,9
TDM (ton/ha)	-	29,6	18,1	25,1	16,6	37,9	27,8
HI (%)	-	55,5	40,2	37,2	27,9	56,1	42,8
Average cob length (cm)	-	19,5	17	19,5	17,2	21	17

**Note:** Total dry mass includes stalks, leaves, cob and grain mass. Yield is grain mass alone.

The values shown for the irrigated crop almost treble that of the dryland crop each growing season. The immense value irrigation with mine water can present to the agricultural industry, as well as the water management of mines in South Africa, is clearly demonstrated.

Crop biomass production is attributed to the following two factors: amount of photosynthetically active radiation (PAR) intercepted by the canopy and efficiency of converting the captured radiation into biomass, so called radiation use efficiency (RUE) (Louarn et al., 2008). Both leaf area and fractional radiant interception are used in crop models to predict the accumulation of dry matter. Measuring the LAI of the crop, as was done in the Mafube trial, considers the crop at a small sampling scale. If the field is not very uniform, as is expected on rehabilitated ground, then considering the greater spatial distribution over the whole pivot using satellite or drone imagery is useful.

The LAI measured at certain positions within the irrigated and dryland areas throughout the growing seasons over the project period can be seen in Figure 2.19. The LAI is a measure of crop canopy cover and is defined as the adaxial green leaf area per ground surface area, measured in  $m^2 \cdot m^{-2}$ . Destructive sampling was done every two weeks from a 2 to 3  $m^2$  area, and analysed at the University of Pretoria's Experimental Farm within a few hours of collection. The LAI curve follows the expected general sigmoidal trend for a maize crop for all growing seasons. A rapid canopy development is seen within the first 30 to 40 days after emergence, until a peak LAI of 4.5 to 5.5  $m^2 \cdot m^{-2} \pm 100$  days after emergence, when the crop reaches its reproductive growth stages. Maize is a determinate crop. Once it has reached the reproductive stage, no further vegetative growth will occur. The LAI of the crop is then expected to plateau, followed by a decline when physiological maturity is reached. This decline will be due to the leaf senesce and the crop drying out in-field before harvest. During the 2018/19 growing season, severe hail damage was experienced approximately 100 days into the season. This is reflected in the sharp decrease in LAI due to loss in the photosynthetically active area of the crop.

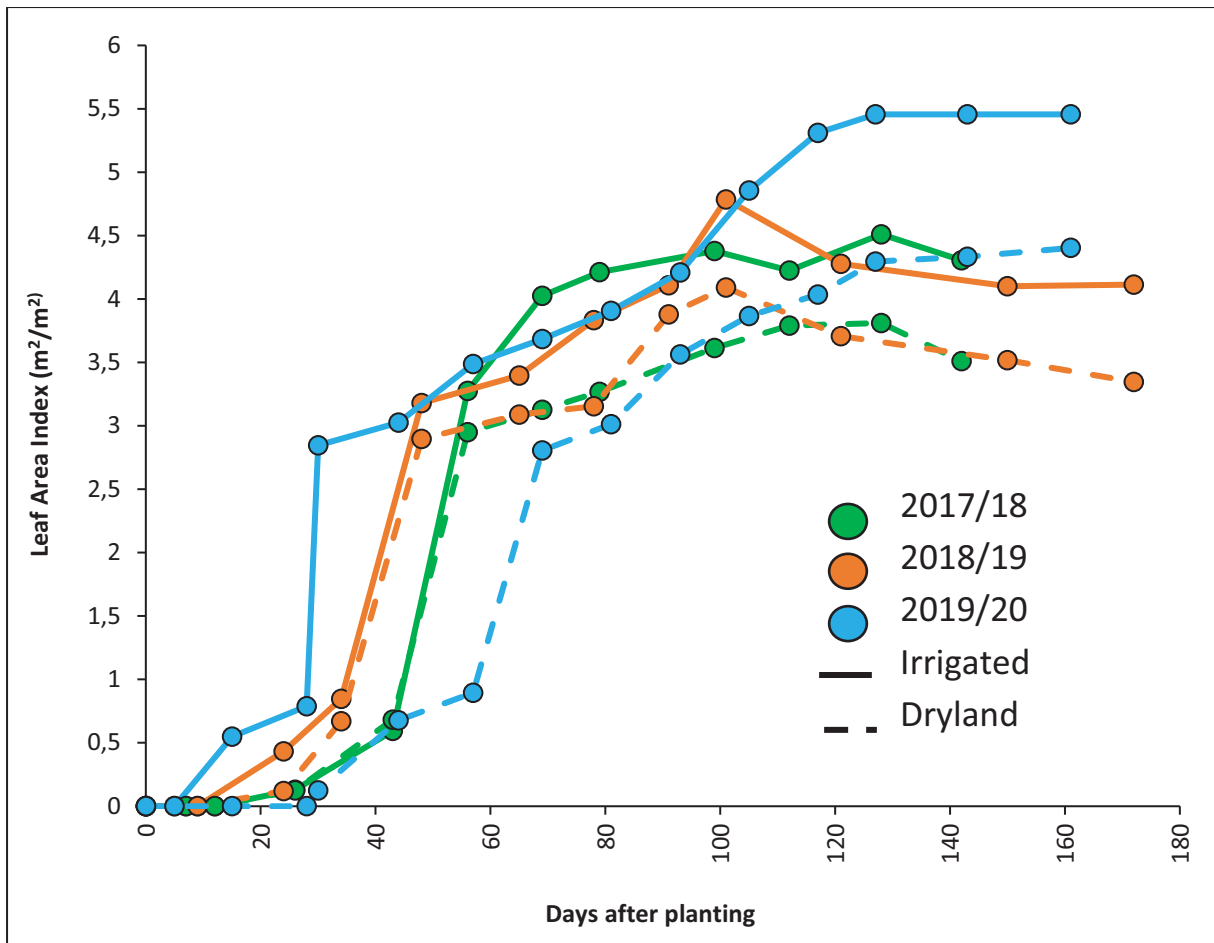


Figure 2.20: Average leaf area index of irrigated and dryland white maize on the Mafube unmined field over the project period

Photosynthetically active radiation is measured at the bottom of the canopy, as well as above it. These values ( $PAR_{bottom}$  and  $PAR_{top}$ ) are then used along with the measured LAI to determine a radiation extinction coefficient. With this coefficient, the fraction of PAR ( $FI_{PAR}$ ) that is intercepted by the canopy (Figure 2.20) can be modelled from the LAI, and is an important parameter for the partitioning of available evaporative energy into that available for transpiration and that available for direct evaporation from the soil. Fractional interception (FI) of PAR gives us insight into whether or not radiation is a limiting factor in crop growth. The fractional interception can be seen in Figure 2.7 and all monitoring stations follow an asymptotic curve. The FI of the crop is expected to plateau, followed by a decline when physiological maturity is reached. This decline will be due to crop leaf senescence and the crop drying out before harvest.

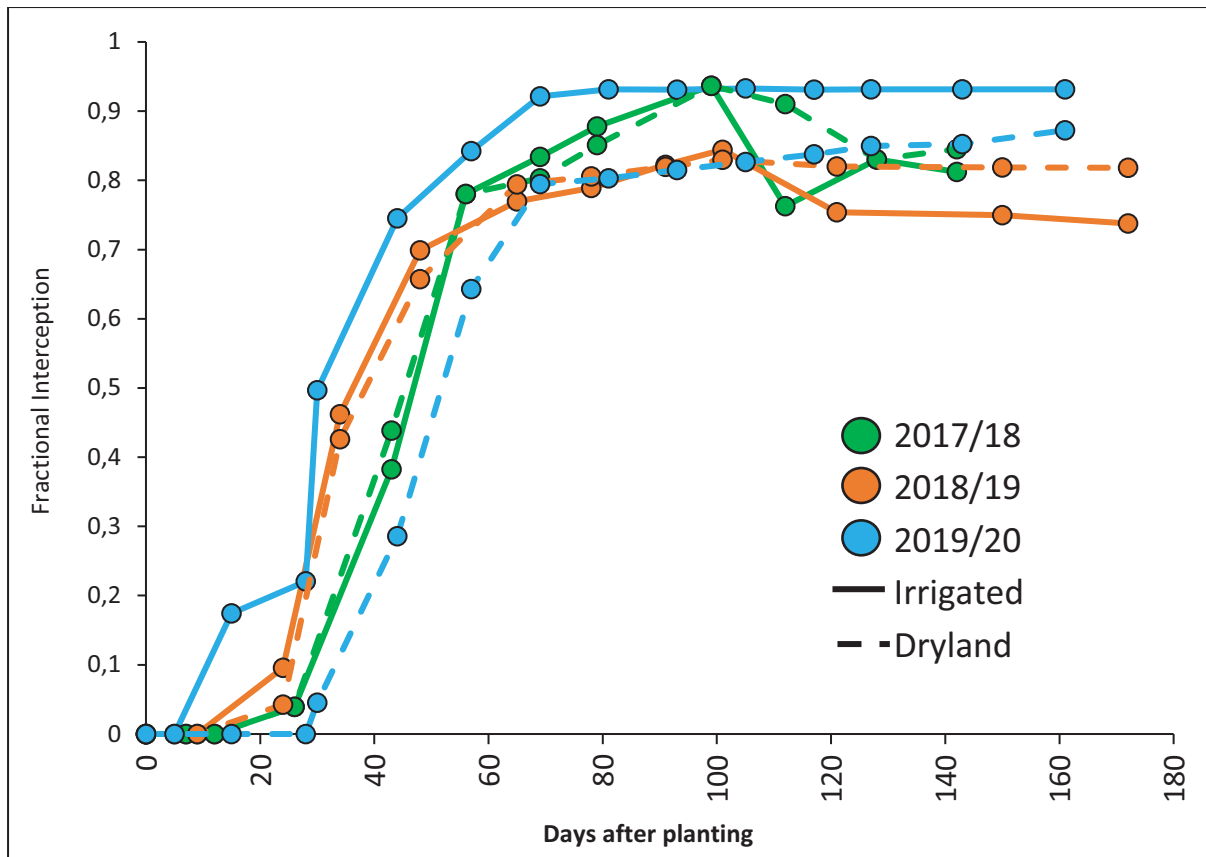


Figure 2.21: Average fractional interception of photosynthetically active radiation for white maize grown at the Mafube unmined field

Plant height was monitored throughout the growing season and has followed the typical maize sigmoidal growth pattern (Figure 2.21). A plateau in plant height is observed as the crop reaches the reproductive stage, and assimilates are directed to grain filling.

During the 2018/19 growing season, severe hail damage was experienced approximately 100 days into the season. This is reflected in the sharp decrease in crop stand area and leaf defoliation.

The difference in planting date between the dryland and irrigated maize has an impact on crop height, biomass production and ultimately yield. Irrigated maize in Middelburg (Mpumalanga) has a supplemented water supply. It is therefore expected that irrigated maize will perform better than a dryland crop, especially in dry years, or when mid-summer droughts are experienced.

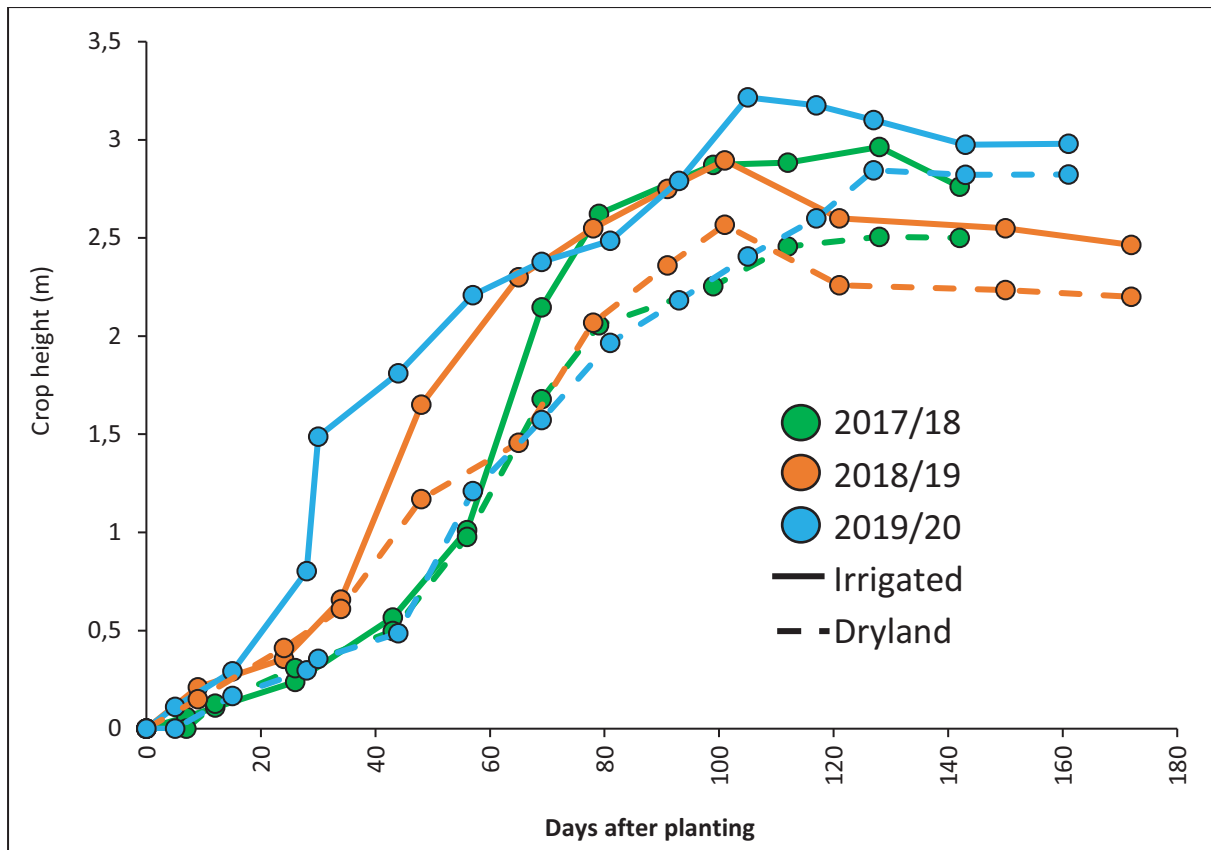


Figure 2.22: Crop height measured for pivot and dryland areas for white maize grown at the Mafube unmined field

## 2.5 COSTING REPORT: SEED, FERTILIZER AND PESTICIDE REGIME

The following section will discuss agronomic inputs and some of the budgeted costs to produce white maize during the three growing seasons at the Mafube unmined site. The full summary can be seen in Appendix A1. The total fertilizers added before, during and after planting per hectare each season amounted to 290 kg nitrogen, 40 kg phosphorus, 64 kg potassium, and 10 kg sulphur. The farmer chose to add a nitrogen (urea) top dressing after crop emergence. Herbicides and pesticides were applied via broadcast sprayers prior to planting. The reasons for use of the crop protection chemicals are for the control of annual broadleaf weeds, grasses, yellow nutsedge, cutworm, stem and stalk borers, and their larvae.

The University of Pretoria's research team's method of determining the predicted yield was by taking whole maize plant samples at various growth stages during the growing season. The sampling procedure was to use seven sampling points, where three 10 m row lengths were sampled, with  $\pm 10$  plants per row length sampled. After sampling, the plants were stripped of their stems, cobs and leaves, and each plant part was weighed separately. The separate plant parts were then oven dried at 70 °C for  $\pm 7$  days, or until plant parts displayed a constant mass. The average masses determined were corrected for plant density in order to estimate yield per unit surface area. The values reported in Table 2.8 are yield and profit/loss estimates of the white maize crop for the three growing seasons.

The full summary of the annual costs of cultivation, harvest, transport, storage and labour can be seen in Appendix A1. The total estimated cost per hectare for 2019/20 is around R19,700 for irrigated land and R17,700 for dryland. Note that the irrigation cost would usually include another R5,000 for pumping costs, but in this case, Mafube Colliery covered these.

Table 2.8: Average tonnage, cost per hectare, maize price, profit or loss per hectare with and without pumping costs for each cropping season.

	2016/17	2017/18		2018/19		2019/20	
	Dryland	Irrigated	Dryland	Irrigated	Dryland	Irrigated	Dryland
<b>Yield (ton/ha)</b>	4.1	13.5	4.5	11.6	5.5	14.3	4.9
<b>Cost per ha</b>	R9 100,00	R18 000,00	R16 000,00	R18 770,00	R16 800,00	R19 980,00	R17 900,00
<b>SAFEX maize price/ton</b>	R1 966,00	R2 103,00		R2 910,00		R2 450,00	
<b>Profit/loss per ha (no pumping costs)</b>	<b>R1 039,00</b>	<b>R10 390,00</b>	<b>R6 540,00</b>	<b>R12 000,00</b>	<b>R4 600,00</b>	<b>R15 055,00</b>	<b>R5 900,00</b>
<b>Profit/loss per ha (with pumping costs)</b>	<b>R1 039,00</b>	<b>R5 390,00</b>	<b>R6 540,00</b>	<b>R7 000,00</b>	<b>R4 600,00</b>	<b>R10 300,00</b>	<b>R5 900,00</b>

This demonstrates that dry land agronomic crop production can be extremely risky, and irrigation can usually be expected to stabilise yields, but cannot mitigate against low commodity prices and high input costs. Irrigation can certainly be used to cost effectively manage large volumes of surplus poor-quality mine water, but this will definitely be a more resilient option if mines are able to somewhat assist growers by, for example, agreeing to cover pumping costs. This is a reasonable request, considering that the liability of managing the water rests with the mine, and alternative treatment options can be very expensive. The benefit of being able to irrigate with mine water over these three seasons is clear.

## 2.6 GRAIN ANALYSES

For food and fodder safety analyses, one needs to determine the elemental composition of the edible portions of the plant. For this, an acid digestion of milled plant parts is undertaken. At the end of each growing season, the relevant plant samples were taken and analysed. Comparisons were made to current food and fodder safety thresholds. The full chemical analyses can be found in Appendix A2. When looking at the elemental partitioning throughout the maize plant over the three growing periods, no major differences can be identified for the grain, stem and leaves. The elemental distribution within the three parts remains similar. It is noted that leaves exhibit far higher concentration of most elements when compared to the grain and stems (figures 2.22 and 2.23).

When looking at food and feed safety, we have to refer to the international, as well as local guidelines on the safety thresholds for grains (see Table 2.9). Although most mine water contains a range of metals, including iron, aluminium and manganese, the important potential elements of concern from a safety perspective were identified as arsenic, cadmium, chromium, lead and mercury. It is therefore important to identify specific elements of potential concern in each body of mine water with which one is proposing to irrigate.

Table 2.9: International guidelines and thresholds of selected elements for grain food and feed safety

Element	Average Mafube white maize grain	China	European Union/ South Africa	Ireland	South African feed safety
	ppm or mg/kg				
As	0.09	0.5	-	-	2
Cd	<0.001	0.1	0.1	0.1	1
Zn	12.5	-	-	-	150
Pb	0.005	0.2	0.2	0.1	10
Hg	<0.001	0.02	-	-	0.1

The Mafube unmined pivot grain falls well below all the identified constituents of concern in the identified guidelines. The data collected from the white maize crop grown on the Mafube unmined site clearly illustrates the opportunity created by the availability of mine-impacted water for irrigation. Under the current irrigation conditions at the Mafube unmined site, the irrigated white maize is producing a good-quality grain, well within the set threshold limits. In summary, the data collected from the white maize crop grown on the Mafube unmined site during the 2017/18, 2018/19 and 2019/20 growing seasons illustrates the opportunity created by the availability of mine-impacted water for irrigation. Under the current irrigation conditions at the Mafube unmined site, the irrigated maize is producing maize grain, leaf and stem material of a similar quality, in terms of elemental concentrations, as the dryland or control maize.

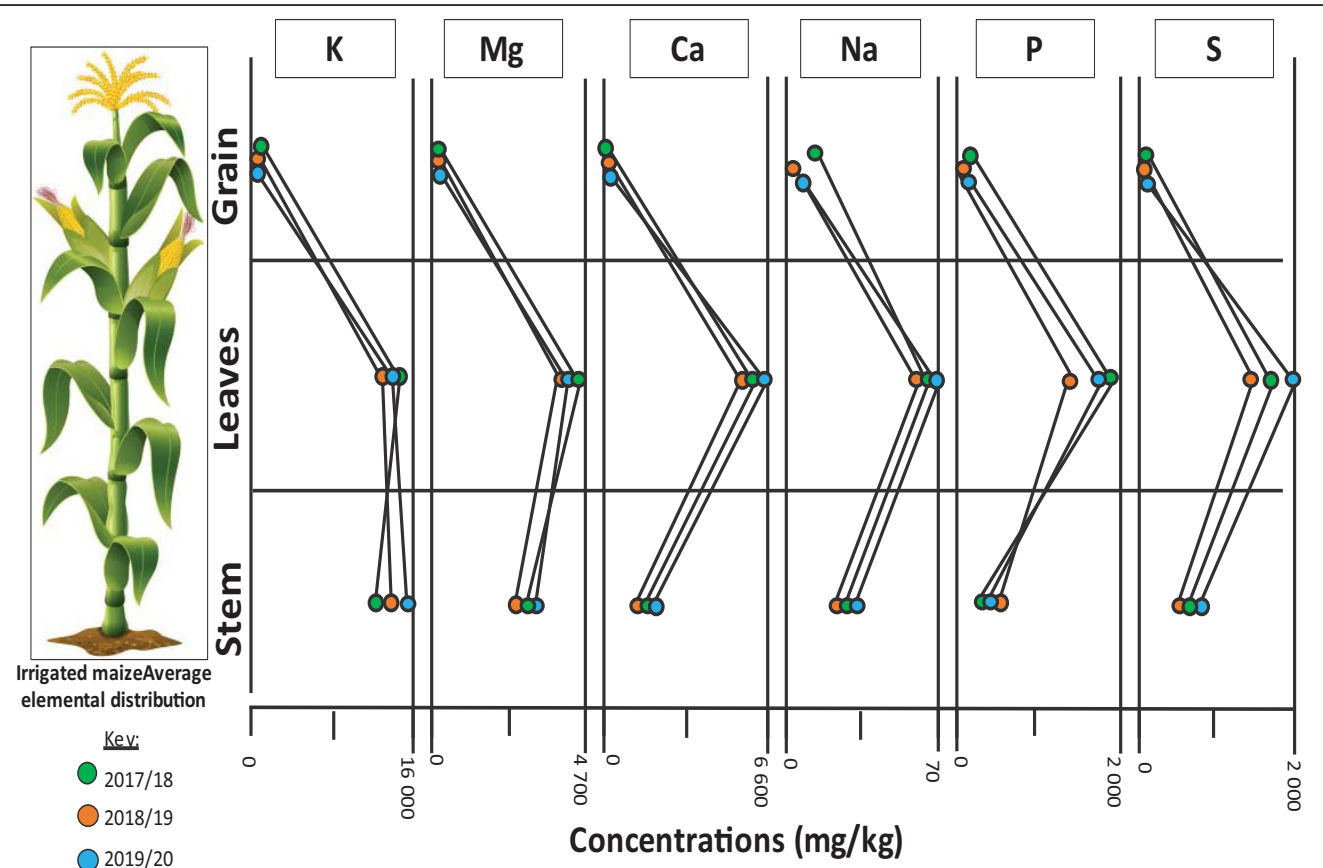


Figure 2.23: Elemental distribution of irrigated maize from the Mafube unmined pivot

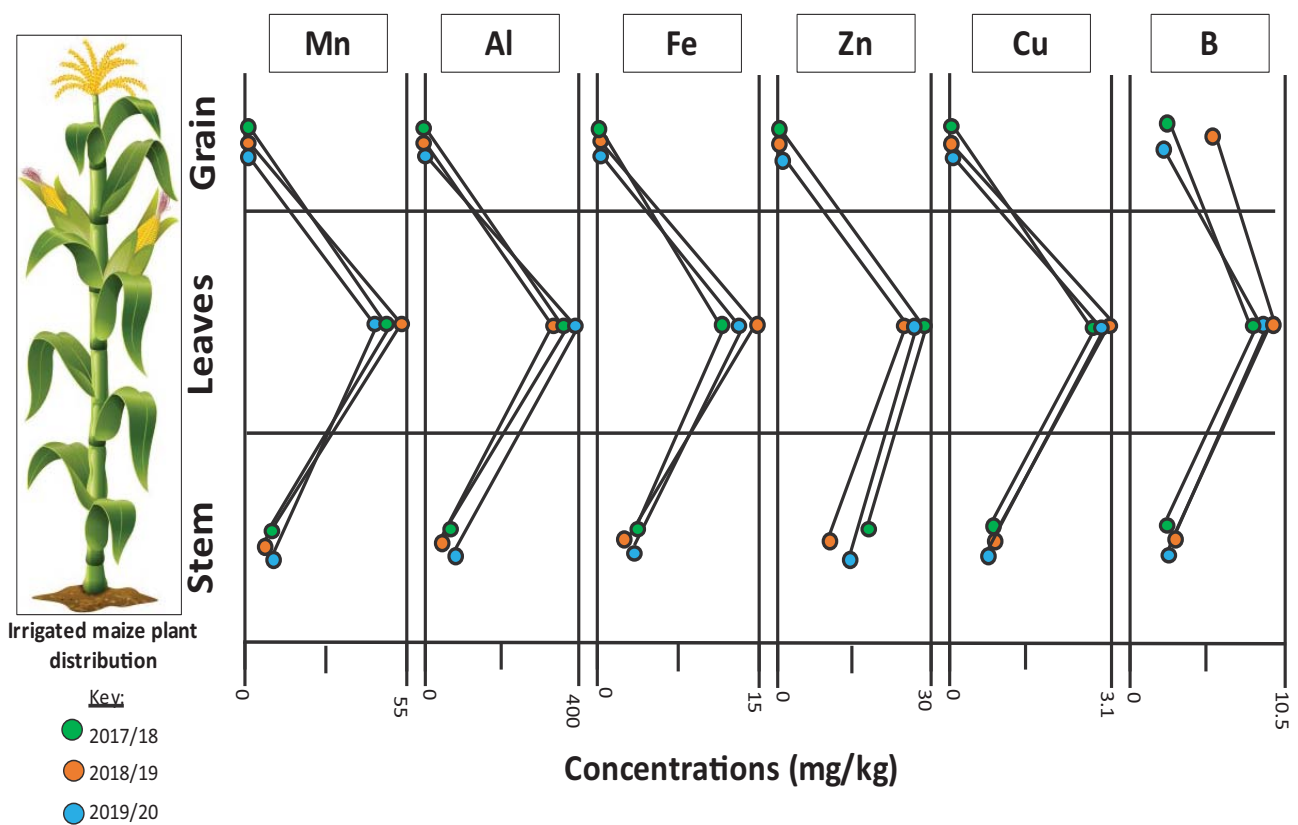


Figure 2.24: Elemental distribution of irrigated maize from the Mafube unmined pivot

## 2.7 SOIL ANALYSES

A soil sampling grid was set up at the start of this project, with 14 sampling locations identified as indicated in Figure 2.24, more or less evenly distributed throughout the pivot and dryland area. Soil samples were taken at the beginning of each irrigation season in three 30 cm increments from the surface down to 0.9 m. The analyses performed on the soils at the beginning of each irrigated season are given in Table 2.10. The full chemical analyses of all sampling sites can be found in Appendix A3.

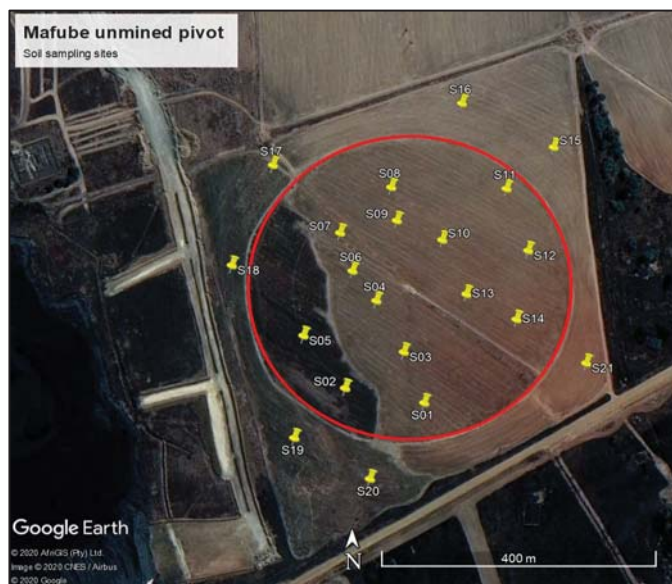


Figure 2.25: Map of soil sampling locations on the Mafube unmined land

Table 2.10: Detailed soil analyses performed

Property	Method	Result
Sulphate as S Ca, Mg, K, Na	Mehlich-3 extraction	This gives the extractable portion
	Saturated paste	This gives the soluble portion
pH	KCl extract and pH electrode	This gives the pH (KCl) of the soil solution
Phosphate as P	P-Bray 1 and P-Bray 2	This gives the extractable P
ECe	EC meter	This gives the EC of the soil solution
	Saturated paste	This gives the EC of a saturated soil extract
Total salt accumulation	Dialysis, solution replacement and EC	This gives the EC measurements as the salts are “washed” out of the soil with subsequent dilutions, and the EC decreases as the salt content decreases. The EC can be related to the ionic strength of the solution and thus give an indication of the salt (gypsum) content of the soil.

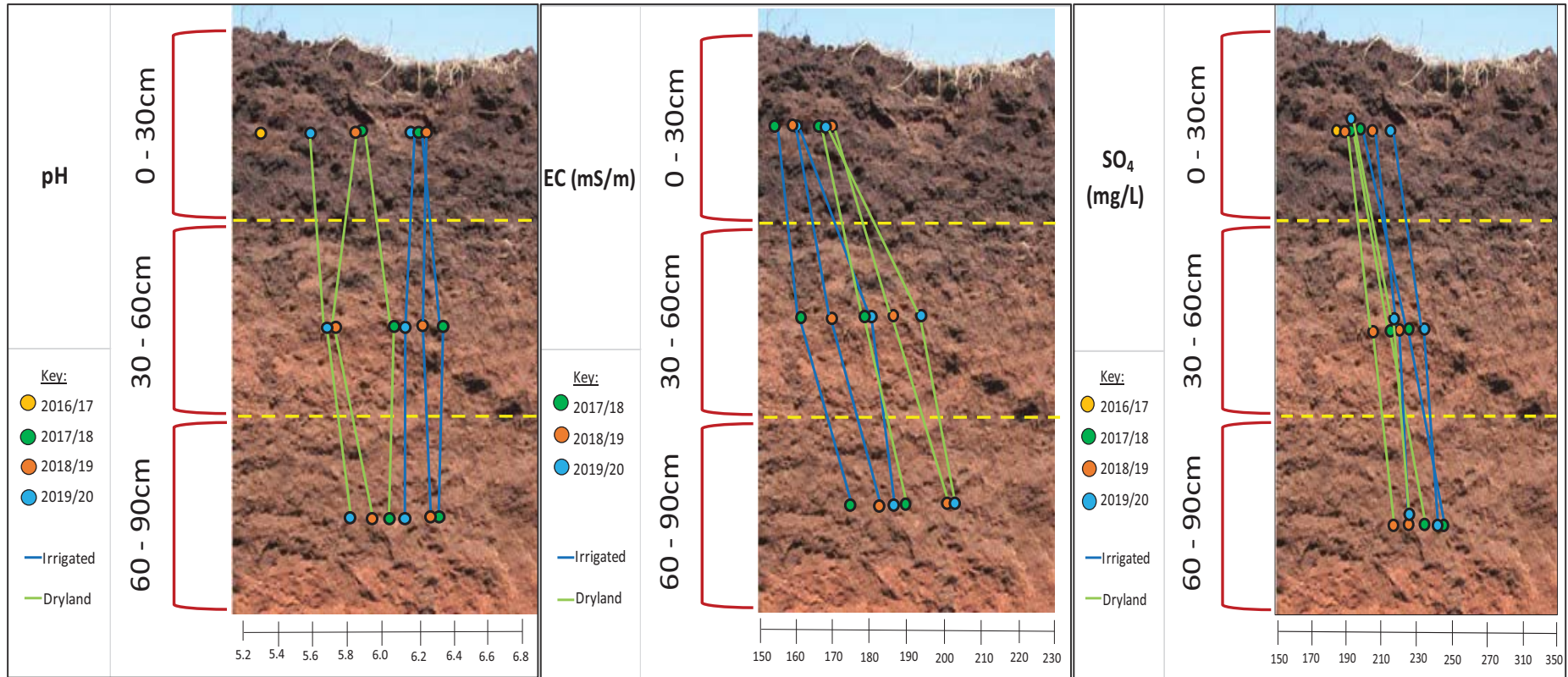


Figure 2.26: Soil profile at the Mafube unmined pivot indicating the change in pH, electrical conductivity (mS/m) and SO<sub>4</sub> (mg/l), over an irrigation period of three years, at three depths (30, 60 and 90 cm)

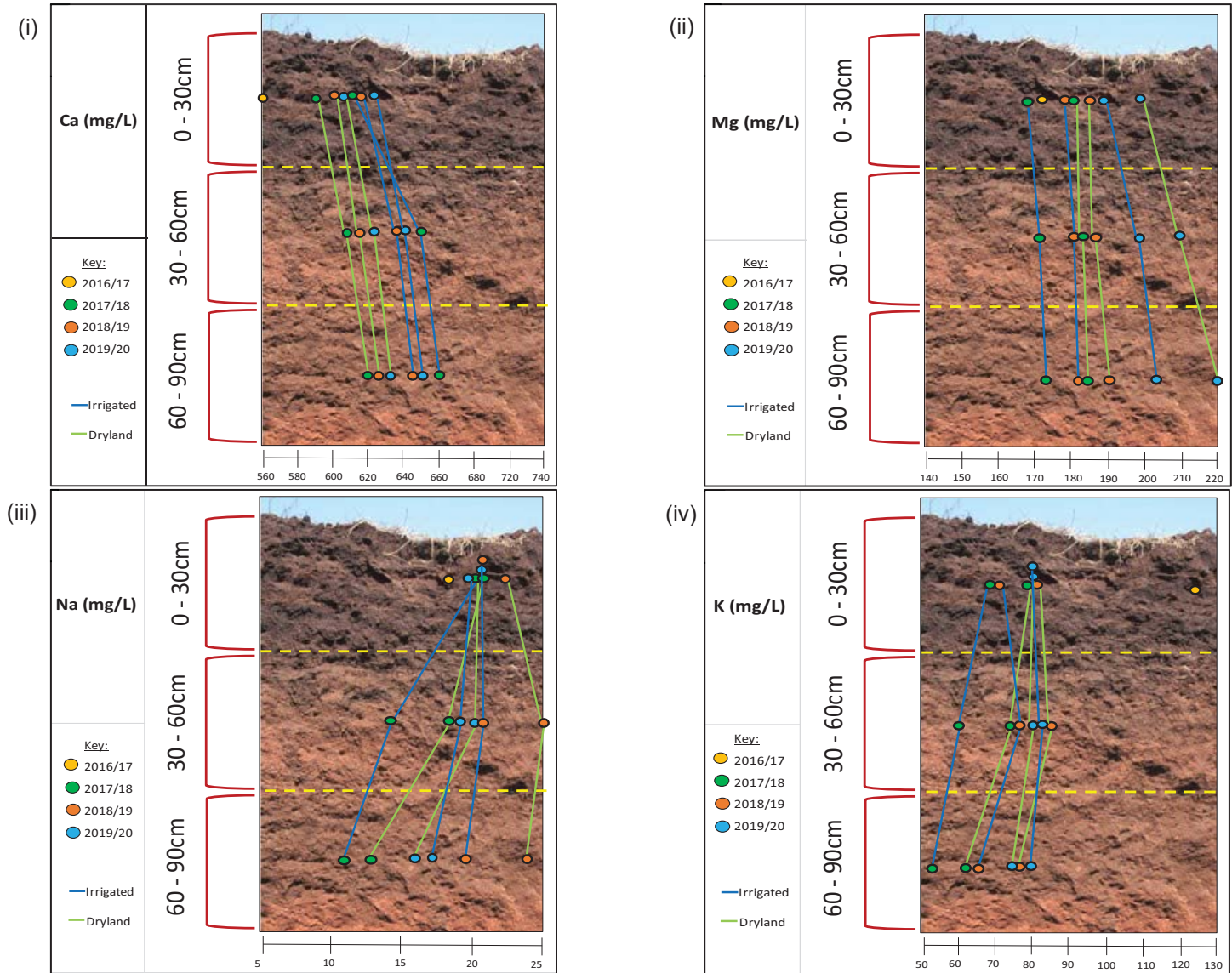


Figure 2.27: Soil profile at the Mafube unmined pivot indicating the change in Ca (i), Mg (ii), Na (iii) and K (iv) (mg/l), over an irrigation period of three years, at three depths (30, 60 and 90 cm).

Appendix A3 presents the full soil elemental analyses table, as well as interpolation maps, where the Kriging statistical analysis method was applied to show the likelihood that a certain concentration of a particular element in the soil would occur within the set boundary.

The pH of the poorly drained western side of the Mafube unmined field increased from 5.3 to 5.7. The pH of the well-drained eastern side of the field remained relatively constant over the three-year period, at 6.2. As expected, there has been a slight increase in salinity (Figure 2.25) after the commencement of irrigation with mine water. The EC in the 0 to 30 cm layer of the soil profile is mostly below the 170 mS m<sup>-1</sup> threshold for maize (Maas and Hoffman, 1977), and therefore no significant yield reduction due to salinity is expected at this stage. The reported EC (mS/m) of the dryland soils are elevated levels due to the increased waterlogging on the western side of the field. This same trend is observed with both potassium and sodium.

The water-soluble elements Ca, Mg and SO<sub>4</sub> increased in concentration with depth after irrigation commenced. The soil is sequestering a large fraction of the salts applied to it, and is thereby keeping these out of adjacent water sources. Although these increases can be attributed to mine water irrigation, the fertilizer regime added before each planting season, as well as crop nutrient uptake, should also be taken into account.

## 2.8 CONCLUSION

The increase in availability of water for irrigation is of benefit to both the mining and agricultural industries. Large areas of agricultural land are located near mines in South Africa, so there is a great opportunity for mine water-irrigated cropping to occur. Owing to the substantial treatment costs mines face, this alternative water utilisation option has a benefit of treatment cost savings, creating employment and empowering the local community through the production of mine water-irrigated crops.

This irrigation with mine-impacted water demonstration pivot at Mafube has shown, at least in the short term, to be a profitable use of the mine water for irrigation. This ongoing research demonstrates the sustainability of irrigating with mine water, and the opportunity presented by mine water irrigation practices.

Large amounts of salts can be immobilised in the soil profile when irrigating with gypsiferous water, as is evident in the following chapter. It is important to monitor salt levels in the irrigation environment and to stop or adaptively manage irrigation if any unacceptable impacts are encountered. One way to estimate the long-term viability is by using models to simulate long-term effects in yield and the irrigation's fitness for use (Chapter 3).

The food and forage safety of the irrigated crops should be assessed for identified constituents of concern to ensure that the thresholds are consistently met. If the food and forage thresholds are not met, a biofuel or fibre crop can be considered. The grain produced at the Mafube pivot is safe for human consumption, which makes grain production for human and animal consumption feasible.

The Mafube unmined pivot has demonstrated a cost-effective and productive utilisation of untreated, circum-neutral mine water. This is a valuable demonstration for prospective mine water irrigators and the regulators who will be approached to approve such projects. On a larger scale than this demonstration, such irrigation projects are expected to contribute to job creation in the area. The success of this project has clearly shown that productive mine water irrigation is possible, and with further long-term studies, stakeholders such as the Department of Human Settlements, Water and Sanitation, the Department of Agriculture, Land Reform and Rural Development, mines and farmers can more confidently enter into the utilisation of mine-impacted waters for irrigation.

## 2.9 REFERENCES

- ABIYE TA, MENGISTU H, MASINDI K and DEMLIE M (2015) Surface water and groundwater interaction in the upper Crocodile River basin, Johannesburg, South Africa: Environmental isotope approach. *South African Journal of Geology* **118 (2)** 109–118.
- AKCIL A and KOLDAS S (2006) Acid mine drainage (AMD): Causes, treatment and case studies. *Journal of Cleaner Production* **14** 1139–1145.
- AKWENSIOGE M, BOWERS T and MATOWANYIKA W (2019) *Monitoring of boreholes*. Mpumamanzi Group Report No. E64495, Anglo Coal, Middelburg, South Africa.
- ANNANDALE JG, JOVANOVIC NZ, PRETORIUS JJB, LORENTZ SA, RETHMAN NFG and TANNER PD (2001) Gypsiferous mine water use in irrigation on rehabilitated open-cast mine land: Crop production, soil water and salt balance. *Journal of Ecological Engineering* **17** 153–164.
- ANNANDALE JG, JOVANOVIC NZ, HODGSON FDI, USHER BH, AKEN ME, VAN DER WESTHUIZEN AM, BRISTOW KL and STEYN JM (2006) Prediction of the environmental impact and sustainability of large-scale irrigation with gypsiferous mine-water on groundwater resources. *Water SA* **32** 21–28.
- BUTLER M, MALINGA O and MABITSELA M (2018) *Tritium analysis on twenty-two (22) water samples*. Laboratory Report, iThemba Labs, Johannesburg, South Africa.
- BRINK A (1983) *Engineering geology of Southern Africa – the Karoo sequence, Vol. 3*. Building Publications, Pretoria, South Africa.
- CRAIG H (1961) Isotopic variations in meteoric waters. *Science* **133** 1702–1703.
- DU PLESSIS HM (1983) Using lime treated acid-mine water for irrigation. *Water Science and Technology* **151** 45–154.
- HE Q, BERG A, LI Y, VALLEJOS E and WU R (2010) Mapping genes for plant structure, development and evolution: Functional mapping meets ontology. *Trends in Genetics* **26 (1)** 39–46.
- JOHNSON DB and HALLBERG KB (2005) Acid mine drainage remediation options: A review. *Science of the Total Environment* **338** 3–14.
- JOVANOVIC NZ, BARNARD RO, RETHMAN NFG and ANNANDALE JG (1998). Crops can be irrigated with lime-treated acid mine drainage. *Water SA* **24** 113–122.
- LOUARN G, LECOEUR J and LEBON E (2008). A three-dimensional statistical reconstruction model of grapevine (*Vitis vinifera*) simulating canopy structure variability within and between cultivar/training system pairs. *Analytical Botany* **101 (8)** 1167–1184.
- MAAS EV and HOFFMAN GJ (1977) Crop salt tolerance – current assessment. *Journal of Irrigation and Drainage Division* **103** 115–134.
- MACKIE AL and WALSH ME (2015) Investigation into the use of cement kiln dust in high density sludge (HDS) treatment of acid mine water. *Water Research* **85** 443–450.
- MAHLANGU S, LORENTZ S, DIAMOND R and DIPPENAAR M (2020) Surface water-groundwater interaction using tritium and stable water isotopes: A case study of Middelburg, South Africa. *Journal of Africa Earth Sciences* **171** 1–14.
- PIONEER GROWTH STAGES OF CORN.  
[https://www.pioneer.com/CMRoot/pioneer/us/images/agronomy/field\\_facts/corn/staging-corn-growth-zoom.jpg](https://www.pioneer.com/CMRoot/pioneer/us/images/agronomy/field_facts/corn/staging-corn-growth-zoom.jpg).
- TANNER PD, ANNANDALE JG and RETHMAN NFG (1999) Converting problems into opportunities – the use of gypsiferous mine-water for crop irrigation. In: *Proceedings of the 22nd Conference Soil Science Society of South Africa*, Pretoria, South Africa, 160–162.
- UNKOVICH M, BALDOCK J and FORBES M (2010) Variability in harvest index of grain crops and potential significance for carbon accounting: Examples from Australian agriculture. In: *Advances in agronomy*, SPARKS DL. Elsevier, Oxford, UK, 173–219.

# CHAPTER 3: IRRIGATION WITH MINE-IMPACTED WATERS: CROP, SALT AND WATER BALANCE MODELLING

SN Heuer, JG Annandale, HM du Plessis, N Benadé and PD Tanner

## 3.1 INTRODUCTION

The SWB-Sci model (Benadé et al., 1995; Annandale et al., 1996; Annandale et al., 1999) that was developed over many years with funding from the WRC and the mine industry was used to predict gypsum precipitation in soil for several mine-affected waters under various cropping system and water management scenarios. The model gives an indication of the amount of water crops will require through irrigation, and the opportunity to sequester salt as gypsum in the profile, which will reduce salt loading to watercourses.

The South African Irrigation Water Quality Guidelines (DWAF, 1996) comprises one of the most widely used tools in water quality management. It aids in the determination of water quality requirements for irrigation water use, as well as quantitative fitness-for-use assessments. An important goal of these guidelines is to maintain the productivity of irrigated agricultural land and associated water resources. A revision of the guidelines was necessary to reflect the most appropriate and latest research and practices in this field. Recently, a computer program-based decision support system (Du Plessis et al., 2017) was developed to assess the fitness for use of bodies of water of different quality for irrigation. This DSS is referred to as the South African Water Quality Guidelines for Irrigation (SAWQI). It makes use of a simplified version of SWB to make predictions.

From regular sampling and monitoring, data is obtained that can be used to parameterise and validate the SWB model to ensure that simulations with mine water irrigation are reasonable. Accurate simulations will enable the potential effect of irrigation in the long term (more than 20 years), as well as the prediction of if and when gypsum will precipitate, and at what depth in the profile it will take place. Such simulations will give an indication of the sustainability of this practice.

## 3.2 SOIL-WATER BALANCE MODEL

The SWB model simulates crop growth and water and salt balances, using weather, water quality, and soil and management data to give a detailed description of the soil-plant-atmosphere continuum. The crop database includes several growth parameters that are crop specific, and values that are not given can be estimated.

### 3.2.1 Crop parameter determination

The SWB model uses transpiration (corrected for vapour pressure deficit) to calculate dry matter accumulation (Tanner & Sinclair, 1983). It also calculates radiation-limited growth (Monteith, 1977) and dry matter partitioning. The partitioning depends on crop phenology, which is calculated with thermal time (growing degree days) and is modified by water stress. Dry matter is partitioned to stems, roots, leaves and grain (Annandale, Benadé, Jovanovic, Steyn, & Du Sautoy, 1999). Crop parameters required in SWB are described in Table 3.1.

Table 3.1: Crop parameters required for SWB modelling

Crop parameter	Unit
Radiation extinction coefficient ( $K_c$ for solar radiation)	-
Dry matter to water ratio (DWR)	Pa
Radiation use efficiency ( $E_c$ )	kg MJ <sup>-1</sup>

Crop parameter	Unit
Base temperature	°C
Optimum light limiting temperature	°C
Cut-off temperature	°C
Emergence day degrees	d °C
Flowering day degrees	d °C
Maturity day degrees	d °C
Transition period day degrees	d °C
Leaf senescence day degrees	d °C
Maximum crop height ( $H_{max}$ )	m
Maximum root depth ( $RD_{max}$ )	m
Minimum leaf water potential	kPa
Specific leaf area (SLA)	m <sup>2</sup> kg <sup>-1</sup>
Leaf-stem partition ( $p$ )	m <sup>2</sup> kg <sup>-1</sup>
Root growth rate	m <sup>2</sup> kg <sup>-0.5</sup>
TDM at emergence	kg m <sup>-2</sup>
Maximum transpiration	mm d <sup>-1</sup>
Stem-grain translocation parameter	-
Canopy storage	mm
Root fraction	-
Stress index	-

### 3.2.2 Weather variables

Weather data is used in the SWB model as the driving variables for evaporation and crop growth. Soil-water balance requires solar radiation, wind speed, temperature and humidity. However, if only the minimum and maximum temperatures are known, SWB will mechanistically estimate missing data, although it is more accurate to have measured values. Penman-Monteith's reference crop evaporation ( $ET_o$ ) (Smith, Allen, & Pereira, 1996) is used to calculate daily evapotranspiration (Annandale et al., 1999). The variables required are listed in Table 3.2.

Table 3.2: Daily weather parameters required for SWB modelling

Weather variable	Unit
Minimum temperature	°C
Maximum temperature	°C
Minimum humidity	%
Maximum humidity	%
Average wind speed	m s <sup>-1</sup>
Average solar radiation	W m <sup>-2</sup>
Precipitation	mm

### 3.2.3 Soil parameters

Actual physical and chemical properties of the soil can be used as input in SWB, otherwise a default soil will be used. This data is used to calculate the soil-water movement and salt balance. By estimating radiation interception by the canopy from crop leaf area, potential evaporation and transpiration are

predicted. A root-density weighted-average soil water potential is estimated, which characterises the water supply capacity of the soil-root system.

This multi-layer soil component gives a realistic simulation of infiltration and water uptake processes, which uses a cascading soil-water balance, once runoff and crop interception have been accounted for (Annandale et al., 1999). Other than soil texture, other parameters and initial conditions required for the soil database are listed in Table 3.3. If initial soil chemical conditions are not specified, the model assumes no salts to start with in the profile.

Table 3.3: Soil parameters and initial conditions required for SWB modelling

Soil variable	Unit
Ca	mg kg <sup>-1</sup>
Mg	mg kg <sup>-1</sup>
K	mg kg <sup>-1</sup>
Na	mg kg <sup>-1</sup>
Cl	mg kg <sup>-1</sup>
SO <sub>4</sub>	mg kg <sup>-1</sup>
pH	-
Exchangeable Ca	mg kg <sup>-1</sup>
Exchangeable Mg	mg kg <sup>-1</sup>
Exchangeable K	mg kg <sup>-1</sup>
Exchangeable Na	mg kg <sup>-1</sup>
Gypsum	g m <sup>-2</sup>
Lime	g m <sup>-2</sup>
Texture	-
Silt content	%
Clay content	%
Field capacity (FC)	kPa or m m <sup>-1</sup> when estimated from texture
Permanent wilting point (PWP)	kPa or m m <sup>-1</sup> when estimated from texture
Root depth limit	m
Drain rate	mm d <sup>-1</sup>

### 3.3 MODELLING MINE WATER IRRIGATION AND CROP GROWTH

The objective of this study was to collect field data to determine crop-specific parameters, which can be used to calibrate and validate the SWB model for this specific scenario (mine water irrigation of maize with circum-neutral water in Mpumalanga). The calibrated model can then be used to simulate potential yields, as well as the salt balance of the soil profile over time (gypsum precipitation, soluble salt storage or leaching). The experimental setup and field measurement methods are described in Chapter 2. Data from the 2017/18 season (maize) was used to parameterise the SWB model.

#### 3.3.1 Crop parameters

Crop parameters like transition period day degrees (d °C), day degrees for leaf senescence (d °C), maximum root depth (m), canopy storage (mm), stem-to-grain translocation, minimum leaf water potential (kPa), leaf-to-stem portioning parameter (m<sup>2</sup> kg<sup>-1</sup>), TDM at emergence (kg m<sup>-2</sup>), root fraction, root growth rate and stress index for maize were obtained from the SWB database (Annandale et al., 1999). Base temperature (°C), optimum light limiting temperature (°C) and cut-off temperature (°C) were acquired from Du Toit et al. (1999). Emergence day degrees (d °C), flowering day degrees (d °C), day

degrees to maturity ( $d\ ^\circ C$ ), extinction coefficient, specific leaf area ( $m^2\ kg^{-1}$ ), dry matter water ratio (Pa) and radiation use efficiency ( $kg\ MJ^{-1}$ ) were calculated based on measurements and observations made in the field. All values used as input can be seen in Table 3.4.

Thermal time is used to simulate crop development (Annandale et al., 1999). Growing degree days (GDD) are calculated at a daily time step after the crop is planted ( $GDD_i$ ), and accumulated to predict development (Monteith, 1977). Accumulated GDD since planting is compared to observed crop phenological stages in the field to determine GDD to emergence, flowering and maturity.

$$GDD = GDD + GDD_i \quad (3.1)$$

$$GDD_i = T_{ave} - T_b \quad (3.2)$$

Where  $GDD_i$  is the daily increment of growing degree days,  $T_{ave}$  is the average daily temperature ( $^\circ C$ ), and  $T_b$  is a crop-specific ( $10\ ^\circ C$  for maize) base temperature ( $^\circ C$ ). Specific leaf area (in  $m^2\ kg^{-1}$ ) is calculated by dividing the LAI (in  $m^2\ m^{-2}$ ) by total leaf dry matter (LDM) (in  $kg\ m^{-2}$ ) as stated by Jovanovic, Annandale, and Mhlauli (1999).

$$SLA = \frac{LAI}{LDM} \quad (3.3)$$

The canopy extinction coefficient for solar radiation ( $K_s$ ) (Monteith, 1977) is needed to partition energy to evaporation and transpiration, as well as dry matter production, and is converted from the canopy extinction coefficient for PAR ( $K_{PAR}$ ), which is calculated using the measured fractional interception of PAR ( $FI_{PAR}$ ) and measured LAI (Campbell & Van Evert, 1994).

$$FI_{PAR} = 1 - e^{-K_{PAR} \times LAI} \quad (3.4)$$

$$K_s = K_{bd} \sqrt{a_s} \quad (3.5)$$

$$K_{bd} = \frac{K_{PAR}}{\sqrt{a_p}} \quad (3.6)$$

$$a_s = \sqrt{a_p \times a_n} \quad (3.7)$$

Where  $K_{bd}$  is the canopy radiation extinction coefficient for “black” leaves with diffuse radiation,  $a_s$  is leaf absorptivity of solar radiation,  $a_p$  is leaf absorptivity of PAR and  $a_n$  is leaf absorptivity of near-infrared radiation. The value of  $a_p$  is assumed to be 0.8 and  $a_n$  is assumed to be 0.2 (Goudriaan, 1977).

Radiation use efficiency ( $E_c$ ) (in  $kg\ MJ^{-1}$ ) is used to calculate dry matter production under conditions where radiation limits growth (Monteith, 1977).

$$DM = E_c \times FI_s \times RS \quad (3.8)$$

Where DM ( $kg\ m^{-2}$ ) is dry matter production,  $FI_s$  is fractional interception of solar radiation and RS ( $W\ m^{-2}$ ) is solar radiation. Radiation use efficiency can also be estimated using the slope of the graph when plotting cumulative dry matter and cumulative  $FI_s \times RS$  (Figure 3.1).

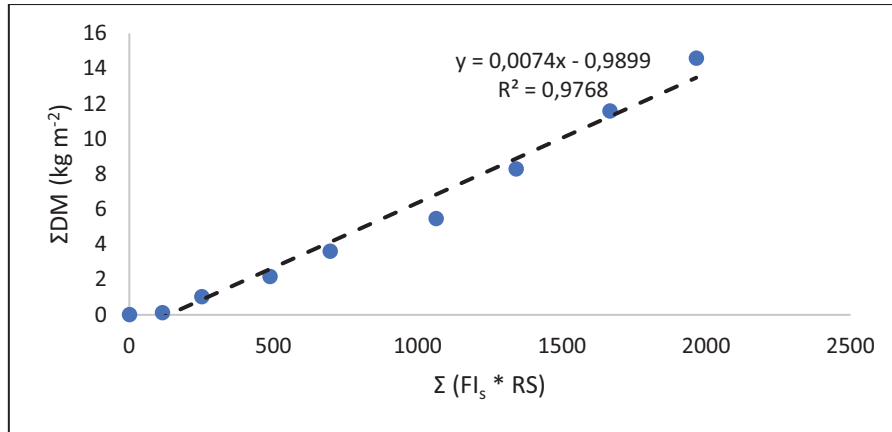


Figure 3.1: Radiation use efficiency as the slope of the relation between cumulative dry matter production and cumulative interception of solar radiation

Seasonal crop evapotranspiration (ET) (in mm or kg m<sup>-2</sup>) (Jovanovic et al., 1999) is used along with seasonal average vapour pressure deficit (VPD) (in Pa) (Jovanovic et al., 1999) to estimate the DWR (in Pa) (Tanner & Sinclair, 1983).

$$ET = P + I - R - D - \Delta Q \quad (3.9)$$

$$VPD = \frac{(e_{sT_{max}} + e_{sT_{min}})}{2} - e_a \quad (3.10)$$

$$e_s = 0.611 \exp \left[ \frac{17.27 T}{(T+273.3)} \right] \quad (3.11)$$

$$e_a = \frac{[e_{sT_{max}} \times \frac{RH_{max}}{100} + e_{sT_{min}} \times \frac{RH_{min}}{100}]}{2} \quad (3.12)$$

$$DWR = \frac{DM \times VPD}{ET} \quad (3.13)$$

Where P is precipitation, I is irrigation, R is runoff, D is drainage and  $\Delta Q$  is the change in soil water storage, all in mm (Jovanovic et al., 1999). The  $e_s$  is saturated vapour pressure (Pa) at maximum ( $T_{max}$ ) and minimum ( $T_{min}$ ) air temperatures ( $^{\circ}C$ ) (Tetens, 1930, as cited by Jovanovic et al. (1999)) and  $e_a$  is the actual vapour pressure (Pa) as a function of relative minimum ( $RH_{min}$ ) and maximum ( $RH_{max}$ ) humidity (Bosen, 1958, as cited by Jovanovic et al. (1999)). DM (kg m<sup>-2</sup>) is dry matter as measured at harvest.

Table 3.4: Crop input parameters used for simulations

Crop parameter	Value
Radiation extinction coefficient for solar radiation*	0.487
DWR (Pa)*	6.0
Radiation use efficiency (kg MJ <sup>-1</sup> )*	0.007
Base temperature ( $^{\circ}C$ )**	10
Optimum temperature under light limiting conditions ( $^{\circ}C$ )**	25
Cut-off temperature ( $^{\circ}C$ )**	30
Emergence day degrees (d $^{\circ}C$ )*	60
Flowering day degrees (d $^{\circ}C$ )*	730
Maturity day degrees (d $^{\circ}C$ )*	1,600
Transition period day degrees (d $^{\circ}C$ )***	10
Leaf senescence day degrees (d $^{\circ}C$ )***	950
Maximum crop height (m)*	3.2
Maximum root depth (m)***	1.5
Stem-grain translocation***	0.05

Canopy storage (mm) <sup>***</sup>	1
Minimum leaf water potential (kPa) <sup>***</sup>	-2,000
Maximum transpiration (mm day <sup>-1</sup> ) <sup>***</sup>	9
Specific leaf area (m <sup>2</sup> kg <sup>-1</sup> ) <sup>*</sup>	12
Leaf-stem partition (m <sup>2</sup> kg <sup>-1</sup> ) <sup>***</sup>	0.8
TDM at emergence (kg m <sup>-2</sup> ) <sup>***</sup>	0.0019
Root fraction <sup>***</sup>	0.01
Root growth rate (m <sup>2</sup> kg <sup>-0.5</sup> ) <sup>***</sup>	8
Stress index <sup>***</sup>	0.95

**Note:** \* Calculated from field measurements

\*\* Obtained from Du Toit et al. (1999)

\*\*\* Obtained from the SWB database (Annandale et al., 1999)

### 3.3.2 Soil parameters

Soil chemical and physical properties were determined by analysing soil samples taken before planting. The soil parameters used as input to SWB can be seen in Table 3.5.

Table 3.5: Soil chemical initial conditions and hydraulic parameters used for simulations

Soil variable	Value
Ca (ppm)	519
Mg (ppm)	111
K (ppm)	126
Na (ppm)	8
pH	5.75
Field capacity (m m <sup>-1</sup> )	0.269
Bulk density (g cm <sup>-3</sup> )	1.6
Permanent wilting point (m m <sup>-1</sup> )	0.148
Clay percentage	25
Silt percentage	10
Texture	Sandy loam

### 3.3.3 Weather variables

Weather variables were obtained by using a combination of two automatic weather stations (Table 3.6): one at Mafube Colliery and an on-site station at the University of Pretoria (UP). Long-term weather data used for scenario simulations and long-term modelling was provided by the Agricultural Research Council (ARC) using the Middelburg Eden Farms (Middelburg, Mpumalanga) station.

Table 3.6: Weather station locations and data provided

	Mafube Colliery	UP fixed station
Location	25°47'36.00" S 29°44'15.00" E Altitude: 1,663 m	25°48'22.38" S 29°45'59.58" E Altitude: 1,674 m
Minimum temperature (°C)	Yes	Yes
Maximum temperature (°C)	Yes	Yes
Minimum humidity (%)	Yes	Yes

Maximum humidity (%)	Yes	Yes
Average wind speed (m s <sup>-1</sup> )	Yes	Yes
Average solar radiation (W m <sup>-2</sup> )	No	Yes
Precipitation (mm)	Yes	-

### 3.3.4 Results

The parameterisation of top (TDM) and harvestable dry matter (HDM) with salts simulation is deemed acceptable if  $r^2$  and  $D > 0.8$  and  $MAE < 20\%$  (as recommended by De Jager (1994)). This can be seen in Figure 3.2. Measured LAI might be somewhat underestimated due to the time delay between harvest in the field and measurement in the laboratory, which could cause leaves to wilt, break or go missing. The 2016/17 dryland season data was used to double check the parameterisation, and the result presented in Figure 3.2 can be described as a relatively good fit, as all the statistical metrics meet or come close to the requirements set by De Jager (1994). Other simulations with determined crop parameters can be seen in Appendix A4.

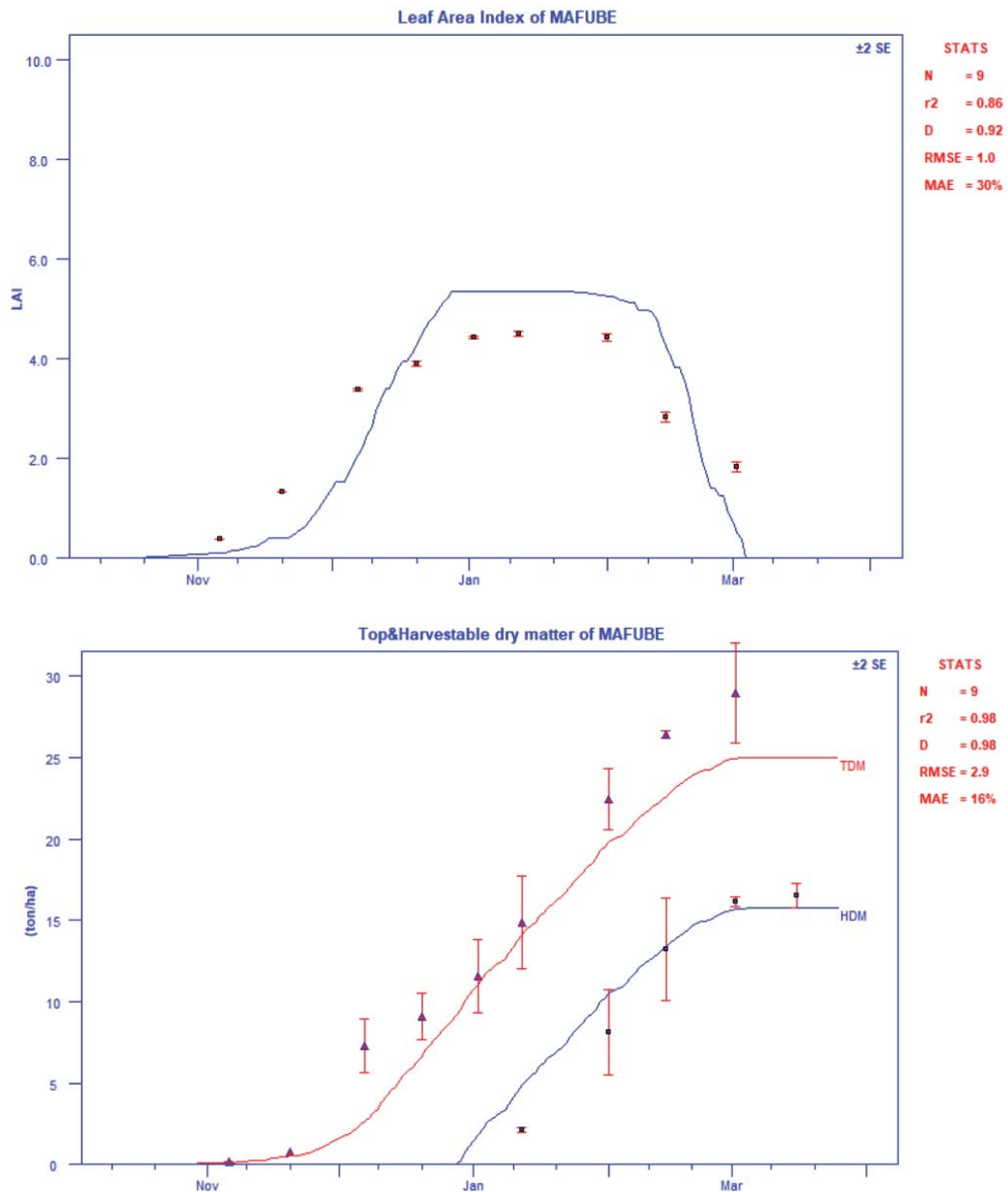


Figure 3.2: Measured (symbols) and simulated (lines) LAI (top), and top and harvestable dry matter (bottom) simulating the effect of saline water irrigation.

**Note:** N = Number of observations;  $r^2$  = Coefficient of determination; D = Willmott's (1982) Index of Agreement; RMSE = Root mean square error; MAE = Mean absolute error

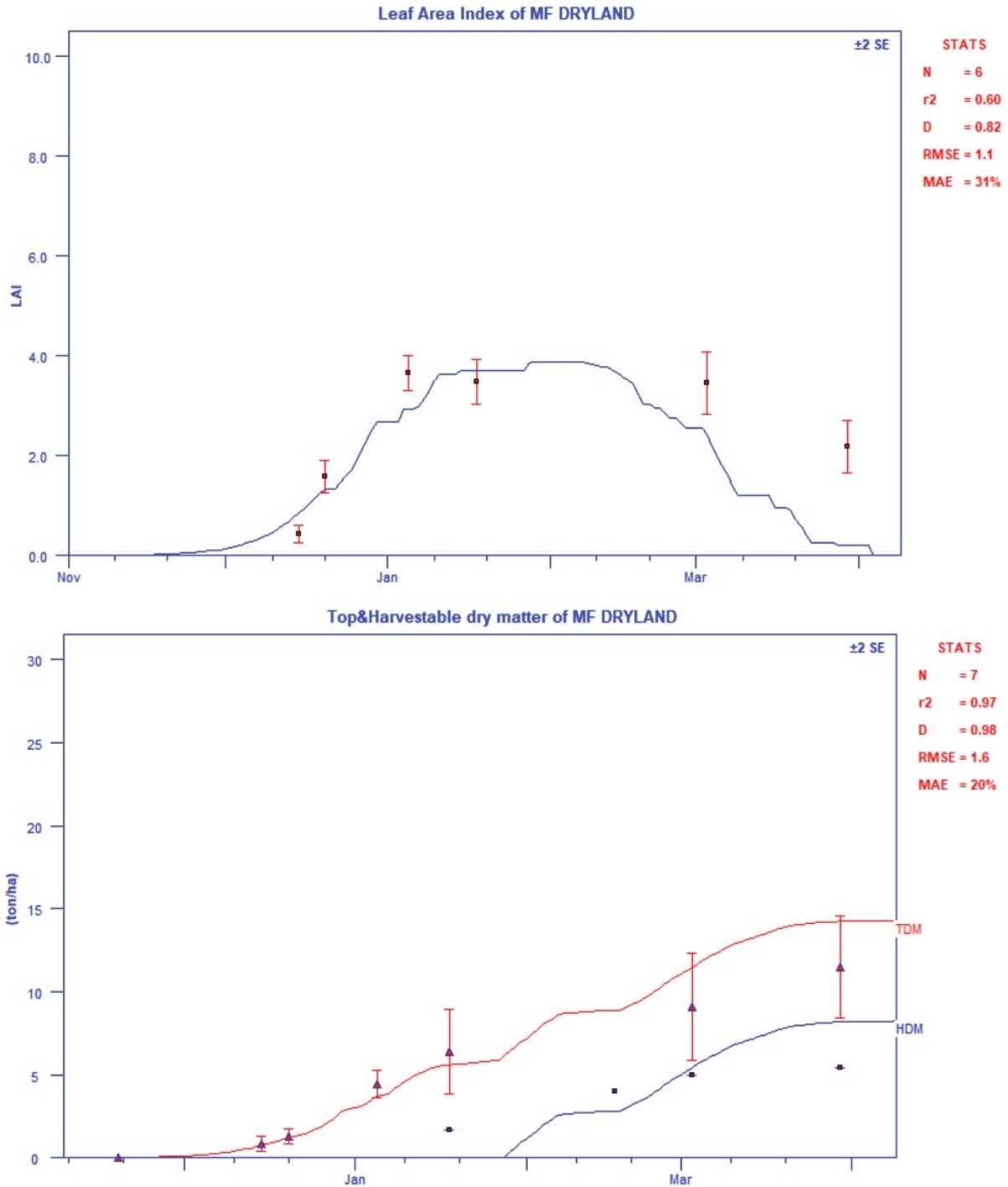


Figure 3.3: Measured (symbols) and simulated (lines) LAI (top), and top and harvestable dry matter (bottom) simulating a dryland season.

**Note:** N = Number of observations;  $r^2$  = Coefficient of determination; D = Willmott's (1982) Index of Agreement; RMSE = Root mean square error; MAE = Mean absolute error

### Scenario simulations

Long-term simulations of about 50 years show that the yields of both maize and wheat remain fairly stable (no consistent increase or decrease is apparent) throughout 50 years of irrigation (Figure 3.4). Maize yield averages around 20 t ha<sup>-1</sup>, with a minimum of 15 and a maximum of 24 t ha<sup>-1</sup>. Wheat yield averages around 10 t ha<sup>-1</sup>, with a minimum of 8 and a maximum of 13 t ha<sup>-1</sup>. Predicted yield fluctuations can be attributed to seasonal variation, with leaching fractions higher in wetter seasons, and with more saline irrigation being applied in drier seasons. Although these yields are likely somewhat overestimated, the important point this simulation brings across is that irrigating with this specific saline mine water is not predicted to cause a decrease in yield over the long term.

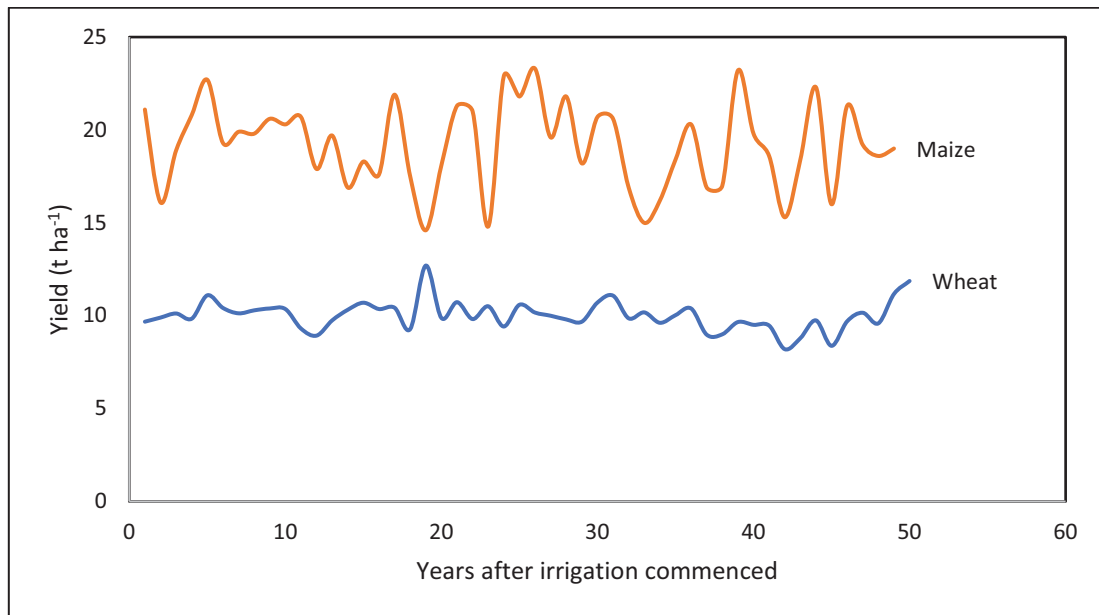


Figure 3.4: Soil-water balance simulation of yields (t ha<sup>-1</sup>) for a maize/wheat rotation over a 50-year period

When using different water qualities (Table 3.7), the salt balance and expected yields change. For example, simulating wheat yield over 50 years (Figure 3.5) with a fairly good-quality water (Mafube void water) and a poorer-quality water (Arnot), it is clear that poorer-quality water is predicted to reduce yield compared to the good-quality water. The simulations with poor-quality water also show significant decreases in yield at about 20-year intervals, coinciding with very dry seasons. In Figure 3.6, the EC<sub>e</sub> (soil profile salinity) is depicted for each of the water qualities in Figure 3.7, along with the published salinity thresholds for maize, soybean and wheat. This simulation shows that only fresh water and water from the raw water dam may be suitable for the irrigation of maize, whereas all four water qualities may be suitable for irrigation of soybean and wheat. Figure 3.7 shows gypsum precipitation and percentage salts removed from water resources for each water quality. Although water from Arnot exhibits the most gypsum precipitation over a 50-year period, it shows that a lower percentage of salts is removed, indicating a lower efficiency in salt removal through gypsum precipitation.

Table 3.7: Different water qualities in the vicinity of Mafube Colliery

	Good quality fresh water	Mafube voids	Raw water dam	Arnot
pH	7.5	7.7	7.8	7.7
EC (mS m <sup>-1</sup> )	60	208	229	558
Ca (mg l <sup>-1</sup> )	50	241	268	526
Mg (mg l <sup>-1</sup> )	29	151	176	585

	Good quality fresh water	Mafube voids	Raw water dam	Arnot
Na (mg l <sup>-1</sup> )	30	103	56	108
K (mg l <sup>-1</sup> )	0.2	35	30	72
Cl (mg l <sup>-1</sup> )	85	28	23	21
SO <sub>4</sub> (mg l <sup>-1</sup> )	120	1065	1414	3580

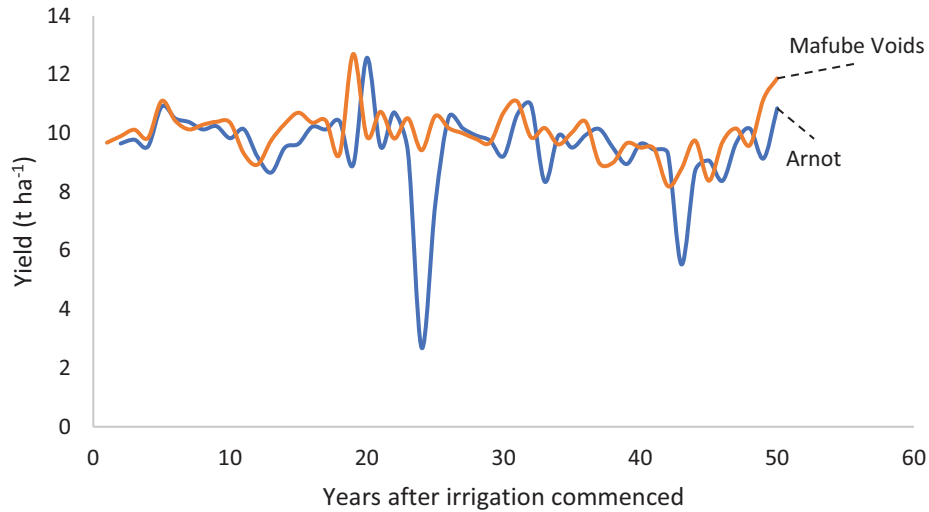


Figure 3.5: Simulated wheat yield (t ha<sup>-1</sup>) over a 50-year period for two different water qualities using soil-water balance

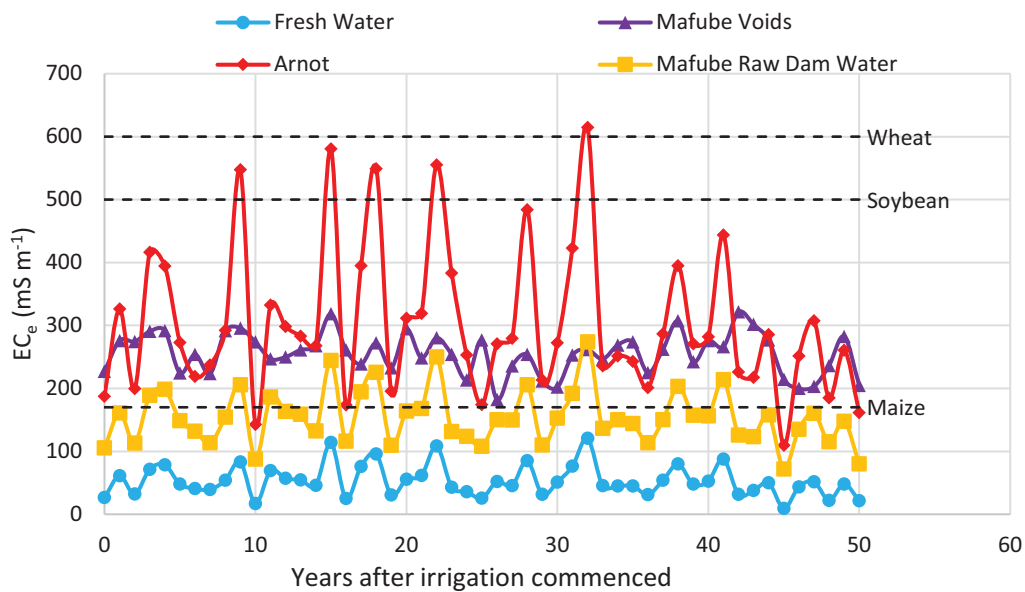


Figure 3.6: Soil profile salinity (EC<sub>e</sub> in mS m<sup>-1</sup>) predicted for 50 years of irrigation with four different water qualities using soil-water balance. Salinity thresholds (Maas and Hoffman, 1977) for maize, wheat and soybean are also indicated.

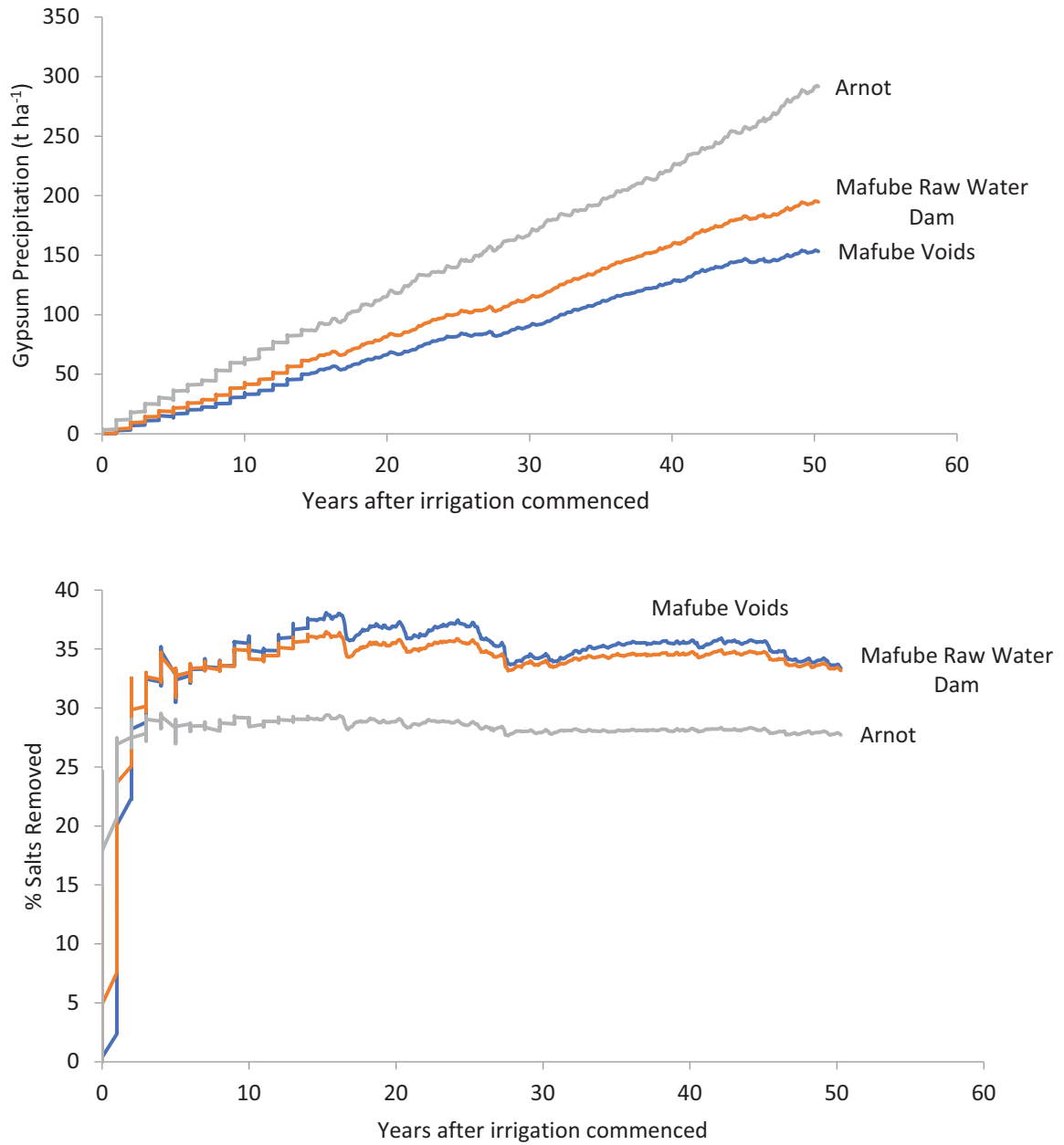


Figure 3.7: Gypsum precipitation (t ha<sup>-1</sup>) and percentage salt removed as predicted by soil-water balance over a 50-year period for three different water qualities

### 3.4 IRRIGATION WATER FITNESS-FOR-USE ASSESSMENT – DECISION SUPPORT SYSTEM

A fitness-for-use assessment of a given water composition can be obtained by running a 45-year simulation with the SAWQI model, which uses a simplified version of SWB to make its predictions. A conservative Tier 1 simulation is usually run first, which considers a generic salt-sensitive crop, receiving 1,000 mm irrigation per annum with no rainfall to dilute salinity. These very conservative assumptions will highlight potential problems, but will likely be too stringent for any mine-impacted waters. Waters shown to be ideal at Tier 1 can be used successfully for irrigation under practically all conditions. Tier 2 simulations are more site specific (soil, weather, crop, irrigation system and management are specified), and more appropriate for mine water irrigation assessments. Here the DSS is used to determine if there are circumstances under which the water will be rendered usable for irrigation.

The mine water used for irrigation at Mafube is untreated and pumped from one of the open-cast voids (Void 3). It is mostly near neutral to slightly alkaline (pH 7.1), with a relatively low EC of around 200 to 300 mS m<sup>-1</sup>. This range is acceptable according to the SAWQI (Du Plessis et al., 2017). The major cations include Ca at 235 mg/l, Mg at 160 mg/l and Na at 70 mg/l. Major anions include HCO<sub>3</sub> at 335 mg/l, Cl at 10 mg/l, and SO<sub>4</sub> at 1,130 mg/l. The water also contains 3.5 mg/l N and 35 mg/l K. The trace elements that could be measured included Al at 510 ug/l, Mn at 390 ug/l, Fe at 110 ug/l, Zn at 40 ug/l, B at 225 ug/l, Co at 3.2 ug/l, V at 7.5 ug/l and F at 0.7 ug/l. As these waters contain high concentrations of Ca and SO<sub>4</sub><sup>2-</sup>, precipitation of gypsum (CaSO<sub>4</sub>) in the soil profile is highly likely. When gypsum precipitates and is retained in soil, these salts are kept out of solution, thereby reducing the salt load to surrounding water bodies.

A Tier 1 fitness-for-use assessment of this water quality highlighted that potential problems with a reduction in yield due to salinity may be expected. It also shows that sodium might cause a negligible to slight scorching of leaves. The irrigation water is not corrosive, but rather slightly scaling, but to an *acceptable* degree. There is also a possibility of the clogging of drippers due to pH. However, this would not present a problem under centre pivot irrigation. The contribution of NPK to the crop is deemed *unacceptable* for both phosphorus and potassium, and *tolerable* for nitrogen. This means that it will be important for the irrigator to take into account what nutrient levels are applied to the crop through irrigation, as this can potentially save on fertilization costs and reduce the likelihood of nutrient imbalances.

A Tier 1 fitness-for-use assessment of this water quality highlighted potential problems with manganese accumulation. It shows that manganese (18 years) has the potential to accumulate to its threshold value in the topsoil in less than 100 years with 1,000 mm irrigation applied per year. It is likely that the current guidelines for manganese, iron and aluminium are too stringent, considering that these elements are abundant in natural soils. It is also noted that the guidelines do not take into account the bioavailable amount of the elements, but rather the total amount.

The quality of the irrigation water used at Mafube during this project has deteriorated over time due to the introduction of water from Arnot Colliery. However, the circum-neutral Void 3 water with a relatively low EC of around 200 mS/m that this project started with is seen as *tolerable* at the conservative Tier 1 level of the DSS. High concentrations of calcium (ranges between 200 and 250 ppm) and SO<sub>4</sub><sup>2-</sup> can lead to gypsum precipitation in soils, which is seen as favourable, as these salts are then retained in the soil and kept out of solution, thereby reducing the salt load to water bodies.

When using this initial water quality, but running the more site-specific Tier 2 simulation with maize, the accumulation of manganese is highlighted once again, showing that it is now estimated to take 40 years to accumulate to the threshold value, which is a slight improvement on Tier 1.

Table 3.8: Tier 1 results of irrigating with Void 3 irrigation water quality

Tier 1 suitability indicators					Irrigation water quality Void 3		
Cation balance error (percentage)					0.1		
Soil quality							
Root zone salinity					Tolerable (400–800 mS/m)		
Soil permeability	Surface infiltration				Slight		
	Soil hydraulic conductivity				None		
Trace elements raised as reaching soil accumulation threshold (in years)		Manganese (Mn)			18		
Trace element accumulation							
Number of years to reach soil accumulation threshold		Trace element			Fitness-for-use		
18		Manganese			Unacceptable		
Yield and quality of crop with 1,000 mm of irrigation/annum							
Relative crop yield (percentage) as affected by:		Salinity (EC)			Unacceptable		
Leaf scorching when wetted		Sodium (Na)			Slight		
Estimated NPK removal at harvest and amount that is applied through irrigation		Nitrogen (N)		Phosphorus (P)		Potassium (K)	
		Removal (%)	Applied (kg/ha)	Removal (%)	Applied (kg/ha)	Removal (%)	Applied (kg/ha)
		Tolerable		Unacceptable		Unacceptable	
		44	22	120	12	2,800	280
Irrigation equipment							
Scaling (Langelier Index)					Acceptable		
Clogging of drippers		Suspended solids			Unacceptable		
		pH			Tolerable		
		Mn			Tolerable		

Table 3.9: Tier 2 results of irrigating only white maize with Void 3 irrigation water quality

Tier 2 suitability indicators						Irrigation water quality Void 3	
Cation balance error (percentage)						0.1	
Soil quality							
Root zone salinity			Percentage of time soil permeability is predicted to fall within a particular Fitness-for-use category			Ideal: 0–200 mS/m (100%)	
Soil permeability		Surface infiltration				Ideal (80%) Acceptable (20%)	
		Soil hydraulic conductivity				Ideal (95%) Acceptable (3%) Tolerable (2%) Unacceptable (1%)	
Trace element accumulation							
Trace element		Number of years to reach soil accumulation threshold				Fitness-for-use	
Manganese		40				Unacceptable	
Yield and quality of crop with 1,000 mm of irrigation/annum							
Relative crop yield (percentage) as affected by:		Salinity (EC)		Percentage of time yield is within relative crop yield category, as affected by:		Ideal (100%)	
Leaf scorching when wetted		Sodium (Na)				Ideal (100%)	
Estimated NPK removal at harvest and amount that is applied through irrigation		Nitrogen (N)		Phosphorus (P)		Potassium (K)	
		Time (%)	Applied (kg/ha)	Time (%)	Applied (kg/ha)	Time (%)	Applied (kg/ha)
		Tolerable				Unacceptable	
		100	10	Ideal (78) Acceptable (22)	Ideal (5) Acceptable (6)	100	125
Irrigation equipment							
Scaling (Langelier Index)						Acceptable	
Clogging of drippers			Suspended solids			Unacceptable	
			pH			Tolerable	
						Tolerable	

When using the initial Void 3 water quality, for the more site-specific Tier 2 simulation with maize, the accumulation of manganese, the presence of suspended solids and high levels of potassium are still seen as problematic. Preliminary studies done by the research team in 2019 indicated that irrigated soils used at the pivot have great potential to oxidise the added  $Mn^{2+}$  ions. These results show that true available soil accumulation may not be of such concern as currently indicated by the SAWQI. The potassium supply can easily be managed by the farmer to his benefit, and with pivot irrigation of maize, suspended solids are likely inconsequential. Long-term simulations with the DSS over 45 years provide indications of annual and seasonal variations in yield and salt balances. Different water, weather and soil qualities will have an effect on the outcome of these simulations and the predictions made.

When looking at crop selection for irrigating with poor-quality waters, it is important to know the crop's salt tolerance. According to Maas and Hoffman (1977), the salinity thresholds for maize, wheat and soybean are 180, 500 and 600 mS/m, respectively. When estimating the soil saturated paste electrical conductivity (ECe), the DSS predicts that there will be an increase in salinity upon irrigation, followed by a stabilisation of the ECe value at around 200 mS/m, which can be a sign of gypsum precipitating with excess soluble salts in the profile being leached. It is clear that maize may not be the best crop choice for summer production, especially if water quality deteriorates, but soybean should do better in summer, and a cool season cereal crop like wheat should show no yield decrease due to salinity.

The ECe measurements were determined to be 35 mS/m after the 2018 irrigated season. In 2019, it reached 60 mS/m, and in 2020 the level was 67 mS/m. These are well below the predicted ECe values produced by the DSS's 45-year simulation (Figure 3.8). This indicates that there is enough gypsum precipitation and leaching of excess salts to prevent the soil profile from becoming too saline, at least in the short term. If the water quality deteriorates, maize may not be the best choice for summer production and may need to be replaced by a more salt-tolerant crop like soybean.

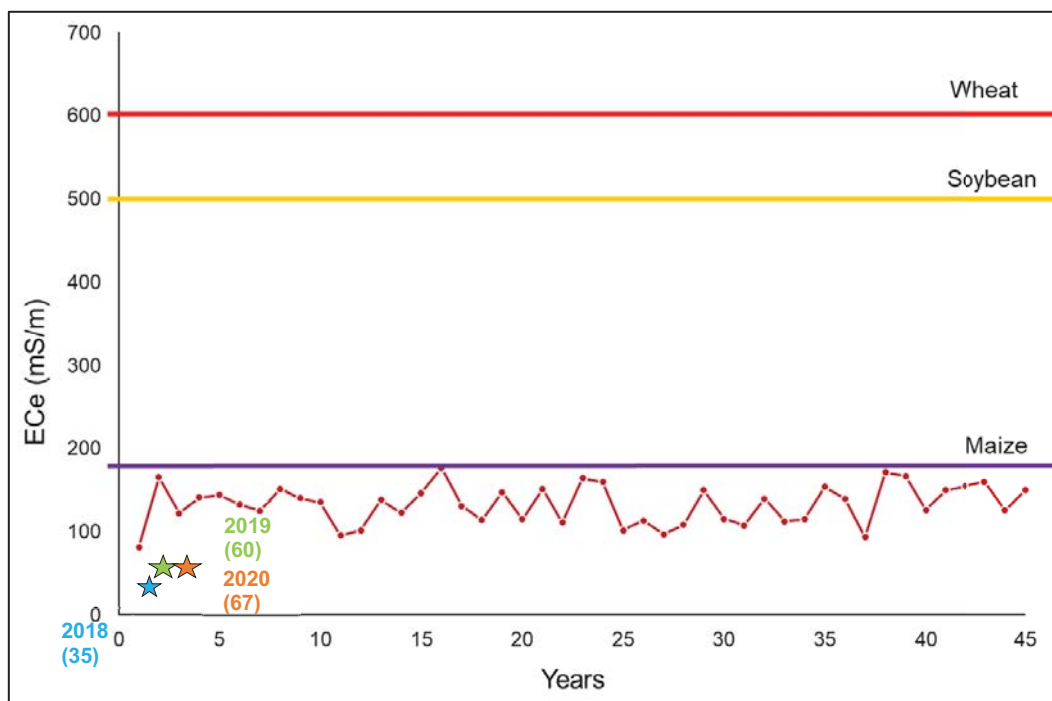


Figure 3.8: The decision support system's 45-year simulation for the soil saturated paste electrical conductivity (ECe) for a single maize crop using Void 3 water. The 2018, 2019 and 2020 ECe soil measurements and the salinity thresholds for maize, wheat and soybean are included.

Long-term (45 years), Tier 2 site-specific DSS simulations were performed using Mafube's Void 3 as the source of irrigation water. An overhead irrigation system was selected to evaluate the potential for scorching, and the sandy loam soil profile was refilled to field capacity after 10 mm depletion. The Gemsbokfontein weather station was selected as it is in close proximity to the colliery, and two cropping systems were compared. These were a rotational cropping system of soybean and wheat, and a maize monocrop.

With a maize-only crop, an average of 1,000 mm of irrigation will be applied per year. Over a 50-year period, this would add 1,037 t ha<sup>-1</sup> salt, of which 620 t ha<sup>-1</sup> is leached, and 357 t ha<sup>-1</sup> is predicted to precipitate as gypsum, with about 35% of the salt added. It would appear that calcium limits gypsum precipitation, as there is twice the amount of SO<sub>4</sub> than that required for precipitation with calcium. However, with an adjusted fertilization programme, precipitation can be increased and, in turn, the salt load to water bodies is reduced. The modelled cumulative salt balance and gypsum precipitation in the soil profile is presented in Table 3.10.

Table 3.10: Cumulative salt balance and gypsum retained in the soil profile after a 45-year simulation of irrigation with Void 3 water

Cropping system	Total salts added	Sum of salt leached	Profile gypsum	Percentage gypsum retained in profile	Soluble salts stored in profile
	(tons/ha)				
Maize only	1,037	620	357	34.4	20

As stated in Chapter 2, the irrigation water qualities were plotted on Piper diagrams and are seen as calcium sulphate hydrofacies. High concentrations of calcium and  $\text{SO}_4^{2-}$  can lead to gypsum precipitation in soils, which is seen as favourable, as these salts are then retained in the soil and kept out of solution, thereby reducing the salt load to water bodies. Running a 45-year simulation, the gypsum precipitation in the soil is predicted using the average irrigation water quality. The 2018, 2019 and 2020 soil gypsum precipitate analyses were all below the 45-year simulated gypsum precipitate values (Figure 3.9).

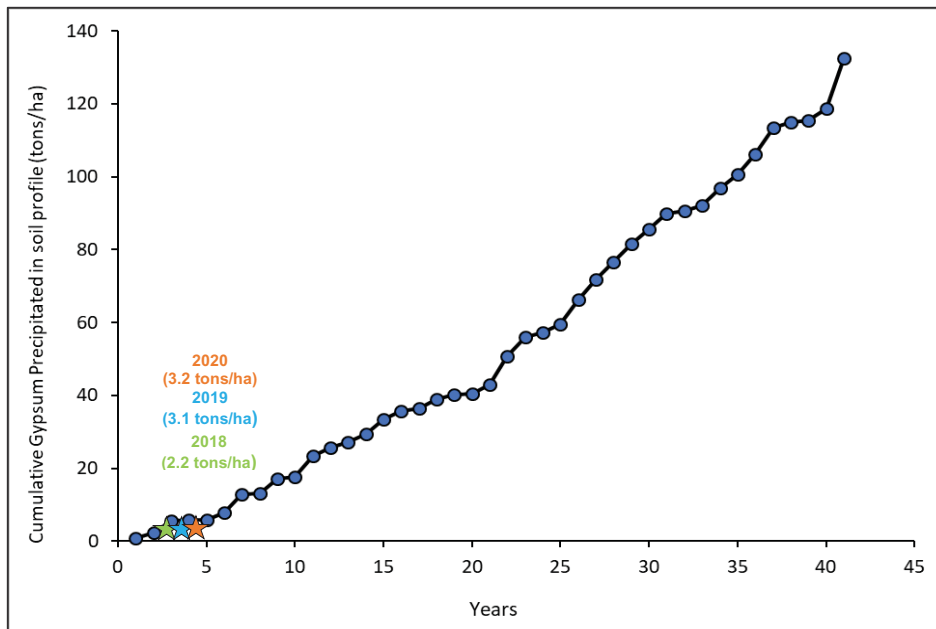


Figure 3.9: The decision support system's 45-year simulation for the soil gypsum precipitation (tons/ha) for a single maize crop using Void 3's average water quality.

### 3.5 CONCLUSIONS

Using models such as SAWQI-DSS, one can assess site-specific factors that influence the suitability of mine waters for irrigation. The careful monitoring of water quality, soil nutrient levels, and food and forage safety is necessary to ensure the feasibility of a mine water irrigation project. Irrigation with mine water over the long term can be viable, sustainable and feasible if the appropriate management practices are in place. The results from this study show that irrigation with Mafube's Void 3 water is a feasible and sustainable alternative mine water utilisation option, as supported by the results in Chapter 2. The circum-neutral waters at Void 3 are ideal for irrigation, and from the simulations run, there are indications of minimal environmental impact on ground and surface waters. The soil environment is slowly starting to precipitate gypsum, thereby sequestering a sizable fraction of the salts applied to it, thereby keeping these out of adjacent water sources.

### 3.6 REFERENCES

- ANNANDALE JG, BENADÉ N, JOVANOVIĆ NZ, STEYN JM and DU SAUTOY N (1999) *Facilitating irrigation scheduling by means of the soil-water balance model*. WRC Report No. 753/1/99. Water Research Commission, Pretoria, South Africa.
- ANNANDALE JG, BENADÉ N, VAN DER WESTHUIZEN AJ and CAMPBELL GS (1996) The SWB (soil water balance) irrigation scheduling model. In: *Proceedings of the International Conference on Evapotranspiration and Irrigation Scheduling*, San Antonio, Texas, USA, 3–6 November 1996, 944–949.
- BENADÉ N, ANNANDALE JG and VAN ZIJL H (1995) *The development of a computerized management system for irrigation schemes*. WRC Report No. 513/1/95. Water Research Commission, Pretoria, South Africa.
- CAMPBELL GS and VAN EVERT FK (1994) Light interception by plant canopies: Efficiency and architecture. In: *Resource capture by crops*, MONTEITH JL, SCOTT RK and UNSWORTH MH, Nottingham University Press, Nottingham, UK, 35–52.
- DE JAGER JM (1994) Accuracy of vegetation evaporation ratio formulae for estimating final wheat yield. *Water SA* **20** 307–315.
- DEPARTMENT OF WATER AFFAIRS AND FORESTRY (DWAf) (1996) *South African irrigation water quality guidelines, Vol. 4: Agricultural use: Irrigation*, 2<sup>nd</sup> ed., DWAf, Pretoria, South Africa.
- DU PLESSIS HM, ANNANDALE JG, BENADÉ N, VAN DER LAAN M, JOOSTE S, DU PREEZ C, BARNARD J, RODDA N, DABROWSKI J and NELL P (2017) *Revision of the 1996 South African water quality guidelines: Development of a risk-based approach using irrigation water use as a case study*. WRC Report No. 2399/1/17. Water Research Commission, Pretoria, South Africa.
- DU TOIT W, FLETT BC, BENSCH MJ, SMIT E, FOURIE H, DRINKWATER TW, BATE R and DU TOIT HA (1999) *Production of maize in the summer rainfall area*. ARC – Grain Crops Institute, Pretoria, South Africa.
- GOUDRIAAN, J. (1977). *Crop micrometeorology: a simulation study*. Pudoc
- JOVANOVIĆ NZ, ANNANDALE JG and MHLAULI NC (1999) Field water balance and SWB parameter determination of six winter vegetable species. *Water SA* **25** 191–196.
- MAAS EV and HOFFMAN GJ (1977) Crop salt tolerance – current assessment. *Journal of Irrigation and Drainage Division* **103** 115–134.
- MONTEITH JL (1977) Climate and efficiency of crop production in Britain. *Royal Society of London Philosophical Transactions* **281** 277–294.
- SMITH M, ALLEN RG and PEREIRA LS (1996) Revised FAO methodology for crop water requirements. In: *Proceedings of the International Conference on Evapotranspiration and Irrigation Scheduling*, San Antonio, Texas, USA, 3–6 November 1996, 133–140.
- TANNER PD and SINCLAIR TR (1983) Efficient water use in crop production: research or re-search? In: *Limitations to efficient water use in crop production*, TAYLOR HM, JORDAN WR and SINCLAIR TR, American Society of Agronomy, Crop Science Society of America, Soil Science Society of America, Madison, WI, USA.

# CHAPTER 4: DEMONSTRATING THE SUSTAINABLE USE OF UNTREATED CIRCUM-NEUTRAL MINE WATER FOR IRRIGATION: REHABILITATED LAND

---

PD Tanner, G van der Walt, W Coetzer and JG Annandale

## 4.1 INTRODUCTION

Mining is a temporary process, while what is left behind after mining is permanent. This is why the rehabilitation of mined areas that meets the standards of the Land Rehabilitation Guidelines for Surface Coal Mines (LaRSSA, 2018) is required. When a mined area is not rehabilitated properly or to a specific standard, it can lead to severe impacts on the environment and local communities through pollution of the soil and water, through soil degradation and through a permanent decrease in land productivity. The process of land degradation is unique and different for every site or area. However, if rehabilitation is not done properly, the outcome is unusable land, or land of lowered productivity. Closure planning has been a requirement in South Africa since the Minerals Act of 1991, which means that financial provisions must be made, rehabilitation must be undertaken, and application made for a closure certificate.

Pre-mining land capability is assessed before mining commences, and post-mining rehabilitation capabilities should meet the requirements and targets that have been set from the pre-mining capabilities. The main focus of rehabilitation is on the environment, productivity and creating the best possible post-mining land capabilities. There are various challenges regarding the rehabilitation process. The physical and chemical properties of soil should be carefully monitored throughout the duration of the rehabilitation process. One of the most common problems that arises with rehabilitation is compaction and the formation of dense layers in the soil. This degrades the soil's physical properties, reduces root development and infiltration, and can limit free drainage of the profile. This can lead to water accumulation in certain areas, which can result in waterlogged soils or ponding in the field.

Mafube Colliery is an open-cast mine in Mpumalanga, where field trials on irrigation with untreated circum-neutral mine-affected water on unmined land have been successfully undertaken. However, it is not only economic and sustainable production that is important with this approach to managing surplus mine-impacted waters. The impact of such irrigation on the environment is a key consideration. The potential advantage of being able to irrigate rehabilitated land is that salts leaching from the irrigated profile can be more easily contained and managed than is the case for previously unmined areas. It is, therefore, essential to demonstrate under what conditions rehabilitated land can be used to successfully produce crops irrigated with mine water.

While there are guidelines for re-establishing land of arable capability, there are currently no specific guidelines on how to rehabilitate a profile to irrigable potential. What is clear, though, is that surface ponding and perched water tables within a field will be problematic for irrigation, especially with saline waters. The reason for this is that, although with many mine waters, a large fraction of the salts applied with irrigation will precipitate as gypsum in the soil profile, thereby removing them from the surface and groundwater environment, salts that remain in solution will need to be leached from the profile for irrigation to be sustainable. The aim of the research at Mafube was to ascertain under what conditions the irrigation of rehabilitated land will be successful and sustainable.

## 4.2 SITE SELECTION AND REHABILITATED FIELD DESCRIPTION

The chosen rehabilitated site for the trial was located adjacent to Mafube Colliery at 25°47'29.04" S 29°46'0.42" E (centre of pivot area). The big advantage of this site was its proximity to the water source (Void 3), as well as to the unmined site, with easy and safe access for the farmer and research team, thereby creating a safer working environment than is generally found on an active mine.

Figure 4.1 indicates the different rehabilitation sites identified and the preferred site that was selected. The sites were augured in order to classify the soils and get an indication of their irrigability. A tractor-loader-back (TLB) vehicle was provided to excavate profile holes for the research team to inspect.

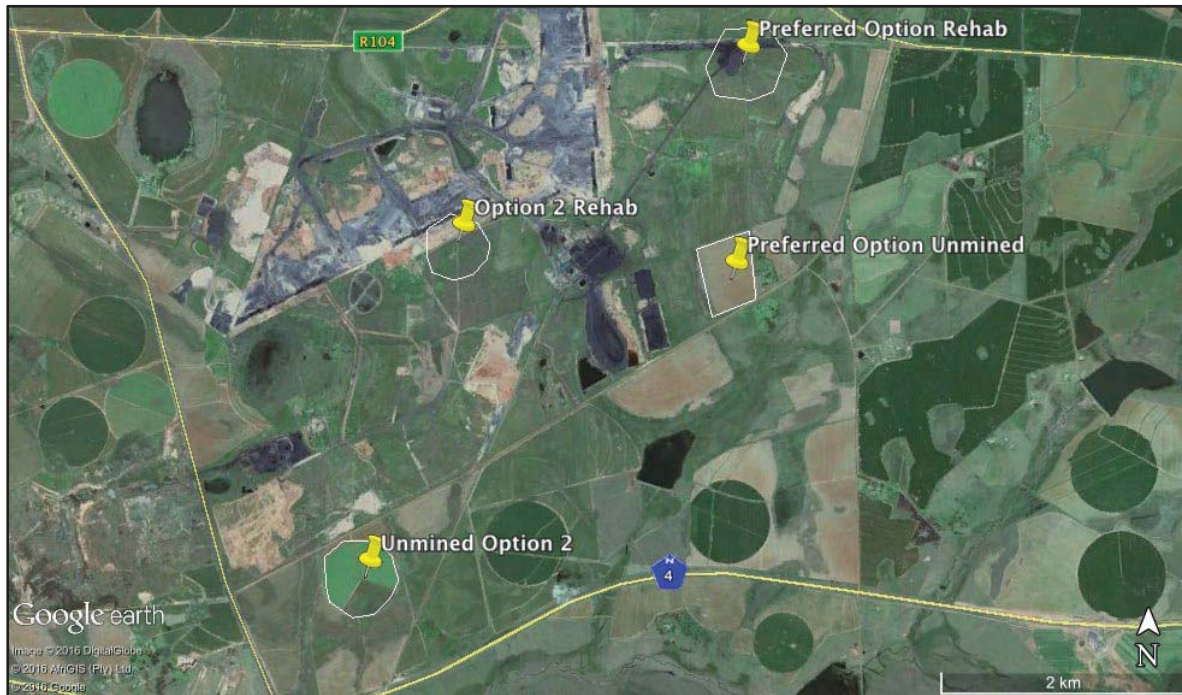


Figure 4.1: Google Earth image of the four potential pivot sites considered, with the preferred rehabilitated and unmined sites indicated

The results from the soil classification studies done in September 2017 indicated that the soil profile in most of the selected rehabilitated area was generally quite uniform, with a typical Witbank soil form. It can be seen that the profile was relatively shallow, with extensive root growth throughout the Orthic A (top soil) and man-made soil deposits, thus throughout the entire anthropogenic soil profile (Figure 4.2) (sequestering a large fraction of the salts applied to it, and thereby keeping these out of adjacent water sources).

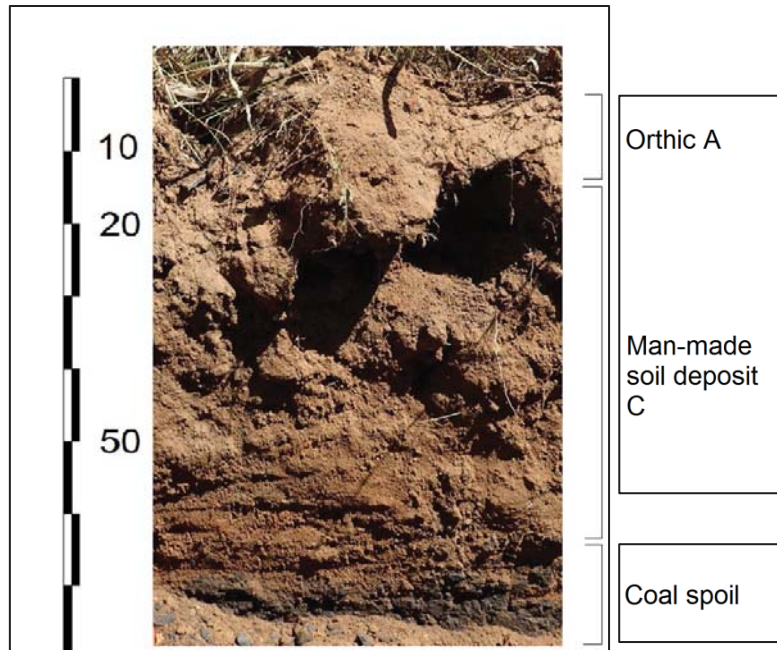


Figure 4.2: Representative soil profile of a rehabilitated site with a Witbank soil form

The research team took 30 soil samples in 2016 (for soil analyses and baseline data before trial commencement) and recorded the depth to spoil layer across the field. A map of the field is provided and sampling points with the depth to spoil layer indicated at each point. This can be found in Appendix A5. A cross-section of the field is presented in figures 4.3 and 4.4, indicating the depth to spoil layer from north to south, and from west to east of the field. The pivot area has deep soils on the southern side, with shallower areas to the north (Figure 4.3). The cross-section of the field from west to east indicates that the soil profile is generally deep with a few shallower areas closer to the centre of the pivot area.

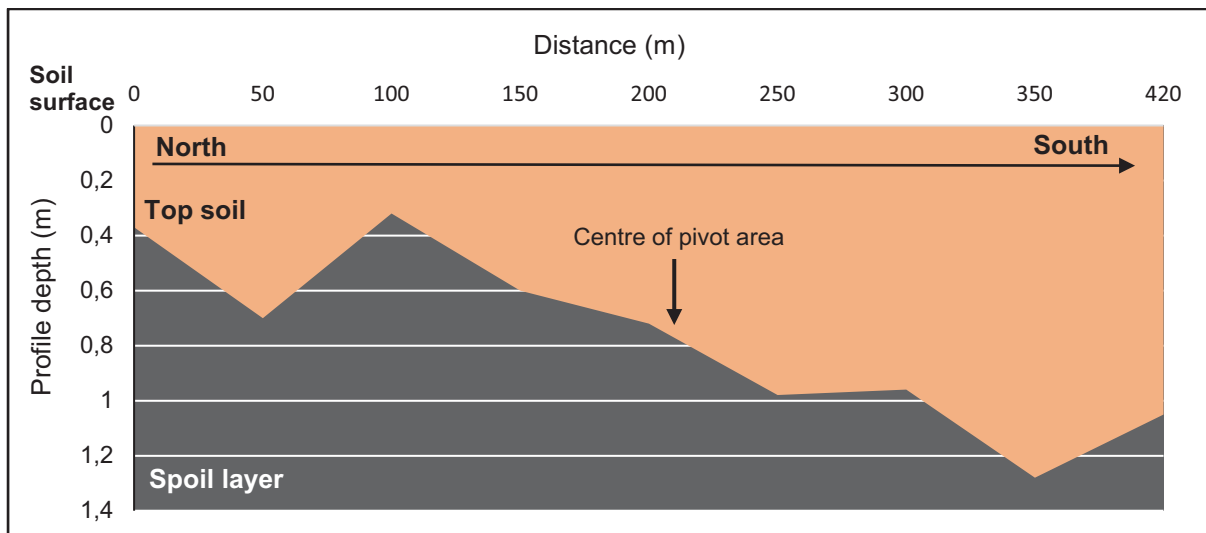


Figure 4.3: Cross-section of the soil depth of the rehabilitated site from north to south

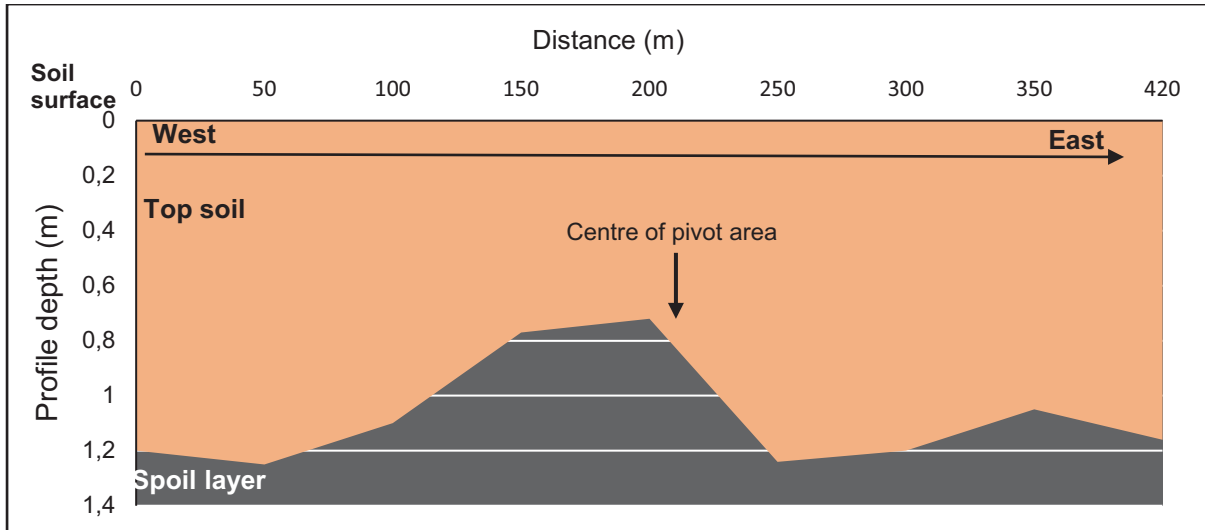


Figure 4.4: Cross-section of the soil depth of the rehabilitated site from west to east

Hydraulic conductivity and internal drainage measurements of profile layers will assist with understanding the potential productivity of the field and the likelihood of sustainable and successful crop production.

#### 4.3 WORK DONE TO ESTABLISH A FUNCTIONING PIVOT SYSTEM ON A SUITABLE SECTION OF REHABILITATED LAND AT MAFUBE COLLIERY

After selecting a suitable site to erect an irrigation system, Mafube Colliery proceeded to procure a centre-pivot irrigation system, and to commission its assembly (Figure 4.5). South32 collaborated with this endeavour by donating an old centre pivot that was not in use on one of its mines. Unfortunately, this pivot had not been disassembled correctly, with many bolts and stays just removed with a cutting torch, causing considerable damage. Costs to refurbish this pivot were significant, with the farmer estimating that it would have been easier and cheaper to install a new pivot from the start. There were also delays with establishing the central foundation for this pivot, and supplying electricity and water at the correct pressure to the site. Theft of the pipeline in 2020 and its replacement also caused delays.



Figure 4.5: Unassembled pivot on the rehabilitation site, mid-2017

Soon after the assembly of the pivot was complete, heavy rain fell that helped to accentuate the unevenness of the field surface through surface ponding, indicating that there were surface drainage problems. This is indicated in Figure 4.6.



*Figure 4.6: Dr Phil Tanner at the centre pivot on the Mafube rehabilitated field with clear signs of water ponding after the heavy rains*

Apart from the ponding, the land surface was too uneven for the pivot to safely make a full circle, and the commercial farmer could not plant the field, as this would result in breakages of his equipment. The unevenness is often caused by subsidence, which is common for rehabilitated mine land as it ages, and the water table re-establishes itself in the rehabilitated land. It is clear that a suitable surface topography is essential before rehabilitated fields can be considered arable and irrigable. Dr Tanner, a mine land rehabilitation expert, selected suitable A and non-plinthic B horizon soil materials from the soil stockpiles on Mafube with which to fill the depressions.

Large volumes of this material were trucked into the field in 2018 to fill the hollows. A grader was subsequently used to create a gently sloping, free-draining surface. However, carting in large volumes of soil, often at times when the soil profile was wet, coupled with the shaping activity of the grader, resulted in heavy compaction across the filled in portions of the site, together with those portions of the site where heavy vehicles had travelled.

Initial efforts to remedy this compaction made use of normal agricultural equipment. This was not able to rip deeply enough, resulting in loosening of only the top 150–300 mm of the profile. A bulldozer with adequate ripping configuration was then hired, which was able to rip the field to depths in excess of 300 mm, providing satisfactory loosening and reducing compaction (Figure 4.7). However, only half of the pivot area was ripped due to it being the start of the rainy season, which resulted in the soil profile becoming too wet for ripping to be done effectively.



Figure 4.7: A bulldozer with a ripper reducing compaction to 300 mm

Figure 4.8 represents the state of the rehabilitation site at the end of this research project. The photograph was taken in January 2021. After the heavy rainfall that occurred in January and February due to Cyclone Eloise, access to the pivot, even by foot, was not possible. Heavy water ponding is suspected in different areas on the site. This will be helpful in identifying areas differing in infiltration, surface runoff and internal drainage.



Figure 4.8: The rehabilitation pivot at the end of the research project (January 2021)

#### 4.4 RECOMMENDATIONS AND CONCLUSION

This site has provided valuable information on the teething problems associated with establishing a pivot on rehabilitated mined land. It is clear that a gentle slope and a field without hollows is required for the surface drainage of surplus rainwater. The subsurface compaction must be corrected to ensure both adequate rooting depth and the free drainage of irrigation water from the profile. Getting a rehabilitated field to meet these requirements will likely involve the use of heavy equipment, and care must be taken to minimise and alleviate any compaction this causes. Another concern is that of internal drainage within the profile, and it is important that water is able to drain through the soil-spoil interface, which is often an area of extreme compaction. If this is not the case, perched water tables will result, thereby waterlogging and salinising the profile. A valuable research site has been established that will be useful to verify the conditions under which rehabilitated land can be used effectively for irrigation with mine water.

#### 4.5 REFERENCES

LAND REHABILITATION SOCIETY OF SOUTHERN AFRICA (LaRSSA) (2018) *Land rehabilitation guidelines for surface coal mines*. Coaltech, Minerals Council of South Africa, Johannesburg, South Africa.

## CHAPTER 5: IRRIGATION WITH UNTREATED OR PARTIALLY TREATED ACID MINE DRAINAGE

BH Sukati, JG Annandale, PD Tanner, PC de Jager and JM Steyn

### 5.1 INTRODUCTION

Acid mine drainage is generated in both underground mining and in open-cast workings through the exposure of sulphide minerals, especially pyrite ( $\text{FeS}_2$ ), to infiltrating water, oxygen and catalytic bacteria (*Thiobacillus ferrooxidans*), which are active in extremely acidic (pH 1.0–3.5) solutions (De Almeida et al., 2015; Yadav and Jamal, 2015). The dissolution of  $\text{FeS}_2$  produces  $\text{H}_2\text{SO}_4$  that increases the acidity of the solution to a pH of between 2.0 and 4.0, and further enhances the release of metals and other pollutants (Du Plessis, 1983; Sheoran and Sheoran, 2006; Vahedian et al., 2014). The acidity, in combination with high concentrations of metals and other contaminants, can be highly toxic to the receiving environment. Therefore, the treatment and safe disposal of any hazardous wastes generated is essential. For this reason, neutralising AMD with the intention to raise its pH and to precipitate most of the transition metals, especially iron, is a requirement (Mackie and Walsh, 2015). However, mine water neutralisation itself is a costly operation and the large volumes of neutral mine water generated still require cost-effective management strategies.

The neutralisation of acidity and removal of metals from AMD with the high-density sludge process results in circum-neutral mine water, with large loads of suspended solids that include metal hydroxides that need to settle out as a sludge through a clarification process (Figure 5.1). Treated water is sometimes released to surface water bodies, or further treatment may be required to reduce salinity and residual metal concentrations. Reverse osmosis (RO) is often used to further treat clarified circum-neutral mine water if the intention is to achieve potable water status.

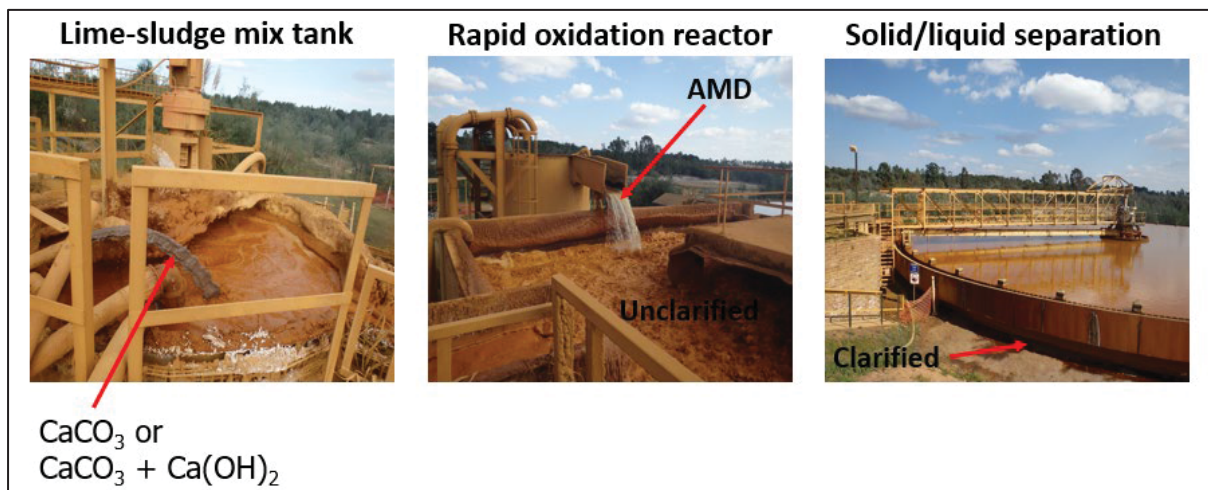


Figure 5.1: Acid mine drainage treatment process and resultant high-density sludge generation

In pursuit of a cost-effective mine water management strategy, Du Plessis (1983) theoretically showed the feasibility of using clarified mine water from HDS treatment for irrigation, as opposed to further purification with expensive and energy-hungry RO technology that also generates brines and sludge that need management. This research concluded that, if this water is used for irrigation, it should be applied to field capacity to ensure that it is a utilisation and not a waste disposal practice.

This would enhance gypsum precipitation and reduce leaching. Root zone salinity was also not expected to negatively impact on soil physical properties, as sodium levels are usually quite low. Subsequent irrigation research with circum-neutral mine water has demonstrated this technology to be a cost-effective, alternative mine water utilisation strategy (Annandale et al., 2006).

Jovanovic et al. (1998) irrigated several crops with clarified, lime-treated acid mine water, monitoring crop response and changes to soil chemical properties. Results indicated that there were no symptoms of foliar injury. However, shallow rooting of most crops, which was attributed to soil acidity, soil compaction and phosphorus deficiency in deeper layers, was recorded. Salinity fluctuated following rainfall patterns and pH increased after three years of irrigation due to residual alkalinity in the water. As alluded to earlier, irrigation with such waters negates the need to further treat water with a technology like RO, which is expensive and energy intensive.

The success of using AMD directly as an irrigation source has, to our knowledge, only been demonstrated under controlled environmental conditions (greenhouse) on a pot scale (Madiseng, 2019). Using limed soil as the “treatment plant” for AMD applied as irrigation under field conditions, if feasible and sustainable, could eliminate the need for an HDS processing plant. This would obviously save enormous capital and some of the running costs of operating such a plant. If this is not feasible, and there is still a need to neutralise AMD in a liming plant, then irrigating with unclarified neutralised mine water, if feasible and sustainable, would eliminate the need for the clarification of limed water and sludge disposal (an expensive operation). Studies on crop and soil response to irrigation with AMD and with unclarified and clarified neutralised mine waters for irrigation are clearly needed.

Because crops differ widely in their acid and salt tolerance, and because these are very unusual waters that have not been used for crop production, a crop-screening trial with irrigation using untreated or partially treated AMD is seen as a sensible point of departure. If this is only successful with specific crops, future research can look at more detailed crop growth, and water and salt balance determinations of those cropping systems with the best chance of success using these unconventional waters for irrigation. In addition, there may be concerns (real or perceived) around food or the feed safety of crops produced with such mine waters. Therefore, the inclusion of non-edible biofuel and fibre crops would be prudent.

## **5.2 CROP SCREENING FIELD TRIAL**

The objectives of the proposed crop screening trial were, firstly, to observe the response of selected cereals, legumes, pasture grasses, biofuel crops and soils to irrigation with AMD, as well as with unclarified and clarified neutralised mine water; secondly, to predict long-term changes in soil chemical properties, environmental effects and crop growth when these three unusual sources of water are used for irrigation.

### **5.2.1 Site selection**

Originally, the research team had planned to execute the trials at Mafube Colliery. This would have been the most convenient logistically, as the pivots for the commercial field scale trials were located there. However, Dr P Tanner and Prof J Annandale found, on closer inspection of the liming plant, that there was no source of unclarified neutralised water. There was just a settling pond that was intermittently desludged. The liming plant was also only operated when the pH of pit water was suboptimal. In addition, the land in close proximity to the plant tended to be waterlogged and unsuitable for irrigation. Therefore, planting could not occur on this site.

In view of the above, Ms R Mühlbauer from Anglo American facilitated a visit to another Anglo American colliery, Kromdraai, Landau Colliery (Emalahleni, 25°46'10.54" S; 29°05'59.66" E; altitude 1,510 m). The liming plant at this location has been in operation for decades and was considered ideal for these trials.

There was also sufficient rehabilitated land in reasonable proximity to the liming plant. Ms A Rossouw from Anglo American, Dr Tanner and Prof Annandale undertook a reconnaissance visit to the rehabilitated site and decided on a suitable location for the trial based on extensive soil auguring. This area was approximately 850 m from the AMD neutralisation plant, and approximately 400 m from the AMD source at Lopies Dam (25°46'19.53" S; 29°05'47.87" E). The total area needed for the trial, depending on the final layout of the plots, was approximately 1 ha. The site that was selected is indicated in Figure 5.2.



Figure 5.2: A: Source for neutral mine water (unclarified and clarified); B: Source for AMD; and C: Rehabilitated land (Source: Theo van Rensburg, 2017 – irrigation engineer)

### 5.2.2 Crop screening trial layout

The focus of the trial was the screening of economically important agronomic, pasture and biofuel/fibre crops that are adapted to the Highveld, and that can potentially produce economic yields under irrigation with mine-impacted waters. A dryland control was also suggested for summer cropping to assess whether crops perform better with mine water than with no additional water at all. The experimental design consisted of three irrigation blocks, one for each water source, and in summer, an additional dryland block for the warm season crops. The dryland plot would only be planted to summer crops, as insufficient winter rainfall is received for winter cropping (Figure 5.3).

Block dimensions were 45 m x 45 m in order to fall within the irrigation system design criteria. Each 2,025 m<sup>2</sup> block was divided into 36 subplots of 7 m x 7 m, allowing four different rotational annual cropping systems, six perennial summer growing biofuel/pasture crops, and two perennial evergreen pasture systems, all replicated three times. Pathways between plots were planted to a salt-tolerant cynodon species. Crops to screen were also selected based on commercial importance and expected acidity and salinity tolerance (Table 5.1). The biofuel/fibre crops were included in the trial as they may have become more important should food or feed safety issues have arisen. The five best-performing biofuel crops out of eight used in another trial executed on UP's Hatfield Experimental Farm were selected for planting in this crop-screening trial (Table 5.2). These crops were selected based on a previous study by Cloete (2018) that focused on assessing the performance of various biofuel crops. The selection was based on performance in descending order, starting with the best-performing crop (column 3 in Table 5.2).

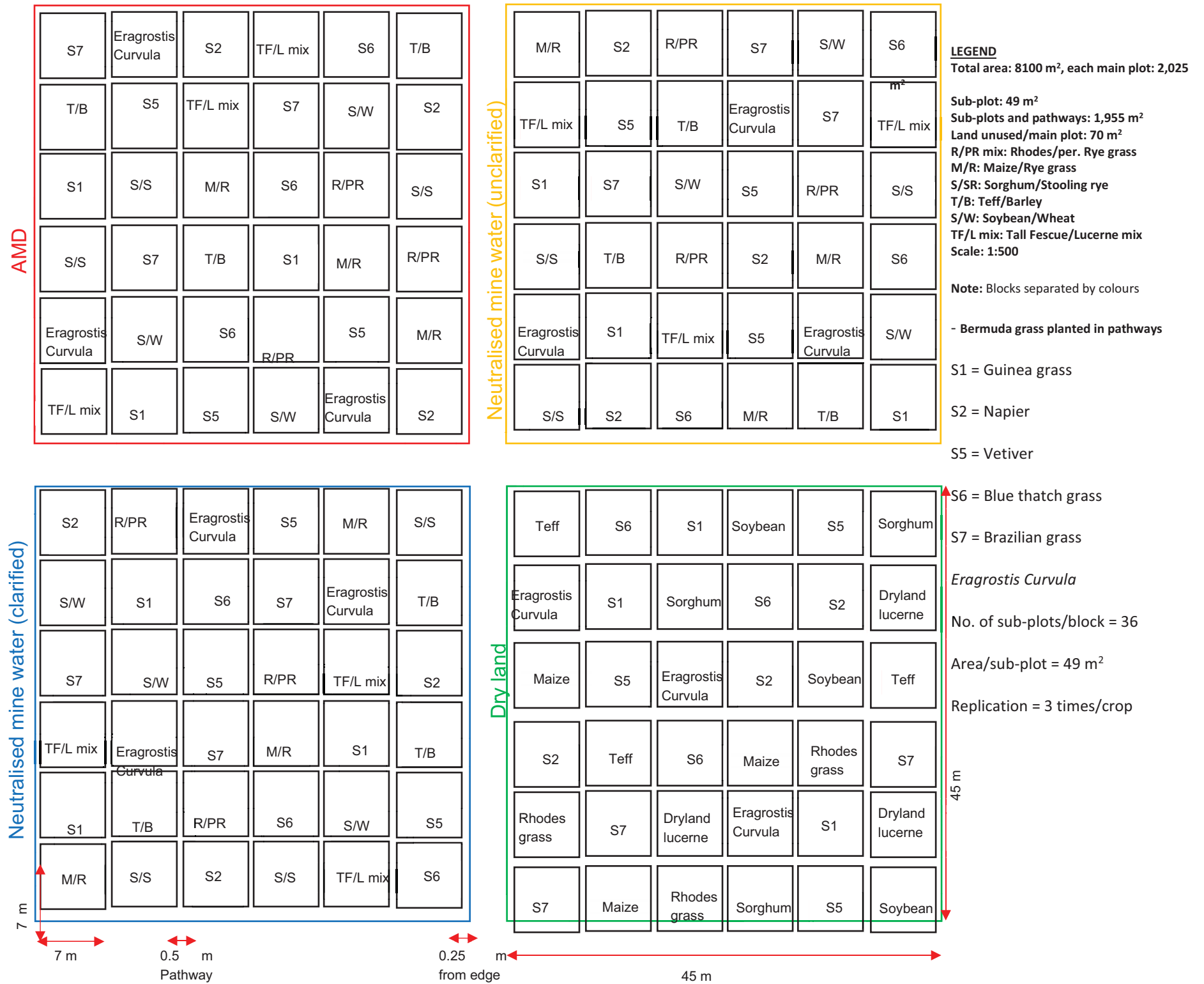


Figure 0.3: Crop screening trial layout

Table 5.1: Selected crops' and pastures' acidity and salinity tolerance (adapted from Jovanovic et al., 1998, AGRICOL, 2016; Pannar Product Catalogue, 2013)

Summer crops						Winter crops					
Crop	Species	Growth form	Optimum pH	Salinity tolerance (dS m <sup>-1</sup> )	Rainfall (mm)	Crop	Species	Growth form	Optimum pH	Salinity tolerance (dS m <sup>-1</sup> )	Rainfall (mm)
Maize	<i>Zea mays</i>	Annual	5.5–6.5	1.8	450–1,500	Wheat	<i>Triticum spp.</i>	Annual	5.5–6.5	6.0	-
Soybeans	<i>Glycine max</i>	Annual	5.5–6.5	5.0	-	Barley	<i>Hordeum vulgare L.</i>	Annual	5.5–6.5	8.0	>300
Sorghum	<i>Sorghum bicolor</i>	Annual	-	6.8	400–600	Annual ryegrass	<i>Lolium multiflorum</i>	Annual, temperate	5.0–8.0	7.6	762–1270
Teff	<i>Eragrostis tef</i> [Zucc]	Annual	4.5–8.5	7.5	432–559	Stooling rye	<i>Secale cereale L.</i>	Annual, temperate	-	11.4	>300
Bermuda grass (for pathways)	<i>Cynodon dactylon</i>	Perennial, subtropical	4.5–8.5	6.9	550–4,300	Tall fescue	<i>Festuca arundinaceae</i>	Perennial, temperate	5.5–8.5 (4.7–9.5)	3.9	375–750
Rhodes grass	<i>Chloris gayana</i>	Perennial subtropical	4.5–10	>10	650	Perennial ryegrass	<i>Lolium perrene</i>	Perennial subtropical	5.0–8.0	5.6	762–1270
Lucerne	<i>Medicago sativa</i>	Perennial, subtropical	Neutral to slightly alkaline	4	400–600						

Table 5.2: List of selected biofuel crops (*Poaceae* sp.) planned to be planted at Kromdraai

Grasses	Species	Performance ranking	Plant spacing	Planting density	Planting procedure	Time of planting
Guinea grass (S1)	<i>Panicum maximum</i>	1	1 x 0.5 m	20,000 plants/ha	Vegetative	February to March
Napier (S2)	<i>Pennisetum purpureum</i>	2	1 x 0.5 m	20,000 plants/ha	Vegetative	March to April
Blue thatch grass (S6)	<i>Hyparrhenia tamba</i>	3	1 x 0.5 m	20,000 plants/ha	Vegetative	March to April
Brazilian grass (S7)	<i>Brachiaria brizantha</i>	4	1 x 0.5 m	20,000 plants/ha	Vegetative	March to April
Vetiver (S5)	<i>Chrysopogon zizanoides</i>	5	1 x 0.5 m	20,000 plants/ha	Vegetative	March to April
Weeping love grass	<i>Eragrostis curvula</i>	Extra	-	10–12 kg/ha	Broadcasted	January to February

**Note:** Ranking: 1 represents best-performing and 5 represents least-performing crop in trial of Cloete (2018). Five of the crops were planted from cuttings and the sixth crop from seeds.

A total of 1,000 rooted plantlets were prepared for each of the biofuel crops to be planted in all blocks.

### 5.2.3 Seedbed establishment, plot demarcation and fertilization

Basic land preparation was undertaken through the services of a contractor who had the required size of tractors and appropriate equipment (Figure 5.4a). Disc harrowing several passes over the 2 ha land with overgrown grasses was the first step, followed by ripping down and across the slope to between a depth of 0.25 and 0.30 m. However, these operations were insufficient, since the land was still uneven with too much plant material at the surface, making cultivation difficult. A plough was then used to turn under excess plant material and prepare an acceptable seed bed. Disc harrowing was once again undertaken as the last step to prepare the seed bed (Figure 5.4b). The marking of blocks and sub-plots followed. The research team's equipment (rotovator) and tools (for the marking out of blocks and sub-plots) were used for final plot preparation.



Figure 5.4: a) Disc-harrowing and ripping operation; b) Field ready for marking of blocks and sub-plots

Four blocks, measuring 45 x 45 m each were marked out using a tape measure, string and white painted pegs, leaving  $\pm 5$  m between blocks to limit irrigation water drift from sprinklers between blocks. The corners of each block were marked at 90° following the 3-4-5 Pythagoras method. A total of 36 sub-

plots measuring 7 m x 7 m were then marked out within each block (Figure 5.5a). After the marking of sub-plots, each was prepared to a fine tilth using a rotovator (Figure 5.5b).

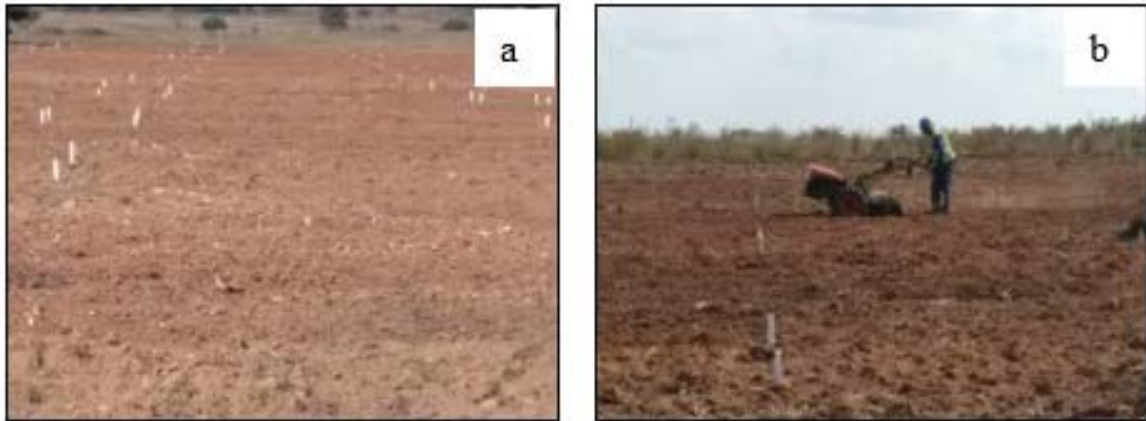


Figure 5.5: a) Marked blocks and sub-plots; b) Rotovating within blocks

Liming requirement calculations for all blocks considered soil chemical properties (tables 5.3 and 5.4). This quantity of lime was determined through the use of a buffer curve (Figure 5.6). However, it should be noted that the block to be irrigated with AMD received extra lime, with this estimated from the acidity of the water. The liming materials were spread by hand (figures 5.7a and b) and incorporated to a depth of 0.1 m in all blocks using the rotovator.

The soils were found to be quite acidic, and a limestone ( $\text{CaCO}_3$ ) requirement of  $5.1 \text{ t ha}^{-1}$  was determined for all blocks. Due to the low manganese levels in these soils (Table 5.4), dolomitic lime ( $\text{CaMg}(\text{CO}_3)_2$ ) was selected for the dryland block (aimed at comparing irrigation with mine water and rainfall/no irrigation), as the mine waters contain significant concentrations of manganese. The AMD and clarified neutralised mine water had manganese concentrations of around  $119$  and  $98 \text{ mg l}^{-1}$ , respectively. Therefore, calcitic lime was selected for the blocks to receive irrigation. In addition, extra lime is required for the block to receive AMD. This was estimated from limestone dosing rates of the lime treatment plant at Kromdraai. The target of the HDS plant is to treat  $8 \text{ Ml}$  of AMD daily, equivalent to  $56 \text{ Ml}$  per week (seven days), consuming  $60$  tons of limestone to neutralise acidity. Therefore, limestone required to treat an estimated  $500 \text{ mm}$  of irrigation for a winter crop ( $5 \text{ Ml/ha}$ ) was calculated to be an additional  $5.4 \text{ t ha}^{-1}$ .

Table 5.3: Soil chemical composition per block

	Block A	Block B	Block C	Block D	Units
$\text{pH}_{\text{H}_2\text{O}}$	3.9	4.5	3.9	4.0	-
$\text{EC}_e$	60	52	66	57	$\text{mS m}^{-1}$

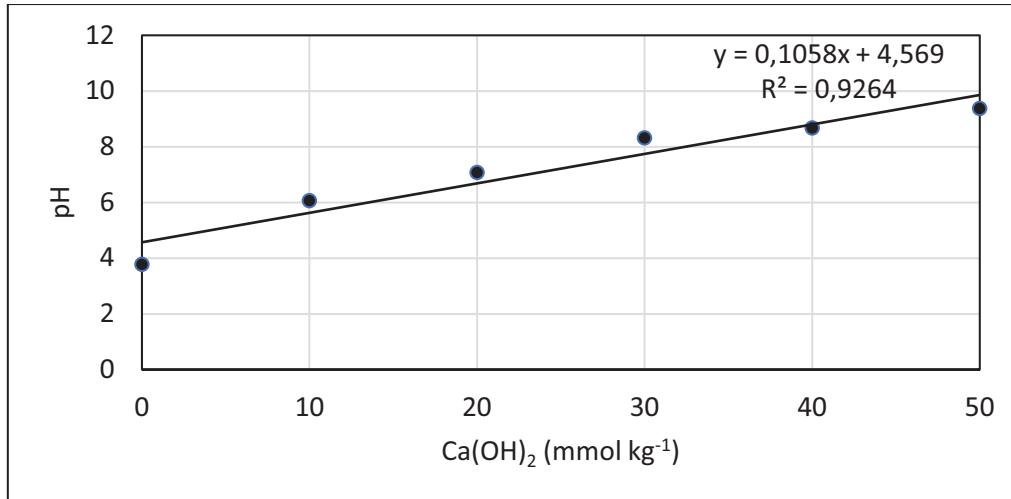


Figure 5.6: Buffer curve used to determine lime requirement

Table 5.4: Concentrations of plant available macro and micronutrients in the soil

Element	Block A (dryland)	Block B (to irrigate with unclarified mine water)	Block C (to irrigate with AMD)	Block D (to irrigate with clarified mine water)	Averages for all blocks
Ca	75	256	167	159	164
S	52	50	83	60	61
K	13	15	13	13	14
P	8	6	2	3	5
Mg	1	2	1	1	1
Fe	52	29	20	29	32
Mn	1	1	1	4	2
Ni	0	0	0	0	0
Pb	5	3	2	3	3
Na	6	4	4	4	5
Al	206	138	184	142	167

Fertilizer requirements were calculated based on soil chemical analysis and recommended specific crop requirements (Table 5.5). The sources of nitrogen, phosphorus and potassium were limestone ammonium nitrate (LAN), single superphosphate (SSP) and potassium chloride (KCl). Phosphate and potassium were applied as basal dressings, while nitrogen was split into two applications (30 kg ha<sup>-1</sup> at planting and 70 kg ha<sup>-1</sup> for top dressing).

Table 5.5: Fertilizers and quantities procured per block

Input	Application rates (kg ha <sup>-1</sup> )
Limestone ammonium nitrate – 28% N	100 N
Single superphosphate – 14% P	40 P
Potassium chloride– 50% K	40 K



Figure 5.7: a) Liming of plots; b) Lime applied per block

#### 5.2.4 Design and installation of irrigation system

The technical specifications and cost of the irrigation system are presented in Appendix A6. Costs do not include installation and commissioning, nor the fittings needed to connect the pump units to the water supply.

The proposed irrigation design required three 7.5 kW pump units, one for each water source (Figure 5.8). The system was to be radio controlled, with one central programmable control unit (by means of a laptop) and three field stations and pump control units. The system could operate as four independent side-by-side systems, three for irrigation and the fourth for flushing the system. The controller can be pre-programmed with a laptop and, as such, is tamper free. To change the program, alterations need to be made on the laptop and downloaded to the control unit by USB connection. Field units are small sealed 12-volt DC radio controllers with small batteries, each operating four valves or pump/flushing valves. The head from the liming plant to the trial site is 90 m, and from Lopies Dam it is 70 m.

The designed flow rate of each pump was 16.4 m<sup>3</sup> hour, with 1,600 m of Class 8 and 1,100 m of Class 10 110 mm high-density polyethylene (HDPE) required. Within each block (45 x 45 m), there were 16 sprinkler emitters to ensure whole block coverage. The 16 sprinkler emitters per block were made up of four sprinklers on each side, and another four in the middle of each block (Figure 5.9). Pipes feeding the four sprinklers were laid in the middle of a block along pathways.

A flushing mechanism for the system had also been included to help reduce the scaling of pipes and pump parts. Scheduling would have ensured the delivery of an average amount of water approximately suitable for all the crops in a block. This would have been achieved by calculating the water requirement for each crop within a block from neutron probe readings and determining an average amount to apply. Irrigation would have been applied once a week for all blocks, as this would save on travelling and other costs linked to irrigation. The plan was to control irrigation through the internet, but manual override was possible if required. A setback occurred before the irrigation system could be commissioned, as a fire in the game farm melted much of the water supply and control hardware in the winter of 2018 (Figure 5.10A and B).



Figure 5.8: Sites for the installation of pump units: A: Sources of neutralised mine water (clarified and unclarified); B: Acid mine drainage (Lopies Dam)



Figure 5.9: Irrigation system installed for each block



Figure 5.10: Fire melted A) pipes and B) connectors

### 5.2.5 Crop schedule and growth

For the summer crops of 2018/19, a devastating fire in the winter of 2018 damaged much of the irrigation system and its water supply network. It was believed that installation and repair of the irrigation system would be achieved for the summer season and a decision was made to plant summer crops despite damage caused to the irrigation system, as precipitation (rain) would allow for crops to at least establish before the water supply was in place. Unfortunately, these crops were never irrigated with any of the mine-impacted waters due to delays experienced in the re-installation and commissioning of the irrigation system that the mine had kindly undertaken to facilitate. These crops were therefore entirely dependent on precipitation. The winter crops of 2019 could also not be planted and the global Coronavirus pandemic prevented any further progress with the mine -water irrigation trial. During lockdown, the research location become very unsafe, with armed robberies and vandals taking advantage of the reduced activities at the colliery.

#### **5.2.6 Summary of challenges encountered at Kromdraai**

Although no experimental results for the crop-screening trial were forthcoming during this project period, much valuable work was done on designing the trial layout, selecting crops to screen and designing appropriate irrigation equipment for future field trials. However, several key aspects related to the concept of irrigation with untreated or partially treated AMD was undertaken in laboratory settings. This will greatly improve the chances of success of any future experimental work. These other research activities are reported on in several chapters to follow.

### 5.3 REFERENCES

- AGRICOL (2016) Go for growth. <http://www.agricol.co.za/about-us/>.
- ANNANDALE JG, JOVANOVIĆ NZ and HODGSON FDI, USHER BH, AKEN ME, VAN DER WESTHUIZEN AM, BRISTOW KL and STEYN JM (2006) Prediction of the environmental impact and sustainability of large-scale irrigation with gypsiferous mine-water on groundwater resources. *Water South Africa* **32** (1).
- CLOETE H (2018) *Water use and bioenergy potential of subtropical Poaceae species as second-generation field crops*. Master's dissertation, University of Pretoria, Pretoria, South Africa.
- DE ALMEIDA RP, ADILSON DO LAGO LEITE A and SOARES AB (2015) Reduction of acid rock drainage using steel slag in cover systems over sulfide rock waste piles. *Waste Management and Research* **33** (4) 353–362.
- DU PLESSIS H (1983) Using lime treated acid mine water for irrigation. *Water Science and Technology* **15** (2) 145–154.
- JOVANOVIĆ NZ, BARNARD RO, RETHMAN NFG and ANNANDALE JG (1998) Crops can be irrigated with lime-treated acid mine drainage. *Water SA* **24** (2) 113–122.
- MACKIE AL and WALSH ME (2015) Investigation into the use of cement kiln dust in high density sludge (HDS) treatment of acid mine water. *Water Research* **85** 443–450.
- MADISENG L (2019) *Crop response to irrigation with acidic and neutralised, saline mine water*. Master's dissertation, University of Pretoria, Pretoria, South Africa.
- PANNAR PRODUCT CATALOGUE (2013) Performance tested seed. [www.pannar.com](http://www.pannar.com).
- SHEORAN AS and SHEORAN V (2006) Heavy metal removal mechanism of acid mine drainage in wetlands: A critical review. *Minerals Engineering* **19** (2) 105–116.
- VAHEDIAN A, ASADZADEH AGHDAEIB SA and MAHINIC S (2014) Acid sulphate soil interaction with groundwater: A remediation case study in East Trinity. *APCBEE Procedia* **9** 274–279.
- YADAV HL and JAMAL A (2015) Removal of heavy metals from acid mine drainage: A review. *International Journal of New Technologies in Science and Engineering* **2** 2349–0780.

## CHAPTER 6: HIGH-DENSITY SLUDGE AS A SOIL AMENDMENT

---

BH Sukati, JG Annandale, PD Tanner, PC de Jager and JM Steyn

### 6.1 EXECUTIVE SUMMARY

Studies on crop and soil response to irrigation with untreated AMD and with unclarified and clarified neutralised mine water for irrigation were planned as part of this project. Chapter 5 outlined the experimental and equipment designs, soil preparation and physical trial layout work that took place over the five years of this project at Kromdraai Colliery, Mpumalanga. Unfortunately, it was not possible, for security reasons, to physically irrigate this site as planned, and the trial will now potentially take place at the Emalahleni water treatment plant, where security should be less of an issue. Studies on the response of crops and soil to irrigation with AMD and with unclarified and clarified neutralised mine water for irrigation are clearly still of significant interest, and these trials should be continued.

In the absence of the field testing of the application of unclarified, but limed water, laboratory and greenhouse studies explored potential issues that could arise if sludges from HDS treatment plants were added to soils. This would simulate part of the situation that would arise if unclarified limed AMD was to be applied directly to the soil. As South African regulations now stand, these sludges are frequently classified as hazardous waste, requiring them to be deposited in appropriate permanent storage facilities.

Chapter 6 examines South African HDS composition and categorisation using the current South African hazardous waste regulations, the impacts of sludge addition on soil physical and chemical status, and finally the effect of sludge addition to soil on plant growth and chemical composition. While the South African waste system classified some HDS as toxic due to its manganese content, this is not the case for classification systems in use in other parts of the world, and a case is made for the current South African system to be revised. The application of HDS to soils increased total Ca, Mg, S, Mn, Al and Fe contents, and also increased the soil pH, decreased soil acidity and increased soil salinity. Soluble and extractable manganese, lead and nickel were not increased by the addition of sludge to soils.

In greenhouse trials on acid soil, plant growth was increased by the addition of HDS, particularly in the presence of added phosphate. Analyses confirmed that the addition of up to the equivalent of 20 t ha<sup>-1</sup> of HDS did not increase concentrations of manganese, nickel or lead in plant tissue, including grain, despite the sludges being tested containing high enough levels of these elements to result in hazardous waste classification.

These encouraging results should be confirmed by the field testing of the application of unclarified treated AMD to a range of field crops, or alternatively, greenhouse trials should examine the impact of much greater levels of application of sludge to soils.

### 6.2 INTRODUCTION

The concept of the use of limed soil as a reactor for the neutralisation of AMD has been proposed. Although it has not been possible to test this novel concept in the field in the current project, additional information on potential issues that may arise has been obtained by examining the nature of the products of AMD neutralisation (i.e. HDS), and investigating, in glasshouse trials, the impact of added HDS on soil properties, plant growth and the content of potentially hazardous elements in grain.

In this chapter, the methods used and results obtained are listed for six investigations associated with the use of HDS as a soil ameliorant, and the validity of the current local classification of this material as hazardous is discussed.

The six investigations are as follows:

- The solubility of constituents of HDS resulting from AMD neutralisation and possible environmental risk
- The physical properties of HDS generated by AMD treatment
- The hazardous waste classification status of HDS from AMD neutralisation
- The soil amelioration effects of HDS as a soil amendment
- The crop response of HDS as a soil amendment
- The food safety of maize grain produced with HDS from AMD as a soil amendment: the uptake and translocation of lead and nickel

### **6.3 THE SOLUBILITY OF CONSTITUENTS OF HIGH-DENSITY SLUDGE FROM ACID MINE DRAINAGE NEUTRALISATION AND POSSIBLE ENVIRONMENTAL RISK**

#### **6.3.1 Materials and methods**

Three sludge samples were collected from an AMD treatment plant that uses a combination of  $\text{CaCO}_3$  and  $\text{Ca}(\text{OH})_2$ . These were designated GypFeMn (gypsum with iron oxides and manganese), GypB (gypsum with brucite) and Gyp (a refined gypsum product). The fourth sludge was sourced from an AMD treatment plant that only uses  $\text{CaCO}_3$  and was designated as GypFe (with gypsum and iron oxides).

#### **Mineralogical and elemental analysis**

*Total elemental analysis using X-ray fluorescence (XRF) and mineral determination using X-ray diffraction (XRD)*

Crystalline phases in HDS were determined using a PANalytical X'Pert Pro Powder diffractometer and total elemental content using an ARL 9400XP+ wavelength dispersive XRF spectrometer. The XRF spectrometer relied on software (UniQuant) to analyse raw spectral data qualitatively and quantitatively, as described by Loubser and Verryn (2008).

#### *Dissolution of sludge constituents*

The determination of solubility, as influenced by different solutions, was aimed at understanding the expected behaviour of the materials if they were to come into contact with organic chelators, or be exposed to reductive, acidic or circum-neutral conditions in the environment.

#### *Aqueous solubility*

A 30 g HDS sample was transferred into a SnakeSkin<sup>®</sup> dialysis tube (from Thermo Fisher Scientific, Rockford, USA). This membrane had 10 kDa molecular weight cut-off (MWCO), with a pore size of approximately 2.9 nm. It was tied at both ends and placed in a 500 ml Schott bottle. A volume of 500 ml deionised water was added to achieve a solid-to-water ratio of 1:16.7. Initial pH and EC were measured immediately after setting up the experiment. After equilibration, the solution was decanted; with 15 ml of the solution reserved for elemental analysis using inductively coupled plasma optical emission spectrometry (ICP-OES), and 50 ml for anion analysis using ion chromatography, a method described by Tabatabai and Frankenberger (1996). The decanted solution was replaced with fresh deionised water. The standard method used to assess the leachability of solid wastes for disposal purposes, the SW-846 test method 1311: toxicity characteristic leaching procedure (TCLP) from the United States Environmental Protection Agency (EPA) (1992), was followed.

#### *Ammonium acetate and organic chelation solubility*

Extractable macro- and micro-elements were determined using standard methods, namely with ammonium acetate (1 mol l<sup>-1</sup>, pH 7) and di-ammonium ethylenediaminetetraacetic acid (EDTA), respectively, as defined by the Soil Science Society of South Africa (1990).

#### *Phosphate sorption capacity*

One-gram samples of air dried HDS were transferred into 50 ml centrifuge tubes and suspended in 30 ml of 2 mmol CaCl<sub>2</sub>, 1 mmol MgCl<sub>2</sub> and 0.5 mmol NaCl containing 0, 50, 100, 250, 500, 1,000 and 2,000 mg P I<sup>-1</sup> prepared from KH<sub>2</sub>PO<sub>4</sub>. The tubes were then stoppered and shaken end to end at 180 oscillations per minute for two hours per day for two days, and stored in the dark at a constant temperature (25 °C). After 48 hours, the samples were centrifuged at 300 revolutions per minute for 10 minutes and filtered through Whatman No. 42 filter paper. The filtered solutions were then analysed for phosphorus using ICP-OES. The amount of phosphorus sorbed was calculated as the difference between the amount of phosphorus added and that remaining in solution. The sorption data was then fitted to a linearised form of the Langmuir equation (Essington, 2004).

#### *Determination of method detection limits for elements*

To ensure the quality of the data generated, method detection limits (MDL) for the different chemical methods (digestion, EDTA, NH<sub>4</sub>OAc, solubility through dialysis) used in this study were determined following a standard procedure of the US EPA (40 CFR Appendix B to Part 136) (2011).

### **6.3.2 Results and discussion**

#### **Mineralogy of sludges**

The XRD showed that the crystalline phase of GypFe ranged from 72 to 77% CaSO<sub>4</sub>·2H<sub>2</sub>O with a further 4% of a carbonate mineral – ankerite (Ca(Fe, Mg, Mn)(CO<sub>3</sub>)<sub>2</sub>). The precipitation of ankerite was not unexpected, since it is one of the minerals abundant in mine wastes (Lollar et al., 2005). Ankerite formation was facilitated by the lower pH (5.5) of GypFe that reduced the kinetics of oxidation and increased the concentration of iron and manganese (Hendry et al., 2000). In addition, solid phases of Fe(II) and Mn(II) decrease their propensity to be oxidised. The magnesium and calcium in this mineral could be traced back to the liming material used to treat AMD. Diffractogram peaks developed and were used to identify some of the minerals in GypFe. It also showed prominent peaks of the iron oxides hematite (Fe<sub>2</sub>O<sub>3</sub>) and goethite (FeOOH). Other minerals identified in GypFe through XRD peaks were calcite (CaCO<sub>3</sub>) and quartz (SiO<sub>2</sub>).

GypFe showed evidence of some amorphous structures dominated by iron and oxygen (suggesting the existence of ferrihydrite), while other structures were dominated by aluminium, potassium and oxygen with traces of sodium, sulphur and iron, resembling Jarosite-Na (NaFe<sup>III</sup><sub>3</sub>(SO<sub>4</sub>)<sub>2</sub>(OH)<sub>6</sub>).

The other sludges, GypFeMn, GypB and Gyp, in addition to their major fractions being composed of CaSO<sub>4</sub>·2H<sub>2</sub>O, showed minor components of CaCO<sub>3</sub>, SiO<sub>2</sub> and brucite (Mg(OH)<sub>2</sub>). No other additional minerals were identified through the use of diffractogram peaks.

Before and after the aqueous solubility test, all the sludges were dominated by gypsum. Deionised water could not completely solubilise CaSO<sub>4</sub>·2H<sub>2</sub>O, possibly because of protection or armouring by iron oxides Ca(Fe, Mg, Mn)(CO<sub>3</sub>)<sub>2</sub> and could not facilitate the dissolution of SiO<sub>2</sub> (as SiO<sub>2</sub> is not water soluble) in the sludge GypFe, and all other minerals were below their detection limits. Diluted HCl at a pH of 4 facilitated the complete dissolution of Ca(Fe, Mg, Mn)(CO<sub>3</sub>)<sub>2</sub> in GypFe, and only CaSO<sub>4</sub>·2H<sub>2</sub>O and SiO<sub>2</sub> were retained.

The SiO<sub>2</sub> in GypFe, as determined by SEM-EDS, is detrital in origin (Zinck et al., 1997), suggesting that it was formed from rock fragments. Similarly, for the sludges GypFeMn, GypB and Gyp, gypsum was also not completely dissolved by diluted HCl at a pH of 4. In addition to gypsum in GypFeMn, CaCO<sub>3</sub> also remained after extraction with deionised water and diluted HCl at a pH of 4, possibly protected by iron oxides through armouring.

### **Acid-base chemistry of sludges**

GypFeMn, GypB and Gyp exhibited alkaline pH values of 8.2, 9.4 and 9.5, and total alkalinity CaCO<sub>3</sub> equivalents (CCE) of 510, 601 and 617 mg kg<sup>-1</sup>. This was expected, because the Ca(OH)<sub>2</sub> used in the process was capable of increasing the pH of the AMD solution to above 9 (Skousen, 2014). GypFe showed an acidic pH of 5.5 and a total alkalinity CCE of 250 mg kg<sup>-1</sup>.

All the materials have the potential to reduce soil acidity if used as soil amendments due to the alkalinity they possess.

### **Total elemental content of GypFe, GypFeMn, GypB and Gyp using X-ray fluorescence**

As expected, a total elemental analysis showed that calcium and sulphur were major components in all four sludges, but GypFeMn and GypB contained, in addition, significant amounts of magnesium (see Table 6.1). The materials can be potential sources of these elements if used as soil amendments. These are considered essential macronutrients, required in large quantities for plant growth, but are often deficient in acidic soils. The calcium can be traced back to the liming material used in the treatment process and the sulphur from the AMD. The magnesium was also likely from the liming material used to treat AMD. Among the trace elements, iron was the most abundant in all the materials, followed by manganese, which were statistically different ( $\alpha < 0.05$ ) for each of the sludges (see Table 6.1). All sludges also contained zinc, but in low concentrations, and as such, these materials cannot be regarded as important sources of this element.

The materials GypFe, GypFeMn and GypB had traces of nickel. The materials GypFeMn, GypB and Gyp contained traces of lead. However, the solubility of lead should be low in these materials, since the process that uses a combination of limestone and lime generated them. Cadmium was below the MDL of 0.18 mg kg<sup>-1</sup> in all the sludges, irrespective of the treatment process.

When compared to similar materials, these sludges seem to have more value as soil amendments than HDS sourced from a coal mine in Canada, as reported by Zinck et al. (1997). The calcium content ranged from 18 to 23.7% in all the sludges investigated in this study, which is slightly higher than the calcium content (14%) reported by Zinck et al. (1997). The sludges in this study also appear to be better sources of iron than those reported by Zinck et al. (1997). The iron content was more concentrated in GypFe (12.5% Fe) and GypFeMn (4.2% Fe), compared to only 1.5% Fe reported by these authors in a similar HDS material. Manganese concentration in all the materials was below 3.6%. The iron and manganese can be traced back to the chemical composition of AMD.

Table 6.1: Total concentration of selected major and trace elements in HDS

Constituents	GypFe	GypFeMn	GypB	Gyp	CV (percentage)	$\alpha$
Major elements (mmol kg <sup>-1</sup> )						
Ca	4,565 <sup>c</sup>	4,499 <sup>d</sup>	5,913 <sup>a</sup>	5,602 <sup>b</sup>	2	<0.05
K	2 <sup>b</sup>	3 <sup>a</sup>	1.7 <sup>b</sup>	1.6 <sup>b</sup>	4	<0.05
Mg	268 <sup>c</sup>	1,946 <sup>a</sup>	1,448 <sup>b</sup>	113 <sup>d</sup>	3	<0.05
S	1,726 <sup>d</sup>	1,914 <sup>c</sup>	2,666 <sup>a</sup>	2,329 <sup>b</sup>	2	<0.05
Trace elements (mmol kg <sup>-1</sup> )						
Cd	< 0.18	< 0.18	< 0.18	< 0.18	-	-
Fe	2,229 <sup>a</sup>	753 <sup>b</sup>	12 <sup>c</sup>	2.7 <sup>d</sup>	4	<0.05
Mn	138 <sup>a</sup>	118 <sup>b</sup>	17 <sup>c</sup>	1.7 <sup>d</sup>	3	<0.05
Ni	2 <sup>a</sup>	2 <sup>b</sup>	0.04 <sup>c</sup>	< 0.01	5	<0.05
Pb	< 0.2	1 <sup>a</sup>	0.8 <sup>a</sup>	0.2 <sup>b</sup>	6	<0.05
Zn	4 <sup>b</sup>	5 <sup>a</sup>	0.1 <sup>c</sup>	0.08 <sup>c</sup>	4	<0.05

**Note:** Any value with a < sign indicates content below the MDL for that element. Means with the same letter across HDS products are not significantly different from each other.

#### Aqueous solubility of sludges using deionised H<sub>2</sub>O

Sulphur was the most soluble element when subjected to weekly extraction with water for five weeks, followed by calcium, magnesium and potassium in descending order in all the sludges (see Table 6.2). Water extracted 99.8, 77, 62 and 66% of sulphur and 22, 31, 28, 29% of calcium from GypFe, GypFeMn, GypB and Gyp, respectively. The abundance of sulphur extracted was an indication that it resided mostly in gypsum, which is water soluble. This showed that both materials could supply sulphur in abundance if used as soil amendments and when in contact with water. However, the reduction in the extraction of calcium was not expected. This was possibly influenced by the armouring of gypsum by iron oxides. Relative to total concentration, water extracted 14, 38.4, 11 and 53% of the magnesium from GypFe, GypFeMn, GypB and Gyp.

When considering the solubility of trace elements, manganese was the element most extracted by water, followed by zinc in GypFe. Manganese releases were below detection limit (BDL) in three of the four sludges, and low in the fourth (the most acid sludge). The iron in GypFe and GypFeMn existed in forms that were of low solubility. The XRD evidence showed that iron occurred as iron oxides and these oxides are sparingly soluble under circum-neutral conditions (Maree et al., 2004)

Table 6.2: Selected water-soluble elements in the sludges (cumulative of five water extractions)

Constituents	GypFe	GypFeMn	GypB	Gyp	CV (percentage)	$\alpha$
Major elements released (mmol kg <sup>-1</sup> )						
Ca	984 <sup>c</sup>	1,378 <sup>b</sup>	1681 <sup>a</sup>	1,643 <sup>ba</sup>	10	<0.05
K	0.6 <sup>c</sup>	2.3 <sup>a</sup>	1.6 <sup>b</sup>	0.8 <sup>c</sup>	13	<0.05
Mg	103 <sup>c</sup>	268 <sup>a</sup>	154 <sup>b</sup>	60 <sup>d</sup>	9	<0.05
S	1,723 <sup>a</sup>	1474 <sup>a</sup>	1,650 <sup>a</sup>	1,539 <sup>a</sup>	8	<0.05

Constituents	GypFe	GypFeMn	GypB	Gyp	CV (percentage)	$\alpha$
Minor elements released (mmol kg <sup>-1</sup> )						
Cd	<0.04	<0.04	<0.04	<0.04	-	-
Fe	<0.2	<0.2	<0.2	<0.2	-	-
Mn	7 <sup>a</sup>	<0.01	<0.01	<0.01	10	<0.05
Ni	<0.3	<0.3	<0.3	<0.3	-	-
Pb	<0.04	<0.04	<0.04	<0.04	-	-
Zn	0.09 <sup>a</sup>	<0.03	<0.03	<0.03	6	<0.05
Anions released (mmol kg <sup>-1</sup> ) by first extraction						
Cl <sup>-</sup>	1.6 <sup>a</sup>	1.4 <sup>a</sup>	1.3 <sup>a</sup>	1.4 <sup>a</sup>	16	<0.05
F <sup>-</sup>	<0.1	0.1 <sup>a</sup>	<0.1	<0.1	-	<0.05
NO <sub>3</sub> <sup>-</sup>	0.2 <sup>b</sup>	1.1 <sup>a</sup>	0.2 <sup>b</sup>	0.2 <sup>b</sup>	22	<0.05
SO <sub>4</sub> <sup>2-</sup>	296 <sup>c</sup>	31 <sup>d</sup>	303 <sup>b</sup>	314 <sup>a</sup>	25	<0.05

**Note:** Any value with a < sign in front represents MDL for that element. Means of the same letter across HDS products are not significantly different from each other.

#### Solubility of sludges in diluted hydrochloric acid at a pH of 4

Diluted HCl at a pH of 4 dissolved sulphur the most, followed by calcium, magnesium and potassium in sludges (see Table 6.3). Relative to total concentration, more sulphur was released from GypFe than from any other sludge. The pH of the GypFeMn sludge (8.2), was reduced by 1.6 units, facilitating the release of elements from this material. However, at this pH (6.6), the dissolution of iron oxides was negligible, since it was still well above a pH of 4. The dissolution of iron minerals is facilitated when the pH falls below 4.

Generally, the diluted acid (pH 4) extracted less calcium and sulphur compared to extraction by deionised water. The pH values of the dilute acid extracts ranged from 6.6 to 10.4, while those from deionised water extraction ranged from 5.7 to 10.7. For both extractants, all materials were extracted with a total of 2.5 l solution.

Acid extraction released the most manganese from GypFe, where 6.5% of the total manganese was extracted. However, only 0.2% of the total manganese was extracted from the more alkaline sludge, GypFeMn, which contained similar amounts of total iron. All other trace elements extracted were close to or at BDL. The low release of metals (e.g. iron and cadmium) showed that all four HDS materials are of low risk to the environment, even when in contact with acidic solutions.

It could be expected that most of the trace elements in sludge are likely to be soluble once in contact with more acidic conditions. It is possible that pH buffering took place due to the solid phases of the CaCO<sub>3</sub> and Mg(OH)<sub>2</sub> contained in the sludges. Generally, metal solubility in HDS increases with decreasing pH levels below 9.5 (Zinck et al., 1997). This is in agreement with results obtained by Maree et al. (2004), who reported that metals in HDS were more soluble at a pH under 6. A gradual increase in the solubility of trace elements is therefore expected once the sludges come into contact with acidic solutions.

Table 6.3: Selected soluble elements extracted with diluted HCl at a pH of 4 (five cumulative extractions)

Constituents	GypFe	GypFeMn	GypB	Gyp	CV (percentage)	$\alpha$
Major elements released (mmol kg <sup>-1</sup> )						
Ca	305 <sup>a</sup>	275 <sup>b</sup>	324 <sup>a</sup>	314 <sup>a</sup>	5	<0.05
K	0.9 <sup>c</sup>	3 <sup>a</sup>	1.9 <sup>b</sup>	0.5 <sup>d</sup>	3	<0.05
Mg	82 <sup>c</sup>	245 <sup>a</sup>	119 <sup>b</sup>	45 <sup>d</sup>	6	<0.05
S	515 <sup>a</sup>	501 <sup>a</sup>	409 <sup>b</sup>	349 <sup>c</sup>	5	<0.05

Constituents	GypFe	GypFeMn	GypB	Gyp	CV (percentage)	$\alpha$
Trace elements released (mmol kg <sup>-1</sup> )						
Cd	<0.04	<0.04	<0.04	<0.04	-	-
Fe	0.34 <sup>a</sup>	<0.2	<0.2	<0.2	7	<0.05
Mn	9 <sup>a</sup>	0.02 <sup>b</sup>	<0.01	<0.01	2	<0.05
Ni	<0.3	<0.3	<0.3	<0.3	-	-
Pb	<0.04	<0.04	<0.04	<0.04	-	-
Zn	0.1 <sup>a</sup>	<0.03	<0.03	<0.03	14	<0.05

**Note:** Any value with a < sign in front represents MDL for that element. Means of the same letter across HDS products are not significantly different from each other.

*Leaching GypFe, GypFeMn, GypB and Gyp with the toxicity characteristic leaching procedure*

With respect to major elements, TCLP extracted more sulphur than calcium from all the sludges (Table 6.4). The release of magnesium and sulphur was significantly different ( $\alpha < 0.05$ ) across the sludges. Among the major elements, magnesium was the next most extracted after calcium, followed by potassium for all sludges. The concentrations of these major elements extracted by TCLP were below those extracted by water and diluted acid.

All trace elements were BDL, except for manganese and zinc in GypFe. Relative to total elemental content, 4% of the manganese and 0.2% of the zinc were extracted from this material. Again, the extraction of these metals (manganese and zinc) from GypFe was facilitated by the lower pH (5.5) of this limestone-generated sludge.

*Table 6.4: Selected TCLP extractable elements*

Constituents	GypFe	GypFeMn	GypB	Gyp	CV (percentage)	$\alpha$
Major elements released (mmol kg <sup>-1</sup> )						
Ca	16 <sup>a</sup>	14 <sup>b</sup>	14 <sup>b</sup>	16 <sup>a</sup>	6	<0.05
K	0.25 <sup>a</sup>	0.12 <sup>b</sup>	0.3 <sup>a</sup>	<0.1	17	<0.05
Mg	3 <sup>c</sup>	4 <sup>b</sup>	5 <sup>a</sup>	0.5 <sup>d</sup>	16	<0.05
S	71 <sup>a</sup>	55 <sup>c</sup>	61 <sup>b</sup>	45 <sup>d</sup>	2	<0.05
Trace elements extracted (mmol kg <sup>-1</sup> )						
Cd	<0.04	<0.04	<0.04	<0.04	-	-
Fe	<0.02	<0.02	<0.02	<0.02	-	-
Mn	5 <sup>a</sup>	<0.01	<0.01	<0.01	4	<0.05
Ni	<0.3	<0.3	<0.3	<0.3		
Pb	<0.04	<0.04	<0.04	<0.04		
Zn	0.06 <sup>a</sup>	<0.03	<0.03	<0.03		<0.05
Anions extracted (mmol kg <sup>-1</sup> )						
Cl <sup>-</sup>	4 <sup>b</sup>	5.8 <sup>a</sup>	1.1 <sup>d</sup>	2.3 <sup>c</sup>	15	<0.05
F <sup>-</sup>	0.8 <sup>b</sup>	1.3 <sup>a</sup>	<0.2	0.8 <sup>b</sup>	8	<0.05
NO <sub>3</sub> <sup>-</sup>	0.1 <sup>a</sup>	<0.1	0.03 <sup>b</sup>	<0.1	18	<0.05
SO <sub>4</sub> <sup>2-</sup>	473 <sup>ab</sup>	367 <sup>b</sup>	316 <sup>c</sup>	595 <sup>a</sup>	7	<0.05

**Note:** Any value with a < sign in front represents MDL for that element. Means of the same letter across HDS products are not significantly different from each other.

### Ammonium acetate and EDTA dissolution of sludges

Calcium and sulphur were the major elements extracted from GypFe, GypFeMn and Gyp (see Table 6.5), while in GypB, magnesium was the most extracted, followed by sulphur and calcium. Relative to total elemental content, NH<sub>4</sub>OAc extracted 15, 17, 12 and 14% of the calcium from GypFe, GypFe, GypB and Gyp. The EDTA extracted 8, 17, 28 and 32% of the sulphur from GypFe, GypFeMn, GypB and Gyp. This indicated that both calcium and sulphur existed in soluble forms and were susceptible to organic chelation in all the materials, but the concentrations extracted were lower than those of water. Among the major elements, potassium was the least extracted from all the sludges. The sludge GypB proved to be a potential source of magnesium if used as a soil amendment, especially for acid soils where this element is often deficient.

With respect to trace elements, EDTA extracted iron, manganese and zinc from the sludges. All other trace elements, including lead and nickel, were BDL in all the sludges. This showed that these materials should be of low risk to the environment.

Table 6.5: Selected elements extractable with EDTA and NH<sub>4</sub>OAc.

Constituents	GypFe	GypFeMn	GypB	Gyp	CV (percentage)	$\alpha$
Major elements extracted with NH <sub>4</sub> OAc (mmol kg <sup>-1</sup> )						
Ca	702 <sup>d</sup>	771 <sup>b</sup>	716 <sup>c</sup>	812 <sup>a</sup>	0.8	<0.05
K	1 <sup>c</sup>	2 <sup>a</sup>	1.7 <sup>b</sup>	0.4 <sup>d</sup>	0.7	<0.05
Mg	31 <sup>d</sup>	324 <sup>b</sup>	1,370 <sup>a</sup>	89 <sup>c</sup>	10	<0.05
S	137 <sup>d</sup>	776 <sup>a</sup>	739 <sup>c</sup>	751 <sup>b</sup>	0.9	<0.05
Trace elements extracted with EDTA (mmol kg <sup>-1</sup> )						
Cd	<0.01	<0.01	<0.01	<0.01	-	-
Fe	7 <sup>a</sup>	0.5 <sup>b</sup>	0.0004 <sup>c</sup>	0.7 <sup>b</sup>	11	<0.05
Mn	5 <sup>a</sup>	3 <sup>b</sup>	0.05 <sup>d</sup>	0.4 <sup>c</sup>	8	<0.05
Ni	<0.08	<0.08	<0.08	<0.08		-
Pb	<0.01	<0.01	<0.01	<0.01		-
Zn	0.4 <sup>a</sup>	0.3 <sup>a</sup>	0.0006 <sup>d</sup>	0.02 <sup>c</sup>	8	<0.05

**Note:** Any value with a < sign in front represents MDL for that element. Means of the same letter across HDS products are not significantly different from each other.

### Phosphate sorption capacity of sludges

The extraction of all trace elements, using the different extractants, including metals of environmental concern (lead, nickel and cadmium), was extremely low from all the sludges. Some of these materials, especially GypFe and GypFeMn, contain large amounts of poorly crystalline iron oxides. Therefore, it is logical to expect these materials to have high phosphorus sorption capacities, which may minimise environmental contamination by these metals. This was investigated by determining the phosphate sorption capacity of the materials. All the sludge adsorption isotherms suggested a high affinity for phosphate (see Figure 6.1). GypFe and GypB had sorption capacities of 887 mmol kg<sup>-1</sup>. Gyp was lower, at 236 mmol kg<sup>-1</sup>, and GypFeMn was by far the greatest at more than 1,800 mmol kg<sup>-1</sup>.

The substantial amount of iron, manganese and aluminium hydroxides in GypFeMn creates specific phosphate adsorption sites (Sposito, 2008; Zinck, 2006). These results indicated that all sludges with aluminium, iron and manganese oxides will have strong sorption capacities that will resist the release of phosphate, even when HDS is in contact with organic chelators, acidic solutions and water in the environment.

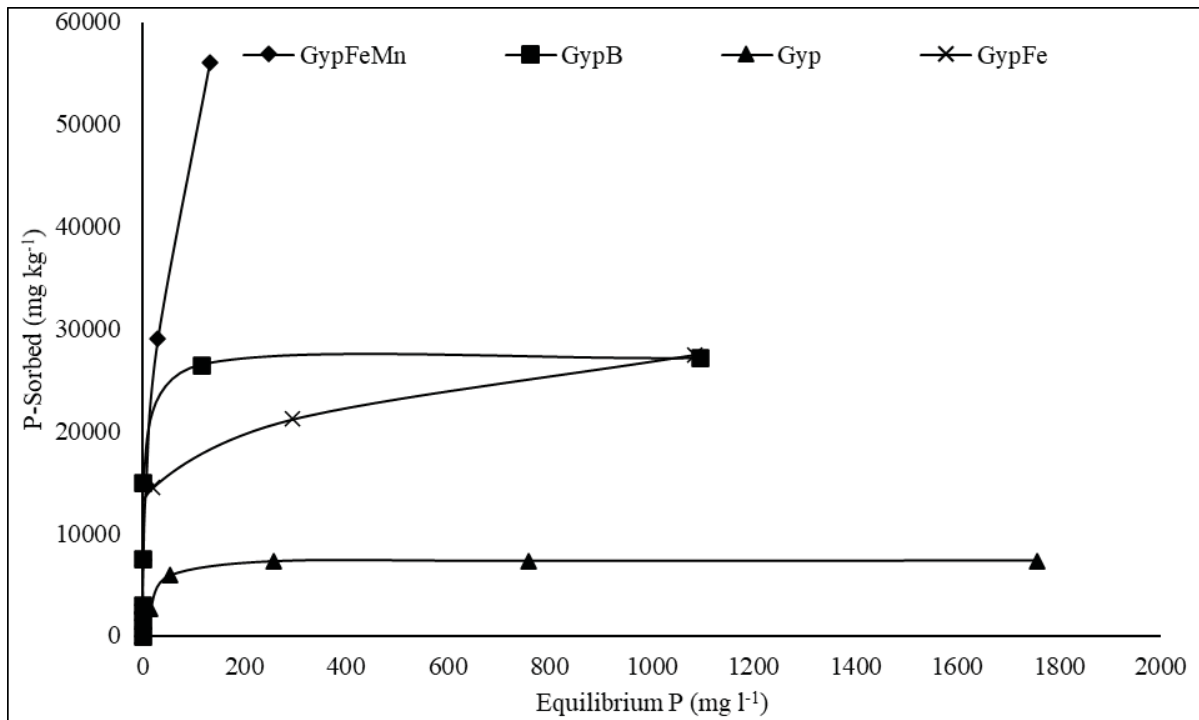


Figure 6.1: High-density sludge phosphate sorption curves

**Note:** GypFe = Ferriferous gypseous; GypFeMn = Ferriferous gypseous with manganese; GypB = Gypseous with brucite; Gyp = Gypseous

## Conclusions

The GypFe sludge was slightly acidic (pH 5.5), with total alkalinity of 250 mg kg<sup>-1</sup>, while the sludges GypFeMn, GypB and Gyp were alkaline with pH values of 8.2, 9.4 and 9.5, and total alkalinity values of 510, 601 and 617 mg kg<sup>-1</sup>. All the materials have the potential to reduce soil acidity if used as soil amendments due to the alkalinity they possess. All the materials were composed mainly of gypsum before and after extraction, with all extractants considered. In addition, GypFe and GypFeMn had substantial amounts of iron oxides that can potentially supply iron and sorb metals of environmental concern. With total elemental content, sulphur was generally dominant in all the sludges, followed by calcium, magnesium and potassium, in descending order.

Iron was the most dominant trace element, followed by manganese, in GypFe, GypFeMn and Gyp. In GypB, manganese was the most dominant, followed by iron. Limited amounts of lead or nickel were detected in the total elemental analyses of the sludges, but neither lead nor nickel were extracted by any of the extractants in levels above the method detection limit. The concentration of other trace elements was extremely low. Cadmium was below detection limits in all the sludges, making it of low risk to the environment.

Extractability tests showed that, in general, both major and trace elements were most soluble in deionised water. Among trace elements, manganese was extractable from GypFe, the least alkaline of the sludges, but not from the other sludges. Manganese is among the constituents of environmental concern in the South African waste classification guidelines. Other metals of environmental concern, cadmium and lead, were below detection limits in all extractants for all the sludges tested. All the materials have the potential to sorb phosphate, with GypFeMn showing the highest potential to sorb phosphate. These results indicated that all sludges considered in this study were potentially safe materials for the environment, and, in addition, have the potential to be used as soil amendments.

## 6.4 THE PHYSICAL PROPERTIES OF HIGH-DENSITY SLUDGE GENERATED BY ACID MINE DRAINAGE TREATMENT

The HDS materials from the coalfields of South Africa in Mpumalanga have potential for use as agricultural soil amendments. The physical properties of these materials have not previously been investigated. In order to be classified as agricultural amendments, the sludges will have to fall within certain specified physical limits.

### 6.4.1 Materials and methods

#### Particle size distribution determination of sludges using the Mastersizer 2000 laser diffractometer and hydrometer sedimentation method

Since the materials contained more than 72% gypsum (which is water soluble), for comparison purposes, particle size distribution was assessed using both a Mastersizer 2000 laser diffractometer and the sedimentation method (hydrometer) (Beuselinck et al., 1998). The hydrometer method assumes that particles are not water soluble and that silt and clay-sized particles can be dispersed. Particles disperse if they possess appreciable surface charge, and non-dispersal shows inadequate surface charge. Sieves were used to separate sand-sized fractions.

With the Mastersizer 2000 laser diffractometer (Malvern Instruments), a slurry was prepared by mixing a small quantity of each of the sludges with deionised water as a dispersant and transferred into its dispersing unit for analysis. At this point, a beam of monochromatic light with a wavelength ( $\lambda$ ) of 750 nm was passed through the sample and particles' diffracted light through a given angle. To calculate the particle size distribution, the Mie scattering principle/theory model was used (Beuselinck et al., 1998). The instrument was capable of measuring materials with particle sizes from 0.045  $\mu\text{m}$  to 2000  $\mu\text{m}$  (Eshel et al., 2004). In addition to the dispersants, ultrasound/ultrasonics was applied to the slurry to enhance the dispersion of particles. The data collected was used to draw particle size distribution curves for each of the samples.

Particle size separates were also determined using the hydrometer method as described by Kroetsch and Wang (2008), but with slight modifications. A 20 g sample was transferred into a mixing flask. A total of 10 ml Calgon<sup>®</sup> solution (50 g l<sup>-1</sup>) (hexametaphosphate) was added as a dispersing agent, in addition to sufficient water for mixing, and mixed for five minutes using a stirrer, Model 1G9850. This process, on average, dissolved 4.1 g of the gypsum from the 20 g sample. After dispersion, the suspensions were transferred into a clear 2 l measuring cylinder through a 0.054 mm sieve. The cylinder had a 1,000 ml mark, which was at 36  $\pm$  2 cm from the bottom. The sieve was rinsed with water to fill the cylinder to the 1,000 ml mark. The particles left on the sieve were transferred back into the pre-weighed beakers and oven dried at 110 °C to determine the sand component. The cylinders were placed and left to stand in a room with a constant temperature (25 °C) for 06:35 hours, after which a first hydrometer reading was taken. A plunger was then used to mix the sample in the cylinder after the first reading and then left to stand for 40 seconds, after which the last hydrometer reading was taken. The readings were taken using a standard hydrometer ASTM E100 No. 152H-TP with Bouyoucos scale in g l<sup>-1</sup>.

Clay and silt-sized particles were calculated from the hydrometer readings using Stoke's Law (Lal and Shukla, 2004). Stokes' Law assumes that particles are rigid and smooth spheres, so the results are expressed as equivalent spherical diameters (Beuselinck et al., 1998). The oven-dried samples were removed after obtaining a constant mass, reweighed and transferred into a column of pre-weighed sieves. The sieves had the following apertures: 53, 100, 250, 500 and 100  $\mu\text{m}$ , and the column was arranged starting with the sieve that had the smallest aperture at the bottom, fitted to a pan, and the top sieve was covered with a lid. The column was gently tapped on a wooden bench approximately 30 times. Each sieve was then weighed with its contents.

Each sample mass was expressed as a percentage of the initial sample mass. Texture for each sludge was then determined based on the percentages of sand, silt and clay as described by Lal and Shukla (2004). The particle separates were matched against several soil textures appearing in the textural triangle.

## 6.4.2 Results and discussion

### Particle size range, specific surface area and uniformity of sludges

GypFe had the largest specific surface area (SSA) ( $1.7 \text{ m}^2 \text{ g}^{-1}$ ), followed by GypB ( $1.2 \text{ m}^2 \text{ g}^{-1}$ ), GypFeMn ( $1.1 \text{ m}^2 \text{ g}^{-1}$ ) and Gyp ( $0.2 \text{ m}^2 \text{ g}^{-1}$ ) (Table 6.6). The SSA of the materials increased with an increase in the content of iron oxides. Iron oxides are known to have a high surface area due to their small particle sizes. For instance, ferrihydrite has a surface area of  $600 \text{ m}^2 \text{ g}^{-1}$  (Schwertmann and Cornell, 2000). The increase in surface area due to iron oxides can increase chemical reactivity in the soil if used as a soil amendment. Hence, increasing gypsum levels reduced the SSA of the materials; GypB, GypFeMn and Gyp had more than 90% gypsum, whereas GypFe had only 72 to 77%. Gyp, had the smallest SSA due to its large particle sizes. This variation in the SSA of the sludges was due to differences in particle size distribution (see Figure 6.2), and possibly differences in the mineralogy of the materials (Ersahin et al., 2006). Surface area is an important property, as it is approximately proportional to surface chemical reactions that could occur within the material and in the soil when added as a soil amendment to cation exchange capacity (CEC) and to the dissolution rates of minerals (Sposito, 2004; Ersahin et al., 2006). Reactivity in the soil is a function of surface area and solubility. Based on uniformity coefficients, the materials GypFe, GypB and GypFeMn had poly-disperse particle sizes, since they had uniformity coefficients of 3.9, 1.5 and 2.2 that all exceed 1 (see Table 6.6). However, Gyp exhibited mono-disperse particle size characteristics, since its uniformity coefficient of 0.6 was less than 1 (Hillel, 1998; Nimmo, 2004; Lal and Shukla, 2004).

Table 6.6: Particle size, surface area, particle density and uniformity of sludges

Sludge	Particle size range ( $\mu\text{m}$ )	SSA ( $\text{m}^2 \text{ g}^{-1}$ )	Uniformity	Particle Density ( $\text{kg m}^{-3}$ )	$D_{0.1}$ ( $\mu\text{m}$ )	$D_{0.5}$ ( $\mu\text{m}$ )	$D_{0.9}$ ( $\mu\text{m}$ )
GypFe	0.4–906	1.7	3.9	2,354	1.1	8.3	92
GypFeMn	0.4–168	1.1	1.5	2,386	2.8	12.8	69
GypB	0.5–250	1.2	2.2	2,313	1.8	11.5	84
Gyp	0.5–906	0.2	0.6	2,312	46	109	234

**Note:** SSA = Specific surface area;  $D_{0.1}$  = Size of particle below which 10% of sample lies;  $D_{0.5}$  = Median particle size,  $D_{0.9}$  = Size of particle below which 90% of sample lies; GypFe = Ferriferous gypseous; Gyp = Gypseous; GypFeMn = Ferriferous gypseous with manganese; GypB = Gypseous with brucite

The materials, GypFe and Gyp showed wider particle size distribution ranges of 0.40–906 and 0.54–906  $\mu\text{m}$ , whereas GypB and GypFeMn had narrower particle size distribution ranges of 0.49–250 and 0.40–168  $\mu\text{m}$ , respectively (see Table 6.6).

All of these particle sizes meet the fertilizer regulations of the Department of Agriculture, Forestry and Fisheries (DAFF) (2012), which state that amendments containing mainly calcium, magnesium and sulphur should have at least 90% of their particles pass through a 2 mm sieve. In addition, these materials are also soluble, as they are largely made up of gypsum. All the gypseous materials investigated here had finer particle size fractions than commercially available agricultural gypsum reported Chen and Dick (2011) to have all particles (100%) exceeding 250  $\mu\text{m}$ .

Gyp had larger particle sizes than the other materials; at 10% ( $D_{0.1}$ ), particles were <46  $\mu\text{m}$ ; at 50% ( $D_{0.5}$ ), particles were < 09  $\mu\text{m}$ ; and at 90% ( $D_{0.9}$ ), particles were <234  $\mu\text{m}$ . GypFe, GypFeMn and GypB had smaller particle sizes. Natural gypsum (crude crushed) reported by Wang et al. (2017) had particle sizes at  $D_{0.1}$  (11  $\mu\text{m}$ ),  $D_{0.5}$  (296  $\mu\text{m}$ ) and  $D_{0.9}$  (653  $\mu\text{m}$ ). Fine crushed natural gypsum, at  $D_{0.1}$  (2.4  $\mu\text{m}$ ),  $D_{0.5}$  (30  $\mu\text{m}$ ) and  $D_{0.9}$  (112  $\mu\text{m}$ ), was finer than Gyp. In general, all the materials studied have particle sizes that are comparable to the particle sizes of agricultural gypsum.

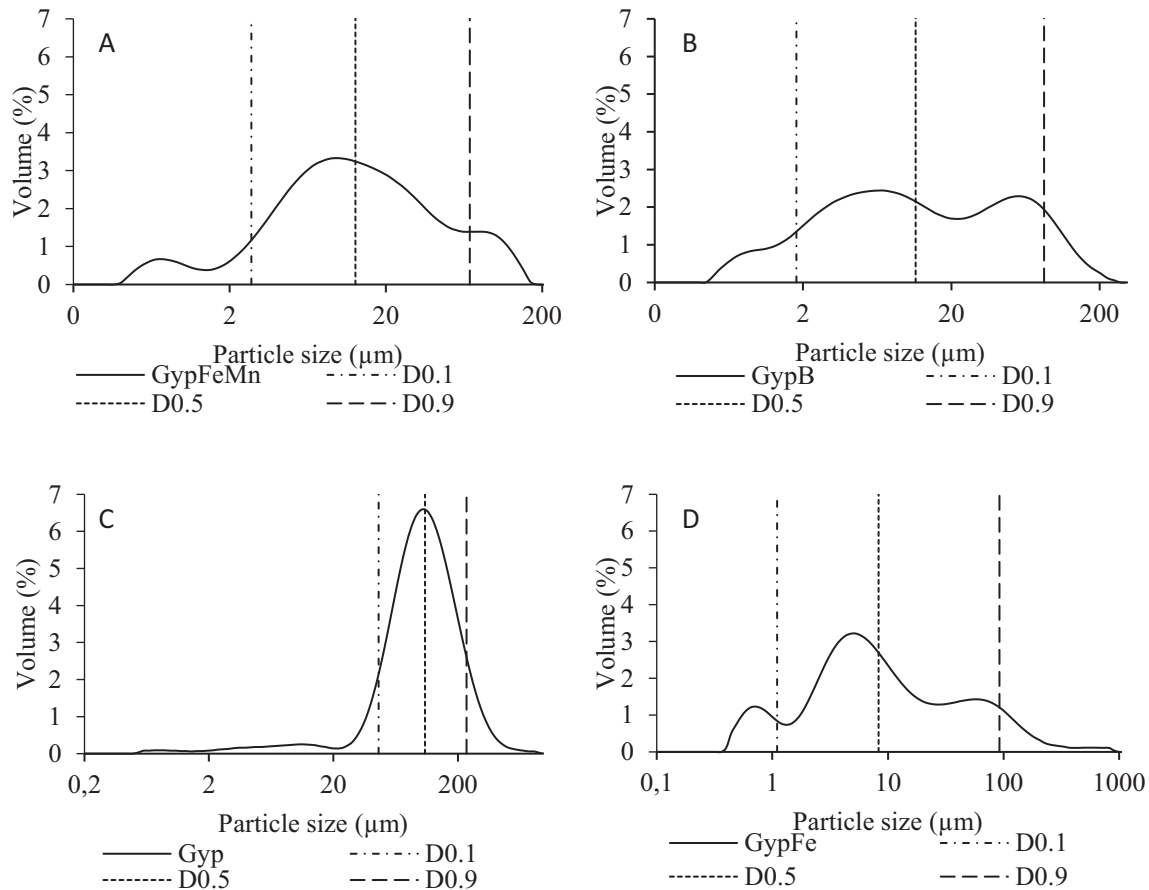


Figure 6.2: Particle size distribution with demarcations for D0.1 (particles at 10%), D0.5 (median particles at 50%) and D0.9 (particles at 90%) for A): GypFeMn; B): GypB; C): Gyp; and D): GypFe sludges

Cumulative particle size distribution curves (Figure 6.3) for all materials other than gypseous indicated a shift towards smaller particle sizes, due to higher iron oxide contents that have small particles (Schwertmann and Cornell, 2000). These curves were smooth and well graded, similar to those of clay or loam soils (Hillel, 1998). This indicates that, if these materials are used as soil amendments, especially in sandy soils, they may be expected to increase microporosity and improve water retention (Mittra et al., 2005). However, this may not be realised if the material dissolves, since it is largely composed of gypsum.

GypFe was generally finer grained, and had the smallest particle sizes. When compared to inorganic soils, GypFe (with  $D_{0.1}$  particle size  $<1.1 \mu\text{m}$ ) and GypB (with  $D_{0.1}$  particle size  $<1.8 \mu\text{m}$ ) had particle sizes falling below the clay/fine silt boundary ( $2 \mu\text{m}$  – clay region) (Figure 6.2). There was a significant shift in the  $D_{0.1}$  particle size for the gypseous and ferriferous gypseous with manganese sludges. The  $D_{0.1}$  particle size for ferriferous gypseous with manganese was  $<2.8 \mu\text{m}$ , falling between  $2 \mu\text{m}$  (clay/fine silt boundary) and  $20 \mu\text{m}$  (fine silt/coarse silt boundary), and that of gypseous was  $<46 \mu\text{m}$ , falling between the  $20 \mu\text{m}$  fine silt/coarse silt boundary, and the  $50 \mu\text{m}$  sand/coarse silt boundary (Figure 6.4). The  $D_{0.5}$  particle sizes for all sludges except gypseous fell between 20 and  $50 \mu\text{m}$ , while that of gypseous fell above  $50 \mu\text{m}$  (in the sand region). The  $D_{0.9}$  particle sizes for all sludges fell in the sand region, i.e. above the sand/coarse silt boundary ( $50 \mu\text{m}$ ).

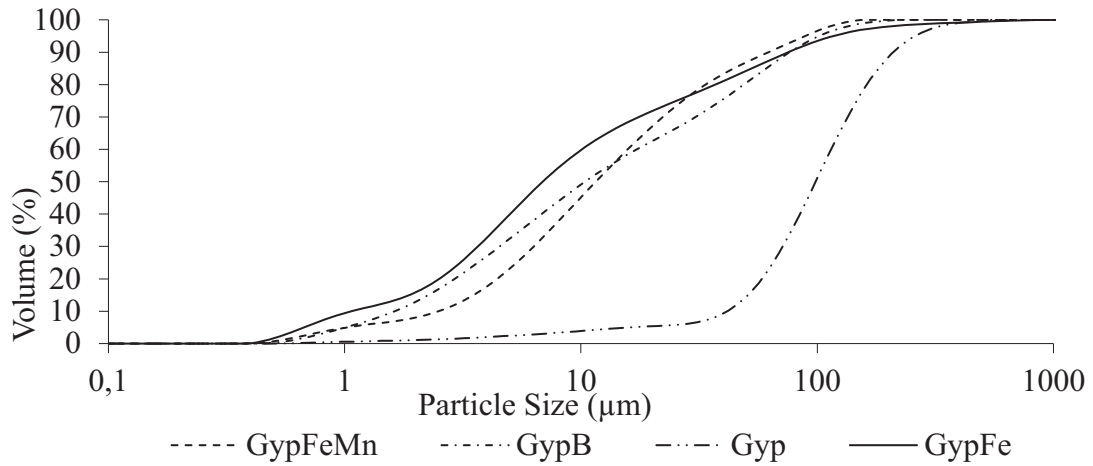


Figure 6.3: Cumulative particle size distribution curves for the sludges GypFeMn, GypFe, GypB and Gyp

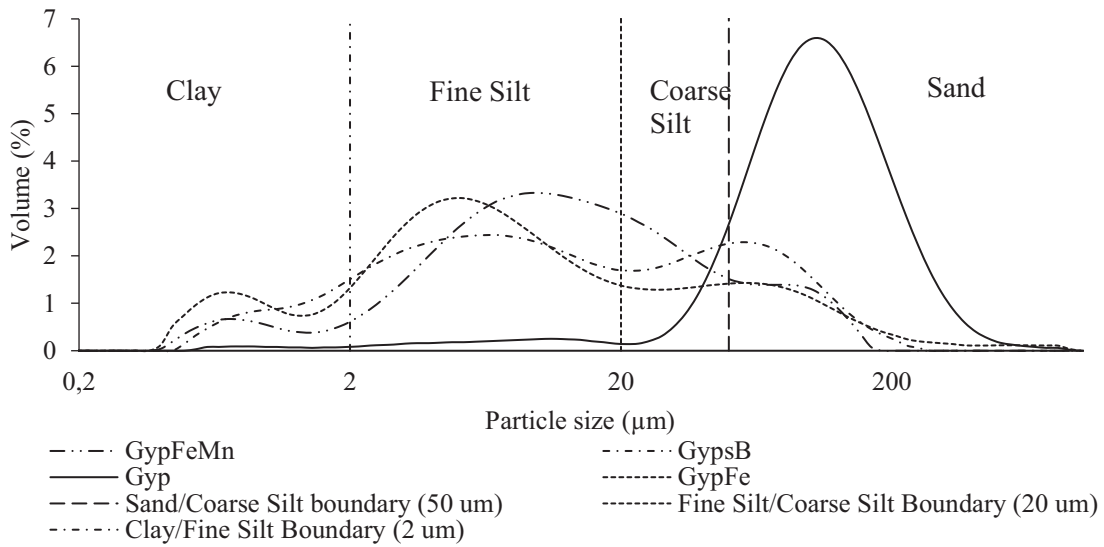


Figure 6.4: Particle size distribution of sludges and particle size boundaries for clay-, silt- and sand- sized particles

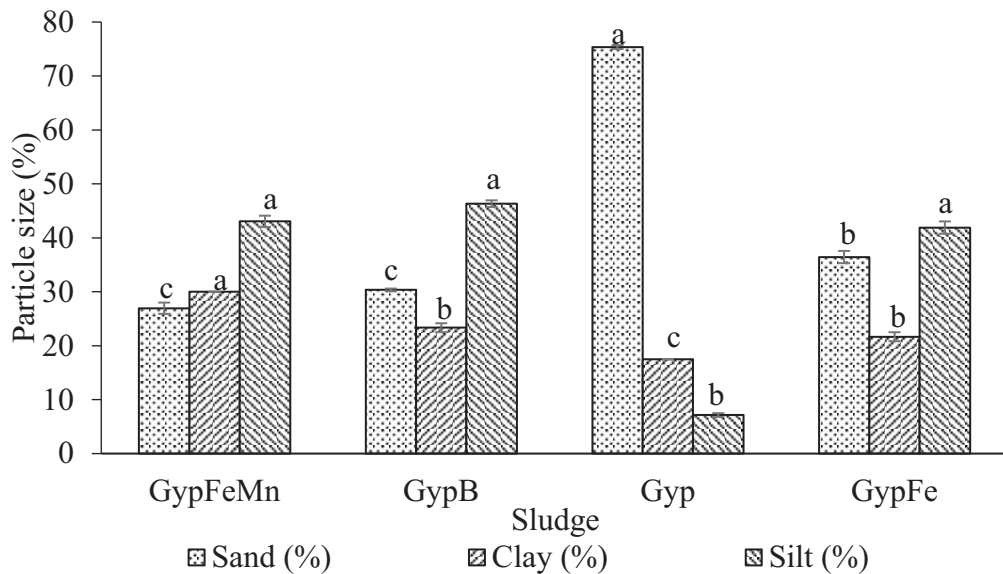


Figure 6.5: Proportions of sand-, silt- and clay-sized particles for each sludge.

**Note:** Sand fraction: Coefficient of variation (CV) = 3.8%, Least significant difference (LSD) = 4.5; silt fraction: CV = 4.6%, LSD = 4.5; Clay fraction: CV = 5.1%, LSD = 3.4.

Based on the hydrometer method, statistically, the sand component in gypseous (75%) was the most dominant (as discussed) and significantly different ( $\alpha < 0.05$ ) from other sludges (Figure 6.5). The data generated by the hydrometer method was in line with that obtained by laser diffractometry, especially for gypseous in the sand fraction.

### Particle density of sludges

Sludge particle density ranged from 2,312 to 2,386  $\text{kg m}^{-3}$ . These values were typical for minerals such as gypsum (2,300–2,470  $\text{kg m}^{-3}$ ) and brucite (2,380–3,400  $\text{kg m}^{-3}$ ) (Eshel et al., 2004; Lal and Shukla, 2004). The particle sizes of all the materials were close to the lower limit of the density range for gypsum. The overall particle densities for GypFe (2,354  $\text{kg m}^{-3}$ ) and GypFeMn (2,386  $\text{kg m}^{-3}$ ) were close to the 2,400  $\text{kg m}^{-3}$  reported by Zinck et al. (1997) for HDS, but densities for GypB (2,313  $\text{kg m}^{-3}$ ) and Gyp (2,312  $\text{kg m}^{-3}$ ) were slightly lower. GypFeMn had the highest particle density, with Gyp the lowest. The increase in particle densities of GypFe and GypFeMn was influenced by the increase in the content of iron oxides that generally have high densities, for example, hematite has a density of 5,260  $\text{kg m}^{-3}$  (Schwertmann and Cornell, 2000). There was a weak correlation between total concentration of iron and particle density (Figure 6.6).

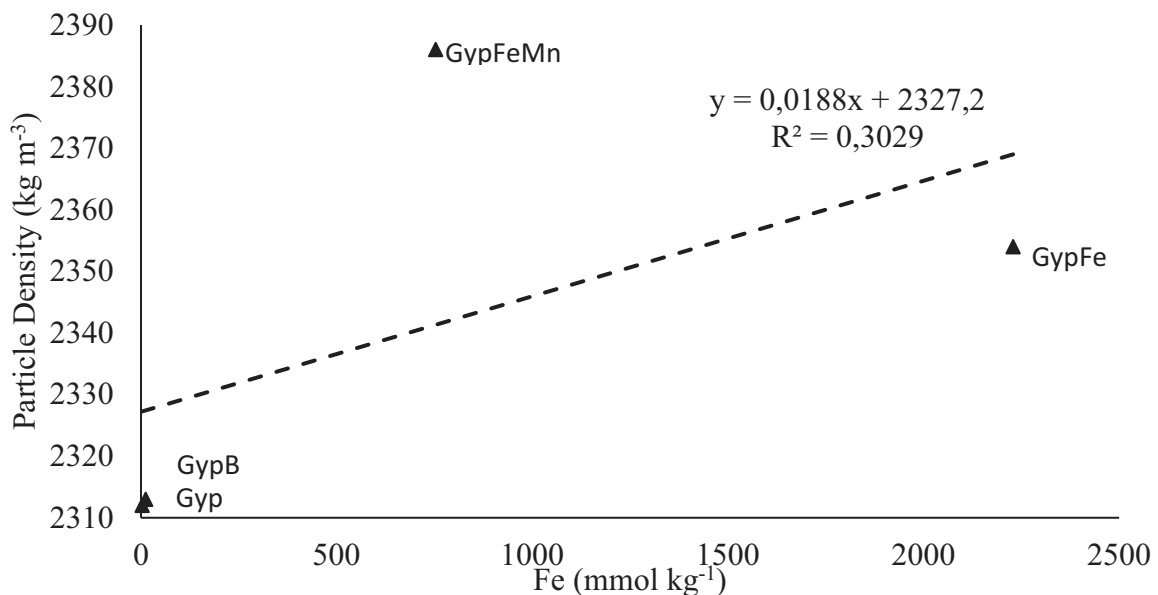


Figure 6.6: Relationship between total iron concentration in gypsum products (GypFe, GypFeMn, GypB, Gyp) and particle density

### Water retention of sludges

The relationship between water content and matric potential depends on the texture and structure of the material as it is determined by total porosity and pore size distribution (Lal and Shukla, 2004). Subjecting the sludges to water potentials of -0.1 (close to saturation), -1, -5 and -10 MPa, reduced the water content of each material (Figure 6.7). The reduction in water content was due to losses of water from pore spaces in the sludges.

The retention curve for Gyp indicated less water lost (5%), between -1 and -10 Mpa potentials, and also a low gravimetric water content (26%) at field capacity, which was assumed to be represented by 0.1 Mpa suction. Contrary to the retention curve of Gyp, the retention curve for GypFeMn resembled that of a clay loam/heavy textured soil, as indicated by the 22% water lost between -1 and -10 Mpa matric potential. It also had 50% gravimetric water content at field capacity. Water contents at field capacity were 39 and 42% for GypB and GypFe, respectively.

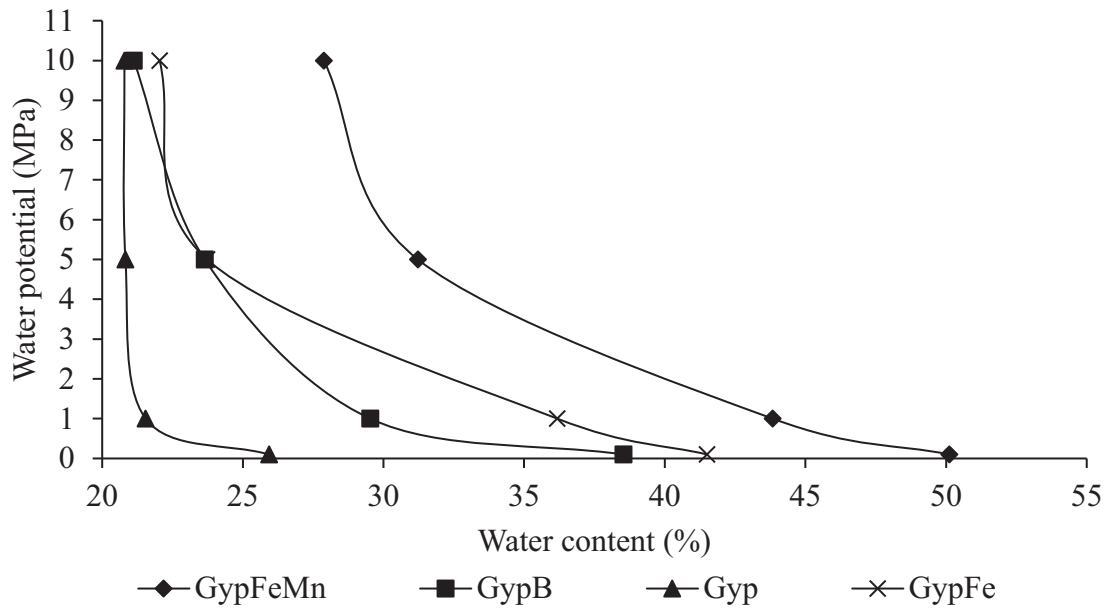


Figure 6.7: Water characteristic curves

### 6.4.3 Conclusions

The focus was on evaluating GypFe, GypFeMn, GypB and Gyp as soil amendments based on their physical properties. Generally, their particle sizes were lower than that of agricultural gypsum. The material Gyp was dominated by sand-sized particles (75%), and if used as a soil amendment, may be expected to increase 87xidizing87ity and improve water movement, especially in clay or silty soils. All the other materials may be expected to increase the microporosity and water-holding capacity of sandy soils. However, these effects may be transient, since the material is largely made up of gypsum, which is water soluble. All the materials had particle densities close to the lower limit of the particle density range expected for gypsum (2,300–2,470 kg m<sup>-3</sup>).

## 6.5 THE HAZARDOUS WASTE CLASSIFICATION STATUS OF HIGH-DENSITY SLUDGE FROM ACID MINE DRAINAGE NEUTRALISATION, AS DETERMINED BY VARIOUS CLASSIFICATION SYSTEMS

### 6.5.1 Materials and methods

#### Regulatory guidelines used to assess HDS

Various hazardous waste classification systems were the “instruments” of this study. The following classification systems were considered: the South African Guidelines, the Australian (New South Wales) Guidelines, the US EPA Guidelines, the Chinese Guidelines and the Canadian (Alberta, British Columbia, Ontario and Manitoba) Guidelines. Briefly, the South African system considers 20 constituents and the Australian system considers nine constituents in terms of their total and leachable content. The US EPA Guidelines, as well as those from China and the Canadian provinces, evaluate eight, eleven and between nine and fourteen constituents, respectively, purely in terms of their leachable content. Details of the classification methodology used for each of these systems is contained in Appendix A7. In the results and discussion section, their respective criteria are used to classify six South African HDS materials, four of which were selected and analysed as defined above, and two of which were analysed for key constituents by other authorities (Maree et al., 2004; Anglo American Thermal Coal, 2015).

## 6.5.2 Results and discussion

### Assessment of HDS using the South African Guidelines

The assessment of the South African Guidelines compared HDS data (on the right) to thresholds (on the left) in Table 6.7. The hazardous classification of each sludge is given in Table 6.8.

Of the six sludges evaluated, the South African system classifies four as low or zero risk. For GypFe, from limestone (Site 1), all elements were classified as Type 3 or Type 4 (low or zero risk,) except for its manganese content. The TCLP extractable manganese of 259 mg  $\ell^{-1}$  in Table 6.8 exceeded the leachable concentration threshold (LCT) LCT3 (200 mg  $\ell^{-1}$ ), resulting in a Type 0 (very high risk) classification for this sludge. GypFe1, also from a limestone plant, had TCLP extractable manganese of 211 mg  $\ell^{-1}$ , also resulting in a Type 0 classification. Hazardous materials classed as Type 0 require treatment and reassessment before disposal in a lined facility. The nickel content of GypFe1 resulted in a Type 1 classification. The nickel content may either be related to the nature of the AMD treated, or to the quality of limestone used (Wang, 2012). The source of the acid waters treated in the limestone plant (Site 2) has not been confirmed as being solely of coal mining origin, and it should be noted that a major metalliferous processing plant is situated upstream of the limestone treatment plant (Site 2). A more detailed discussion of this is beyond the scope of this study.

Table 6.7: South African waste classification limits and analytical status of six HDS samples.

Constituents	TC standards (mg kg <sup>-1</sup> )			LC standards (mg ℓ <sup>-1</sup> )				HDS TC and LC data compared to standards on the left											
	<sup>1</sup> TCT0	<sup>1</sup> TCT1	<sup>1</sup> TCT2	<sup>2</sup> LCT0	<sup>2</sup> LCT1	<sup>2</sup> LCT2	<sup>2</sup> LCT3	Limestone (Site 1)		Limestone (Site 2)				Limestone/Lime site					
								GypFe		GypFe1		GypFe2		GypFeMn		GypB		Gyp	
								mg/ℓ	mg/kg	mg/ℓ	mg/kg	mg/ℓ	mg/kg	mg/ℓ	mg/kg	mg/ℓ	mg/kg	mg/ℓ	mg/kg
As	5.8	500	2,000	0.01	0.5	1	4	<0.01	0.1	0.2	NR	0.003	NR	<0.05	0.5	<0.05	<0.5	<0.05	<0.5
B	150	15,000	60,000	0.5	25	50	200	<0.01		NR	NR	NR	NR	<0.24	4.87	<0.24	6.39	<0.24	0.96
Ba	62.5	6,250	25,000	0.7	35	70	280	<0.01	465	NR	NR	NR	NR	<0.1	12	<0.1	4	<0.1	1
Cd	7.5	260	1,040	0.003	0.15	0.3	1.2	<0.01	<1	0.3	NR	0.01	NR	<0.04	<0.1	<0.01	<0.1	<0.01	<0.1
Co	50	5,000	20,000	0.5	25	50	200	2.9	73	13	NR	0.2	NR	<0.04	97.2	<0.04	2.9	<0.04	0.6
Cr	46,000	800,000	N/A	0.1	5	10	40	0.03	68	2	60	0.03	60	<0.03	2.5	<0.03	<0.5	<0.03	<0.5
Cr(VI)	6.5	500	2,000	0.05	2.5	5	20		-	-	-	-	-	-	-	-	-	-	-
Cu	16	19,500	78,000	2.0	100	200	800	<0.01	80	0.1	NR	0.002	NR	<0.14	3	<0.14	1	<0.14	<1
Hg	0.93	160	640	0.006	0.3	0.6	2.4	NA	NA	NR	NR	NR	NR	<0.02	<0.1	<0.01	<0.1	<0.02	<0.1
Mn	1000	25,000	100,000	0.5	25	50	200	259	7590	211	1000	4	1000	<0.04	6473	<0.04	949	<0.04	95
Mo	40	1,000	4,000	0.07	3.5	7	28	<0.01	3.3	NR	NR	NR	NR	<0.04	<0.1	<0.04	0.1	<0.04	<0.1
Ni	91	10,600	42,400	0.07	3.5	7	28	2.9	108	16.5	NR	0.3	NR	<0.04	104.9	<0.04	2.2	<0.04	<0.7
Pb	20	1,900	7,600	0.01	0.5	1	4	<0.1	<1	NR	NR	NR	NR	<0.1	143	<0.1	163	<0.1	40
Sb	10	75	300	0.02	1.0	2	8	NA	NA	NR	NR	NR	NR	<0.04	<1	<0.04	<1	<0.04	<1
Se	10	50	200	0.01	0.5	1	4	<0.01	25	NR	NR	NR	NR	<0.06	2	<0.06	<1	<0.06	<1
V	150	2,680	10,720	0.2	10	20	80	<0.01	56	NR	NR	NR	NR	<0.03	4	<0.03	<1	<0.03	<1
Zn	240	160,000	640,000	5.0	250	500	2000	3.7	285	20.3	400	0.3	400	<0.1	330	<0.1	7	<0.1	5
Cl				300	15,000	30,000	120,000	7		NR		NR		10.2		25		1.3	
SO <sub>4</sub>				250	12,500	25,000	100,000	2270	55,343	NR		NR		1761		1946		1456	
NO <sub>3</sub>				11	550	1100	4400	0.1		NR		NR		<0.2		0.9		<0.2	
F				1.5	75	150	600	0.8		NR		NR		1.2		0.3		<0.3	

<sup>1</sup>TCT = Total concentration threshold; <sup>2</sup>LCT = Leachable concentration threshold; NA = Not analysed; NR = Not reported

Table 6.8: Classification results obtained from Table 6.5 using the South African Guidelines

Constituents	Limestone (Site 1)	Limestone (Site 2)		Limestone/ lime site		
	GypFe	GypFe1	GypFe2	GypFeMn	GypB	Gyp
As	4	3	4	Inconclusive	Inconclusive	Inconclusive
B	-	-	-	4	4	4
Ba	3	-	-	4	4	4
Cd	Inconclusive	Inconclusive	Inconclusive	Inconclusive	Inconclusive	Inconclusive
Co	3	3	4	3	4	4
Cr	4	3	4	4	4	4
Cr(VI)	-	-	-	-	-	-
Cu	3	4	4	4	4	4
Hg	-	-	-	Inconclusive	Inconclusive	Inconclusive
Mn	0	0	3	3	4	4
Mo	4	-	-	4	4	4
Ni	3	1	3	3	4	4
Pb	Inconclusive	-	-	Inconclusive	Inconclusive	Inconclusive
Sb	-	-	-	Inconclusive	Inconclusive	Inconclusive
Se	3	-	-	Inconclusive	Inconclusive	Inconclusive
V	4	-	-	4	4	4
Zn	3	3	3	3	4	4
Cl	4	-	-	4	4	4
SO <sub>4</sub>	3	-	-	3	3	3
NO <sub>3</sub>	4	-	-	4	4	4
F	4	-	-	4	4	4
Overall type	0	0	3	3	4	4

**Notes:** Inconclusive evaluation, usually because set limit is below analytical detection limit.

Class: 0 = Very high risk; 1 = High risk; 2 = Moderate risk; 3 = Low risk; 4 = Inert material

For both GypB and Gyp sludges, total lead content exceeded the TCT0 threshold of 20 mg kg<sup>-1</sup>, resulting in a low-risk classification.

The South Africa guidelines have set low minimum TCLP values (LCT0), especially for arsenic, cadmium, lead, mercury and selenium. Due to detection limit difficulties, this has given inconclusive results and technically also an incomplete classification for some of the more important elements.

### Assessment of HDS using the Australian (New South Wales) Guidelines

The Australian Guidelines include total fluorine, silver and beryllium levels, where the South African Guidelines do not. As a result, these elements could be analysed and evaluated with the Australian system. Sludge evaluations against Australian standards are shown in Table 6.9.

Table 6.9: Assessment of sludge hazardous status based on both TCLP and SCC thresholds (first and second screening stages) (New South Wales Environment Protection Authority, 2014)

Element	Standards				HDS TCLP extracted and TC data compared to the standards on the left											
	<sup>2</sup> TCLP1	<sup>1</sup> SCC1	<sup>2</sup> TCLP2	<sup>1</sup> SCC2	Limestone (Site 1)		Limestone (Site 2)				Limestone/ Lime Site					
	mg/ℓ	mg/kg	mg/ℓ	mg/kg	GypFe		GypFe1		GypFe2		GypFeMn		GypB		Gyp	
					mg/ℓ	mg/kg	mg/ℓ	mg/kg	mg/ℓ	mg/kg	mg/ℓ	mg/kg	mg/ℓ	mg/kg	mg/ℓ	mg/kg
Ag	5.0	180	20	270	-	-	-	-	-	-	-	-	-	-	-	-
As	5.0	200	20	500	<0.01	0.1	-	-	-	-	<0.05	0.5	<0.05	<0.5	<0.05	<0.5
Be	1.0	100	4	400	-	-	-	-	-	-	-	-	-	-	-	-
Cd	1.0	100	4	400	<0.01	<1	0.3	-	0.01	-	<0.01	<0.1	<0.01	<0.1	<0.01	<0.1
Cr	5.0	1900	20	7,600	0.03	68	2	60	0.03	60	<0.03	2.5	<0.03	<0.5	<0.03	<0.5
F	2.0	75	8	300	0.8	-	-	-	-	-	1.2	-	0.3	-	<0.3	-
Pb	5.0	1500	20	6,000	<0.1	<1	-	-	-	-	<0.1	143	<0.1	163	<0.1	40
Hg	0.2	50	0.8	200	NA	NA	-	-	-	-	<0.02	<0.1	<0.01	<0.1	<0.02	<0.1
Mo	5.0	1000	20	4,000	<0.01	3.3	-	-	-	-	<0.04	<0.1	<0.04	0.1	<0.04	<0.1
Ni	2.0	1050	8	4,200	2.9	108	16.5	-	0.3	-	<0.04	104.9	<0.04	2.2	<0.04	<0.7
Se	1.0	50	4	200	<0.01	25	-	-	-	-	<0.06	2	<0.06	<1	<0.06	<1
Classification					RSW		HW		GSW		RSW		RSW		GSW	

<sup>1</sup>SCC = Specific contaminant concentrations; <sup>2</sup>TCLP = Toxicity characteristic leaching procedure, NA = Not analysed.

If TC > SCC1, but LC ≤ TCLP1: General solid waste (GSW), TC ≤ SCC2 and LC ≤ TCLP2: Restricted solid waste (RSW), TC > SCC2 and LC > TCLP2: Hazardous waste (HW).

At the first screening stage, the Australian Regulations indicate that total nickel ( $108 \text{ mg kg}^{-1}$ ) for GypFe from limestone (Site 1) exceeded SCC1 ( $40 \text{ mg kg}^{-1}$ ), thereby allocating a restricted solid waste (RSW) status to the material.

This sludge was then assessed against both specific contaminant concentrations (SCC) and TCLP in the second screening stage. All elements other than nickel were found to be below SCC1 thresholds, while nickel at  $2.9 \text{ mg l}^{-1}$  marginally exceeded TCLP1 ( $2.0 \text{ mg l}^{-1}$ ), confirming the classification of the material as RSW. This categorisation is equivalent to Type 1 to Type 2 in the South African system. Only nickel was highlighted as an element of concern by the Australian Guidelines as they do not consider manganese.

The sludge GypFe1 from limestone (Site 2) was allocated a hazardous status (equivalent to Type 0 of the South African system), since its TCLP nickel ( $16.5 \text{ mg l}^{-1}$ ) exceeded TCLP2 ( $8.0 \text{ mg l}^{-1}$ ), while GypFe2 from the same site was categorised as GSW, since all its total concentrations (TCs) and leachable concentrations (LCs) were below the SCC1 and TCLP1 thresholds.

GypFeMn had TCs for lead ( $143 \text{ mg kg}^{-1}$ ) and nickel ( $104.9 \text{ mg kg}^{-1}$ ) marginally exceeding the lower threshold, as did GypB for lead ( $163 \text{ mg kg}^{-1}$ ), thus categorising these materials as RSW. Gyp from the same site was categorised as GSW (allowing exploration for use by either the construction industry or agriculture).

#### **Assessment of high-density sludge based on the US EPA, Canadian and Chinese guidelines**

Guidelines for these countries only rely on TCLP data (Table 6.10). Analyses for GypFe, GypFe2, GypFeMn, GypB and Gyp were all below TCLP thresholds considered by the US EPA, Canadian and Chinese guidelines, assigning these materials a non-hazardous status. This suggests that no restrictions are needed for the disposal of these five sludges and the potential for their use in agriculture or the construction industry could be explored.

GypFe1 from limestone (Site 2) had an LC for nickel ( $16.5 \text{ mg l}^{-1}$ ) exceeding the TCLP threshold of Canada (Alberta) and China (of  $5 \text{ mg l}^{-1}$ ), thereby classifying the material as hazardous waste. The other three systems classified this sludge as non-hazardous.

The source of the acid waters treated in the limestone (Site 2) has not been confirmed as being solely of coal mining origin, and it should be noted that a major metalliferous processing plant is situated upstream of the limestone (Site 2) treatment plant, which could be the source of the elevated nickel levels.

Table 6.10: Assessment of HDS based on leachable concentrations using regulatory guidelines for Canada, US EPA and China (Zinck et al., 1997 and US EPA (1990))

Constituents	Standards (mg ℓ <sup>-1</sup> )					HDS TCLP extracted data (mg ℓ <sup>-1</sup> )					
	Canada			US EPA	China	Limestone (Site 1)	Limestone (Site 2)		Limestone/ Lime site		
	Ontario and Manitoba	British Columbia	Alberta				GypFe	GypFe1	GypFe2	GypFeMn	GypB
Ba	100	100	100	100	100	<0.01	-	-	<0.1	<0.1	<0.1
B	500	500	500	-	-	<0.01	-	-	<0.24	<0.24	<0.24
Cd	5	5	1	1	1	<0.01	0.3	0.01	<0.01	<0.01	<0.01
Cr	5	5	5	5	5	0.03	2	0.03	<0.03	<0.03	<0.03
Co	-	-	100	-	-	2.9	13	0.2	<0.04	<0.04	<0.04
Cu	-	100	100	-	100	<0.01	0.1	0.002	<0.14	<0.14	<0.14
Fe	-	-	1000	-	-	<0.1	26	0.4	<0.4	<0.4	<0.4
Pb	5	5	5	5	5	<0.1	-	-	<0.1	<0.1	<0.1
Hg	0.1	0.1	0.2	0.2	0.1	-	-	-	<0.02	<0.01	<0.02
Ni	-	-	5	-	5	2.9	16.5	0.3	<0.04	<0.04	<0.04
Se	1	1	1	1	-	<0.01	-	-	<0.06	<0.06	<0.06
Ag	5	5	5	5	5	-	-	-	-	-	-
U	2	10	2	-	-	-	-	-	-	-	-
Zn	-	500	500	-	100	3.7	20.3	0.3	<0.1	<0.1	<0.1
As	-	-	-	5	5	<0.01	0.2	0.003	<0.05	<0.05	<0.05
Be	-	-	-	-	0.02	-	-	-	-	-	-

**Note:** If LC < TCLP: Non-hazardous; LC > TCLP: Hazardous

### Comparison of assessments using US, Australian, Canadian, Chinese and South African classification systems

The US EPA classification allocated a non-hazardous status to all six sludges assessed. Accordingly, all would be open for exploration for use in the construction industry or agriculture.

With the Australian system, nickel and lead were the elements responsible for either a RSW or HW status for three of the sludges. Soluble nickel was the only factor that resulted in the allocation of a hazardous status to one sludge with the Canadian (Alberta) and Chinese guidelines.

The GypFe1 product, from limestone (Site 2), was flagged by the majority of the guidelines (Canada, China and Australia) based on soluble nickel (the US EPA does not consider nickel). Two elements, manganese and nickel, resulted in Type 0 or Type 1 categorisation by the South African system for two of the sludges from the limestone treatment plants (Table 6.11).

Table 6.11: Summary of elements affecting classification of high-density sludge by the different systems

Element	High-density sludge						
	Limestone (Site 1)	Limestone (Site 2)			Limestone/Lime site		
	GypFe	GypFe1	GypFe2	GypFeMn	GypB	Gyp	
Mn	South Africa	South Africa	None	None	None	None	
Ni	Australia	South Africa, Australia, Alberta and China	None	Australia	None	None	
Pb	None	None	None	Australia	Australia	None	

#### Should manganese form part of hazardous waste classification?

GypFe, from limestone (Site 1), and GypFe1, from limestone (Site 2), were both flagged as hazardous based on their manganese content, but only by the South African guidelines. The South African guidelines are very thorough in the number of elements they consider (20). The South African system is the only system that considers manganese. However, it omits iron and aluminium.

Like iron, manganese forms sparingly soluble oxides. This is most likely the reason why most countries do not consider it to be an element of major concern.

The two AMD treatment plants where the sludge has been classed as hazardous due to its manganese status are both limestone plants. If only limestone is used, more time is needed at a lower pH for complete oxidation and formation of Mn(IV) oxides. Lime accelerates oxidation kinetics because of the higher pH. Once formed, Mn(IV) oxides are exceedingly insoluble as demonstrated by the GypFeMn sludge, which had almost 7,000 mg kg<sup>-1</sup> of total manganese, yet the TCLP solubility was below 0.04 mg l<sup>-1</sup>.

Manganese is also a common soil constituent, especially in the South African context. This is another environment where the low solubility of manganese from Mn(IV) oxides is demonstrated. The best example is the manganiferous soils derived from the Malmani dolomites in South Africa, which have been used for irrigation for 150 years or longer and have been critical in providing food for the large urban and peri-urban Gauteng population. These soils span important agricultural areas in Gauteng, and parts of the North West and Mpumalanga, and contain up to 13,000 mg Mn kg<sup>-1</sup> soil, more than double the total manganese content of the GypFeMn sludge (Mudaly, 2016). This means that these soils would be Type 1 (high risk) wastes if they were to be classified using the South African system based on TC.

Apart from their low solubility, Mn(IV) oxides also have various other benefits. Their metal-scavenging abilities are well known and have a particularly high affinity for B-type cations (soft metals), especially lead (Feng et al., 2007). They also have the ability to oxidise organic pollutants in the soil and are more likely to play a critical role in protecting environmental quality, rather than harming it. Furthermore, the oxidizing propensity it lends to environments is well known in soil research, and commonly observed in dolomite-derived soils (Skousen, 2014). Mn(IV) oxides will not only help buffer ferric oxide reduction and dissolution, but also actively oxidise (or re-oxidise) ferrous iron and  $Mn^{2+}$ . If arsenic occurs in the waste, the presence of manganese will result in its oxidation to the less soluble As(V) arsenate (Fischel et al., 2015).

Based on the arguments made on the low solubility of Mn(IV) oxides and of the potential environmental benefits, it seems prudent to omit total manganese content from the South African system, as has already been done with iron and aluminium.

### **6.5.3 Conclusions**

The hazardous waste classification of various sludges generated from HDS processes has been determined using various international waste classification systems. One consistency between the Canadian, Chinese, Australian and South African systems was the classification of GypFe1 sludge from limestone (Site 2) as hazardous waste. In the case of the Canadian, Chinese and Australian systems, it was due to nickel solubility. For the South Africa system, it was due to both nickel and manganese solubility. Apart from this specific HDS material, the Canadian and Chinese systems did not consider any other sludge to be hazardous.

None of the sludges was considered as hazardous by the US EPA guidelines because nickel is not included in its system. The Australian system further classified three other sludges (GypFe, GypFeMn, GypB) as RSW, based on either their nickel or their lead content, while two (GypFe2, Gyp) were classed as GSW.

LCT0 values for several elements in TCLP extracts are below detection limits using methods commonly available in South Africa. Consequently, incomplete classification of waste is a risk. Changing the LCT0 values for these elements to below the MDL in TCLP would still be lower than the single soluble screening levels used in the other national systems.

Considering all the systems, the probability for the HDS investigated to be classified as hazardous waste increases if the material is only subjected to limestone, as opposed to limestone plus lime.

Based on the arguments made on the low solubility of Mn(IV) oxides and of the potential environmental benefits, it seems prudent to omit total manganese content from the South African system, as has already been done with iron and aluminium.

## **6.6 THE SOIL AMELIORATION EFFECTS OF HIGH-DENSITY SLUDGE AS A SOIL AMENDMENT**

### **6.6.1 Materials and methods**

A pot trial was set up to assess the response of an acid soil when treated with HDS. The study focused on three aspects: the response of the soil, the response of the crop and the uptake of the manganese, lead and nickel present in HDS. This part of the study reports on soil responses.

#### **Sources of sludges and soil used**

Two sludges were selected. The one, sourced from a limestone treatment plant (GypFe), contained both gypsum and iron oxides. The other was collected from a limestone and lime treatment plant, Gyp, a refined product dominated by gypsum.

To assess their effects as soil amendments, an acid soil with a pH of 3.75, low in bases and with low salinity (7.98 mS m<sup>-1</sup>), indicative of the substantially low salt content, was selected. This soil was collected from a field that had been intentionally acidified over the years for research purposes. Several treatment combinations were considered, with one soil, given the symbol S in the treatment combinations, with or without liming (L), two levels of potassium (40 or 100 kg ha<sup>-1</sup>) and two levels of the sludges Gyp and GypFe (10 and 20 t ha<sup>-1</sup>).

### Elemental contents, pH and electrical conductivity of sludges and soil

Before the establishment of HDS-soil mixtures, the individual sludges and soil were analysed. The HDS-soil mixtures were also assessed for changes in chemical properties after cropping.

Total elemental content in sludge and soil was determined following the digestion method of the US EPA 3052. A 0.3 g sample was treated with concentrated nitric acid (HNO<sub>3</sub>) at a solid-to-solution ratio of 1:30 and transferred into a digestion tube. The sample was digested at 180 °C ±5 °C by the Anton Paar Multiwave 3000 digester for 15 to 19.5 minutes, after which it was transferred into a 50 ml centrifuge tube. Extractable elements in the sample were determined with inductively coupled plasma atomic emission spectroscopy (ICP-AES). Plant-available elements were also determined in the HDS-soil mixtures and soil using ammonium acetate (NH<sub>4</sub>Oac) to extract Fe, Mn, Ni, Zn, Pb, Cd and S, using EDTA or Mehlich 3 to extract K, Ca, Na and Mg, and P-Bray 1 solution to extract phosphorus.

Standard methods, as described by Thomas (1996) and Rhoades (1996), were followed to determine the pH and EC of HDS-soil mixtures (after harvesting), and individual sludges and soil. A multi-parameter analyser (Consort C830) with a 0.01 pH resolution, coupled with epoxy electrode, was used, as well as an electrical conductivity meter (Consort C861), with a 0.001 µS cm<sup>-1</sup> resolution.

### Determination of exchangeable acidity and exchangeable hydrolysable cations of the soils

Potassium chloride extraction was used to determine exchangeable aluminium, and soluble and exchangeable acidity in the soil, as described by Thomas (1982), both before and after cropping in the greenhouse trial.

## 6.6.2 Results and discussion

### Physical and chemical status of soil used

The soil used was acidic (pH 3.75) and of low salinity (7.98 mS m<sup>-1</sup>), indicative of the substantially low salt content (Table 6.14). This soil was collected from a field that had been intentionally acidified over the years for research purposes. This soil was therefore expected to respond positively to the liming effects of the sludges. With regard to elemental content, this soil was dominated by iron, while other elements such as Ca, Mg, S, Pb, Ni and Cd were very low. The low calcium content suggests that this element was possibly leached from the topsoil.

Table 6.12: Selected physicochemical soil properties

pH(H <sub>2</sub> O)	3.75
Salinity (EC) (mS m <sup>-1</sup> ) at 2.5 soil /solid ratio	7.8
CEC (cmol <sub>c</sub> kg <sup>-1</sup> )	7.98
Texture	Clay loam

	Acid digestion (mg kg <sup>-1</sup> )	Extractable elements (mg kg <sup>-1</sup> )	Extraction methods
<b>Major elements</b>			
Ca	26	18	NH <sub>4</sub> Oac
K	894	68	NH <sub>4</sub> Oac
Mg	338	12	NH <sub>4</sub> Oac
P	244	8	P-Bray 1
S	69	25	EDTA
<b>Metals</b>			
Cd	< 0.18	< 0.01	EDTA
Fe	37,363	25	EDTA
Mn	301	167	EDTA
Na	38	< 0.01	EDTA
Ni	35	0.9	EDTA
Pb	36	7.2	EDTA
Zn	20	1.2	EDTA

**Note:** NH<sub>4</sub>Oac = Ammonium acetate; EDTA = Ethylenediaminetetraacetic acid.

Values with the smaller than sign (<) indicate MDL of those elements.

### Chemical and mineralogical status of high-density sludge materials used

GypFe was slightly acidic with a pH of 5.5 and an alkalinity of 250 mg kg<sup>-1</sup> (Table 6.13). The material was from a limestone treatment plant where limestone is only capable of increasing pH close to neutral. A further increase in pH may be prevented by armouring where the insoluble precipitation of metals, especially iron and manganese, occurs on the surfaces of the limestone particles preventing further dissolution and chemical reactions (Sun, McDonald Jr, & Skousen, 2000).

Gyp was alkaline with a pH of 9.4 and an alkalinity of 617 mg kg<sup>-1</sup> due to the use of CaCO<sub>3</sub> plus Ca(OH)<sub>2</sub> in the HDS plant. Gyp was therefore expected to be a better liming material than GypFe. Both sludges showed high calcium and sulphur concentrations and some magnesium, presumably contributed by the neutralising materials (Table 6.13). GypFe contained much more total iron and manganese than Gyp. The cadmium concentration was extremely low (<0.18 mg kg<sup>-1</sup>) in both sludges, nickel content was greater in GypFe and lead content was greater in Gyp. As described in Section 6.2, the mineral composition indicated that both sludges were largely composed of gypsum.

Table 6.13: Selected chemical sludge properties and selected total elemental content

Parameter	GypFe	Gyp
pH(H <sub>2</sub> O) at 2.5 solution/solid ratio	5.5 <sup>b</sup>	9.4 <sup>a</sup>
Salinity (EC) (mS m <sup>-1</sup> ) at 2.5 solution/solid ratio	364 <sup>a</sup>	274 <sup>b</sup>
Total alkalinity as CaCO <sub>3</sub> (mg kg <sup>-1</sup> )	250 <sup>b</sup>	617 <sup>a</sup>
Concentrations extracted by acid digestion (mg kg <sup>-1</sup> )		

Major elements	GypFe	Gyp
Ca	182,961 <sup>b</sup>	224,500 <sup>a</sup>
K	83 <sup>a</sup>	61 <sup>b</sup>
Mg	6,513 <sup>a</sup>	2,736 <sup>b</sup>
P	44 <sup>b</sup>	129 <sup>a</sup>
S	132,974 <sup>b</sup>	216,189 <sup>a</sup>
Other metals	GypFe	Gyp
Cd	< 0.18	<0.18
Fe	124,500 <sup>a</sup>	152 <sup>b</sup>
Mn	7,590 <sup>a</sup>	95 <sup>b</sup>
Na	74 <sup>b</sup>	279 <sup>a</sup>
Ni	108 <sup>a</sup>	0.7 <sup>b</sup>
Pb	< 0.2	40 <sup>a</sup>
Zn	285 <sup>a</sup>	5 <sup>b</sup>

**Note:** Values with the smaller than sign (<) indicates MDL of those elements.

### Liming effect of the different sludges

A significant ( $\alpha < 0.05$ ) increase in soil pH occurred when sludge was applied. The incremental addition of phosphate from 40 to 100 kg ha<sup>-1</sup> significantly ( $\alpha < 0.05$ ) increased soil pH (Table 6.14). This was due to phosphate sorption, which involves the co-sorption of not only cations, but also hydrogen ions (H<sup>+</sup>). The interaction of phosphate with either of the sludges was also significantly different ( $\alpha < 0.05$ ) in increasing pH.

This increase in pH was marginal, and soils were still not ideal for the growth of plants. Liming alone increased the soil pH to >5 as expected. A further increase in pH in the limed soil was obtained when the phosphate rate was increased. Applying sludges on their own and the co-application of phosphate with sludge significantly increased soil pH.

Table 6.14: Effect of treatments on soil pH

P	Sludges (t ha <sup>-1</sup> )						
	Soil	Soil (limed)	10Gyp	20Gyp	10GypFe	20GypFe	Average
P0	3.75 <sup>fgh</sup>	5.10 <sup>c</sup>	3.56 <sup>h</sup>	3.79 <sup>fgh</sup>	3.83 <sup>efg</sup>	3.74 <sup>fgh</sup>	3.8 <sup>c</sup>
P40 (kg ha <sup>-1</sup> )	3.63 <sup>gh</sup>	5.68 <sup>b</sup>	3.81 <sup>efgh</sup>	3.91 <sup>ef</sup>	3.90 <sup>ef</sup>	3.90 <sup>ef</sup>	3.89 <sup>b</sup>
P100 (kg ha <sup>-1</sup> )	3.80 <sup>efgh</sup>	5.95 <sup>a</sup>	3.91 <sup>ef</sup>	4.06 <sup>de</sup>	3.93 <sup>ef</sup>	4.21 <sup>d</sup>	4.04 <sup>a</sup>
Average	3.73 <sup>c</sup>	5.43 <sup>a</sup>	3.73 <sup>c</sup>	3.91 <sup>b</sup>	3.88 <sup>b</sup>	3.91 <sup>b</sup>	

**Note:**  $\alpha < 0.05$ ; CV = 0.2%; LSD = 0.1375

Chemical and biological reactions in the soil are controlled by pH (Hendershot and Lalande, 2008). Under strongly acidic conditions, the bioavailability of some of the elements (Ca, P, K and Mg) essential for plant growth are reduced, but some, such as manganese and aluminium, are increased (Agegnehu et al., 2019). Acidity is composed of exchangeable H<sup>+</sup> and exchangeable Al as either Al<sup>3+</sup> or partially neutralised compounds (Al-OH), for example AlOH<sup>2+</sup>, Al(OH)<sub>2</sub><sup>+</sup> and organic acids (Hendershot and Lalande 2008). When the acidity is coupled with Al<sup>3+</sup> toxicity, this leads to poor soil fertility and reduces soil productivity (Han et al., 2019).

Liming is generally used to increase the bioavailability of essential plant nutrients and reduce the toxicity of  $Al^{3+}$ . In this study, therefore, the sludges were expected to ameliorate the acid soil used since they contain solid phases of  $CaCO_3$  and  $Mg(OH)_2$  that can contribute to alkalinity.

### Sludge effects on exchangeable acidity and aluminium

The soil initially showed an exchangeable acidity of  $14.7 \text{ mmol}_c \text{ kg}^{-1}$  (Figure 6.8A). Application of either sludge decreased exchangeable acidity. Applying phosphate on its own at 40 and  $100 \text{ kg ha}^{-1}$  significantly ( $\alpha < 0.05$ ) reduced acidity by 3 and 16% relative to the initial acidity of  $14.7 \text{ mmol}_c \text{ kg}^{-1}$ . This was expected, because phosphate is known to precipitate protons in soils and facilitate an increase in soil pH. The co-application of phosphate with either sludge also significantly ( $\alpha < 0.05$ ) reduced soil acidity. Generally, treatments with the sludge Gyp reduced acidity more than GypFe. As expected, liming reduced soil acidity the most, from 92 to 94% relative to the initial soil acidity.

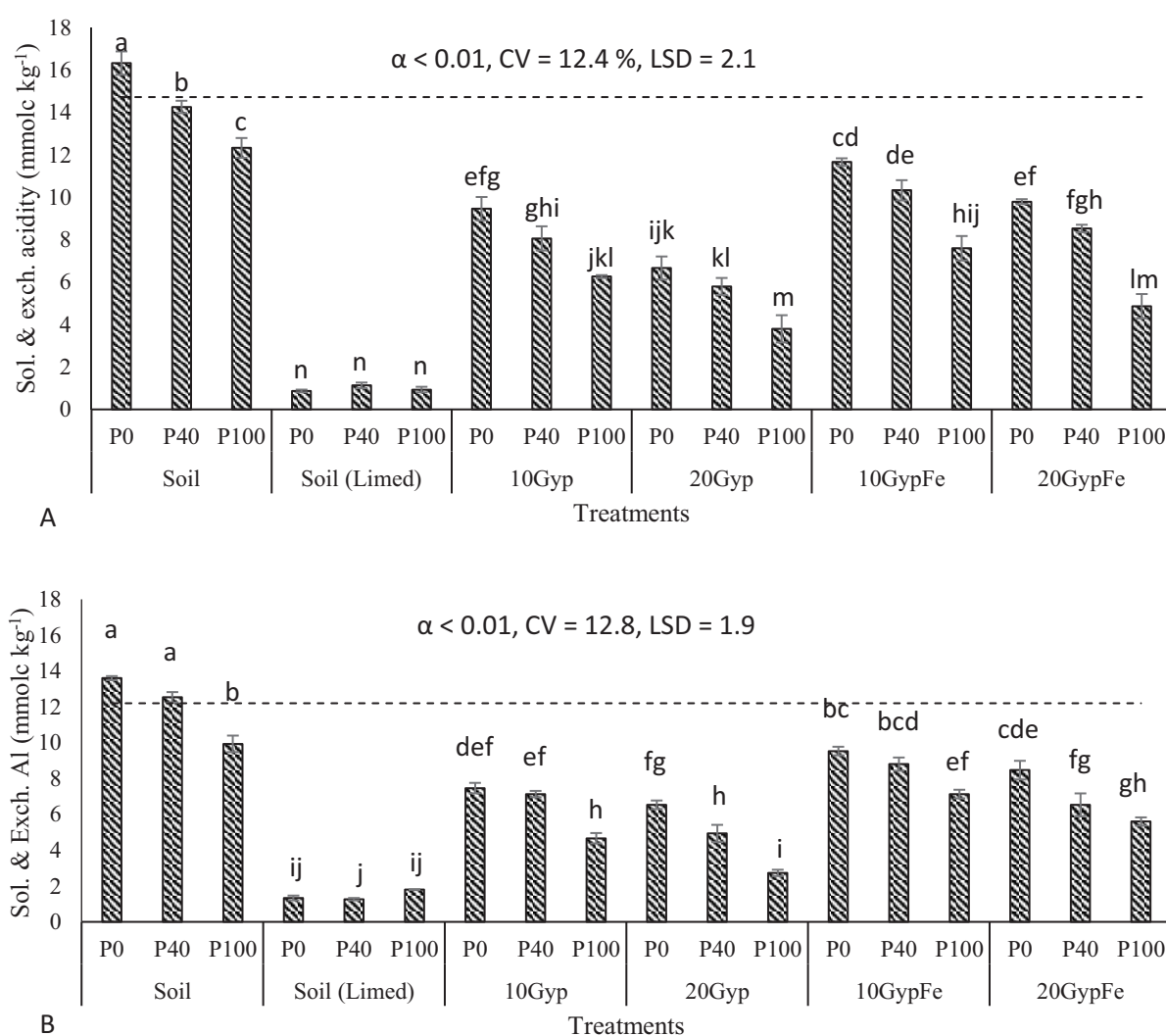


Figure 6.8: A): Exchangeable acidity reduction, dotted line indicates initial exchangeable acidity; B): Exchangeable hydrolysable cations, dashed line indicates initial exchangeable hydrolysable cations.

**Note:** Gyp ( $t \text{ ha}^{-1}$ ) = Gypseous; GypFe ( $t \text{ ha}^{-1}$ ) = Ferriferous gypseous; P ( $\text{kg ha}^{-1}$ ) = Phosphorus

The soil showed initial exchangeable hydrolysable cations (EHC) of  $12.2 \text{ mmol}_c \text{ kg}^{-1}$ . The application of phosphate on its own, or either sludge, significantly ( $\alpha < 0.05$ ) reduced EHC (Figure 6.8B). However, the decrease in EHC was more evident where sludge was applied in combination with phosphate.

It should be noted that treatments with Gyp generally reduced EHC more than those with GypFe. The combined effect of the sludge Gyp applied at 20 t ha<sup>-1</sup> with phosphate at 100 kg ha<sup>-1</sup> reduced EHC the most by 78%. This was expected because phosphate is known to precipitate soluble aluminium under acidic soil conditions, forming sparingly soluble minerals such as variscite (AlPO<sub>4</sub>·2(H<sub>2</sub>O)).

Liming, as expected, reduced EHC more than any other treatment, reducing it by 90% relative to the initial EHC.

### Salinity of soil-sludge mixtures

Although sludges containing iron oxides are known to adsorb elements, they also contain salts, as indicated in Section 6.2, which can increase soil salinity, possibly to levels toxic to plants. There was a significant ( $\alpha < 0.05$ ) increase in salinity with the addition of either sludge.

The application of phosphate on its own significantly ( $\alpha < 0.05$ ) reduced soil salinity (Table 6.15) due to the sequestration of salts through precipitation and co-sorption. The combined effect of either sludge with phosphate was also significant ( $\alpha < 0.05$ ). However, the significant differences were more evident when either of the sludges was applied either on its own or in combination with phosphate. When Gyp and GypFe were applied on their own at 20 t ha<sup>-1</sup>, they significantly increased soil salinity by 813 mS m<sup>-1</sup> and 560 mS m<sup>-1</sup>, levels which are only suitable for salt-tolerant plants. The lesser increase in salinity that occurred with GypFe was probably because this material contained iron oxides that possibly sequestered some of the soluble salts through surface precipitation, complexation or co-sorption. Liming the soil drastically reduced soluble salts as expected, hence salinity was extremely low in these treatments (Table 6.15).

Table 6.15: Effect of treatments on salinity (mS m<sup>-1</sup>) in soil-sludge mixtures

P	Sludges (t ha <sup>-1</sup> )						
	Soil	Soil (limed)	10Gyp	20Gyp	10GypFe	20GypFe	Average
P0	160 <sup>ghi</sup>	13 <sup>i</sup>	576 <sup>cde</sup>	981 <sup>a</sup>	348 <sup>efgh</sup>	728 <sup>bc</sup>	468 <sup>a</sup>
P40 (kg ha <sup>-1</sup> )	122 <sup>hi</sup>	14 <sup>i</sup>	443 <sup>def</sup>	865 <sup>ab</sup>	338 <sup>fgh</sup>	644 <sup>bcd</sup>	404 <sup>b</sup>
P100 (kg ha <sup>-1</sup> )	161 <sup>ghi</sup>	14 <sup>i</sup>	347 <sup>efgh</sup>	818 <sup>ab</sup>	371 <sup>efg</sup>	449 <sup>def</sup>	360 <sup>b</sup>
Average	148 <sup>d</sup>	14 <sup>e</sup>	455 <sup>c</sup>	888 <sup>a</sup>	352 <sup>c</sup>	607 <sup>b</sup>	

Note:  $\alpha < 0.05$ ; CV = 2.1%; LSD = 126

### Is HDS a source of Ca, S and other nutrients?

Total sulphur was extremely low in soil (SP0, SP40, SP100) and in treatments with lime (SLP0, SLP40, SLP100) compared to those with sludges (Figure 6.9A). Total sulphur increased with an increase in the addition of either sludge from 10 to 20 t ha<sup>-1</sup> due to the gypsum it contained. Gyp contributed more total sulphur compared to the same rates of GypFe. This was because Gyp contained more than 95% gypsum compared to GypFe, at 72–77% of this mineral. Similarly, total calcium increased with an increase in the addition of either sludge. This trend was also observed in its availability (Figure 6.9B). Gyp contributed more total and soluble calcium than GypFe to the soil. This was due to the differences in gypsum composition. Both total and available calcium were extremely low in all treatments, with soil alone and with phosphate (SP0, SP40 and SP100).

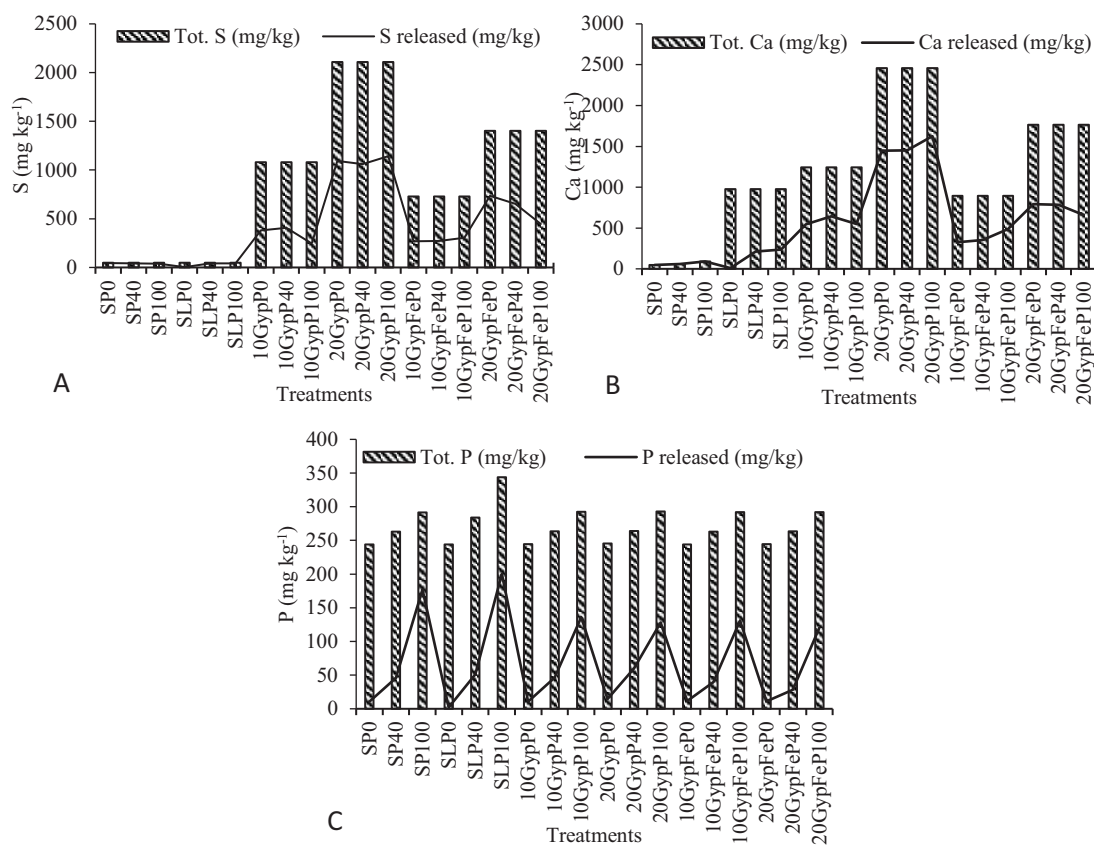


Figure 6.9: Selected major plant nutrients, total and available: A): sulphur; B): calcium; C): phosphorus

An increase in the addition of phosphate increased soil total phosphorus content and its solubility in all treatments (Figure 6.9C). The addition of both sludges reduced soluble phosphorus slightly.

Total manganese in the soil was not affected by the addition of lime, phosphate or Gyp sludge (Figure 6.10A). However, the addition of GypFe significantly increased total manganese, as would be expected, because it contained more than 7,000 mg Mn kg<sup>-1</sup>. Available manganese was greatest for soil alone, but liming soil to pH >5 drastically reduced availability. The addition of either sludge reduced the solubility of this element compared to soil alone, through either precipitation or sorption on reactive mineral surfaces.

Similarly, total iron in treatments with soil alone, soil and phosphate, soil with lime and treatments with Gyp were mostly contributed by soil (Figure 6.10B), as it contained 37,363 mg kg<sup>-1</sup> Fe. Gyp and phosphate source had minimal iron concentration. Increasing the application of GypFe increased total iron as this material contained the most iron (124,500 mg kg<sup>-1</sup>). Soluble iron was extremely low in all treatments (Figure 6.10B).

Total zinc in soil, soil with lime and soil with Gyp was contributed by soil (Figure 6.10C) as it contained 20 mg kg<sup>-1</sup> Zn. Total zinc concentration increased with an increase in the application of GypFe as it contained a significant amount of zinc (285 mg kg<sup>-1</sup>). The solubility of zinc was, on average, greatest in unlimed soils and was increased by the application of phosphate in both unlimed and limed soils. The solubility of zinc in soils containing sludges was, on average, lower than for soils without sludges, and neither phosphate application nor increasing the rate of sludge applied from 10 to 20 t ha<sup>-1</sup> affected the solubility of zinc in soils to which sludge had been added.

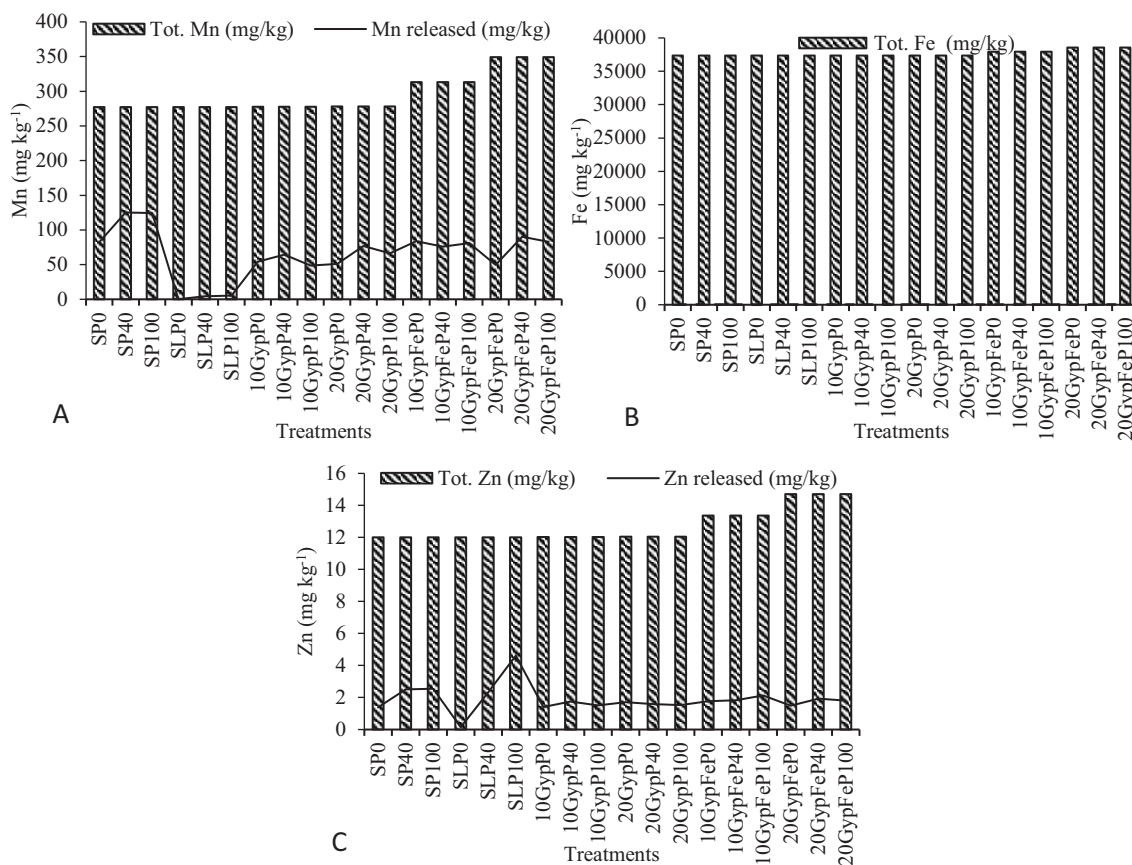


Figure 6.10: Total and available trace elements: A): manganese; B): iron; C): zinc

The effects of nickel and lead in sludges on soil total content and solubility were evaluated because these elements are present in some sludges and have been flagged as being potentially hazardous. Total nickel in soil was contributed mostly by the soil (Figure 6.11A). Total soil nickel was not affected by the addition of phosphorus, lime or Gyp, but was slightly increased by an increase in the application of GypFe, as this material contained 108 mg kg<sup>-1</sup> total nickel. Relative to total concentration, soluble nickel was low in all treatments. The low soil pH (3.75) increased nickel solubility, but liming reduced its availability. Increasing the application of either sludge slightly increased the solubility of nickel, but not greater than soil alone. The application of phosphate did not substantially influence nickel availability.

Total lead in soil, soil with lime and soil with GypFe remained constant at 13.0 mg kg<sup>-1</sup>. Total lead concentration increased to 13.2 mg kg<sup>-1</sup>, with the application of 10 t ha<sup>-1</sup>, and to 13.4 mg kg<sup>-1</sup> with 20 t ha<sup>-1</sup> Gyp, as this material contained 40 mg kg<sup>-1</sup> lead. Keeping the pH of the soil at 3.75 facilitated the solubility of this element, but liming drastically reduced solubility. Adding either sludge increased lead solubility above that shown by the acid soil, but soils with Gyp had more soluble lead than any other treatment.

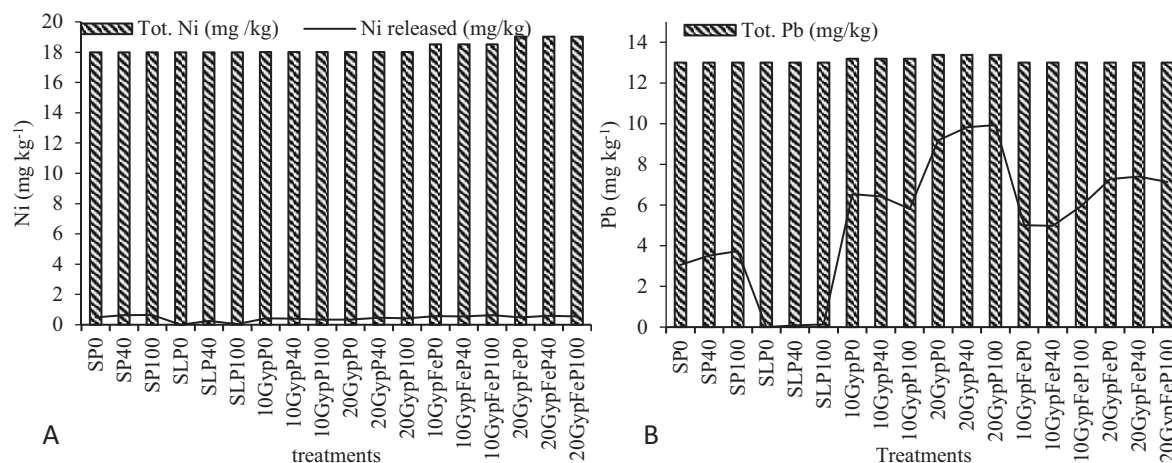


Figure 6.11: Total and available metals: A) nickel; B) lead

### 6.6.3 Conclusions

Applying either sludge with phosphate increased soil pH marginally, and reduced soil acidity significantly, but neither reduced soil acidity to levels ideal for plant growth. Therefore, to use these sludges solely to raise soil pH to >5 would require quantities in excess of 20 t ha<sup>-1</sup>, but this could increase salinity, metal solubility and the sorption of added inorganic plant nutrients like phosphate.

The application of either sludge increased the solubility of calcium and sulphur (through gypsum solubility), but reduced that of phosphate due to sorption by iron oxides in GypFe and precipitation with calcium from both sludges.

Increasing the application of GypFe increased total nickel and manganese in soils, but marginally decreased the solubility of these elements. Increasing Gyp marginally increased total lead in soils, and also increased lead solubility. Irrespective of the sludge source, both are suitable for the supply of calcium and sulphur in acid soils.

## 6.7 THE CROP RESPONSE OF HIGH-DENSITY SLUDGE AS A SOIL AMENDMENT

### 6.7.1 Materials and methods

#### Development of sludge-soil mixtures

A homogeneous mixture of sludge and soil was required for plant growth. Each of the sludges was applied at two rates (10 and 20 t ha<sup>-1</sup> on a mass/mass basis) and thoroughly mixed with 8.8 kg of soil that was prepared by sieving through a 5 mm sieve. The mass of soil per hectare was estimated to be 2.1 x 10<sup>6</sup> kg assuming a 0.15 depth and a density of 1,400 kg m<sup>-3</sup>. Each HDS-soil mixture was then transferred into pots with 26 cm top and 20 cm bottom diameters and a height of 25 cm. They also had three small openings at the bottom to allow for drainage.

#### Experimental design

The experiment had 18 treatments with a total of six controls. Three of the controls received lime (Ca(OH)<sub>2</sub>) at 3.7 t ha<sup>-1</sup> and different levels of phosphorus, and were considered “positive controls”, while the other three received no lime at three phosphorus levels and were considered to be “negative controls” (Table 6.16). The other 12 treatments were made up of the two HDS materials, each at two rates of HDS, and each with three levels of phosphorus application. All treatments were replicated three times. This experiment was arranged in a randomised complete block design (RCBD).

Table 6.16: Treatments

Treatment	Comments	Description of treatments
Soil + lime SoilP40+lime SoilP100+lime	Positive control	3.7 t ha <sup>-1</sup> lime 40 kg ha <sup>-1</sup> P; 3.7 t ha <sup>-1</sup> lime 100 kg ha <sup>-1</sup> P; 3.7 t ha <sup>-1</sup> lime
Soil SoilP40 SoilP100	Negative control – soil unlimed	40 kg ha <sup>-1</sup> P 100 kg ha <sup>-1</sup> P
10GypP0 10GypP40 10GypP100 20GypP0 20GypP40 20GypP100 10GypFeP0 10GypFeP40 10GypFeP100 20GypFeP0 20GypFeP40 20GypFeP100		10 t ha <sup>-1</sup> Gyp; 0 kg ha <sup>-1</sup> P 10 t ha <sup>-1</sup> Gyp; 40 kg ha <sup>-1</sup> P 10 t ha <sup>-1</sup> Gyp; 100 kg ha <sup>-1</sup> P 20 t ha <sup>-1</sup> Gyp; 0 kg ha <sup>-1</sup> P 20 t ha <sup>-1</sup> Gyp; 40 kg ha <sup>-1</sup> P 20 t ha <sup>-1</sup> Gyp; 100 kg ha <sup>-1</sup> P 10 t ha <sup>-1</sup> GypFe; 0 kg ha <sup>-1</sup> P 10 t ha <sup>-1</sup> GypFe; 40 kg ha <sup>-1</sup> P 10 t ha <sup>-1</sup> GypFe; 100 kg ha <sup>-1</sup> P 20 t ha <sup>-1</sup> GypFe; 0 kg ha <sup>-1</sup> P 20 t ha <sup>-1</sup> GypFe; 40 kg ha <sup>-1</sup> P 20 t ha <sup>-1</sup> GypFe; 100 kg ha <sup>-1</sup> P

**Note:** Gyp (t ha<sup>-1</sup>) = Gypseous; GypFe (t ha<sup>-1</sup>) = Ferriferous gypseous; P (kg ha<sup>-1</sup>) = Phosphate

### Sources of sludges and soil used

Two sludges from the Mpumalanga coalfields of South Africa, selected based on the different processes used to generate them, were tested. One of the sludges was sourced from a limestone treatment plant (GypFe) containing largely gypsum and iron oxides. The other (Gyp) was refined from limestone plus lime treatment and was dominated by gypsum. To assess their full potential as soil amendments, an acid soil with a pH of 3.75, low in base elements, was selected.

### Determination of basic chemical properties of both sludges and soil

Basic chemical properties of both sludges and soil were determined before and after the establishment of HDS-soil mixtures. The individual sludges and soil were analysed for chemical status as defined in Section 6.6 above. The determination of pH and EC was done after harvesting in the soil-sludge mixtures and before the start of the experiment in the individual sludges and soil.

### Fertilizer choice, application and planting

The GypFe had the potential to sequester some of the essential applied plant nutrients, especially phosphate, due to the abundance of ferric hydroxide. To test this, a prior phosphate sorption study was carried out and the sludge was shown to have the ability to sequester 27 kg of phosphate per ton. Three phosphate application rates were adopted: a control (0 kg ha<sup>-1</sup>), a recommended rate of 40 kg ha<sup>-1</sup> (Mengel and Kirkby, 2001; MIG, 2017) and a rate (100 kg ha<sup>-1</sup>) well above the recommendation. Phosphate was also added to test if it can aid in decreasing the uptake of nickel and lead from HDS. To minimise the introduction of any impurities, a reagent grade potassium dihydrogen phosphate (KH<sub>2</sub>PO<sub>4</sub>) was used as the source of phosphate. This source also provided some of the potassium needed by the maize, but as this was insufficient to supply the recommended 40 kg K ha<sup>-1</sup>, additional potassium was applied as reagent grade potassium chloride. Nitrogen was applied at a recommended rate of 100 kg ha<sup>-1</sup> as reagent grade diammonium hydrogen phosphate ((NH<sub>4</sub>)<sub>2</sub>HPO<sub>4</sub>). This source of nitrogen provided additional phosphate that was taken into account to achieve the selected rates of 40 and 100 kg P ha<sup>-1</sup>.

To benefit from the addition of nitrogen and potassium,  $\text{KH}_2\text{PO}_4$  (70%) and 30%  $(\text{NH}_4)_2\text{PO}_4$  were added to the HDS-soil mix. As an application strategy, sources of phosphorus and potassium were applied in a single dose and spread 5 mm below the seed, while the nitrogen application was split into two applications during vegetative growth. Maize (*Zea mays*) (variety DKC73 – 74BRGEN) was selected based on its acidity (pH 5.5–6.5) and salinity ( $180 \text{ mS m}^{-1}$ ) tolerance and since it is the most common crop planted in Mpumalanga. Five seeds were planted in each pot at a depth of 5 mm. The five seeds were intended to allow plant sampling at different time intervals. The maize was harvested at physiological maturity (after 140 days) to determine final yield and enable food safety assessment of the grain.

### **Crop management and data collection**

Tap water was used for irrigation. Initially, all treatments were irrigated to field capacity, which was calculated to be 2.55 l per pot, but water added to reach field capacity after three days was calculated to be approximately 1 l, which was determined as a difference by weighing the pots. During active vegetative growth, the litre of water needed to refill the pots to field capacity was required every two days. This amount was applied every second day until harvesting. Samples were collected by destructive sampling, cutting one of the plants off at soil level at the following development stages: V3 (third leaf collar evident), V7 (seventh leaf collar evident), V10 (tenth leaf collar evident), VT (tasselling) and R6 (physiological maturity, milk line no longer evident, black layer formed). Data collected at the V3 to VT stages included plant height, leaf area, plant biomass and assessment of metal uptake in leaves. At R6, data collected included the number of cobs, yield (leaves, stems and grains) and concentrations of potentially toxic metals in leaves and grains.

### **Grain and leaf chemical composition**

The grain was harvested at physiological maturity. To assess nutritional value, the chemical composition of both grain and leaves was determined following the US EPA 3052 method, as described under the section on the determination of the total elemental status of sludges and soil. The focus was on selected major plant nutrients (calcium, sulphur and phosphorus) and trace elements (manganese and iron), as calcium, sulphur, manganese and iron were expected to be a contribution of both sludges. The phosphorus was included to assess the potential of the sludges to reduce the availability of this element. Nickel and lead were analysed as both elements have been identified as providing potential risk to food security as they identified components of concern in the sludges tested.

### **Statistical analysis**

All statistical analyses were carried out using SAS Version 9.4. ANOVA to establish differences among treatments. To separate means, the LSD separation test was used. To assess the main effects, averages were calculated across the sludges and phosphate levels applied.

### **Food safety assessment**

Food safety standards for humans were assessed using Codex Alimentarius (2006). Codex is a collection of internationally adopted standards (developed by different countries) and related texts aimed at protecting consumers' health and ensuring fair practices in the food trade (Codex Alimentarius Commission, 2010). The main concern in this study was the concentration of lead and nickel in maize grain. While cereal grain contaminants of concern in Codex Alimentarius include lead, with a threshold set at  $0.2 \text{ mg kg}^{-1}$ , they do not include nickel. Accordingly, a different food safety standard had to be selected to assess nickel toxicity in the grain. Several food standards (European, Canadian, US, Australian and South African) were scrutinised to see if nickel was included, but none consider it a toxic contaminant in food. The Chinese food standards only assess nickel in fats in their products, i.e. in hydrogenated vegetable oils and hydrogenated vegetable oil-based products. The threshold for nickel was set at  $1.0 \text{ mg kg}^{-1}$  on a dry basis (National Standard of the People's Republic of China, 2012).

Also investigated was animal feed safety in case the fodder, including grain, is fed to animals. Standards of the Food and Agricultural Organisation (FAO) (1997), the European Commission (2002) and the Department of Agriculture of South Africa (Department of Agriculture, 2006) were considered.

The European Commission (2002), together with its member states, does not consider nickel as toxic in animal feed, and accordingly, it is excluded from its standards, but the lead threshold was set at 40 mg kg<sup>-1</sup>. The Standards of the FAO (1997) and the Department of Agriculture of South Africa (Department of Agriculture, 2006) were considered because they include thresholds for both nickel and lead. With lead, both guidelines have set the threshold at 40 mg kg<sup>-1</sup>. The FAO (1997) considers nickel moderately toxic, and has set its threshold at 100 mg kg<sup>-1</sup>, while the South African Department of Agriculture (2006) has set it at 50 mg kg<sup>-1</sup>.

## 6.7.2 Results and discussion

### Sludge effects on the germination of maize seeds

Seeds in the limed soil treatments took the shortest time (four days) to germinate, compared to five to eight days taken by all other treatments. This was expected, as the soil was limed to a pH >5, which is conducive for plant growth, whereas the other treatments were still acidic with an initial pH of 3.75. There was no clear effect of the other treatments in the percentage germination of seeds (Figure 6.12).

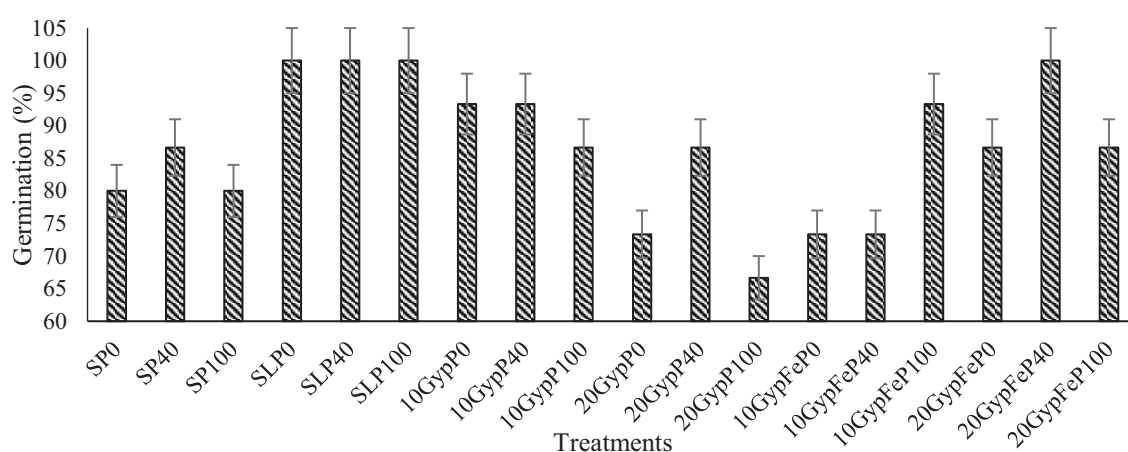


Figure 6.12: Germination (percentage) in the pot trial with different sludge-soil treatment combinations

### The influence of sludge on plant growth of maize

Adding sludges on their own at both rates (10 and 20 t ha<sup>-1</sup>) or in co-application with phosphate increased average plant height (Table 6.17). The application of phosphate on its own significantly increased plant height, but the heights recorded at 40 and 100 kg ha<sup>-1</sup> phosphorus were not significantly different from each other.

Table 6.17: Final height (cm) of maize plants in a pot trial with different sludge-soil treatment combinations as growth medium

Sludge	Soil	SL	10Gyp	20Gyp	10GypFe	20GypFe	Average
P0	65 <sup>e</sup>	63 <sup>e</sup>	96 <sup>d</sup>	141 <sup>abcd</sup>	118 <sup>bcde</sup>	102 <sup>cde</sup>	97 <sup>b</sup>
P40	133 <sup>abcd</sup>	184 <sup>a</sup>	132 <sup>abcd</sup>	131 <sup>abcd</sup>	130 <sup>abcd</sup>	151 <sup>abcd</sup>	143 <sup>a</sup>
P100	136 <sup>abcd</sup>	182 <sup>a</sup>	149 <sup>abcd</sup>	160 <sup>abc</sup>	123 <sup>abcde</sup>	166 <sup>ab</sup>	153 <sup>a</sup>
Average	111 <sup>b</sup>	143 <sup>a</sup>	126 <sup>ab</sup>	144 <sup>a</sup>	124 <sup>ab</sup>	140 <sup>a</sup>	

$\alpha < 0.05$ ; CV = 3.6%; LSD = 33.2

The increase in crop height was rapid from germination for all treatments except treatments SP0 and SLP0 until the 90th day (figures 6.13A to 6.13D), after which some started to exhibit slowed growth responses. However, as expected from a determinate crop, all treatments stopped increasing in height after tasselling, which occurred after 100 days (figures 6.13A to 6.13C). Tasselling occurred earlier, i.e. after 90 days, for the limed soil where phosphate was applied at 40 and 100 kg ha<sup>-1</sup> phosphorus (Figure 6.13D). The addition of phosphate or any of the sludge products on their own increased plant growth significantly compared to soil receiving neither phosphate nor sludge. The crop growing in treatments without phosphate and sludge were only able to reach a height of 65 cm (Table 6.18). This suggested that the individual sludges had the potential to increase plant growth. Any combination of either sludge or phosphate increased growth more than when phosphate or sludge was applied on its own.

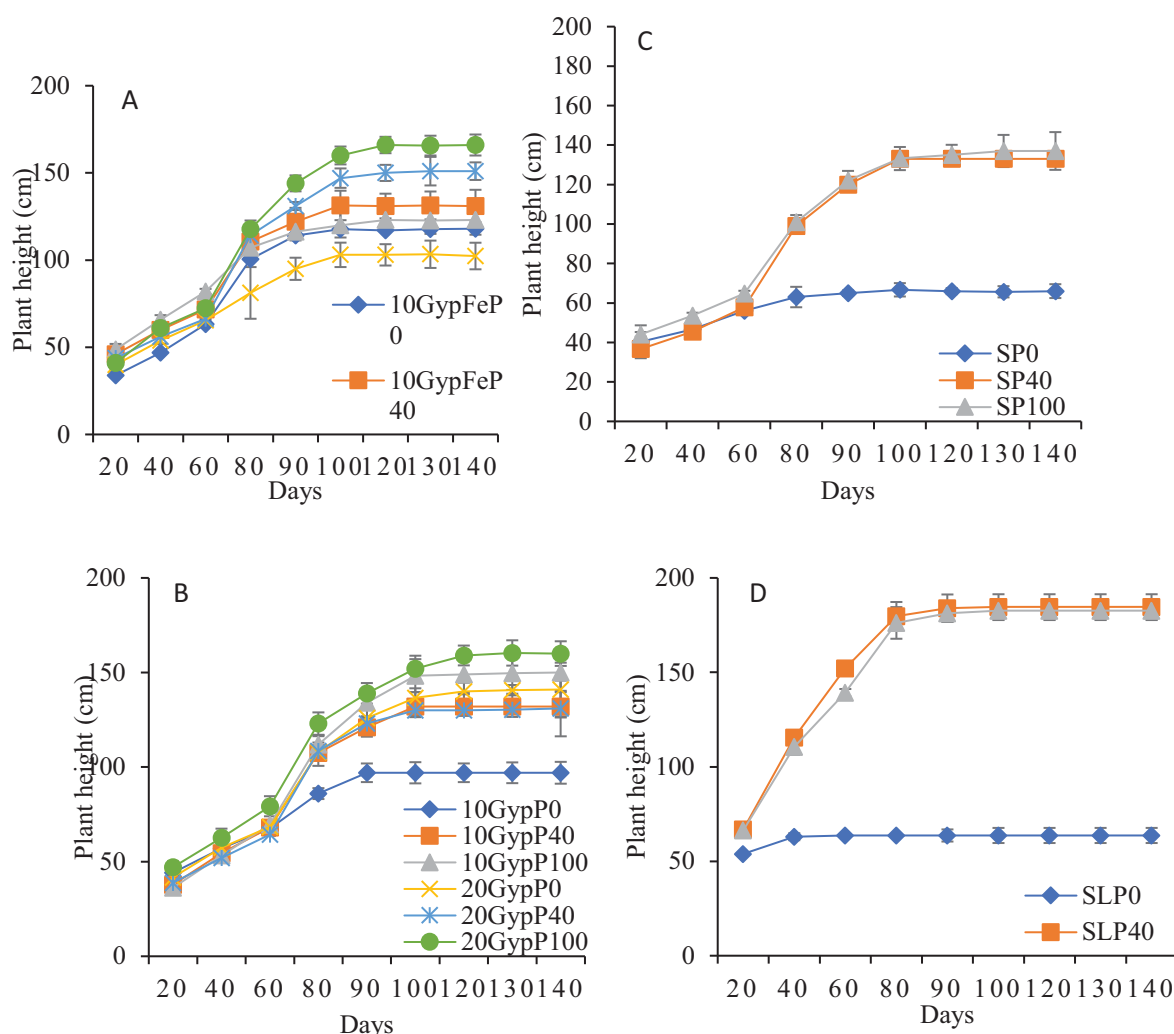


Figure 6.13: Plant height for: A: Soil + GypFe; B: Soil + Gyp; C: Soil only; D: Limed soil

### The influence of sludge on total biomass of maize

The application of phosphate, whether on its own or in combination with sludge, increased total plant biomass. This was more evident and significant ( $\alpha < 0.05$ ) in treatments with and without lime and where the sludge GypFe was applied at 20 t ha<sup>-1</sup> (Figure 6.14).

The addition of either sludge at 20 t ha<sup>-1</sup> (on its own, as well as in combination with phosphorus) showed a slight increase in plant biomass. However, this increase was not statistically significant, compared to the lower rate (10 t ha<sup>-1</sup>). Liming the soil and applying phosphate at 40 and 100 kg ha<sup>-1</sup> significantly increased biomass relative to that of soil without lime.

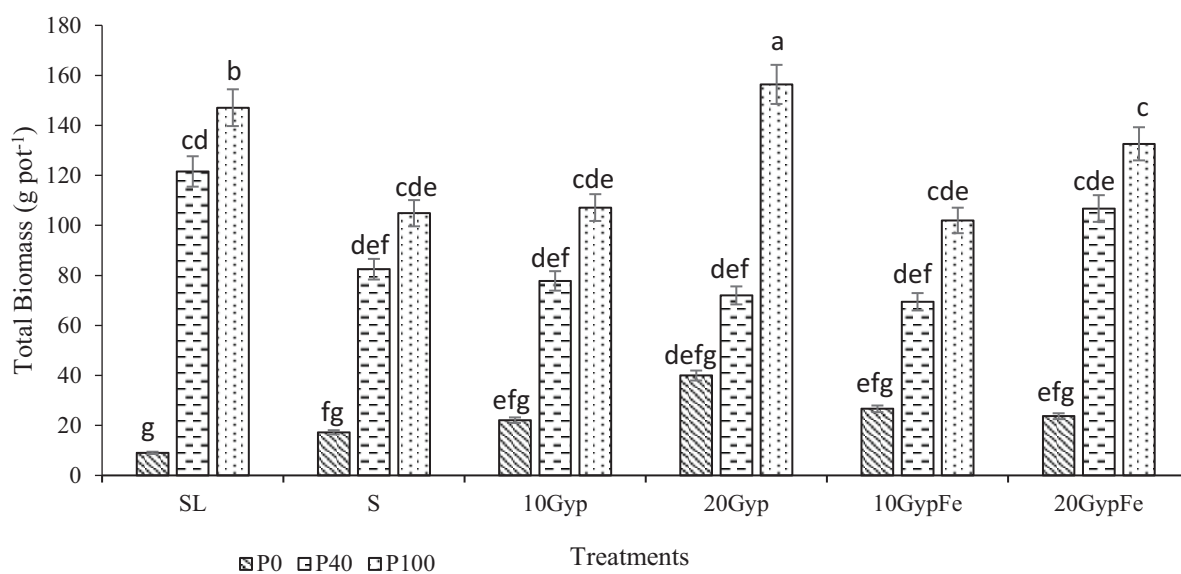


Figure 6.14: Total plant biomass comparisons

### The influence of sludge on calcium, sulphur and phosphorus uptake by leaves, stem and tassels of maize

#### Calcium

Sludge treatment resulted in much greater concentrations of calcium in all plant parts in comparison to soils with and without lime (Table 6.18). Calcium concentrations were lowest for plants grown on limed soils. Phosphate increased the calcium content of all plant parts, but had a much smaller effect than sludge. The concentration of calcium in leaf dry matter for all treatments with sludges was above 5,000 mg kg<sup>-1</sup>, which was reported as adequate for plant growth (Jones, 2012; Bindraban et al., 2015).

Table 6.18: Sludge, lime and phosphate effects on calcium concentration ( $\text{mg kg}^{-1}$ ) in maize stems, leaves and tassels

Plant part	Calcium							
	Sludge	S	SL	10Gyp	20Gyp	10GypFe	20GypFe	Average
Leaves	P0	3,404 <sup>f</sup>	4,384 <sup>ef</sup>	6,581 <sup>cdef</sup>	8,740 <sup>abcde</sup>	7,356 <sup>bcdef</sup>	7,025 <sup>bcdef</sup>	<b>6,248<sup>b</sup></b>
	P40	6,290 <sup>cdef</sup>	8,615 <sup>abcde</sup>	10,175 <sup>abc</sup>	10,930 <sup>abc</sup>	8,692 <sup>abcde</sup>	1,1537 <sup>ab</sup>	<b>9,373<sup>a</sup></b>
	P100	4,738 <sup>def</sup>	7,338 <sup>bcdef</sup>	10,377 <sup>abc</sup>	13,257 <sup>a</sup>	9,202 <sup>abcd</sup>	9,724 <sup>abc</sup>	<b>9,106<sup>a</sup></b>
	<b>Average</b>	<b>4,811<sup>d</sup></b>	<b>6779<sup>cd</sup></b>	<b>9,044<sup>abc</sup></b>	<b>10,976<sup>a</sup></b>	<b>8,417<sup>bc</sup></b>	<b>9,429<sup>ab</sup></b>	
Stem	P0	1,178 <sup>ef</sup>	ND	3,923 <sup>ab</sup>	3,515 <sup>abc</sup>	3,419 <sup>abc</sup>	2,594 <sup>cd</sup>	<b>2,438<sup>b</sup></b>
	P40	1,158 <sup>ef</sup>	2,118 <sup>de</sup>	3,672 <sup>abc</sup>	4,468 <sup>a</sup>	2,802 <sup>bcd</sup>	3,177 <sup>bcd</sup>	<b>2,899<sup>a</sup></b>
	P100	1,240 <sup>e</sup>	1,239 <sup>e</sup>	3,116 <sup>bcd</sup>	3,948 <sup>ab</sup>	2,967 <sup>bcd</sup>	2,679 <sup>cd</sup>	<b>2,532<sup>b</sup></b>
	<b>Average</b>	<b>1,192<sup>d</sup></b>	<b>1119<sup>d</sup></b>	<b>3,570<sup>ab</sup></b>	<b>3,977<sup>a</sup></b>	<b>3,063<sup>bc</sup></b>	<b>2,817<sup>c</sup></b>	
Tassel	P0	538 <sup>ef</sup>	ND	2,052 <sup>de</sup>	2,954 <sup>abcd</sup>	2,522 <sup>bcde</sup>	2,223 <sup>cde</sup>	<b>1,715<sup>b</sup></b>
	P40	2,779 <sup>abcd</sup>	2,801 <sup>abcd</sup>	3,383 <sup>abcd</sup>	4,622 <sup>a</sup>	2,712 <sup>abcd</sup>	4,331 <sup>ab</sup>	<b>3,438<sup>a</sup></b>
	P100	2,455 <sup>bcde</sup>	2,454 <sup>bcde</sup>	4,097 <sup>abc</sup>	4,381 <sup>ab</sup>	3,454 <sup>abcd</sup>	3,300 <sup>abcd</sup>	<b>3,357<sup>a</sup></b>
	<b>Average</b>	<b>1,924<sup>c</sup></b>	<b>1,752<sup>c</sup></b>	<b>3,177<sup>ab</sup></b>	<b>3,986<sup>a</sup></b>	<b>2,896<sup>b</sup></b>	<b>3,285<sup>ab</sup></b>	

**Notes:** Leaves:  $\alpha < 0.05$ ; CV = 3.3%; LSD = 2,537; Stem:  $\alpha < 0.05$ ; CV = 3.3%; LSD = 667; Tassel:  $\alpha < 0.05$ ; CV = 2.1%; LSD = 1,093. Note: ND = Not determined

### Sulphur

The application of either sludge significantly increased the concentration of sulphur in all plant parts in comparison to soil alone or limed soil. Liming, if anything, slightly reduced plant sulphur content. Sulphur was mostly concentrated in the leaves, compared to the stem and tassels (Table 6.19). The sulphur concentration for all plant leaves still exceeded 1,000  $\text{mg kg}^{-1}$ , which is considered adequate for plant growth (Jones, 2012; Bindraban et al., 2015).

Table 6.19: Sludge, lime and phosphate effects on sulphur concentration ( $\text{mg kg}^{-1}$ ) in leaves, stems and tassels of maize

Plant parts	Sulphur							
	Sludge	S	SL	10Gyp	20Gyp	10GypFe	20GypFe	Average
Leaves	P0	1,957 <sup>e</sup>	1,582 <sup>e</sup>	4,601 <sup>bcd</sup>	8,567 <sup>a</sup>	4,217 <sup>bcd</sup>	5,989 <sup>b</sup>	<b>4,486<sup>a</sup></b>
	P40	2,572 <sup>de</sup>	1,564 <sup>e</sup>	4,233 <sup>bcd</sup>	4,998 <sup>bc</sup>	3,325 <sup>cde</sup>	4,491 <sup>bcd</sup>	<b>3,531<sup>b</sup></b>
	P100	2,389 <sup>de</sup>	1,865 <sup>e</sup>	3,194 <sup>cde</sup>	4,907 <sup>bc</sup>	3,201 <sup>cde</sup>	3,455 <sup>cde</sup>	<b>3,169<sup>b</sup></b>
	<b>Average</b>	<b>2,306<sup>c</sup></b>	<b>1,670<sup>c</sup></b>	<b>4,009<sup>b</sup></b>	<b>6,158<sup>a</sup></b>	<b>3,581<sup>b</sup></b>	<b>4,645<sup>b</sup></b>	
Stem	P0	712 <sup>cde</sup>	ND	1,699 <sup>ab</sup>	1,879 <sup>a</sup>	1,399 <sup>abc</sup>	1,348 <sup>abc</sup>	<b>1,173<sup>a</sup></b>
	P40	825 <sup>bcde</sup>	279 <sup>de</sup>	1,604 <sup>abc</sup>	1,849 <sup>a</sup>	9,75 <sup>abcd</sup>	1,537 <sup>abc</sup>	<b>1,178<sup>a</sup></b>
	P100	686 <sup>cde</sup>	352 <sup>de</sup>	1,443 <sup>abc</sup>	1,801 <sup>a</sup>	1,515 <sup>abc</sup>	1,599 <sup>abc</sup>	<b>1,233<sup>a</sup></b>
	<b>Average</b>	<b>741<sup>c</sup></b>	<b>210<sup>d</sup></b>	<b>1,582<sup>ab</sup></b>	<b>1,843<sup>a</sup></b>	<b>1,296<sup>b</sup></b>	<b>1,495<sup>ab</sup></b>	
Tassel	P0	714 <sup>de</sup>	ND	1,384 <sup>bcd</sup>	2,110 <sup>ab</sup>	1,420 <sup>bcd</sup>	1,482 <sup>bcd</sup>	<b>1,185<sup>b</sup></b>
	P40	1,730 <sup>abc</sup>	929 <sup>cd</sup>	1,613 <sup>abc</sup>	2,425 <sup>a</sup>	1,554 <sup>bcd</sup>	1,866 <sup>ab</sup>	<b>1,686<sup>a</sup></b>
	P100	1,909 <sup>ab</sup>	977 <sup>cd</sup>	1,999 <sup>ab</sup>	2,156 <sup>ab</sup>	1,954 <sup>ab</sup>	2,022 <sup>ab</sup>	<b>1,836<sup>a</sup></b>
	<b>Average</b>	<b>1,451<sup>b</sup></b>	<b>635<sup>c</sup></b>	<b>1,665<sup>b</sup></b>	<b>2,230<sup>a</sup></b>	<b>1,643<sup>b</sup></b>	<b>1,790<sup>b</sup></b>	

**Notes:** Leaves:  $\alpha < 0.05$ ; CV = 4.6%; LSD = 1,212.8; Stem:  $\alpha < 0.05$ ; CV = 5.5%; LSD = 504; Tassel:  $\alpha < 0.05$ ; CV = 1.7%; LSD = 464. Note: ND = Not determined

*Phosphorus*

The application of phosphate resulted in a substantial increase in the concentration of this element in all plant parts (Table 6.20). The application of either sludge had no significant effect ( $\alpha > 0.05$ ) on the phosphate concentration in the stem and tassels, but incremental sludge application slightly reduced the phosphorus concentration in leaves.

Table 6.20: Sludge, lime and phosphorus effects on phosphorus concentration ( $\text{mg kg}^{-1}$ ) in maize leaves, stems and tassels

Plant parts	Phosphorus							
	Sludge	S	SL	10Gyp	20Gyp	10GypFe	20GypFe	Average
Leaves	P0	709 <sup>b</sup>	1087 <sup>b</sup>	940 <sup>b</sup>	874 <sup>b</sup>	749 <sup>b</sup>	925 <sup>b</sup>	<b>881<sup>b</sup></b>
	P40	1,602 <sup>b</sup>	521 <sup>b</sup>	1,195 <sup>b</sup>	840 <sup>b</sup>	781 <sup>b</sup>	690 <sup>b</sup>	<b>938<sup>b</sup></b>
	P100	3,750 <sup>a</sup>	1,709 <sup>b</sup>	1,675 <sup>b</sup>	1,366 <sup>b</sup>	1,859 <sup>b</sup>	1544 <sup>b</sup>	<b>1,984<sup>a</sup></b>
	<b>Average</b>	<b>2,020<sup>a</sup></b>	<b>1,106<sup>b</sup></b>	<b>1,270<sup>ab</sup></b>	<b>1,027<sup>b</sup></b>	<b>1,130<sup>b</sup></b>	<b>1,053<sup>b</sup></b>	
Stem	P0	625 <sup>bc</sup>	<b>ND</b>	578 <sup>bc</sup>	498 <sup>bc</sup>	640 <sup>bc</sup>	749 <sup>bc</sup>	<b>515<sup>b</sup></b>
	P40	1,018 <sup>bc</sup>	270 <sup>c</sup>	660 <sup>bc</sup>	707 <sup>bc</sup>	703 <sup>bc</sup>	527 <sup>bc</sup>	<b>648<sup>b</sup></b>
	P100	1,454 <sup>b</sup>	2,684 <sup>a</sup>	739 <sup>bc</sup>	596 <sup>bc</sup>	706 <sup>bc</sup>	964 <sup>bc</sup>	<b>1,191<sup>a</sup></b>
	<b>Average</b>	<b>1,032<sup>a</sup></b>	<b>985<sup>a</sup></b>	<b>659<sup>a</sup></b>	<b>600<sup>a</sup></b>	<b>683<sup>a</sup></b>	<b>747<sup>a</sup></b>	
Tassel	P0	522 <sup>bc</sup>	<b>ND</b>	620 <sup>bc</sup>	857 <sup>bc</sup>	715 <sup>bc</sup>	929 <sup>bc</sup>	<b>607<sup>c</sup></b>
	P40	1,964 <sup>ab</sup>	1,281 <sup>bc</sup>	1,232 <sup>bc</sup>	1,251 <sup>bc</sup>	927 <sup>bc</sup>	760 <sup>bc</sup>	<b>1,236<sup>b</sup></b>
	P100	3,487 <sup>a</sup>	3,617 <sup>a</sup>	1,957 <sup>ab</sup>	2,172 <sup>ab</sup>	2,005 <sup>ab</sup>	2,164 <sup>ab</sup>	<b>2,567<sup>a</sup></b>
	<b>Average</b>	<b>1,991<sup>a</sup></b>	<b>1,633<sup>a</sup></b>	<b>1,270<sup>a</sup></b>	<b>1,427<sup>a</sup></b>	<b>1,216<sup>a</sup></b>	<b>1,284<sup>a</sup></b>	

Notes: Leaves:  $\alpha < 0.05$ ; CV = 9.6%; LSD = 938; Stem:  $\alpha < 0.05$ ; CV = 10.9%; LSD = 635; Tassel:  $\alpha < 0.05$ ; CV = 10.8%; LSD = 973. Note: ND = Not determined

### The influence of sludge on the uptake of trace elements (iron and manganese) by plant parts

*Iron*

The concentration of iron in plant leaves and tassels was much greater for plants grown in limed soil than it was for plants grown in soil with added sludges. Adding sludges resulted in the same concentrations of iron in plant parts as was found for plant parts grown in soils without lime or sludge. Iron was more concentrated in the leaves than in the stem and tassels (Table 6.21). Phosphorus application significantly decreased ( $\alpha < 0.05$ ) the concentration of iron in the leaves, tassels and stems. The concentration of this element in plant leaves exceeded  $100 \text{ mg kg}^{-1}$ , which was reported by Jones (2012) and Bindraban et al. (2015) as adequate for plant growth.

Table 6.21: Iron ( $\text{mg kg}^{-1}$ ) in biomass of maize

Plant parts	Iron							
	Sludge	S	SL	10Gyp	20Gyp	10GypFe	20GypFe	Average
Leaves	P0	265 <sup>b</sup>	1231 <sup>a</sup>	132 <sup>b</sup>	187 <sup>b</sup>	308 <sup>b</sup>	181 <sup>b</sup>	<b>384<sup>a</sup></b>
	P40	168 <sup>b</sup>	370 <sup>b</sup>	132 <sup>b</sup>	137 <sup>b</sup>	176 <sup>b</sup>	188 <sup>b</sup>	<b>195<sup>ab</sup></b>
	P100	131 <sup>b</sup>	436 <sup>b</sup>	123 <sup>b</sup>	150 <sup>b</sup>	142 <sup>b</sup>	129 <sup>b</sup>	<b>185<sup>b</sup></b>
	<b>Average</b>	<b>188<sup>b</sup></b>	<b>679<sup>a</sup></b>	<b>129<sup>b</sup></b>	<b>158<sup>b</sup></b>	<b>209<sup>b</sup></b>	<b>166<sup>b</sup></b>	
Stem	P0	36 <sup>ab</sup>	ND	53 <sup>a</sup>	14 <sup>b</sup>	17 <sup>ab</sup>	23 <sup>ab</sup>	<b>24<sup>a</sup></b>
	P40	24 <sup>ab</sup>	15 <sup>ab</sup>	16 <sup>ab</sup>	13 <sup>b</sup>	11 <sup>b</sup>	15 <sup>ab</sup>	<b>16<sup>a</sup></b>
	P100	17 <sup>ab</sup>	15 <sup>ab</sup>	15 <sup>ab</sup>	15 <sup>ab</sup>	30 <sup>ab</sup>	10 <sup>b</sup>	<b>17<sup>a</sup></b>

Plant parts	Iron							
	Sludge	S	SL	10Gyp	20Gyp	10GypFe	20GypFe	Average
	Average	26 <sup>a</sup>	10 <sup>a</sup>	28 <sup>a</sup>	14 <sup>a</sup>	20 <sup>a</sup>	16 <sup>a</sup>	
Tassel	P0	26 <sup>b</sup>	ND	24 <sup>b</sup>	37 <sup>b</sup>	32 <sup>b</sup>	23 <sup>b</sup>	24 <sup>b</sup>
	P40	37 <sup>b</sup>	140 <sup>a</sup>	31 <sup>b</sup>	49 <sup>b</sup>	47 <sup>b</sup>	45 <sup>b</sup>	58 <sup>a</sup>
	P100	48 <sup>b</sup>	140 <sup>a</sup>	35 <sup>b</sup>	51 <sup>b</sup>	32 <sup>b</sup>	52 <sup>b</sup>	60 <sup>a</sup>
	Average	37 <sup>b</sup>	93 <sup>a</sup>	30 <sup>b</sup>	45 <sup>b</sup>	37 <sup>b</sup>	40 <sup>b</sup>	

**Notes:** Leaves:  $\alpha < 0.05$ ; CV = 4.8%; LSD = 397; Stem:  $\alpha < 0.05$ ; CV = 12.5%; LSD = 21.4; Tassel:  $\alpha < 0.05$ ; CV = 2.5%; LSD = 33.6. Note: ND = Not determined

### Manganese

The application of either sludge significantly reduced the concentration of manganese in leaves, stems and tassels in comparison to soils without lime or sludge. Liming resulted in the greatest decrease in manganese concentration in all plant parts. Manganese was concentrated more in the leaves than in the stem and tassels (Table 6.21). The stem showed substantially lower manganese levels than the leaves and tassels. Phosphate application significantly increased ( $\alpha < 0.05$ ) the concentration of manganese in all plant parts (Table 6.22). The concentration of manganese greatly exceeded the 50 mg kg<sup>-1</sup> that was reported by Jones (2012) and Bindraban et al. (2015) as adequate for plant growth.

The plant concentrations of manganese from plants grown with GypFe, which contains in excess of 7,000 mg kg<sup>-1</sup>, were lower than those in plants grown with Gyp, which contained very little manganese. This would indicate that the manganese contained in sludges is very poorly available to plants grown with this ameliorant, even when the soil/sludge mixture is acidic, and well below a pH of 4.5.

Table 6.22: Manganese (mg kg<sup>-1</sup>) in biomass of maize

Plant parts	Manganese							
	Sludge	S	SL	10Gyp	20Gyp	10GypFe	20GypFe	Average
Leaves	P0	1,592 <sup>bcd</sup>	102 <sup>e</sup>	1,243 <sup>cde</sup>	1,935 <sup>abc</sup>	1,178 <sup>cde</sup>	1,178 <sup>cde</sup>	1,205 <sup>b</sup>
	P40	3,100 <sup>a</sup>	207 <sup>de</sup>	1,583 <sup>bcd</sup>	1,596 <sup>bcd</sup>	1,548 <sup>bcd</sup>	1,760 <sup>abc</sup>	1,632 <sup>a</sup>
	P100	2,697 <sup>ab</sup>	198 <sup>de</sup>	1,964 <sup>abc</sup>	1,954 <sup>abc</sup>	1,881 <sup>abc</sup>	1,536 <sup>bcd</sup>	1,705 <sup>a</sup>
	Average	2,463 <sup>a</sup>	169 <sup>c</sup>	1,597 <sup>b</sup>	1,828 <sup>ab</sup>	1,536 <sup>b</sup>	1,491 <sup>b</sup>	
Stem	P0	163 <sup>ab</sup>	BMDL	135 <sup>bc</sup>	116 <sup>bc</sup>	114 <sup>bc</sup>	71 <sup>cde</sup>	100 <sup>ab</sup>
	P40	160 <sup>ab</sup>	7 <sup>de</sup>	100 <sup>bc</sup>	85 <sup>bcd</sup>	69 <sup>cde</sup>	92 <sup>bc</sup>	86 <sup>b</sup>
	P100	241 <sup>a</sup>	3 <sup>de</sup>	123 <sup>bc</sup>	86 <sup>bcd</sup>	125 <sup>bc</sup>	85 <sup>bcd</sup>	110 <sup>a</sup>
	Average	188 <sup>a</sup>	3 <sup>c</sup>	120 <sup>b</sup>	96 <sup>b</sup>	103 <sup>b</sup>	83 <sup>b</sup>	
Tassel	P0	319 <sup>cde</sup>	<0.001	344 <sup>cde</sup>	489 <sup>cde</sup>	346 <sup>cde</sup>	234 <sup>cde</sup>	289 <sup>b</sup>
	P40	1257 <sup>a</sup>	65 <sup>de</sup>	587 <sup>cd</sup>	658 <sup>bc</sup>	427 <sup>cde</sup>	535 <sup>cde</sup>	588 <sup>a</sup>
	P100	1179 <sup>ab</sup>	59 <sup>de</sup>	699 <sup>bc</sup>	619 <sup>c</sup>	570 <sup>cd</sup>	578 <sup>cd</sup>	617 <sup>a</sup>
	Average	918 <sup>a</sup>	41 <sup>c</sup>	543 <sup>b</sup>	589 <sup>b</sup>	448 <sup>b</sup>	449 <sup>b</sup>	

**Notes:** Leaves:  $\alpha < 0.05$ ; CV = 3.3%; LSD = 760; Stem:  $\alpha < 0.05$ ; CV = 7.3%; LSD = 46; Tassel:  $\alpha < 0.05$ ; CV = 2.0%; LSD = 291. Note: BMDL = Below method determination limit

### The influence of sludge on the uptake and distribution of nickel and lead in maize plant parts

Nickel concentrations were highest for plant parts produced with soil alone. All nickel concentrations determined were close to the detection limit, but the two sludges showed lower nickel concentrations than the soil-alone treatments. Phosphate application did not significantly increase ( $\alpha > 0.05$ ) the concentration of nickel in plant parts (Table 6.23).

Table 6.23: Sludge and phosphate influence on nickel ( $\text{mg kg}^{-1}$ ) in biomass

Plant part	Nickel							
	Treatment	S	SL	10Gyp	20Gyp	10GypFe	20GypFe	Average
Leaves	P0	1.14 <sup>a</sup>	0.93 <sup>a</sup>	0.98 <sup>a</sup>	1.23 <sup>a</sup>	<0.93	1.55 <sup>a</sup>	1.17 <sup>a</sup>
	P40	1.25 <sup>a</sup>	<0.93	<0.93	1.38 <sup>a</sup>	1.22 <sup>a</sup>	1.28 <sup>a</sup>	1.28 <sup>a</sup>
	P100	1.11 <sup>a</sup>	1.03 <sup>a</sup>	<0.93	<0.93	<0.93	<0.93	1.07 <sup>a</sup>
	<b>Average</b>	1.17 <sup>a</sup>	0.98 <sup>a</sup>	0.98 <sup>a</sup>	1.31 <sup>a</sup>	1.22 <sup>a</sup>	1.42 <sup>a</sup>	
Stem	P0	1.15 <sup>a</sup>	<0.93	1.32 <sup>a</sup>	<0.93	<0.93	0.25 <sup>a</sup>	0.91 <sup>a</sup>
	P40	<0.93	<0.93	<0.93	<0.93	<0.93	<0.93	<0.93
	P100	<0.93	<0.93	<0.93	<0.93	<0.93	<0.93	<0.93
	<b>Average</b>	1.15 <sup>a</sup>	<0.93	1.32 <sup>a</sup>	<0.93	<0.93	0.25 <sup>a</sup>	
Tassel	P0	1.66 <sup>a</sup>	<0.93	<0.93	1.06 <sup>a</sup>	<0.93	<0.93	1.36 <sup>a</sup>
	P40	<0.93	1.40 <sup>a</sup>	1.00 <sup>a</sup>	<0.93	1.07 <sup>a</sup>	<0.93	1.15 <sup>a</sup>
	P100	2.26 <sup>a</sup>	<0.93	<0.93	<0.93	<0.93	1.36 <sup>a</sup>	1.81 <sup>a</sup>
	<b>Average</b>	1.96 <sup>a</sup>	1.40 <sup>a</sup>	1.00 <sup>a</sup>	1.06 <sup>a</sup>	1.07 <sup>a</sup>	1.36 <sup>a</sup>	

**Notes:** Leaves:  $\alpha < 0.05$ ; CV = 4.3%; LSD = 1.1; Stem:  $\alpha < 0.05$ ; CV = 17.3%; LSD = 0.8; Tassel:  $\alpha < 0.05$ ; CV = 7.8%; LSD = 1.5. Note: MDL for nickel was  $0.93 \text{ mg kg}^{-1}$

Plant parts grown in limed or unlimed soils, on average, had greater lead concentrations than plant parts grown on soils with sludges (Table 6.24). There was no significant difference in lead concentrations in plant parts grown with Gyp as opposed to GypFe, despite the former containing  $40 \text{ mg kg}^{-1}$  Pb.

According to Kumpiene et al. (2008), calcium compounds, including gypsum and phosphogypsum, as well as iron and manganese oxides, have the potential to immobilise lead. As discussed earlier, both sludge materials are composed of gypsum, but GypFe also contains ferric oxides that can sorb lead.

Liming soil increased the concentration of lead in the leaves due to the combined effect of the  $\text{Ca(OH)}_2$ , which contained  $30 \text{ mg kg}^{-1}$  lead, and soil that already had  $36 \text{ mg kg}^{-1}$  lead.

Table 6.24: Sludge, lime and phosphate influence on lead ( $\text{mg kg}^{-1}$ ) in biomass

Plant part	Lead							
	Treatment	S	SL	10Gyp	20Gyp	10GypFe	20GypFe	Average
Leaves	P0	1.27 <sup>b</sup>	2.4 <sup>ab</sup>	1.21 <sup>b</sup>	1.48 <sup>b</sup>	0.97 <sup>b</sup>	1.1 <sup>b</sup>	1.41 <sup>a</sup>
	P40	3.01 <sup>ab</sup>	3.46 <sup>ab</sup>	1.41 <sup>b</sup>	1.43 <sup>b</sup>	1.9 <sup>ab</sup>	1.79 <sup>ab</sup>	2.17 <sup>a</sup>
	P100	0.96 <sup>b</sup>	4.22 <sup>a</sup>	0.97 <sup>b</sup>	0.93 <sup>b</sup>	1.08 <sup>b</sup>	0.97 <sup>b</sup>	1.52 <sup>ab</sup>
	<b>Average</b>	1.75 <sup>b</sup>	3.36 <sup>a</sup>	1.20 <sup>b</sup>	1.28 <sup>b</sup>	1.32 <sup>b</sup>	1.29 <sup>b</sup>	
Stem	P0	0.46 <sup>ab</sup>	<0.2	0.29 <sup>ab</sup>	0.43 <sup>ab</sup>	<0.2	0.29 <sup>ab</sup>	0.37 <sup>a</sup>
	P40	0.93 <sup>a</sup>	0.2 <sup>ab</sup>	0.34 <sup>ab</sup>	0.40 <sup>ab</sup>	0.55 <sup>ab</sup>	0.32 <sup>ab</sup>	0.46 <sup>a</sup>
	P100	0.48 <sup>ab</sup>	<0.2	<0.2	0.35 <sup>ab</sup>	<0.2	0.60 <sup>ab</sup>	0.48 <sup>a</sup>
	<b>Average</b>	0.62 <sup>a</sup>	0.2 <sup>b</sup>	0.32 <sup>ab</sup>	0.40 <sup>ab</sup>	0.55 <sup>ab</sup>	0.40 <sup>ab</sup>	
Tassel	P0	0.65 <sup>bc</sup>	<0.2	0.33 <sup>c</sup>	0.41 <sup>bc</sup>	0.59 <sup>bc</sup>	0.46 <sup>bc</sup>	0.49 <sup>b</sup>
	P40	0.67 <sup>bc</sup>	1.64 <sup>ab</sup>	0.79 <sup>bc</sup>	0.92 <sup>abc</sup>	0.87 <sup>abc</sup>	0.69 <sup>bc</sup>	0.93 <sup>a</sup>
	P100	0.38 <sup>c</sup>	2.05 <sup>a</sup>	1.01 <sup>abc</sup>	0.81 <sup>bc</sup>	0.31 <sup>c</sup>	1.13 <sup>abc</sup>	0.95 <sup>a</sup>
	<b>Average</b>	0.57 <sup>b</sup>	1.85 <sup>a</sup>	0.71 <sup>ab</sup>	0.71 <sup>ab</sup>	0.59 <sup>b</sup>	0.76 <sup>ab</sup>	

**Notes:** Leaves:  $\alpha < 0.05$ ; CV = 19.4%; LSD = 1.5; Stem:  $\alpha < 0.05$ ; CV = 14.3%; LSD = 0.5; Tassel:  $\alpha < 0.05$ ; CV = 3.7%; LSD = 0.7. MDL for lead was  $0.2 \text{ mg kg}^{-1}$

The application of sludge, even with a content of 40 mg kg<sup>-1</sup> lead, did not increase the concentration of lead in the plants, while liming soil with a lead content of 36 mg kg<sup>-1</sup> with a lime containing 30 mg kg<sup>-1</sup> lead did. Lead was concentrated more in the leaves than in the stem and tassels, and generally increased with an increase in phosphate application.

### The influence of sludge on the yield of maize grain yield

Grain was only produced in treatments that received phosphate. Increasing the addition of phosphate from 40 to 100 kg ha<sup>-1</sup> increased grain yield significantly by 45%. On average, the yield of maize grain was lowest from limed soils, slightly higher from unlimed soils, and highest from soils that had received either of the sludges. Yields were significantly higher ( $\alpha < 0.05$ ) on soils with 20 t ha<sup>-1</sup> than on those with 10 t ha<sup>-1</sup> sludge (Table 6.25). The increase in yield by treatments with sludges was an indication that these materials improved soil fertility.

Table 6.25: Yield of maize planted in different sludge-soil mixtures (g pot<sup>-1</sup>)

Sludge	Soil	Soil (limed)	10Gyp	20Gyp	10GypFe	20GypFe	Average
P40	40.4 <sup>b</sup>	41.2 <sup>b</sup>	39.3 <sup>b</sup>	31.4 <sup>b</sup>	32.1 <sup>b</sup>	66.3 <sup>b</sup>	<b>41.8<sup>b</sup></b>
P100	58.4 <sup>ab</sup>	43.5 <sup>b</sup>	65.5 <sup>ab</sup>	101.7 <sup>a</sup>	61.3 <sup>ab</sup>	82.18 <sup>ab</sup>	<b>68.8<sup>a</sup></b>
<b>Average</b>	<b>49.4<sup>b</sup></b>	<b>42.3<sup>c</sup></b>	<b>52.4<sup>b</sup></b>	<b>66.6<sup>a</sup></b>	<b>46.7<sup>b</sup></b>	<b>74.23<sup>a</sup></b>	

Notes:  $\alpha < 0.05$ ; CV = 14.4%; LSD = 2.4

### The influence of sludge on the concentration of calcium, sulphur and phosphorus in maize grain

Applying either of the sludges at both rates slightly increased concentrations of sulphur and phosphorus in the grain. Increasing phosphate from 40 to 100 kg ha<sup>-1</sup> had a non-significant effect on the concentration of calcium in the grain, but showed a small, but significant effect on the concentration of sulphur and phosphorus (Table 6.26).

The concentration of calcium in grain from plants that received neither lime nor sludge was extremely low at <1 mg kg<sup>-1</sup> and was increased to between 2.5 and 4.4 mg kg<sup>-1</sup> by sludge application. Liming the soil resulted in by far the greatest contents of calcium, sulphur and phosphorus in grain.

Table 6.26: Major elements in maize grain (mg kg<sup>-1</sup>)

	Sludge	S	SL	10Gyp	20Gyp	10GypFe	20GypFe	Average
<b>Sulphur</b>	P40	94 <sup>cd</sup>	937 <sup>a</sup>	108 <sup>c</sup>	114 <sup>c</sup>	110 <sup>c</sup>	105 <sup>c</sup>	<b>245<sup>a</sup></b>
	P100	93 <sup>cd</sup>	789 <sup>b</sup>	89 <sup>cd</sup>	94 <sup>cd</sup>	99 <sup>cd</sup>	98 <sup>cd</sup>	<b>210<sup>b</sup></b>
	<b>Average</b>	<b>93<sup>b</sup></b>	<b>863<sup>a</sup></b>	<b>99<sup>b</sup></b>	<b>104<sup>b</sup></b>	<b>104<sup>b</sup></b>	<b>102<sup>b</sup></b>	
<b>Phosphorus</b>	P40	285 <sup>c</sup>	2023 <sup>b</sup>	289 <sup>c</sup>	302 <sup>c</sup>	300 <sup>c</sup>	262 <sup>c</sup>	<b>577<sup>b</sup></b>
	P100	312 <sup>c</sup>	3043 <sup>a</sup>	317 <sup>c</sup>	287 <sup>c</sup>	349 <sup>c</sup>	374 <sup>c</sup>	<b>780<sup>a</sup></b>
	<b>Average</b>	<b>299<sup>b</sup></b>	<b>2533<sup>a</sup></b>	<b>303<sup>b</sup></b>	<b>295<sup>b</sup></b>	<b>325<sup>b</sup></b>	<b>318<sup>b</sup></b>	
<b>Calcium</b>	P40	0.5 <sup>a</sup>	63.6 <sup>a</sup>	2.8 <sup>a</sup>	4.3 <sup>a</sup>	4.3 <sup>a</sup>	4.0 <sup>a</sup>	<b>13<sup>a</sup></b>
	P100	0.8 <sup>a</sup>	56.4 <sup>a</sup>	2.2 <sup>a</sup>	2.0 <sup>a</sup>	2.1 <sup>a</sup>	4.7 <sup>a</sup>	<b>11<sup>a</sup></b>
	<b>Average</b>	<b>0.7<sup>b</sup></b>	<b>60.0<sup>a</sup></b>	<b>2.5<sup>b</sup></b>	<b>3.1<sup>b</sup></b>	<b>3.2<sup>b</sup></b>	<b>4.4<sup>b</sup></b>	

Notes: S:  $\alpha < 0.05$ ; CV = 3.6%; LSD = 55.9; P:  $\alpha < 0.05$ ; CV = 4.1%; LSD = 213; Ca:  $\alpha < 0.05$ ; CV = 17%; LSD = 8.3

### The influence of sludge on the concentration of Fe and Mn in maize grain

The application of either sludge resulted in relatively small decreases in the concentrations of iron and manganese in grain compared to unlimed soil. The addition of phosphate showed no significant effects on the concentration of manganese and iron (Table 6.27). Liming the soil resulted in marked increases in grain iron concentration, but manganese concentration was below detection limits in grain grown with lime.

Table 6.27: Manganese and iron in maize grain ( $\text{mg kg}^{-1}$ )

	Sludge	S	SL	10Gyp	20Gyp	10GypFe	20GypFe	Average
Manganese	P40	0.798 <sup>a</sup>	BMDL	0.381 <sup>bc</sup>	0.427 <sup>bc</sup>	0.528 <sup>abc</sup>	0.352 <sup>bcd</sup>	<b>0.41<sup>a</sup></b>
	P100	0.683 <sup>ab</sup>	BMDL	0.387 <sup>bc</sup>	0.292 <sup>cd</sup>	0.532 <sup>abc</sup>	0.480 <sup>abc</sup>	<b>0.40<sup>a</sup></b>
	<b>Average</b>	<b>0.741<sup>a</sup></b>	<b>BMDL</b>	<b>0.384<sup>b</sup></b>	<b>0.360<sup>b</sup></b>	<b>0.530<sup>ab</sup></b>	<b>0.416<sup>b</sup></b>	
Iron	P40	1.090 <sup>b</sup>	16.680 <sup>a</sup>	0.890 <sup>b</sup>	0.990 <sup>b</sup>	0.660 <sup>b</sup>	2.530 <sup>b</sup>	<b>3.81<sup>a</sup></b>
	P100	1.040 <sup>b</sup>	18.090 <sup>a</sup>	0.770 <sup>b</sup>	0.660 <sup>b</sup>	0.650 <sup>b</sup>	0.880 <sup>b</sup>	<b>3.68<sup>a</sup></b>
	<b>Average</b>	<b>1.065<sup>b</sup></b>	<b>17.385<sup>a</sup></b>	<b>0.830<sup>b</sup></b>	<b>0.825<sup>b</sup></b>	<b>0.655<sup>b</sup></b>	<b>1.705<sup>b</sup></b>	

Notes: Iron:  $\alpha < 0.05$ ; CV = 13.2%; LSD = 2.45; Manganese:  $\alpha < 0.05$ ; CV = 15.5%; LSD = 0.19.

BMDL = Below method detection limit

### The influence of sludge on the concentration of nickel and lead in maize grain

Nickel and lead in the grain were below the MDL for all treatments (Table 6.28). Even loading the soil with 20 t ha<sup>-1</sup> sludge containing more than 100 mg kg<sup>-1</sup> nickel (in the case of GypFe) and 40 mg kg<sup>-1</sup> lead (in the case of Gyp) did not result in elevating the levels of these elements in the grain relative to the control. This could be a result of either the sorption or precipitation of these metals by the sludges, reducing their phyto-availability.

Table 6.28: Nickel and lead ( $\text{mg kg}^{-1}$ ) in grain

	Sludge	S	SL	10Gyp	20Gyp	10GypFe	20GypFe	Average
Lead	P40	<0.2	<0.2	<0.2	<0.2	<0.2	<0.2	<0.2
	P100	<0.2	<0.2	<0.2	<0.2	<0.2	<0.2	<0.2
	<b>Average</b>	<b>&lt;0.2</b>	<b>&lt;0.2</b>	<b>&lt;0.2</b>	<b>&lt;0.2</b>	<b>&lt;0.2</b>	<b>&lt;0.2</b>	
Nickel	P40	<0.93	<0.93	<0.93	<0.93	<0.93	<0.93	<0.93
	P100	<0.93	<0.93	<0.93	<0.93	<0.93	<0.93	<0.93
	<b>Average</b>	<b>&lt;0.93</b>	<b>&lt;0.93</b>	<b>&lt;0.93</b>	<b>&lt;0.93</b>	<b>&lt;0.93</b>	<b>&lt;0.93</b>	

Note: Method detection limits for nickel and lead were 0.93 mg kg<sup>-1</sup> (0.01 mg l<sup>-1</sup>) and 0.2 mg kg<sup>-1</sup> (0.002 mg l<sup>-1</sup>)

### Food and feed safety of the grain and fodder

For all treatments, lead concentration in the grain was below the threshold (0.2 mg kg<sup>-1</sup>) stipulated by Codex Alimentarius (2006). This threshold was close to the lead MDL of 0.2 mg kg<sup>-1</sup>. Using HDS from the coal fields as a soil amendment, even at application rates of 20 t ha<sup>-1</sup>, did not elevate lead levels in grain above the Codex threshold. Similarly, nickel concentration in the grain was below the threshold of 1 mg kg<sup>-1</sup> stipulated by the National Standard of the People's Republic of China (2012). This threshold was also close to the nickel MDL of 0.93 mg kg<sup>-1</sup>. Applying GypFe containing the most nickel (108 mg kg<sup>-1</sup>) did not increase the concentration of this element above the threshold. This indicates that the use of the sludges to improve crop yield will not induce nickel or lead toxicity if the grain is ingested.

With respect to the safety of the fodder and grain as animal feed, applying sludges on their own, even at 20 t ha<sup>-1</sup>, or co-applying them with phosphate, did not increase the concentration of lead to above the threshold of 40 mg kg<sup>-1</sup> as stipulated by the FAO (1997), the European Commission (2002) and the South African Department of Agriculture (2006). These treatments did not increase the concentration of nickel in both fodder and grain to above the 50 and 100 mg kg<sup>-1</sup> thresholds stipulated by the South African Department of Agriculture (2006) and the FAO (1997) either.

### 6.7.3 Conclusions

Both sludges showed value as ameliorants, since they contained macro and micronutrients (S, Ca, Mg, K, Mn, Fe and Zn). Both Gyp and GypFe exhibited a liming effect, marginally increasing soil pH, and decreasing acidity and hydrolysable cations.

Co-application with phosphate had the strongest liming effect. Both sludges reduced exchangeable hydrolysable cations and exchangeable acidity. However, the application of these materials on their own at 20 t ha<sup>-1</sup> increased soil salinity to levels suitable for more salt-tolerant plants.

When sludges were used in plant growth trials at rates equivalent to 10 or 20 t ha<sup>-1</sup>, they increased plant growth in comparison to plants grown without sludge on an acidic soil. The two sludges selected for testing had been categorised by various waste classification systems as posing some environmental risk. In the case of Gyp, this was because of its lead content of 40 mg kg<sup>-1</sup>, and for GypFe, this was because of its total nickel content of 105 mg kg<sup>-1</sup> and its total manganese content of 7,000 mg kg<sup>-1</sup>.

Plants grown with these two sludges exhibited increased concentrations of calcium, sulphur and phosphorus and decreased concentrations of iron and manganese in comparison to plants grown on unlimed soils. Plant or grain lead or nickel content was not increased as a result of sludge application. With respect to food safety, both lead and nickel were below the standards set by Codex Alimentarius (2006) and the National Standard of the People's Republic of China (2012) for grain for all treatments.

Both fodder and grain were safe as feed for animals since levels of both metals in all treatments were well below the thresholds stipulated by the European Commission (2002), the FAO (1997) and the South African Department of Agriculture (2006).

It can be concluded, therefore, that the use of HDS, on its own, as a soil ameliorant, or in combination with phosphate up to the levels trialled in this study, poses no food or feed safety risk, and can be beneficially used as a crop nutrient source through soil amelioration.

### 6.8 REFERENCES

- AGEGNEHU G, YIRGA C, AND ERKOSSA T (2019) *Soil Acidity Management*. Ethiopian Institute of Agricultural Research (EIAR), Addis Ababa, Ethiopia, p 13
- ANGLO AMERICAN THERMAL COAL (2015) Classification and Assessment of Brine and Sludge; Report Number 1538858-298217-1; Anglo American: EMalahleni, South Africa.
- BEUSELINCK L, GOVERS G, POESEN J, DEGRAER G, FROYEN L (1998) Grain-size analysis by laser diffractometry: comparison with the sieve-pipette method. *Catena* 32 (3-4) 193–208. [https://doi.org/10.1016/S0341-8162\(98\)00051-4](https://doi.org/10.1016/S0341-8162(98)00051-4).
- BINDRABAN PS, DIMKPA C, NAGARAJAN L, ROY A and RABBINGE R (2015) Revisiting fertilisers and fertilisation strategies for improved nutrient uptake by plants. *Biology and Fertility of Soils* 51(8): 897-911. <https://doi.org/10.1007/s00374-015-1039-7>
- CHEN L and DICK WA. (2011). Gypsum as an agricultural amendment: General use guidelines: Ohio State University Extension.
- CODEX ALIMENTARIUS COMMISSION (2006) *Understanding the Codex Alimentarius*. 3rd ed. Joint Food and Agricultural Organization of the United Nations (FAO)/World health Organization (WHO) Food Standards Programme, FAO, Rome
- CODEX ALIMENTARIUS COMMISSION (2010). Procedural manual, Joint FAO. In: WHO Food Standards Programme.

- COSTLEY S (2013) Waste classification and management regulations and supporting norms and standards. Waste Khoro.
- DEPARTMENT OF AGRICULTURE FORESTRY AND FISHERIES (DAFF) (2012). Fertilizers, Farm Feeds, Agricultural Remedies And Stock Remedies Act, 1947 (Act No. 36 Of 1947).
- DEPARTMENT OF AGRICULTURE, D. O. A. (2006). Fertilizers, Farm Feeds, Agricultural Remedies And Stock Remedies Act, 1947.
- DEPARTMENT OF ENVIRONMENTAL AFFAIRS (DEA) (2008) National Environmental Management: Waste Act, Act No. 59 of 2008. Waste classification and management regulations. DEA, Pretoria, South Africa.  
[https://www.environment.gov.za/sites/default/files/legislations/nemwa59of2008\\_wasteclassification](https://www.environment.gov.za/sites/default/files/legislations/nemwa59of2008_wasteclassification).
- DEPARTMENT OF WATER AFFAIRS AND FORESTRY (DWAF) (1998) Waste management series. Minimum requirements for waste disposal by landfill, 2nd ed. <http://www.dwaf.gov.za/Documents/Other/WQM/RequirementsWasteDisposalLandfillSep05Part1.pdf>.
- ERSAHIN, S., GUNAL, H., KUTLU, T., YETGIN, B., & COBAN, S. (2006). Estimating specific surface area and cation exchange capacity in soils using fractal dimension of particle-size distribution. *Geoderma* **136**( 3-4) 588-597. <https://doi.org/10.1016/j.geoderma.2006.04.014> .
- ESHEL, G, LEVY GJ, MINGELGRIN U and SINGER MJ (2004) Critical Evaluation of the Use of Laser Diffraction for Particle-Size Distribution Analysis. *Soil Science Society of America Journal* **68**(3) 736-743. <https://doi.org/10.2136/sssaj2004.7360>
- ESSINGTON ME (2004) Organic matter in soils. pp 129-180. In: Soil and water chemistry: An integrative approach. CRC Press LLC, 200 N.W.
- ESSINGTON ME (2003) Organic matter in soils. In: *Soil and Water Chemistry*. CRC Press, Baton Rouge, UNITED STATES.
- EUROPEAN COMMISSION (2002). REGULATION (EC) No 178/2002 OF THE EUROPEAN PARLIAMENT AND OF THE COUNCIL of 28 January 2002.
- FENG XH, ZHAI LM, TAN WF, LIU F and HE JZ (2007) Adsorption and redox reactions of heavy metals on synthesized Mn oxide minerals. *Environmental Pollution* **147**(2) 366-373. <https://doi.org/10.1016/j.envpol.2006.05.028> .
- FISCHEL MHH, FISCHEL JS, LAFFERTY BJ and SPARKS DL (2015) The influence of environmental conditions on kinetics of arsenite oxidation by manganese-oxides. *Geochem. Trans.*, 16, 15, doi:10.1186/s12932-015-0030-4.
- FOOD AND AGRICULTURE ORGANIZATION OF THE UNITED NATIONS (FAO) (1997). Animal Feeding And Food Safety: Report of an FAO Expert Consultation Rome, Italy, 10 to 14 March 1997.
- HAN T, CAI A, LIU K, HUANG J, WANG B, LI D, QASWAR M, FENG G and ZHANG H (2019) The links between potassium availability and soil exchangeable calcium, magnesium, and aluminum are mediated by lime in acidic soil. *Journal of Soils and Sediments* **19**(3) 1382-1392. <https://doi.org/10.1007/s11368-018-2145-6> .
- HENDERSHOT WH AND LALANDE H (2008) Soil Reaction and Exchangeable Acidity, In: *Soil Sampling and Methods of Analysis*, 2nd Ed. Taylor & Francis Group, LLC, Canadian Society of Soil Science, p 163

- HENDRY JP, WILKINSON M, FALLICK AE and HASZELDINE RS (2000) Ankerite cementation in deeply buried Jurassic sandstone reservoirs of the central North Sea. *Journal of Sedimentary Research* **70**(1) 227-239. <https://doi.org/10.1306/2DC4090D-0E47-11D7-8643000102C1865D>.
- HILLEL, D. (1998). Environmental soil physics: Fundamentals, applications, and environmental considerations: Elsevier.
- JONES JR JB (2012) Plant nutrition and soil fertility manual. CRC press.
- KROETSCH D AND WANG C (2008) Particle size distribution. Soil sampling and methods of analysis, 2, 713-725.
- KUMPIENE J, LAGERKVIST A and MAURICE C (2008) Stabilization of As, Cr, Cu, Pb and Zn in soil using amendments – A review. *Waste Management* **28**(1) 215-225. <https://doi.org/10.1016/j.wasman.2006.12.012> .
- LAL R and SHUKLA MK. 2004. Principles of soil physics. Marcel Dekker, Inc. New York, USA. pp 271 – 275
- LIU A, REN F, LIN WY and WANG JY (2015) A review of municipal solid waste environmental standards with a focus on incinerator residues. *International Journal of Sustainable Built Environment* 4 165–188. DOI: 10.1016/j.ijbsbe.2015.11.002.
- LOLLAR BS, HOLLAND HD and TUREKIAN KK (2005) Environmental Geochemistry. Elsevier, The Boulevard, Langford Lane, Kidlington, Oxford OX5, IGB, UK.
- LOUBSER M and VERRYIN S (2008) Combining XRF and XRD analyses and sample preparation to solve mineralogical problems. *S. Afr. J. Geol.*, 111, 229–238, doi:10.2113/gssajg.111.2-3.229.
- MAREE JP, STRYDOM WF, ADLEM CJL, DE BEER M, VAN TONDER GJ and VAN DIJK BJ (2004) Neutralization of acid mine water and sludge disposal. Division of Water, Environment and Forestry Technology, CSIR, WRC Report No. 1057/1/04, Water Research Commission, Pretoria, South Africa.
- MENGEL K and KIRKBY E (2001) Fertilizer application. In: Principles of plant nutrition, Springer Science and Business Media. Dordrecht, The Netherlands, 337–596.
- MIG (2017) Fertilization. In: Maize information guide, Grain Crops Institute ARC, Pretoria, South Africa, 69–94.
- MITTRA B, KARMAKAR S, SWAIN D and GHOSH B (2005) Fly ash—a potential source of soil amendment and a component of integrated plant nutrient supply system. *Fuel* **84**(11) 1447-1451. <https://doi.org/10.1016/j.fuel.2004.10.019>
- MUDALY L (2016) The Contribution of Manganese Oxides to Redox Buffering in Selected Soils of the South African Highveld. Master's Thesis, University of Pretoria, Pretoria, South Africa,
- NATIONAL HEALTH AND MEDICAL RESEARCH COUNCIL (NHMRC), NATIONAL RESOURCE MANAGEMENT MINISTERIAL COUNCIL (NRMCC) (2011) Australian Drinking Water Guidelines Paper 6: National water quality management strategy. <https://nhmrc.gov.au/about-us/publications/australian-drinking-waterguidelines>.
- NATIONAL STANDARD OF THE PEOPLE'S REPUBLIC OF CHINA (2012). National Food Safety Standard for Maximum Levels Of Contaminants In Foods. Gb 2762-2012.
- NEW SOUTH WALES ENVIRONMENT PROTECTION AUTHORITY (EPA) (2014) Waste classification guidelines. Part 1: Classifying waste. [www.epa.nsw.gov.au](http://www.epa.nsw.gov.au).

- NEW SOUTH WALES ENVIRONMENT PROTECTION AUTHORITY (EPA) (2018) ACT's environmental standards: Assessment and classification of liquid and non-liquid wastes. <http://www.act.gov.au/environ/>.
- NIMMO JR (2004) Porosity and Pore Size Distribution. in Hillel, D., ed. Encyclopedia of Soils in the Environment: London, Elsevier 3: pp 295-303
- RHOADES JD (1996) Salinity: Electrical conductivity and Total dissolved solids. In: Methods of Soil Analysis, Part 3 – Chemical methods. SSSA Book Series No. 5, pp 417
- SCHWERTMANN U and CORNELL RM (2000). Iron oxides in the laboratory: preparation and *preparation and characterization*. Wiley-VCH.
- SKOUSEN J (2014) Overview of Acid Mine Drainage Treatment with Chemicals. In Acid Mine Drainage, Rock Drainage, and Acid Sulfate Soils: Causes, Assessment, Prediction, Prevention, and Remediation; Jacobs, J.A., Lehr, J.H., Testa, S.M., Eds.; John Wiley & Sons, Inc.: Hoboken, NJ, USA, , doi:10.1002/9781118749197.ch29.
- SOIL SCIENCE SOCIETY OF SOUTH AFRICA (1990) Handbook of standard soil testing methods for advisory purposes. The non-affiliated soil analysis work committee. ISBN0620148004.
- SPOSITO G (2008) Mineral stability and weathering. pp119-135. In: The Chemistry of Soils. 2nd Ed. Published by Oxford University Press, Inc. 198 Madison Avenue, New York.
- SPOSITO, G (2004) The surface chemistry of natural particles: Oxford University Press on Demand.
- SUN Q, MCDONALD JR LM and SKOUSEN JG (2000) Effects of armoring on limestone neutralization of AMD. pp. 1-10.
- TABATABAI MA. FRANKENBERGER WT (1996) Liquid chromatography. In: Methods of Soil Analysis, Part 3 – Chemical methods. SSSA Book Series No. 5, pp 225
- THOMAS GW (1982) Exchangeable Cations, In Methods of Analysis, Part 2. American Society of Agronomy, Madison, Wisconsin, USA. PP 159 – 165
- THOMAS GW (1996) Soil pH and Soil Acidity. In: Methods of Soil Analysis, Part 3 – Chemical methods. SSSA Book Series No. 5, pp 475
- UNITED STATES ENVIRONMENTAL PROTECTION AGENCY (EPA ) (2011) USEPA procedure 40 CFR Appendix B to Part 136. 2011. Definition and Procedure for the Determination of the Method Detection Limit—Revision 2. <https://www.epa.gov/cwa-methods> (Accessed March 2019)
- UNITED STATES ENVIRONMENTAL PROTECTION AGENCY (EPA) (1990) Hazardous waste management system, identification and listing of hazardous waste, toxicity characteristics revisions. Federal Register, Rules and Regulations.
- UNITED STATES ENVIRONMENTAL PROTECTION AGENCY (EPA) (1992). SW-846 Test Method 1311. 1992. Toxicity Characteristic Leaching Procedure (TCLP). Available online: <https://www.epa.gov/hw-sw846/sw-846-test-method-1311-toxicity-characteristic-leaching-procedure> (accessed on 9 March 2018).
- WANG CY, LIU JQ and GUO P (2012) An Analysis of Limestone Gypsum Desulfurization Systems; Trans Tech Publ.: Zurich, Switzerland; Volume 550–553, pp. 667–670.
- WANG S, CHEN Q, LI Y, ZHUO Y and XU, L. (2017). Research on saline-alkali soil amelioration with FGD gypsum. Resources, Conservation and Recycling, 121, 82-92.
- ZINCK JM and GRIFFITH W (2006) Utilizing industrial wastes and alterative reagents to treat acidic drainage. The 7th International Conference on Acid Rock Drainage (ICARD), American Society

of Mining and Reclamation (ASMR) 3134 Montavesta Road, Lexington, KY 40502.  
<https://nrcca.cals.cornell.edu/soil/CA2/CA0212.1-3.php> (accessed 21 August 2017)

ZINCK JM, WILSON LJ, CHEN TT, GRIFFITH W, MIKHAIL S and TURCOTTE A.M (1997)  
Characterization and Stability of Acid Mine Drainage Treatment Sludges. Mining and Mineral  
Sciences Laboratories Report MMSL 96-079 (CR). MEND Project 3.42.2a, Job No. 51144,  
Canada. <http://mend-nedem.org/wp-content/uploads/2013/01/3.42.2a.pdf>. Accessed 22  
November 2018

# CHAPTER 7: RESPONSE OF SELECTED CROPS TO FOLIAR APPLICATION OF SIMULATED ACID MINE DRAINAGE

---

M Mabuza, W Coetzer, JG Annandale, PD Tanner and JM Steyn

## 7.1 INTRODUCTION

The possibility of irrigating crops directly with AMD on soils that are strategically limed has been identified as a potentially fruitful research area. One of the questions that arises when considering this unusual practice is whether or not crop foliage will be scorched, thereby reducing photosynthetic leaf area, and reducing production to below economic levels. Foliar injury and yield losses have been observed in crops following treatment with simulated acid rain under both laboratory and field conditions (Lal, 2016; Conkling et al., 1991). Field-grown soybean sprayed with simulated acid rain with a pH of 2.7 in outdoor experiments (which excluded ambient rain) resulted in 23% lower seed yields than those that were sprayed with simulated rain at a pH of 4.1 (Lal, 2016).

In an experiment by Jacobson et al. (1989), working on red spruce seedlings, these authors reported that visual foliar symptoms were produced by acidic mist. These were in the form of loss of the green colouration and development of tan to reddish brown necrotic lesions on the distal portion of the needles. Sulphuric acid mist at its lowest pH of 2.5 was reported to have caused the greatest increase in foliar injury. Caporn and Hutchinson (1986) attributed leaf scorching to the collapse of the epidermal cells after wetting with simulated acid rain.

According to Lal (2016) and Jacobson (1984), monocotyledons are relatively less affected by acid rain compared to dicotyledonous plants. This is due to the presence of a waxy covering on the leaves of the former. The same authors indicated that the most sensitive plant parts for the foliar application of AMD are leaves and shoots. In a study by Dhere (2009), sorghum leaves showed signs of necrosis on leaf blades after the eighth day of wetting with simulated acid rain at a pH of 2, while chlorosis was observed for acid rain with a pH of 3 to 5. According to Odiyi and Eniola (2015), when cowpeas were sprinkled with simulated acid rain at a pH of 2, 3 and 4, leaves turned from brown to red, with 60% leaf abscission. At a pH of 2, plants died from the base of the shoot. In a similar study, soybean showed small amounts of foliar injury, seen as white or tan lesions on young leaves at a pH of 2.4 and 2.8.

The oxidation of pyrite ( $\text{FeS}_2$ ) creates AMD, which needs to be neutralised through liming before being released into the environment (Jovanovic et al., 2004). Upon exposure to water and oxygen, pyrite reacts to form sulphuric acid ( $\text{H}_2\text{SO}_4$ ) and ferric hydroxide ( $\text{Fe}(\text{OH})_3$ ) (Sparks 2003). The use of AMD for irrigation may lead to inhospitable conditions for growth, especially for non-acidophilic crops. The AMD also causes excessive loading and mobilisation of iron, aluminium and manganese. In this study, sulphuric acid without these acid-generating cations was used to simulate potential foliage scorching through acid mine water irrigation.

In a study by Golden et al. (2016), damaged leaf regions, as seen by grey or brown flecking and localised chlorosis and necrosis, were visually estimated as a percentage of the total leaf area to ensure consistent injury ratings. However, in this study, a more objective, quantitative approach was employed over and above the visual scoring method. Several digital platforms have become popular in recent times, such as CompuEye, Adobe Photoshop, ImageJ and WinFoliar, which all use a colour scheme to distinguish between damaged and healthy leaf parts. When evaluating the efficacy of CompuEye, Bakr (2005) reported mean values with no significant difference when compared with manual measurements, at a 95% confidence level. In CompuEye, images are scanned in rather than photographed, which made this platform lose popularity.

Adobe Photoshop is the most versatile platform. It goes a step further to calculate leaf area and land area. It does not require a uniform-coloured background (Li et al., 2007). ImageJ is the preferred option, as it also requires standard conditions to take photographs of plants, and there is no need for a pure white or black background. It also allows for the manual selection of specific colours for analysis (Schneider et al., 2012). In this study, ImageJ was used as it is freely available and easy to manipulate.

This study therefore had the objective of using quantitative methods to determine the degree of foliar damage to selected crops under low pH conditions in the absence of transition metals. The use of AMD for irrigation may lead to inhospitable conditions for the growth of crops, especially non-acidophilic crops. This may be through soil acidification and the excessive loading and mobilisation of iron, aluminium and manganese. The acidic water may also lead to leaf scorching and damage or compromise the economic yield of crops if overhead irrigation is used. Nonetheless, there are factors to consider that influence the degree to which such water qualities will have a negative influence on crop growth.

## 7.2 MATERIALS AND METHODS

### 7.2.1 Location of study

The study involved both a greenhouse pot trial and a field trial. Both experiments were conducted at the University of Pretoria's Agricultural Farm in the 2020/21 season. Acid mine waters were synthesised in the University of Pretoria's Soil Science Laboratory.

Sulphuric acid (98%) was used as the source of acidity because most acidic mine waters are dominated by sulphates. Four pH levels, based on an AMD analysis by Sukati (2016), who reported an AMD pH of 3, were selected. These pH levels were 2, 3 and 4, with a neutral control treatment of distilled water at a pH of 7. All treatments excluded metals commonly found in AMD (aluminium, iron and manganese), as these acidifying elements could potentially confound results.

### 7.2.2 Crop selection and synthesis of acid mine waters

Four summer crops were selected for the trial and consisted of two monocotyledonous crops (sorghum and maize) and two dicotyledonous crops (soybean and cowpeas) (Table 7.1). The desired pH values were made using concentrated sulphuric acid and deionised water. A pH meter was used to confirm the dilutions (Table 7.2).

Table 7.1 Minimum and maximum soil pH requirements of the selected crops

Crop	Species	Variety	Minimum pH	Maximum pH	Reference
Sorghum	<i>Sorghum bicolor</i>		5.0	8.5	Butchee et al., 2012
Maize	<i>Zea mays</i>	PAN 3A157	5.5	6.5	Edje and Ossom, 2016
Soybean	<i>Glycine max</i>	PAN 1454R	6.0	7.0	Staton, 2012
Cowpeas	<i>Vigna unguiculata</i>	Agriawa	5.5	8.3	Ngalamu et al., 2015

Table 7.2: Treatments and sulphuric acid volumes added to water

Treatment	H <sub>2</sub> SO <sub>4</sub> concentration (M)	Target pH	Measured pH	mℓ H <sub>2</sub> SO <sub>4</sub> per ℓ water
Foliar wetting at pH 2	0.005	2	2.32	0.27
Foliar wetting at pH 3	0.0005	3	3.01	0.027
Foliar wetting at pH 4	0.00005	4	3.88	0.0027
Foliar wetting (H <sub>2</sub> O at pH 7)	N/A	7	6.60	N/A

### 7.2.3 Part 1: Pot trial

The pot trial was laid out in a completely randomised design (CRD). Each treatment was represented by one pot. This trial evaluated one pH level (pH 2). Flower pots (6 l by volume) with a top diameter of 26 cm were filled with soil and coir at a ratio of 5:1. Coir assisted with free drainage. The soil was sourced from the University of Pretoria's Agricultural Farm. It has a sandy loam texture and is classified as a deep Hutton loamy, kaolinite, mesic, typic, highly weathered soil (Soil Classification Working Group, 1991). The pH of this soil averaged 5.49, and no lime was added. There were four treatments in the pot trial (maize, sorghum, cowpea and soybean). These were replicated five times. Five seeds were planted per pot.

Both maize and sorghum received the recommended amounts of nitrogen (100 kg/ha), phosphorus (40 kg/ha) and potassium (40 kg/ha). Cowpea and soybean also received similar amounts, but nitrogen was halved. Fertilizer to be applied per pot was based on the assumption that the plough layer is 0.15 m. Bulk density was assumed to be 1,400 kg m<sup>-3</sup>. The mass of the soil was then calculated to be 2,100,000 kg/ha (10,000 m<sup>2</sup>/ha x 0.15 m x 1,400 kg m<sup>-3</sup>). To calculate the volume of each pot, its base diameter was measured, as well as its height and top diameter. Height was reduced by 2 cm to allow for irrigation. The volume was found to be 0.00628 m<sup>3</sup> ( $\pi r^2 = 3.14 \times (0.24/2)^2 \times 0.25$ ). The mass of the soil and coir per pot was calculated using the formula  $(0.00628 \times 2,100,000)/(10,000 \times 0.15) = 8.8$  kg. The final calculation was done using cross multiplication to come up with the mass of the fertilizer per pot. For crop irrigation, tap water from the municipality was used for the duration of the trial. Irrigation was done every other day to prevent water stress from occurring. All treatments were allowed to drain freely.

Beginning two days after crop emergence, simulated AMD at a pH of 2 was sprayed onto the leaves with a spray bottle on a daily basis. This pH level and wetting frequency were selected to increase the chances of getting scorched leaves in order to have bases for the field trial. The leaves were sprayed to just below the point of runoff. To eliminate acid drip into the growth media when spraying foliage, the soil was covered with plastic discs. The plastic was sliced to allow plants to grow through it (Figure 7.1). Spraying was carried out after irrigation to avoid acid run-off with irrigation water. The pot trial was terminated five weeks after planting.



Figure 7.1: Cowpeas grown in sliced plastic discs to prevent acid drip into soil during foliar wetting

#### **7.2.4 Part 2: Field trial**

Land preparation was undertaken with a tractor-drawn plough, which was followed by disc-harrowing as the last step to prepare a fine seed bed. The soil for this trial is as described for the pot trial. A split plot design with three replicates was used in this trial. Each main plot consisted of a single pH level, while subplots were planted to the four different crops. The marking of plots began with the demarcation of main plots and sub-plots. Twelve main plots, measuring 20 m x 3.4 m, were marked out. These were further divided into four sub-plots, each measuring 4 m x 2.4 m. The four crops were randomly assigned to the sub-plots. Maize was planted in rows with 0.8 m between rows and 0.25 m between plants. Sorghum was planted at 0.8 m x 0.2 m between plants. Three seeds were planted per station. Both cowpea and soybean were planted in rows 0.6 m apart. The spacing within rows was 0.15 m for cowpea and 0.1 m for soybean. Due to the non-availability of an irrigation system during the time of planting, fertilizer was applied after crop emergence to avoid fertilizer burn. A week after emergence, fertilizer was applied using the dollop method based on crop recommendations. Nitrogen was applied at 100 kg/ha for maize and sorghum, and 50 kg/ha for both cowpea and soybean. Phosphorus and potassium were applied at 40 kg/ha across all crops.

Soybean failed to germinate due to a dry spell when it was at the emergence stage. Replanting was done after the irrigation system had been set up. However, the crop did not emerge again following the failure of the water pump at the farm. Soybean's high moisture requirement is highly critical at the time of germination. The other crops were able to germinate since they are not hindered by a hard soil cap during emergence. Nonetheless, the other three crops performed well. Supplemental irrigation commenced after the pump was fixed. Weeds were controlled through hand-hoeing. The trial was terminated eight weeks after planting.

#### **Foliar spraying with acid waters**

In the pot trial, foliar spraying began two days after crop emergence, while it began in the third week after crop emergence in the field trial. The variation in the commencement of foliar spraying was to determine if susceptibility to acid injury will vary with crop growth stage. Pot trial plants were sprayed daily, while field-grown crops were sprayed once in two days. A hand-held sprayer was used in both experiments to ensure that all leaves were adequately wetted to just below the point of run-off. Leaf wetting with simulated acid water continued until the trials were terminated.

#### **7.2.5 Data collection**

##### **Agronomic data**

To collect plant data, three plants were selected per plot. This is where crop growth and canopy-related data were measured (plant height, number of leaves per plant, number of scorched leaves per plant and percentage of foliar damage). At the end of the experiment, chlorophyll content and LAI were measured using a SPAD meter and a ceptometer, respectively. Destructive sampling was done at the end of the experiment. Three plants were cut off at ground level and oven dried at 65 °C until a constant mass was achieved.

##### **Leaf scorching data**

Every second day after treatment commenced, crops were observed for the inception of scorching. Data was collected once a week and included days after the commencement of wetting when scorching occurred, as well as the number of leaves showing injury per plant. Crops were visually assessed for symptoms of stress and foliar injury. If there were noticeable symptoms of stress, control crops were checked for similar symptoms. If the control crops did not display similar symptoms, the symptom was attributed to the water quality.

Damaged leaves were visually estimated and recorded on a score chart ranging from 0 to 100%. The same person did the scoring to ensure consistent injury ratings. Damaged or scorched leaves were also photographed, and images imported into ImageJ to determine fractional leaf area damage.

### ***ImageJ***

Standard conditions were used to take photographs of leaves. Once the leaves had been photographed, images were imported into ImageJ. Using the “threshold” option, the images were automatically filtered using the “filter” and “select” tools. At first, the whole leaf was selected to get its total pixel count. Total pixel counts were generated using the “measure” option under “analyse”. To select scorched sections of the leaf, the navigation bars under “brightness” and “saturation” were used. In crops like maize, where the midrib is white, like scorched sections, the “polygon selection” option was used to cut out the midrib. This was followed by selecting the “clear outside” option under “edit”. Navigating between “filtered” and “original” bars enabled cross-checking if the selection was done correctly. Injured leaf area was calculated using the “measure” option. The total damaged fraction of leaf area was then calculated by dividing the total pixels of the damaged area by the total pixels of the entire leaf area.

## **7.3 RESULTS**

### **7.3.1 Part 1: Pot trial**

Results on pot trials show that cowpeas were the most vulnerable to foliar spraying with acid water. Cowpeas had a significantly higher percentage of injured leaves ( $P < 0.05$ ), followed by soybean and sorghum. Maize was significantly lower ( $P < 0.05$ ) with only 12.6% of its leaves showing signs of scorching (Figure 7.2). The percentage of scorching from both estimated and calculated data showed an upward trend as time progressed. There was a significant difference in visual foliar injury assessment ( $P < 0.05$ ) among the different crops (Figure 7.3). Cowpea exhibited significantly more injury in the beginning, while that of sorghum was significantly higher than the other crops 24 days after planting. Foliar injury quantification using ImageJ showed no significant differences in scorching among the different crops. However, a trend similar to the visual assessment was observed (Figure 7.4).

It was noted that foliar injury was concentrated on leaves that had been formed earlier and progressed in those leaves with time. Undeveloped trifoliolate leaves were not injured in either cowpea or soybean. Leaf injury began with the development of white lesions common with sun-scorching (Figure 7.5).

These white lesions later became necrotic in all crops except maize. Chlorosis, necrosis, stunted growth, lesions, the suppression of leaf development, leaf curling, the withering of leaves, leaf abscission and even the death of plants are symptoms of plants that are injured by simulated AMD, which leads to the collapse of epidermal cells (Odiyi and Eniola, 2015; Hutchinson, 1986). Lal (2016) observed severe epidermal layer degradation and cytoplasm depletion in the palisade cells of treated crop leaves. The differences in degree of injury among the different crops may be attributed to ease of wettability, rate of cuticular permeation and the resistance or tolerance of exposed leaves to altered extracellular characteristics (Keevar, 1982). Leaf curling or cupping was evident in soybean plants. The same observation was made by MacLean et al. (1982), who reported that young leaves showed moderate tip and marginal necrosis, while older leaves crinkled and cupped following exposure to hydrofluoric acid at a pH of 2.

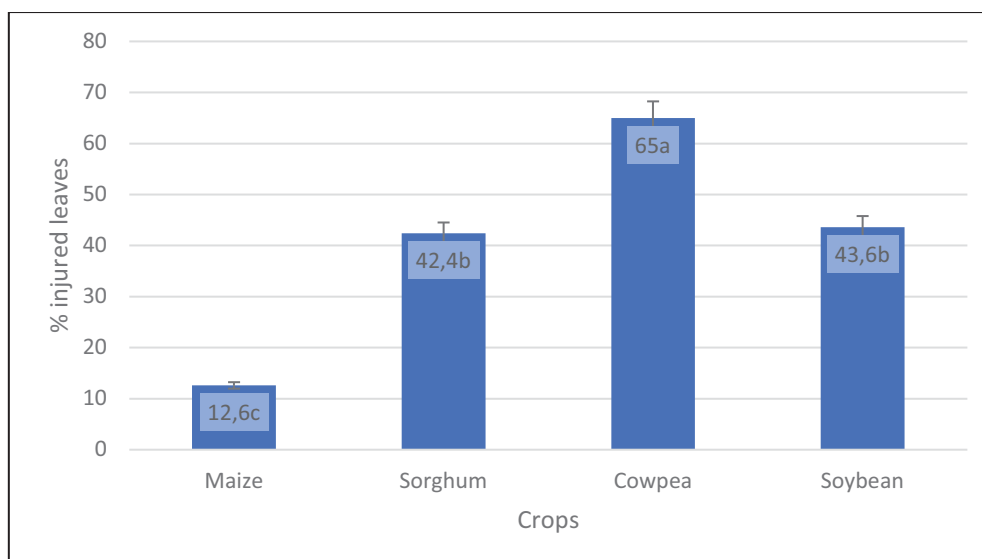


Figure 7.2: Fraction of injured leaves as a percentage of total leaves per plant for crops sprayed with synthetic acid mine water at a pH of 2 at 24 days after planting

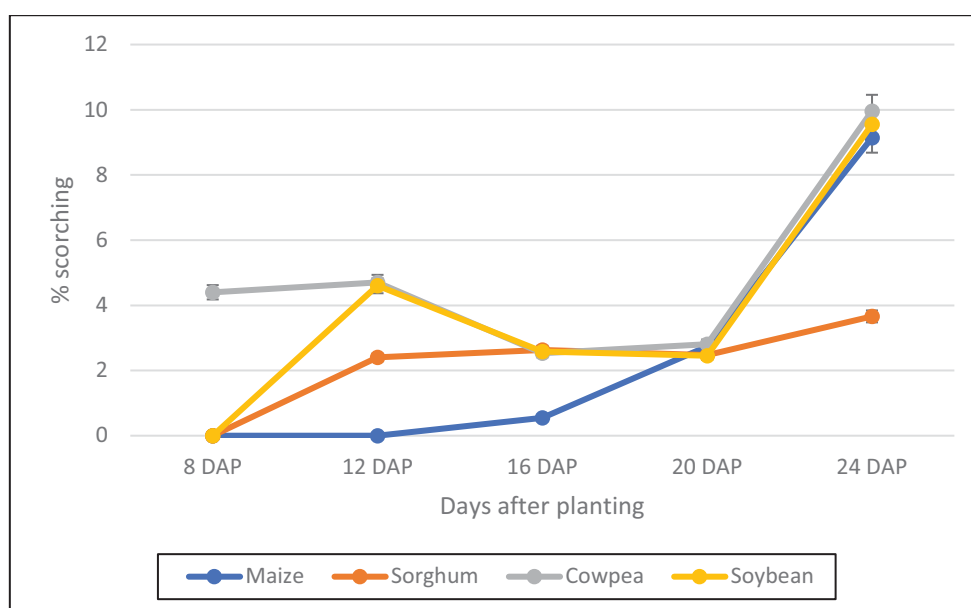
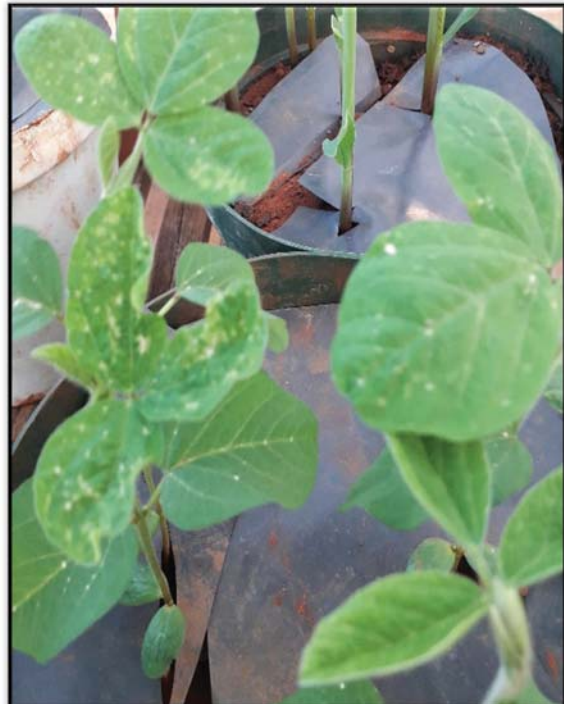
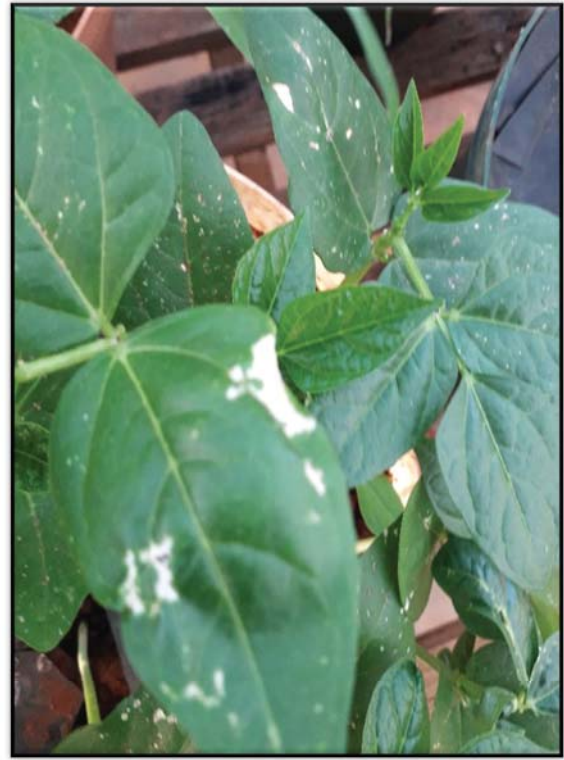


Figure 7.3: Percentage of scorched leaves visually estimated for crops sprayed with synthetic acid mine water at a pH of 2



*Figure 7.4 (clockwise): Scorched maize, cowpea, soybean and sorghum at 20 days after planting following wetting with synthetic acid mine water at a pH of 2*

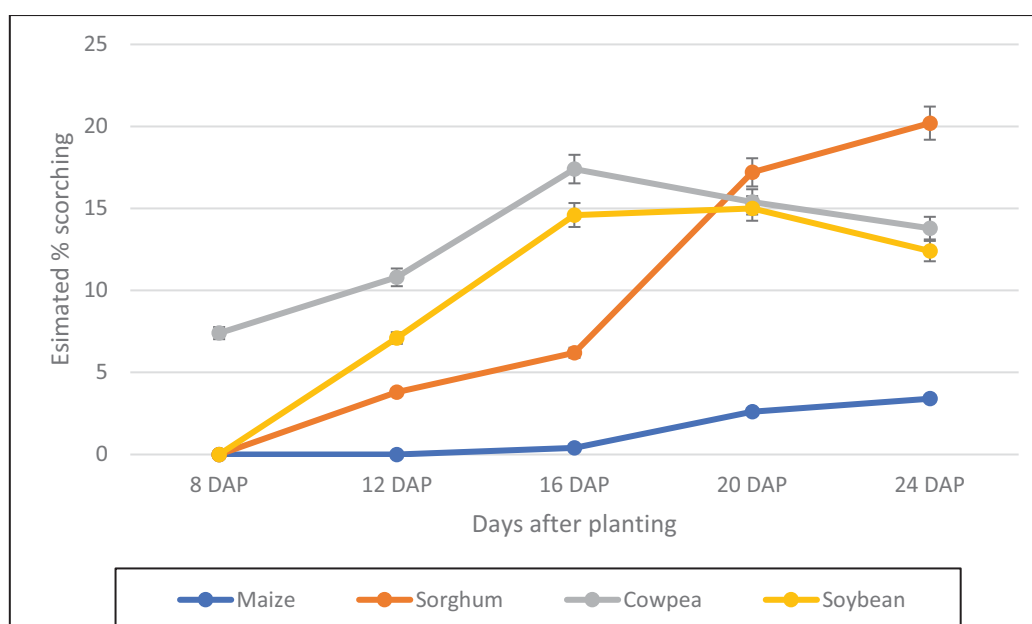


Figure 7.5: Percentage of scorched leaves calculated using ImageJ for crops sprayed with synthetic acid mine water at a pH of 2

Cowpeas showed signs of foliar injury earlier than the other crops. However, this was not significantly different from sorghum or soybean. It took cowpeas less than 48 hours to show signs of foliar damage, while scorching was only seen after eight days in maize (Figure 7.6). These findings are in line with those of Odiyi and Eniola (2015), who reported that cowpeas showed signs of scorching within 24 hours of sprinkling with simulated acid rain at a pH of 2. On the other hand, maize took significantly longer ( $P < 0.05$ ) to show symptoms of foliar injury. This delay in foliar injury in maize is attributed to the cuticle, which is made up of the epidermis and the outermost layer of cells. It is composed of cutin. This complex lipid is formed by linking several fatty acids and waxes to a strong polymer (Salt, 2019). The wax is primarily composed of different types of compounds, which contain long hydrocarbon chains, in addition to other minor components that play a key role in protecting the leaves. The difference in the onset of scorching between maize and sorghum is attributed to the early development of trichomes in sorghum leaves, while these usually only form from the fifth leaf in maize (Traore et al., 1989). Trichomes trap acid waters in sorghum leaves, while water simply runs off maize leaves.

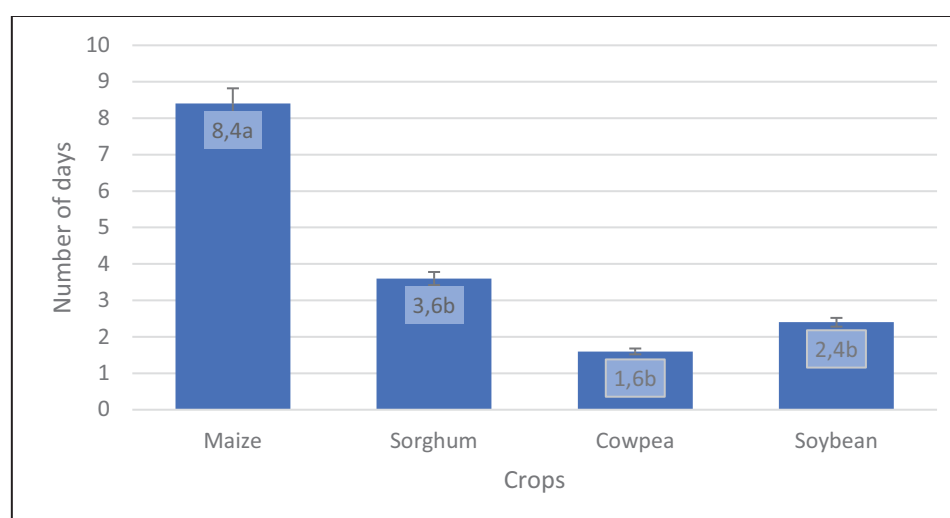


Figure 7.6: Number of days to showing signs of leaf scorching for crops sprayed with synthetic acid mine water at a pH of 2

### 7.3.2 Part 2: Field trial

There was no visible foliar scorching in field-grown crops across all pH levels. Foliar spraying began in the third week after crop emergence, at which point the crops may have developed some tolerance or resistance to acid injury. A similar observation was made by Keevar and Jacobson (1983), that foliar absorption rate is influenced by both the degree of cuticular development and the quantity, chemical composition and physical form of epicuticular waxes, which all vary with leaf maturity. This observation is contrary to Odiyi and Eniola (2015), who reported leaf injury following spraying with acid waters in cowpeas until 15 weeks after planting.

Plant height for the three crops that were successfully grown in the field is shown in Table 7.3. The results show that there was no significant difference across the four pH levels for all crops. Wetting leaves with acid waters would be expected to negatively affect plant height. It appears that by the beginning of foliar wetting three weeks after crop emergence, leaves were already resistant to acid injury. This is contrary to what was reported by Odiyi and Eniola (2015), who found that plant height was significantly higher in control treatments (pH 7) compared to lower acidity treatments.

Data on dry mass is shown in Table 7.3. There was no significant difference in dry mass across the different pH levels for each of the three crops. This is an indication that yield would not have been reduced in these crops had they been grown to maturity. In a study by Lee et al. (1981), no statistically significant effects were observed on yield for 15 crops aerially irrigated with simulated acid rain at a pH of 2. Most findings from simulated acid rain exposure studies have shown that rain acidity below a pH of 3 can induce direct or indirect deleterious effects on crops and other herbaceous plants, with noticeable growth and yield injury, and reduction (Cohen et al., 1981). However, plants display different acid sensitivities below a pH of 3 in terms of visible acute injury or growth and yield reduction (Kohno, 2017).

Table 7.3: Plant height for crops sprayed with synthetic acid mine water

Crop/pH	Weeks after planting			
	3	4	5	6
<b>Maize</b>				
pH 2	47.2	68.5	96.8	141.4
pH 3	41.0	60.7	89	121.9
pH 4	39.6	59.9	89.5	126.7
pH 7	44.0	68.0	97.8	142.3
Significance	ns	ns	ns	ns
<b>Sorghum</b>				
pH 2	43.2	55.1	80.2	100.7
pH 3	46.5	59.6	81.1	96.8
pH 4	37.7	54.4	75.6	106.9
pH 7	45.1	62.2	84.5	108.9
Significance	ns	ns	ns	ns
<b>Cowpea</b>				
pH 2	20.77	24.50	33.00	50.4
pH 3	21.33	23.70	29.50	42.2
pH 4	23.67	25.50	33.80	47.6
pH 7	21.10	27.00	35.10	55.40
Significance	ns	ns	ns	ns

ns = Non-significant at P = 0.05

Table 7.4: Above-ground dry mass (kg/ha) of crops sprayed with acid mine water

pH	Crop		
	Maize	Sorghum	Cowpea
pH 2	4,433	6,562	3,926
pH 3	7,967	7,167	2,741
pH 4	7,200	8,458	3,037
pH 7	5,350	6,083	2,667
Significance	ns	ns	ns

ns = Non-significant at P = 0.05

Wetting crop leaves with acid water did not have an effect on the LAI (Table 7.5). The same observation was made with the chlorophyll content of specific crops, which was not significantly different for the different pH levels (Table 7.6). This was not expected, as foliar wetting with acid water is associated with chlorosis, scorching and necrosis in plant leaves, which should lower the chlorophyll content. Contrary to this study, Odiyi and Eniola (2015) report that plants that were sprayed with simulated acid rain had a relative growth rate (RGR), chlorophyll content and a Harvest Index that was significantly lower ( $P < 0.05$ ) than the control that had a pH 7.

Table 7.5: Leaf Area Index of crops sprayed with synthetic acid mine water

pH	Crop		
	Maize	Sorghum	Cowpea
pH 2	2.62	2.08	4.87
pH 3	2.16	2.20	4.61
pH 4	1.96	2.33	4.75
pH 7	2.05	2.94	6.15
Significance	ns	ns	ns

ns = Non-significant at P = 0.05

Table 7.6: Chlorophyll content (SPAD units) of crops sprayed with synthetic acid mine water

pH	Crop		
	Maize	Sorghum	Cowpea
pH 2	51.4	45.8	50.9
pH 3	53.2	46.7	51.5
pH 4	54.8	51.9	49.6
pH 7	56.0	50.5	48.5
Significance	ns	ns	ns

ns = Non-significant at P = 0.05

## 7.4 CONCLUSION

Based on the observations and results obtained in this study, it is concluded that cowpea, soybean and sorghum produced significant morphological defects as a result of foliar wetting with AMD at the early seedling stage. It is furthermore concluded that field-planted crops are resistant to foliar wetting with acid mine water after the seedling stage, and that wetting crops with these waters does not lead to a reduction in crop growth.

## 7.5 RECOMMENDATIONS

- The field experiment should be repeated with crops being grown to maturity with daily foliar wetting beginning two days after crop emergence.
- Another experiment should be carried out with the addition of the three potentially toxic elements found in AMD (manganese, iron and aluminium). In addition, the quantities of these elements should be based on typical mine water analyses.
- Crops planted in wet soil can be sprayed with a waxy anti-desiccant after germination prior to irrigating them with acidic mine water to prevent foliar injury until the crops are no longer susceptible.
- A follow-up trial is needed where the crops, grown on adequately limed soil, will be irrigated with acid mine water to evaluate the response of both the soil and the crops.

## 7.6 REFERENCES

- BAKR E (2005) A new software for measuring leaf area, and area damaged by *Tetranychus urticae* Koch. *Journal of Applied Entomology* **129** 173–175.
- BUTCHEE K, GODSEY C, ARNAL B and ZHANG H (2012) Determining critical soil pH for grain sorghum production. *International Journal of Agronomy* 1–6.
- CAPORN SJ and HUTCHINSON TC (1986) The influence of temperature, water and nutrient conditions during growth on the response of *Brassica oleracea* L. to a single, short treatment with simulated acid rain. *The New Phytologist* **106** (2) 251–259.
- COHEN CJ, GROTHAUS LC and PERRIGAN SC (1981) *Effects of simulated sulfuric acid rain on crop plants*. Agricultural Experiment Station, Oregon State University, Corvallis, OR, USA.
- CONKLING BL, BLANCHARD RW and NIBLACK TL (1991) Effects of foliar and soil acidity on the rhizosphere pH of alfalfa, corn, and soybean. *Journal of Environmental Quality* **20** (2) 381–386.
- DEPARTMENT OF WATER AFFAIRS AND FORESTRY (DWA) (1996) *South African water quality*
- DHERE A (2009) Impact of simulated acid rain on the growth of *Sorghum vulgare*. *Journal of Phytological Research* 22(2): 315-318.
- EDJE OT and OSSOM EM (2016) *Crop science handbook*, 2<sup>nd</sup> ed., BlueMoon Publishers, Manzini, Swaziland.
- GOLDEN BR, ORLOWSKI JM and BOND JA (2016) Corn injury from foliar zinc application does not affect grain yield. *Agronomy Journal* 108(5): 2071-2075.
- HUTCHINSON T, DIXON M and SCOTT M (1986) The effect of simulated acid rain on feather mosses and lichens of the boreal forest. *Water, Air, and Soil Pollution* 31(1): 409-416
- JACOBSON JS (1984) Effects of acidic aerosol, fog, mist and rain on crops and trees. *Transactions of the Royal Society of London* **305** 327–338.
- JACOBSON JS, HELLER LI, YAMADA KE, OSMELOSKI JF and BETHARD T (1989) *Foliar injury and growth response of red spruce to sulfate and nitrate acidic mist*. Environmental Biology Program, Boyce Thompson Institute for Plant Research, Ithaca, NY, USA.
- JAMES A (2016) Increase the pH of acidic water to neutral. <https://www.inspireliving.com/>.

- JOVANOVIC N, ANNANDALE J, CLAASSENS A, LORENTZ S, TANNER P, AKEN M and HODGSON F (2004) Commercial production of crops irrigated with gypsiferous mine water. *Water SA* 28(4): 413-422.
- KEEVAR GJ (1982) Plant response to simulated acid rain with special reference to foliar injury, foliar leaching, trichome status and plant nutrition. <https://www.osti.gov/biblio/6577719>}journal={}
- KEEVAR GJ and JACOBSON JS (1983) Response of glycine max (L.) merrill to simulated acid rain II. Localization of foliar injury and growth response. *Field Crops Research* 6 251--259.
- KOHNO Y (2017) Effects of simulated acid rain on Asian crops and garden plants. In: *Air pollution impacts on plants in east Asia*, IZUTA T, Springer, Tokyo, Japan. [https://doi.org/10.1007/978-4-431-56438-6\\_14](https://doi.org/10.1007/978-4-431-56438-6_14).
- KRSTIC D, DJALOVIC I, NIKEZIC D and BJELIC D (2012) *Aluminium in acid soils: Chemistry, toxicity and impact on maize plants, food production – approaches, challenges and tasks*, ALADJADJIYAN A, INTECH, China.
- LAL N (2016) Effects of acid rain on plant growth and development. *E-Journal of Science and Technology* 11 (5) 85–108.
- LEE JJ, NEELY GE, PERRIGAN SC and GROTHAUS LC (1981) Effects of simulated sulfuric acid rain on yield, growth and foliar injury of several crops. <https://www.osti.gov/biblio/6577719>}technical report={}
- LI Q, CHEN J, MCCONNELL DB and HENNY RJ (2007) A simple and effective method for quantifying leaf variegation. *HortTechnology* 17(3): 285-288.
- MACLEAN DC, SCHNEIDER RE and WEINSTEIN LH (1982) Fluoride-induced foliar injury in solanum pseudo-capsicum: Its induction in the dark and activation in the light. *Environmental Pollution* 29 27–33.
- NGALAMU T, ODRA J and TONGUN N (2015) *Cowpea production handbook*, College of Natural Resources and Environmental Studies University of Juba, Juba, South Sudan.
- ODIYI BO and ENIOLA AO (2015) The effect of simulated acid rain on plant growth component of cowpea (*Vigna unguiculata*) L. Walps. *Jordan Journal of Biological Sciences* 1 51–54.
- SALT A (2019) A new study reveals how cuticle protects the leaf. <https://www.botany.one/2019/09/>.
- SCHNEIDER CA, RASBAND WS and ELICEIRI KW (2012) NIH Image to ImageJ: 25 years of image analysis. *Nature Methods* 9 (7) 671–675.
- SOIL CLASSIFICATION WORKING GROUP (1991) *Soil classification: A taxonomic system for South Africa*. Department of Agricultural Development, Pretoria, South Africa.
- SPARKS DL (2003) *Environmental soil chemistry*. Academic press, pp.
- STATON M (2012) *Managing soil pH for optimal Soybean production*. Michigan State University Extension, East Lansing MI, USA.
- SUKATI B (2020) *The Use Of Mine Impacted Water And Its Treatment By-Products In Agriculture*. PhD Thesis, University of Pretoria.

TRAORE M, SULLIVAN CY, ROSOWSKI JR and LEE KW (1989) Comparative leaf surface morphology and the glossy characteristic of sorghum, maize, and pearl millet. *Annals of Botany* **64** (4) 447–453.

## CHAPTER 8: EVALUATION OF IRRIGATION WATER QUALITY GUIDELINES FOR ARSENIC AND LEAD, WITH IMPLICATIONS FOR FOOD SAFETY

---

C McGladdery, JG Annandale, PD Tanner and PC de Jager

### 8.1 INTRODUCTION

As competition for land and water resources, as well as the need to feed a growing population, increases, the agricultural industry will be progressively driven to utilise ever-more contaminated lands and irrigation water sources for crop production (Thiam et al., 2015). Consequently, the probability of producing crops that pose a human health risk is likely to increase.

Research has demonstrated that the edible parts of crops grown in soils or irrigated with water containing elevated levels of potentially hazardous trace elements, such as arsenic and lead, have repeatedly exceeded international food safety guidelines (Alexander et al., 2006; Nayek et al., 2010; Baig and Kazi, 2012; Schreck et al., 2014; Yañez et al., 2019). In the local context, South African water sources have been shown to contain arsenic and lead in excess of the maximum South African Irrigation Water Quality Guideline (DWA, 1996) limit of 2 mg l<sup>-1</sup> of arsenic or lead, particularly in areas that have been impacted on by mining and industry (Dzoma et al., 2010; Mzini and Winter, 2015). Therefore, irrigating crops with water containing the maximum allowable concentration of potentially hazardous trace elements in irrigation water may pose a health risk to those who consume the produce. As far as we are aware, the impact of irrigation water quality guidelines for trace elements, such as arsenic and lead, on the safety of fresh produce has yet to be directly investigated.

Trace elements may enter a plant via two pathways: root uptake and translocation mechanisms, or foliar absorption and phloem mobilisation (Schreck et al., 2014). The uptake pathway (root or shoot) also determines the extent of compartmentalisation and speciation of these elements within plant tissues, which may consequently influence their bioavailability and toxicity (Schreck et al., 2014). Therefore, the way trace elements enter a plant directly affects the location in which they will accumulate and have a potentially hazardous effect. While irrigating crops with trace elements may result in the aboveground biomass coming into contact with those elements (foliar uptake pathway), the medium- to long-term effect of trace element build-up in the soil as a consequence of irrigation with poor-quality waters should also be considered (root uptake pathway). The primary objective of this study was to evaluate whether the uptake of arsenic or lead present in irrigation water, or built-up in soil as a result of irrigation, results in the edible plant parts exceeding food safety thresholds for those elements.

To assess this, two glasshouse trials were conducted:

- The glasshouse foliar absorption trial was established to evaluate whether arsenic or lead present in irrigation water at the “target water quality” or “maximum acceptable” concentrations, applied to the aboveground biomass, results in crop plant parts exceeding modern food safety thresholds for those elements over one growing season.
- The glasshouse root uptake trial was conducted to determine whether arsenic or lead present in the soil as a consequence of medium- to long-term irrigation at the “target water quality” or “maximum acceptable concentration” results in crop plant parts exceeding modern food safety thresholds for those elements over one growing season.

## 8.2 GLASSHOUSE FOLIAR ADSORPTION TRIAL

### Materials and methodology

The glasshouse foliar absorption trial comprised 60 pots. Four crops (barley, beetroot, Swiss chard and garden pea) were evaluated against five treatments (control, arsenic irrigation at 0.1 mg/l, arsenic irrigation at 2.0 mg/l, lead irrigation at 0.2 mg/l and lead irrigation at 2.0 mg/l) with three replicates each. Data from the crops was collected for 10 different plant parts (barley grain, barley leaves, barley stems, beetroot root, beetroot leaves, Swiss chard leaves, peas, pea pods, pea leaves and pea stems), which yielded 150 samples for analysis.

### Results and discussion

#### *Yield responses*

No significant difference in yield response was found between the control and treatment yields for all crops (barley, garden pea, Swiss chard and beetroot) (Table 8.1). The foliar treatments had no effect on the dry mass accumulation in the plant parts (stem, leaf, grain, pea, pod and root) in all the crops. These results were expected, as it was anticipated that the element concentrations applied in the foliar treatments were too low to influence crop growth and yield. The results thus confirmed that foliar applications at the concentrations applied in this study do not influence yield.

Table 8.1: Yield response of crops following irrigation with arsenic- or lead-enriched irrigation water

Crop	Plant part	Average yield $\pm$ SD, dry mass (g.pot <sup>-1</sup> )				
		Control	As [0.1]	As [2.0]	Pb [0.2]	Pb [2.0]
Barley	Grain	9.29 $\pm$ 1.54	9.68 $\pm$ 1.99	9.71 $\pm$ 2.11	10.47 $\pm$ 1.08	9.99 $\pm$ 1.09
	Leaf	5.41 $\pm$ 0.61	4.55 $\pm$ 0.54	5.63 $\pm$ 1.05	4.65 $\pm$ 1.06	4.69 $\pm$ 0.69
	Stem	8.61 $\pm$ 1.15	7.63 $\pm$ 1.52	6.57 $\pm$ 0.69	7.55 $\pm$ 1.09	7.74 $\pm$ 0.41
Garden pea	Pea	2.56 $\pm$ 0.21	2.61 $\pm$ 0.74	2.47 $\pm$ 0.19	1.97 $\pm$ 0.14	2.08 $\pm$ 0.39
	Pod	0.69 $\pm$ 0.05	0.82 $\pm$ 0.17	0.87 $\pm$ 0.08	0.70 $\pm$ 0.05	0.84 $\pm$ 0.05
	Leaf	1.05 $\pm$ 0.20	1.18 $\pm$ 0.29	1.07 $\pm$ 0.23	1.15 $\pm$ 0.01	1.05 $\pm$ 0.11
	Stem	1.78 $\pm$ 0.27	1.42 $\pm$ 0.16	1.45 $\pm$ 0.36	1.47 $\pm$ 0.47	1.64 $\pm$ 0.08
Swiss chard	Leaf	3.37 $\pm$ 0.51	4.25 $\pm$ 0.55	4.00 $\pm$ 0.35	3.23 $\pm$ 0.63	3.29 $\pm$ 0.47
Beetroot	Root	2.63 $\pm$ 0.68	3.80 $\pm$ 1.06	2.91 $\pm$ 0.17	3.86 $\pm$ 1.19	4.06 $\pm$ 0.12
	Leaf	2.96 $\pm$ 1.81	2.57 $\pm$ 0.36	2.35 $\pm$ 0.31	2.02 $\pm$ 0.19	2.78 $\pm$ 0.51

#### *Influence of irrigation treatments on crop quality*

Crop quality was visually assessed by qualitatively assessing phenology, colour (according to the Munsell colour chart) and the presence or absence of treatment residues. No noticeable differences between control and treated plants were observed for each of the four crops under investigation. Arsenic and lead applied via irrigation water did not result in a visible deposit or residue. No difference in size, shape or quantity of barley grains and pea pods was observed. Similarly, the size, shape and colour of Swiss chard, beetroot leaves and beetroot roots did not differ from the control plants.

#### *Arsenic accumulation in plant parts*

Arsenic accumulation in the aboveground biomass was analysed according to plant part (Table 8.2). Fisher's LSD test was performed by combining all arsenic irrigation trial data and comparing the results against the crop controls, where all controls tested below the detection limit and were thus assigned a value of zero. Note that the Chinese (not the South African) food safety guidelines were used to determine the human food safety thresholds for arsenic and lead.

While both guidelines share the same range of allowable arsenic in human foods, the Chinese guidelines specify trace element limits for fruit, vegetables and grains, while the South African guidelines do not.

Table 8.2: Mean arsenic accumulation in dry mass following irrigation with arsenic-enriched irrigation water in relation to food and feed thresholds

Crop	Plant part	As concentration $\pm$ SD, DM (mg.kg <sup>-1</sup> )				Regulated threshold, DM (mg.kg <sup>-1</sup> )
		As [0.1 mg.ℓ <sup>-1</sup> ]	LSD <sup>**</sup>	As [2.0 mg.ℓ <sup>-1</sup> ]	LSD <sup>**</sup>	
Barley	Grain	BDL	a	BDL	a	0.5 <sup>Δ</sup>
	Leaf	10.32 $\pm$ 0.91	b	21.46 $\pm$ 2.42	c	4.0 <sup>*</sup>
	Stem	BDL	a	1.30 $\pm$ 0.55	a	4.0 <sup>*</sup>
Garden pea	Pea	BDL	a	BDL	a	0.7 <sup>Δ</sup>
	Pod	BDL	a	0.46 $\pm$ 0.18	a	0.6 <sup>Δ</sup>
	Leaf	4.04 $\pm$ 1.04	a	19.50 $\pm$ 3.19	c	4.0 <sup>*</sup>
	Stem	BDL	a	2.09 $\pm$ 0.73	a	4.0 <sup>*</sup>
Swiss chard	Leaf	1.56 $\pm$ 0.51	a	33.38 $\pm$ 4.48	d	6.3 <sup>Δ</sup>
Beetroot	Root	BDL	a	BDL	a	3.6 <sup>Δ</sup>
	Leaf	1.09 $\pm$ 0.39	a	10.57 $\pm$ 1.21	b	6.3 <sup>Δ</sup>

<sup>\*\*</sup> Means assigned the letter "a" are not significantly different from the control at the 95% probability level (Fisher's LSD test).  
BDL: Below method detection limit of 0.70 mg.kg<sup>-1</sup>.  
<sup>Δ</sup> Food safety threshold derived from the National Food Safety Standards, People's Republic of China (2012).  
<sup>\*</sup> DAFF Act No. 36 of 1947, Annexure 4: Undesirable substances in farm feeds.

Whole barley grains (inclusive of bran) did not accumulate arsenic above the MDL of 0.70 mg.ℓ<sup>-1</sup> in either of the arsenic irrigation treatments: 0.1 mg.ℓ<sup>-1</sup> (target water quality) and 2.0 mg.ℓ<sup>-1</sup> (maximum acceptable water quality). In contrast, barley leaves, and to a lesser extent, stems, accumulated most of the arsenic applied to the aboveground biomass. Since these plant parts are not consumed by humans, arsenic accumulation in these parts does not pose a risk to human food safety. In terms of animal feed, barley leaves in both arsenic irrigation treatments accumulated arsenic in excess of the regulated 4 mg.kg<sup>-1</sup> (relative to a farm feed with a moisture content of 120 g kg<sup>-1</sup>) for hay, straw, lucerne, roughage and bagasse, while the stems did not (DAFF, 1947). Peas and pods did not accumulate arsenic above the human food safety threshold when irrigated with arsenic at both treatment levels. Similar to barley, pea leaves accumulated most of the arsenic applied to the aboveground biomass. Leaves that received the 2 mg ℓ<sup>-1</sup> arsenic treatment far exceeded the animal feed threshold, while leaves that received the 0.1 mg.ℓ<sup>-1</sup> arsenic treatment only marginally exceeded the animal feed threshold of 4.0 mg kg<sup>-1</sup> arsenic (DAFF, 1947). Swiss chard leaves irrigated with the 0.1 mg ℓ<sup>-1</sup> arsenic treatment did not exceed the food safety threshold of 6.3 mg kg<sup>-1</sup>.

However, similar to the findings of Mahmood and Malik (2014), Swiss chard leaves that received the 2 mg ℓ<sup>-1</sup> arsenic irrigation treatment readily absorbed foliar-applied arsenic and accumulated the largest amount of arsenic of all the crops and plant parts, with an average of 33.4 mg kg<sup>-1</sup> arsenic on a dry mass basis. This concentration was five times more than the regulated food safety threshold and is likely due to the large surface area of Swiss chard leaves (Nayek et al., 2010; Mahmood and Malik, 2014). Beetroot roots did not accumulate arsenic above the detection limit of 0.70 mg kg<sup>-1</sup> at either irrigation treatment level. While, according to Page and Feller (2015), arsenate and arsenite can be remobilised in the phloem and translocated to the roots, this process did not seem to occur, possibly because the phosphate fertilizer supplied adequate phosphorous to the roots throughout the growing period and therefore did not initiate the remobilisation process.

Similar to Swiss chard leaves, the foliar accumulation of arsenic was significant at both treatment levels, but only exceeded the food safety threshold at the "maximum acceptable" irrigation concentration, accumulating 10.6 mg arsenic kg<sup>-1</sup> dry mass. The highest rate of arsenic absorption occurred on the leaf surfaces of all four crops. This is likely due to the larger surface area and more complex cuticle morphology of leaves, as well as the increased concentration of epidermal structures through which arsenic may be absorbed (Nayek et al., 2010; Mahmood and Malik, 2014).

The lower rate of arsenic uptake via stems may also suggest that arsenite was oxidised to arsenate when applied to the stem surface, which may then have strongly associated with pre-existing iron and aluminium oxide soil and dust particles, and later been washed off the leaf surface during subsequent irrigations or during the sample washing process in the laboratory after harvest. Owing to the small number of replicates per treatment (three for each plant part of each crop), mean values may not have accurately reflected true values where large variability among replicates occurred.

To evaluate the validity of using the means, the medians were also investigated and are recorded in Table 8.3. Comparison of the median and mean values demonstrated that, in all but one instance, the selection of this statistical parameter did not change the result of whether or not the treatment exceeded dry mass food safety thresholds. Only in pea leaves irrigated with  $0.1 \text{ mg } \ell^{-1}$  arsenic did the median reflect a value below the animal feed threshold of  $4.0 \text{ mg kg}^{-1}$ , while the median value just exceeded the threshold at  $4.04 \text{ mg kg}^{-1}$ . Owing to the similarities in results between the median and mean values, both serve to validate the other, thereby justifying the use of means for this data set.

Table 8.3: Median arsenic accumulation in dry mass following irrigation with arsenic-enriched irrigation water in relation to food and feed thresholds

Crop	Plant part	As concentration, DM ( $\text{mg.kg}^{-1}$ )				Regulated threshold, DM ( $\text{mg.kg}^{-1}$ )
		As [ $0.1 \text{ mg.}\ell^{-1}$ ]	Above threshold frequency	As [ $2.0 \text{ mg.}\ell^{-1}$ ]	Above threshold frequency	
Barley	Grain	BDL		BDL		0.5 <sup>Δ</sup>
	Leaf	9.62	***	24.26	***	4.0 *
	Stem	BDL		0.99		4.0 *
Garden pea	Pea	BDL		BDL		0.7 <sup>Δ</sup>
	Pod	BDL		0.53		0.6 <sup>Δ</sup>
	Leaf	2.74	*	16.81	***	4.0 *
	Stem	0.11		1.22		4.0 *
Swiss chard	Leaf	1.16		29.01	***	6.3 <sup>Δ</sup>
Beetroot	Root	BDL		BDL		3.6 <sup>Δ</sup>
	Leaf	1.55		11.04	***	6.3 <sup>Δ</sup>

\* Number of replicates that were above the regulated threshold (maximum of 3).  
BDL: Below method detection limit of  $0.70 \text{ mg.}\ell^{-1}$ .  
<sup>Δ</sup> Food safety threshold derived from the National Food Safety Standards, People's Republic of China (2012).  
\* DAFF Act No. 36 of 1947, Annexure 4: Undesirable substances in farm feeds.

The above threshold frequency, recorded in Table 8.3, serves to illustrate the number of replicates that exceeded the food or feed safety threshold for arsenic. Note that, in all cases where the median value exceeded either the human food or animal feed arsenic threshold, all three replicates were above the threshold value. Only in the case of garden pea leaves did one of the three replicates exceed the animal feed arsenic threshold. Figure 8.1 provides a visual representation of which edible parts exceeded the food safety thresholds for arsenic and which did not.

The results of this study demonstrate that barley grains, pea pods and beetroot roots irrigated with arsenic-loaded water to the “maximum acceptable” concentration did not accumulate enough arsenic to pose a risk to human health. Similarly, none of the crops investigated exceeded food safety thresholds when irrigated with arsenic at  $0.1 \text{ mg } \ell^{-1}$ . However, when irrigated at  $2.0 \text{ mg } \ell^{-1}$  arsenic, Swiss chard and beetroot leaves exceeded the food safety thresholds and may thus pose a risk to human health if consumed as a regular dietary component. Swiss chard leaves accumulated an exceptionally large amount of arsenic at over five times the food safety threshold.

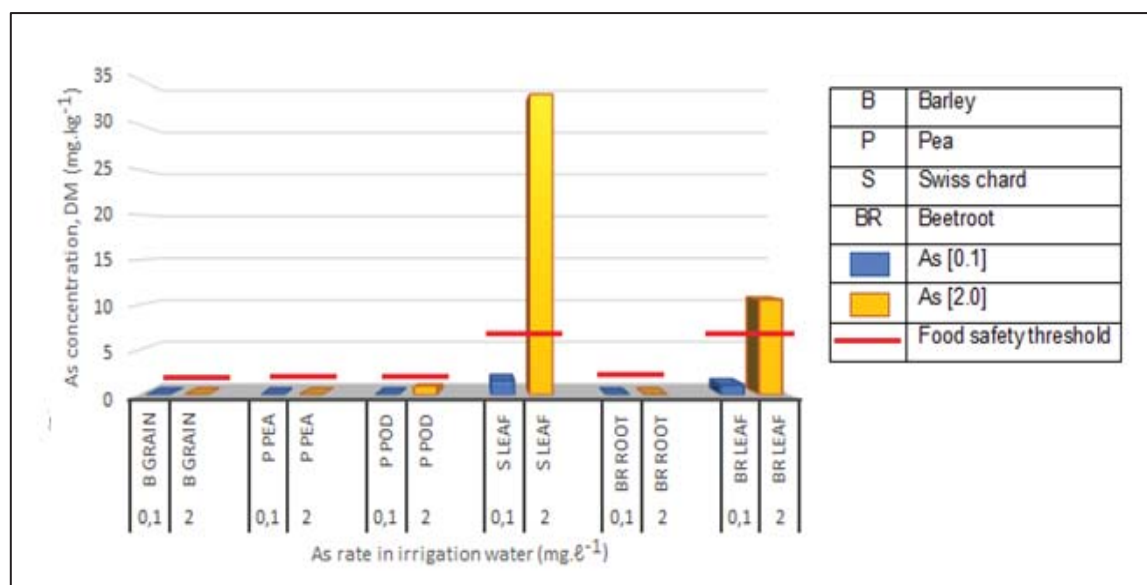


Figure 8.1: Arsenic accumulation on a dry mass basis, within edible plant parts of crops wetted with arsenic-enriched water every one to three days throughout the growing period, in relation to food safety thresholds

#### Lead accumulation in plant parts

The results of the lead irrigation treatments showed a similar trend to that of the arsenic irrigation treatments, with leaves accumulating by far the greatest quantity of lead applied via irrigation water (Table 8.4). The major difference between the two treatments was that leaves irrigated with lead treatments tended to accumulate lead at a rate almost double that of the arsenic treatments. One possible explanation is that the source of lead, lead nitrate, used when formulating the irrigation treatments, was more easily adsorbed via the leaf cuticular surface than the arsenic source, sodium arsenite. However, the complexation of lead and nitrate is relatively low (Category 5), according to Sposito (2008). It is more likely that the industry standard of reporting concentration on a mass basis has artificially inflated the relative concentration of lead in comparison to arsenic because the atomic mass of lead is approximately three times greater than that of arsenic.

Table 8.4: Lead accumulation in dry mass following irrigation with lead-enriched irrigation water in relation to food safety thresholds

Crop	Plant part	Mean Pb concentration $\pm$ SD, DM (mg.kg <sup>-1</sup> )				Food safety threshold, DM (mg.kg <sup>-1</sup> )
		Pb [0.2 mg.l <sup>-1</sup> ]	LSD <sup>~</sup>	Pb [2.0 mg.l <sup>-1</sup> ]	LSD <sup>~</sup>	
Barley	Grain	BDL	a	BDL	a	0.2 <sup>Δ</sup>
	Leaf	BDL	a	46.26 $\pm$ 8.78	e	40.0 *
	Stem	4.26 $\pm$ 1.51	a	17.57 $\pm$ 3.84	bc	40.0 *
Garden pea	Pea	BDL	a	BDL	a	0.3 <sup>Δ</sup>
	Pod	BDL	a	BDL	a	0.2 <sup>Δ</sup>
	Leaf	26.26 $\pm$ 6.92	bcd	27.91 $\pm$ 2.40	bcd	40.0 *
	Stem	BDL	a	BDL	a	40.0 *
Swiss chard	Leaf	32.42 $\pm$ 2.97	cd	62.41 $\pm$ 7.21	f	3.8 <sup>Δ</sup>
Beetroot	Root	BDL	a	BDL	a	0.7 <sup>Δ</sup>
	Leaf	8.34 $\pm$ 3.10	ab	19.91 $\pm$ 3.19	bc	3.8 <sup>Δ</sup>

<sup>~</sup> Means assigned the letter "a" are not significantly different from the control at the 95% probability level (Fisher's LSD test).  
BDL: Below method detection limit of 1.4 mg.kg<sup>-1</sup>.  
<sup>Δ</sup> Food safety threshold derived from the National Food Safety Standards, People's Republic of China (2012).  
\* DAFF Act No. 36 of 1947, Annexure 4: Undesirable substances in farm feeds.

Swiss chard and beetroot leaves accumulated lead well beyond the food safety guidelines at both lead irrigation levels. At the “maximum acceptable” lead concentration of 2.0 mg  $\ell^{-1}$ , beetroot leaves accumulated five times more than the regulated food safety limit, and Swiss chard leaves accumulated 16 times more lead than the regulated limit. Apart from barley stems, only the leaves of each crop accumulated lead above the method detection limit of 1.4 mg  $\text{kg}^{-1}$ . These results are comparable to Schreck et al. (2014), where lettuce leaves accumulated 171.5 mg arsenic  $\text{kg}^{-1}$  dry mass after six weeks of exposure to atmospheric deposition of lead. In terms of animal feed, only barley leaves exceeded the maximum lead threshold of 40 mg  $\text{kg}^{-1}$  (relative to a farm feed with a moisture content of 120 g  $\text{kg}^{-1}$ ) for green roughages. Barley stems, pea stems and pea leaves were fit for use as animal feed under both lead irrigation treatments. More leaves and stems were considered fit for animal consumption, not because they accumulated less lead when compared to the arsenic irrigation trials, but because the lead feed guideline is 10 times higher (40 mg  $\text{kg}^{-1}$ ) than the arsenic feed guideline (4 mg  $\text{kg}^{-1}$ ).

As with the arsenic analysis, median values were also investigated to evaluate the validity of using the mean scores and are recorded in Table 8.5. Comparison of the median and mean values demonstrated that the selection of the statistical parameter did not change the result of whether the treatment exceeded the dry mass food safety threshold. Owing to the similarities in results between the median and mean values, both serve to validate the other, thereby justifying the use of means for this data set.

Table 8.5: Median lead accumulation in dry mass following irrigation with lead-enriched irrigation water in relation to food and feed thresholds

Crop	Plant part	Pb concentration, DM (mg.kg <sup>-1</sup> )				Regulated threshold, DM (mg.kg <sup>-1</sup> )
		Median Pb [0.2 mg.ℓ <sup>-1</sup> ]	Replicates Above threshold frequency	Median Pb [2.0 mg.ℓ <sup>-1</sup> ]	Above threshold frequency	
Barley	Grain	BDL		BDL	•	0.2 <sup>Δ</sup>
	Leaf	BDL		44.93	**	40.0 *
	Stem	6.34		21.96		40.0 *
Garden pea	Pea	BDL	•	BDL		0.3 <sup>Δ</sup>
	Pod	BDL		BDL		0.2 <sup>Δ</sup>
	Leaf	33.56		30.5		40.0 *
	Stem	BDL		BDL		40.0 *
Swiss chard	Leaf	33.63	***	52.5	***	3.8 <sup>Δ</sup>
Beetroot	Root	BDL		BDL		0.7 <sup>Δ</sup>
	Leaf	14.9	***	28.91	***	3.8 <sup>Δ</sup>

• Number of replicates that were above the regulated threshold (maximum of 3).  
BDL: Below method detection limit of 1.4 mg.ℓ<sup>-1</sup>.  
<sup>Δ</sup> Food safety threshold derived from the National Food Safety Standards, People's Republic of China (2012).  
\* DAFF Act No. 36 of 1947, Annexure 4: Undesirable substances in farm feeds.

Generally, the variability of the lead data was higher than that of the arsenic data, which is further explained by the method detection limit differences (arsenic at 0.7 mg  $\ell^{-1}$  and lead at 1.4 mg  $\ell^{-1}$ ). For example, the high standard deviation ( $\pm 1.51$ ) associated with the mean of lead in barley stems irrigated with the 0.2 mg  $\ell^{-1}$  lead treatment (4.26) is explained by a low replicate below the MDL that skewed the mean.

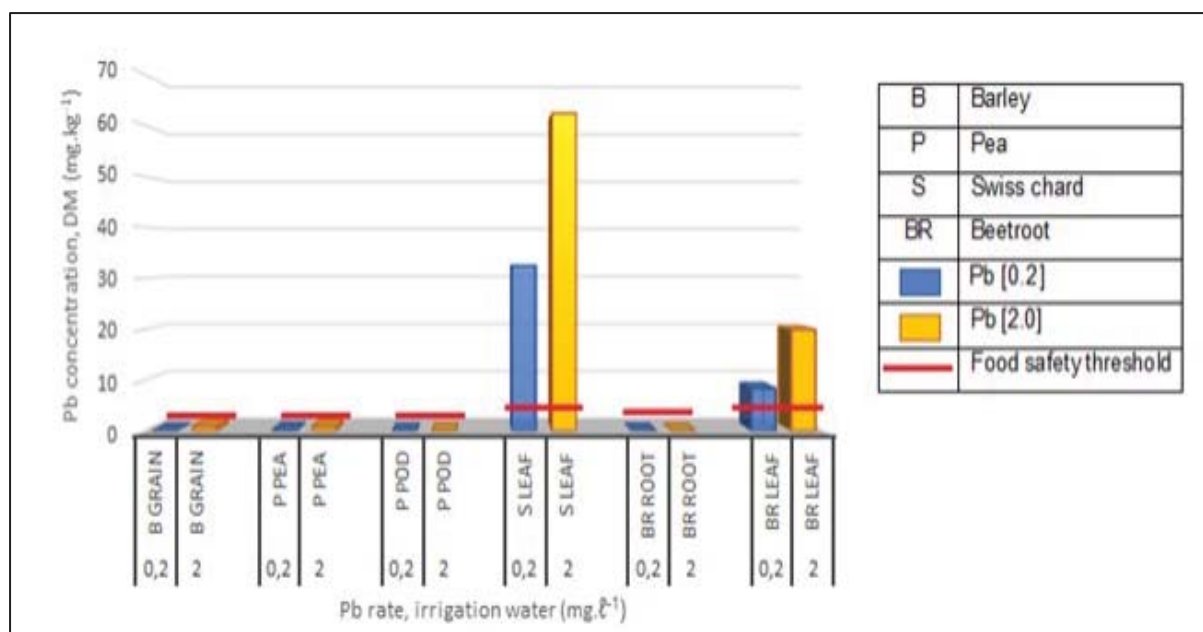


Figure 8.2: Lead accumulation, dry mass basis, within edible parts of crops wetted with lead-enriched water every two days throughout the growing period in relation to food safety thresholds

Beetroot leaves and, more significantly, Swiss chard leaves, accumulated lead well beyond the food safety threshold at both “target water quality” and “maximum acceptable” lead irrigation treatments. In contrast, no edible parts of the remaining crops accumulated lead above the MDL.

### 8.3 GLASSHOUSE ROOT UPTAKE TRIAL

#### Materials and methods

The glasshouse root uptake trial comprised 60 pots. Four crops (barley, beetroot, Swiss chard and garden pea) were evaluated against five treatments (control, soil enriched with 43.5 mg kg<sup>-1</sup> arsenic, soil enriched with 168.9 mg kg<sup>-1</sup> arsenic, soil with 88.1 mg kg<sup>-1</sup> lead and soil dosed with 168.9 mg.kg<sup>-1</sup> lead) with three replicates of each. Data from the crops was collected for ten different plant parts (barley grain, barley leaves, barley stems, beetroot root, beetroot leaves, Swiss chard leaves, pea pods, pea leaves and pea stems), which yielded 150 samples for analysis.

#### Effect of treatment applications on soil properties

Soil samples from pots were analysed approximately two weeks after harvest. A summary of the effect of the soil treatments on pH and EC is recorded in Table 8.6. As anticipated, the addition of arsenic and lead salts during the soil treatment dosing process increased the EC of the soil. The dosing of sodium arsenite increased soil EC from 0.071 mS m<sup>-1</sup> to 0.219 mS m<sup>-1</sup> at 43.5 mg.kg<sup>-1</sup> arsenic and 0.229 mS m<sup>-1</sup> at 168.9 mg kg<sup>-1</sup> arsenic. Similarly, the addition of lead nitrate salts increased the soil EC to 0.205 mS m<sup>-1</sup> at 88.1 mg.kg<sup>-1</sup> lead and 0.208 mS m<sup>-1</sup> at 168.9 mg.kg<sup>-1</sup> lead. The resulting increase in EC was below the 0.250 mS m<sup>-1</sup> threshold at which salt-sensitive crops may begin to show signs of osmotic stress (FERTASA, 2016).

Table 8.6: Effect of arsenic and lead treatments on soil pH and EC

Element	Target concentration (mg.kg <sup>-1</sup> )	pH <sub>water</sub> ± SD	pH <sub>CaCl</sub> ± SD	EC ± SD (mS.m <sup>-1</sup> )
Control	0.0	6.71 ± 0.30	6.17 ± 0.21	0.071 ± 0.002
As	43.5	7.14 ± 0.17	6.56 ± 0.13	0.219 ± 0.047
	168.9	6.98 ± 0.36	6.66 ± 0.20	0.229 ± 0.099
Pb	88.1	7.03 ± 0.23	6.63 ± 0.14	0.205 ± 0.050
	168.9	6.96 ± 0.13	6.57 ± 0.16	0.207 ± 0.056

Approximately two weeks after harvest, soil from each pot in the root uptake glass house trial was sampled and analysed to determine the total (acid extractable) and bioavailable (salt extractable) concentrations of applied arsenic or lead (Table 8.7). Three additional pots enriched with 168.9 mg kg<sup>-1</sup> arsenic and three at 168.9 mg kg<sup>-1</sup> lead were left unplanted and occasionally irrigated to simulate the effects of a fallow period on arsenic and lead sequestration.

Table 8.7: Bioavailability of arsenic and lead 22 weeks after soil application

Element	Target concentration (mg.kg <sup>-1</sup> )	Crop	Acid extraction (mg.kg <sup>-1</sup> )	Salt extraction (mg.kg <sup>-1</sup> )
As	43.5	Barley	36.18	BDL
		Garden pea	34.66	1.71
		Swiss chard	36.26	BDL
		Beetroot	35.42	1.49
As	168.9	Barley	101.48	23.73
		Garden pea	127.96	28.45
		Swiss chard	156.95	33.97
		Beetroot	115.19	36.61
		Unplanted *	173.40	98.17
Pb	88.1	Barley	85.89	BDL
		Garden pea	77.97	BDL
		Swiss chard	93.54	BDL
		Beetroot	91.92	BDL
Pb	168.9	Barley	158.87	BDL
		Garden pea	182.53	BDL
		Swiss chard	152.78	BDL
		Beetroot	163.19	BDL
		Unplanted *	160.17	9.57

BDL: Below method detection limit of 0.70 mg.kg<sup>-1</sup> for As or 1.40 mg.kg<sup>-1</sup> for Pb.

On a mass balance basis, less than 1% of the total applied arsenic or lead was incorporated into the plant biomass, while the rest underwent physicochemical transformations to be incorporated into the soil mineral structure. In pots enriched with 43.5 mg kg<sup>-1</sup> arsenic, only 3.1% of the arsenic was plant available after 22 weeks. For pots with 168.9 mg kg<sup>-1</sup> arsenic, 24.5% of the total arsenic was plant available. Therefore, the soil's ability to buffer arsenic was dose dependent, as it could effectively immobilise approximately 95 mg kg<sup>-1</sup> arsenic after 22 weeks. These results would suggest that arsenite from the sodium arsenite source used to dose the soil may have been oxidised to arsenate over time. Therefore, like phosphate, arsenate may have strongly associated with iron and aluminium oxyhydroxides, resulting in far less remaining exchangeable and salt extractable arsenic. The soil used in this trial exhibited a high propensity for lead attenuation. When dosed with both 88.1 mg kg<sup>-1</sup> and 168.9 mg kg<sup>-1</sup> lead, all salt extractable lead was below the MDL. Lead immobilisation was likely a result of multiple physicochemical factors: lead may have been buffered by the soil's cation exchange; phosphate fertilizer applications may have resulted in insoluble lead phosphate precipitates, and lead may have undergone sorption onto the relatively high concentration of amorphous iron, aluminium and manganese oxyhydroxides.

Interestingly, soils in which crops were grown were shown to significantly increase the rate of arsenic and lead immobilisation when compared to unplanted “fallow” soils. When dosed with the higher trace element rates, 56.6% of the arsenic and 6% of the lead in the unplanted pots were salt extractable after 22 weeks, compared to 24.5% arsenic and 0% lead in planted pots. This significant decrease of bioavailability in planted pots may be attributed to the effect of plant root exudates and/or the more regular wetting and drying cycle of the soils in planted pots, which was shown to increase the incidence of reactive amorphous iron, aluminium and manganese oxyhydroxides.

## Results and discussion

### *Yield response*

No significant difference in yield response was found between the control and the arsenic- or lead-treated pots for all crops (barley, garden pea, Swiss chard and beetroot) (Table 8.8). The soil dosing treatments of arsenic had no effect on dry mass accumulation in all crops' plant parts (stem, leaf, grain, pea pod and root). However, while the lead treatments did not affect yield, an increase in leaf dry mass was noted when barley and garden pea was grown in the higher lead-dosed soils (168.9 mg kg<sup>-1</sup>). This is most likely a consequence of the increased nitrogen input, as lead nitrate salt was used to simulate lead accumulation. These results were expected because “food safety-limited trace elements” are deemed more likely to accumulate in plant tissues, to the extent that they may become a zootoxic risk before phytotoxicity symptoms are exhibited. The results thus confirmed that the soil dose concentrations of arsenic and lead applied in this study did not have an impact on yield.

Table 8.8: Yield response of crops grown in arsenic- or lead-enriched soil

Crop	Plant part	Average yield ± SD, dry mass (g.pot <sup>-1</sup> )				
		Control	As [43.5]	As [168.9]	Pb [88.1]	Pb [168.9]
Barley	Grain	9.89 ± 1.06	9.65 ± 0.24	9.66 ± 0.79	9.68 ± 2.37	8.82 ± 2.50
	Leaf	4.90 ± 0.73	3.62 ± 0.40	4.08 ± 0.93	6.42 ± 0.56	5.08 ± 0.26
	Stem	7.65 ± 0.96	7.59 ± 0.64	7.86 ± 1.40	10.37 ± 1.25	9.59 ± 2.78
Garden pea	Pea	2.01 ± 0.41	2.68 ± 0.69	3.12 ± 0.51	3.76 ± 0.67	4.64 ± 0.50
	Pod	0.82 ± 0.10	1.34 ± 0.15	1.19 ± 0.21	1.19 ± 0.03	1.43 ± 0.16
	Leaf	1.22 ± 0.26	1.77 ± 0.09	1.30 ± 0.09	1.53 ± 0.15	2.09 ± 0.11
Swiss chard	Stem	1.52 ± 0.33	2.35 ± 0.40	2.08 ± 0.15	2.08 ± 0.11	2.33 ± 0.09
	Leaf	3.79 ± 0.61	2.75 ± 0.75	2.15 ± 0.10	3.99 ± 0.92	2.59 ± 0.71
Beetroot	Root	3.13 ± 0.70	2.52 ± 0.63	3.30 ± 0.59	2.31 ± 0.09	3.01 ± 0.41
	Leaf	2.48 ± 0.88	2.06 ± 0.17	1.91 ± 0.91	2.26 ± 0.42	1.72 ± 0.53

### *Influence of soil dose treatments on crop quality*

Crop quality was visually assessed by qualitatively assessing phenology, colour (according to the Munsell colour chart) and the presence or absence of treatment residues. No noticeable differences between control and treated plants were observed for each of the four crops under investigation. No difference in size, shape and quantity of barley grains and pea pods was observed. Similarly, the size, shape and colour of Swiss chard, beetroot leaves and beetroot roots did not seem to differ from that of the control plants.

### *Arsenic accumulation in plant parts*

Results for arsenic accumulation in plant parts under the different arsenic-enriched soils are recorded in Table 8.9. The arsenic-enriched soils were aimed at simulating arsenic accumulation in the soil after 19 years of irrigation at the “maximum allowable water quality” of 2.0 mg l<sup>-1</sup> and after 99 years of irrigation at the “target water quality” of 0.2 mg l<sup>-1</sup>. Fisher's LSD test was performed by combining all arsenic irrigation trial data and comparing the results against the crop controls. All controls tested below the detection limit and were thus assigned a value of 0 mg kg<sup>-1</sup> arsenic.

Note that the Chinese (not the South African) food safety guidelines were used to determine the human food safety thresholds for arsenic and lead. While both guidelines share the same range of allowable arsenic in rice, the Chinese guidelines specify trace element limits for fruit, vegetables and other grains, while the South African guidelines do not.

Plant parts that may be used as animal feed were compared to the farm feed guidelines of the South African Department of Agriculture, Forestry and Fisheries (DAFF, 1947).

Table 8.9: Mean arsenic accumulation in the dry mass of crops grown in arsenic-enriched soils in relation to food and feed thresholds

Crop	Plant part	Mean As concentration $\pm$ SD, DM (mg.kg <sup>-1</sup> )				Regulated threshold, DM (mg.kg <sup>-1</sup> )
		As [43.5 mg.kg <sup>-1</sup> ]	LSD <sup>™</sup>	As [168.9 mg.kg <sup>-1</sup> ]	LSD <sup>™</sup>	
Barley	Grain	0.93 $\pm$ 0.42	a	0.96 $\pm$ 0.32	a	0.5 <sup>Δ</sup>
	Leaf	12.64 $\pm$ 1.74	bc	28.64 $\pm$ 14.90	d	4.0 *
	Stem	1.52 $\pm$ 1.10	a	2.67 $\pm$ 1.32	a	4.0 *
Garden pea	Pea	BDL	a	BDL	a	0.7 <sup>Δ</sup>
	Pod	0.86 $\pm$ 0.66	a	1.47 $\pm$ 0.32	a	0.6 <sup>Δ</sup>
	Leaf	13.25 $\pm$ 5.06	bc	14.48 $\pm$ 2.10	bc	4.0 *
	Stem	5.62 $\pm$ 1.76	a	6.55 $\pm$ 1.38	ab	4.0 *
Swiss chard	Leaf	2.67 $\pm$ 2.02	a	12.31 $\pm$ 2.22	bc	6.3 <sup>Δ</sup>
Beetroot	Root	3.91 $\pm$ 1.30	a	4.88 $\pm$ 3.18	a	3.6 <sup>Δ</sup>
	Leaf	3.03 $\pm$ 1.96	a	16.67 $\pm$ 6.20	bc	6.3 <sup>Δ</sup>

<sup>™</sup> Means assigned the letter "a" are not significantly different from the control at the 95% probability level (Fisher's LSD test).  
BDL: Below method detection limit of 0.70 mg.kg<sup>-1</sup>.  
<sup>Δ</sup> Food safety threshold derived from the National Food Safety Standards, People's Republic of China (2012).  
\* DAFF Act No. 36 of 1947, Annexure 4: Undesirable substances in farm feeds.

In crops grown in soils enriched with 43.5 mg kg<sup>-1</sup> arsenic, none of the edible parts of the four tested crops, except for barley grains, exceeded the food safety threshold. The grains of barley grown in 168.9 mg kg<sup>-1</sup> arsenic also exceeded the food safety threshold of 0.5 mg kg<sup>-1</sup> arsenic on a dry mass basis. However, at both arsenic soil concentrations, the results were not statistically differentiable from the control. However, proportionally more arsenic in the root uptake trial accumulated in the stems, compared to the foliar uptake trial. This was expected, since all arsenic was initially taken up by the roots, and then translocated to the leaves via the stems. Swiss chard and beetroot leaves were shown to accumulate arsenic well beyond the food safety threshold when grown in soil enriched with 168.9 mg kg<sup>-1</sup> arsenic. In terms of animal feed, both garden pea leaves and stems exceeded the animal feed threshold of 4.0 mg kg<sup>-1</sup> arsenic (DAFF, 1947) at both arsenic soil treatments. Similarly, barley leaves were also found to be unfit for use as animal feed when grown in both arsenic-treated soils. However, barley stems did not accumulate arsenic in excess of the regulated animal feed guidelines. While the peas did not accumulate arsenic beyond the method detection limit, pods were found to accumulate arsenic beyond the food safety guideline threshold at both soil treatment levels. Similarly, beetroot roots accumulated arsenic at both soil treatment levels that exceed the food safety guidelines. Note that food safety testing standards require all root vegetables to be peeled first. Therefore, unpeeled beetroot may have shown considerably higher arsenic contamination and posed an even greater food safety risk. The results of this trial indicated that arsenic taken up by roots exhibited a tendency to accumulate in leaf and stem tissues in all four crops. This is of concern if the roughage is to be used for animal feed. Therefore, with the exception of cultivating leafy vegetables, and possibly grains, and owing to the stricter animal feed thresholds for arsenic, soils containing elevated levels of arsenic may be better suited for the production of crops for human food instead of animal feed.

Owing to the small number of replicates per treatment (three for each plant part of each crop), mean values may not have accurately reflected true values where large variability among the replicates occurred. To evaluate the validity of using the means, the medians were also investigated and are recorded in Table 8.10. Comparison of the median and mean values demonstrated that the selection of the statistical parameter did not change the result of whether the treatment exceeded the dry mass food safety or animal feed threshold. Owing to the similarities in results between the median and mean values, both serve to validate the other, thereby justifying the use of means for this data set.

Table 8.10: Median arsenic accumulation in the dry mass of crops grown in arsenic-enriched soils in relation to food and feed thresholds

Crop	Plant part	Median As concentration, DM (mg.kg <sup>-1</sup> )				Regulated threshold, DM (mg.kg <sup>-1</sup> )
		As [43.5 mg.kg <sup>-1</sup> ]	Above threshold frequency	As [168.9 mg.kg <sup>-1</sup> ]	Above threshold frequency	
Barley	Grain	0.96	**	1.28	***	0.5 <sup>Δ</sup>
	Leaf	13.00	***	33.88	***	4.0*
	Stem	2.01		2.45	*	4.0*
Garden pea	Pea	BDL		BDL		0.7 <sup>Δ</sup>
	Pod	0.98		1.33		0.6 <sup>Δ</sup>
	Leaf	10.85	***	15.88	***	4.0*
	Stem	4.41	**	6.06	***	4.0*
Swiss chard	Leaf	3.14		13.56	***	6.3 <sup>Δ</sup>
Beetroot	Root	3.05	*	5.00	*	3.6 <sup>Δ</sup>
	Leaf	1.92		17.82	***	6.3 <sup>Δ</sup>

\* Number of replicates that were above the regulated threshold (maximum of 3).  
BDL: Below method detection limit of 0.70 mg.kg<sup>-1</sup>.  
<sup>Δ</sup> Food safety threshold derived from the National Food Safety Standards, People's Republic of China (2012).  
\* DAFF Act No. 36 of 1947, Annexure 4: Undesirable substances in farm feeds.

The threshold frequency recorded in Table 8.10 serves to illustrate the number of replicates that exceeded the food or feed safety threshold for arsenic. Note that, in all cases where the median value exceeded either the human food or animal feed arsenic threshold, all three replicates were above the threshold value. Only in the case of garden pea stems did two of the three replicates exceed the animal feed arsenic threshold. However, this is explained by the fact that the mean and median values for garden pea stems are very close to the food safety threshold, so some variability above and below the threshold was to be expected. A summary of the results of the arsenic soil dosing treatments on barley, garden pea, Swiss chard and beetroot on human food safety is recorded in Figure 8.3. Owing to the criteria of food safety thresholds, only arsenic concentrations within the edible parts of each crop are presented.

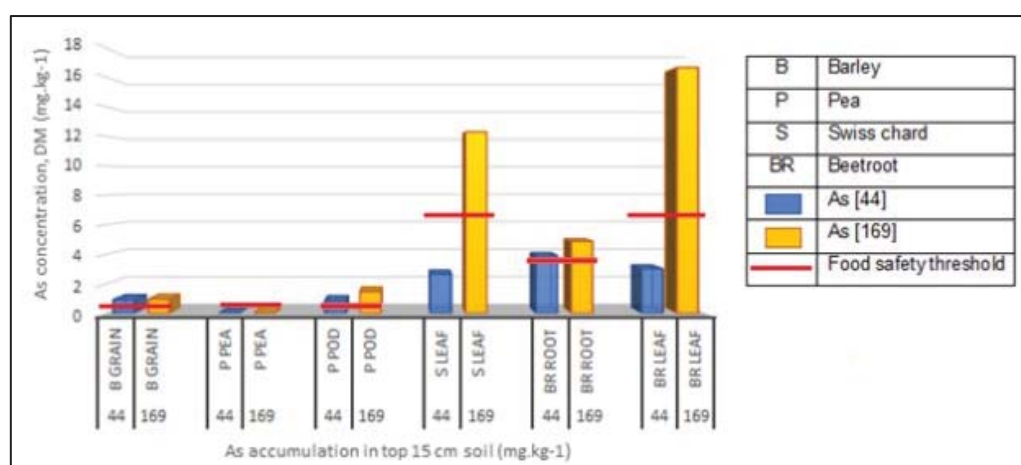


Figure 8.3: Arsenic accumulation on a dry mass basis, within edible parts of crops grown in arsenic-enriched soil at 43.5 mg kg<sup>-1</sup> (simulating 99 years of irrigation at 0.1 mg ℓ<sup>-1</sup>) and 168.9 mg kg<sup>-1</sup> (19 years of irrigation at 2.0 mg ℓ<sup>-1</sup>) in relation to food safety thresholds

Only Swiss chard and beetroot leaves grown in soils contaminated with 168.9 mg kg<sup>-1</sup> arsenic, representing 19 years of irrigation at 2.0 mg l<sup>-1</sup> arsenic, significantly exceeded the human food safety threshold. Barley grains exceeded food safety guidelines at both concentrations. However, the results were not statistically significant and therefore the findings are inconclusive. Pea pods and beetroot roots were shown to accumulate arsenic in a typical dose response. However, arsenic in those tissues was not found to be in excess of the arsenic limit in foods.

#### Lead accumulation in plant parts

Similar to the findings with regard to arsenic uptake, the majority of lead taken up by each crop accumulated in the leaf and stem tissue, with very little being translocated into the edible fruits (peas and pods) and grains (barley). However, more lead was shown to accumulate in the beetroot roots when compared to arsenic that had accumulated in beetroot roots grown in arsenic-enriched soils. A likely explanation is that, according to Dollard (1986), lead is not remobilised in the phloem and would therefore be expected to remain in the roots, stems and leaves. Table 8.11 details the mean and standard deviation of lead accumulation in each plant part.

Table 8.11: Mean lead accumulation in the dry mass of crops grown in lead-enriched soil in relation to food and feed thresholds

Crop	Plant part	Mean Pb concentration, DM (mg.kg <sup>-1</sup> )				Regulated threshold, DM (mg.kg <sup>-1</sup> )
		Pb [88.1 mg.kg <sup>-1</sup> ]	LSD <sup>™</sup>	Pb [168.9 mg.kg <sup>-1</sup> ]	LSD <sup>™</sup>	
Barley	Grain	BDL	a	BDL	a	0.2 <sup>Δ</sup>
	Leaf	BDL	a	2.52 ± 1.02	ab	40.0 *
	Stem	1.86 ± 0.74	ab	3.96 ± 1.22	b	40.0 *
Garden pea	Pea	BDL	a	BDL	a	0.3 <sup>Δ</sup>
	Pod	BDL	a	2.78 ± 2.00	ab	0.2 <sup>Δ</sup>
	Leaf	3.49 ± 1.18	b	32.97 ± 10.52	d	40.0 *
	Stem	BDL	a	14.10 ± 3.50	c	40.0 *
Swiss chard	Leaf	BDL	a	8.04 ± 3.78	c	3.8 <sup>Δ</sup>
Beetroot	Root	11.56 ± 4.44	c	12.87 ± 6.28	c	0.7 <sup>Δ</sup>
	Leaf	BDL	a	30.62 ± 6.10	d	3.8 <sup>Δ</sup>

<sup>™</sup> Means assigned the letter "a" are not significantly different from the control at the 95% probability level (Fisher's LSD test).  
BDL: Below method detection limit of 1.4 mg.kg<sup>-1</sup>.  
<sup>Δ</sup> Food safety threshold derived from the National Food Safety Standards, People's Republic of China (2012).  
\* DAFF Act No. 36 of 1947, Annexure 4: Undesirable substances in farm feeds.

Relatively low amounts of lead accumulated in the aboveground biomass of barley when grown in lead-enriched soil. While most lead accumulated in the leaves and stems, the lead concentrations were far lower than the animal feed threshold and would therefore be fit for animal consumption. This trend was repeated in all crops, with none of the aboveground biomass accumulating lead at concentrations in excess of the animal feed limit of 40.0 mg kg<sup>-1</sup> (DAFF, 1947).

Garden peas grown in arsenic-enriched soil and peas grown in lead-enriched soil did not accumulate lead above the MDL of 1.40 mg l<sup>-1</sup>. Pods grown in soil containing 168.9 mg kg<sup>-1</sup> lead did, however, accumulate enough lead to pose a food safety risk, although the results were not statistically significant.

Swiss chard leaves grown in lead-enriched soils simulating 99 years of irrigation at the "target water quality" of 0.2 mg l<sup>-1</sup> did not accumulate lead in excess of the food safety guidelines. However, the leaves of Swiss chard grown in 168.9 mg kg<sup>-1</sup> lead accumulated more than double the food safety threshold of 3.8 mg kg<sup>-1</sup> lead on a dry mass basis. Peeled beetroot roots were found to have accumulated lead in excess of the food safety guidelines at both soil lead concentrations (88.1 and 168.9 mg kg<sup>-1</sup>) and, in both cases, the results were statistically significant.

The leaves of beetroot grown in soil containing 88.1 mg kg<sup>-1</sup> lead did not pose a risk to human health if consumed. However, when grown in soil containing 168.9 mg kg<sup>-1</sup> lead, leaves accumulated over eight times the lead food safety limit. As with the arsenic analysis, median values were also investigated to evaluate the validity of using the mean scores, and are recorded in Table 8.12. Comparison of the median and mean values demonstrated that the selection of the statistical parameter did not change the result of whether or not the treatment exceeded the dry mass food safety threshold.

Table 8.12: Median lead accumulation in the dry mass of crops grown in lead-enriched soils in relation to food and feed thresholds

Crop	Plant part	Median Pb concentration, DM (mg.kg <sup>-1</sup> )				Regulated threshold, DM (mg.kg <sup>-1</sup> )
		Median Pb [88.1 mg.kg <sup>-1</sup> ]	Above threshold frequency	Median Pb [168.9 mg.kg <sup>-1</sup> ]	Above threshold frequency	
Barley	Grain	BDL		BDL		0.2 <sup>Δ</sup>
	Leaf	BDL		2.16		40.0 *
	Stem	1.69		4.03		40.0 *
Garden pea	Pea	BDL		BDL		0.3 <sup>Δ</sup>
	Pod	BDL		3.73	***	0.2 <sup>Δ</sup>
	Leaf	3.16		38.16	*	40.0 *
Swiss chard	Stem	BDL		12.92		40.0 *
	Leaf	BDL		6.26	**	3.8 <sup>Δ</sup>
Beetroot	Root	12.00	***	14.42	***	0.7 <sup>Δ</sup>
	Leaf	BDL		59.76	***	3.8 <sup>Δ</sup>

\* Number of replicates that were above the regulated threshold (maximum of 3).  
BDL: Below method detection limit of 1.4 mg.kg<sup>-1</sup>.  
<sup>Δ</sup> Food safety threshold derived from the National Food Safety Standards, People's Republic of China (2012).  
\* DAFF Act No. 36 of 1947, Annexure 4: Undesirable substances in farm feeds.

Generally, the variability of the lead data was higher than that of arsenic, which is reiterated by the MDL differences (arsenic at 0.7 mg l<sup>-1</sup> and lead at 1.4 mg l<sup>-1</sup>). For example, the high standard deviation ( $\pm 3.78$ ) associated with the mean of lead in Swiss chard leaves grown in soils at 168.9 mg lead kg<sup>-1</sup> (8.04 mg kg<sup>-1</sup>) is explained by a low replicate below the MDL, which skewed the mean. The increased variability among the lead results may have been due to inter-element interferences or contamination during the sample preparation and digestion process (EAG, 2007). Figure 8.4 summarises the results of the lead soil-dosing treatments on the edible plant parts of barley, garden pea, Swiss chard and beetroot with regard to human food safety. Swiss chard and beetroot leaves accumulated lead well in excess of the food safety threshold, with beetroot leaves accumulating over eight times the acceptable limit. Peeled beetroot roots grown in both lead-treated soils accumulated lead at over double the acceptable limit. Since uptake in the edible parts of all four crops either exceeded the food safety threshold or was inconclusive, it is advisable that site-specific crop cultivar trials be performed before utilising a field with elevated levels of lead in order to gauge the human food safety risk.

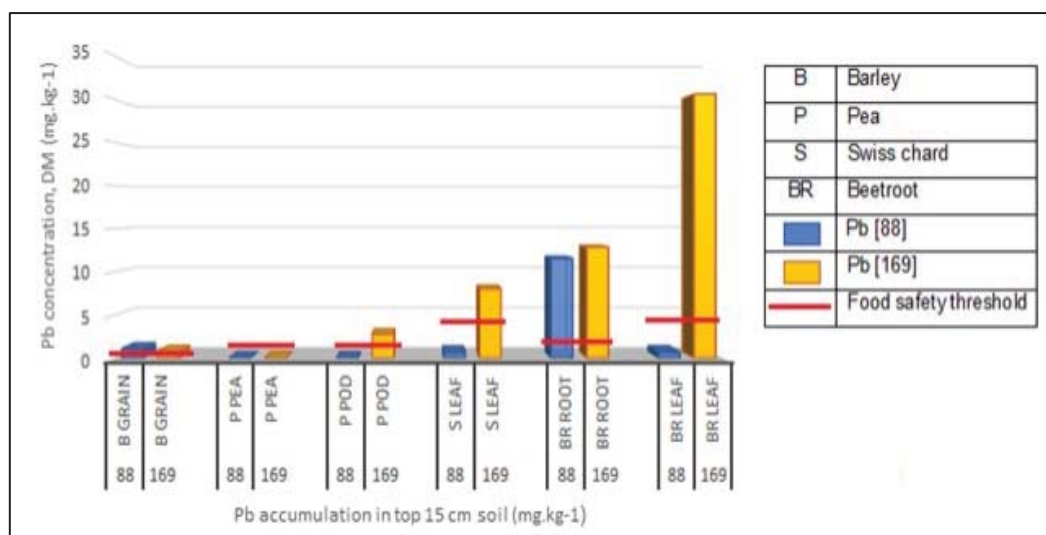


Figure 8.4: Lead accumulation, dry mass basis, within edible parts of crops grown in lead-enriched soil at 88.1 mg kg<sup>-1</sup> (simulating 99 years of irrigation at 0.2 mg l<sup>-1</sup>) and 168.9 mg kg<sup>-1</sup> (19 years of irrigation at 2 mg l<sup>-1</sup>) in relation to food safety thresholds

#### 8.4 CONCLUSION

As competition for land and the need to feed a growing population increases, the agricultural industry will be progressively driven to utilise ever-more contaminated lands and irrigation water sources. Consequently, the probability of producing crops that pose a human health risk are likely to increase. Therefore, the results of this study have highlighted the urgent need for agricultural policy makers to revise irrigation water quality guidelines to ensure sustainable food safety. It is noted that the food safety thresholds were developed after the irrigation water quality guidelines, and that foliar absorption and differences between crops or edible parts are not considered in current guidelines. In conclusion, this study has demonstrated that if food safety thresholds for fresh produce are to be adhered to in South Africa, the South African Irrigation Water Quality Guidelines (1996) for arsenic and lead need to be revised so as to negate all possible future contamination of fresh produce resulting from irrigation inputs.

#### 8.5 REFERENCES

- ALEXANDER PD, ALLOWAY BJ and DOURADO AM (2006) Genotypic variations in the accumulation of Cd, Cu, Pb and Zn exhibited by six commonly grown vegetables. *Environmental Pollution* **144** 736–745.
- BAIG JA and KAZI TG (2012) Translocation of arsenic contents in vegetables from growing media of contaminated areas. *Ecotoxicology and Environmental Safety* **75** 27–32.
- DEPARTMENT OF AGRICULTURE, FORESTRY AND FISHERIES (DAFF) (1947) *Fertilizers, Farm Feeds, Agricultural Remedies and Stock Remedies Act, Act No. 36 of 1947*. DAFF, Pretoria, South Africa.
- DEPARTMENT OF WATER AFFAIRS AND FORESTRY (DWAf) (1996) *South African irrigation water quality guidelines, Vol. 4: Agricultural use: Irrigation, 2<sup>nd</sup> ed.*, DWAf, Pretoria, South Africa.
- DOLLARD G (1986) Glasshouse experiments on the uptake of foliar applied lead. *Environmental Pollution Series A, Ecological and Biological* **40**(2): 109-119.

- DZOMA BM, MORALO RA, MOTSEI LE, NDOU RV and BAKUNZI FR (2010) Preliminary findings on the levels of five heavy metals in water, sediments, grass and various specimens from cattle grazing and watering in potentially heavy metal polluted areas of the North West province of South Africa. *Journal of Animal and Veterinary Advances* **9 (24)** 3026–3033.
- EVANS ANALYTICAL GROUP EAG (2007) ICP-OES and ICP-MS detection limit guidelines. URL: <https://www.eag.com/resources/appnotes/icp-oes-and-icp-ms-detection-limit-guidance/> (Accessed 22 March 2019).
- FERTILIZER SOCIETY OF SOUTH AFRICA (FERTASA) (2016) Fertilizer Handbook. FERTASA, Pretoria.
- MAHMOOD A and MALIK RN (2014) Human health risk assessment of heavy metals via consumption of contaminated vegetables collected from different irrigation sources in Lahore, Pakistan. *Arabian Journal of Chemistry* **7** 91–99.
- MZINI LL and WINTER K (2015) Analysis of grey-water used for irrigating vegetables and possible effects on soils in the vicinity of Umtata Dam, Eastern Cape. *Water SA* **41 (1)** 115–120.
- NAYEK S, GUPTA S and SAHA RN (2010) Metal accumulation and its effects in relation to biochemical response of vegetables irrigated with metal contaminated water and wastewater. *Journal of Hazardous Materials* **178** 588–595.
- PAGE V and FELLER U (2015) Heavy metals in crop plants: Transport and redistribution processes on the whole plant level. *Agronomy* **5** 447–463.
- SCHRECK E, DAPPE V, SARRET G, SOBANSKA S, NOWAK D, NOWAK J, STEFANIAK EA, MAGIN V, RANIERI V and DUMAT C (2014) Foliar or root exposures to smelter particles: Consequences for lead compartmentalization and speciation in plant leaves. *Science of the Total Environment* **476** 667–676.
- SPOSITO G (2008) *The chemistry of soils*. Oxford university press, USA.
- THIAM DR, MUCHAPONDWA E, KIRSTEN J and BOURBLANC M (2015) Implications of water policy reforms for agricultural productivity in South Africa: Scenario analysis based on the Olifants River basin. *Water Resources and Economics* **9** 60–79.
- WARREN GP, ALLOWAY BJ, LEPP NW, SINGH B, BOCHEREAU FJM and PENNY C (2003) Field trials to assess the uptake of arsenic by vegetables from contaminated soils and soil remediation with iron oxides. *The Science of the Total Environment* **311** 19–33.
- YAÑEZ LM, ALFARO JA, NMEA CARRERAS and GB MITRE (2019) Arsenic accumulation in lettuce (*Lactuca sativa* L.) and broad bean (*Vicia faba* L.) crops and its potential risk for human consumption. *Heliyon* **5** 1–22.

## **CHAPTER 9: LIMESTONE NEUTRALISATION OF SYNTHETIC ACIDS IN AN AQUEOUS ENVIRONMENT AND SAND COLUMNS**

---

V Moodley, JG Annandale, PD Tanner and PC de Jager

### **9.1 INTRODUCTION**

For irrigation with untreated AMD to be successful, a better understanding is needed of the factors that influence the efficiency with which a limed soil will be able to neutralise acidity from the irrigation water applied. This will guide the way in which profiles receiving AMD are strategically managed to best treat infiltrating acidic waters. Considerations are types of liming material and factors that affect its reactivity, as well as the placement within or on top of the soil profile to ensure sufficient contact with acidic mine water.

A crucial limitation of limestone as a neutralising agent for acid mine water is its susceptibility to armouring by metal hydroxides and gypsum. The relatively slow dissolution rate of limestone is another limitation. However, the following approaches can partially overcome these limitations:

- Maximise the available surface area of limestone (De Beer, 2005)
- Increase the contact time between limestone and acid mine water (Brahaita et al., 2017)

The aim of this study is to assess calcitic limestone as a neutralising agent for synthetic acidic solutions and to determine whether a soil profile containing limestone can act as a mine water neutralisation reactor and aid in the treatment of acid mine water percolating through the root zone. This reactor could essentially serve as a geochemical barrier that may form part of a containment strategy for acid mine water. Considerations around neutralisation ability, such as limestone particle size in relation to neutralisation efficiency, and the aggressiveness of the acidic solutions stemming from acidity already present and the contribution of additional acidity due to the presence of acid-generating metal cations in AMD were investigated. The location of limestone within the sand column, which emanates from its placement in the soil profile in relation to the cultivation of perennial and annual crops, and lastly, the leaching procedure for synthetic acid mine water that relates to the contact time between the limestone and this leachate, were also considered.

For this sand column trial, it was hypothesised that limestone particle size becomes less important for neutralisation as acidity increases, as the more aggressive the water, the more effective the dissolution will be. Additionally, the location of limestone within sand columns is less important for neutralisation than frequent wetting, which increases the contact time between limestone and the synthetic acid mine water, thus aiding neutralisation.

### **9.2 MATERIALS AND METHODS – NEUTRALISATION OF THE SYNTHETIC ACIDS IN AN AQUEOUS ENVIRONMENT**

The first experiment involved neutralisation of sulphuric acid and synthetic acid metal cation mine water at two pH levels, 2 and 3, using limestone particles of various sizes. The intention was to determine whether limestone particle size is less important for achieving neutralisation as acidity increases. The concept of increasing acidity refers to the presence of iron, aluminium and manganese ions, which can undergo hydrolysis reactions and generate acidity in the form of protons ( $H^+$  ions). Additionally, these ions may precipitate as metal hydroxides and armour the limestone, which is identified to be a limitation associated with limestone neutralisation. Limestone has a relatively slow dissolution rate, and for this experiment, a mechanical mixing table was used to hasten dissolution and ensure sufficient mixing for the duration of the experiment.

A variety of limestone particle sizes was used to address the aim of the experiment. The idea of performing neutralisation in an aqueous system emanates from the treatment of mine-impacted waters by active treatment systems (such as a high-density sludge plant). This is because, in this system, the neutralisation process occurs within the mine-impacted waters as alkaline agents are added to the water to raise the pH.

The following limestone particle sizes were used for this experiment:

- < 0.1 mm
- ≥ 0.1 mm < 1 mm
- ≥ 1 mm < 4 mm
- ≥ 4 mm < 10 mm

The average mass of single limestone grains of the largest particle size fraction (≥ 4 mm < 10 mm) was found to be about 0.20 g. This mass was used as the dosage of limestone for the experiment. A mass of 0.20 g of each of the particle sizes was added to Schott bottles of 100 ml to execute the experiment. This was conducted in triplicate for each particle size.

To prevent spillage of the acidic solutions from the bottles, 30 ml aliquots of the freshly prepared acids (sulphuric and synthetic acid metal cation mine water) were added to each of the bottles. The pH of each acid was directly measured in the Schott bottles using a calibrated Consort C830 pH electrode. Measurements were taken every 20 minutes. The duration of the experiment was 100 minutes.

### 9.2.1 Preparation of synthetic acids

The formation of sulphuric acid in mine water contributes to its acidic nature. The sulphuric acid also facilitates mineral dissolution, which further contributes to the toxic character of mine water by introducing a variety of soluble metals to it. It is identified that iron, aluminium and manganese are the principal metals that occur in most mine waters globally. In view of the above, it was decided to include the synthesis of two types of acid in the project: sulphuric acid and sulphuric acid that had been dosed with iron, aluminium and manganese ions (which will be referred to as synthetic acid metal cation mine water).

Since most mine-affected waters have a low pH range of 2 to 6, the pH for each of the acids was targeted at the lower end of this spectrum. Therefore, a pH of 2 and 3 was chosen as the target pH level for each of the acids used in the experiments. To reach the targeted pH for each acid, it was necessary to produce a stock solution (1 M H<sub>2</sub>SO<sub>4</sub>) from which dilutions could be produced (Table 9.1).

*Table 9.1: The required volume of stock solution needed per litre to produce the target pH levels and actual pH values obtained*

Targeted pH	Concentration of H <sub>2</sub> SO <sub>4</sub> synthesised (M)	Required volume of 1 M H <sub>2</sub> SO <sub>4</sub> stock solution (cm <sup>3</sup> )	Measured pH
2	0.005	5	2.08
3	0.0005	0.5	3.01

*Note: The dilution was prepared according to the formula  $C_1V_1 = C_2V_2$ , where  $C_1$  denotes the concentration of the stock solution (1 M),  $V_1$  is the volume of the stock solution used,  $C_2$  is the concentration of the target pH level and  $V_2$  is the volume of the target pH to be made (1 ℓ).*

The synthetic acid metal cation mine water (Table 9.2) was prepared by dosing the sulphuric acid at the targeted pH level with iron, aluminium and manganese ions. These metal cations were available as sulphate salts in the laboratory and the following were used:

- $\text{FeSO}_4 \cdot 7\text{H}_2\text{O}$
- $\text{Al}_2(\text{SO}_4)_3 \cdot 18\text{H}_2\text{O}$
- $\text{MnSO}_4 \cdot \text{H}_2\text{O}$

Aqion was used to simulate cases whereby the abovementioned metals, at concentrations that could be encountered in actual AMD, could be combined with sulphuric acid at a concentration of 0.005 and 0.0005 M without causing deviations in the targeted pH of 2 and 3.

From the outputs, those concentrations that were closest to attaining the targeted pH level of 2 and 3 were used to derive the mass of each salt that would be needed. The synthetic acid metal cation mine water was then produced by dosing sulphuric acid with the required amounts of the chosen salts as calculated by Aqion (Table 9.2).

Table 9.2: The mass of each sulphate salt required to produce a litre of synthetic acid metal cation mine water for each target pH level and the concentration of metals present in the acids

Target pH	Mass of salt required (g)			Concentration of metal present ( $\text{mg}\cdot\ell^{-1}$ )		
	$\text{FeSO}_4 \cdot 7\text{H}_2\text{O}$	$\text{Al}_2(\text{SO}_4)_3 \cdot 18\text{H}_2\text{O}$	$\text{MnSO}_4 \cdot \text{H}_2\text{O}$	$\text{Fe}^{2+}$	$\text{Al}^{3+}$	$\text{Mn}^{2+}$
2	4.98	6.17	0.77	1831	973	280
3	2.49	2.47	0.31	915	390	113

### 9.3 MATERIALS AND METHODS – NEUTRALISATION OF SYNTHETIC ACID METAL CATION MINE WATER IN SAND COLUMNS

The second experiment focused on neutralising a synthetic acid metal cation mine water in a sand column that contained limestone. Synthetic acid metal cation mine water corresponding to a target pH of 2 (see Table 9.2) was used as the percolating solution for this experiment. It was decided to execute this experiment by conducting a soil column leaching experiment. This experiment aimed to determine whether the location of limestone in a sand column was less important for the neutralisation of a synthetic acid metal cation mine water compared to the leaching procedure of the synthetic acid mine water that relates to the contact time between the limestone and this percolating solution. The focus of this work was neutralisation by limestone. Therefore, it was motivated that silica sand (2–4 mm) be used as the medium for the columns as it is representative of a material that has limited to no inherent buffering ability and facilitates percolation efficiently because of its high hydraulic conductivity.

The concept of the location of limestone emanates from its placement in or on the soil in relation to the cultivation of perennial versus annual crops. Commonly employed methods of lime application for perennial grasses involve broadcasting limestone on the surface without physical incorporation. However, with annual crops, lime is applied to the field and incorporated into the soil. As a result, it was decided to include treatments where limestone was applied to the surface of some columns, and where it was mixed with the sand before being packed into other columns.

#### 9.3.1 Soil column components

The columns were essentially clear polyvinyl chloride cylinders with an inner diameter of 10.5 cm, a length of 30 cm and a volume of  $2,598 \text{ cm}^3$ . The columns fit into a polypropylene base, which held them in a vertical position. The base had a grid-like sieve on the inside that allowed leachate to exit the column. A mesh-filter membrane barrier was placed above the sieve to prevent sand from passing through the column. This barrier consisted of a 2 mm nylon gridded mesh, followed by 5  $\mu\text{m}$ , 10  $\mu\text{m}$  and 20  $\mu\text{m}$  filter membranes before being capped by another 2 mm nylon mesh.

A black rubber O-ring was recessed around the inner diameter of the base to provide a tight seal between the column and the base (Figure 9.1). The columns were filled to a depth of 25 cm with the sand, leaving a 5 cm gap to provide space to accommodate the applied volume of synthetic mine water to pass through the porous medium. Underneath each base, Schott bottles were attached so that the leachate exiting the columns could be collected and analysed (Figure 9.2).



Figure 9.1: The column ensemble, which consists of a polyethylene tube and its base, with a gridded sieve to allow leachate to exit the column and prevent the loss of soil



Figure 9.2: The ensemble that was utilised for the percolation and collection of the synthetic acid mine water that was passed through sand columns containing limestone

### 9.3.2 Estimating the dosage of limestone applied to the columns

From the aqueous experiment, it was established that the mass of limestone used to induce neutralisation of the synthetic acid metal cation mine water with an initial pH of 2 was 0.2 g per 30 ml of acid water used. The approach for the sand column experiment was to use the same amount of limestone per unit volume of synthetic acid mine water (with a pH of 2) to be passed through each column. Since a total of 1.8 l was percolated through the columns, the amount of limestone added to each column was 12.6 g. Limestone particle sizes of less than 0.1 mm and larger than 4 mm, but less than 10 mm, were considered for this experiment.

### 9.3.3 Treatments and experimental procedure

The treatments for the experiment were as follows:

- Surface application of limestone to the sand columns
- Mixing limestone with the sand before packing it into columns
- Percolating 300 ml of synthetic acid mine water twice a week for three weeks (LP1)
- Percolating 100 ml of synthetic acid mine water per day for six consecutive days for three weeks (LP2)
- Limestone particle sizes of less than 0.1 mm and larger than 4 mm, but less than 10 mm

A total of 24 columns were used in this experiment. Of this total, 12 received limestone applied to the surface of the sand column (Figure 9.3) and the remaining 12 received limestone that was mixed with the sand before being packed into each column. Six of the 12 columns that received a surface application of limestone had limestone particle sizes of less than 0.1 mm. The other six received limestone particle sizes of larger than 4 mm, but less than 10 mm. The same division was used for the 12 columns that received limestone that was mixed with sand before being packed.



Figure 9.3: Surface application of 12.6 g limestone with a particle size of larger than 4 mm, but less than 10 mm (left) and less than 0.1 mm (right)

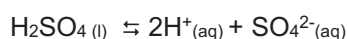
The leachate from each column was collected in Schott bottles attached beneath the columns. Before application of the next percolation event, the leachate was transferred into 50 ml centrifuge tubes for analysis. The leachates were analysed for pH only.

## 9.4 RESULTS

A summary of the results that were obtained for the individual experiments is included in Appendix A8.

### 9.4.1 Effect of limestone particle size on the neutralisation (increasing of pH) of sulphuric acid

Sulphuric acid is the primary source of acidity that affects mine-impacted waters, and its acidifying potential is attributed to the presence of hydrogen ions (Dold, 2014). This strong diprotic acid will disassociate releasing hydrogen and sulphate ions into solution as follows:



Upon contact with an alkaline material such as limestone, the hydrogen ions consume the limestone, resulting in its dissolution. This causes the release of  $\text{Ca}^{2+}$  ions in addition to decreasing the concentration of hydrogen ions in solution and essentially marks neutralisation as the pH increases (Fusi et al., 2012).



In addition to neutralisation, partial sulphate removal can be achieved by the precipitation of calcium sulphate as gypsum, hemihydrate or anhydrite, depending on neutralisation conditions (Geldenhuys et al., 2003; Petkov et al., 2017).

Figures 9.4 and 9.5 represent the influence of a series of limestone particle sizes on increasing the pH (neutralisation) of sulphuric acid at a pH of 2 and 3, respectively. Both figures indicate fine-textured limestone with a particle size of less than 0.1 mm, which generated a pH slightly higher than 7, and was the highest increase overall. This particle size proved to be the most efficient as this rapid increase in pH occurred during the first 20 minutes of the reaction. As limestone particle size became coarser, it was less effective in increasing the pH of the sulphuric acid, with a larger hydrogen ion concentration (symbolic of a lower pH).

Figure 9.4 shows that sulphuric acid with an initial pH of 2 required longer than 80 minutes to initiate a marked increase in pH when coarser limestone particle sizes were used. A particle size of less than 1 mm generated a pH slightly lower than 5; particle sizes larger than 1 mm, but less than 4 mm, generated a pH slightly lower than 4; and particle sizes larger than 4 mm, but less than 10 mm, yielded a pH lower than 3 over the duration of the experiment. Sjoeborg and Rickard (1984) found that, at a low pH, the rate of limestone dissolution in an aqueous environment is almost directly proportional to the concentration of hydrogen ions present in that system. That is, the lower the pH of an acid, the greater the concentration of hydrogen ions ( $\text{H}^+$ ) present in solution. A shorter period is consequently required to dissolve the limestone, consume acidity and reach neutrality. Subsequently, it can be expected that the higher the pH of an acid, the lower the concentration of hydrogen ions present in the solution and consequently the longer the period needed to dissolve the limestone and achieve neutrality.

Figure 9.5 explains that, within a period of 20 to 40 minutes, the coarser particle sizes begin to cause a noticeable increase in the pH of the sulphuric acid. Limestone with a particle size of less than 1 mm generated a pH slightly higher than 7; that greater than 1 mm, but less than 4 mm, produced a pH slightly higher than 6; and a particle size greater than 4 mm, but less than 10 mm, resulted in a pH of about 5 over the duration of the experiment.

A slight delay, after the initially rapid increase in pH was observed for fine-textured limestone (Figure 9.4). It is plausible that, when fine-textured limestone is used, the slight delay experienced could be attributed to the formation of gypsum precipitate in solution due to the process of homogenous nucleation. This step is identified to be responsible for sequestering sulphate concentrations in solution. The homogenous nucleation is likely due to the product of the concentration of  $\text{Ca}^{2+}$  and  $\text{SO}_4^{2-}$  ions exceeding the solubility product ( $K_{\text{sp}}$ ) of  $\text{CaSO}_4$  (Ahmad, 2006). As a result, the ion activity product (IAP) would theoretically be larger than the  $K_{\text{sp}}$  for  $\text{CaSO}_4$ , implying that the aqueous system (solution) is supersaturated with respect to the elements that form this solid, and that its precipitation in this environment is possible (Essington, 2003).

A slight delay after the initially rapid increase in pH was noted for both fine-textured limestone and limestone with a particle size less than 1 mm, which occurred after 40 minutes with the pH appearing to plateau (Figure 9.5). This suggests that limestone with a particle size of less than 1 mm was slightly constrained in its capacity to further increase pH, which could have been the result of the precipitation of calcium sulphate (gypsum). Potgieter-Vermaak et al. (2006) mention that a slight delay after the initial fast increase is due to a layer of precipitate on limestone particles that prevents further dissolution and consequently neutralising ability. This explains the plateau in the pH that is observed for the solution.

This precipitate is referred to as armouring. Hammarstrom et al. (2003) call this layer of precipitate, which has developed on the surface of the particles, a rind of  $\text{CaSO}_4$ . This coat is formed because of heterogenous nucleation, a surface-induced precipitation process. Sparks (2003) explains the surface-induced precipitation process as follows: There are zones around the limestone surface where the dielectric constant of the solution will be less than that of the bulk solution. This results in a decrease in the solubility around these zones and causes the formation of surface precipitates.

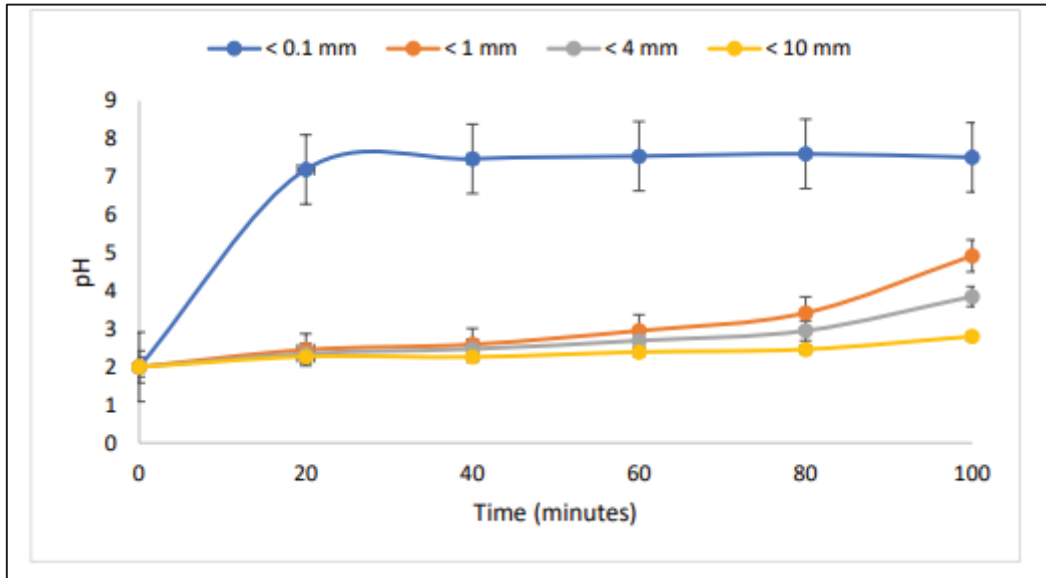


Figure 9.4: Neutralisation of sulphuric acid with an initial pH of 2 as influenced by a series of limestone particle sizes

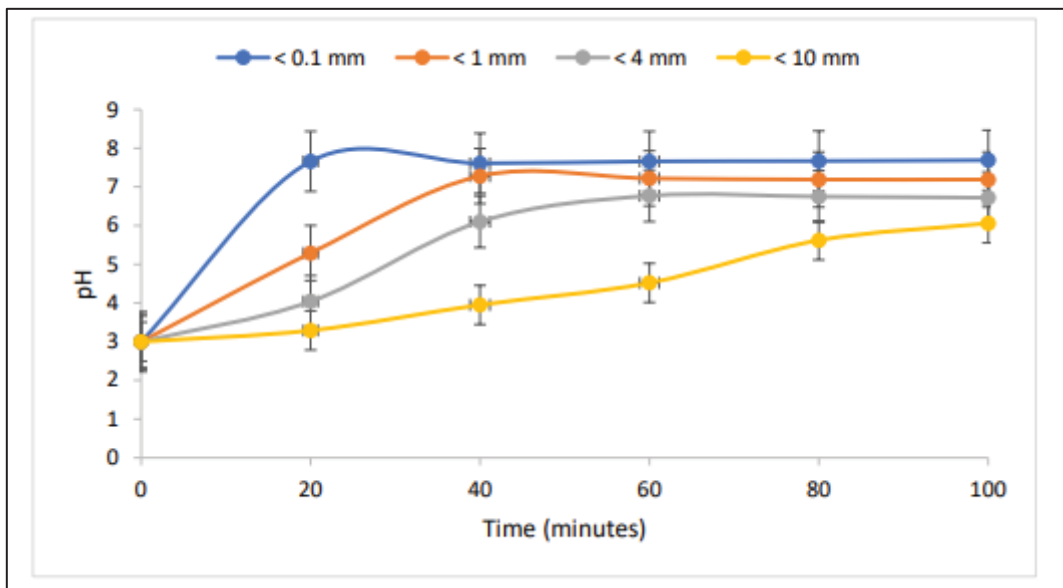


Figure 9.5: Neutralisation of sulphuric acid with an initial pH of 3 as influenced by a series of limestone particle sizes

#### 9.4.2 Effect of limestone particle size on the neutralisation (increasing of pH) of synthetic acid metal cation mine water

Synthetic acid metal cation mine water is essentially sulphuric acid that contains metal cations such as  $\text{Fe}^{2+}$ ,  $\text{Al}^{3+}$  and  $\text{Mn}^{2+}$ . The assumption is that two sources of acidity are contained within the synthesised mine water. The concentration of hydrogen ions in the sulphuric acid is the primary source of acidity, while the ability of these metal cations to facilitate hydrolysis reactions is the secondary source of acidity, referred to as mineral acidity (Madiseng, 2019).

Figures 9.6 and 9.7 represent the influence of a series of limestone particle sizes on increasing the pH of synthetic acid metal cation mine water with a pH of 2 and 3, respectively. Both figures show that limestone with the finest texture, i.e. with a particle size of less than 0.1 mm, generated a pH slightly higher than 5 (the highest increase in pH overall) and plateaued at this range. A slight delay, after the initially rapid increase in pH for limestone with the finest texture, was also observed with the synthetic mine water with a pH of 3 (Figure 9.7). This suggests that metal hydroxide and hydroxysulphate precipitation had occurred within these systems. At a pH of 5.5,  $\text{Fe}^{3+}$  had precipitated as ferric hydroxide in solution, which has a characteristic orange-ochre-like colour (Figure 9.8). No other particle size fraction considered visibly demonstrated this precipitate.

The development of this precipitate can be attributed to the oxidation of  $\text{Fe}^{2+}$  to  $\text{Fe}^{3+}$ , which is influenced by increasing the pH of the aqueous system. The increase in pH essentially drives redox conditions, which prevents dissolved iron ( $\text{Fe}^{2+}$ ) from being stable and consequently causes its oxidation and precipitation as ferric mineral species (Clarke et al., 1985). Bailey (2016) supports that at a pH of greater than 4.5,  $\text{Fe}^{3+}$  is likely to precipitate as  $\text{Fe}(\text{OH})_3$ . This precipitation is also likely to have generated acidity by producing additional hydrogen ions in solution. The mineral acidity that has been generated is supposedly responsible for causing the plateau in the increase in pH (neutralisation).

As particle size increased, the coarser sizes stimulated only a slight increase in pH (to about 3.5 at most) with the pH appearing to be restricted or buffered against further increases as the experiment continued (figures 9.6 and 9.7). The minimal increase in pH is attributed to limestone dissolution kinetics, which is influenced by the surface area of the limestone particle (Sun et al., 2000), and miniscule precipitate formation on the surfaces of the coarser size fractions is supposedly the main factor, resulting in the only slight observed increase in pH.

Smaller specific surface areas are associated with coarser particle sizes, implying that a longer period is needed to initiate an increase in pH, thus favouring the precipitation of metal hydroxides and hydroxysulphates. These precipitates are responsible for contributing additional acidity, which must be consumed in conjunction with the present quantity in the system.

This is suggested to prolong the dissolution of coarser particles of limestone, in particular, and increase the probability of the surfaces of these particles being armoured by these precipitates. Jones et al. (2014) mention that the precipitation of metal hydroxides, such as  $\text{Fe}(\text{OH})_3$ , is not a rapid process and requires some time to occur. Furthermore, there will be zones or areas around the coarser particles that may experience higher pH conditions than the bulk solution. This can oxidise ferrous iron around these zones into ferric iron, which can enable hydrolysis reactions and precipitation as iron hydroxide minerals such as Schwartmenite, Goethite or even Lepidocrocite (Jones et al., 2014).

By the process of heterogenous nucleation, surface-induced precipitation of iron hydroxide and hydroxysulphate minerals may coat the limestone that can eventually build up over time. The precipitation of these minerals can contribute additional acidity due to the generation of hydrogen ions because of the hydrolysis reaction involved (Madiseng, 2019). The additional hydrogen ions could well act as a buffer to increasing the pH of the acid (neutralise it), especially if coarser limestone particles are used.

It then appears that, as the particle size of limestone used increases, its reactivity would essentially decrease and be demonstrated to be ineffective in neutralising acidic solutions, which contain metals that can liberate additional acidity, like acid mine water.

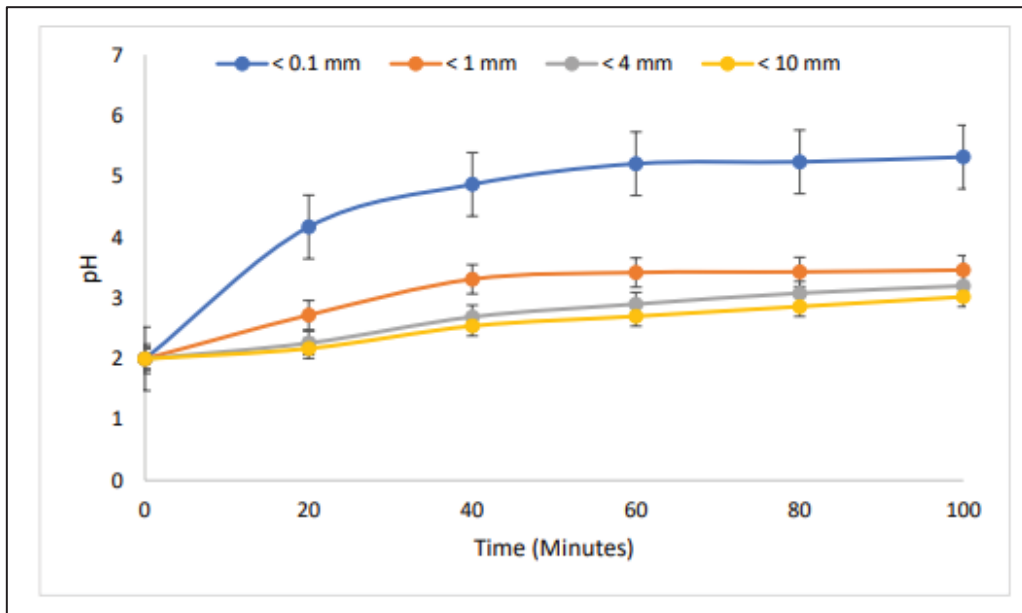


Figure 9.6: Neutralisation of synthetic acid metal cation mine water with an initial pH of 2 as influenced by a series of limestone particle sizes

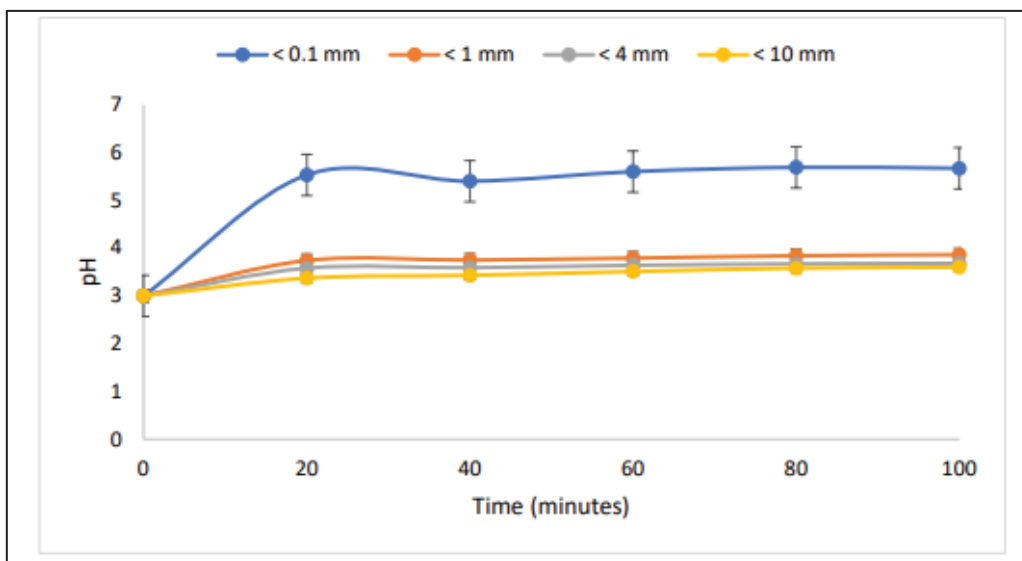


Figure 9.7: Neutralisation of synthetic acid metal cation mine water with an initial pH of 3 as influenced by a series of limestone particle sizes



Figure 9.8: The precipitation of ferric hydroxide, represented by the orange-rust-like colour at a pH of about 5.5

#### 9.4.3 Neutralisation of a synthetic acid metal cation mine water in a sand column

The approach was to pass synthetic mine water through sand columns, which contained limestone that was mixed with sand before being packed into the columns (Figure 9.9), and which was applied to the surface of the columns (Figure 9.10). Motivation for these application methods emanates from the placement of lime in relation to the cultivation of annual and perennial crops. Lime is incorporated (mixed) into the soil for annual crops, whereas for perennial crops, surface application is a commonly employed technique. The ability of limestone to neutralise acid mine water is constrained by the slow dissolution rate. Increased contact time between the limestone and acid mine water should overcome this limitation to some extent.

Therefore, two leaching treatment procedures were used: LP1 and LP2. LP1 involved leaching 300 mℓ of the synthetic mine water twice a week, whereas LP2 involved leaching 100 mℓ of the synthetic mine water daily. Figure 9.9 shows that fine-textured limestone, i.e. a particle size of less than 0.1 mm was the most effective in neutralising the leached synthetic mine water for both procedures with a pH higher than 4. However, leaching 100 mℓ of the synthetic mine water daily (LP2) was more effective in facilitating the neutralisation of synthetic acid mine water in sand columns with limestone that was mixed with sand. It was observed that the pH for both procedures decreased after the initial increase, probably due to the limestone being consumed, thus the concentration of limestone is thought to have decreased over time.

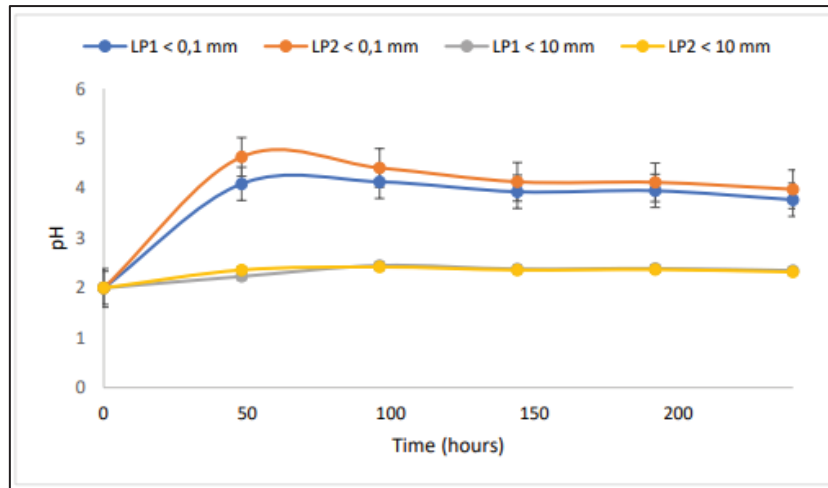


Figure 9.9: Neutralisation of synthetic acid metal cation mine water according to two leaching procedures (LP1 and LP2) in a sand column with limestone of less than 0.1 mm and less than 10 mm in size that is mixed with sand

Coarse limestone, that has a particle size greater than 4 mm, but less than 10 mm, performed poorly in terms of neutralising the percolate, and showed a minimal increase in pH for both leaching procedures (LP1 and LP2) (Figure 9.9).

Figure 9.10 illustrates that fine-textured limestone is also most effective at increasing the pH of the leached synthetic mine water in sand columns with the limestone applied to the surface. Initially, leaching 300 ml of synthetic mine water twice a week (LP1) led to a pH slightly higher than 5. As leaching progressed according to LP1, the pH markedly decreased for these columns. However, leaching 100 ml of synthetic mine water daily (LP2) was slightly more effective at facilitating an increase in pH (neutralisation) than LP1.

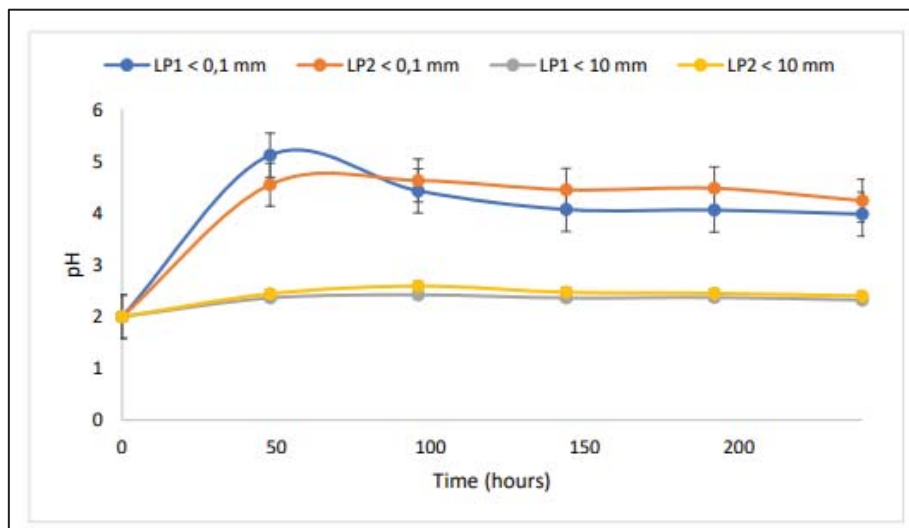


Figure 9.10: Neutralisation of synthetic acid metal cation mine water according to two leaching procedures (LP1 and LP2) in a sand column with limestone of less than 0.1 mm and less than 10 mm in size applied to the surface of the columns

Coarse limestone performed poorly in terms of neutralising the percolate and showed a minimal increase in pH for both leaching procedures where limestone is applied to the surface of the sand columns (Figure 9.10).

Shorter contact time with LP1 is not as effective in neutralising leached synthetic mine water for both the surface application of limestone and mixing limestone with sand, whereas an increased contact time with more frequent leaching, as with LP2, is more effective for both locations of limestone in the sand columns. Limestone particle size also has an effect in that fine-textured limestone is more effective for both application methods, but is more effective with frequent leaching at a smaller volume/fraction (LP2). In a study conducted by Brahaita et al. (2017), similar results were obtained. They concluded that by increasing the length of their limestone channel, reducing the water flow rate and adding more limestone, the time of contact could be increased, which resulted in the highest efficiency in terms of neutralisation. Therefore, it is probable that leaching synthetic mine water with 100 m<sup>l</sup> daily reduced the flow rate, which allowed for an increased contact time between the limestone and the leachate, which neutralised the leachate more effectively.

## 9.5 CONCLUSIONS

The first hypothesis states that limestone particle size is less important for neutralisation as acidity increases and the concentration of hydrogen ions increases, which will allow for effective dissolution and increase the pH. The study rejected this hypothesis based on the following experiments:

- Neutralising sulphuric acid with a pH of 2 and 3 by using a series of limestone particle sizes
- Neutralising synthetic acid metal cation mine water with a pH of 2 and 3 by using a series of limestone particle sizes

The primary finding was that coarser particle sizes of calcite would essentially require prolonged periods to attain an end-point pH of 7 as the acidity of the solution increased or its pH decreased (demonstrated by the experiment that involved sulphuric acid). Furthermore, the capacity of these particles to increase the pH of solutions, which can generate additional acidity, is buffered against (demonstrated by the experiment involving synthetic acid metal cation mine water).

It is suggested, however, that, to overcome these challenges, a larger dosage of limestone of coarse size fractions could be considered to lessen the duration required and to compensate for additional acidity introduced. The concern raised, however, is that, by applying excessive quantities of larger particles to overcome these challenges, the potential of their surfaces to experience precipitate accumulation increases. This may render the limestone ineffective as it would be armoured by gypsum, hydrosulphates and metal hydroxide precipitates.

The abovementioned experiments suggest that the particle size of limestone considered will be important for increasing the pH (neutralisation) of acidic solutions as they had demonstrated that fine-textured limestone was more efficient than coarse-textured limestone in neutralising the acid because it enabled quicker dissolution of the limestone. The study confirmed that fine-textured limestone can increase the pH of the acid so that ferrous iron can be oxidised to ferric iron, which precipitated into ferric hydroxide. This precipitation is beneficial, as it would sequester metals.

This indicates that particle size remains a key factor for neutralisation, and if a limed soil profile is to receive AMD, then fine particle size is required to do the following:

- Increase the surface area for the neutralisation reaction
- Reduce armouring concerns, which restrict the dissolution potential and neutralisation efficiency of limestone
- Enable the sequestration of metals through precipitation, which could then be stored in the soil profile

The second hypothesis states that the location of limestone in sand columns becomes less important for neutralisation with more frequent leaching at a lower volume, which increases the contact time between the limestone and the synthetic acid mine water, thus aiding neutralisation.

The study accepted this hypothesis based on the column leaching experiment. The ability of limestone to neutralise synthetic acid mine water is not dependent on the location of limestone in the sand columns. The study showed that increased contact time between the limestone and synthetic acid mine water was more effective in neutralisation by leaching 100 ml of synthetic acid mine water daily, which probably reduced the flow rate, thus aiding neutralisation by increasing contact time. Additionally, the particle size of the limestone considered in the sand column remained crucial with fine-textured limestone demonstrated to be the most appropriate. Therefore, it is suggested that if AMD is applied as irrigation to limed soil, appropriate irrigation techniques must be carefully considered and managed to favour the contact time between the soil solution and the liming material to enable neutralisation.

## 9.6 REFERENCES

- AHMAD Z (2006) *Principles of corrosion engineering and corrosion control*. Elsevier, 500 pp.
- BAILEY AT (2016) *The application of sandstone to reduce limestone armoring in acid mine drainage*. Master's dissertation, Wichita State University, Wichita, KS, USA.
- BRAHAITA ID, POP IC, BACIU C, MIHAIESCU R, MODOI C, POPITA G and TRUTA RM (2017) The efficiency of limestone in neutralising acid mine drainage – a laboratory study. *Carpathian Journal of Earth and Environmental Sciences* **12** 347–356.
- CLARKE ET, LOEPPERT RH and EHRMAN JM (1985). Crystallization of iron oxides on calcite surfaces in static systems. *Clays and Clay Minerals* **33** 152–158.
- DE BEER M (2005) *Treatment of acid mine drainage and acidic effluents*. Master's dissertation, North-West University, Potchefstroom, South Africa.
- DOLD B (2014) Evolution of acid mine drainage formation in sulphidic mine tailings. *Minerals* **4** 621 Potchefstroom 641.
- ESSINGTON ME (2005) *Soil and water chemistry: An integrative approach*, Taylor & Francis.
- FUSI L, MONTI A and PRIMICERIO, M (2012) Determining calcium carbonate neutralisation kinetics from experimental laboratory data. *Journal of Mathematical Chemistry* **50** 2492–2511.
- GELDENHUYS AJ, MAREE JP, DE BEER M and HLABELA P (2003) An integrated limestone/lime process for partial sulphate removal. *The Journal of The South African Institute of Mining and Metallurgy* 345–354.
- HAMMARSTROM JM, SIBRELL PL and BELKIN HE (2003) Characterisation of limestone reacted with acid-mine drainage in a pulsed limestone bed treatment system at the Friendship Hill National Historical Site, Pennsylvania, USA. *Applied Geochemistry* **18** 1705–1721.
- JONES AM, GRIFFIN PJ, COLLINS RN and WAITE TD (2014) Ferrous iron oxidation under acidic conditions – the effect of ferric oxide surfaces. *Geochimica et Cosmochimica Acta* **145** 1–12.
- MADISENG L (2019). *Crop response to irrigation with acidic and neutralised, saline mine water*. Master's dissertation, University of Pretoria, Pretoria, South Africa.
- PETKOV K, STEFANOVA V, STAMENOV L and ILIEV P (2017) An analytical study of the neutralisation process of solutions with high concentration of Fe(III) Ions. *Journal of Chemical Technology and Metallurgy* **52** 242–251.

POTGIETER-VERMAAK SS, POTGIETER JH, MONAMA P and VAN GRIEKEN R (2005) Comparison of limestone, dolomite and fly ash as pre-treatment agents for acid mine drainage. *Minerals Engineering* **19** 454–462.

SJOEBERG EL and RICKARD D (1984) Temperature dependence of calcite dissolution kinetics between 1 and 62°C at pH 2.7 to 8.4 in aqueous solutions. *Geochimica et Cosmochimica Acta* **48** 485–493.

SPARKS DL (2003) Inorganic soil components. In: *Environmental soil chemistry*, SPARKS DL, Elsevier Science, USA.

SUN Q, MCDONALD LM and SKOUSEN JG (2000) Effects of armoring on limestone neutralisation of AMD, 1–10.

# CHAPTER 10: MANGANESE(II) OXIDISING POTENTIAL OF SELECTED SOILS UNDER DIFFERING OXIDATION CONDITIONS

---

SN Heuer, PC de Jager, PD Tanner, JG Annandale and HM du Plessis

## 10.1 INTRODUCTION

Using mine-affected water for irrigation may alleviate water treatment costs post-mine closure, and an additional and supplemented water supply may assist in the reclamation of valuable agricultural lands (Rodda et al., 2011). According to Annandale et al. (2006), irrigation with mine-affected water offers a plausible solution to the environmental and economic problem mine-affected waters pose, as long as it is effectively implemented, monitored and managed.

Many mine-affected waters contain appreciable concentrations of manganese. Understanding the extensive relationships manganese has in the soil is thus of utmost importance if this manganese mine-affected water is to be responsibly used. The South African Irrigation Water Quality Guidelines, published by the Department of Water Affairs and Forestry in 1996 (DWAF, 1996), has set manganese irrigation threshold concentrations. The manganese concentrations in these guidelines are as follows: 0.2 mg/l when irrigating with this water quality for 100 years; 10 mg/l when irrigating with this water quality for 20 years; and 100 mg/kg when irrigating with this water quality for 100 years. The speciation of manganese in irrigation waters and the soils to which they are applied determine whether manganese is bioavailable, environmentally mobile or toxic. Manganese is highly redox active in the soil, and rapid rates of Mn(II) oxidation in soils render Mn(II) unavailable. The rate of the biotic and abiotic oxidation of Mn(II) depends on the specific environmental conditions and sorbents present (Elzinga, 2011; Lefkowitz et al., 2013). If some soils and conditions rapidly oxidise and render Mn(II) unavailable, a blanket manganese threshold value, as stated in the Irrigation Water Quality Guidelines, may need to be reconsidered. A better understanding of the Mn(II) oxidation potential of soil allows users, researchers and authorities to make better-informed decisions about the utilisation of manganese-rich mine water in agriculture and its considered environmental impact.

The aim of this study is to determine the impact a changing oxidising environment and a soil's inherent manganese concentration will have on a soil's Mn(II) oxidising propensity. The hypotheses of this study are that soils with elevated inherent manganese oxide concentrations in oxidised environments will have a greater Mn(II)-oxidising propensity than soils with little to no inherent manganese concentrations. The objectives of the study are to investigate the Mn(II) oxidation of soils with different total manganese concentrations under differing oxidising conditions.

## 10.2 MATERIALS AND METHODS

After the completion of the Mn(II) batch sorption trial, a quantitative mass balance can be determined. By analysing the soil before and after the trial, a quantitative comparison can be made as to what each soil sorbed, and the degree of sorption and manganese speciation. By analysing the solution's manganese content using ICP-AES analyses, the Mn(II) amount sorbed and removed from solution can be determined. The adsorption coefficients and isotherms for each soil for Mn(II) determine the efficiency and theoretical adsorption type for Mn(II) in the soils. Determining the oxidisable and reducible fractions of manganese in the soil before and after the experiment will allow one to determine the effectiveness of the soil in oxidising Mn<sup>2+</sup> to Mn(III + IV), and therefore its Mn(II)-oxidising propensity.

## 10.2.1 The soil's physical and chemical characterisation

### Soil description

Four selected soils were used for this study: sand, andesitic-derived soil, dolomitic-derived soil and manganese oxide-coated sand. After soil sample sourcing and the collection of these four soils, they were stored in a temperature control room at 4 °C. Field moist conditions were maintained until the sorption batch study began. Table 10.1 shows the general characterisation, classification and description of the four selected soils used in this study.

The andesitic-derived soil was sourced from the University of Pretoria's Experimental Farm. The soil samples were collected up to a depth of 20 cm, and appeared reddish-brown in colour, indicative of the presence of clays, with intermittent small manganese concretions visible. The dolomitic-derived soil was sourced in the Irene area near Pretoria. This dolomitic-derived soil is rich in manganese. The soil samples were collected up to a depth of 30 cm. Basement dolomite was intermittently intersected during the sample collection process due to the undulating bedrock profile. This dark brown soil had calcitic (white) and manganese oxide (black) concretions dispersed throughout the sample. This is indicative of the composition of the dolomitic bedrock, as both the bedrock and the *in situ* soil were rich in calcium and manganese.

Two of the soil samples used were not sourced *in situ* from the environment: the sand and the manganese oxide-coated sand. The sand filter media and the manganese oxide-coated sand were bought from a water treatment company, which states that it sources its manganese oxide sand from the USA, where it is manufactured. The sand is sourced from a quartzite quarry outside Pretoria.

Table 10.1: General soil sample description and classification

Soil sample	Source	Soil description	Geology
Sand	Water treatment company	99% silica sand (< 2mm)	-
Andesite-derived soil	University of Pretoria Experimental Farm	Hutton soil classification 0–20 cm depth Orthic A	Hekpoort Formation andesite, Pretoria Group, Transvaal Supergroup (Eriksson et al., 2006)
Dolomite-derived soil	Irene shooting range, Pretoria	Mispah soil classification 0–30 cm depth Orthic A hard rock	Lyttleton Formation, Malmani Subgroup, Chuniespoort Group, Transvaal Supergroup (Obbes 2000)
Magnesium-coated sand	Water treatment company	Also known as "Birm" By weight, a 90% aluminium silicate core is coated in a 10% manganese dioxide	-

### Soil physical characterisation

Soil colour and texture analyses were performed. The dry soil colour was visually determined using the Munsell 7.5 YR colour chart. The soil texture analysis used is a method adapted from Bouyoucos (1962). The soil preparation and pre-treatment for the soil texture analysis were as follows: Remove the organic matter, 20 ml of hydrogen peroxide was added to each 50 g soil sample. The samples were placed on sand baths where they were heated and where excess water could evaporate. De-ionised water was added intermittently to slow the soil and hydrogen peroxide reaction as this is a very aggressive exothermic reaction.

Soil texture determination was as follows: Following the removal of the organic matter, pre-treatment, 10 ml of a Calgon-dispersing agent and 200 ml of deionised water was added to each soil sample. The samples were decanted into separate dispersion cups and mixed with an electric beater for five minutes. Samples were then passed through a 0.053 mm wire mesh sieve until the solution appeared clear. This is to ensure that the sand fraction was separated from the clay and silt fractions. Deionised water was added to the silt and clay fractions to make up a 1 l container.

Sand fraction determination was as follows: The fraction of the samples that did not pass through the 0.053 mm sieve, were carefully collected and transferred to containers and dried overnight in an oven. The dry mass sand fraction was weighed and the sand fraction percentage determined.

Clay fraction determination was as follows: A blank sample of 1 l was made up of a 10 ml Calgon dispersing agent and deionised water. The 1 l samples were thoroughly mixed with a plastic plunger. After 06:35 hours of the sampling being undisturbed, a standard hydrometer (ASTM No 152 H) was slowly placed into the 1 l cylinders and the hydrometer readings were taken. The clay fraction percentage was determined using the appropriate temperature column.

Silt fraction determination was as follows: The silt fraction percentage was calculated by subtracting the clay and sand fractions from 100%.

### **Soil chemical characterisation**

The soil pH and cation exchange capacity were determined to chemically classify the soils. Soil pH was calculated to determine the relative hydrogen ion activity in the soil. To each 10 g soil sample, 25 ml of 1 M potassium chloride solution was added. The samples were agitated and left undisturbed for an hour, after which a calibrated pH meter was used to measure the pH of the supernatant. This process was repeated with 25 ml of deionised water, still having the 1:2.5 soil/water mass basis ratio (FSSA, 1974).

The soils' cation exchange capacity analysis used an adapted method from Zelazny et al. (1996): A quantity of 0.2 M KCl was added to 5 g of each soil. The samples were agitated for 20 minutes and then centrifuged for 10 minutes. The clear supernatants were decanted. This procedure was repeated four times. The samples were then washed with 30 ml of 0.04 M KCl three times over, and the supernatants were again decanted. The samples were weighed to determine the volume of the entrained solutions. Finally, 30 ml of 0.2 M ammonium chloride (NH<sub>4</sub>Cl) was added to the washed and weighed samples, agitated and centrifuged a final time. This process was repeated four times, with the supernatants collected each time. The collected supernatants were analysed for K<sup>+</sup> using ICP-AES (Zelazny et al., 1996).

### **10.2.2 Manganese batch sorption experiment**

#### **Experimental description and layout**

The Mn(II) batch sorption trial comprised four soils (sand, andesitic-derived soil, dolomitic-derived soil and manganese oxide-coated sand), exposed to a 200 mg Mn(II)/kg soil loading in solution. The soil-solution system consisted of 500 ml of manganese sulphate solution (MnSO<sub>4</sub> · 4H<sub>2</sub>O) exposed to 300 g of each selected soil. The soils were not pre-treated or air-dried, and the experiment began with soils at field moist conditions. These soils were split into three batches, and each batch was exposed to different oxidation regimes: a 20-day oxidation/aeration, a 40-day oxidation/aeration, and a 15-day oxidation/aeration plus a 25-day cycle increasingly reducing oxidation/aeration. This Mn(II) batch sorption trial was carried out in duplicates for each soil and oxidising regime. Figure 10.1 shows the basic experimental set-up of this Mn(II) batch sorption trial.

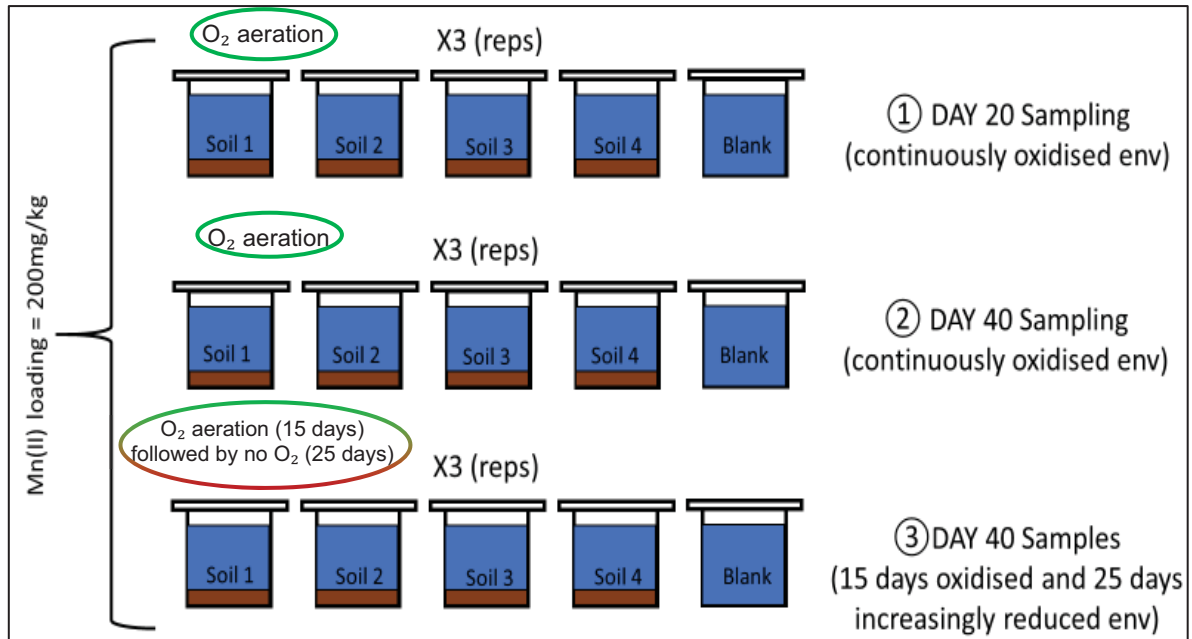


Figure 10.1: Basic experimental set-up of the Mn(II) batch sorption trial

The Mn(II) loading used in this Mn(II) batch sorption trial is double that of the stated South African Irrigation Water Quality Guidelines' manganese threshold. This Mn(II) loading of 200 mg Mn(II)/kg was chosen to determine whether soils are capable of oxidising larger applied amounts of Mn(II) than stated in the guidelines.

The following calculations indicate how the Mn(II) loading and salt concentrations were determined:

Using 500 ml of deionised water and 300 g of soil, a set Mn(II) loading of 200 mg/kg, the concentration of Mn(II) (mg/l) can be determined as follows:

$$\text{Mn (II) loading (mg/kg)} = \frac{\text{Mn (II) concentration } \left(\frac{\text{mg}}{\text{L}}\right) * \text{volume (L)}}{\text{soil mass (kg)}}$$

$$200 \text{ mg/kg} = \frac{(X \frac{\text{mg}}{\text{L}})(0.5\text{L})}{0.3\text{kg}}$$

$$X = 120 \text{ mg Mn (II)/ l}$$

Knowing the Mn(II) concentration (mg/l), the total salt concentration ( $\text{MnSO}_4 \cdot 4\text{H}_2\text{O}$ ) can be determined:

$$\text{Total salt concentration (g/l)} = \frac{\text{Mn (II) loading } \left(\frac{\text{g}}{\text{L}}\right) * \text{Total salt (MnSO}_4 \cdot 4\text{H}_2\text{O) molecular mass } \left(\frac{\text{g}}{\text{mol}}\right)}{n * \text{Mn molecular mass } \left(\frac{\text{g}}{\text{mol}}\right)}$$

$$= \frac{0.12 * 223.08}{1 * 54.94}$$

Therefore, adding 0.495 g  $\text{MnSO}_4 \cdot 4\text{H}_2\text{O}$  to 1 l of water.

The contact time determined to be suitable for the maximum removal of Mn(II) by the soils was split into two contact or sampling time periods: 20 days and 40 days. Samples were agitated for 30 minutes daily at room temperature. Each sample was aerated daily for five minutes (specific for each batch's allotted time) and stored in a temperature-controlled room ( $21 \pm 0.3$ ) °C, after the daily redox, pH, EC ( $\mu\text{S/cm}$ ) and TDS (mg/l) measurements had been taken. Figure 10.2 shows the samples before daily aeration took place. Figure 10.2(ii) shows an example of the daily measurements being taken for samples of the batch sorption trial.



Figure 10.2: Samples after measurements were taken, before daily aeration; (ii) daily measurements using an ORP probe

### 10.2.3 Soil monitoring, analyses and extractions

#### Soil redox monitoring

As the pH of the soils was unaltered by any pre-treatments, the changes to the soil's natural pH, EC and TDS conditions were observed throughout the experiment. Manganese speciation would thus have been under conditions similar to those found of the soils *in situ*. This allows for simulating, in a laboratory-scale experiment, similar conditions if the experiment was to be *in situ*. Monitoring the redox conditions of the system ensured that the system remained oxidative during the aeration phases so that the oxidation conditions were not viewed as a hindrance to the soils' Mn(II)-oxidising propensity. This ensured that the manganese species present reflected a system under oxidative conditions. Monitoring the redox conditions of the system during the periods of no aeration allows the effect of the system's oxidative conditions on the Mn(II)-oxidising propensity of the soils to be determined.

The HM digital ORP 200 meter was used in this experiment to measure the daily redox potentials of the solution. The oxidation reduction potential (ORP) probe uses a glass sensor and platinum reference electrode cell. The HM digital COM 300 meter, a combined probe, was used to make daily pH, EC ( $\mu\text{S}/\text{cm}$ ) and TDS ( $\text{mg}/\ell$ ) measurements. The HM digital COM 300 meter uses platinum electrodes and a pH glass sensor with reference tube electrodes.

After 30 minutes of daily agitation, the redox probe is inserted until it is completely covered by the system's solution. After the system has stabilised, a potential difference reading is obtained and transformed into a standardised redox potential (Eh) reading. This value was recorded for all the soils under both oxidising regimes daily over the entire time frame of the experiment. The same process was followed for the use of the combined probe, and daily pH, EC ( $\mu\text{S}/\text{cm}$ ) and TDS ( $\text{mg}/\ell$ ) measurements were recorded.

#### Manganese adsorption coefficients

The batch sorption experiments were carried out, and from the Mn(II) ions left in solution at the end of the experiment, the adsorption coefficient and isotherms of the different soils were determined under differing oxidising conditions. The batch sorption experiment was carried out at a constant concentration of Mn(II) and a constant soil-to-liquid ratio of 1:1.67, 300 g soil and 500 m $\ell$  manganese sulphate solution. ICP-AES readings of Mn(II) were taken of the solution added to the different soils at the start of the experiment and at the end of the experiment.

Using known relationships between adsorption and adsorbents, a comparison of the Mn(II) adsorption efficiencies, the adsorption capacities and modelling of the adsorption isotherms could be determined.

Using these calculations, a better understanding of the adsorption capacities of the manganese in these soils could be obtained.

The Mn(II) adsorption capacity (mg/g) was calculated using the following expression (Langmuir, 1918):

$$q_e = \frac{(C_o - C_e) \cdot V}{m}$$

Where  $C_o$  is the initial manganese concentration in solution (mg/l),  $C_e$  is the final manganese concentration in solution (mg/l),  $V$  is the volume of solution (ml), and  $m$  is the mass of sorbent used (g).

The manganese sorption efficiency (MSE) (as a percentage) was calculated using the following expression (Igwe and Abia, 2007):

$$MSE\% = \frac{(C_o - C_e)}{C_o} \times 100$$

Where  $C_o$  is the initial manganese concentration in solution (mg/l), and  $C_e$  is the final manganese concentration in solution (mg/l).

### Total electron demand

A volume of 4 ml 0.2 M KI and 12 ml 0.1 M HCl was added to 2 g field moist soil. All samples were centrifuged for 15 minutes and membrane filtered. A starch solution (0.2 g potato starch boiled with 30 ml water) was added to the extractants as the indicator solution. The extractants were titrated to a colourless endpoint using 2 mM  $\text{Na}_2\text{S}_2\text{O}_3$  (Bartlett, 1988).

Figure 10.3 gives a graphic representation of the manganese mass balance, and how determining each fraction should provide more accurate and quantitative answers as to the speciation and oxidation of manganese by these different soils. The KCl extraction analyses the exchangeable and oxidisable manganese fraction of the soil, while the hydroxyl amine extraction analyses the reducible manganese in the soil. Knowing the concentrations of these three main fractions of the soil-solution system before and after treatment should allow one to determine the manganese adsorption and oxidisable potential of the different soils.

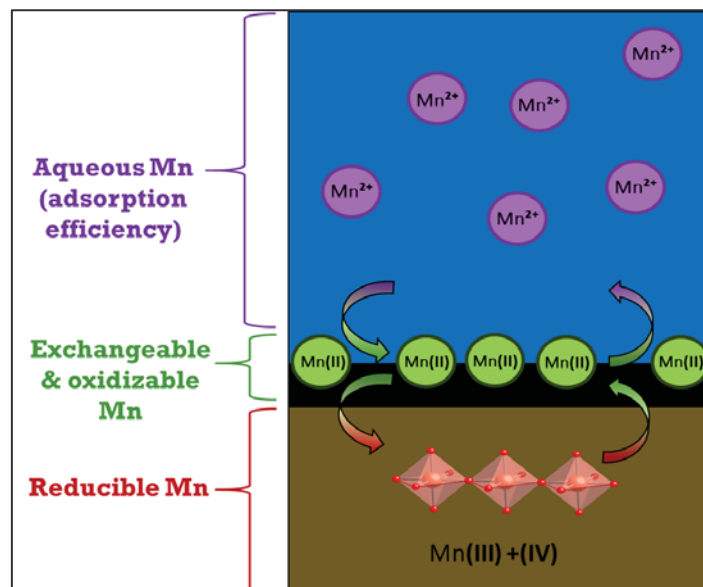


Figure 10.3: A simplification of the soil-solution system as seen in the manganese batch sorption experiment, showing the concept of manganese mass balance determination

## 10.3 RESULTS

### 10.3.1 Soil physical and chemical characterisation

#### Soil physical properties

The results of the adapted soil texture analyses from Bouyoucos (1962) or the “rapid method”, and the use of the Munsell colour chart provided an overall representation of the different soils’ physical characteristics (Table 10.2).

Table 10.2: Texture analyses of the selected soils

Soil sample	Dry soil colour	Textural class	Soil texture		
			Clay fraction	Silt fraction	Sand fraction
Sand	7.5 YR 7/6	Sand	1	2	98
Andesite-derived soil	2.5 YR 4/8	Clay	60	5	35
Dolomite-derived soil	7.5 YR 2.5/3	Sandy loam	18	28	54
Manganese-coated sand	7.5 YR 2.5/1	Sand	2	4	94

#### Soil chemical properties

The results provided in Table 10.3 provide a basic chemical characterisation of the selected soils used in the batch sorption experiment.

Table 10.3: Basic chemical characterisation of the selected soils

Soil sample	pH (H <sub>2</sub> O)	pH (KCl)	CEC (cmol <sub>c</sub> /kg)
Sand	4.45	3.32	1.36
Andesite-derived soil	5.65	4.09	5.45
Dolomite-derived soil	6.39	4.1	9.32
Manganese-coated sand	10.78	7.6	112.5

The pH (KCl) values were between two to three units lower than that measured by the pH (H<sub>2</sub>O). This can be assumed to be an experimental error and these values are taken as being less accurate than the pH (H<sub>2</sub>O). The pH of the manganese oxide-coated sand was surprisingly high, indicating the presence of residual alkalinity, presumed to be from the production process of this sand. The sand and andesitic-derived soil are slightly acidic, and the dolomitic-derived soil is near neutral. The baseline pH assessment of these soils allows for comparison with any changes in the soils’ pH after the experiment is complete.

The manganese oxide-coated sand and the andesite- and dolomite-derived soils have a higher inherent manganese oxide content. The surface charge of the manganese oxides, coupled with the presence of clay minerals, both contribute to the cation retention capacity of the soils. Based on the above cation exchange capacity results, the manganese oxide-coated sand is expected to show the highest manganese cation retention of all the soils, while the sand is expected to have the lowest manganese cation retention. These results do not indicate the manganese-oxidising potential of the soils, but rather the ability of the soils to retain dissolved manganese cations on surface adsorption sites.

### 10.3.2 Manganese batch sorption experiment

The following section looks at the adsorption efficiencies and adsorption coefficients, using linearised Langmuir and Freundlich adsorption isotherms to model the adsorption capacities of the four soils.

The  $Mn^{2+}$  adsorption efficiencies of the four soils provides insight into how well the soils adsorb manganese from solution. The type and number of surface adsorption sites depends on how well the specific soil adsorbs  $Mn^{2+}$  from solution.

Table 10.4: Summary of the Mn(II) adsorption efficiencies (as a percentage) for the four selected soils in the batch experiment

Soil type	Oxidation regime		
	20 days oxidative	40 days oxidative	15 days oxidative and 25 days reducing
	Mn(II) sorption percentage		
Sand	23.9	53.8	25.4
Andesitic-derived soil	99.9	99.9	99.8
Dolomitic-derived soil	99.9	99.9	99.8
Manganese oxide-coated sand	94.3	98.9	96.6

As seen in Table 10.4, the sand samples had the lowest sorption efficiencies, indicating that the soil with the lowest manganese oxide content and lowest CEC has the least surface adsorption sites for  $Mn^{2+}$ , and the presumed lowest oxidising ability.

Maximum removal of  $Mn^{2+}$  from solution is within 20 days for the andesitic-derived, dolomitic-derived and manganese oxide-coated sand samples. Adsorption by these soil samples is thus rapid. The sand samples were only able to remove a bit more than half the  $Mn^{2+}$  ions in solution after 40 days under oxidising conditions. Sand has a low adsorption capacity for manganese in solution, and irrigating with manganese-rich waters on very sandy soils means that large amounts of manganese remain environmentally available and will easily leach through the soil profile.

The 15-day oxidation followed by 25-day reducing conditions had little impact on the manganese adsorption of the andesitic-derived, dolomitic-derived and manganese oxide-coated sand samples. The decrease in the oxygen content (Eh) of the sand-solution system saw a great decrease in the  $Mn^{2+}$  adsorption of the sand.

The soils with an increased inherent Mn(III + IV) content had increased surface adsorption sites for the removal of  $Mn^{2+}$  ions, and were better able to remove  $Mn^{2+}$  from solution, making it less environmentally mobile. An analysis of the oxidisable and reducible manganese content of the soils will indicate the manganese-oxidising potential and intensity of these soils.

The amount of adsorption at equilibrium and the adsorption coefficients provide an indication of effect of the different oxidising regimes on the different soils' manganese adsorption capacities.

Table 10.5: Summary of adsorption coefficients for Mn(II) of the four selected soils for the three different oxidising regimes

Soil type	Oxidation regime		
	20 days oxidative	40 days oxidative	15 days oxidative and 25 days reducing
	q <sub>e</sub> (mg/g)		
Sand	46.3	109.2	50.3
Andesitic-derived soil	188.6	196.4	193.3
Dolomitic-derived soil	199.9	199.8	199.7
Manganese oxide-coated sand	199.9	199.8	199.6

The adsorption capacities indicate that the 15-day oxidation followed by 25-day reducing conditions impact on the adsorption capacity. Sand is most greatly affected by the removal of oxygen from the soil-solution system, showing a decrease in its adsorption capacity by half when compared to the 40-day oxidising regime. This provides the premise that oxygen, as an oxidant, has an impact on the adsorption capacity of some soils. A greater impact is seen on soils with lower inherent manganese oxide concentrations. The adsorption capacity of the andesitic-derived soil indicates that this soil's manganese adsorption capacity is positively influenced by the increased exposure time to an oxidised system. The increased levels of oxygen present provide higher adsorption capacities.

The adsorbents' performance is studied by adsorption isotherm data. This adsorption data is obtained from the batch sorption experiment. The adsorption isotherm data is modelled to predict and compare the adsorption performance of different materials, to optimise adsorption mechanism pathways, to determine the adsorbents capacities, and to effectively design adsorption systems to treat water that has undesired contaminants (Thompson et al., 2001).

The two-parameter linear Langmuir and Freundlich isotherm models are used to predict the overall adsorption behaviour of sorbents. Using the linearised forms of these isotherm models is the most widely adopted method to determine the isotherm parameters due to their mathematical simplicity. In recent years, a linear analysis has been found to cause discrepancies between the predicted and experimental data (Chen, 2015).

Table 10.6: Summary of linearised Langmuir isotherm parameters for Mn(II) on the four selected soils

Linearised Langmuir adsorption isotherm					
Soil type	$q_e$ (mg/g)	$K_L$ (L/mg)	$q_{max}$ (mg/g)	$R^2$	$R_L$
Sand	68.7	-0.599	45.9	0.9971	-0.014
Andesitic-derived soil	199.8	-0.922	49.8	0.9991	-0.002
Dolomitic-derived soil	193.2	-10 000	200	1	$-8.3 \times 10^{-7}$
Manganese oxide-coated sand	199.8	-4.38	108.7	0.9999	-0.009

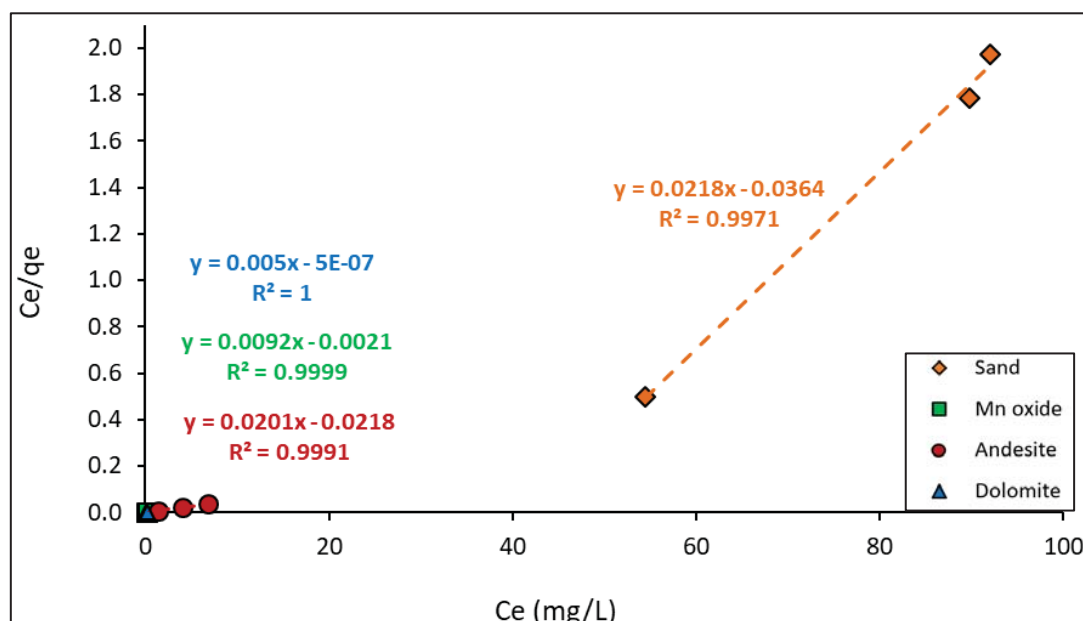


Figure 10.4: Linearised Langmuir isotherm for the adsorption of Mn(II) for the four selected soils

Due to sand not adsorbing a great deal of the applied  $Mn^{2+}$  ions, the Langmuir isotherm is a completely separate population when compared to the manganese oxide-coated sand, the dolomite-derived soil and the andesite-derived soil.

Even though the coefficient of determination suggests extremely good correlation for these soils, the linearised Langmuir isotherm constants determined suggest otherwise. Due to the intercepts of linear regression lines being negative, the Langmuir constant is also determined to be negative, which affects the separation factor. Negative  $K_L$  and  $R_L$  values indicate that the linearised Langmuir adsorption isotherm does not correctly depict the adsorption process of  $Mn^{2+}$  onto the surfaces of the selected adsorbents. The assumptions used in the description of the Langmuir model of a monolayer of adsorbed ions and the homogenous distribution of adsorption sites of the adsorbent are therefore not suited to any of the adsorbents in this batch study.

### 10.3.3 Soil monitoring, analyses and extractions

#### Soil redox monitoring

Appendix A9 shows the monitored pH, EC ( $\mu S/cm$ ) and TDS ( $mg/l$ ) measurements for the four soils over the period of the experiments for all the oxidation regimes. None of the different oxidative regimes and the addition of Mn(II) seemed to have an effect on the pH, EC or TDS of the four soil systems. After the first four days of exposure of the soil to Mn(II) and oxidation, the soil systems stabilised and the pH, EC ( $\mu S/cm$ ) and TDS ( $mg/l$ ) remained relatively constant over the period of the experiment.

Figures 10.5A and 10.5C show the Pourbaix diagrams (Eh vs pH) for the 40-day oxidation and the 15-day oxidation followed by 25-day reducing regimes for the four soils. Using the theoretical Pourbaix diagram, a prediction can be made of the expected manganese speciation over the monitoring period of the different oxidation regimes. Monitoring the system's Eh confirms the system's oxygen status, and ensures that reducing conditions are not occurring when oxidation conditions should be taking place.

From Figure 10.5B, a steady increase in Eh is observed over the 40-day period, while the pH is constant over the experimental period. The increase in the system's Eh provides the premise to assume that the speciation of manganese tends towards an increase in the solid Mn(III) and Mn(IV) phases present in the system. As the number of days of oxidation increases, the manganese species present in the system changes from  $Mn^{2+}$  to the more insoluble  $Mn_2O_3$  and  $MnO_2$  phases.

Figure 10.5D shows the change in Eh of the soil systems over the 15-day oxidising followed by 25-day reducing conditions. The manganese oxide-coated sand, even at its high pH, had a theoretical manganese species change from a manganese oxide to a manganese hydroxide form. This is due to the decrease in the redox status of the soil system. The other three soils showed an increase in the system's Eh, followed by a period of about two or three days of constant Eh, and finally a period of sharp decrease in the system's Eh. There were brief periods of Mn  $Mn_2O_3$  and  $MnO_2$  phases at around Day 15 to Day 20, followed by the bulk of the solution being in the  $Mn^{2+}$  phase for the three soils. This specific change in the systems' Eh showed how a system's manganese speciation is highly dependent on the system's Eh. It can also be said that the system's Eh therefore has a great influence, theoretically, on the oxidation and manganese oxide species that would form under different oxidation conditions.

It is noted that, due to the residual alkalinity present in the manganese oxide-coated sand, and that no pre-treatment of acid washing was administered, the very alkaline pH of this system will influence the manganese speciation seen throughout the experiment for this soil.

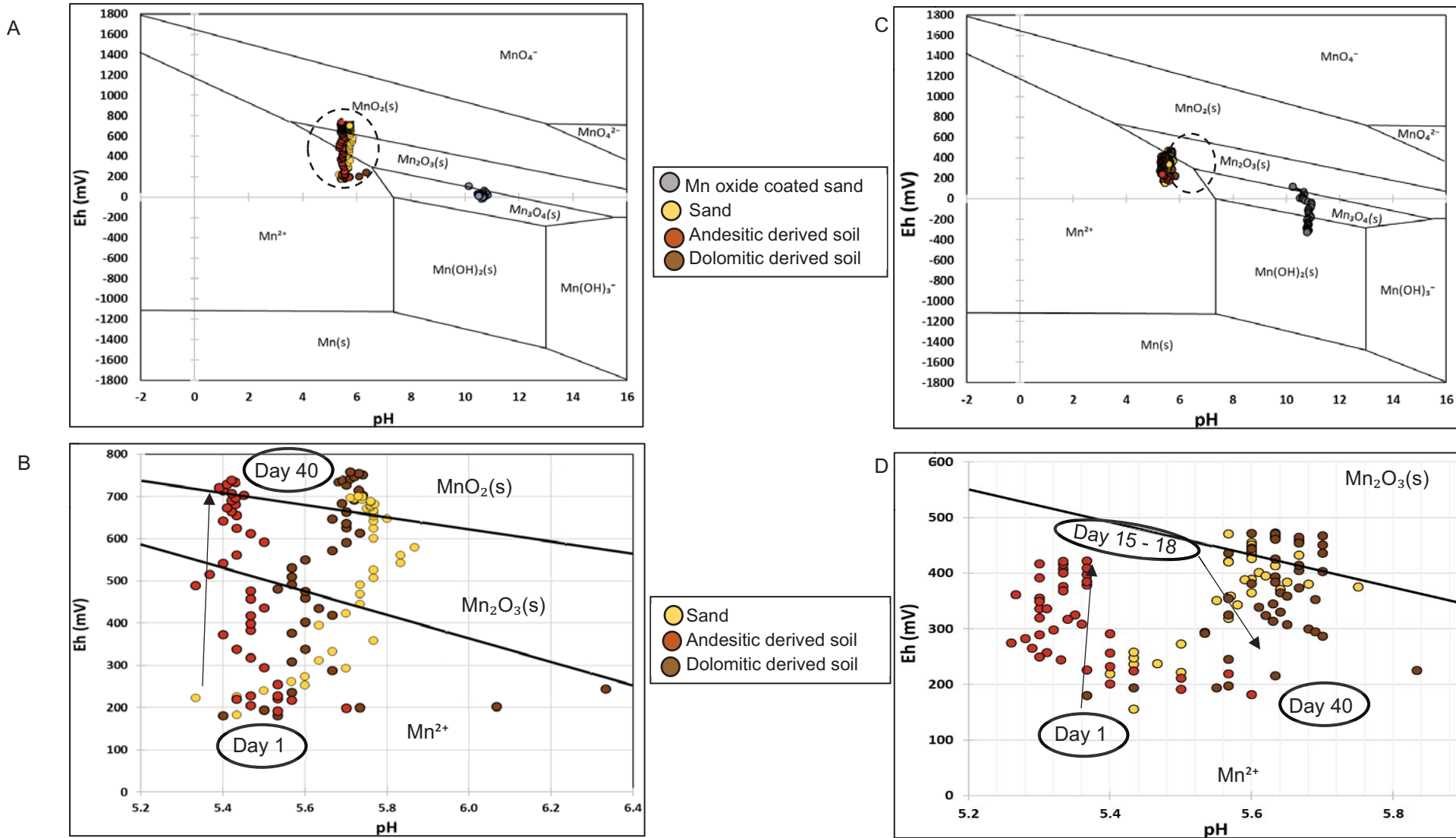


Figure 10.5: The redox potential (mV) vs the pH of the four soils over the 40-day aeration/oxidising period (A and B), as well as for the four soils over the 15-day aeration/oxidising followed by 25-day reducing period (C and D)

**Hydroxyl amine extraction**

The results of inherent manganese oxide concentrations, as well as the effects of different oxidising regimes on the easily reducible forms of manganese from the experiment, are seen in Table 10.7.

*Table 10.7: Easily reducible manganese fractions for the four soils under three different oxidising regimes*

Soils	Contact time		
	20-days oxidative	40-days oxidative	15-days oxidative and 25-days reducing
	Reducible Mn(III and IV) (mg/kg)		
Sand	36.8	58.8	38.6
Andesitic-derived soil	735.8	933.2	682.6
Dolomitic-derived soil	2710.5	2880.4	2620.7
Manganese oxide-coated sand	802.7	922.7	794.6

It was observed that all soils showed an increase in the Mn(III + IV) fractions of the soil when Mn<sup>2+</sup> was added to the system. Under the 40-day oxidising conditions, higher amounts of the added Mn<sup>2+</sup> was converted to Mn(III + IV), indicating that increased time under highly oxidised conditions allows for greater quantities of manganese oxidation of Mn<sup>2+</sup> to Mn(III + IV).

The soil with the highest easily reducible forms of manganese was dolomite. This is due to its inherently high amount of manganese, visually seen in the soil profile as black manganese nodules. The soil expected to have the highest Mn(III + IV) was the manganese oxide-coated sand, yet it did not. The reason for this was that the hydroxylamine extraction solution was most likely not a strong enough reductant to remove the greater portions of Mn(III + IV) coated on the sand. The way in which the manganese oxide coating is chemically bound to the sand during the production process requires a stronger reductant, possibly dithionite-citrate or acid ammonium oxalate, to reduce and remove these fractions.

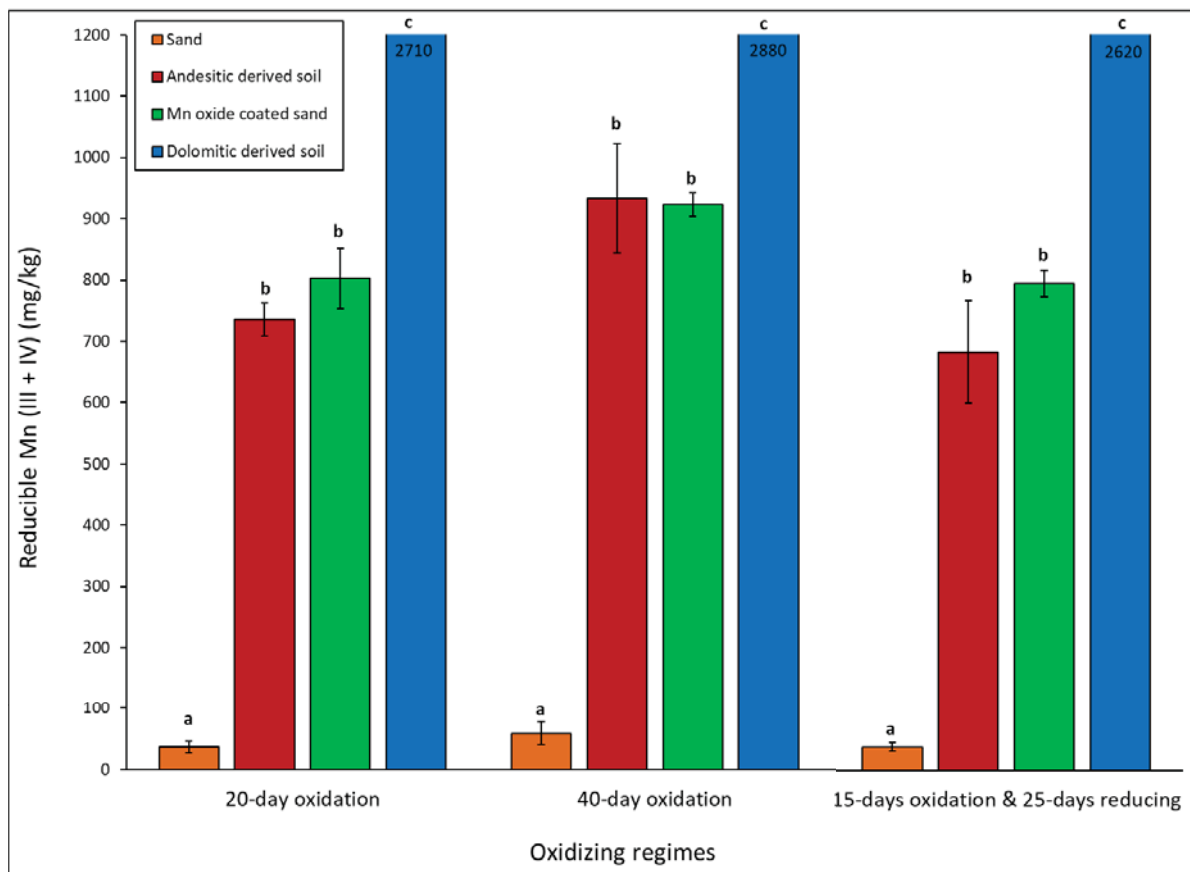


Figure 10.6: Easily reducible fraction of manganese in the four soils for the three different oxidising regimes

No significant differences were observed among the three oxidising regimes of the sand soil samples. This means that sand's reducible manganese fraction is not statistically affected by the change in oxygen levels in the system. As sand has a low CEC and inherent manganese oxide content, the reducible manganese values seen are due to the oxidation and subsequent precipitation induced by the aeration.

Dolomite had the largest Mn(III +IV) fraction. This is due to its inherently large manganese oxide concentration, directly related to its residual formation from the parent material. The large Mn(III +IV) concentrations indicate that this dolomite soil has a large potential to accept electrons and be a strong oxidising agent. There was a slight decrease in Mn(III +IV) content for the reducing conditions. This can be attributed to some Mn(III +IV) being reduced to Mn(II) during the time of low redox potential.

The andesitic-derived soil saw a greater decrease in Mn(III +IV) content during the reduced conditions. This can be attributed to its low ability to buffer changes in the system to reduced conditions. A greater fraction of the soil's inherent Mn(III +IV) was reduced to Mn(II). All the soils showed an increase in Mn(III +IV) concentrations with increasing oxidation conditions. An increase in the oxidising period shows an increase in the oxidation of the added  $Mn^{2+}$  ions. Soils with higher Mn(III +IV) contents oxidise  $Mn^{2+}$  more readily and rapidly, and irrigating these soils with manganese-rich waters would render most of the  $Mn^{2+}$  unavailable, as it would be rapidly oxidised.

Table 10.8 shows the relationship and correlation between total electron demand (TED) and the hydroxylamine extractable manganese fraction of the soils, or the reducible manganese fraction of the soil (Mn(III + IV)), as well as the relationship of all the oxidising agents present in the soil on the soil's overall  $Mn^{2+}$  oxidising capacity, especially the influence of Mn(III + IV) content on the soil's TED.

Table 10.8: The regression analysis and coefficient of determination for the total electron demand and hydroxylamine values of the four soils under three oxidising regimes

Soil type	Oxidising regime					
	20-days oxidative		40-days oxidative		15-days oxidative and 25-days reducing	
	R <sup>2</sup>	Regression line equation	R <sup>2</sup>	Regression line equation	R <sup>2</sup>	Regression line equation
Sand	0	Y = 0	0	Y = 0	0	Y = 0
Andesitic-derived soil	0.41	Y = -0.009x + 8.7	0.04	Y = -0.005x + 6.4	0.01	Y = 0.005x + 1.9
Dolomitic-derived soil	0.74	Y = 0.03x - 56.3	0.002	Y = -0.0005x + 22.1	0.09	Y = -0.001x + 21.7
Manganese oxide-coated sand	0.89	Y = 0.01x + 22.7	0.04	Y = -0.0.3x + 60.9	0.95	Y = -0.13x + 138.6

The sand has no linear regression and coefficient of determination due to sand having zero TED for all samples. The 20-day oxidative conditions for the remaining three soils show a linear regression, with the points being relatively near one another. For the 40-day oxidative and 15-day oxidative followed by 25-day reducing conditions, the R<sup>2</sup> values do not show a strong correlation. The reason for this is that no trend was seen in the values, instead there was a close cluster of the data points. Even though a poor correlation is observed between the TED and reducible manganese content in these samples, this relationship is possibly not a true reflection of the actual relationship usually seen with TED and reducible manganese. If more data points were to be included, an increase in the accuracy of the conclusion can be obtained.

#### Potassium chloride extraction

The results of inherent manganese oxide concentrations, as well as the effects of different oxidising regimes on the easily oxidisable forms of manganese from the experiment, are seen in Table 10.9.

Table 10.9: Easily oxidisable manganese fractions for the four soils under three different oxidising regimes

Soils	Contact time		
	20-days oxidative	40-days oxidative	15-days oxidative and 25-days reducing
	Oxidisable Mn (II) (mmol/kg)		
Sand	22.5	27.1	30.7
Andesitic-derived soil	7.3	4.9	58.4
Dolomitic-derived soil	2.4	4.06	4.09
Manganese oxide-coated sand	0.17	0.16	0.05

The only significant differences between the oxidising regimes were for the andesitic-derived soil. This is attributed to a decreasing redox potential of the system (decreasing Eh and O<sub>2</sub> content), which means that there is an increase in the amount of easily oxidisable Mn(II) present. A decrease in surplus electron acceptors, O<sub>2</sub>, means that the Mn(III +IV) also becomes reduced, and there is an increase in the amount of exchangeable Mn(II) present in the soil. The Eh of the andesite-derived soil was at an optimum value for the Mn(III +IV) to be more readily reduced than in the other soils.

The abnormally high Mn(II) value for the 15-day oxidation followed by 25-day reducing conditions can be seen as a possible experimental error, but the decrease in the Mn(III +IV) content for this soil under this oxidising regime, as clearly seen in Figure 10.7, attributes the higher Mn(II) fraction to the Mn(III +IV) reduction. Statistically, in the andesite soil, there is a significant difference between the two oxidising regimes and the 15-day oxidation followed by 25-day reducing regime.

The sand soil had the highest fraction of exchangeable or oxidisable Mn(II). This is due to the fact that sand has a low inherent CEC, low clay content and a low inherent manganese oxide content, all characteristics that greatly contribute to manganese adsorption and oxidation.

All soils showed an increase in Mn(II) content, however slight, with a decrease in the O<sub>2</sub> content of the system. This is attributed to the increased reduction of the Mn(III +IV) fraction in the soils.

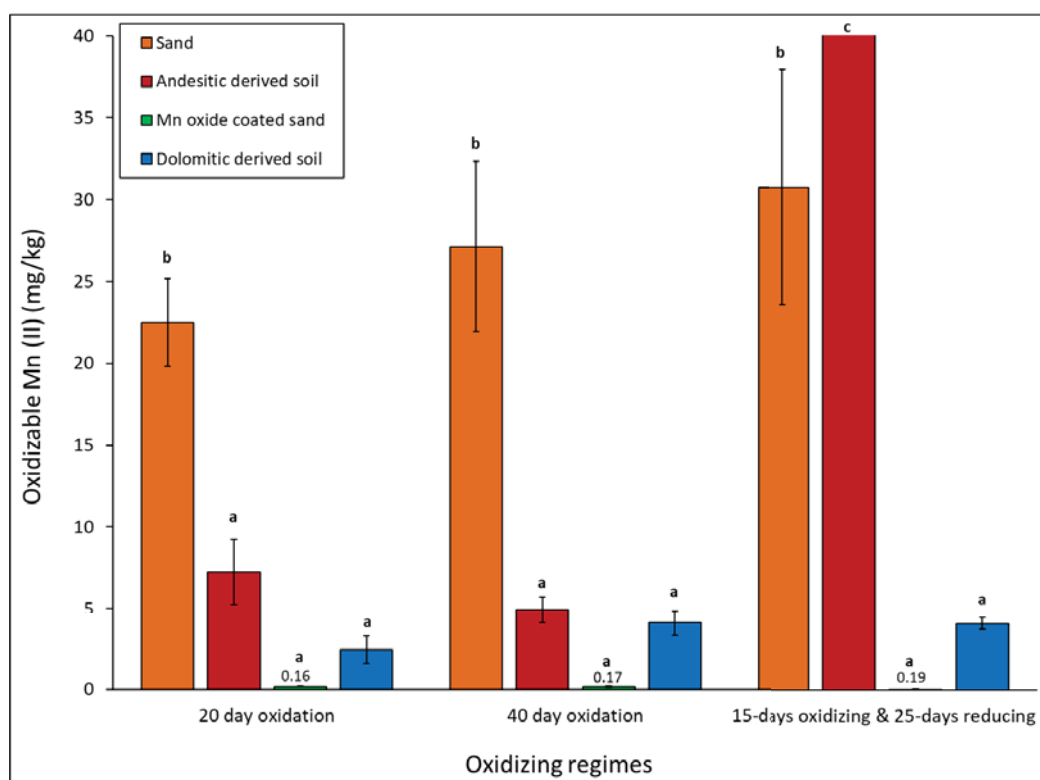


Figure 10.7: Easily oxidisable fraction of manganese in the four soils for the three different oxidising regimes

Combining figures 10.6 and 10.7, Figure 10.8 shows the total manganese analysed. The ratio between oxidisable and reducible manganese in each soil for each oxidation regime can be seen.

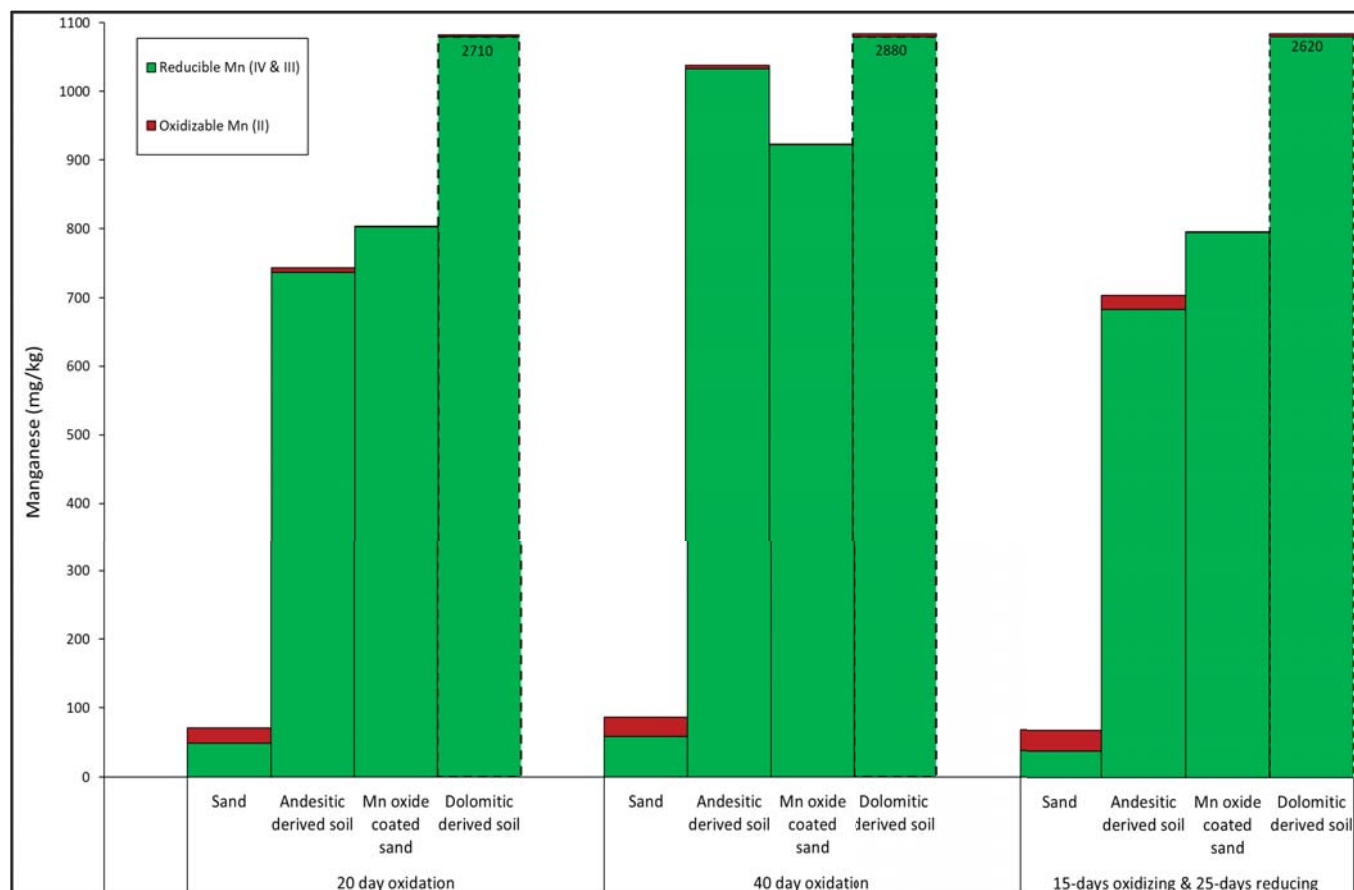


Figure 10.8: Easily oxidisable and reducible fractions of manganese making up the total manganese fraction of the four soils for three oxidising regimes

### 10.3.4 Manganese (II) oxidising potentials

Variations in the oxidising abilities and states within a soil profile result in the variable oxidation-reduction status and adsorption, dissolution and precipitation throughout the profile (Somera, 1967). Knowing the distribution of Eh throughout the soil will provide a provisional profile distribution of manganese oxide formation. The ability of the soil to buffer a change in the Eh conditions also influences the soil's response to changes in the addition or removal of electrons and the speciation of many elements (Von de Kammer et al., 2000).

As stated by Heron et al. (1994), the oxidising capacity of soils helps predict the movement and development of a contaminant plume, and can help to understand aquifer redox zones. Heron et al. (1994) defined oxidation capacity as depending on the availability of electron acceptors or oxidised species. This influences the ability of a system to restrict changes in the development of reduced conditions.

Based on these results and the understanding gained throughout this experiment, a simple analysis or categorisation can be determined. Figure 10.9 provides a generalised summary of predicting a soil's manganese-oxidising potential when looking at the inherent manganese oxide concentration of soils and their manganese-adsorption capacities.

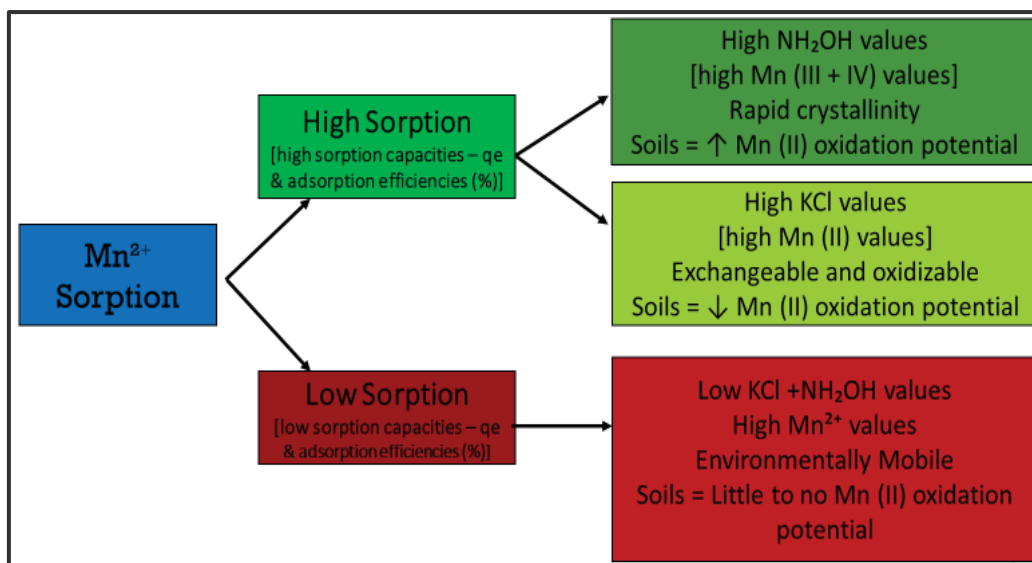


Figure 10.9: A simplified breakdown of how measuring adsorption and the oxidisable and reducible fraction of manganese can be used to determine a soil's manganese oxidising potential

The following two calculations are used to determine the manganese-oxidising potential percentage and the manganese-adsorption efficiency percentage.

$$MOP (\%) = \frac{(NH_2OH \text{ extractable Mn} - KCl \text{ extractable Mn})}{Total Mn} * 100$$

$$\% Mn \text{ adsorption efficiency} = \frac{(C_o - C_e)}{C_o} * 100$$

When comparing the two calculations, the accuracy and applicability of using solely the manganese adsorption coefficient is questioned. Only looking at how much Mn<sup>2+</sup> is removed from the solution system does not report on the speciation and availability of manganese after adsorption and oxidation. If all the added Mn<sup>2+</sup> ions are adsorbed, the manganese adsorption coefficient would be 100%. If the speciation of the adsorbed and oxidised Mn<sup>2+</sup> ions is analysed, there will be a higher fraction of oxidisable Mn(II) than reducible Mn(III +IV), for example, providing an MOP value a lot smaller than that first determined by the manganese adsorption coefficient.

Table 10.10: Manganese adsorption efficiency percentage and manganese oxidising potential percentage for the four soils under three different oxidising regimes

Soil type	20-days oxidation		40-days oxidation		15-days oxidising and 25-days reducing	
	Manganese adsorption (%)	MOP (%)	Manganese adsorption (%)	MOP (%)	Manganese adsorption (%)	MOP (%)
Sand	23.9	37.4	53.8	36.9	25.4	11.28
Andesitic-derived soil	99.9	98.1	99.9	99.1	99.8	82.5
Manganese oxide-coated sand	94.3	99.9	98.9	99.9	96.6	99.9
Dolomitic-derived soil	99.9	99.8	99.9	99.8	99.8	99.7

For soils with a higher inherent manganese oxide content, there is not much difference between the adsorption efficiency values and the MOP. For soils with little to no inherent manganese oxide content, the MOP would be a more accurate calculation and determination of the manganese oxidation. The MOP considers the chemical speciation of manganese, and not merely what is adsorbed from solution. This provides important information as to the reactivity and mobility of manganese in the soil.

When looking at the factors that affect the MOP of soils, this chapter focuses on two aspects, the inherent manganese oxide content and the redox potential of the system. Relating the MOP percentage of the soil to the change in the system's Eh can provide possible insight into the influence the system's Eh would have on the soils' MOP. This relationship can be seen in Figure 10.10.

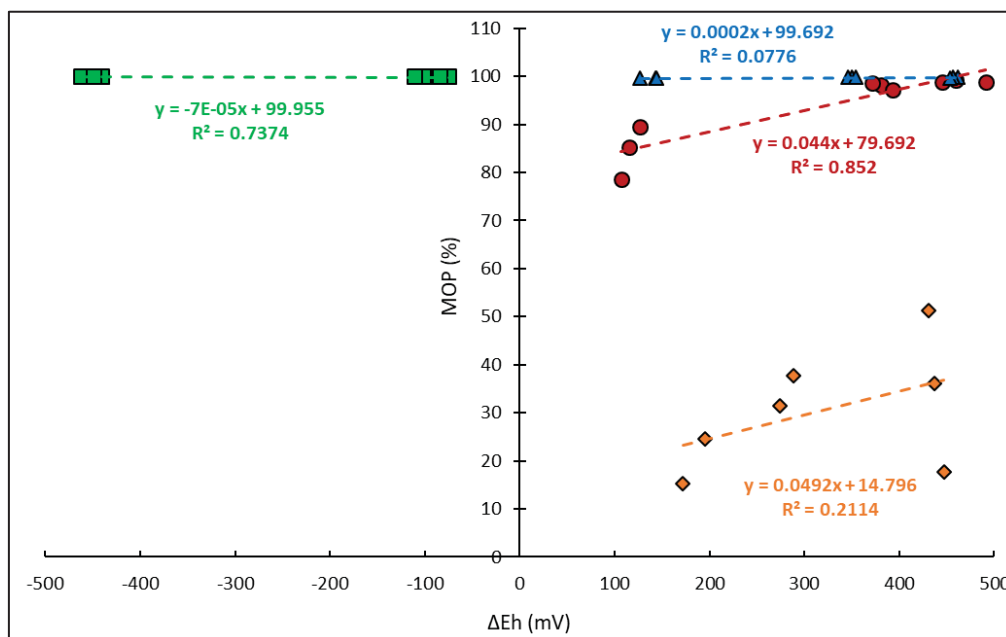


Figure 10.10: The MOP percentage of the soils in correlation with the change in Eh (mV) of the different soil systems over the period of the batch sorption experiment

Sand has a lower coefficient of determination due to some outliers being a bit high and a bit low, and shows a positive linear regression relationship between MOP and  $\Delta Eh$ . As the system's Eh increased, the MOP percentage of the sand also increased. Sand's MOP is, therefore, controlled by a combination of the soil's inherent manganese oxide concentration, and the Eh conditions of the system. As sand has a low inherent manganese oxide content, the system's Eh is possibly more influential when it comes to the adsorption, oxidation and precipitation of  $Mn^{2+}$  to  $Mn(III + IV)$ .

Manganese oxide-coated sand does not show a great difference in MOP for the great changes in Eh experienced by the soil-solution system. A big decrease in the system's Eh barely affected the soil's MOP. This means that the oxidising potential of the manganese oxide-coated sand is mainly controlled by the inherent manganese oxide content and, to a much lesser extent, the system's Eh. This soil has a high inherent manganese oxide content. This shows that  $Mn^{2+}$  oxidation is mainly controlled by surface oxidation processes.

The dolomitic-derived soil had a similar result, as seen by the manganese oxide-coated sand. A change in the system's Eh had very small effect on the dolomite-derived soils' MOP. With an extremely low coefficient of determination, no strong correlation can be determined between Eh and MOP. As with manganese oxide-coated sand, the dolomitic-derived soil has a high inherent manganese oxide content, and surface oxidation processes mainly control the MOP of this system.

It is also noted that the system's rate of oxidation was not examined in this experiment. The relationship between the rate of  $Mn^{2+}$  oxidation and the system's change in Eh is an aspect to examine in further work. Over longer periods of contact time and aeration periods, the effect of Eh alone on the  $Mn^{2+}$  oxidation is not solely a factor that affects MOP.

The andesitic-derived soil had the strongest correlation between MOP and change in the system's Eh. With an increase in the system's Eh showing an increase in MOP between 10 and 15%, the MOP and Eh of the andesitic-derived soil system can be seen to be greatly affected by these two factors.

Knowing the soil type, its inherent manganese oxide content and the Eh fluctuations in the soil profile can provide invaluable information to users looking to irrigate with manganese-rich water. Knowing the soil's potential to oxidise  $Mn^{2+}$  can help determine the fitness for use of water, and accurately project any environmental risks or concerns associated with irrigation practices.

#### 10.4 CONCLUSION

Four selected soils with varying inherent manganese concentrations were exposed to a manganese loading of 200 mg Mn(II)/kg in a batch sorption experiment with differing oxidation conditions. The purpose of this experiment was to determine how effectively these soils adsorb and oxidise the added  $Mn^{2+}$ , and how fractions of the adsorbed  $Mn^{2+}$  have speciated into easily oxidisable Mn(II) and easily reducible Mn(III + IV). Using such determinations of adsorption and manganese speciation, a better understanding can be established of how well soils are able to oxidise manganese, and how feasible it is to consider irrigating specific soils with large amounts of  $Mn^{2+}$  without expecting to negatively affect soils and subsequently ecosystems.

The order of the adsorption capacities of the selected soils was found to be dolomite-derived soil > manganese-coated sand > andesitic-derived soil > sand. This is fairly consistent with what was predicted in the hypotheses, that soils with higher inherent manganese content would adsorb and oxidise higher concentrations of  $Mn^{2+}$  from solution.

The data of the adsorption of Mn(II) by all four soils cannot be effectively expressed with the Langmuir- and Freundlich-type adsorption isotherms. The linearisation of these models did not sufficiently describe the Mn(II) adsorption process and the experimental data either. Other more accurate adsorption models can be used to determine the adsorption parameters for such manganese batch sorption studies.

A batch sorption experiment can provide abundant contact time for the system to reach equilibrium, and for the system to adsorb and oxidise the maximum amount of  $Mn^{2+}$  possible. Quantifying the MOP of soil is possible by looking at the speciation of the adsorbed and oxidised manganese species. The dolomitic-derived soil and the manganese oxide-coated sand were the soils with the highest inherent manganese oxide content. These soils were the most effective in adsorbing and oxidising  $Mn^{2+}$  from solution under oxidising conditions. These soils had the lowest exchangeable and oxidisable Mn(II) content, and were therefore classified as the soils with the highest manganese-oxidising potential in this experiment.

Soils with a high electron-accepting ability can ideally oxidise larger quantities of  $Mn^{2+}$  ions if they were to be irrigated with manganese-rich mine waters. This study concludes that current manganese concentrations in the Irrigation Water Quality Guidelines should take the MOP of soils to be irrigated into account.

## 10.5 REFERENCES

- AGUIAR A, XAVIER G and LADEIRA A (2010) The use of limestone, lime and MnO<sub>2</sub> in the removal of soluble manganese from acid mine drainage. *Water Pollution* **135** 267–276.
- AGUIAR AO, DUARTE RA and LADEIRA ACQ (2013) The application of MnO<sub>2</sub> in the removal of manganese from acid mine water. *Water, Air, and Soil Pollution* **224** 1690–1698.
- AKPOMIE KG, DAWODU FA and ADEBOWALE KO (2015) Mechanism on the sorption of heavy metals from binary-solution by a low cost montmorillonite and its desorption potential. *Alexandria Engineering Journal* **54** 757–767.
- ALBY D, CHARNY C, HERAN M, PRELOT B and ZAJAC J (2018) Recent developments in nanostructured inorganic materials for sorption of cesium and strontium: Synthesis and shaping, sorption capacity, mechanisms, and selectivity – a review. *Journal of Hazardous Material* **344** 511–530.
- ANNANDALE JG, JOVANOVIC NZ, HODGSON FDI, USHER BH, AKEN ME, VAN DER WESTHUIZEN AM, BRISTOW KL and STEYN JM (2006) Prediction of the environmental impact and sustainability of large-scale irrigation with gypsiferous mine-water on groundwater resources. *Water SA* **32** 21–28.
- BAIZE D (2009) Cadmium in soils and cereal grains after sewage-sludge application on French soils: A review. In: *Sustainable agriculture, Vol. 1*, LICHTFOUSE E, NAVARRETE M, DEBAEKE P, SOUCERE V and ALBEROLA C, Springer Science and Business Media, NY, USA, 847.
- BAMFORTH SM, MANNING DAC, SINGLETON I, YOUNGER PL and JOHNSON KL (2006) Manganese removal from mine waters – investigating the occurrence and importance of manganese carbonates. *Applied Geochemistry* **21** 1274–1287.
- BARTLETT RJ (1988) Manganese redox reactions and organic interactions in soils. In: *Manganese in soils and plants*, GRAHAM RD, HANNAM RJ and UREN NC, Kluwer Academic Publishers, The Netherlands, 59–73.
- BOURG ACM and LOCH JPG (1995) Mobilization of heavy metals as affected by pH and redox conditions. In: *Biogeochemistry of pollutants in soils and sediments*, 1<sup>st</sup> ed., SALOMONS W and STIGLIANI WM, Environmental Science, Springer, Berlin, Germany, 87–102.
- BOUYOUCOS GJ (1962) Hydrometer method improved for making particle size analysis of soils. *Agronomy Journal* **54** 464–465.
- BRUINS JH, PETRUSEVSKI B, SLOKAR YM, KRUIHOF JC and KENNEDY MD (2014) Manganese removal from groundwater: Characterisation of filter media coating. *Desalination and Water Treatment* **55** 1851–1863.
- CHAUDHRY SA, KHAN TA and ALI I (2016) Adsorptive removal of Pb(II) and Zn(II) from water onto manganese oxide-coated sand: Isotherm, thermodynamic and kinetic studies. *Egyptian Journal of Basic and Applied Sciences* **3** 287–300.
- CHEN X (2015) Modeling of experimental adsorption isotherm data. *Information* **6** 14–22.
- CHEN BR, SUN W, KITCHAV DA, MANGUM JS, THAMPY V, GARTEN LM, GINLEY DS, GORMAN BP, STONE KH, CEDER G, TONEY MF and SCHELHAS LT (2018) Understanding

- crystallization pathways leading to manganese oxide polymorph formation. *Nature Communications* **9** 2553–2562.
- CURKO J, MATOSIC M, CRNEK V, STULIC V and MIJATOVIC I (2016) Adsorption characteristics of different adsorbents and iron(III) salt for removing As(V) from water. *Food Technology and Biotechnology* **54** 250–255.
- DATTA S, TAGHVAEIAN S and STIVERS J (2017) *Understanding soil water content and thresholds for irrigation management*. Technical Report No. BAE-1537, Oklahoma Cooperative Extension Service, OK, USA.
- DELAUNE RD and REDDY KR (2005) Redox potential. *Encyclopedia of soil in the environment. In: Reference module in earth systems and environmental sciences*, 366–371.
- DEPARTMENT OF WATER AFFAIRS AND FORESTRY (DWAF) (1996) *South African irrigation water quality guidelines, Vol. 4: Agricultural use: Irrigation*, 2<sup>nd</sup> ed., DWAF, Pretoria, South Africa.
- DESTA MB (2013) Batch sorption experiments: Langmuir and freundlich isotherm studies for the adsorption of textile metal ions onto teff straw (*Eragrostis tef*) agricultural waste. *Journal of Thermodynamics* 1–6.
- DIEM D and STUMM W (1984) Is dissolved Mn<sup>2+</sup> being oxidised by O<sub>2</sub> in absence of Mn-bacteria or surface catalysts? *Geochimica et Cosmochimica Acta* **48** 1571–1573.
- DORAU K and MANSFELDT T (2015) Manganese-oxide-coated redox bars as an indicator of reducing conditions in soils. *Journal of Environmental Quality* **44** 696–703.
- EL-SHERIF IY, FATHY NA and HANNA AA (2013) Removal of Mn (II) and Fe (II) ions from aqueous solution using precipitation and adsorption methods. *Journal of Applied Sciences Research* **9** 233–239.
- ELZINGA EJ (2011) Reductive transformation of birnessite by aqueous Mn(II). *Environmental Science and Technology* **45** 6366–6372
- ERIKSSON PG, ALTERM ANN W and HARTZER FJ (2006) The Transvaal supergroup and its precursors. In: *The geology of South Africa*, JOHNSON MR, ANHAEUSSER CR and THOMAS RJ, Geological Society of South Africa, Council for Geoscience, Pretoria, South Africa, 237–260.
- FERTILIZER SOCIETY OF SOUTH AFRICA (FSSA) (1974) *Manual of soil analysis methods*. FSSA Publication No. 37.
- FRANSWORTH CE, VOEGELIN A and HERING JG (2012) Manganese oxidation induced by water table fluctuations in a sand column. *Environmental Science and Technology* **46** 277–284.
- FREUNDLICJ H (1922) *Kapillarchemie*. Akademische Verlagsgesellschaft.
- FUKUSHI K (2018) Modelling sorption processes of trace elements by earth surface materials. *Journal of Geography-Chigaku Zasshi* **126** 325–341.
- GAMBRELL RP (1996) Manganese. In: *Methods of soil analysis. Part 3: Chemical methods*, SPARKS DL, PAGE AL, HELMKE PA, LOEPPERT RH, SOLTANPOUR PN, TOBATABAI MA, JOHNSTON CT and SUMMER MA, Soil Science Society of America, Madison, USA, 678.

- GILKES RJ and MCKENZIE RM (1988) Geochemistry and mineralogy of manganese in soils. In: *Manganese in soils and plants*, GRAHAM RD, HANNAM RJ and UREN NC, Kluwer Academic Publishers, Dordrecht, The Netherlands, pp 23–95.
- GOLDANI E, MORO CC and MAIA SM (2013) A study employing different clays for Fe and Mn removal in the treatment of acid mine drainage. *Water, Air and Soil Pollution* **224** 1401–1404.
- GOTOH S and PATRICK JR (1972) Transformations of manganese in a waterlogged soil as affected by redox potential and pH. *Soil Science Society of America Journal* **36** 738–742.
- HERON G, TJELL JC and CHRISTENSEN TH (1994) Redox buffering capacity of aquifer sediment. *Environmental Science and Technology* **28** 153–158.
- HOSSAIN MA, NGO HH and GUO W (2013) Introductory of microsoft excel SOLVER function – spreadsheet method for isotherm and kinetics modelling of metals biosorption in water and wastewater. *Journal of Water Sustainability* **3** 223–237.
- HUGHES NP and WILLIAMS RJP (1988) An introduction to manganese biological chemistry. In: *Manganese in soils and plants*, GRAHAM RD, HANNAM RJ and UREN NC, Kluwer Academic Publishers, Dordrecht, The Netherlands, 7–20.
- IGWE JC and ABIA AA (2007) Equilibrium sorption isotherm studies of Cd(II), Pb(II) and Zn(II) ions detoxification from waste water using unmodified and EDTA-modified maize husk. *Electronic Journal of Biotechnology* **10** 33–42.
- JEZ-WALKOWIAK J, DYMACZEWSKI Z, SZUSTER-JANIACZYK A, NOWICKA AB and SCYBOWICS M (2017) Efficiency of Mn removal of different filtration materials for groundwater treatment linking chemical and physical properties. *Water* **9** 498–510.
- JOSHUA PA, SUNDAY EB, OLASEKAN AA, JONATHAN AA, OLADAPO OM and BW TOMORI (2019) Dithionite and oxalate extractable iron and aluminium oxides amount in soils of Ekiti State, Nigeria. *Applied Science Reports* **24** 5–14.
- JUANG RS, WU FC and TSENG RL (1997) The ability of activated clay for the adsorption of dyes from aqueous solutions. *Environmental Technology* **18** 525–531.
- JUNTA JL and HOHELLA MF (1994) Manganese (II) oxidation at mineral surfaces: a microscopic and spectroscopic study. *Geochimica et Cosmochimica Acta* **58** 4985–4999.
- KIM JG, DIXON JB, CHUSUEI CC and DENG Y (2002) Oxidation of chromium(III) to (VI) by manganese oxides. *Soil Science Society of America Journal* **66** 306–315
- KOCAOBA S (2009) Adsorption of Cd(II), Cr(III) and Mn(II) on natural sepiolite. *Desalination* **244** 24–30.
- LAN S, WANG X, XIANG Q, YIN H, TAN W, QIU G, LIU F, ZHANG J and FENG X (2017) Mechanisms of Mn(II) catalytic oxidation on ferrihydrite surfaces and the formation of manganese (oxyhydr)oxides. *Geochimica et Cosmochimica Acta* **211** 79–96.
- LANGMUIR I (1918) The absorption of gases on plane surface of glass, mica and platinum. *Journal of the American Chemical Society* **40** 1361–1403.
- LEFKOWITZ JP, ROUFF AA and ELZINGA EJ (2013) Influence of pH on the reductive transformation of birnessite by aqueous Mn(II). *Environmental Science and Technology* **47** 10364–10371.

- LOVETT RJ (1997). Removal of manganese from acid mine drainage. *Journal of Environmental Quality* **26** 1017–1024.
- MCKENZIE RM (1972) The manganese oxides in soils – a review. *Z. Pflanzenerahr. Bodenk* **131** 221–242.
- METZ PC (2017) *Total scattering analysis of disordered nanosheet materials*. PhD thesis, Alfred University, New York, NY, USA.
- MOGHADDAM HK and PAKIZEH M (2015) Experimental study on mercury ions removal from aqueous solution by MnO<sub>2</sub>/CNTs nanocomposite adsorbent. *Journal of Industrial Engineering* **21** 221–229.
- MORGAN JJ (2005) Kinetics of reaction between O<sub>2</sub> and Mn(II) species in aqueous solutions. *Geochimica et Cosmochimica Acta* **69** 35–48.
- MORGAN JJ and STUMM W (1964) Colloid-chemical properties of manganese dioxide. *Journal of Colloid Science* **19** 347–359.
- NEGRAC C, ROSS DS and LANZIROTTI A (2005) Oxidising behaviour of soil manganese: Interactions among abundance, oxidation state, and pH. *Soil Science Society of America Journal* **69** 87–95.
- OBES AM (2000) *The structure, stratigraphy and sedimentology of the Blackreef – Malmani – Rooihogte succession of the Transvaal supergroup southwest of Pretoria*. Bulletin No. 127, Council for Geoscience, Pretoria, South Africa.
- OTTOW JCG (2011) *Microbiology of soils*, Springer, Heidelberg, Germany.
- PHILLIPS DH, AMMONS JT, LEE SY and LIETZKE DA (1998) Deep weathering of calcareous sedimentary rock and the redistribution of iron and manganese in soils and saprolite. *Soil Science* **163** 71–81.
- POST JE (1999) Manganese oxide minerals: Crystal structures and economic and environmental significance. *Proceedings of the National Academy of Science* **96** 3447–3454.
- REDDY KR and DELAUNE RD (2008) *Biogeochemistry of wetlands: Science and applications*, CRC Press, Boca Raton, FL, USA.
- RELIC D, DORDEVIC D, POPOVIC A and BLAGOJEVIC T (2005) Speciation of trace metals in the Danube alluvial sediments within an oil refinery. *Environmental International* **31** 661–669.
- RODDA N, CARDEN K, ARMITAGE N and DU PLEISIS HM (2011) Development of guidance for sustainable irrigation use of greywater in gardens and small-scale agriculture in South Africa. *Water SA* **37** 727–737.
- PIISPANEN JK and SALLANKO JT (2010) Mn(II) removal from groundwater with manganese oxide-coated filter media. *Journal of Environmental Science and Health* **45** 1732–1740.
- SAHADI DM, TAKEDA M, SUZUKI I and KOIZUMI J (2009) Removal of Mn<sup>2+</sup> from water by “aged” biofilter media: The role of catalytic oxides layers. *Journal of Bioscience and Bioengineering* **107** 151–157.

- SHANG C and ZELAZNY LW (2008) Selective dissolution techniques for mineral analysis of soils and sediments. In: *Methods of soil analysis. Part 5: Mineralogical methods*, ULERY AL and DREES, LR, Soil Science Society of America, Madison, WI, USA.
- SOMERA RD (1967) Iron and manganese distribution and seasonal oxidation changes in soils of the Willamette drainage sequence. Masters Thesis, Oregon State University.
- SPARKS DL (2003) *Environmental soil chemistry*, 2<sup>nd</sup> ed., Academic Press, CA, USA.
- SPARKS DL (1998) *Soil physical chemistry*, 2<sup>nd</sup> ed., CRC Press, Boca Raton, FL, USA.
- SPOSITO G (1994) *Chemical equilibria and kinetics in soils*, Oxford University Press, New York, NY, USA.
- SUNG W and MORGAN JJ (1981) Oxidative removal of Mn(II) from solution catalysed by the  $\gamma$ -FeOOH (lepidocrocite) surface. *Geochim. Geochimica et Cosmochimica Acta* **45** 2377–2383.
- SUN X, DONER HE and ZAVARIN M (1999) Spectroscopy study of arsenite [As(III)] oxidation on Mn-substituted goethite. *Clays Clay Minerals* **47** 474v480.
- SUN W, KITCHEAV DA, KRAMER D and CEDER G (2019) Non-equilibrium crystallization pathways of manganese oxides in aqueous solution. *Nature Communications* **10** 573–582.
- THOMPSON G, SWAIN J, KAY M and FORSTER CF (2001) The treatment of pulp and paper mill effluent: A review. *Bioresources Technology* **77** 275–286.
- THORNTON FC (1995) Manganese removal from water using limestone-filled tanks. *Ecological Engineering* **4** 11–18.
- TONKIN JW, BALISTRERI LS and MURRAY JW (2004) Modeling sorption of divalent metal cations on hydrous manganese oxide using the diffuse double layer model. *Applied Geochemistry* **19** 29–53.
- VAN HUYYSSTEEN CW (2008) A review of advances in hydrogeology for application in South Africa. *South African Journal of Plant and Soil* **125** 245–254.
- VON DE KAMMER, THÖMING J and FÖRSTNER U (2000) Redox buffer capacity concept as a tool for the assessment of long-term effects in natural attenuation/intrinsic remediation. In: *Redox: fundamentals, processes and applications*, SCHÜRING J, SCHULTZ HD, FISCHER WR, BÖTTCHER J and DUIJNISVELD WHM, Springer-Verlag, Berlin, Germany, 189–202.
- WANG Z, LEE SW, CATALANO JG, LEZAMA-PACHECO JS, BARGAR JR, TEBO BM and GIAMMAR DE (2012) Adsorption of uranium(VI) to manganese oxides: X-ray absorption spectroscopy and surface complexation modeling. *Environmental Science and Technology* **47** 850–858.
- WANG X, LAN S, ZHU M, GINDER-VOGEL M, YIN H, LIU F, TAN W and FENG X (2015) The presence of ferrihydrite promotes abiotic Mn(II) oxidation and formation of birnessite. *Soil Science Society of America Journal* **79** 1297–1305.
- YOUNGER PL, BANWART SA and HEDIN RS (2002) *Mine water: Hydrology, pollution, remediation*. Kluwer, Amsterdam, The Netherlands.
- ZELAZNY LW, LIMINGM HE and VANWORMHOUDT AN (1996) Charge analysis of soils and anion exchange. In: *Methods of soil analysis. Part 3: Chemical methods*, SPARKS DL, PAGE AL, HELMKE PA, LOEPPERT RH, SOLTANPOUR PN, TOBATABAI MA, JOHNSTON CT and SUMMER MA, Soil Science Society of America, Madison, WI, USA.

# CHAPTER 11: ECONOMIC FEASIBILITY AND ANALYSIS OF MINE WATER-IRRIGATED CROPPING SYSTEMS

---

H Oosthuizen, GR Backeberg, JG Annandale, PD Tanner, M Aken, HM du Plessis and SN Heuer

## 11.1 INTRODUCTION

There is much interest in the use of mine-affected water for irrigation, especially if these saline waters are gypsiferous (dominated by calcium and sulphate). Extensive research has been done on the agronomic productivity of mine water-irrigated crops and the effects such waters have on soil and water resources. Questions are now being asked about the economic feasibility of this practice, especially considering that alternative approaches to managing mine-impacted waters are normally very expensive, especially when considering the large volumes of waters that need to be managed.

SAPWAT4 was used to determine typical crop irrigation requirements in the Mpumalanga Highveld. The calculation of crop irrigation requirements was based on climate data from Quaternary B11F, assuming a loam soil under centre pivot irrigation. This quaternary falls in a summer rainfall area and the climate is described as warm temperate, warm summer. Irrigation water availability assumed that the mine generated an average of 10 Mℓ per day. Provision was made for a small buffer storage dam of 40 Mℓ, the equivalent of four days' water supply to assist with short-term water management. For the purpose of this study, no other storage costs were assumed, but if the mine had to pump at a constant rate, additional storage would need to be built if on-site storage in mine voids was not possible. The assumption was also made that the farmer rents the land at R750/ha per annum.

Two scenarios were modelled to utilise a water supply of 10 Mℓ per day:

- Scenario 1: Maize mono-cropping (1,400 ha) (summer crop)
- Scenario 2: Maize (450 ha) and soybean (225 ha) (summer rotation) and oats (675 ha) as a winter crop (double-cropping) for high-density grazing for weaner backgrounding

The Mine-Fin model was developed for this project as a user-friendly financial assessment model that integrates the following:

- Whole-farm planning (20-year period)
- Financial analysis
- Comparison of different scenarios

The modelling framework consists of six modules:

- Enterprise crop budgets
- Projected capital budget
- Whole-farm cash flow projection over a 20-year period
- Income statement projection
- Projected balance sheet
- Economic and financial analysis

## 11.2 COMPARATIVE ECONOMIC VIABILITY SCENARIOS

In order to determine economic viability and financial feasibility, the model provides for the following set of criteria: internal rate of return (IRR), net present value (NPV), cash flow ratio, debt ratio and highest debt.

Table 11.1 displays comparative indicators for the two scenarios. Production assumptions include hectares cultivated, crop yield expectations and stocking rate per ha on irrigated oats. Higher crop yields are expected for Scenario 2 due to the benefits of a crop rotation system compared to the monocrop system of Scenario 1.

Scenario 2 has a lower capital investment due to the much smaller area cultivated per season. However, with a double-cropping system (summer and winter crop), hectares cultivated annually are more or less the same for the two scenarios, resulting in a much lower capital investment per hectare cultivated (R33,218 for Scenario 2 as opposed to R53,308 for Scenario 1). Although Scenario 2 cultivates less than half the area of Scenario 1, its production income is much higher due to the high gross turnover realised from weaners on the high-density grazing system of irrigated oat pastures during winter months. The higher production cost ratio (82% for Scenario 2 compared to 51% for Scenario 1), however, results in a lower rate of return on capital invested.

The 20-year average cash flow ratio (155%) for Scenario 1 illustrates solid repayment capacity (norm:  $\geq 115\%$ ). The highest debt ratio (94%) is above the norm of 50%, which means that the farming operation will not be financially feasible without subsidisation or own capital contribution. The debt ratio decreases substantially over time. The maximum loan amount, including working capital, and without any own capital contribution or subsidies, amounts to R107 million. Scenario 1 has an IRR of 27.2% and an NPV of R38.1 million. The NPV/m<sup>3</sup> was calculated at R10,48 m<sup>-3</sup>.

The 20-year average cash flow ratio (113%) for Scenario 2 is marginally below the norm of  $\geq 115\%$ , but still illustrates repayment capacity. The highest debt ratio (106% in Year 2) exceeds 100%, which means that the operation is technically insolvent during the first two years of operation. From Year 5 onwards, the debt ratio is within acceptable financing norms, i.e. under 50%. It is clear that the operation will not be bankable from a commercial point of view without own capital contribution or subsidy. The maximum loan amount, including working capital, amounts to R103 million. Scenario 2 has an IRR of 21.7% and an NPV of R16.6 million. The NPV/m<sup>3</sup> was calculated at R4,55 m<sup>-3</sup>.

Table 11.1: Comparative indicators for Scenario 1 (monocrop) and Scenario 2 (crop rotation)

Production assumptions		Scenario 1	Scenario 2
Total ha cultivated - seasonal crop		1 400	675
Total ha cultivated annually		1 400	1 350
Crop yield	Maize yr 1 (t/ha)	12.48	13.02
	Maize yr 3 (t/ha)	13.00	13.51
	Maize yr 5 (t/ha)	13.00	14.00
	Maize yr 7 (t/ha)	13.00	14.00
	Soybeans yr 1 (t/ha)		3.60
	Soybeans yr 3 (t/ha)		4.05
	Soybeans yr 5 (t/ha)		4.50
	Soybeans yr 7 (t/ha)		4.50
Stocking rate	(weaners / ha oats)		8.00
Financial indicators		Scenario 1	Scenario 2
Capital investment *		74 631 000	44 844 000
Capital investment per ha cultivated		53 308	33 218
Production income	Yr 1	48 048 000	64 858 050
	Yr 5	50 050 000	67 144 050
Direct and non-allocated costs	Yr 1	25 278 337	54 691 253
	Yr 5	25 278 337	54 691 253
20-yr avg prod cost ratio		51%	82%
20-yr avg cash flow ratio		155%	113%
Highest debt ratio		94%	106%
Debt ratio	Yr 3	62%	98%
	Yr 6	8%	25%
	Yr 10	5%	6%
Bank balance	Yr 3	-29 391 151	-30 598 844
	Yr 6	30 975 560	-2 926 547
	Yr 10	116 058 457	38 275 168
Maximum loan amount (end of year)		61 816 359	42 023 397
Maximum loan amount including working capital		107 884 025	103 019 302
Breakeven		Yr 3	Yr 7
Net Present Value (NPV)		38 147 917	16 600 092
Internal Rate of Return (IRR)		27.2%	21.7%
Irrigation water requirement (m3)		3 640 000	3 593 250
<b>NPV per m3</b>		<b>R 10.48</b>	<b>R 4.55</b>

\* Initial investment - vehicles, equipment and machinery - no land

Table 11.2 displays the sensitivity and modelling results of the different scenarios. Scenarios are defined as follows:

- **Scenario 1:** Irrigated maize – monocrop production system (1,400 ha): base case irrigation water salinity (EC of 150 mS/m)
- **Scenario 1a:** Same as Scenario 1, but with 50% own capital contribution
- **Scenario 1b:** Same as Scenario 1, but EC 350 mS/m yield levels apply
- **Scenario 1c:** Same as Scenario 1, but EC 650 mS/m yield levels apply
- **Scenario 2:** A 450 ha short season maize, and 225 ha soybeans (summer crop rotation) and 675 ha oats as a winter crop for grazing with beef weaners (double-cropping): base case EC 150 mS/m

- **Scenario 2a:** Same as Scenario 2, but with 50% own capital contribution
- **Scenario 2b:** Same as Scenario 2, but with 70% own capital contribution
- **Scenario 2c:** Same as Scenario 2, but EC 350 mS/m yield levels apply
- **Scenario 2d:** Same as Scenario 2, but EC 650 mS/m yield levels apply

The 50% own capital contribution (i.e. 50% of capital investment) has a positive impact on highest debt ratio, as well as loan amount required. Both scenarios 1 and 2 will not be commercially viable without own capital contribution or subsidisation. A 50% own capital contribution (R37.315 million) for Scenario 1 is required to get the annual financial indicators within acceptable financing norms. Without any own contribution, a loan of R108 million in Year 1 will be required to start the operation (including operational expenditure). With the 50% own contribution (R37.315 million), the required loan amount decreases to R67.3 million.

For Scenario 2, a 70% own capital contribution (R31.390 million) is sufficient to get the project within acceptable financing norms measured annually. Without any own contribution, the project will require a loan of R103 million to finance capital and operational expenditure. With the 70% own contribution (R31.390 million), the required loan amount decreases to R69 million.

The negative impact of increasing EC levels on yield and profitability is clearly illustrated in the declining NPV, IRR and NPV/m<sup>3</sup>.

Large-scale crop production maximises economies of scale, but is not that efficient at creating jobs. Settling several emerging commercial farmers on such a scheme would be beneficial from a social perspective (increased job creation and improved livelihoods of more people compared to the large commercial farm option). However, economies of scale would be lost, making such farming activities less resilient and riskier, and government or industry support would be required to get these producers on their feet. It may be ideal if this could be done with existing farmer support programmes.

All scenarios modelled, including those with EC 650 mS/m levels, demonstrate positive financial returns. Scenario 2d (EC 650 mS/m) shows the lowest NPV per m<sup>3</sup>, i.e. R2,22 NPV per m<sup>3</sup> irrigation water applied. This is, however, still a positive return on investment compared to the expected cost of around R26/m<sup>3</sup> for alternative mine water treatment.

Table 11.2: Sensitivity analysis

		Scenario 1				Scenario 2				
		Base case EC150 mS/m	50% own contr	Base case EC350 mS/m	Base case EC650 mS/m	Base case EC150 mS/m	50% own contr	70% own contr	Base case EC350 mS/m	Base case EC650 mS/m
		Scenario 1	Scenario 1a	Scenario 1b	Scenario 1c	Scenario 2	Scenario 2a	Scenario 2b	Scenario 2c	Scenario 2d
<b>Production assumptions</b>										
Total ha cultivated - seasonal crop		1 400	1 400	1 400	1 400	675	675	675	675	675
Total ha cultivated annually		1 400	1 400	1 400	1 400	1 350	1 350	1 350	1 350	1 350
Crop yield	Maize yr 1 (t/ha)	12.48	12.48	12.30	10.13	13.02	13.02	13.02	13.02	10.91
	Maize yr 3 (t/ha)	13.00	13.00	12.30	10.13	13.51	13.51	13.51	13.24	10.91
	Maize yr 5 (t/ha)	13.00	13.00	12.30	10.13	14.00	14.00	14.00	13.24	10.91
	Maize yr 7 (t/ha)	13.00	13.00	12.30	10.13	14.00	14.00	14.00	13.24	10.91
	Soybeans yr 1 (t/ha)					3.60	3.60	3.60	3.60	3.60
	Soybeans yr 3 (t/ha)					4.05	4.05	4.05	4.05	4.05
	Soybeans yr 5 (t/ha)					4.50	4.50	4.50	4.50	4.46
	Soybeans yr 7 (t/ha)					4.50	4.50	4.50	4.50	4.46
Stocking rate	(weaners / ha oats)					8.00	8.00	8.00	8.00	8.00
<b>Financial indicators</b>										
Capital investment *		74 631 000	74 631 000	74 631 000	74 631 000	44 844 000	44 844 000	44 844 000	44 844 000	44 844 000
Capital investment per ha cultivated		53 308	53 308	53 308	53 308	33 218	33 218	33 218	33 218	33 218
Production income	Yr 1	48 048 000	48 048 000	47 347 300	38 988 950	64 858 050	64 858 050	64 858 050	64 858 050	62 241 975
	Yr 5	50 050 000	50 050 000	47 347 300	38 988 950	67 144 050	67 144 050	67 144 050	66 208 500	63 266 929
Direct and non-allocated costs	Yr 1	25 278 337	25 278 337	25 278 337	25 278 337	54 691 253	54 691 253	54 691 253	54 691 253	54 691 253
	Yr 5	25 278 337	25 278 337	25 278 337	25 278 337	54 691 253	54 691 253	54 691 253	54 691 253	54 691 253
20-yr avg prod cost ratio		51%	51%	53%	65%	82%	82%	82%	83%	87%
20-yr avg cash flow ratio		155%	158%	150%	128%	113%	114%	115%	111%	107%
Highest debt ratio		94%	49%	94%	111%	106%	63%	47%	106%	126%
Debt ratio	Yr 3	62%	8%	69%	110%	98%	42%	21%	98%	124%
	Yr 6	8%	5%	8%	94%	25%	6%	5%	36%	119%
	Yr 10	5%	4%	5%	10%	6%	4%	4%	6%	14%
Bank balance	Yr 3	-29 391 151	7 096 240	-33 607 354	-59 392 254	-30 598 844	-12 030 886	-4 881 419	-30 964 228	-40 489 985
	Yr 6	30 975 560	69 793 393	20 058 827	-30 512 187	-2 926 547	18 466 908	26 085 047	-5 450 190	-24 377 946
	Yr 10	116 058 457	158 340 389	95 886 705	14 446 371	38 275 168	61 514 804	69 812 785	32 714 180	3 269 786
Maximum loan amount (end of year)		61 816 359	20 182 753	62 536 506	71 126 824	42 023 397	22 429 488	15 994 972	42 023 397	44 712 076
Maximum loan amount including working capital		107 884 025	67 374 669	107 884 025	107 884 025	103 019 302	103 019 302	103 019 302	103 019 302	103 019 302
Breakeven		Yr 5	Yr 3	Yr 3	Yr 9	Yr 7	Yr 5	Yr 4	Yr7	Yr10
Net Present Value (NPV)		38 147 917	44 753 002	31 632 145	10 489 892	16 600 092	23 593 029	26 342 261	14 794 057	8 111 848
Internal Rate of Return (IRR)		27.2%	40.7%	24.6%	15.0%	21.7%	36.7%	50.0%	20.8%	15.8%
Irrigation water requirement (m3)		3 640 000	3 640 000	3 640 000	3 640 000	3 593 250	3 593 250	3 593 250	3 593 250	3 593 250
<b>NPV per m3</b>		<b>R 10.48</b>	<b>R 12.29</b>	<b>R 8.69</b>	<b>R 2.88</b>	<b>R 4.55</b>	<b>R 6.46</b>	<b>R 7.22</b>	<b>R 4.05</b>	<b>R 2.22</b>

\* Initial investment - vehicles, equipment and machinery - no land

### 11.3 CONCLUSION

The objective of this study was to determine the economic viability of irrigating with poor-quality mine water. Two different scenarios were modelled: Scenario 1: Maize mono-cropping (summer crop, long grower) – 1,400 ha, and Scenario 2: Maize (450 ha) and soybean (225 ha) (rotation) and oats (675 ha) as a winter crop (double-cropping) for grazing for weaner production. DSS modelled yields for EC 150 mS/m were applied for maize, soybean and oats in the base case for each scenario.

The NPV for Scenario 1 was calculated at R38.147 million and the IRR at 27%. Both indicators demonstrate economic viability, although the highest projected debt ratio (94%) exceeded financing norms. The NPV per m<sup>3</sup> mine water was calculated at R10,48/m<sup>3</sup>. The NPV for Scenario 2 was calculated at R16.6 million and the IRR at 22%. The NPV per m<sup>3</sup> mine water was calculated at R4,55/m<sup>3</sup>. Although the NPV and IRR demonstrate economic feasibility, the highest projected debt ratio (106%) again, similar to Scenario 1, exceeded financing norms. Both these scenarios are economically viable, but will not be financially feasible without own capital contribution.

Increasing EC levels, as can be expected, led to decreased yields that have a negative impact on economic viability. However, even with very poor-quality water at an EC of 650 mS/m, a positive return on investment (R2,22 NPV per m<sup>3</sup> irrigation water applied) is realised, compared to the expected cost of around R26 per m<sup>3</sup> for alternative mine water treatment.

### 11.4 REFERENCES

- ALLEN RG, PEREIRA LS, RAES D and SMITH M (1998). *Crop evapotranspiration – guidelines for computing crop water requirements*. FAO Irrigation and Drainage Paper 56, FAO, Rome, Italy.
- DU PLESSIS M, ANNANDALE JG, BENADE N, VAN DER LAAN M, JOOSTE S, DU PREEZ CC, BARNARD J, RODDA N, DABROWSKI J, GENTHE B and NELL P (2017) *Risk based, site-specific, irrigation water quality guidelines. Vol. 1: Description of decision support system*. WRC Report No. TT 727/17, Water Research Commission, Pretoria, South Africa.
- DU PLESSIS M (2020) *Personal communication*. Department of Plant and Soil Sciences, University of Pretoria, Pretoria, South Africa.
- GITMAN LJ (2009) *Principles of managerial finance*, 12<sup>th</sup> ed., Boston Pearson Addison Wesley.
- GROVE B (2020) *Personal communication*. Department of Agricultural Economics, University of the Free State, Bloemfontein, South Africa.
- LOUW A and PIENAAR JS (2002) ABSA commercial bank agribusiness financial model. Personal discussions with the model developers.
- OOSTHUIZEN HJ (2014) *Modelling the financial vulnerability of farming systems to climate change in selected case study areas in South Africa*. PhD thesis, Stellenbosch University, Stellenbosch, South Africa.
- SCHULZE RE and HORAN MJC (2008) Soils: Hydrological attributes. In: *South African atlas of climatology and agrohydrology*, SCHULZE RE. WRC Report No. 1489/1/08, Water Research Commission, Pretoria, South Africa.
- VAN HEERDEN PS, CROSBY CT, GROVE B, BENADE N, THERON E, SCHULZE RE and TEWOLDE MH (2009) *Integrating and updating of SAPWAT and PLANWAT to create a powerful and user-friendly irrigation planning tool. Program version 1.0*. WRC Report No. TT 391/08, Water Research Commission, Pretoria, South Africa.

## CHAPTER 12: CONCLUSION

---

JG Annandale, PD Tanner and SN Heuer

### 12.1 PROJECT OVERVIEW

The expensive treatment and discharge of effluent from a mine into water resources is normal practice for most South African mines, and decanting mine water is now exacerbating South Africa's water quality challenges. The beneficial use of poor-quality mine water for irrigation has proven to be a cost-effective, alternative re-use of mine-affected water. If mines can assist in creating irrigated cropping systems that can produce food for local needs, as well as additional income, this can empower local communities and create economic opportunities.

This WRC project has demonstrated that irrigation can be responsibly used as part of an integrated poor-quality mine water treatment strategy, and the guidelines developed (TT 855/2/21) can assist key decision makers to reduce risks when considering irrigation with mine water. The long-term impact and sustainability of mine water irrigation was quantified from the 19-ha unmined land monitoring data and the modelling of this system. On a small experimental scale, the use of untreated AMD on limed soil, limed and clarified AMD, and limed AMD that still contains metal hydroxide sludge (unclarified), showed promising results on crop growth, with limited negative effect on soil properties.

Not all mine-impacted water is suitable for irrigation purposes, thus risk-based approaches and long-term monitoring are imperative for ensuring sustainable irrigation with acceptable environmental impact. All potential risk factors associated with the soil, water and crops irrigated with mine waters should be assessed to indicate monitoring requirements and identify means of setting thresholds for action when monitoring indicates that constituents of concern are outside acceptable limits. Using models such as SWB and the SAWQI-DSS, assessments on site-specific factors that influence the suitability of mine water for irrigation can be undertaken.

Irrigation with mine water over the long term can be viable, sustainable and feasible if the appropriate management practices are in place.

### 12.2 RECOMMENDATIONS

Possible future studies that may reinforce the notion that irrigation with poor-quality mine water is a feasible alternate water utilisation strategy can include the following:

- Further investigating the impacts through foliar injury or damage of selected agronomic and pasture crops irrigated with mine-affected water
- Assessing food safety guidelines through field-based trials on historically contaminated sites
- Assessing irrigation water quality guidelines and food safety guidelines for other potentially hazardous trace elements like cadmium, chromium and mercury
- Reviewing the method detection limits and the toxicity characteristic leaching procedure for assessment of high-density sludge using the South African Guidelines
- Investigating the impact of irrigating limed soil with untreated AMD on soil chemical properties and the potential of the profile to act as a neutralising reactor

### 12.3 REFERENCES

HEUER SN, ANNANDALE JG, TANNER PD and DU PLESSIS M (2021) Technical Guidelines for Irrigation with Mine-Affected Waters, WRC TT Report 855/2/21.

- ANNANDALE JG, BENADÉ, N., JOVANOVIĆ, N. Z., STEYN, J. M., & DU SAUTOY, N. . (1999). Facilitating Irrigation Scheduling by Means of the Soil-Water Balance Model. (753/1/99). Pretoria: Water Research Commission.
- CAMPBELL G and VAN EVERT F (1994) Light interception by plant canopies: Efficiency and architecture. Resource capture by crops 35-52.
- DE JAGER J (1994) Accuracy of vegetation evaporation ratio formulae for estimating final wheat yield. Water SA 20(4) 307-314.
- DU PLESSIS HM, ANNANDALE, J. G., BENADÉ, N., VAN DER LAAN, M., JOOSTE, S., DU PREEZ, C., NELL, P. (2017). Revision of the 1996 South African Water Quality Guidelines: Development of a risk-based approach using irrigation water use as a case study. (2399/1/17). Pretoria: Water Research Commission.
- DU TOIT W, FLETT B, BENSCH M, SMIT E, FOURIE H, DRINKWATER T, BATE R and DU TOIT H (1999) Production of maize in the summer rainfall area. ARC-Grain Crops Institute, pp.
- GOUDRIAAN J (1977) Crop micrometeorology: a simulation study. Doctoral dissertation, Pudoc, Wageningen.
- HILLEL D (1998) Environmental soil physics: Fundamentals, applications, and environmental considerations. Elsevier, pp.
- JOVANOVIĆ N, ANNANDALE J and MHLAULI N (1999) Field water balance and SWB parameter determination of six winter vegetable species. WATER SA-PRETORIA- 25 191-196.
- KROETSCH D and WANG C (2008) Particle size distribution. Soil sampling and methods of analysis 2 713-725.
- MITTRA B, KARMAKAR S, SWAIN D and GHOSH B (2005) Fly ash—a potential source of soil amendment and a component of integrated plant nutrient supply system. Fuel 84(11) 1447-1451.
- MONTEITH JL (1977) Climate and the efficiency of crop production in Britain. Philosophical Transactions of the Royal Society of London. B, Biological Sciences 281(980) 277-294.
- SMITH M, ALLEN R and PEREIRA L (1998) Revised FAO methodology for crop-water requirements. Paper presented at the Evapotranspiration and Irrigation Scheduling, San Antonio, Texas, USA.
- SUN Q, MCDONALD JR LM and SKOUSEN JG (Year) Effects of armoring on limestone neutralization of AMD. In: Proceedngs of the 2000 West Virginia surface mine drainage task force symposium, Morgantown, WV, Session.
- TANNER C and SINCLAIR T (1983) Efficient water use in crop production: Research or re-search? Limitations to efficient water use in crop production 1-27. Madison, Wisconsin: American Society of Agronomy, Crop Science Society of America, Soil Science Society of America.

## APPENDICES

---

### TABLE OF CONTENTS

APPENDIX A1: Mafube unmined land costing report.....	195
APPENDIX A2: Mafube unmined pivot: grain chemical analyses .....	199
APPENDIX A3: Mafube unmined pivot: average soil constituent concentrations .....	200
APPENDIX A4: Soil-water balance simulations.....	220
APPENDIX A5: Mafube rehabilitated land .....	229
APPENDIX A6: Kromdraai irrigation system design.....	231
APPENDIX A7: South African and international hazardous waste classification systems .....	237
APPENDIX A8: Limestone neutralisation results.....	242
APPENDIX A9: Soil redox monitoring.....	244

**APPENDIX A1: Mafube unmined land costing report****Fertilizer regime and budget***Table A1:1: Fertilizers applied to the field at the Mafube unmined site*

Fertilizer type	Details	N (kg/ha)	P (kg/ha)	K (kg/ha)	S (kg/ha)	Cost (R per ha)
Pre-plant broadcast	9.1.2 (38) 0.5% Zn @ 500 kg ha <sup>-1</sup>	161.3	17.9	35.8	-	R2 572,59
Planting fertilizer	3.2.1 (38) 0.5% Zn @ 200 kg ha <sup>-1</sup>	38	25.3	12.7	-	R1 343,00
Top dressing	None	-	-	-	-	R0,00
<b>Total cost for 2016/17 season</b>						<b>R3 915,59</b>
Pre-plant broadcast	9.1.2 (38) 0.5% Zn @ 500 kg ha <sup>-1</sup>	142.5	15.8	31.6	-	R2 526,00
Planting fertilizer	4.3.4 (36) 0.4% Zn + 3.9% S @ 250 kg ha <sup>-1</sup>	32.7	24.5	32.7	9.75	R1 400,00
Top dressing	Urea 46% @ 250 kg ha <sup>-1</sup>	115	-	-	-	R1 088,75
<b>Total cost for 2017/18 season</b>						<b>R5 014,75</b>
Pre-plant broadcast	9.1.2 (38) 0.5% Zn @ 500 kg ha <sup>-1</sup>	142.5	15.8	31.6	-	R2 580,00
Planting fertilizer	4.3.4 (36) 0.4% Zn + 3.9% S @ 250 kg ha <sup>-1</sup>	32.7	24.5	32.7	9.75	R1 490,00
Top dressing	Urea 46% @ 250 kg ha <sup>-1</sup>	115	-	-	-	R1 150,50
<b>Total cost for 2018/19 season</b>						<b>R5 220,50</b>
Pre-plant broadcast	9.1.2 (38) 0.5% Zn @ 500 kg ha <sup>-1</sup>	142.5	15.8	31.6	-	R2 640,00
Planting fertilizer	4.3.4 (36) 0.4% Zn + 3.9% S @ 250 kg ha <sup>-1</sup>	32.7	24.5	32.7	9.75	R1 520,00
Top dressing	Urea 46% @ 250 kg ha <sup>-1</sup>	115	-	-	-	R1 210,00
<b>Total cost for 2019/2020 season</b>						<b>R5 370,00</b>

Table A1.2: Pre-planting herbicide sprays at Mafube unmined site

Herbicide/insecticide	Quantity	Cost per hectare
Eptam Super (EPTC)	2 l ha <sup>-1</sup>	R196,00
Guardian S (840 EC)	700 ml ha <sup>-1</sup>	R62,89
Insectido (50 g L <sup>-1</sup> )	200 ml ha <sup>-1</sup>	R13,40
Allbuff	2 l per 2 000 l water	R2,90
Boron (10%)	2 l ha <sup>-1</sup>	R51,00
<b>Total cost for 2016/17 season</b>		<b>R 326,19</b>
Galago (480)	256 ml ha <sup>-1</sup>	R52,47
Guardian S (840 EC)	1.2 l ha <sup>-1</sup>	R98,40
Atrazine 500 (Atraflo)	2 l ha <sup>-1</sup>	R73,80
Lamda (5EC)	100 ml ha <sup>-1</sup>	R6,30
Correcto	100 ml ha <sup>-1</sup>	R3,40
Liquibor (10%)	2 l ha <sup>-1</sup>	R56,00
<b>Total cost for 2017/18 season</b>		<b>R 290,38</b>
Galago (480)	260 ml ha <sup>-1</sup>	R55,00
Guardian S (840 EC)	1.2 l ha <sup>-1</sup>	R104,40
Atrazine 500 (Atraflo)	2 l ha <sup>-1</sup>	R76,50
Lamda (5EC)	100 ml ha <sup>-1</sup>	R6,80
Correcto	100 ml ha <sup>-1</sup>	R3,60
Liquibor (10%)	2 l ha <sup>-1</sup>	R58,00
<b>Total cost for 2018/19 season</b>		<b>R 304,30</b>
Galago (480)	280 ml ha <sup>-1</sup>	R59,50
Guardian S (840 EC)	1.2 l ha <sup>-1</sup>	R105,00
Atrazine 500 (Atraflo)	2 l ha <sup>-1</sup>	R78,60
Lamda (5EC)	100 ml ha <sup>-1</sup>	R7,00
Correcto	100 ml ha <sup>-1</sup>	R3,80
Liquibor (10%)	2 l ha <sup>-1</sup>	R59,50
<b>Total cost for 2019/20 season</b>		<b>R 313,40</b>

Table A1:3: Post-planting herbicide sprays at Mafube unmined site

Herbicide	Quantity	Cost per hectare
Terbuzine	2.5 l ha <sup>-1</sup>	R196,00
Acetochlor (900EC)	682 ml ha <sup>-1</sup>	R62,89
Campertop (225)	800 ml ha <sup>-1</sup>	R13,40
Allbuff	2 l per 2 000 l water	R2,90
<b>Total cost for 2016/17 season</b>		<b>R 326,19</b>
Galago (480)	200 ml ha <sup>-1</sup>	R52,47
Acetochlor (900EC) no safener	682 ml ha <sup>-1</sup>	R98,40
Terbuzine/Cheetah 600	2 l ha <sup>-1</sup>	R73,80
Lamda (5EC)	100 ml ha <sup>-1</sup>	R6,30
Correcto	100 ml ha <sup>-1</sup>	R3,40
<b>Total cost for 2017/18 season</b>		<b>R 290,38</b>
Galago (480)	200 ml ha <sup>-1</sup>	R55,00
Acetochlor (900EC) no safener	690 ml ha <sup>-1</sup>	R104,40
Terbuzine/Cheetah 600	2 l ha <sup>-1</sup>	R76,50
Lamda (5EC)	120 ml ha <sup>-1</sup>	R6,80
Correcto	100 ml ha <sup>-1</sup>	R3,60
<b>Total cost for 2018/19 season</b>		<b>R 304,30</b>
Galago (480)	210 ml ha <sup>-1</sup>	R59,50
Acetochlor (900EC) no safener	690 ml ha <sup>-1</sup>	R105,00
Terbuzine/Cheetah 600	2 l ha <sup>-1</sup>	R78,60
Lamda (5EC)	120 ml ha <sup>-1</sup>	R7,00
Correcto	100 ml ha <sup>-1</sup>	R3,80
<b>Total cost for 2019/20 season</b>		<b>R 313,40</b>

Table A1:4: Post-planting fungicide sprays at Mafube unmined site

Fungicide	Quantity	Cost per hectare
Spanta S.C.	500 ml ha <sup>-1</sup>	R107,75
Performer	500 ml ha <sup>-1</sup>	R14,25
<b>Total cost for 2016/17 season</b>		<b>R 326,19</b>

Table A1:5: Beestepan Boerdery Costing Report

Direct input costs	2016/17 Dryland	2017/18		2018/19		2019/20	
		Dryland	Irrigated	Dryland	Irrigated	Dryland	Irrigated
	R per ha						
Fertilizer and minerals	3 915,59	2 200,00	5 014,75	4 358,00	5 265,5	4 663,10	5 634,10
Herbicides and insecticides	556,63	394,05	394,05	399,20	399,20	427,15	427,15
Fungicides	122,00	-	-	-	-	-	-
Seeds	1 727,68	1 745,30	2 706,30	1 776,00	2 841,62	1 882,60	2 983,70
Fuel	1 441,59	1 528,09	1 528,09	1 604,45	1 604,45	1 716,76	1 716,76
Repairs and maintenance	1 577,65	1 672,31	1 672,31	1 755,95	1 755,95	1 878,90	1 878,90
Rent	450,00	477,00	477,00	500,85	500,85	535,90	535,90
Depreciation	1 625,43	1 722,96	1 722,96	1 809,11	1 809,11	1 935,75	1 935,75
Fixed improvements	74,01	78,45	78,45	82,40	82,40	86,50	86,50
Wages (temporary staff)	367,27	389,31	389,31	408,78	408,78	429,22	429,22
Indirect fixed costs	2016/17	2017/18		2018/19		2019/20	
	Dryland	Dryland	Irrigated	Dryland	Irrigated	Dryland	Irrigated
Salaries (permanent staff)	2 675,83	2 836,38	2 836,38	2 978,20	2 978,20	3 196,30	3 196,30
Medical aid (Provident Fund)	209,37	221,93	221,93	233,03	233,03	247,02	247,02
Electricity	326,97	346,59	346,59	363,92	363,92	382,12	382,12
Transport for contractors	80,88	85,73	85,73	90,00	90,00	94,50	94,50
Insurance and licences	85,68	90,82	90,82	95,36	95,36	102,04	102,04
Silo cost and packaging	3,67	3,89	3,89	4,09	4,09	4,30	4,30
Telephones	24,86	26,35	26,35	27,70	27,70	29,70	29,70
Statutory levies and WCC	130,86	138,71	138,71	145,65	145,65	155,85	155,85
Sundry operating expenses	118,45	125,56	125,56	131,88	131,88	138,50	138,50
<b>Total cost per hectare</b>	<b>R15 514,42</b>	<b>R15 980,09</b>	<b>R17 859,17</b>	<b>R16 779,10</b>	<b>R18 752,15</b>	<b>R17 906,20</b>	<b>R19 978,30</b>

Note: Irrigation and pumping costs (estimated at R5 000 per ha) are covered by Mafube Colliery.

**APPENDIX A2: Mafube unmined pivot: grain chemical analyses**

Table A2.1: Chemical constituents of the grain of white maize from the irrigated Mafube unmined pivot

	Dryland	Year			Irrigated	Year		
		2017/18	2018/19	2019/20		2017/18	2018/19	2019/20
<b>Grain (mg/kg)</b>	K	18,3	14,5	12,92	K	17,3	21,5	18,3
	Mg	8,9	9,63	9,11	Mg	9,8	9,5	10,1
	Ca	0,4	0,61	0,68	Ca	0,3	0,6	0,85
	Na	0,022	0,009	0,01	Na	0,024	0,029	0,03
	S	9,5	8,2	8,9	S	9,9	8,3	9,1
	P	32,3	24	27,5	P	31,2	26,8	29,7
	B	0,015	0,066	0,04	B	0,017	0,03	0,01
	Fe	0,112	0,12	0,15	Fe	0,142	0,12	0,163
	Mn	0,044	0	0,013	Mn	0,045	0,055	0,053
	Al	0,01	0,011	0,015	Al	0,01	0,03	0,021
	Cu	0,008	0,005	0,003	Cu	0,008	0,004	0,004
	Zn	0,143	0,125	0,2	Zn	0,157	0,17	0,26
	Hg	0,001	0,001	0,001	Hg	0,001	0,001	0,001
	Cd	0,001	0,001	0,001	Cd	0,001	0,001	0,001
	Cr	0,0009	0,0004	0,0007	Cr	0,0004	0,0006	0,0003
Pb	0,006	0,006	0,006	Pb	0,006	0,006	0,006	
<b>Stem</b>	K	11870	12405	12655	K	12350	14840	15890
	Mg	2620	2450	2905	Mg	2510	2423	2630
	Ca	1895	2120	2230	Ca	2000	1975	2015
	Na	85	92	95	Na	31	30	33
	S	445	425	450	S	775	763	790
	P	350	355	341	P	419	433	421
	B	3,9	3,3	4,5	B	3,5	4,7	3,8
	Fe	2,6	2	2,4	Fe	3,5	3,2	3,3
	Mn	3	2,7	3,1	Mn	6,9	5	6,5
	Al	43	42	58	Al	43	36	49
	Zn	12	6,8	14	Zn	19	12	15
	<b>Leaves</b>	K	12630	10895	11210	K	13780	12105
Mg		4015	3928	4210	Mg	4650	4380	4515
Ca		6200	6110	6450	Ca	6430	6085	6570
Na		8,9	8,7	9,2	Na	67	65	70
S		1080	880	1230	S	1870	1633	1950
P		980	850	1100	P	1810	1440	1750
B		6,2	5,9	7	B	9,7	10,3	10,1
Fe		20	22	18	Fe	11	15	13
Mn		41	45	38	Mn	51	55	48
Al		497	519	489	Al	396	385	401
Cu		2,4	2,6	2,3	Cu	2,8	3	2,9
Zn		27	29	28	Zn	29	25	27

**APPENDIX A3: Mafube unmined pivot: average soil constituent concentrations**

Table A3.1: Laboratory analysis results for soil sampling sites within the pivot boundary (0–30 cm depth)

Year	Point	Depth	Chemical Constituents (mg/L)													
			pH	EC	Na	K	Ca	Mg	SO <sub>4</sub>	P	Fe	Mn	Al	Cu	Zn	
2017-2018	S01 S02 S03 S04 S05 S06 S07 S08 S09 S10 S11 S12 S13 S14	0 - 30cm	5,8	181	24	62	632	201	223	48	80	18	812	2	4	
			5,7	213	27	69	627	191	250	56	91	23	893	3	4	
			6,1	173	22	79	623	176	211	45	76	16	798	2	3	
			6,3	166	19	71	642	169	204	39	74	14	801	3	3	
			5,6	201	26	78	622	186	243	63	82	26	876	3	3	
			6,4	142	17	70	639	181	210	41	72	15	810	3	3	
			6,4	170	19	67	631	189	202	43	70	16	809	3	3	
			6,5	145	17	59	639	181	197	38	66	17	778	2	3	
			6,3	134	15	57	626	176	200	41	65	13	766	2	3	
			6,4	122	17	55	640	160	189	46	63	14	793	2	3	
			6,5	130	14	61	597	133	161	39	60	11	763	1	2	
			6,4	126	16	59	602	151	152	43	59	10	770	2	2	
			6,6	133	17	56	589	146	176	48	68	13	781	2	3	
			6,5	126	18	61	578	161	185	58	74	14	759	2	3	
	S15	6,4	112	13	64	567	146	117	48	63	13	743	2	3		
	S16	6,2	108	15	71	574	170	106	55	61	14	756	2	3		
	S17	5,8	180	21	84	563	183	239	69	71	25	887	3	4		
	S18	5,5	191	23	81	613	195	248	71	77	29	912	3	4		
	S19	5,4	220	29	96	619	198	251	69	83	31	956	3	4		
	S20	5,3	231	26	101	626	203	261	74	88	34	970	4	5		
	S21	6,5	134	17	68	580	172	133	41	59	13	734	2	3		
2018-2019	S01 S02 S03 S04 S05 S06 S07 S08 S09 S10 S11 S12 S13 S14	0 - 30cm	5,9	190	26	59	643	197	230	41	85	20	841	2,5	3	
			5,9	211	28	74	624	181	262	52	81	25	905	2,5	3,5	
			6,2	190	18	80	630	185	226	52	61	18	812	2,5	2,5	
			6,2	175	22	65	637	176	197	43	68	15	826	3	3	
			5,8	212	29	74	631	199	251	57	77	24	887	2,5	3	
			6,2	136	18	80	626	190	218	43	60	16	823	2,5	2,5	
			6,2	181	21	63	614	199	220	38	67	18	813	2,5	3,5	
			6,3	151	18	62	627	195	213	42	73	14	801	2,5	3	
			S09	6,3	141	16	67	620	187	212	37	65	12	794	2	3
			S10	6,3	130	14	63	631	173	196	48	60	16	802	2	3,5
			S11	6,5	125	16	60	607	141	170	42	51	12	778	1,5	2,5
			S12	6,6	120	14	69	619	155	155	41	48	9	784	2	2
			S13	6,6	141	18	47	599	142	173	50	43	12	795	1,5	2,5
			S14	6,5	136	19	60	563	172	190	56	52	14	765	2,5	3
	S15	6,3	123	14	60	577	150	123	45	59	16	730	2	3		
	S16	6,1	91	13	65	589	174	113	53	54	18	745	2,5	3,5		
	S17	5,7	185	25	74	614	191	240	70	69	29	901	3,5	4,5		
	S18	5,4	203	26	79	631	193	250	68	76	32	923	3	4,5		
	S19	5,5	216	31	99	623	206	243	70	86	30	1003	3	4,5		
	S20	5,4	246	28	97	616	200	254	76	93	36	998	3,5	5,5		
	S21	6,4	141	19	71	564	189	141	46	52	15	745	2,5	3,5		
2019-2020	S01 S02 S03 S04 S05 S06 S07 S08 S09 S10 S11 S12 S13 S14	0 - 30cm	5,8	202	29	68	650	210	245	55	90	23	856	2,5	3,5	
			5,8	220	30	75	634	197	267	59	78	30	912	3	4	
			6,3	201	19	84	641	191	232	62	65	22	826	1,5	3,5	
			6,3	183	25	62	649	184	209	57	73	16	839	2,5	3,5	
			S05	5,7	210	26	78	650	206	260	69	83	22	897	2,5	3,5
			S06	6,3	131	22	85	639	198	225	58	64	17	839	3	3,5
			S07	6,3	178	28	70	627	208	231	49	78	20	840	3	3
			S08	6,2	161	20	68	630	212	229	54	72	15	821	1,5	3,5
			S09	6,3	145	19	74	635	193	227	49	78	15	804	1,5	3
			S10	6,2	128	21	69	625	188	212	60	62	17	810	2	3,5
			S11	6,4	130	22	71	621	165	191	63	56	14	791	1,5	2
			S12	6,5	116	20	78	626	161	161	65	55	11	799	2	2,5
			S13	6,6	135	25	59	610	155	187	70	50	13	807	1,5	3
			S14	6,3	128	24	67	580	180	204	71	58	15	778	2	3
	S15	6,2	117	18	65	591	162	139	58	64	18	745	2,5	2,5		
	S16	6	121	16	70	576	180	125	66	60	17	756	2,5	3,5		
	S17	5,6	171	26	75	623	200	253	78	80	26	918	3	3,5		
	S18	5,3	210	29	84	636	199	261	84	84	34	930	3	3,5		
	S19	5,1	204	33	102	630	212	258	80	92	32	1019	3	4		
	S20	5	232	29	106	629	206	250	88	97	40	1008	3,5	4,5		
	S21	6,3	157	21	83	587	194	146	56	60	20	756	2,5	3,5		

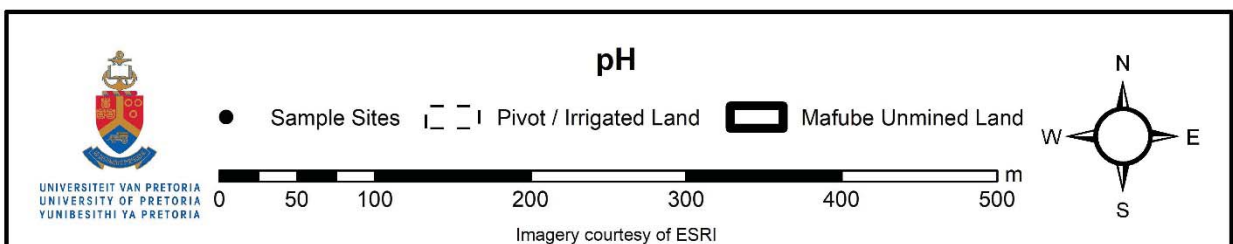
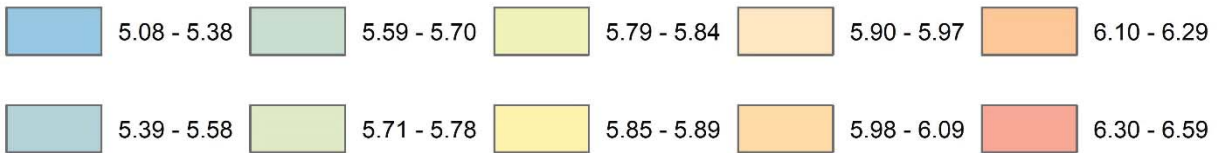
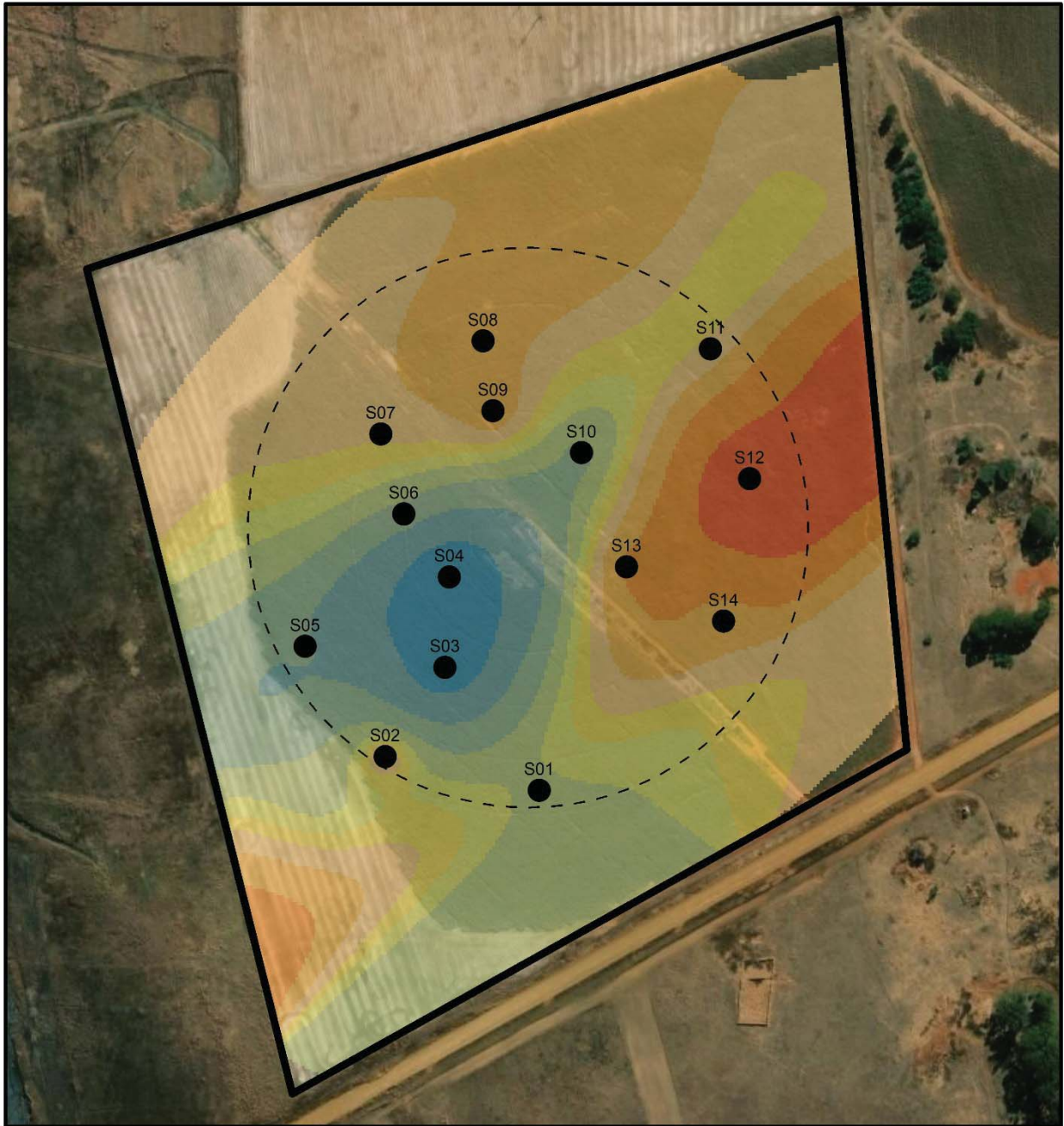
Table A3:2: Laboratory analysis results for soil sampling sites within the pivot boundary (30–60 cm depth)

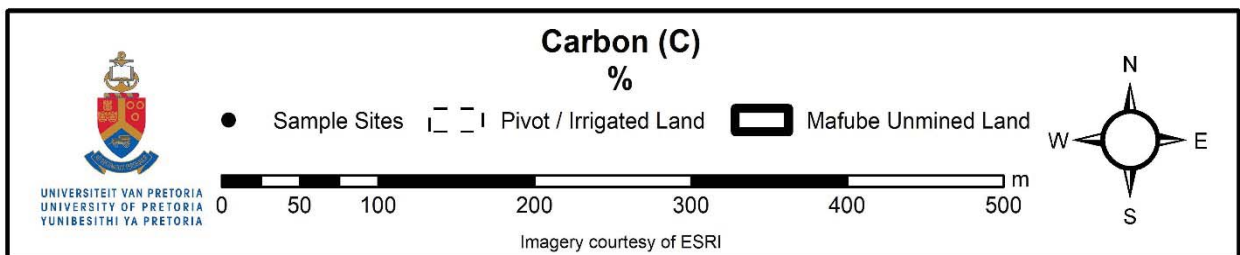
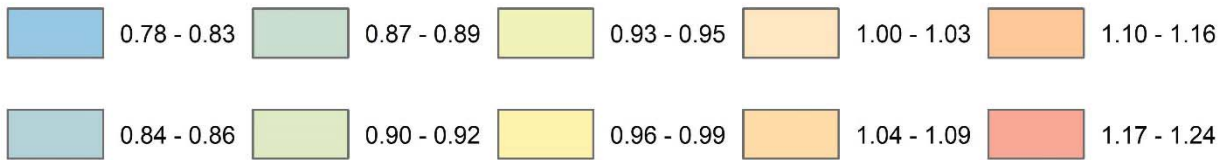
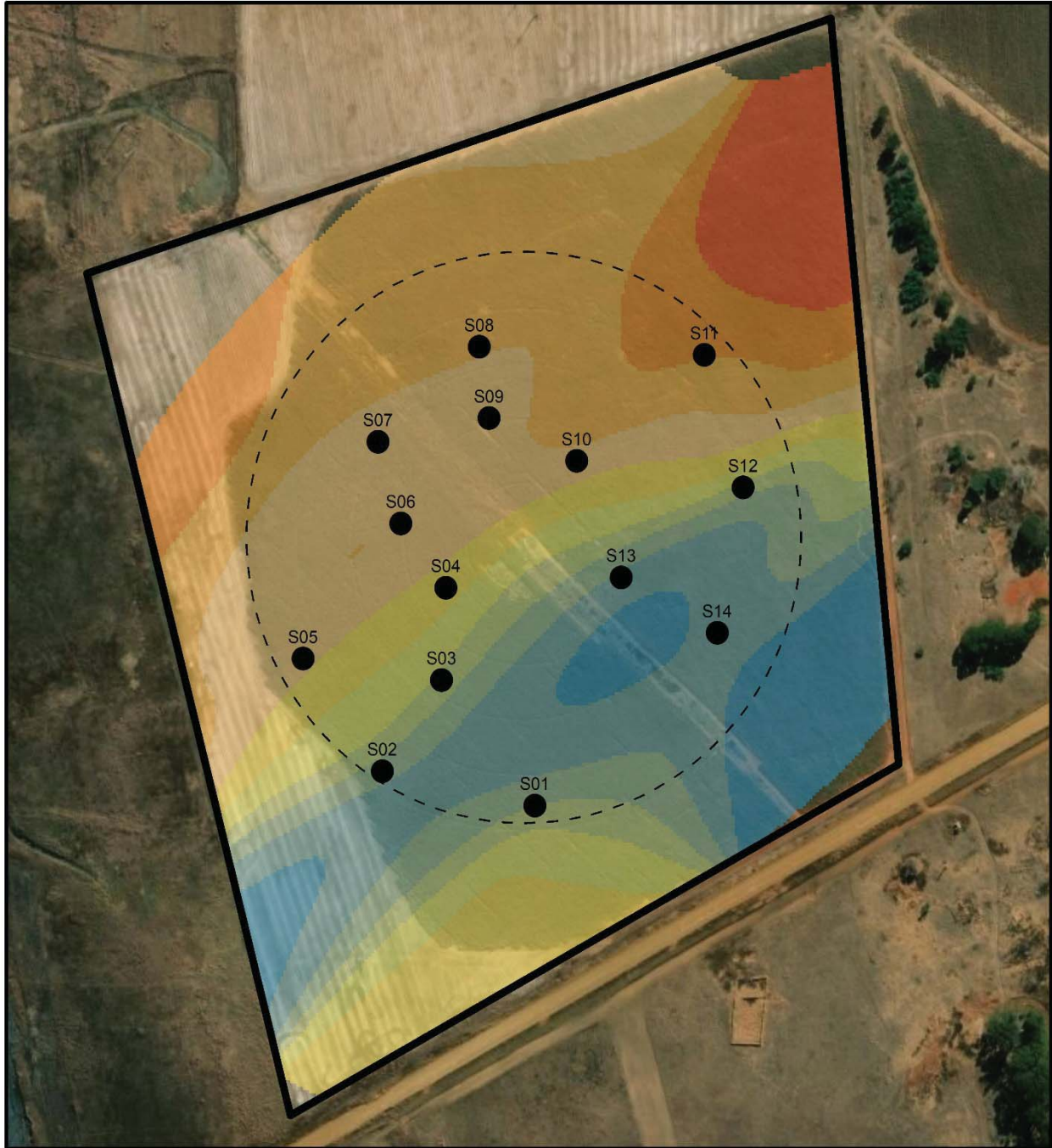
Year	Point	Depth	Chemical Constituents (mg/L)												
			pH	EC	Na	K	Ca	Mg	SO <sub>4</sub>	P	Fe	Mn	Al	Cu	Zn
2017-2018	S01 S02 S03 S04 S05 S06 S07 S08 S09 S10 S11 S12 S13 S14	30 - 60cm	5,8	176	22	58	645	205	260	37	74	16	854	2	3,5
			5,8	232	24	62	650	190	287	45	83	21	906	2,5	3
			6,2	186	16	70	641	174	236	26	71	15	816	2	2,5
			6,5	171	12	65	669	175	235	22	68	12	843	2,5	2
			5,9	221	22	72	635	190	270	44	75	22	899	2,5	1
			6,6	146	10	60	651	176	246	29	62	13	843	2,5	2
			6,5	165	13	59	659	188	236	30	59	12	829	2	3
			6,6	149	15	55	664	183	229	28	53	14	805	2,5	2,5
			6,4	140	12	53	671	178	231	32	50	12	798	2,5	3
			6,5	136	13	52	673	161	207	39	59	11	816	2	2,5
			6,5	136	11	57	623	134	186	30	57	10	785	1,5	2
			6,5	131	8	55	630	147	196	31	45	12	794	1,5	2
			6,7	139	10	50	619	149	208	37	57	15	796	2	3
			6,6	140	12	58	615	163	219	37	61	13	774	2	3
	S15	S16	6,5	120	10	60	591	150	143	34	52	13	765	1,5	2,5
	S17	S18	6,4	118	11	65	598	168	136	41	58	12	769	1,5	2,5
	S19	S20	6	189	18	74	588	181	289	55	70	26	923	2,5	4
	S21	S22	5,7	206	20	76	630	197	299	59	70	27	936	3	4,5
			5,8	229	27	83	628	199	288	56	77	30	1012	2,5	4
			5,6	249	23	105	643	205	306	50	75	31	998	3,5	4,5
			6,6	139	14	59	601	170	156	20	54	13	754	2,5	3
2018-2019	S01 S02 S03 S04 S05 S06 S07 S08 S09 S10 S11 S12 S13 S14	30 - 60cm	5,8	211	30	63	655	192	239	39	80	17	855	2,5	3
			5,9	220	24	84	639	183	257	43	77	21	912	2,5	3,5
			6,1	199	24	86	632	174	237	23	58	14	826	2,5	2,5
			6,2	184	23	77	645	166	206	26	62	12	834	3	3
			6,4	219	31	87	649	203	267	46	69	17	899	2,5	3
			6,1	161	20	89	636	188	221	32	55	10	834	2,5	2,5
			6,1	170	20	68	630	190	228	34	63	11	833	2,5	3,5
			6,2	155	16	70	637	197	231	30	68	12	826	2,5	3
			6,1	153	18	73	645	184	226	35	62	11	810	2	3
			6,2	144	20	69	640	170	209	42	55	11	816	2	3,5
			6,4	140	14	62	630	143	182	35	48	9	791	1,5	2,5
			6,5	150	11	71	640	151	167	28	44	6	806	2	2
			6,5	157	15	53	633	148	182	40	41	10	816	1,5	2,5
			6,4	153	21	65	587	179	201	38	47	12	789	2,5	3
	S15	S16	6,3	131	16	67	594	156	134	32	50	14	746	2	3
	S17	S18	6	122	19	75	606	171	120	46	48	16	758	2,5	3,5
	S19	S20	5,6	199	27	81	625	196	256	58	66	21	913	3,5	4,5
	S21	S22	5,3	221	32	84	641	187	263	56	71	22	930	3	4,5
			5,4	232	36	106	638	201	254	64	81	24	1010	3	4,5
			5,3	255	34	102	629	196	269	61	93	27	1009	3,5	5,5
			6	163	20	80	587	181	167	26	48	13	756	2,5	3,5
2019-2020	S01 S02 S03 S04 S05 S06 S07 S08 S09 S10 S11 S12 S13 S14	30 - 60cm	5,9	218	26	72	666	212	252	51	86	20	863	3	3,5
			6	236	29	73	647	200	273	54	71	27	926	2,5	3,5
			6,4	225	18	89	658	189	241	57	62	20	840	3	3
			6,3	209	22	66	650	196	216	50	71	15	851	2,5	3
			5,8	229	21	72	659	210	271	63	84	20	906	3	2,5
			6,1	231	20	81	647	205	234	52	65	13	856	3	3
			6,1	155	23	76	639	216	240	45	73	14	851	3	4
			6	141	16	70	641	220	245	50	70	12	843	2,5	3
			6,2	146	15	78	650	195	236	44	66	11	819	2,5	3,5
			6,1	150	17	82	638	197	229	49	60	14	823	2	3,5
			6,1	169	16	80	643	173	210	51	55	10	812	2	3
			6,2	139	17	85	641	174	189	56	51	8	809	2,5	2,5
			6,4	145	20	66	635	164	201	62	49	11	821	2	3
			6	163	16	74	597	194	211	63	51	13	798	2	2,5
	S15	S16	6	146	15	70	604	170	151	50	62	14	761	2,5	3,5
	S17	S18	6,1	131	15	78	589	186	149	61	55	16	765	2	4
	S19	S20	5,8	209	22	80	631	195	261	69	74	22	926	3	4,5
	S21	S22	5,5	229	24	88	648	208	278	74	81	24	947	3,5	4,5
			5,2	239	27	112	641	223	260	72	79	28	1029	3,5	4
			5,3	256	25	110	637	217	267	80	81	34	1016	3	5
			6,2	169	16	90	591	206	159	45	53	16	768	3	4

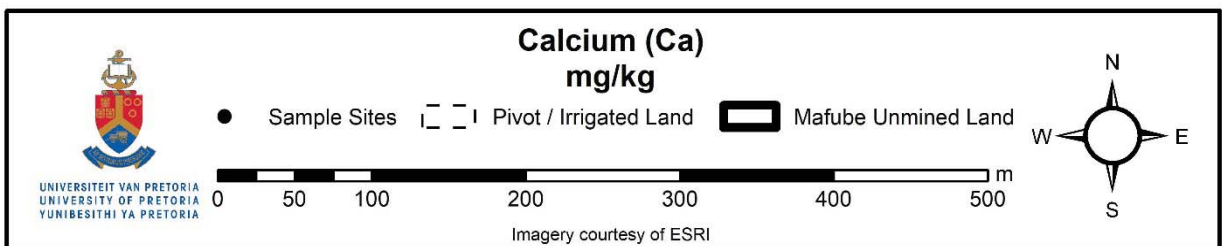
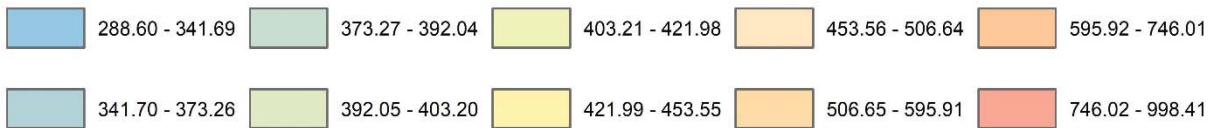
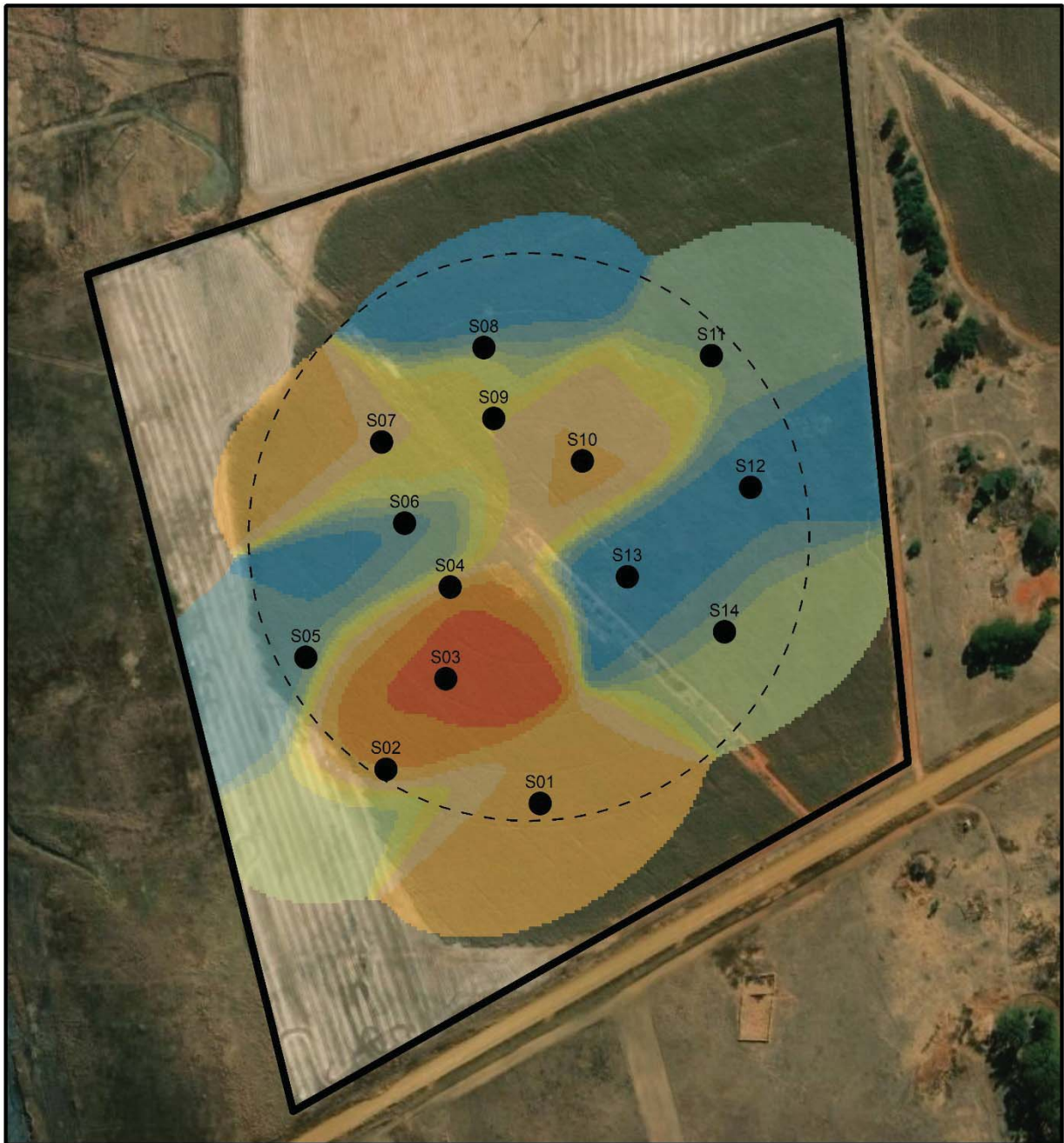
Table A3:3: Laboratory analysis results for soil sampling sites within the pivot boundary (60–90 cm depth)

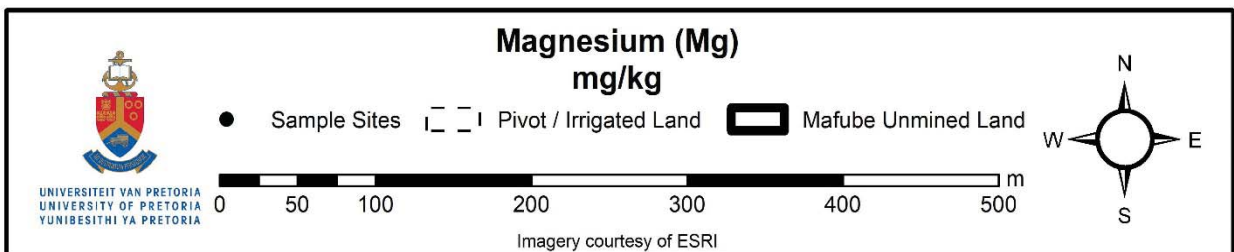
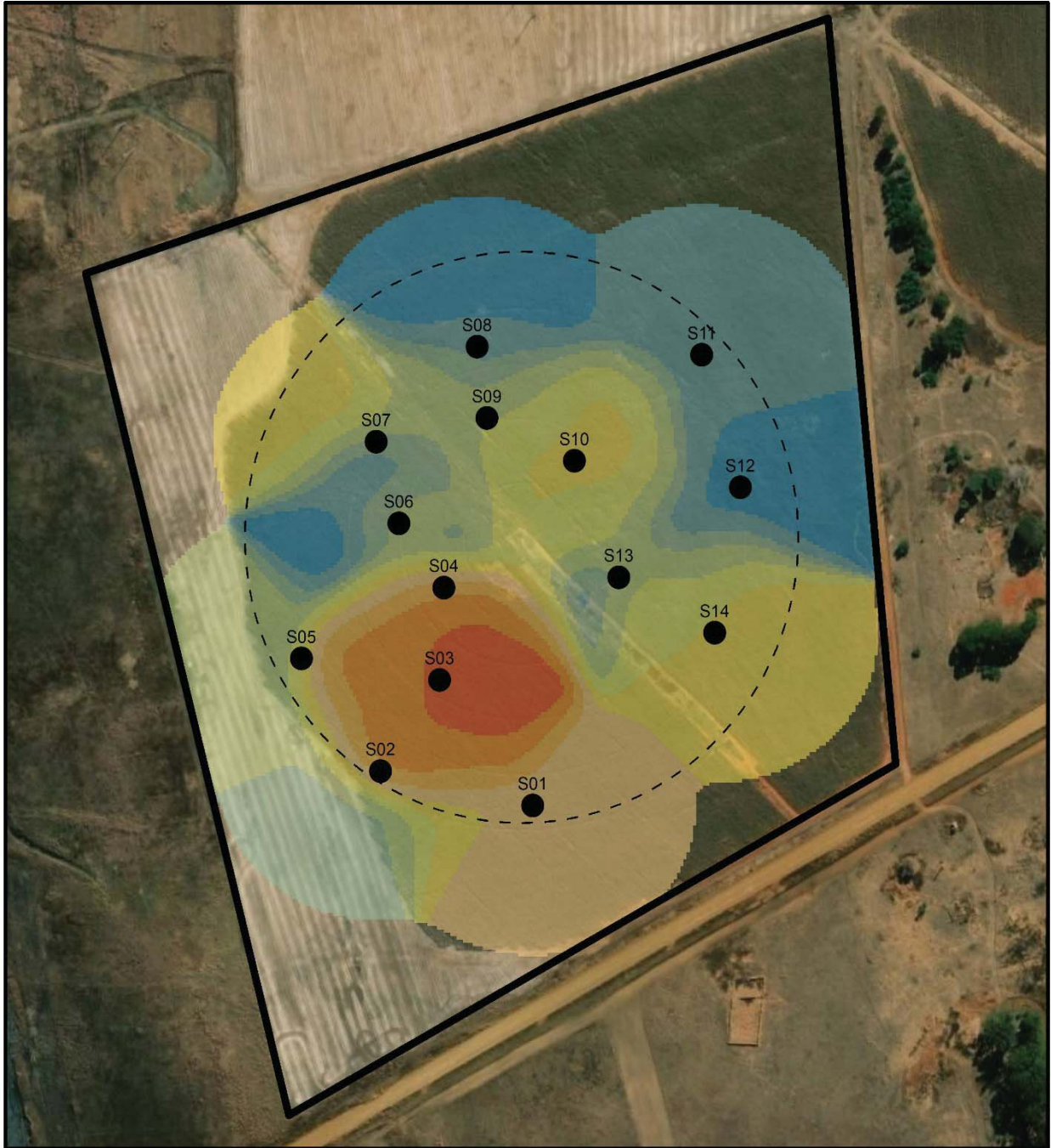
Year	Point	Depth	Chemical Constituents (mg/L)												
			pH	EC	Na	K	Ca	Mg	SO <sub>4</sub>	P	Fe	Mn	Al	Cu	Zn
2017-2018	S01 S02 S03 S04 S05 S06 S07 S08 S09 S10 S11 S12 S13 S14	60 - 90cm	5,9	185	18	53	649	209	270	41	79	20	860	2	3
			5,8	240	12	51	663	193	302	52	86	26	910	2	2,5
			6	199	10	66	671	170	245	34	74	23	820	1,5	2
			6,3	180	8	56	689	171	251	28	78	20	855	2	2
			6	245	16	67	654	189	286	46	80	26	907	2,5	1,5
			6,4	165	7	45	673	182	261	37	67	24	856	2,5	2
			6,5	189	12	51	698	197	249	41	63	23	831	1,5	2,5
			6,5	161	14	49	645	190	241	36	58	18	812	2	2
			6,4	152	11	56	683	175	257	40	59	20	809	2	2,5
			6,5	149	10	59	691	163	229	42	64	19	822	1,5	2
			6,5	142	8	45	647	137	200	34	62	16	795	1,5	2,5
			6,4	140	5	41	626	151	224	37	50	17	806	1,5	2,5
			6,5	151	8	43	627	155	226	40	63	18	810	2	2,5
			6,3	163	11	47	632	169	230	42	67	16	789	2	3
	S15	6,4	143	9	53	605	147	160	38	60	17	770	1,5	2	
	S16	6,3	127	8	47	609	170	151	46	64	20	754	2	2,5	
	S17	6,1	199	16	62	601	188	307	59	74	30	936	2,5	3,5	
	S18	5,8	212	15	68	645	195	321	63	76	30	947	3	5	
	S19	5,8	239	13	65	633	203	306	64	83	36	1023	2	3,5	
	S20	5,5	264	15	89	651	201	329	54	81	37	1005	3,5	4	
	S21	6,4	151	11	49	612	178	179	30	62	16	764	2	3,5	
Year	Point	Depth	Chemical Constituents (mg/L)												
			pH	EC	Na	K	Ca	Mg	SO <sub>4</sub>	P	Fe	Mn	Al	Cu	Zn
2018-2019	S01 S02 S03 S04 S05 S06 S07 S08 S09 S10 S11 S12 S13 S14	60 - 90cm	5,7	206	26	60	662	202	243	36	74	16	862	2,5	3
			5,8	229	22	76	647	186	263	40	71	17	923	2,5	2,5
			6	213	20	82	640	175	247	26	60	13	843	2	2
			6,1	201	22	75	652	171	211	22	56	10	851	2,5	2
			6,3	236	25	81	657	206	273	45	61	14	906	2,5	1,5
			6,2	172	19	84	643	191	230	33	52	8	854	3	2
			6,2	197	21	63	633	193	233	31	60	9	850	2	2,5
			6,3	153	14	62	641	201	237	27	61	10	841	2	2
			6,2	165	16	67	650	187	236	31	55	10	822	2	2,5
			6,3	159	19	61	645	174	216	40	52	11	829	2	2
			6,6	167	15	56	640	150	199	33	46	10	803	1,5	2,5
			6,6	162	12	66	649	155	175	26	40	7	814	1,5	2,5
			6,4	155	13	50	644	157	189	36	36	10	825	1,5	2,5
			6,4	163	19	61	602	186	212	35	40	11	791	1,5	3
	S15	6,3	143	15	60	603	164	142	30	42	12	753	1,5	2,5	
	S16	6,3	126	17	67	614	180	129	44	46	14	769	2	3	
	S17	6	223	24	74	632	207	266	51	61	18	932	3	3	
	S18	5,7	239	30	80	649	192	273	50	65	20	956	2,5	4,5	
	S19	5,8	261	32	100	649	206	260	53	73	22	1023	2,5	4	
	S20	5,6	251	35	94	636	200	273	55	85	24	1020	3	4,5	
	S21	6,1	172	15	76	599	183	179	17	41	14	767	2	3	
Year	Point	Depth	Chemical Constituents (mg/L)												
			pH	EC	Na	K	Ca	Mg	SO <sub>4</sub>	P	Fe	Mn	Al	Cu	Zn
2019-2020	S01 S02 S03 S04 S05 S06 S07 S08 S09 S10 S11 S12 S13 S14	60 - 90cm	5,7	223	22	76	658	216	248	49	82	16	271	2,5	3
			5,9	226	24	79	640	197	271	50	66	20	940	2	3
			6,2	231	16	90	659	184	243	51	57	14	862	1,5	3
			6,4	211	20	71	654	189	218	46	64	11	867	2	3
			6	225	18	75	661	215	268	55	73	13	923	2	2
			5,9	236	16	84	652	212	241	46	59	9	874	2,5	3
			6	159	18	80	648	226	246	40	61	10	869	2	3
			6,2	147	14	78	651	237	251	44	60	8	851	2	2,5
			6,1	152	12	86	649	209	240	39	58	7	832	2,5	3
			6,4	159	13	90	636	210	231	41	50	12	830	1,5	2,5
			6,3	173	12	85	647	189	218	43	49	8	826	2	2
			6,5	141	11	87	653	178	194	51	46	8	827	1,5	2
			6,2	149	14	70	648	170	214	57	41	10	834	1,5	2,5
			6,1	179	12	73	603	204	226	61	50	11	809	2	2,5
	S15	5,9	151	12	69	610	181	160	47	56	12	777	2	3	
	S16	6	139	11	80	697	193	153	56	51	11	779	1,5	2,5	
	S17	6	216	15	83	647	204	270	76	66	15	936	2,5	2,5	
	S18	5,8	235	17	90	655	216	281	69	70	17	957	2,5	4	
	S19	5,4	257	18	120	658	236	269	62	64	21	1039	2,5	3,5	
	S20	5,5	261	19	113	649	228	271	76	75	27	1025	2	4	
	S21	6	170	11	92	609	212	170	42	43	13	779	2,5	3	

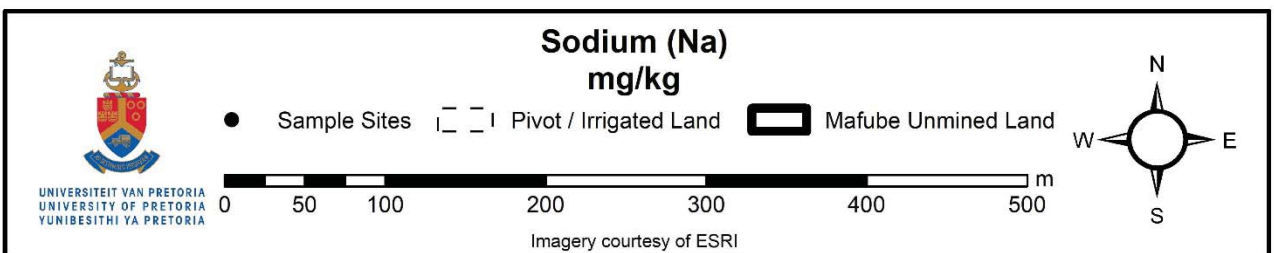
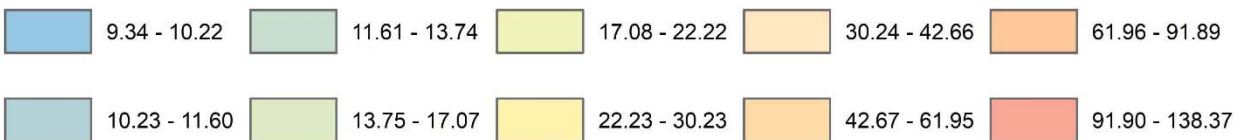
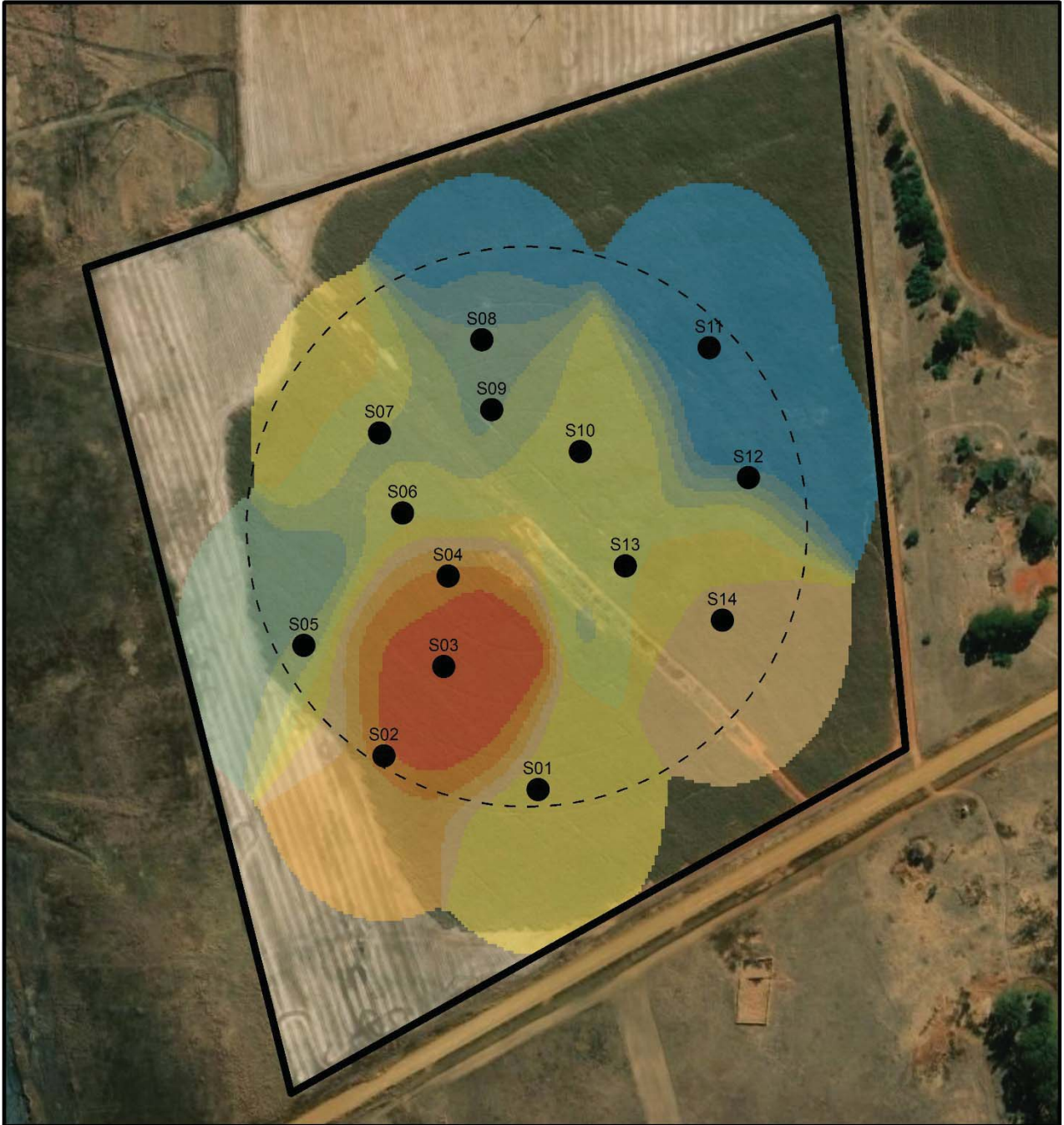
Interpolation maps for soil analyses within pivot boundary

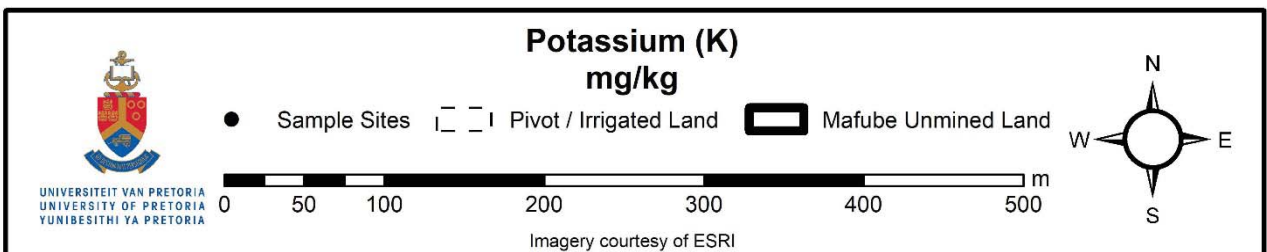
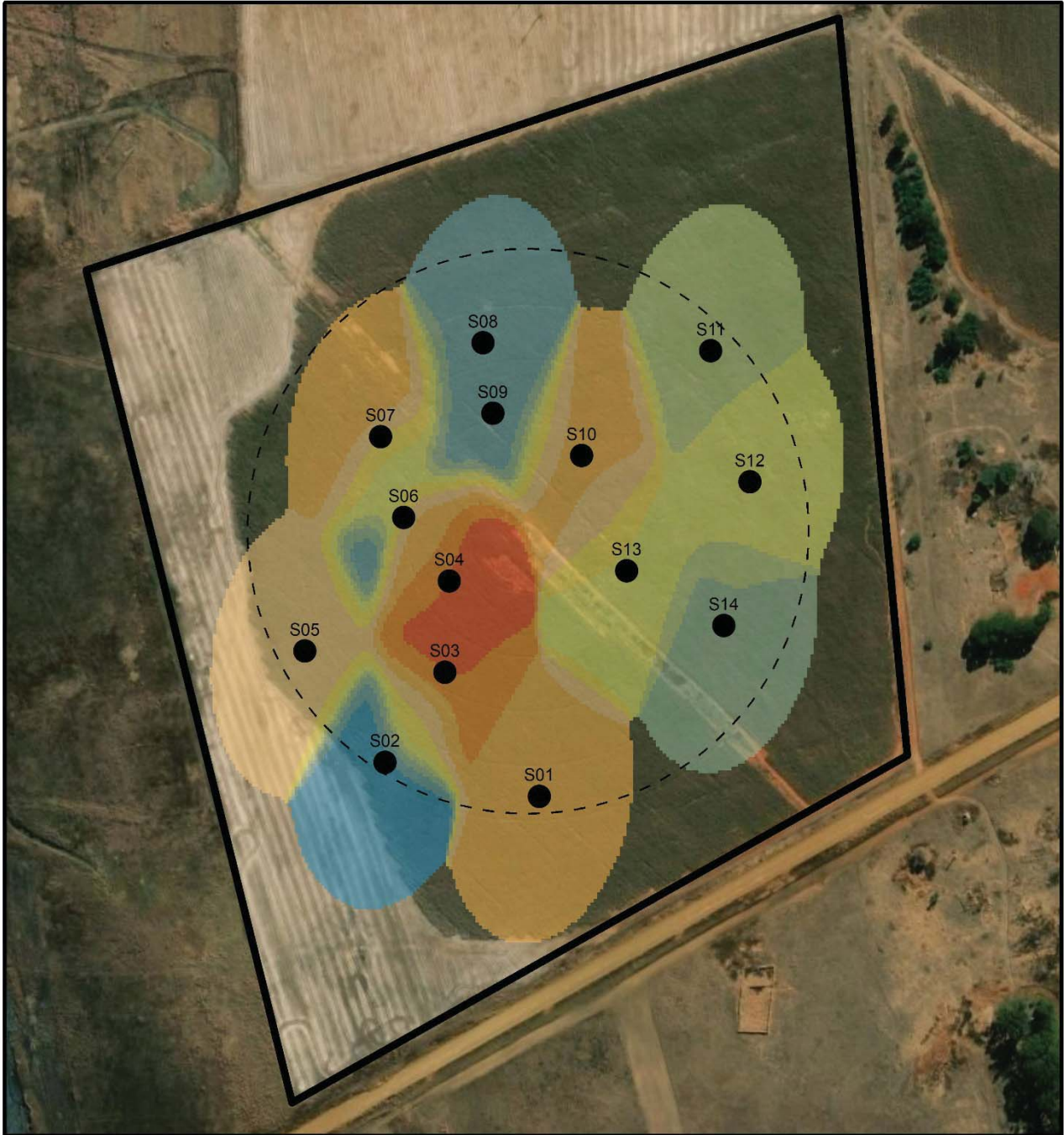


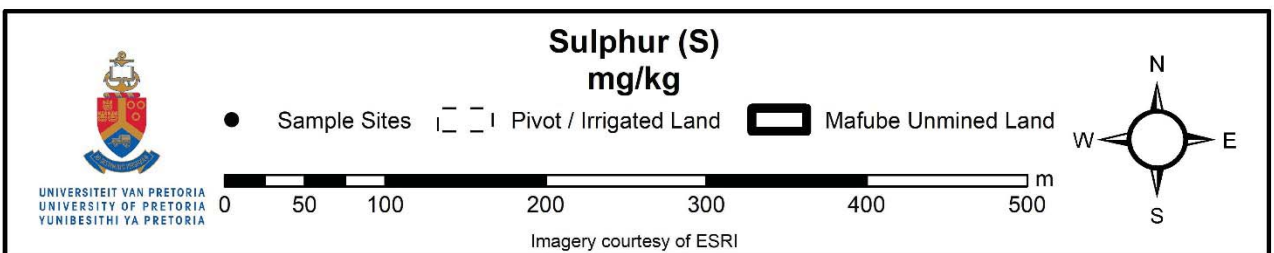
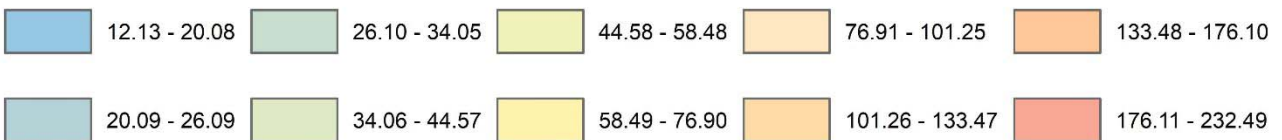
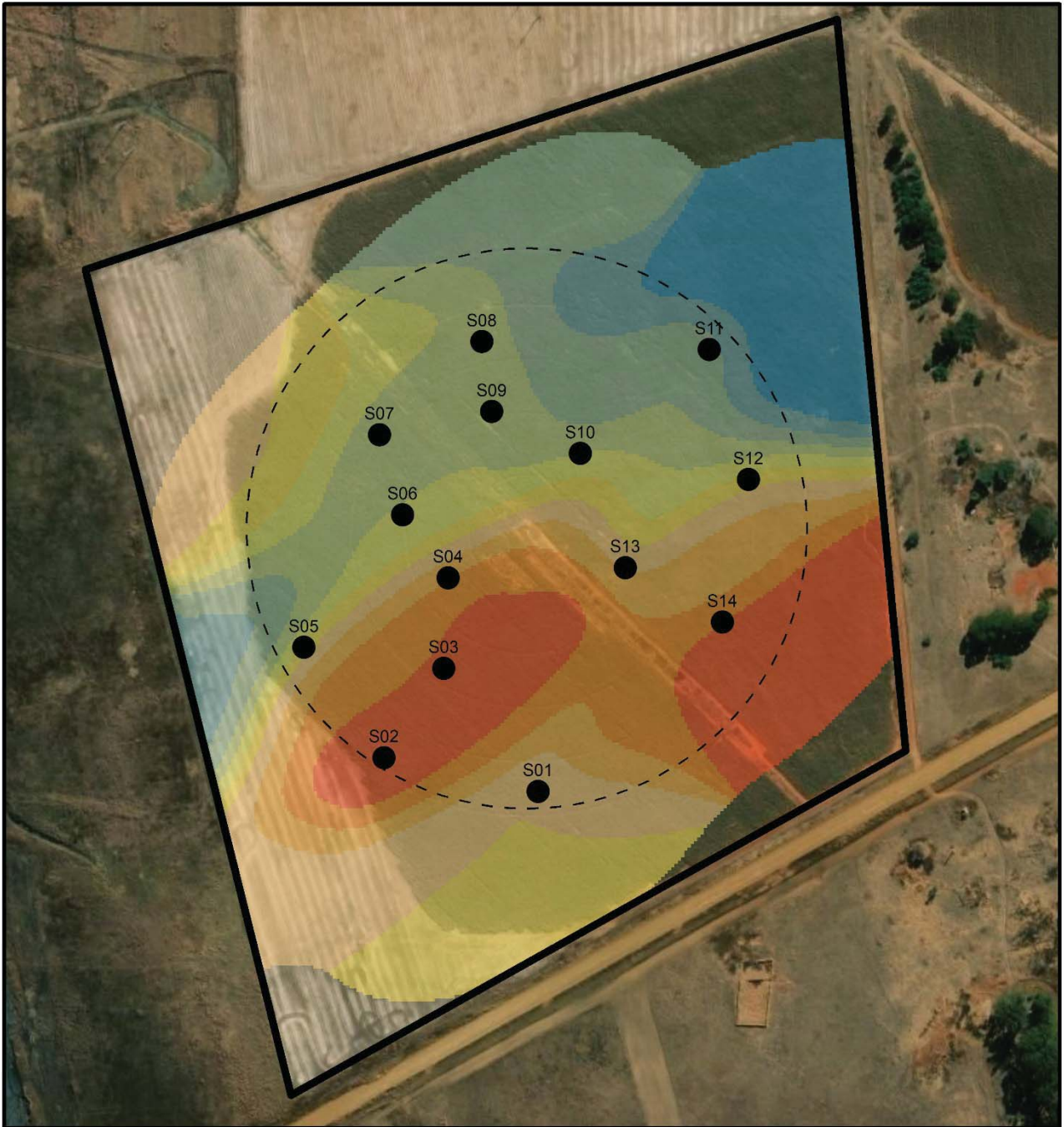


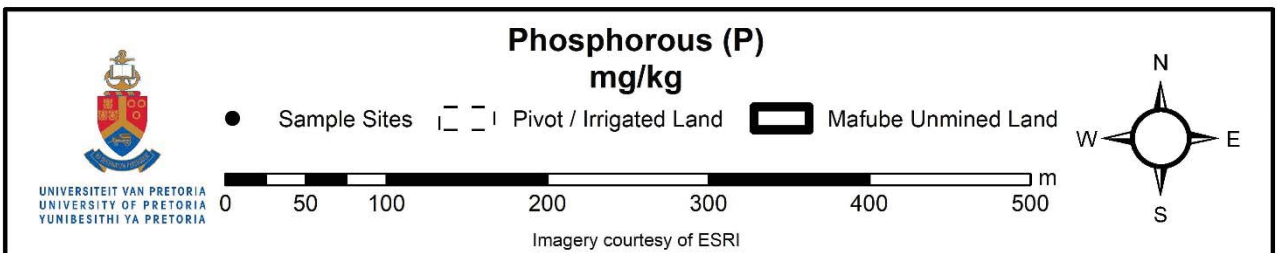
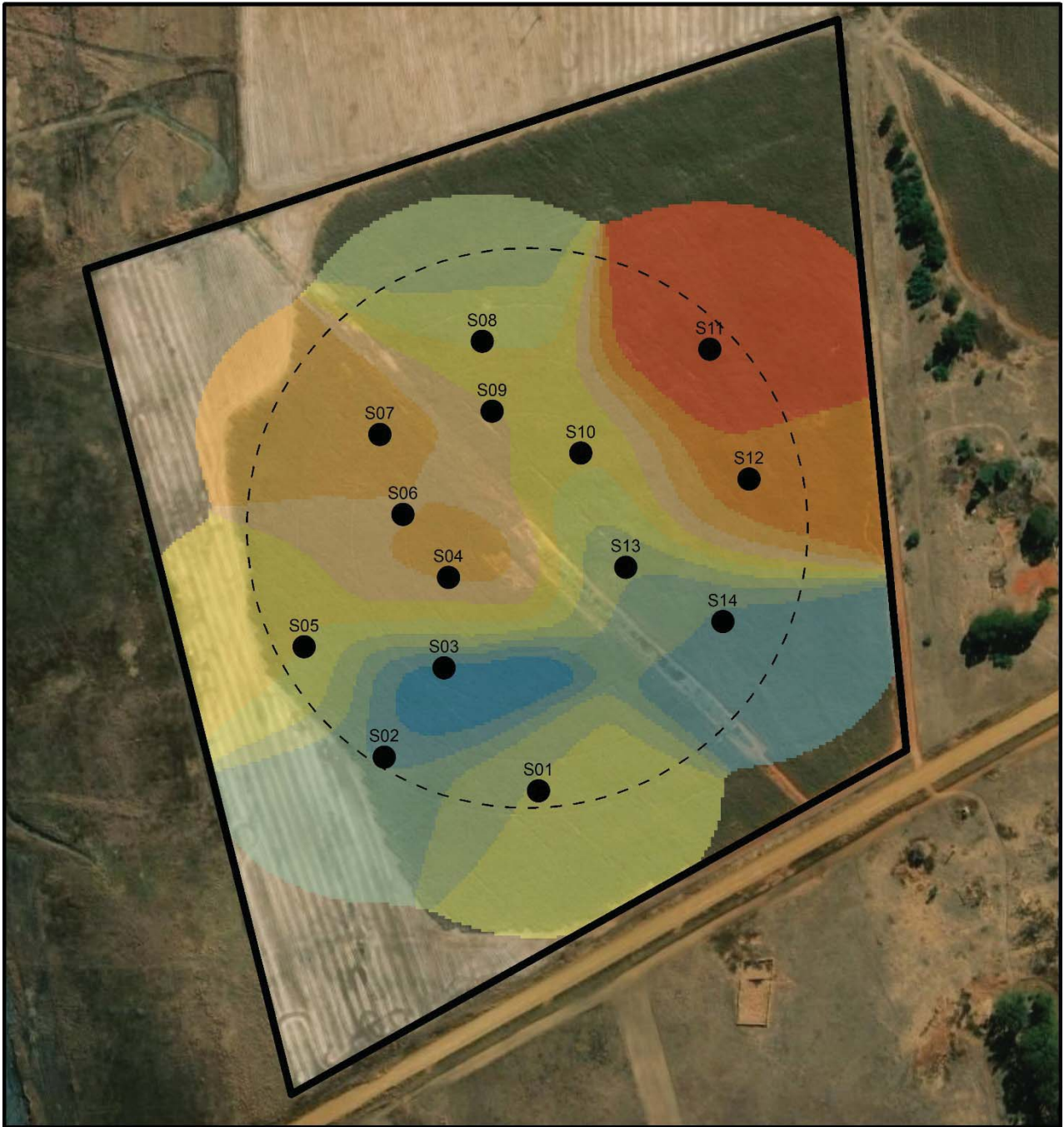


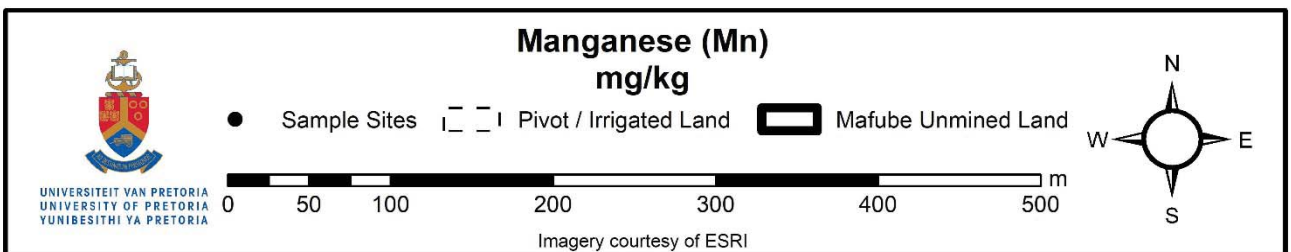
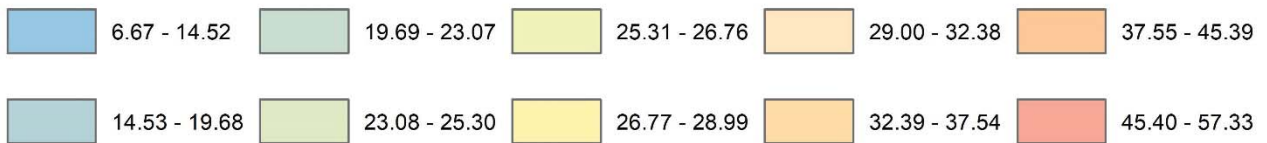
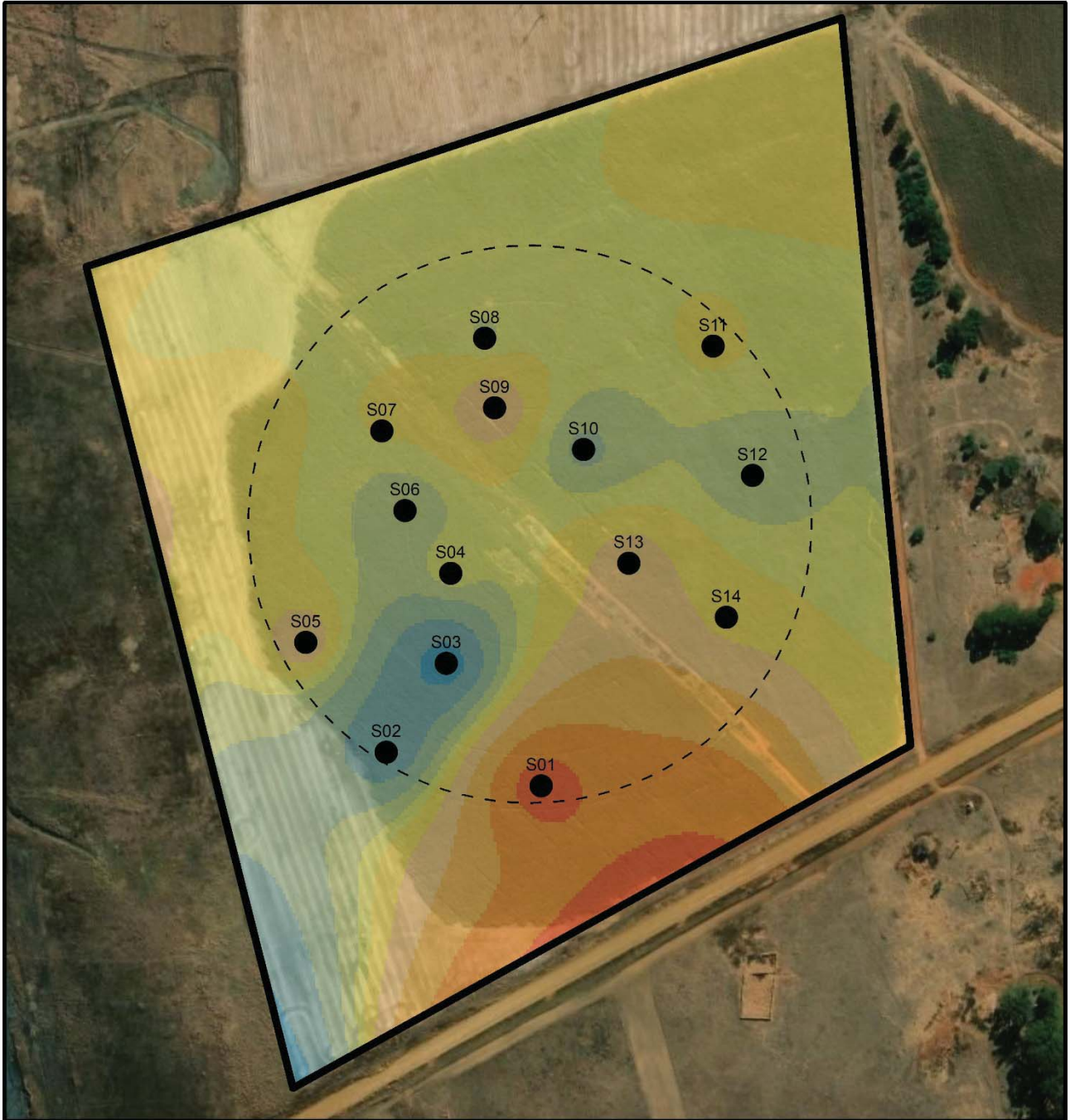


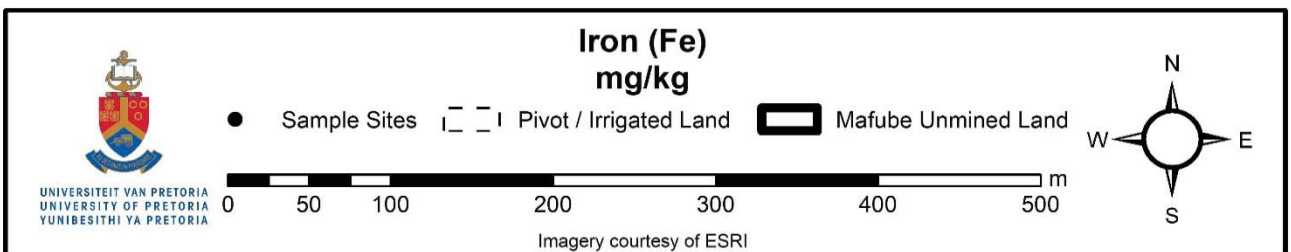
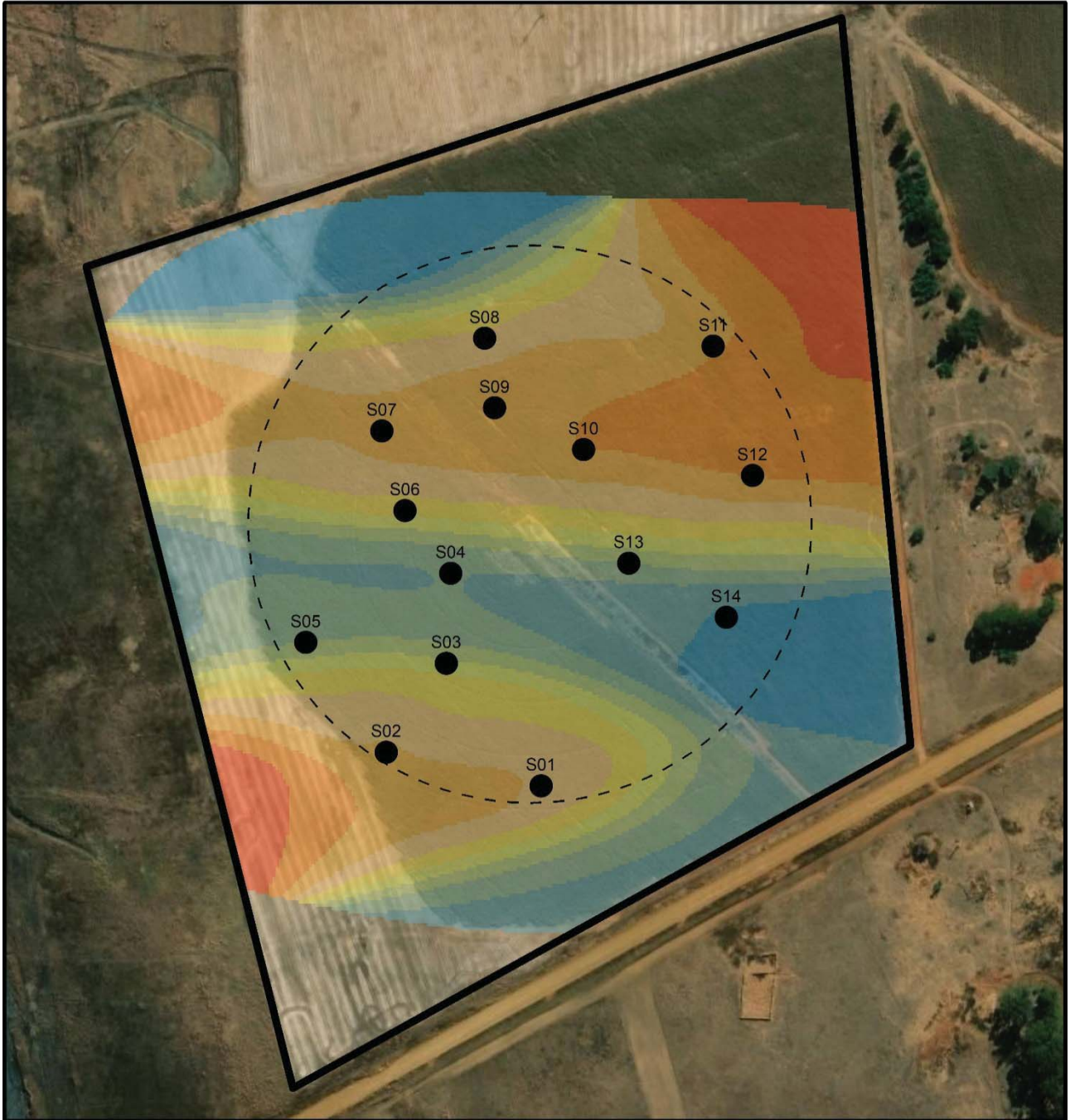


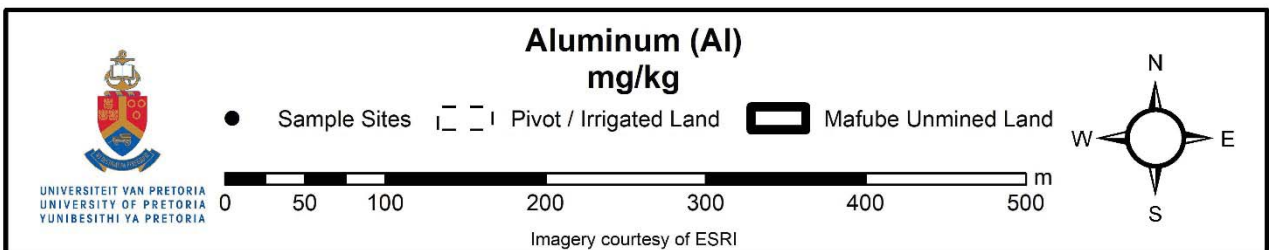
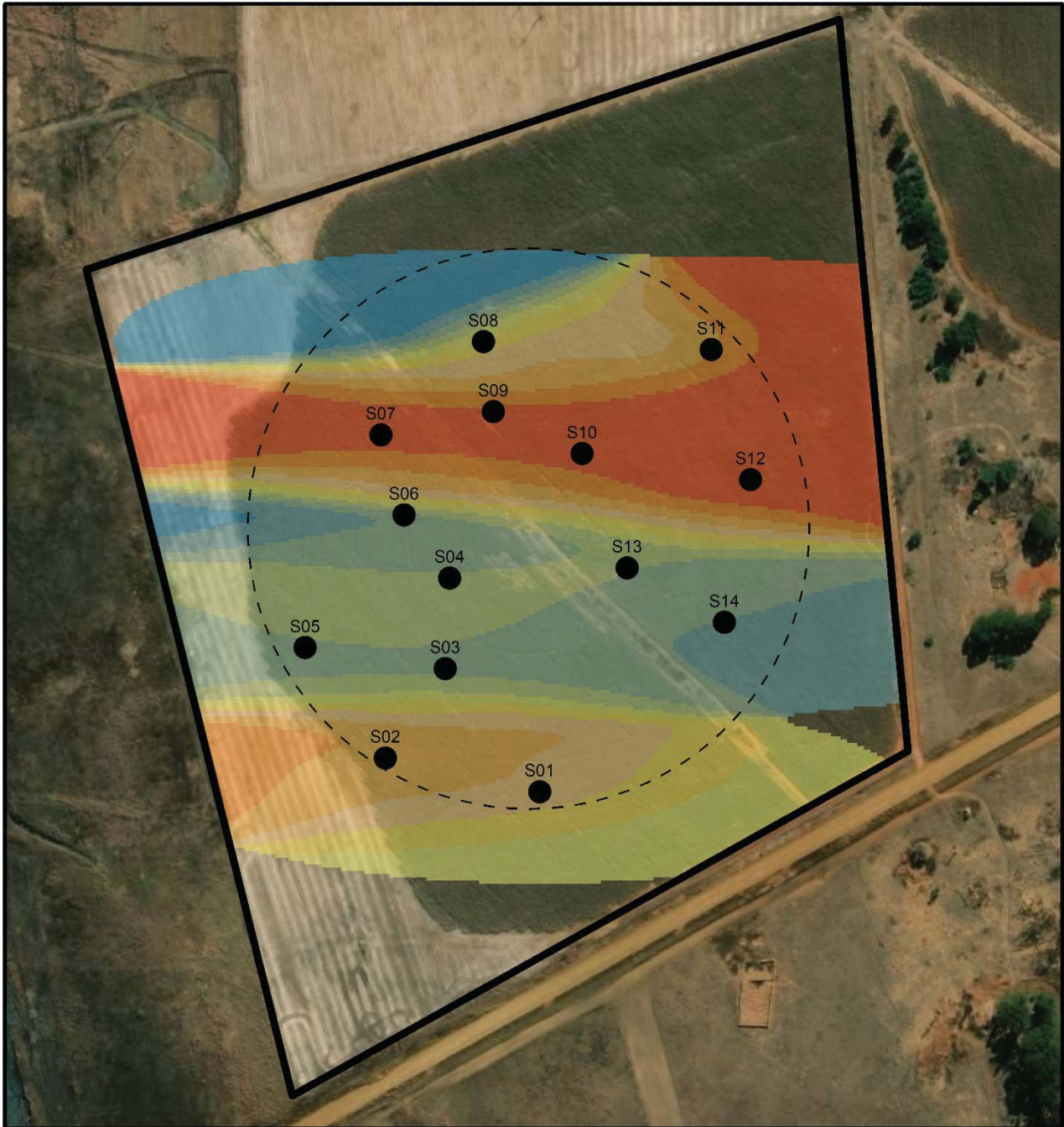


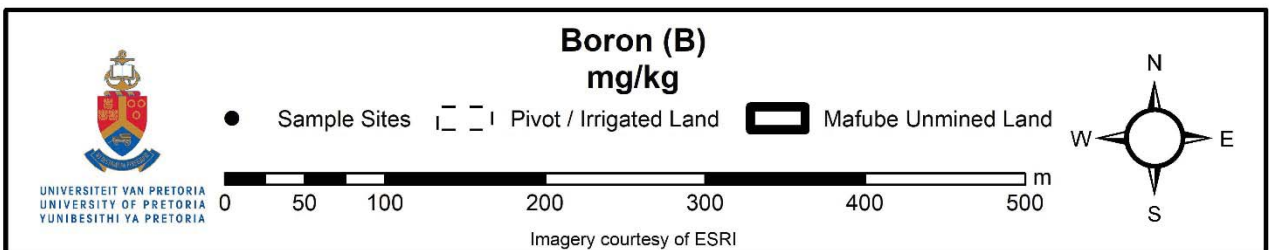
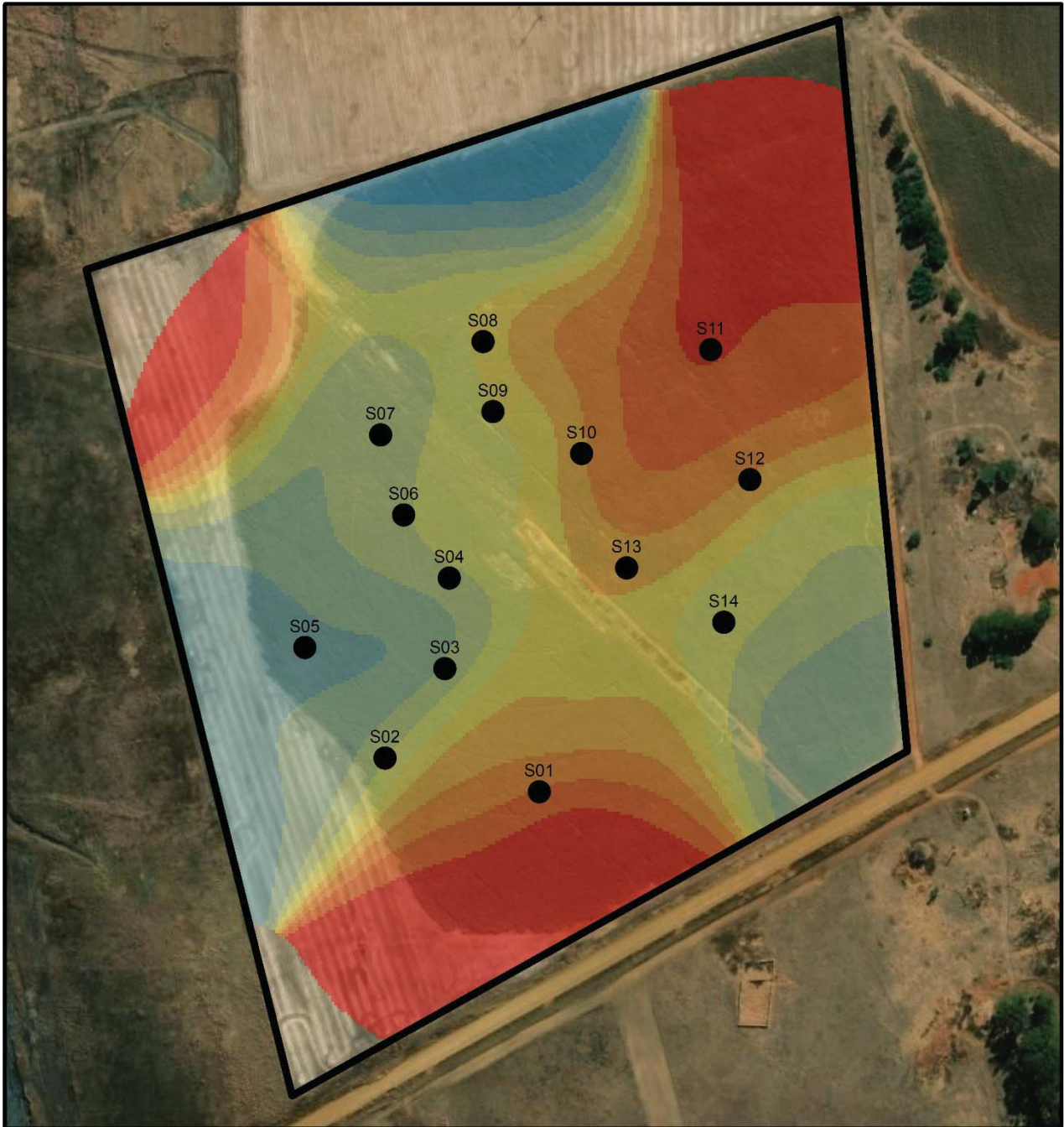


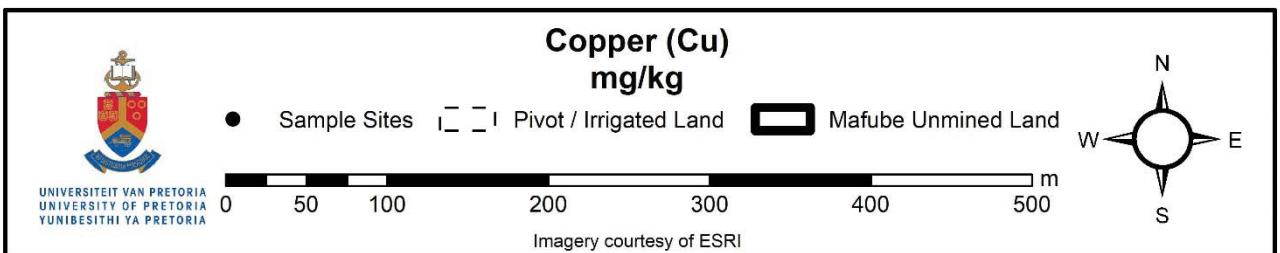
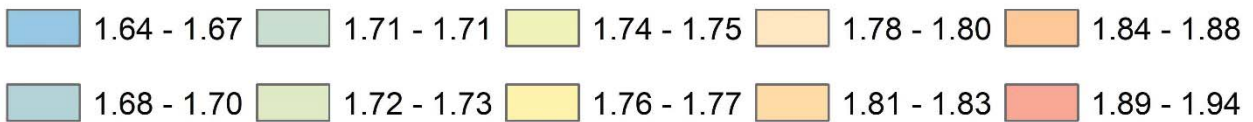
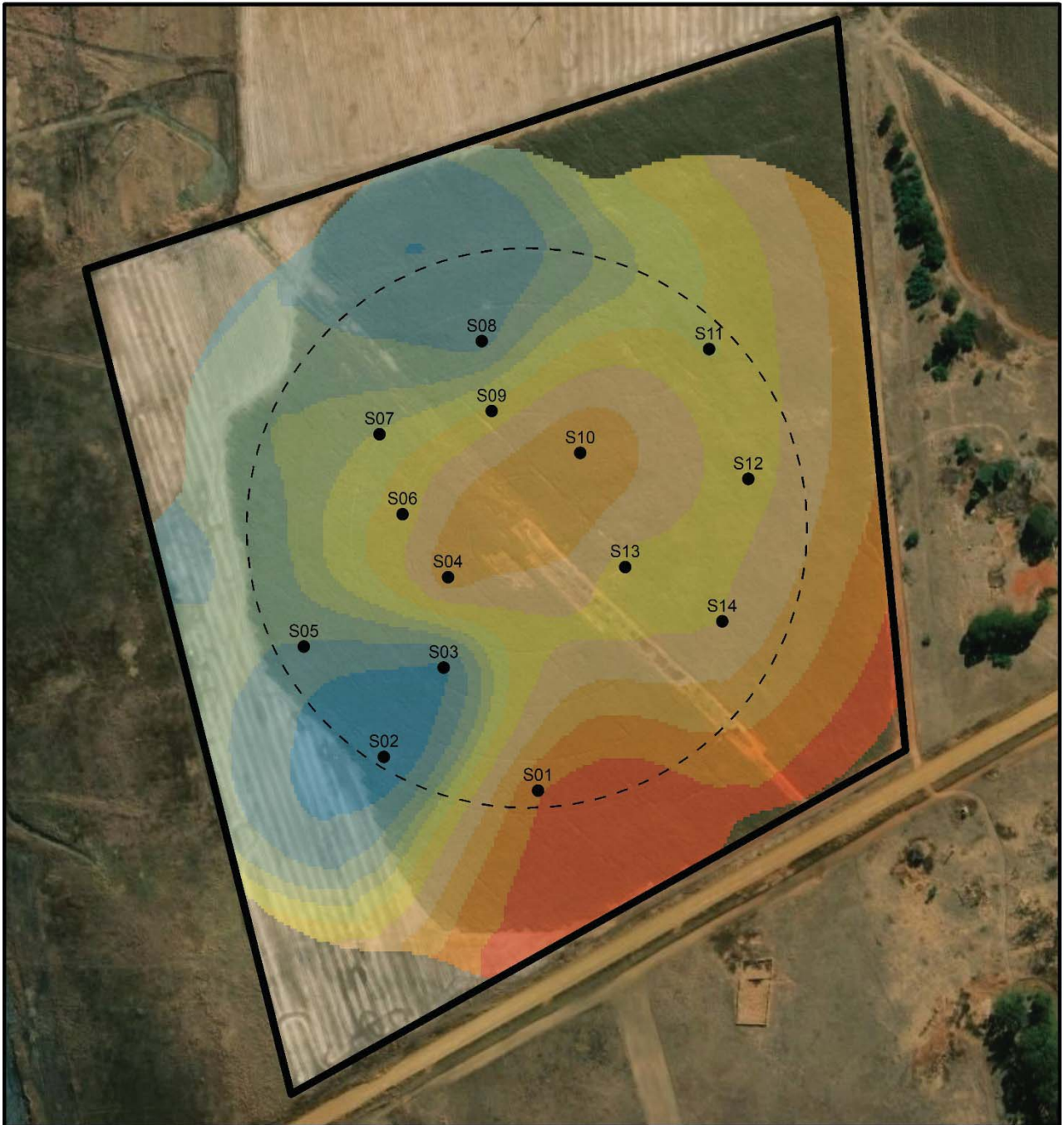


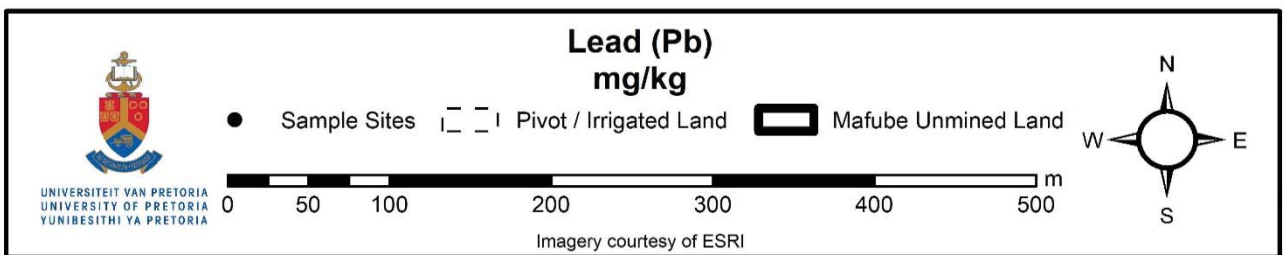
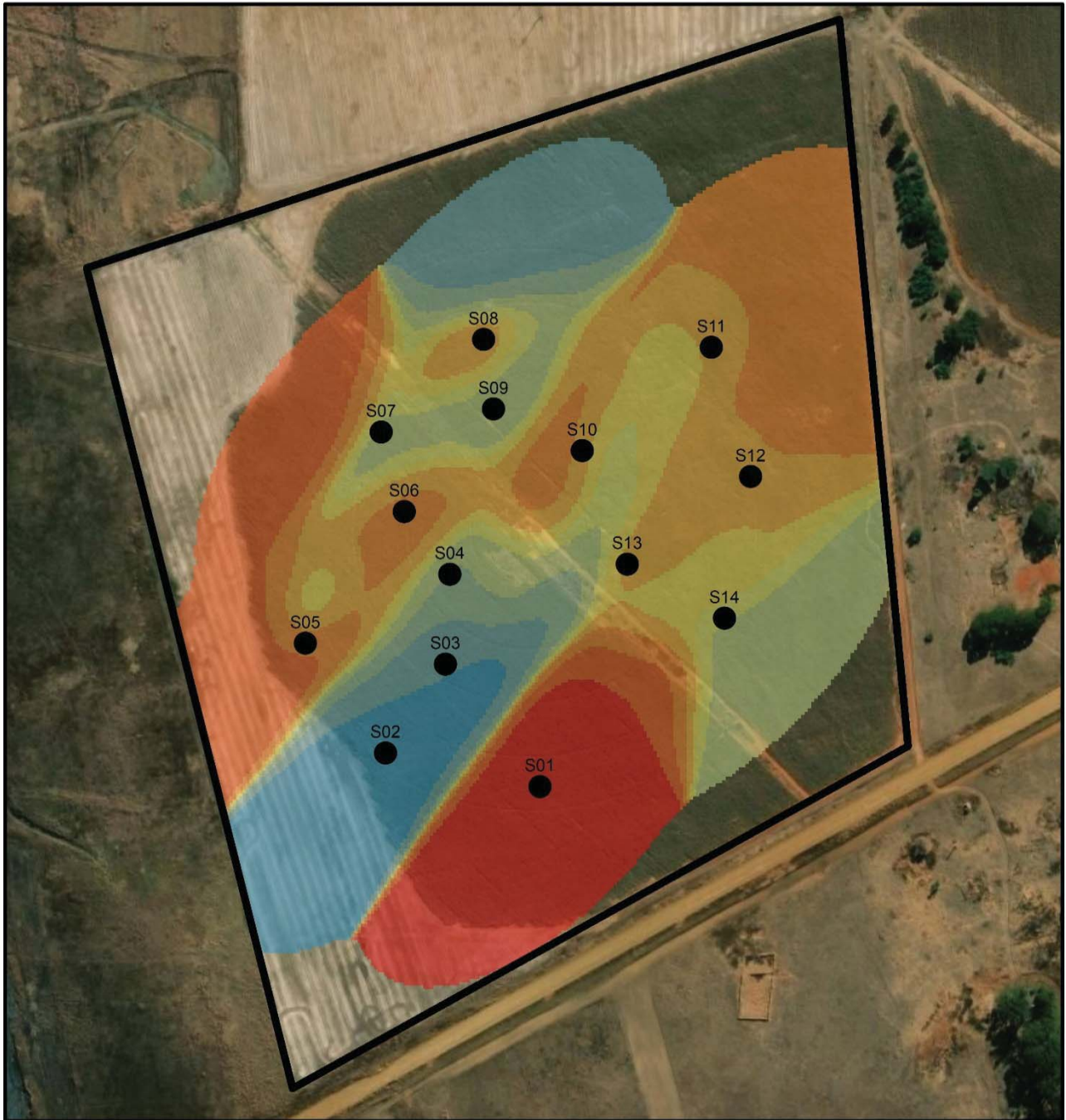


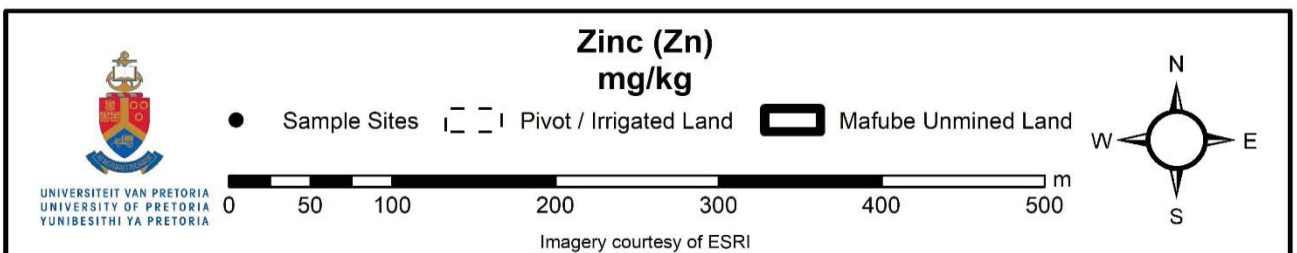
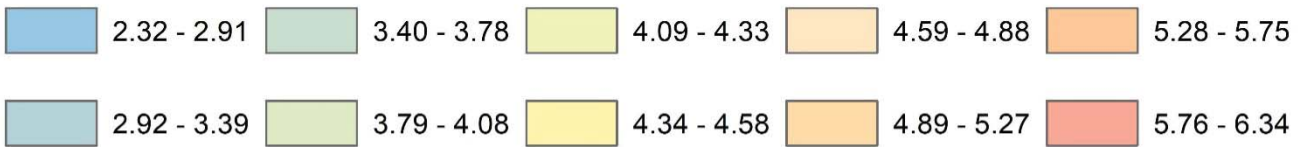
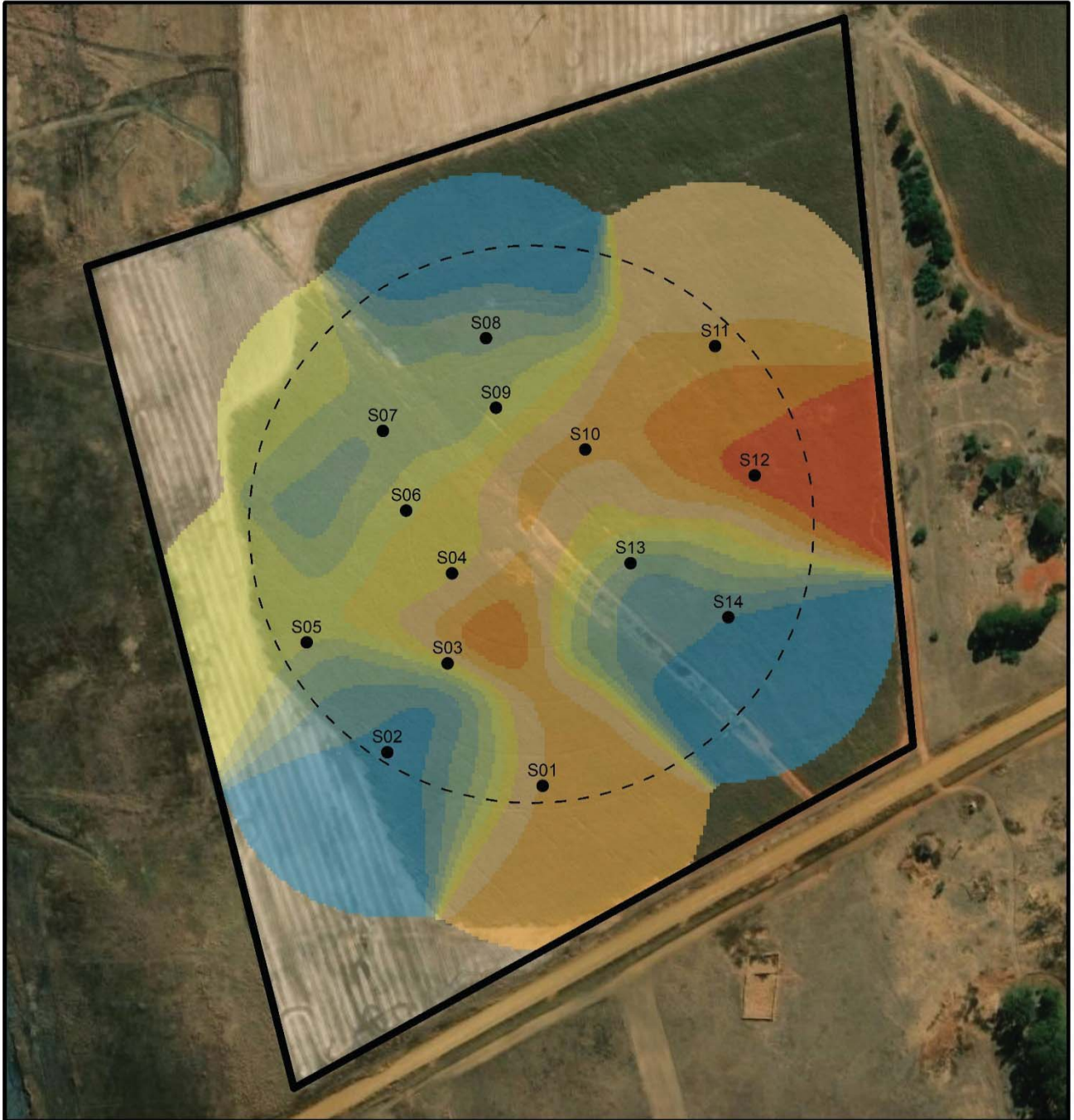


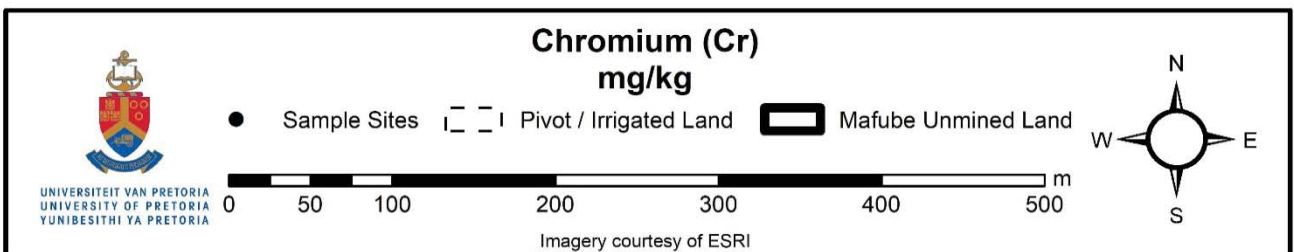
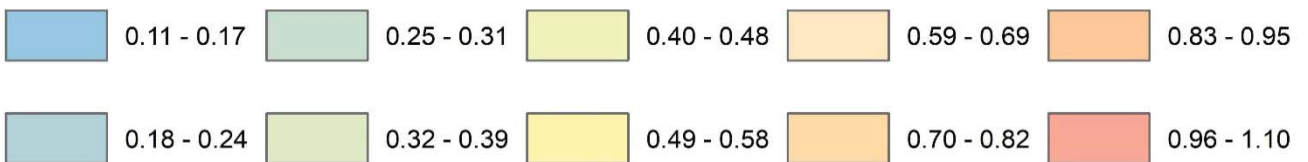
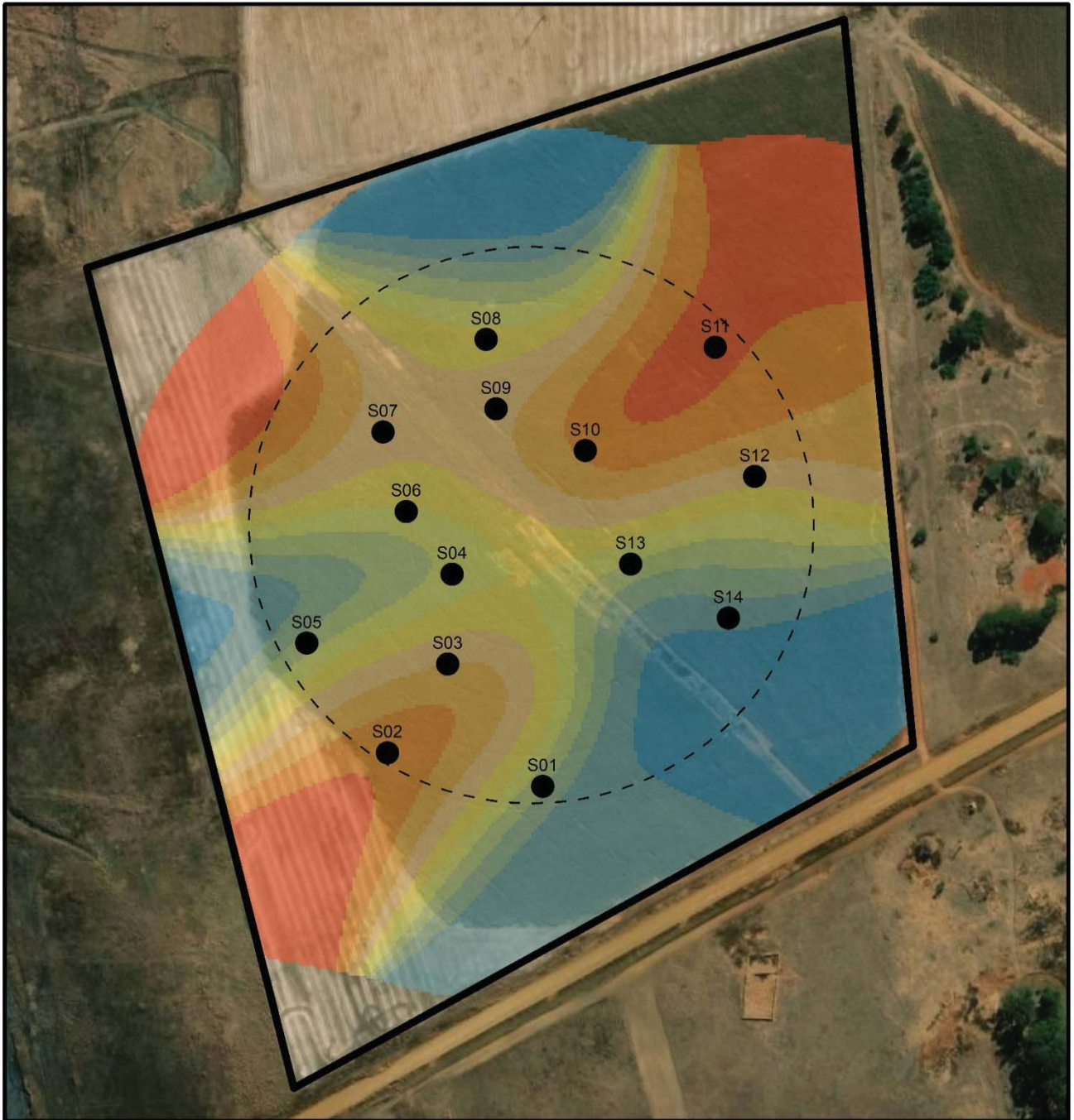


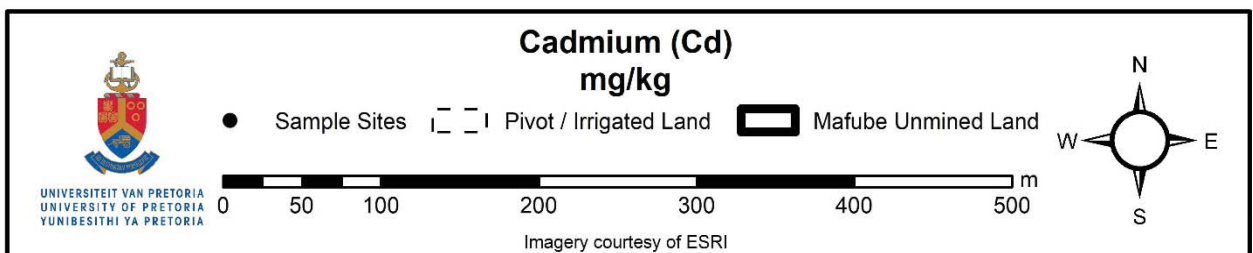
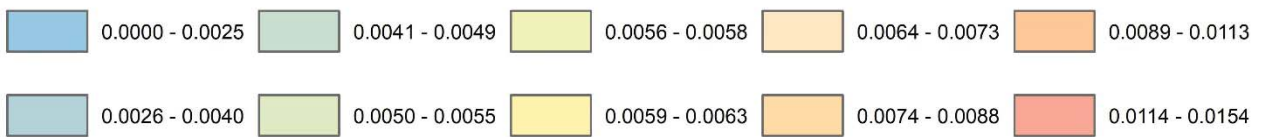
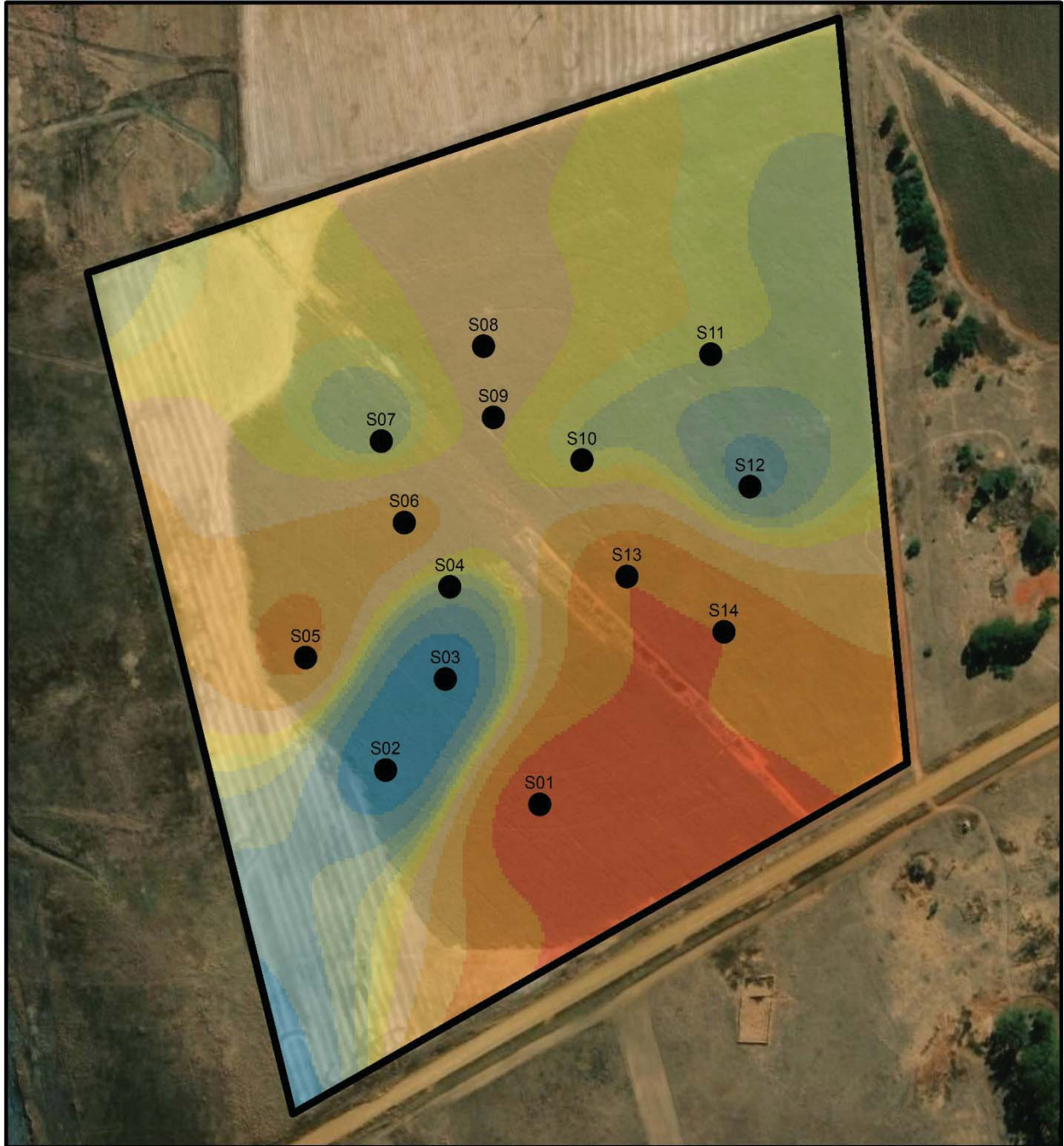












**APPENDIX A4: Soil-water balance simulations**

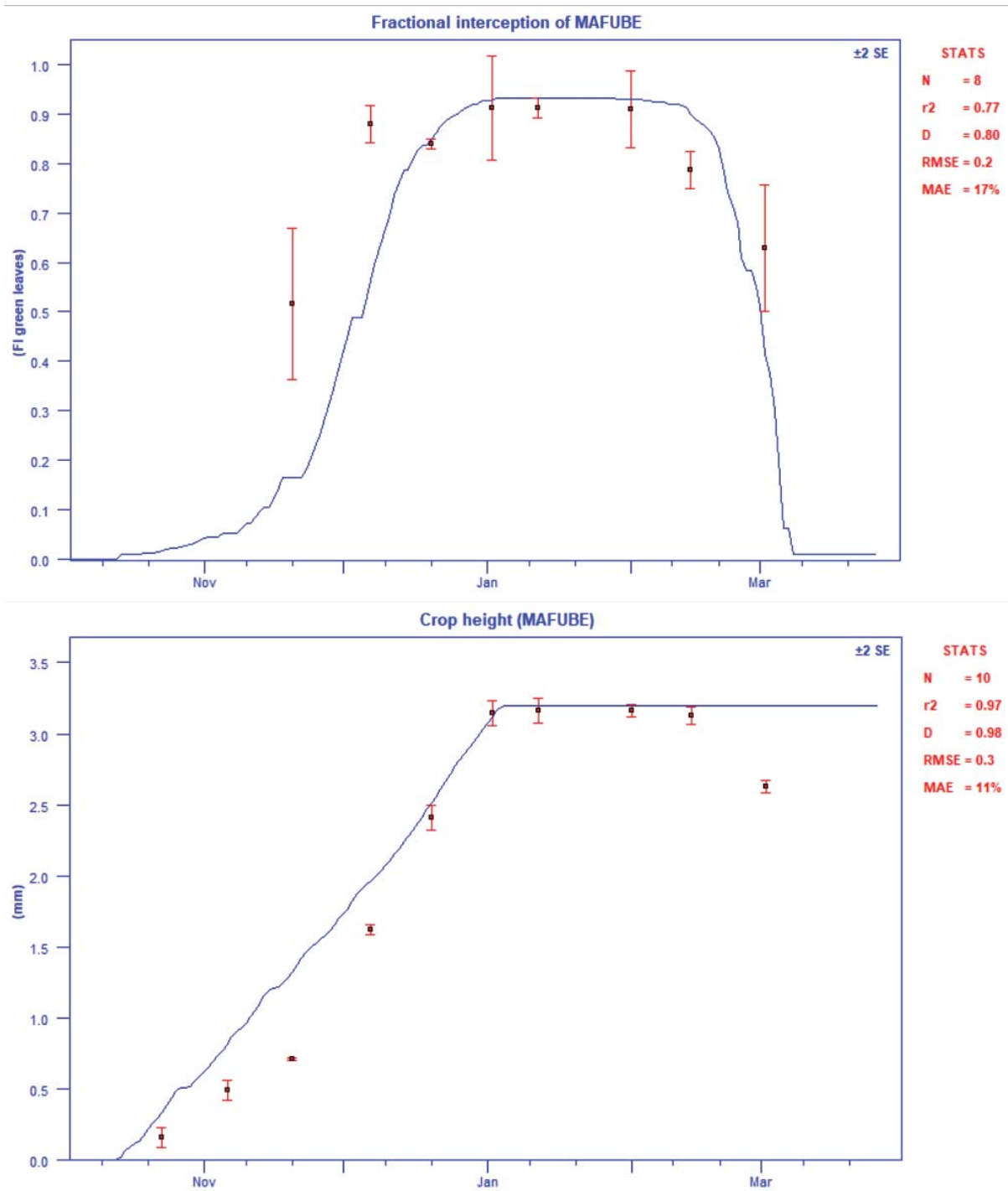


Figure A4:1: Measured (symbols) and simulated (lines) fractional interception (top), and crop height (bottom) simulating the effect of saline mine water irrigation

**Note:** N = Number of observations; r<sup>2</sup> = Coefficient of determination; D = Willmott's (1982) Index of Agreement; RMSE = Root mean square error; MAE = Mean absolute error

Table A4.1: SAWQI decision support system (DSS) – Tier 1 results

**Irrigation Water Fitness-for-Use (Tier 1)**

Sample identification:	45: Mafube Unmined Pivot - Irrigation Water
Site description:	45: Generic using conservative assumptions

**Water Analysis**

Major constituents (mg/L)					
Calcium	221.0		Bicarbonate	250.0	
Magnesium	130.0		Chloride	22.0	
Sodium	54.0		Sulphate	965.0	
pH	7.8		Total Dissolved Solids (TDS)	1642.0	
Electrical Conductivity (mS/m)	215.0		Suspended Solids (SS)	120.0	
SAR (mol/L) <sup>0.5</sup>	0.7		Charge balance error: -0.1%		TDS / EC: 7.64
Biological Constituents			Nutrients (mg/L)		
E. coli (counts/100 mL)			Total inorganic nitrogen (N) 2.2		
Chemical Oxygen Demand (mg/L)			Total inorganic phosphorous (P) 1.2		
			Total inorganic potassium (K) 28.0		
Pesticides (µg/L)					
Atrazine					
Trace Elements in irrigation water (µg/L) and soil (mg/kg)					
	Water	Soil		Water	Soil
Aluminium	315	0	Lead		0
Arsenic		0	Lithium		0
Beryllium		0	Manganese	1125	0
Boron		0	Mercury		0
Cadmium		0	Molybdenum		0
Chromium		0	Nickel		0
Cobalt		0	Selenium		0
Copper		0	Uranium		0
Fluoride	480	0	Vanadium		0
Iron	160	0	Zinc	90	0

**Tier 1: Fitness-for-Use  
Soil Quality**

Soil profile salinity	Fitness-for-use	ECe (mS/m)	Predicted equilibrium soil profile salinity (mS/m)
	Ideal	0 - 200	
	Acceptable	200 - 400	
	Tolerable	400 - 800	404
	Unacceptable	> 800	

Soil Permeability	Fitness-for-use	Degree of reduced Permeability	Qualitative indication of the impact on soil permeability as manifested by reduced:	
			Surface Infiltrability	Soil Hydraulic Conductivity
	Ideal	None		None
	Acceptable	Slight	Slight	
	Tolerable	Moderate		
Unacceptable	Severe			

Oxidisable Carbon Loading	Fitness-for-use	COD Load (kg/ha per month)	Chemical Oxygen Demand (COD) Load (kg/ha per month)
	Ideal	0 - 400	No data
	Acceptable	400 - 1000	
	Tolerable	1000 - 1600	
	Unacceptable	>1600	

Trace Element Accumulation	Fitness-for-use		Number of years of 1000 mm irrigation before Trace Elements reach accumulation threshold in topsoil			
	Ideal		> 200 years to reach soil accumulation threshold			
	Acceptable		150 to 200 years to reach soil accumulation threshold			
	Tolerable		100 to 150 years to reach soil accumulation threshold			
	Unacceptable		< 100 years to reach soil accumulation threshold			
	Trace Element	Soil Accumulation Threshold (mg/kg)	No of years to reach Soil Accumulation Threshold	Trace Element	Soil Accumulation Threshold (mg/kg)	No of years to reach Soil Accumulation Threshold
	Al	2500	> 1000	Li	1250	No data
	As	50	No data	Mn	100	18
	Be	50	No data	Hg	1	No data
	Cd	5	No data	Mo	5	No data
	Cr	50	No data	Ni	100	No data
	Co	25	No data	Se	10	No data
	Cu	100	No data	U	5	No data
F	1000	417	V	50	No data	
Fe	2500	> 1000	Zn	500	> 1000	
Pb	100	No data				

**Tier 1: Fitness-for-Use**  
Yield and Quality of a Generic Sensitive Crop with 1000 mm irrigation p.a.

Root Zone Effects	Fitness-for-use	Relative crop yield (%)	Predicted relative crop yield (%) as affected by:			
			Salinity (EC)	Boron (B)	Chloride (Cl)	Sodium (Na)
	Ideal	90 - 100		No data	100	100
	Acceptable	80 - 90				
	Tolerable	70 - 80				
	Unacceptable	<70	0			

Leaf scorching when wetted	Fitness-for-use	Degree of leaf scorching	Degree of leaf scorching under sprinkler irrigation caused by:	
			Chloride (Cl)	Sodium (Na)
	Ideal	None	None	
	Acceptable	Slight		Slight
	Tolerable	Moderate		
	Unacceptable	Severe		

Contribution to NPK removal by generic sensitive crop	Fitness-for-use	Contribution to estimated N P K Removal by crop	% of estimated N P K removal at harvest and amount that is applied through irrigation (High nutrient concentrations may impact development of sensitive crops)					
			Nitrogen (N)		Phosphorous (P)		Potassium (K)	
			Removal (%)	Applied (kg/ha)	Removal (%)	Applied (kg/ha)	Removal (%)	Applied (kg/ha)
	Ideal	0 - 10%						
	Acceptable	10 - 30%						
	Tolerable	30 - 50%	44	22				
	Unacceptable	>50%			120	12	2800	280

Microbial Contamination	Fitness-for-use	Excess infections per 1000 persons p.a.	Predicted excess infections per 1000 people p.a.
	Acceptable	1 - 3	
	Tolerable	3 - 10	
	Unacceptable	>10	

Qualitative Atrazine Damage	Fitness-for-use	Atrazine load (g/ha)	Estimated Atrazine load (g/ha)
	Acceptable	50 - 75	
	Tolerable	75 - 100	
	Unacceptable	>100	

**Tier 1: Fitness-for-Use**  
Irrigation Equipment

Corrosion or Scaling of Irrigation Equipment				
Fitness-for-use	Fitness for Use Category determined by the corrosion or scaling potential indicated by the Langelier Index			
	Corrosion (Langelier Index)		Scaling (Langelier Index)	
Ideal	-0.5 to 0	Not Corrosive	0 to +0.5	
Acceptable	-0.5 to -1.0		+0.5 to +1.0	0.85
Tolerable	-1.0 to -2.0		+1.0 to +2.0	
Unacceptable	<-2.0		>+2.0	

Clogging of Drippers										
Fitness-for-use	Fitness for Use Category determined by the potential of a constituent to cause clogging of drippers									
	Suspended Solids (mg/L)		pH		Manganese (Mn) (mg/L)		Total Iron (Fe) (mg/L)		<i>E. coli</i> (10 <sup>6</sup> per 100 mL)	
Ideal	<50		<7.0		<0.1		<0.2	0.2	<1	No data
Acceptable	50 - 75		7.0 - 7.5		0.1 - 0.5		0.2 - 0.5		1 - 2	
Tolerable	75 - 100		7.5 - 8.0	7.8	0.5 - 1.5	1.1	0.5 - 1.5		2 - 5	
Unacceptable	>100	120	>8.0		>1.5		>1.5		>5	

Table A4:2: SAWQI DSS – Tier 2 results

## Irrigation Water Fitness-for-Use (Tier 2)

Sample identification:	44: Mafube Unmined Pivot Irrigation water
Site description:	47: Mafube Unmined Pivot - White Maize-Wheat Rotation

## Water Analysis

Major constituents (mg/L)					
Calcium	221.0		Bicarbonate	250.0	
Magnesium	129.0		Chloride	21.0	
Sodium	55.0		Sulphate	963.0	
pH	7.8		Total Dissolved Solids (TDS)	1639.0	
Electrical Conductivity (mS/m)	214.0		Suspended Solids (SS)	28.0	
SAR (mol/L) <sup>0.5</sup>	0.7		Charge balance error: 0.1%		TDS / EC: 7.66
Biological Constituents			Nutrients (mg/L)		
E. coli (counts/100 mL)			Total inorganic nitrogen (N)		
Chemical Oxygen Demand (mg/L)			Total inorganic phosphorous (P)		
			Total inorganic potassium (K)		
Pesticides (µg/L)					
Atrazine					
Trace Elements in irrigation water (µg/L) and soil (mg/kg)					
	Water	Soil		Water	Soil
Aluminium	312	0	Lead		0
Arsenic		0	Lithium		0
Beryllium		0	Manganese	1123	0
Boron		0	Mercury		0
Cadmium		0	Molybdenum		0
Chromium		0	Nickel		0
Cobalt		0	Selenium		0
Copper		0	Uranium		0
Fluoride	480	0	Vanadium		0
Iron	157	0	Zinc	86	0

## Site Specific Characteristics

Crop		Soil	
Summer crop	Maize (Corn)	Soil texture	Sandy loam
Plant date (DD/MM)	1/10	Soil depth (m)	2.0
Winter crop	Wheat	Initial water content	Wet (FC)
Plant date (DD/MM)	1/5	Profile available water (mm)	240
Irrigation management		Plant available water (mm/m)	120
Irrigation system	Overhead	Field capacity (m/m)	0.22
Irrigation timing	Amount (mm) 10	Wilting point (m/m)	0.10
Refill option	Field capacity	Bulk density (Mg/m <sup>3</sup> )	1.40
<b>Weather station</b>	GEMSBOKFONTEIN (45 years)	MAP (mm)	723

## Water Balance

Water balance components	Maize (Corn)	Wheat
Mean seasonal irrigation (mm)	415	692
Mean seasonal rainfall (mm)	662	62
Mean seasonal evaporation (mm)	329	349
Mean seasonal transpiration (mm)	469	386
Mean seasonal evapotranspiration (mm)	798	735
Mean seasonal drainage (mm)	279	18
Effective seasonal leaching fraction (%)	25.9	2.4
Effective annual leaching fraction (%)		16.2

Version: 28 Jan 2021

**Tier 2: Fitness-for-Use**  
Soil Quality of a Sandy loam soil with 447 mm irrigation p.a.

Soil profile salinity	Fitness-for-use	ECe (mS/m)	% of time soil profile salinity is predicted to fall within a particular Fitness-for-use category
	Ideal	0 - 200	100
	Acceptable	200 - 400	
	Tolerable	400 - 800	
	Unacceptable	> 800	

Soil Permeability	Fitness-for-use	Degree of reduced Permeability	% of time soil permeability is predicted to fall within a particular Fitness-for-use category	
			Surface Infiltrability	Soil Hydraulic Conductivity
	Ideal	None	80	95
	Acceptable	Slight	20	3
	Tolerable	Moderate		2
Unacceptable	Severe		1	

Oxidisable Carbon Loading	Fitness-for-use	COD Load (kg/ha per month)	% of time Chemical Oxygen Demand (COD) Load is predicted to fall within a particular Fitness-for-use category
	Ideal	0 - 400	No data
	Acceptable	400 - 1000	
	Tolerable	1000 - 1600	
	Unacceptable	>1600	

Trace Element Accumulation	Fitness-for-use		Number of years of 447 mm irrigation before Trace Elements reach accumulation threshold in topsoil			
	Ideal		> 200 years to reach soil accumulation threshold			
	Acceptable		150 to 200 years to reach soil accumulation threshold			
	Tolerable		100 to 150 years to reach soil accumulation threshold			
	Unacceptable		< 100 years to reach soil accumulation threshold			
	Trace Element	Soil Accumulation Threshold (mg/kg)	No of years to reach Soil Accumulation Threshold	Trace Element	Soil Accumulation Threshold (mg/kg)	No of years to reach Soil Accumulation Threshold
	Al	2500	> 1000	Li	1250	No data
	As	50	No data	Mn	100	40
	Be	50	No data	Hg	1	No data
	Cd	5	No data	Mo	5	No data
	Cr	50	No data	Ni	100	No data
	Co	25	No data	Se	10	No data
	Cu	100	No data	U	5	No data
	F	1000	932	V	50	No data
	Fe	2500	> 1000	Zn	500	> 1000
Pb	100	No data				

**Tier 2: Fitness-for-Use**  
Yield and Quality of a Maize (Corn) crop with 447 mm irrigation per season

Root Zone Effects	Fitness-for-use	Relative crop yield (%)	% of time yield is within relative crop yield category, as affected by:			
			Salinity (EC)	Boron (B)	Chloride (Cl)	Sodium (Na)
Ideal	90 - 100	100	No data	100	100	
Acceptable	80 - 90					
Tolerable	70 - 80					
Unacceptable	<70					

Leaf scorching when wetted	Fitness-for-use	Degree of leaf scorching	Degree of leaf scorching under sprinkler irrigation caused by:	
			Chloride (Cl)	Sodium (Na)
Ideal	None	None	None	None
Acceptable	Slight			
Tolerable	Moderate			
Unacceptable	Severe			

Contribution to NPK removal	Fitness-for-use	Contribution to estimated N P K Removal by crop	Mean applied N P K at harvest and % of time N P K removal at harvest is within fitness-for-use categories (High nutrient concentrations may impact development of sensitive crops)					
			Nitrogen (N)		Phosphorous (P)		Potassium (K)	
			Time (%)	Applied (kg/ha)	Time (%)	Applied (kg/ha)	Time (%)	Applied (kg/ha)
Ideal	0 - 10%	100	10	78	5			
Acceptable	10 - 30%			22	6			
Tolerable	30 - 50%							
Unacceptable	>50%					100	125	

Microbial Contamination	Fitness-for-use	Excess infections per 1000 persons p.a.	Predicted excess infections per 1000 people p.a.
			Ideal
Acceptable	1 - 3		
Tolerable	3 - 10		
Unacceptable	>10		

Qualitative Atrazine Damage	Fitness-for-use	Atrazine load (Maize, SaLm) (g/ha)	% of time Atrazine load is predicted to fall within particular fitness-for-use category
			Ideal
Acceptable	900 - 1300		
Tolerable	1300 - 1800		
Unacceptable	>1800		

**Tier 2: Fitness-for-Use**  
Irrigation Equipment

Corrosion or Scaling of Irrigation Equipment				
Fitness-for-use	Fitness for Use Category determined by the corrosion or scaling potential indicated by the Langelier Index			
	Corrosion (Langelier Index)		Scaling (Langelier Index)	
Ideal	0 to -0.5	Not Corrosive	0 to +0.5	
Acceptable	-0.5 to -1.0		+0.5 to +1.0	0.85
Tolerable	-1.0 to -2.0		+1.0 to +2.0	
Unacceptable	<-2.0		>+2.0	

Clogging of Drippers										
Fitness-for-use	Fitness for Use Category determined by the potential of an irrigation water constituent to cause clogging of drippers									
	Suspended Solids (mg/L)		pH		Manganese (Mn) (mg/L)		Total Iron (Fe) (mg/L)		<i>E.coli</i> (10 <sup>6</sup> per 100 mL)	
Ideal	<50		<7.0		<0.1		<0.2	0.2	<1	No data
Acceptable	50 - 75		7.0 - 7.5		0.1 - 0.5		0.2 - 0.5		1 - 2	
Tolerable	75 - 100		7.5 - 8.0	7.8	0.5 - 1.5	1.1	0.5 - 1.5		2 - 5	
Unacceptable	>100	120	>8.0		>1.5		>1.5		>5	

**APPENDIX A5: Mafube rehabilitated land***Table A5.1: Rehabilitated site sampling point coordinates and depth to spoil layer, pre-infilling (2018)*

<b>Mark</b>	<b>Coordinates</b>		<b>Depth to spoil (cm)</b>
A	S 25°47.498	E 029°45.891	120
B	S 25°47.439	E 029°45.945	85
C	S 25°47.490	E 029°45.953	110
D	S 25°47.541	E 029°45.957	125
E	S 25°47.368	E 029°45.998	37
F	S 25°47.420	E 029°46.005	32
G	S 25°47.484	E 029°46.007	72
H	S 25°47.476	E 029°46.076	120
I	S 25°47.472	E 029°46.139	116
J	S 25°47.430	E 029°46.085	92
K	S 25°47.539	E 029°46.008	96
L	S 25°47.526	E 029°46.079	132
M	S 25°47.593	E 029°46.014	105
N	S 25°47.558'	E 29°46.002'	128
O	S 25°47.513'	E 29°46.006'	98
P	S 25°47.475'	E 29°46.082'	124
Q	S 25°47.506'	E 29°46.039'	60
R	S 25°47.487'	E 29°45.977'	77
S	S 25°47.506'	E 29°45.922'	125
T	S 25°47.455'	E 29°45.999'	60
U	S 25°47.423'	E 29°46.030'	42
V	S 25°47.433'	E 29°45.968'	47
W	S 25°47.400'	E 29°45.998'	70



Figure A5:1: Map of rehabilitated site indicating sampling points and depth of profile

## APPENDIX A6: Kromdraai irrigation system design

<b>WRC IRRIGATION PROJECT</b>
<b>KROMDRAAI MINE, WITBANK</b>
<b>DESIGN DATA &amp; BUDGET COSTING VER 6</b>

NR	DESCRIPTION	UNIT	QUANTITY	ALG	1	2	3	4
					blue	red	green	
	<b>IN-BLOCK:</b>							
1.01	Vyrsa 66 Plastic Sprinklers, with 3.96 x 2.38mm nozzles	unit	12		4	4	4	
1.02	Vyrsa 66 Plastic Sprinklers, with 3.96 x 2.38mm nozzles	unit	24		8	8	8	
1.03	Vyrsa 36 Plastic Sprinklers, with 3.96 x 2.38mm nozzles	unit	12		4	4	4	
1.04	Camlock, Type D, Female Coupler x Female BSP, 20mm	unit	48		48			
1.05	Camlock, Type A, Male Adaptor x Female BSP, 20mm	unit	48		48			
1.06	Polyprop Reducing Hex Nipple, 25 x 20mm BSP	unit	48		48			
1.07	Polyprop Male Adaptor, 25mm x 25 M-BSP	unit	96		96			
1.08	LDPE Pipe, Class 6, 25mm	100m Roll	2		120			
1.09	Stainless Steel Pipe Clamp, 17 - 38mm	unit	96		96			
1.10	PTFE Thread Sealing Tape, 19mm x 10m	unit	16		16			
1.11	25mm Black Steel Socket	unit	48		48			
1.12	25mm x 6mm Flatbar	6,1m	1		1			
1.13	Y-Section Fence Droppers, 2450mm length	unit	48		48			
1.14	Fabrication of Sprinkler Risers	unit	48		48			
1.15	Plastic Saddle, 32mm x 25mm BSP	unit	23	2	2	3	2	
1.16	Plastic Saddle, 40mm x 25mm BSP	unit	23	2	2	4	1	
1.17	Plastic Saddle, 50mm x 25mm BSP	unit	20	2		3	3	
1.18	Compression Male Adator & Ball-Lock Valve, 32mm x 25BSP	unit	23	2	2	3	2	
1.19	Compression Straight Coupling, 32mm	unit	6	6				
1.20	Compression Straight Coupling, 40mm	unit	6	6				
1.21	Compression Straight Coupling, 50mm	unit	3	3				
1.22	Compression Elbow, 32mm	unit	2	2				
1.23	Compression Elbow, 40mm	unit	14	2	1	2	1	
1.24	Compression Elbow, 50mm	unit	11	2		1	2	
1.25	Compression Reducer, 40 x 32mm	unit	20	2	2	3	1	
1.26	Compression Reducer, 50 x 32mm	unit	5	2			1	
1.27	Compression Reducer, 50 x 40mm	unit	5	2		1		

Irrigation with poor-quality mine water in Mpumalanga

NR	DESCRIPTION	UNIT	QUANTITY	ALG	1	2	3	4
1.28	Compression Equal Tee, 40mm	unit	5	2	1			
1.29	Compression Equal Tee, 50mm	unit	5	2		1		
1.30	Compression Reducing Tee, 40 x 32mm	unit	11	2		3		
1.31	Compression Reducing Tee, 50 x 32mm	unit	2	2				
1.32	Compression Reducing Tee, 50 x 40mm	unit	11	2		2	1	
1.33	HDPE Pipe, SDR17, PN10, 32mm	100m Roll	5		80	42	28	
1.34	HDPE Pipe, SDR17, PN10, 40mm	100m Roll	5		44	82	14	
1.35	HDPE Pipe, SDR17, PN10, 50mm	100m Roll	3			32	32	
<b>VALVE CLUSTERS:</b>								
1.36	Compression Male Adaptor, 40mm x 40 BSP	unit	5	2	1			
1.37	Compression Male Adaptor, 50mm x 40 BSP	unit	8	2		1	1	
1.38	Netafim Control Valve with Plastic 3-Way selector - S 75 PP 2" H BSP MAN 3WNC S	unit	9		1	1	1	
1.39	Compression Male Threaded Tee, 50mm x 40 BSP	unit	3		1			
1.40	Compression Male Threaded Elbow, 50mm x 40 BSP	unit	6		2			
1.41	Compression Female Threaded Tee, 50mm x 50 BSP	unit	3		1			
1.42	Compression Reducing Male Adaptor, 75mm x 50 BSP	unit	3		1			
<b>WATER METERS:</b>								
1.43	Arad 40 mm Multi - Jet Water meter with EV -10 l	unit	3		1	1	1	
1.44	Polyprop Reducing Bush, 50 x 40mm	unit	6		2	2	2	
1.45	Compression Female Adaptor, 75mm x 50 BSP	unit	6		2	2	2	
<b>FLUSHING CONNECTIONS:</b>					<u>Inter</u>	<u>Away</u>		
1.46	Compression Female Threaded Reducing Tee, 75mm x 50 BSP	unit	3		2	1		
1.47	Polyprop Barrel Nipple, 50mm	unit	4		2	2		
1.47	Netafim Control Valve with Plastic 3-Way selector - S 75 PP 2" H BSP MAN 3WNC S	unit	2		1	1		
1.48	Compression Female Adaptor, 75mm x 50 BSP	unit	1			1		
<b>SUB-TOTAL (excluding 15% VAT)</b>								
<b>2</b>	<b><u>MAIN LINES &amp; PUMPS</u></b>							
<b>MAIN LINE:</b>								
2.01	HDPE Pipe, SDR17, PN10, 75mm	50m Roll	32	45.99	660	652	221	

Irrigation with poor-quality mine water in Mpumalanga

NR	DESCRIPTION	UNIT	QUANTITY	ALG	1	2	3	4
2.02	Compression Straight Coupling, 75mm	unit	35	3	32			
2.03	Plastic Saddle, 75mm x 50mm BSP	unit	3		1	1	1	
2.04	Double Air Valve, 50mm BSP	unit	3		1	1	1	
	<b>SUCTION SIDE: (ALL SYSTEMS)</b>							
2.05	Compression Male Adaptor, 75mm x 80 BSP	unit	3		1	1	1	
2.06	Compression Male Adaptor, 75mm x 50 BSP	unit	3		1	1	1	
2.07	PVC Full Face Threaded Flange, PN16, 50mm	unit	3		1	1	1	
2.08	M16 x 55mm Galv Hex Bolts & Nuts	unit	12		4	4	4	
2.09	50mm IR Rings	unit	6		2	2	2	
	<b>PUMPS:</b>							
2.10	CRI MVS-16/05T Vertical Pump Unit, 5.5kW Motor	unit	1		1			
	- Inlet/Outlet: 50mm T16							
2.11	CRI MVS-16/07T Vertical Pump Unit, 7.5kW Motor	unit	2			1	1	
	- Inlet/Outlet: 50mm T16							
2.12	Starter, USB with Blackbox Protection, 5.5kW	unit	1		1			
2.13	Starter, USB with Blackbox Protection, 7.5kW	unit	2			1	1	
	<b>DELIVERY SIDE: (ALL SYSTEMS)</b>							
2.14	PVC Full Face Threaded Flange, PN16, 50mm	unit	3		1	1	1	
2.15	Polyprop Hex Barrel Nipple, 50mm BSP	unit	9		3	3	3	
2.16	Tommy PVC Threaded Compact Ball Valve, 50mm BSP	unit	3		1	1	1	
2.17	Tommy PVC Threaded Check Valve, 50mm	unit	3		1	1	1	
2.18	Compression Male Adaptor, 75mm x 80 BSP	unit	3		1	1	1	
2.19	M16 x 55mm Galv Hex Bolts & Nuts	unit	12		4	4	4	
2.20	50mm IR Rings	unit	6		2	2	2	
	<b>FLUSHING AT PUMP:</b>							
2.21	Compression Female Threaded Tee, 75mm x 80 BSP	unit	1		1			
2.22	PVC Reducer Male x Female Threaded, 3" x 2"	unit	1		1			
2.23	Polyprop Hex Barrel Nipple, 50mm BSP	unit	1		1			
2.23	Netafim Control Valve with Plastic 3-Way selector	unit	1		1			
	- S 75 PP 2" H BSP MAN 3WNC S							
2.24	Compression Male Adaptor, 75mm x 50BSP	unit	1		1			
2.25	Compressio Elbow, 75mm x 90°	unit	2		2			
	<b>PRESSURE RELIEF:</b>							
2.26	Compression Female Threaded Tee, 75mm x 50 BSP	unit	3		1	1	1	
2.27	Mipel Pressure Relief Valve, 50mm BSP x 10 Bar	unit	3		1	1	1	
2.28	PTFE Thread Sealing Tape, 19mm x 10m	unit	60		20	20	20	

Irrigation with poor-quality mine water in Mpumalanga

NR	DESCRIPTION	UNIT	QUANTITY	ALG	1	2	3	4
	<b>CONTROL SYSTEM: IRRIGATION AND SYSTEM FLUSHING</b>							
2.29	Galcon CSI 24AC radio control system, inclusive of	unit	1		1			
	- Internet/remote based programmable							
	- 3 x Control computers							
	- 3 x Transmitters, Relays, Solenoids							
	- Steel Enclosures							
	- Installation, Travelling & Expenses							
	- Field comissioning after installation							
2.30	General procurement cost - Irrigation Unlimited	unit	1					
2.31	Delivery on site	unit	1					
	<b>SUB-TOTAL (excluding 15% VAT)</b>							

<b>SUB-TOTAL</b>	<b>R</b>	<b>-</b>
<b>+ 15% VAT</b>	<b>R</b>	<b>-</b>
<b>TOTAL</b>	<b>R</b>	<b>-</b>

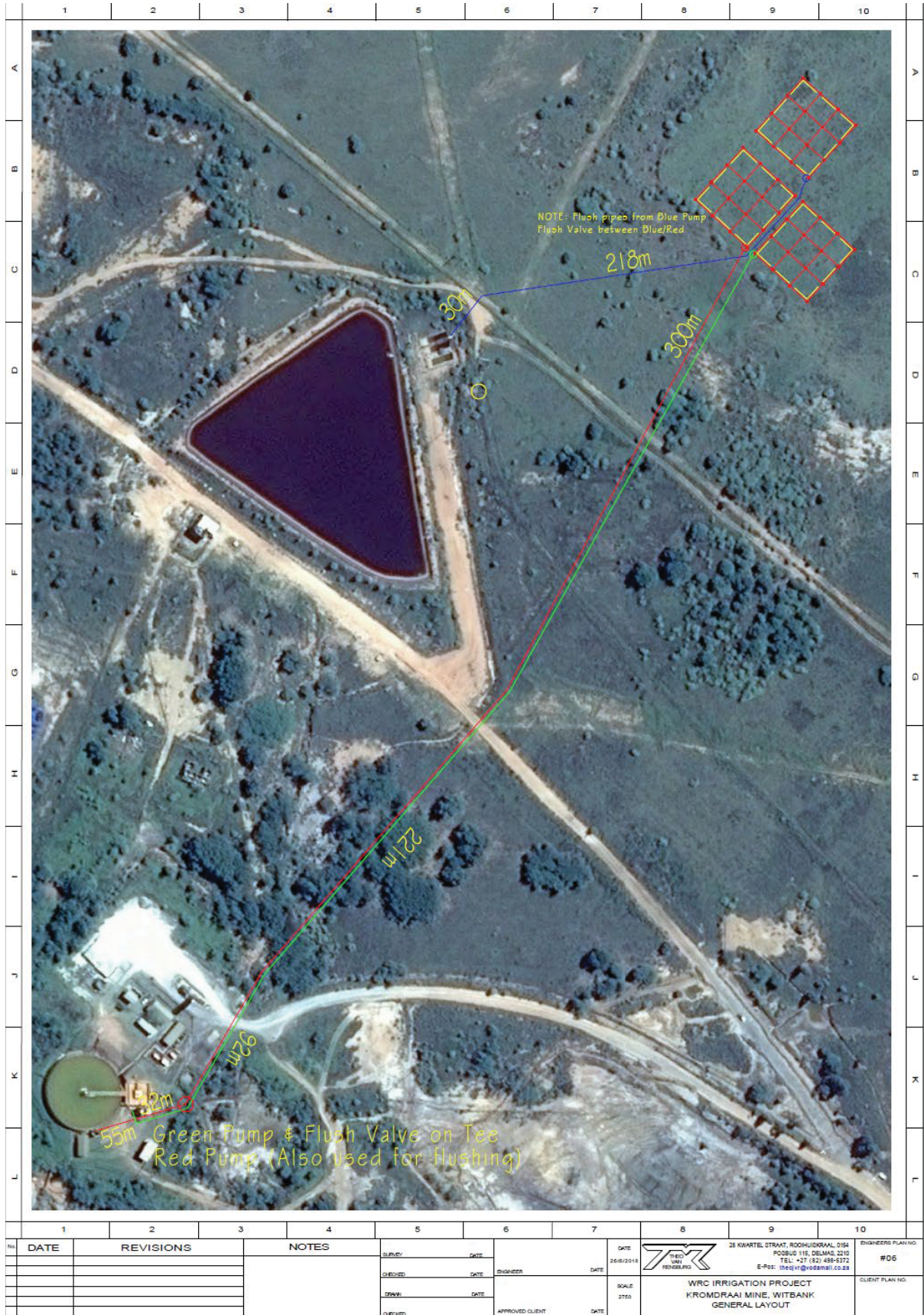


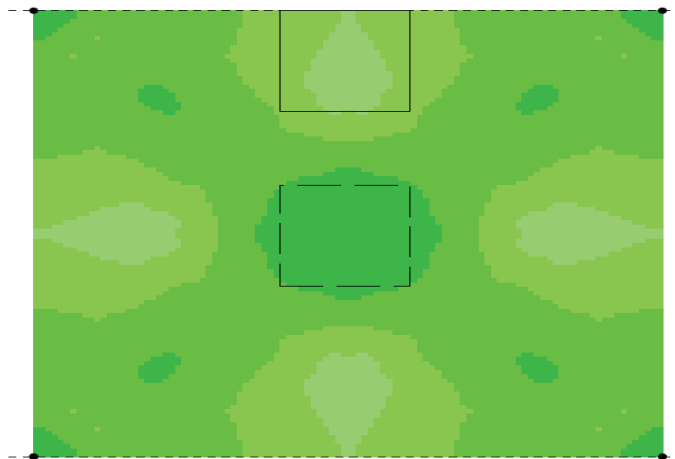
Figure A6:1: Irrigation design layout

Irrigation uniformity evaluation

### Uniformity Evaluation

<b>Sprinkler Name</b>	VYRSA	<b>Base Pressure (KPA)</b>	344.8
<b>Sprinkler Model</b>	VYR66	<b>Riser Height (CM)</b>	30.5
<b>Nozzle Size</b>	4mm x 2.4mm P/C	<b>Set Screw Setting</b>	
<b>Flow Rate (LPM)</b>	23.09	<b>Degree of Arc</b>	360
<b>Date/Time of Test</b>	06/20/02 07:18	<b>Mins./Revolution</b>	0.84
<b>Testing Facility</b>	C. I. T.	<b>Record Number</b>	2911-P
<b>Comment</b>	Sprinkler provided by: VALPLASTIC		

<b>Distr. Uniformity</b>	85%	<b>Min (mm/Hr)</b>	5.0	<b>Spacing</b>	Rectangular
<b>CU (Christiansen)</b>	91%	<b>Mean (mm/Hr)</b>	6.6 6.2 (Theor.)		15.0M x 15.0M
<b>Sched Coeff (5%)</b>	1.2	<b>Max (mm/Hr)</b>	8.4		



## APPENDIX A7: South African and international hazardous waste classification systems

### *Systems using total and soluble concentrations to classify wastes*

#### *Republic of South Africa (RSA) Guidelines*

The South African guidelines consider 20 constituents, with six of them (Mn, Sb, V, Cl, SO<sub>4</sub>, NO<sub>3</sub>) appearing only in this system (Department of Environmental Affairs, 2008; Costley, 2013; Department of Water Affairs and Forestry, 1998). The guidelines compare the toxicity characteristic leaching procedure (TCLP) analysis of the material against leachable concentration thresholds (LCTs) (Table A7.1, summarised in Figure A7.1). These thresholds are divided into LCT0 (minimum threshold), LCT1 and LCT2 (intermediate thresholds) and LCT3 (the maximum threshold). According to Department of Environmental Affairs (2008) and Costley (2013) the LCT1 values were derived from the minimum values (LCT0) of the Standards for Human Health Effects for Drinking Water in South Africa by multiplying them by 50 (a generic dilution attenuation factor (DAF)). This factor was suggested by the Industrial Waste Resource Guidelines: Solid Industrial Waste Hazard Categorization and Management of June 2009. The LCT2 values were derived by doubling the LCT1 values, while the maximum threshold (LCT3) values were derived by multiplying the LCT2 values with a factor of 4 to raise the thresholds. This multiplication factor is also used by the Environment Protection Authority (EPA) of Australia, Victoria State, to calculate some of their thresholds from drinking water values.

The South African regulation further compares the total elemental analysis of the material against stipulated total concentration thresholds (TCTs). The TCTs are divided into TCT0 (minimum threshold), TCT1 (intermediate threshold) and TCT2 (maximum threshold). The TCT0 values were obtained from South African soil screening values that are protective of water resources, while the TCT1 values were derived from the land remediation values for commercial/industrial land determined by the Department of Environmental Affairs' Framework for the Management of Contaminated Land of March 2010. The TCT2 values were derived by multiplying the TCT1 values by a factor of 4 (Department of Environmental Affairs, 2008; Costley 2013). After the total and soluble concentrations of the waste have been compared to the various TCT and LCT levels, the waste is classified into one of five types, as outlined in Table A7.2.

*Table A7.1: Classification of waste according to the South African system (Department of Environmental Affairs, 2008; Costley, 2013; Department of Water Affairs and Forestry, 1998)*

<b>Element or chemical substance concentration</b>	<b>Waste type</b>	<b>Risk</b>	<b>Management</b>
LC > LCT3 or TC > TCT2	Type 0	Very high risk	Direct landfilling not allowed, needs to be treated first, reassessed/classified, needs structure with lining ( <sup>1</sup> H:H facility) for disposal to prevent leaching
LCT2 < LC ≤ LCT3 or TCT1 < TC ≤ TCT2	Type 1	High risk	Treatment not a prerequisite, needs a structure with lining ( <sup>1</sup> H:H facility) for disposal to prevent leaching
LCT1 < LC ≤ LCT2 and TC ≤ TCT1	Type 2	Moderate risk	Needs a structure with lining ( <sup>1</sup> H:H facility) for disposal to prevent leaching
LCT0 < LC ≤ LCT1 and TC ≤ TCT1	Type 3	Low risk	Leaching is not a major concern, as such a structure without lining ( <sup>2</sup> H:h facility) is used for disposal (can be explored for use in construction industry and agriculture)
LC ≤ LCT0 and TC ≤ TCT0	Type 4	Inert	A structure without lining ( <sup>2</sup> H:h facility) is used for disposal as leaching is not a major concern (can be explored for use in construction industry and agriculture)

<sup>1</sup>H:H = Hazardous waste landfill with lining to prevent leaching, can receive from 1 to 4 rated wastes; but  
<sup>2</sup>H:h = Hazardous waste landfill without lining to prevent leaching, can only receive 3 and 4 rated wastes

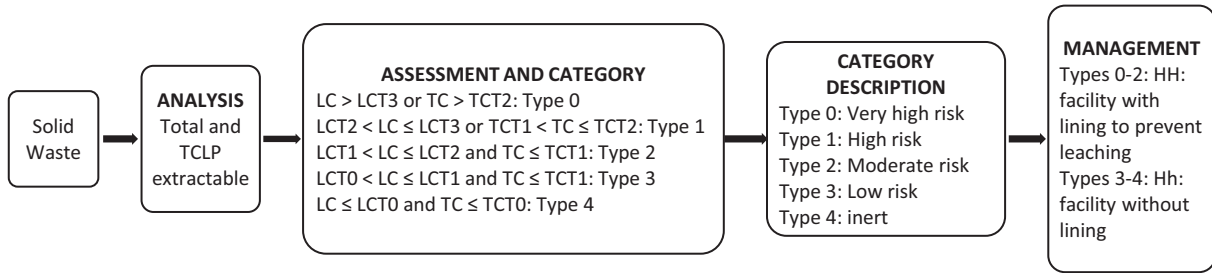


Figure A7.1: Simplified solid waste classification system of the Republic of South Africa

### Australian (New South Wales) Guidelines

The Australian Guidelines were considered as they are partially aligned to the national waste classification system that forms part of the Australian Waste Database. These guidelines consider a total of nine elements (Table A7.2) (New South Wales Environment Protection Authority (EPA), 2014). Some of these element limits (fluorine, molybdenum and nickel) were sourced from the Australian Drinking Water Guidelines of the National Health and Medical Research Council (NHMRC) (New South Wales EPA, 2000), but arsenic, cadmium, Cr(VI), lead and silver were adapted from the United States EPA (2012). The threshold for beryllium was calculated based on beryllium in The Health Risk Assessment and Management of Contaminated Sites. Waste is initially screened (first screening stage) by considering total content only (referred to as specific contaminant concentrations (SCC)) (Figure A7.2). In the case of general solid waste, i.e. putrescible (liable to decay), non-putrescible (equivalent to Type 3 and Type 4 of the South African system) the total concentration (TC) ≤ minimum SCC (SCC1). Restricted solid waste TC ≤ maximum SCC (SCC2)) refers to wastes that have the potential to pollute the environment (equivalent to Type 1 and Type 2 of the South African system). If the TC of a constituent exceeds SCC1, further assessment with the toxicity characteristic leaching procedure (TCLP) may be carried out, and if TC is equal to or exceed SCC2 thresholds, then a TCLP assessment (second screening stage) must be done. At the second screening, using both SCC and TCLP thresholds, final clarity on the status of the waste is obtained, i.e. if TC > SCC1. At the second screening, TCLP is divided into TCLP1 (minimum threshold) and TCLP2 (maximum threshold). Hazardous solid waste is equivalent to Type 0 of the South African system (Department of Water Affairs and Forestry, 1998). The application of this system for high-density sludge classification can be seen under the results section of Chapter 6.

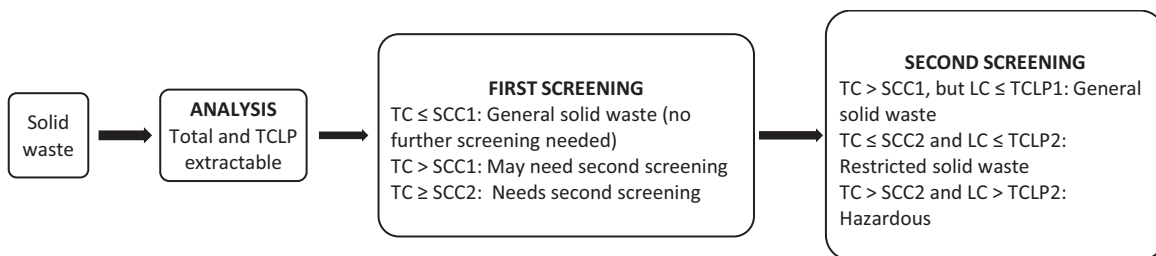


Figure A7.2: Simplified solid waste classification system for Australia (New South Wales)

Systems using only soluble concentrations of constituents to classify waste.

### The USA Guidelines

The US Environmental Protection Agency (EPA)'s Regulations are managed by the Resource Conservation and Recovery Act of 1976, which classifies waste based on hazardous properties. It considers eight elements (Table A7.3) of concern. These elements are considered to cause acute or chronic health effects via the groundwater route.

The consideration of these inorganic constituents was further facilitated by available and appropriate chronic toxicity reference levels (CTRLs) on which to base the calculation of thresholds. These elements also had adequate data for the fate and transport model used to establish element-specific dilution attenuation factors used to convert CTRLs to thresholds. Furthermore, these constituents have been shown to have toxic, carcinogenic, mutagenic or teratogenic effects (United States EPA, 1990). The main concern is the solubility of these constituents, and the only analysis performed is a TCLP extraction, after which the data is evaluated against threshold level (summarised in Figure A7.3).

The critical difference between the US EPA Guidelines and the other guidelines considered is that essential trace elements for plants or crops do not form part of their hazardous waste classification. These are boron, manganese, iron, zinc and copper. The US EPA Regulations, therefore, open the possibility for waste materials/by-products from industry and mining that have low solubilities of non-essential elements for plants and environmentally harmful constituents, to be considered for use in agriculture.

**Chinese and Canadian (Alberta, British Columbia, Ontario and Manitoba) Guidelines**

The Canadian and Chinese regulations also only require a toxicity characteristic leaching procedure (TCLP) extract, after which the data is compared against leachability thresholds (summarised in Figure A7.3). China adopted the US EPA Guidelines (Liu et al., 2015), except that they consider copper, nickel, beryllium and zinc in addition, but do not consider selenium (Table A7.3). Thresholds for all other elements, except for mercury in both guidelines (the Chinese and the US EPA Guidelines) are identical. The Canadian guidelines are also similar to those of the US EPA, except that, in addition, Alberta considers boron, cobalt, copper, nickel, iron, uranium and zinc. British Columbia considers boron, copper, uranium and zinc, while Ontario and Manitoba consider boron and uranium.

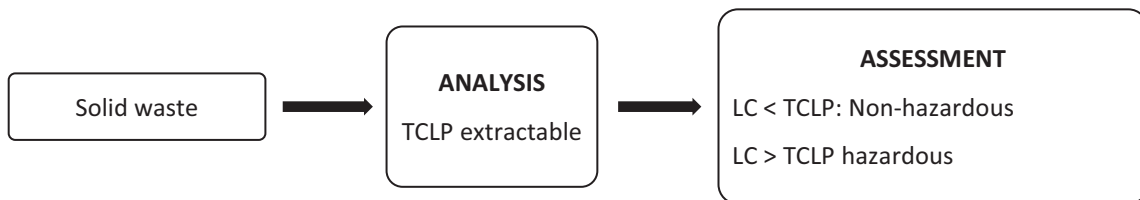


Figure A7.3: Simplified solid waste classification system for US EPA, China and Canada (Alberta, British Columbia, Ontario and Manitoba)

In summary, the South African system considers the most elements (20) and is the most stringent. Both the total elemental content (referred to as total concentration, determined by X-ray fluorescence (XRF)), and the solubility of the elements are assessed (referred to as leachable concentration). Five hazardous categories have been established (Types 0–4). Currently, all waste, including Type 4 (inert waste), must go to a managed storage facility. The Australian system has two screening levels. The first uses only total elemental content (referred to as specific contaminant concentration (SCC), divided into SCC1 and SCC2, determined by XRF. If the total elemental content of a waste exceeds SCC1 thresholds, further assessment against TCLP thresholds (second screening stage) may be carried out, but, if the total concentration exceeds SCC2 thresholds, then TCLP assessment must be done. A material can therefore be classified as a general, restricted or hazardous solid waste. With the US EPA, Canadian and Chinese guidelines, the main concern is the solubility of constituents in a waste, and as such, the approach adopted considers leachable concentration data that is evaluated against TCLP thresholds.

The elements considered by the various systems are summarised below (Table A7.3).

Table A7.1: Summary of elements considered by each system.

Constituent	South Africa	Australia (New South Wales)	Canada			US EPA	China
			Ontario and Manitoba	British Columbia	Alberta		
As	X	X				X	X
Ag		X	X	X	X	X	X
B	X		X	X	X		
Ba	X		X	X	X	X	X
Be		X					X
Cd	X	X	X	X	X	X	X
Co	X				X		
Cr	X	X	X	X	X	X	X
Cu	X			X	X		X
Fe					X		
Hg	X		X	X	X	X	X
Mn	X						
Mo	X	X					
Ni	X	X			X		X
Pb	X	X	X	X	X	X	X
Sb	X						
Se	X		X	X	X	X	
U			X	X	X		
V	X						
Zn	X			X	X		X
Cl	X						
SO <sub>4</sub>	X						
NO <sub>3</sub>	X						
F	X	X					
Total	20	9	9	11	14	8	11

## REFERENCES

- COSTLEY S (2013) Waste classification and management regulations and supporting norms and standards. Waste Khoro.  
[https://www.environment.gov.za/sites/default/files/docs/wasteclassification\\_regulations\\_disposalstandards.pdf](https://www.environment.gov.za/sites/default/files/docs/wasteclassification_regulations_disposalstandards.pdf).
- DEPARTMENT OF ENVIRONMENTAL AFFAIRS (2008) *National Environmental Management: Waste Act, Act No. 59 of 2008. Waste classification and management regulations*. DEA, Pretoria, South Africa.  
[https://www.environment.gov.za/sites/default/files/legislations/nemwa59of2008\\_wasteclassification.pdf](https://www.environment.gov.za/sites/default/files/legislations/nemwa59of2008_wasteclassification.pdf).
- DEPARTMENT OF WATER AFFAIRS AND FORESTRY (DWAF) (1998) *Waste management series: Minimum requirements for waste disposal by landfill, 2<sup>nd</sup> ed.*, DWAF, Pretoria, South Africa.  
<http://www.dwaf.gov.za/Documents/Other/WQM/RequirementsWasteDisposalLandfillSep05Part1.pdf>.
- LIU A, REN F, LIN WY and WANG JY (2015) A review of municipal solid waste environmental standards with a focus on incinerator residues. *International Journal of Sustainable Built Environment* **4** 165–188. DOI: 10.1016/j.ijbsbe.2015.11.002.
- NEW SOUTH WALES ENVIRONMENT PROTECTION AUTHORITY (EPA) (2000) ACT's Environmental Standards: Assessment & Classification of Liquid & Non-Liquid Wastes. URL: <http://www.act.gov.au/environ/> (accessed on 22 April 2018).
- UNITED STATES ENVIRONMENTAL PROTECTION AGENCY (EPA) (1990) Hazardous waste management system, identification and listing of hazardous waste, toxicity characteristics revisions. Federal Register, Rules and Regulations.

NEW SOUTH WALES ENVIRONMENT PROTECTION AUTHORITY (EPA) (2014) Waste classification guidelines. Part 1: Classifying waste. [www.epa.nsw.gov.au](http://www.epa.nsw.gov.au).

UNITED STATES OF AMERICA ENVIRONMENT PROTECTION AUTHORITY EPA (2012) Waste Classification Guidelines–Part 1: Classification of Waste. URL: <https://www.govinfo.gov/content/pkg/CFR-2012-title40-vol27/xml/CFR-2012-title40-vol27-part261.xml>.

**APPENDIX A8: Limestone neutralisation results***Table A8:1: Summary of the neutralisation results of 0.005 M sulphuric acid (pH = 2) that was reacted with 0.20 g CaCO<sub>3</sub> of various particle size fractions*

Reaction time (minutes)	Limestone particle size (mm)			
	< 0.1	≥ 0.1 < 1	≥ 1 < 4	≥ 4 < 10
	pH of the aqueous system			
20	7.19	2.45	2.35	2.27
40	7.47	2.59	2.47	2.26
60	7.54	2.95	2.69	2.39
80	7.60	3.42	2.95	2.46
100	7.51	4.92	3.85	2.80

*Table A8:2: Summary of the neutralisation results of 0.0005 M sulphuric acid (pH = 3) that was reacted with 0.20 g CaCO<sub>3</sub> of various particle size fractions*

Reaction time (minutes)	Limestone particle size (mm)			
	< 0.1	≥ 0.1 < 1	≥ 1 < 4	≥ 4 < 10
	pH of the aqueous system			
20	7.66	5.29	4.04	3.29
40	7.61	7.28	6.10	3.95
60	7.66	7.22	6.77	4.52
80	7.67	7.19	6.75	5.62
100	7.69	7.19	6.72	6.06

*Table A8:3: Summary of the neutralisation results of synthetic acid metal cation mine water with an initial pH of 2 that was reacted with 0.20 grams of CaCO<sub>3</sub> of various particle size fractions*

Reaction time (minutes)	Limestone particle size (mm)			
	< 0.1	≥ 0.1 < 1	≥ 1 < 4	≥ 4 < 10
	pH of the aqueous system			
20	4.17	2.72	2.26	2.17
40	4.87	3.31	2.69	2.54
60	5.21	3.42	2.90	2.70
80	5.24	3.43	3.08	2.86
100	5.32	3.46	3.20	3.02

Table A8:4: Summary of the neutralisation results of synthetic acid metal cation mine water with an initial pH of 3 that was reacted with 0.20 grams of CaCO<sub>3</sub> of various particle size fractions

Time (minutes)	Limestone particle size (mm)			
	< 0.1	≥ 0.1 < 1	≥ 1 < 4	≥ 4 < 10
	pH of the aqueous system			
20	5.53	3.74	3.58	3.37
40	5.40	3.75	3.59	3.43
60	5.60	3.79	3.64	3.51
80	5.69	3.84	3.67	3.58
100	5.67	3.86	3.68	3.60

Table A8:5: Summary of the neutralisation results of percolating synthetic acid metal cation mine water with an initial pH of 2 through a sand column that contained limestone

Leaching procedure	Particle size fraction of limestone used in column (mm)	Placement of limestone in column	pH of the leachate exiting column				
			Time (hours)				
			48	96	144	192	240
LP 1	< 0.1	Surface	5.12	4.43	4.07	4.05	3.98
		Mixed	4.09	4.13	3.93	3.95	3.77
	≥ 4 < 10	Surface	2.36	2.42	2.36	2.37	2.32
		Mixed	2.23	2.45	2.38	2.39	2.35
LP2	< 0.1	Surface	4.55	4.63	4.45	4.48	4.24
		Mixed	4.63	4.41	4.13	4.12	3.98
	≥ 4 < 10	Surface	2.44	2.59	2.47	2.45	2.40
		Mixed	2.43	2.60	2.54	2.52	2.45

**APPENDIX A9: Soil redox monitoring**

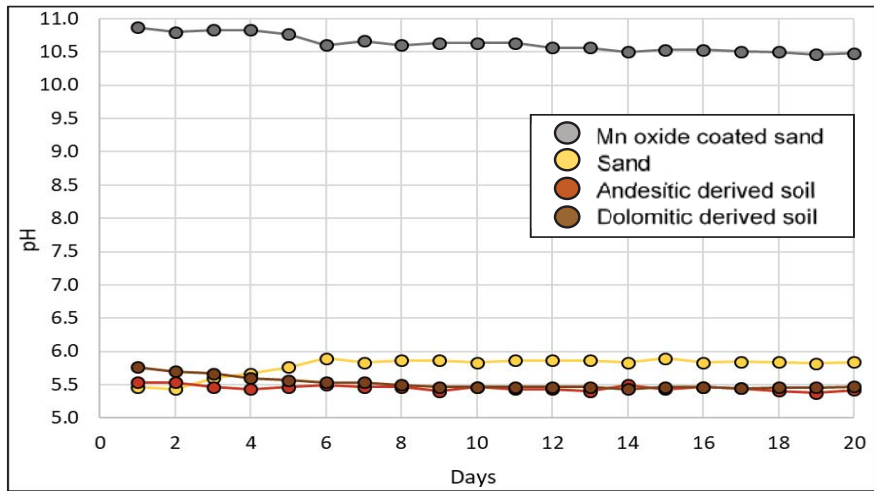


Figure A9.1: Change in pH of the four soils over the 20-day aeration/oxidizing period.

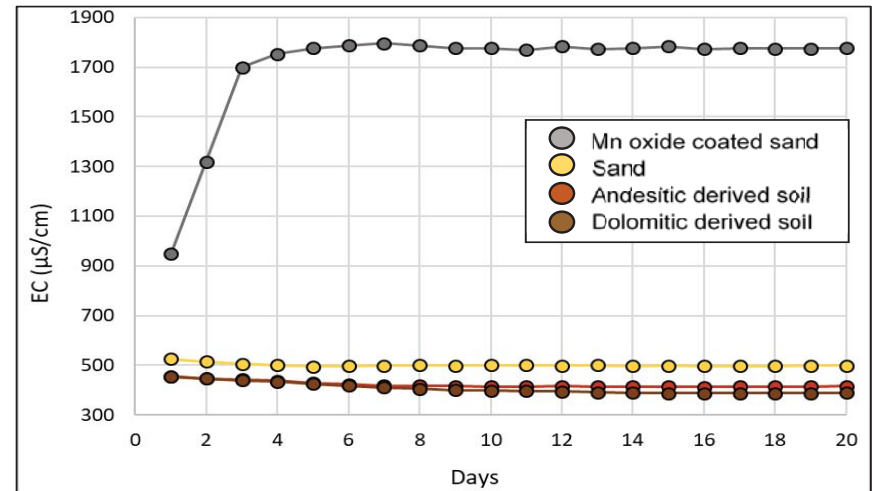


Figure A9.2: Change in Electrical Conductivity (EC -  $\mu\text{S}/\text{cm}$ ) of the four soils over the 20-day aeration/oxidizing period.

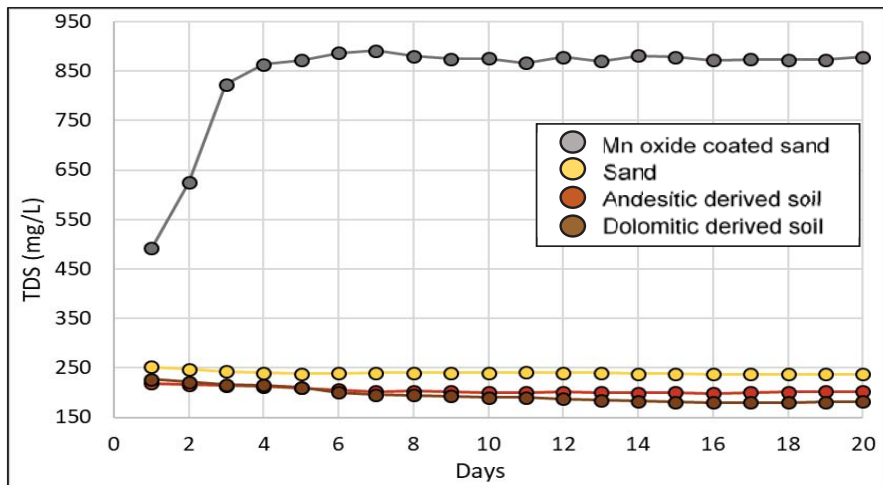


Figure A9.3: Change in Total Dissolved Solids (TDS -  $\text{mg}/\text{L}$ ) of the four soils over the 20-day aeration/oxidizing period.

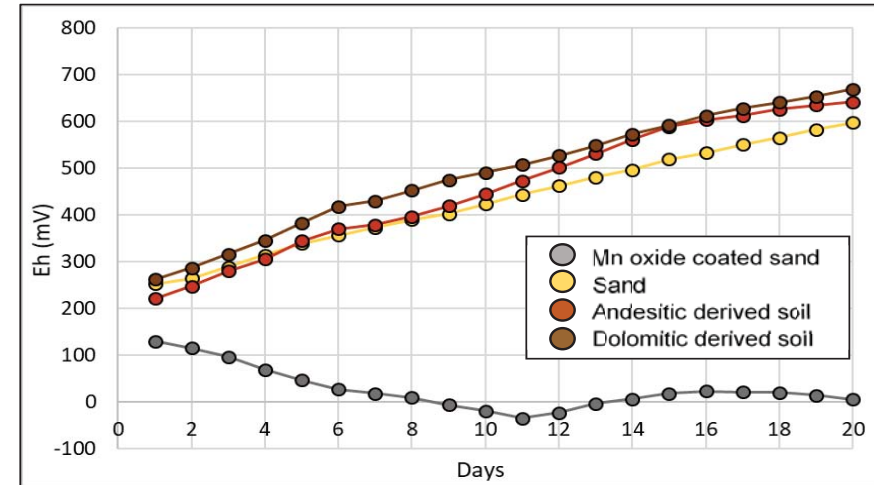


Figure A9.4 Change in Redox Potential (Eh -  $\text{mV}$ ) of the four soils over the 20-day aeration/oxidizing period.

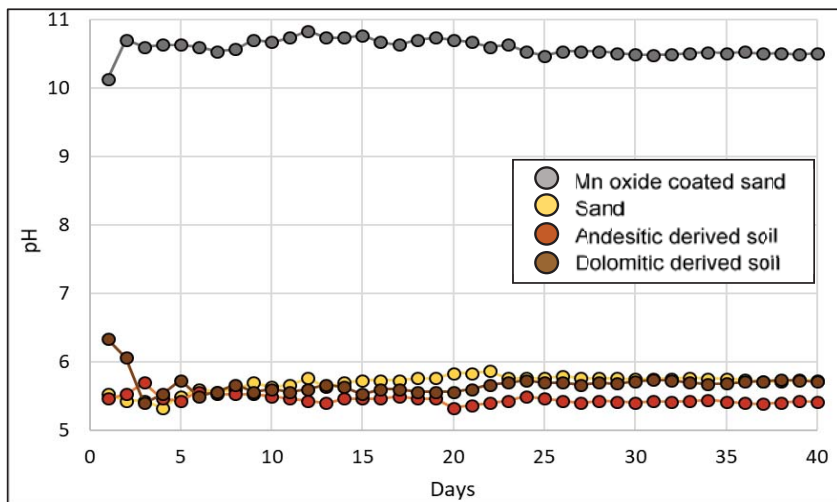


Figure A9.5: Change in pH of the four soils over the 40-day aeration/oxidizing period.

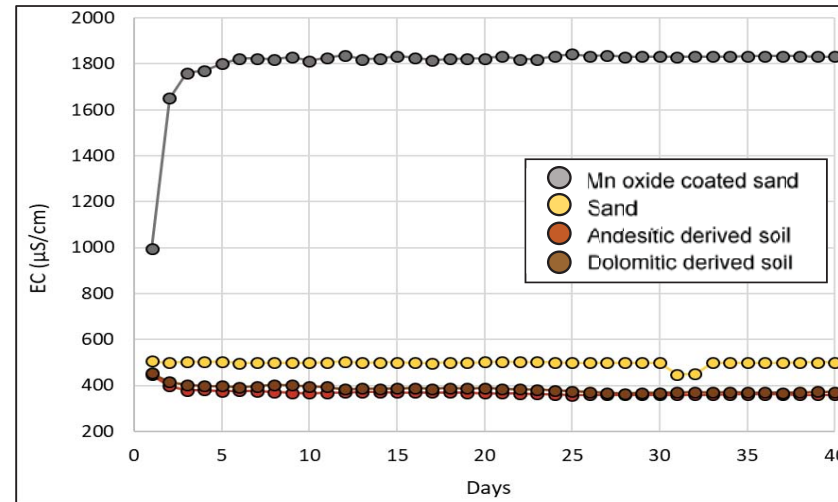


Figure A9.6: Change in Electrical Conductivity (EC -  $\mu\text{S}/\text{cm}$ ) of the four soils over the 40-day aeration/oxidizing period.

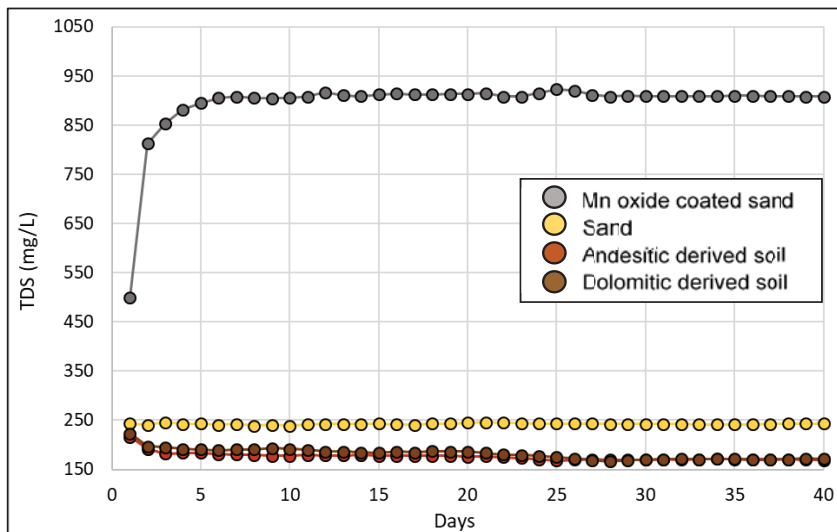


Figure A9.7: Change in Total Dissolved Solids (TDS -  $\text{mg}/\text{L}$ ) of the four soils over the 40-day aeration/oxidizing period.

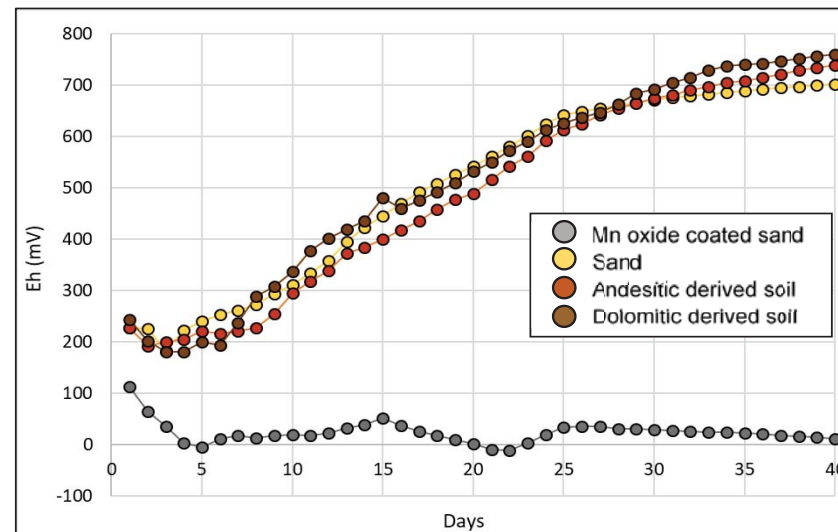


Figure A9.8: Change in Redox Potential (Eh -  $\text{mV}$ ) of the four soils over the 40-day aeration/oxidizing period.

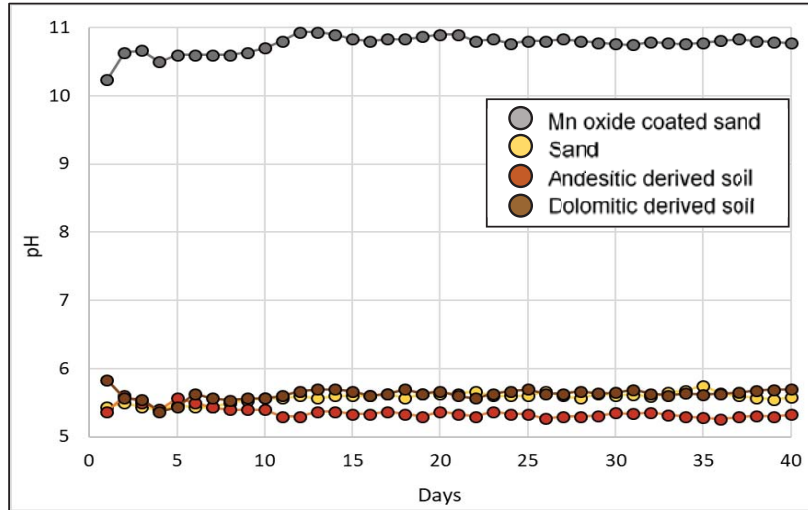


Figure A9.9: Change in pH of the four soils over the 15-day aeration/oxidizing and 25-day increasingly reducing period.

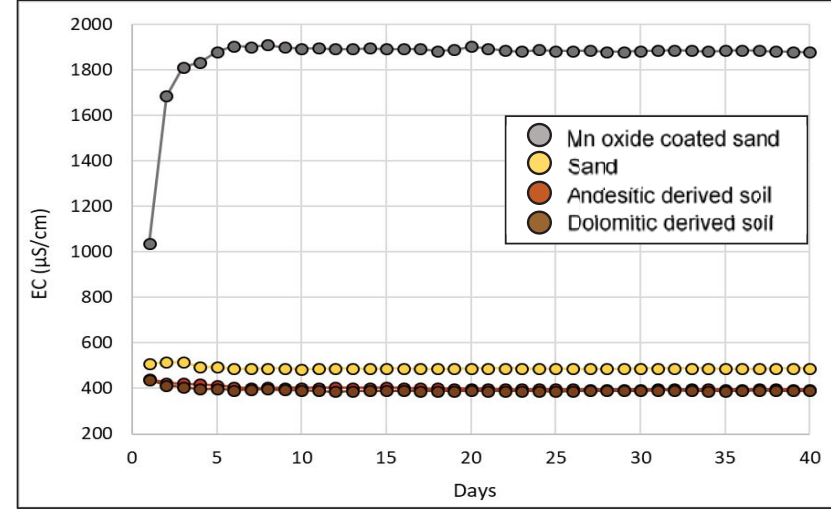


Figure A9.10: Change in Electrical Conductivity (EC -  $\mu\text{S}/\text{cm}$ ) of the four soils over the 15-day aeration/oxidizing and 25-day increasingly reducing period.

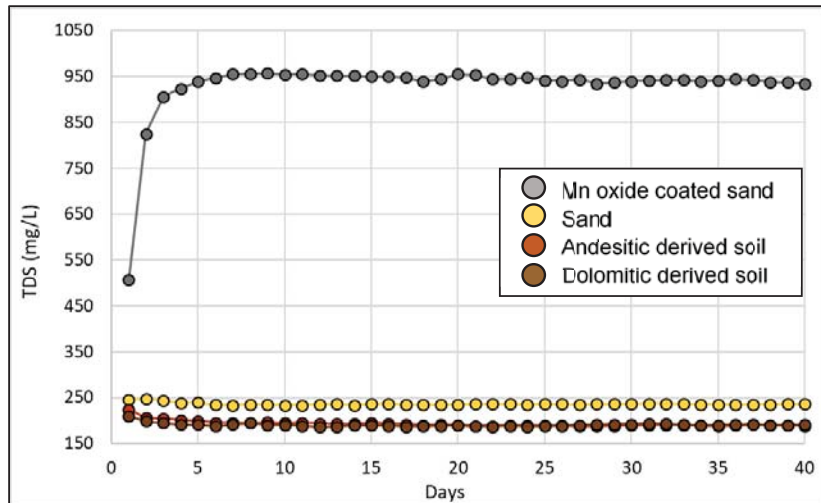


Figure A9.11: Change in Total Dissolved Solids (TDS -  $\text{mg}/\text{L}$ ) of the four soils over the 15-day aeration/oxidizing and 25-day increasingly reducing period.

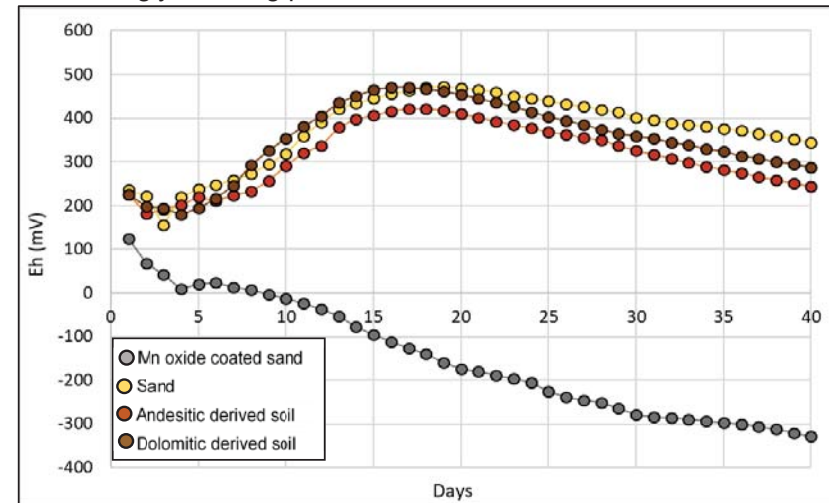


Figure A9.12: Change in Redox Potential (Eh -  $\text{mV}$ ) of the four soils over the 15-day aeration/oxidizing and 25 day increasingly reducing period.



